UNIVERSITY OF KWAZULU-NATAL
INYUVESI YAKWAZULU-NATALI

THE MICROMORPHOLOGICAL CHARACTERIZATION, HISTO-PHYTOCHEMICAL ANALYSIS AND BIOACTIVITY OF *TABERNAEMONTANA VENTRICOSA* HOCHST. EX A. DC. (APOCYNACEAE)

BY

CLARISSA MARCELLE NAIDOO

A research thesis submitted in fulfilment of the academic requirements for the degree of

DOCTOR OF PHILOSOPHY

In the School of Life Sciences,

College of Agriculture, Engineering and Science

University of KwaZulu-Natal

Westville Campus

South Africa

November 2021

As the candidate 's supervisor and co-supervisors, we have approved submission of this thesis.

Signed: [redacted]

Professor Y. Naidoo

Supervisor

30th November 2021

Signed: [redacted]

Professor Y. H. Dewir

Co-Supervisor

30th November 2021

Signed: [redacted]

Professor M. Singh

Co-Supervisor

30th November 2021

ABSTRACT

Medicinal plants are universally important due to their healing properties and pharmacological effects. *Tabernaemontana ventricosa* Hochst. ex A. DC. is a curative plant belonging to the Apocynaceae. The bark, stem, leaves, flowers, and latex of *T. ventricosa* are frequently used in ethnomedicine to palliate fever, treat wounds, and reduce high blood pressure. Due to the inconsistencies in the interpretation of specialized secretory structures within the Apocynaceae, the current study aimed to distinguish, for the first time, the type and distribution of the laticifers in the embryos, seedlings, and adult plants of *T. ventricosa*. Various microscopy techniques such as light microscopy, stereomicroscopy, fluorescence microscopy, Scanning Electron Microscopy (SEM), and Transmission Electron Microscopy (TEM) were used for anatomical and morphological analysis. The histochemical, phytochemical, and biological activities (antibacterial, antioxidant, and cytotoxicity) were assessed using screening standard protocols. Moreover, Gas Chromatography-Mass Spectrometry (GC-MS) was conducted to identify the chemical composition of leaf, stem, and latex extracted with various solvents. Silver nanoparticles (AgNPs) were synthesized using various leaf, stem, and latex extracts. The AgNPs were characterized using UV-visible spectral analysis, Elemental Dispersive X-ray (EDX) spectroscopy, Fourier-Transform Infrared (FTIR) spectroscopy, Nanoparticle Tracking Analysis (NTA), and various microscopy methods. Additionally, AgNPs were evaluated for their biological activity using antibacterial and cytotoxicity assays. The current study indicated the presence of articulated anastomosing laticifers. The laticifers were found to have originated from ground meristematic and procambium cells and were randomly distributed in all ground and vascular tissue, displaying complex branching conformations. The presence of chemical constituents within the laticifers and latex revealed alkaloids, phenolics, neutral lipids, terpenoids, mucilage, pectin, resin acids, carboxylated polysaccharides, lipophilic and hydrophilic substances, and proteins. The GC-MS analysis revealed α-linolenic acid, pentadecanoic acid, α-d-mannofuranoside, methyl, 13-docosenamide, (Z)-, 9,12-octadecadienoic acid (Z,Z)-, lup-20(29)-en-3-ol, acetate, (3β), 9,19-cyclolanost-24-en-3-ol, (3β) and β-amyrin as significant components of the leaf, stem, and latex extracts. It is suggested that these major compounds are responsible for the considerable antibacterial, antioxidant, and cytotoxic activities of *T. ventricosa* extracts. Biologically synthesized AgNPs displayed a spherical, ovate, and triangular shape ranging from 4-80 nm across all treatments. The FTIR analysis showed that alcohols, carboxylic acids, phenolics, and alkanes are possibly responsible for the capping of silver (Ag) ions, and the NTA data suggests that synthesized AgNPs fluctuated from stable to unable particles, which was treatment dependent. Due to the outcomes of biologically active compounds produced by this species, further studies are necessary to establish the potential medicinal properties of *T. ventricosa*.

PREFACE

The research contained in this thesis was completed by the candidate while based in the Discipline of Biological Sciences, School of Life Sciences of the College of Agriculture, Engineering and Science, University of KwaZulu-Natal, Westville, South Africa. The financial assistance of the National Research Foundation (NRF) towards this research is hereby acknowledged. Opinions expressed, and conclusions arrived at, are those of the author and are not necessarily to be attributed to the NRF.

The contents of this work have not been submitted in any form to another university and, except where the work of others is acknowledged in the text, the results reported are due to investigations by the candidate.

[redacted]

Signed: Professor Y. Naidoo (Supervisor)

30th November 2021

[redacted]

Signed: Professor Y. H. Dewir (Co-supervisor)

30th November 2021

[redacted]

Signed: Professor M. Singh (Co-supervisor)

30th November 2021

DECLARATION 1: PLAGIARISM

I, **Clarissa Marcelle Naidoo**, declare that:

1. The research reported in this thesis, except otherwise indicated, is my original research.

2. This thesis has not been submitted for any degree or examination at any other university.

3. This thesis does not contain any other persons' data, pictures graphs or other information, unless specifically acknowledged as being sourced from other persons.

4. This thesis does not contain other persons' writing unless specifically acknowledged as being sourced from other researchers. Where other written sources have been quoted, then:

> **a.** Their words have been re-written but the general information attributed to them has been referenced.
>
> **b.** Where their exact words have been used, then their writing has been placed in italics and inside quotation marks, and referenced.

5. This thesis does not contain text, graphics or tables copied and pasted from the internet, unless specifically acknowledged, and the source being detailed in the thesis and in the Reference Section.

Signed: **Clarissa Marcelle Naidoo**

Date: 30th November 2021

Declaration Plagiarism 22/05/08 FHDR Approved

DECLARATION 2: PUBLICATIONS

DETAILS OF CONTRIBUTION TO PUBLICATIONS that form part and/or include research presented in this thesis (include publications in preparation, submitted, *in press* and published and give details of the contributions of each author to the experimental work and writing of each publication.

Abstract

Naidoo, C.M. and Naidoo, Y., **2018**. Laticifers in the leaves of *Tabernaemontana ventricosa*: Structure, distribution and histophytochemical analysis. South African Journal of Botany 115, 325. 44th Annual Conference of the South African Association of Botanists, Pretoria, South Africa. *Published.*

Research papers

Naidoo, C., Naidoo, Y. and Dewir, Y.H., **2020**. The secretory apparatus of *Tabernaemontana ventricosa* Hochst. ex A. DC. (Apocynaceae): Laticifer identification, characterization and distribution. Plants 9, 686, https://doi.org/10.3390/plants9060686. *Published.*

Naidoo, C.M., Naidoo, Y., Dewir, Y.H., Singh, M. and Lin, J., **2021**.Phytochemical composition and antibacterial evaluation of *Tabernaemontana ventricosa* Hochst. ex A. DC. leaf, stem, and latex extracts. *Publication in preparation*.

Naidoo, C.M., Naidoo, Y., Dewir, Y.H., Singh, M., and Daniels, A.N. **2021**. *In vitro* investigation of the antioxidant and cytotoxic potential of *Tabernaemontana ventricosa* Hochst. ex A. DC. leaf, stem, and latex extracts. *Publication in preparation*.

Naidoo, C.M., Naidoo, Y., Dewir, Y.H., Singh, M., Daniels, A.N. and Lin, J., **2021**. Synthesis, characterization, and bioactivity of silver nanoparticles (AgNPs) using methanolic, fresh, and powdered leaf and stem extracts of *Tabernaemontana ventricosa* Hochst. ex A. DC. *Publication in preparation*.

Naidoo, C.M., Naidoo, Y., Dewir, Y.H., Singh, M., Daniels, A.N. and Lin, J., **2021**. Antibacterial and cytotoxic activity of biologically synthesized silver nanoparticles (AgNPs) using latex extracts of *Tabernaemontana ventricosa* Hochst. ex A. DC. *Publication in preparation*.

Review paper

Naidoo, C.M., Naidoo, Y., Dewir, Y.H., Murthy, H.N., El-Hendawy, S. and Al-Suhaibani, N., **2021**. Major bioactive alkaloids and biological activities of *Tabernaemontana* species (Apocynaceae). Plants 10, 313, https://doi.org/10.3390/plants10020313. *Published.*

Book Chapter

Naidoo, C.M., Munsamy, A., Naidoo, Y., Dewir, Y.H., **2021**. Chemistry, biological activities and uses of latex from selected species of Apocynaceae. In: Murthy H.N. (eds) Reference Series in Phytochemistry: Gums, Resins and Latexes of Plant Origin. Springer Cham. https://doi.org/10.1007/978-3-030-76523-1_36-1. *Published.*

Signed: **Clarissa Marcelle Naidoo**

Date: 30th November 2021

Declaration Publications FHDR 22/05/08 Approved

CONFERENCE CONTRIBUTIONS FROM THIS THESIS

Naidoo, C.M. and Naidoo, Y., **2018**. Laticifers in the leaves of *Tabernaemontana ventricosa*: Structure, distribution and histophytochemical analysis. South African Journal of Botany 115, 325. 44th Annual Conference of the South African Association of Botanists, Pretoria, South Africa **&** School of Life Sciences (SLS) Research Day. University of KwaZulu-Natal (Westville), College of Agriculture, Engineering, and Sciences (**22nd May 2019**).

Naidoo, C.M., Naidoo, Y., Dewir, Y.H., Lin, J. **2019**. Phytochemical analysis and preliminary anti-bacterial activity of *Tabernaemontana ventricosa* Hochst. ex A. DC. leaf and stem crude extracts. 2nd International Conference on Traditional Medicine, Phytochemistry and Medicinal Plants, Berlin, Germany **&** Postgraduate Research, and Innovation Symposium (PRIS). University of KwaZulu-Natal (Westville), College of Agriculture, Engineering, and Sciences (**17TH October 2020**).

Naidoo, C.M., Naidoo, Y., Dewir, Y.H. **2019**. Laticifers in *Tabernaemontana ventricosa*: Micromorphology, histochemical analysis, and ultrastructure. The 56th Congress of the Microscopy Society of Southern Africa, Langebaan, Cape Town.

Naidoo, C.M., Naidoo, Y., Dewir, Y.H., Lin, J. **2020**. Preliminary green synthesis of silver nanoparticles using leaf and stem methanolic extracts of *Tabernaemontana ventricosa.* Postgraduate Research and Innovation Symposium (PRIS). University of KwaZulu-Natal (Westville), College of Agriculture, Engineering, and Sciences **&** The International Conference on Traditional Medicine (TMED-2021) and Phytochemistry (virtual) (**July 2021**).

Naidoo, C.M., Naidoo, Y., Dewir, Y.H., Singh, M., Lin, J. **2021**. Phytochemical composition and anti-bacterial evaluation of *Tabernaemontana ventricosa* Hochst. ex A. DC. leaf, stem, and latex extracts. Postgraduate research and innovation symposium (PRIS). University of KwaZulu- Natal- Westville, College of Agriculture, Engineering, and Sciences. *Abstract submitted presentation to be held on the* ***8th and 9th of December 2021***.

TABLE OF CONTENTS

LIST OF TABLES

LIST OF FIGURES

LIST OF ABBREVIATIONS AND SYMBOLS

3PS31	Leukemia
A2780	Ovarian cancer
A375	Human melanoma cell lines
A431	Human epidermoid carcinoma
A-549	Human gastric carcinoma
A549	Human non-small lung carcinoma
AA	Ascorbic acid
Abs	Absorbance
ABTS	2,2-azino-bis-(3ethylbenzothiazoline-6-sulphonic acid
AChE	Acetylcholinesterase
ACT	Asclepiadinae, Cynanchinae, and Tylophorinae
AD	Alzheimer's disease
Ag	Silver
$AgNO_3$	Silver nitrate
AgNPs	Silver nanoparticles
APG	Angiosperm Phylogeny Group system
APSA	Apocynoideae, Periplocoideae, Secamonoideae, and Asclepiadoideae
AR	Analytical reagent
Asclep	Asclepiadaceae s.str.
ATCC	American Type Tissue Culture Collection
ATP	Adenosine triphosphate
Au	Gold
BHT	Butylated hydroxytoluene
BL	Branched laticifer
BS	*Bacillus subtilis*
c	Collenchyma
C33A	Human cervical carcinoma
Ca	Calcium
Cam	Cambium
CaOx	Calcium oxalate
CC-1-59Sk	Normal skin cell line
CCSCS	Colorectal cancer stem cells
CEM-WT	Lymphoblastoid
Cl	Chloride

CLSI	Clinical and Laboratory Standards Institute
cm	Centimetre
cm^2	Square centimetre
Co	Cortex
CO_2	Carbon dioxide
Col2	Human colon cancer
COLO 320DM	Human colon adenocarcinoma
COR-L23	Lung carcinoma large cell
Cu	Copper
cw	Cell wall
cwd	Cell wall dissolution
DENV	Dengue virus strains
DMSO	Dimethylsulphoxide
DNA	Deoxyribonucleic acid
DPPH	2,2-diphenyl-1-picrylhydrazyl
DR	Democratic republic
dt	Dictyosomes
E	East
EBA-EA	Epstein-Barr virus early antigen
EC	*Escherichia coli*
EDX	Energy-Dispersive X-ray
EMCV	*Encephalomyocarditis* virus
EMEM	Eagles Minimum Essential Medium
er	Endoplasmic reticulum
EtOH	Ethanol
FBS	Foetal bovine serum
Fe^{3+}	Ferric ion
FL	Fresh leaf
Flo	Flowers
FRAP	Ferric Reducing Antioxidant Power
FS	Fresh stem
Fs	Fruit sap
FTIR	Fourier Transform Infrared
g	Gram
GA	Gallic acid
GAE	Gallic acid equivalents

gb	Golgi body
GC-MS	Gas Chromatography-Mass Spectrometry
GM	Ground meristem
h	Hours
H_2SO_4	Sulphuric acid
HCl	Hydrochloric acid
HCT-116	Human colon colorectal
HCT-116	Human hepatoma
HCT-15	Human colon cancer
HEK293	Human embryonic kidney cell line
HeLa	Cervical carcinoma cell line
Hep-2	Laryngeal carcinoma
Hep-G2	Human hepatoma
HL-60	Human myeloid leukemia
HP-1	Leukemia
HRTEM	High-Resolution Transmission Electron Microscopy
HSL	H-shaped laticifer
HSV-1	Herpes simplex virus type 1
HT	Human fibrosarcoma
HT-29	Human colon colorectal
HUH-7	Human hepatoma
IAV	Influenza A virus
IC_{50}	Half minimal inhibitory concentration
IL	Interleukin
itw	Irregular thickened walls
K	Potassium
KB, KB-VIN Cells	Human carcinoma
KM-12	Human colon cancer
kV	Kilovolt
La	Latex
Lb	Lipid body
LC_{50}	Half minimal lethal concentration
le	Lower epidermis
Le	Leaves
LNCaP	Human prostate cancer
LPS	Reduction of lipopolysaccharide

Lu1	Human lung cancer
M	Molar
Ma	Mega-annum
MALOUET	Malouetieae
MCF-7	Human breast adenocarcinoma cell line
MDA-468	Human breast cancer
MDA-M231	Breast cancer cells
MDA-MB-231	Human breast adenocarcinoma
MDR	Multidrug resistance
Mel2	Human melanoma
MESECHIT	Mesechiteae
Mg	Magnesium
mg	Milligram
mg/kg	Milligram per killogram
mg/mL	Milligram per millilitre
MH	Mueller- Hinton
MIC	Minimum Inhibitory Concentration
Min	Minutes
mL	Millilitre
mL/min	Millilitre per minute
mM	Milli molar
MMT	3-(4,5-dimethylthiazol-2-yl)-2,5-diphenyl-2H-tetrazolium bromide
Mn	Manganese
MNZ	Metronidazole
MOG	Metastelmatinae, Oxypetalinae, and Gonolobinae
MOLT4	Human leukemia
MRSA	*Methicillin-Resistant Staphylococcus aureus*
mt	Mitochondria
mV	Millivolt
NaOH	Sodium hydroxide
NCI-H460	Human lung cancer
ND	Not determined
NIST	National institute of science and technology
nm	Nanometer
NO	Nitric acid
NOR	Novel object recognition test

NP	Nanoparticle
NTA	Nanoparticle Tracking Analysis
O_2	Oxygen
ob	Osmiophilic bodies
OD	Optical density
ODONTAD	Odontadenieae
OVCAR-3	Ovarian carcinoma
OW	Old world
p	Plastid
P388	Murine, lymphocytic leukemia
pa	Parenchyma
PA	*Pseudomonas aeruginosa*
pal	Palisade
PBS	Phosphate buffered saline
PC	Procambium
PC-3	Prostate cancer
ph	Phloem
pH	Potential of Hydrogen
pi	Pith
QE	Quercetin equivalents
QR	Quinone reductase induction
Rf	Retention factor
RNS	Reactive nitrogen species
ROS	Reactive oxygen species
rp	Rubber particles
rpm	Revolutions per minute
RPMI-8226	Myeloma
S	Sulphur
SA	*Staphylococcus aureus*
SANBI	South African National Biodiversity institute
SD	Standard deviation
SEM	Scanning Electron Microscopy
SF-268	Human glioblastoma
sg	Starch grain
SH	Stem hexane
SK-BR-3	Human breast carcinoma

SK-MEL-28	Human melanoma cell lines
SK-Mel-28	Melanoma
SM	Stem methanol
SMMC-7721	Human hepatoma
SNB-19	Glioblastoma
Spp	Several species
SPR	Surface Plasmon Resonance
SW480	Colon carcinoma
SW620	Human hepatoma
TEM	Transmission Electron Microscopy
Temp	Temperature
THP-1	Human leukemia cells
TLC	Thin Layer Chromatography
TNF	Tumour necrosis factor
TPA	Terephthalic acid
U-2 OS-WT	Osteosarcoma
U373	Human glioma
UBL	Un-branched laticifer
UK	United Kingdom
USA	United States of America
USL	U-shaped laticifer
UV	Ultra-violet
V	Volt
v	Vacuole
VACV-WR	Vaccina virus Western Reserve
vb	Vascular bundles
Vis	Visible
WHO	World Health Organisation
WM1366	Human melanoma cell lines
ZR-75-1	Hormone-dependent breast cancer
µg	Microgram
µg/mL	Microgram per millilitre
µg/µL	Microgram per Microlitre
µL	Microlitre
µM	Micrometer
°	Degree

%	Percent
v/*v*	Volume to Volume ratio
λ	Wavelength (lambda)
α	Alpha
β	Beta

DEDICATION

This thesis is dedicated to

my dad Mr. Lenny Naidoo, my uncle Mr. Louis Naidoo

and my grandparents Mr. and Mrs. Naidoo, and Mr. and Mrs. Subroyen.

Thank you for your never-ending inspiration, guidance, and love from above.

I am forever grateful for your presence in my life.

ACKNOWLEDGEMENTS

Foremost, I am thankful to the Almighty God, the completion of my research would have been impossible without the comfort, strength, and guidance received from above.

I would like to express my sincere gratitude to my supervisor Prof. Yougasphree Naidoo, thank you for your invaluable supervision, scientific expertise, endless support, encouragement, and care throughout my research. I am extremely grateful to my co-supervisors, Prof. Moganavelli Singh and Prof. Yaser Hassan Dewir for their guidance, comprehensive scientific knowledge, prompt feedback, and valuable suggestions. I would like to thank Prof. Johnson Linn for his leadership and resources for the antibacterial component of this research, and Prof. Shahidul Islam for assistance with antioxidant assays. A genuine thank you to Dr. Sadashiva Thimmegowda, Dr. Nneka Akwu, Dr. Aliscia Daniels, and Dr. Sarisha Singh for their knowledge and assistance with my research components.

A sincere thank you to the University of KwaZulu-Natal (UKZN-Westville) for providing me with the necessary support and facilities required for the completion of my research. I would also like to thank the National Research Foundation (NRF) for assisting me with financial support throughout my research. Thank you to the staff of the Microscopy and Microanalysis Unit (MMU) at UZKN-Westville, especially Dr. Vishal Bharuth, Mr. Subashen Naidu, and Mr. Phillip Christopher for their invaluable assistance, support, and guidance with the microscopy components. I would like to extend my thanks to Mrs. Neervana Rambaran and Mr. Yegandran Pillay for their guidance and kind assistance.

To my dearest friends and colleagues from the UKZN Westville campus, I am thankful for your continuous support, kindness, motivation, inspiring discussions, and infinite cheerfulness. I would also like to thank Ms. Vineshree Shadamorgan for her motivation, patience, and editorial assistance. A special thank you to my colleague and laboratory partner, Serisha Gangaram. I am sincerely grateful for your kind assistance, encouragement, and friendship throughout our immensely challenging journey. Your continuous enthusiasm, support, and guidance are truly appreciated.

Finally, I would like to express my deep gratitude to my supermom Salome Naidoo. Thank you for your constant support and prayers, being my inspiration and an exceptional role model. To my sister Loreal Naidoo, Brother, Jared Naidoo, and partner Nicolan Reddy, I am thankful for your never-ending support, kind assistance, understanding, and continuous reassurance throughout my research. I would also like to thank my Dog Max for being the best companion and keeping me company during many late nights of research. Lastly, I am thankful to my entire Naidoo family, this achievement would have been relentless without your love, support, and care.

CHAPTER 1:

INTRODUCTION

1.1 Traditional medicine

"The healing comes from nature and not from the physician. Therefore, the physician must start from nature with an open mind."

~Paracelsus~

For centuries, nature has been our pharmaceutical dispensary that man was dependent upon plants to cure numerous infectious diseases and illnesses (Rios and Recio, 2005; Kinghorn et al., 2011; Dias et al., 2012). These curative plants are generally recognized as medicinal plants and are comprised of biochemical compounds known as secondary metabolites (Shruthi et al., 2012). These plants have contributed to the enhancements in ancient and contemporary medicine by discovering novel compounds that led to the refinement of medicinal drugs (Thomas et al., 2009; Pan et al., 2010; Cragg and Newman, 2013). The biochemical constituents of various medicinal plants have been applied therapeutically in pharmacological industries (Shruthi et al., 2012; Yuan et al., 2016). The secondary metabolites of plants contain biochemical compounds that can be extracted from the entire plant or plant organs, such as the leaves, stems, bark, roots, fruit, and flowers (Shakya, 2016). Traditional healers incorporate medicinal plants into their treatment practices, as particular plant organs contain a myriad of secondary metabolites that aid in combating specific illnesses (Shruthi et al., 2012; Boadu and Asase, 2017).

Traditional healers have exploited traditional medicine since the ancient practice of general world healthcare (WHO, 2001). The World Health Organization (WHO) has defined traditional medicine as:

"*Health practices, approaches, knowledge, and beliefs incorporating plant, animal and mineral-based medicines, spiritual therapies, manual techniques, and exercises, applied singularly or in combination to treat, diagnose and prevent illnesses and maintain well-being,*" (WHO, 2001).

This form of traditional medicine has been used solely to prevent and treat physical and mental sicknesses in many countries such as China, Japan, India, and Africa (Abdullahai, 2011; Yuan et al., 2016). The latter countries have developed a deep understanding of ancient and modern systems of traditional medicine. According to Li (2000), the vital source of remedies used by traditional healers in China is botanical and accountable for approximately one-fifth of the Chinese pharmaceutical

market. Saito (2000) explained that the adoption of these medical practices in Japan was based on the abundance of native traditional herbs classified in the pharmacopeia of Japanese medicine in the ninth century. Yuan et al. (2016) reported that the traditional medical systems in India, frequently referred to as Ayurveda was practiced for ~ 5000 years. This practice integrated a holistic treatment process on the body, mind, and spirit (Yuan et al., 2016). Furthermore, the fact sheet compiled by WHO (2003) specified that ~ 80% of the African population are reliant on traditional medicines as their basic healthcare system.

Southern Africa countries embrace a remarkable diversity of more than 30 000 higher plant species (Drewes, 2012). It has been reported that traditional healers and individuals utilize over 3 000 of South Africa's indigenous plants in rural areas (Van Vuuren, 2008; Van Wyk, 2008). Due to severe limitations and restrictions of medicinal facilities, several African communities often rely exclusively on medicinal plants for their primary healthcare (Van Vuuren, 2008; Van Wyk, 2008). The medicinal plant market in South Africa is currently garnering attention with the principal purpose of improving the well-being and health of people in rural areas that are exceedingly vulnerable to illness and disease (Yuan et al., 2016). Factors such as the rapid rise in the global population, poverty, and increased transmission of diseases have prompted the full acceptance of medicinal plant species in South Africa over the past 15 years (Erasto et al., 2005).

Recently, phytochemical, and pharmacological researchers have developed an augmented interest in medicinal plants (Wadood et al., 2013). Currently, these research fields support studies relating to homeopathic medicine (Street, 2012; Wadood et al., 2013). Pharmacological studies involve determining the drug action of natural compounds present within medicinal plants (Debnath et al., 2006). In addition, researchers are attentive to understanding the biochemical and physiological effects or mechanisms that therapeutic compounds exert on cells, tissues, organs, or organisms (Jäger and Van Staden, 2000; Debnath et al., 2006). Therefore, it is imperative to improve the use of natural medicinal compounds in modern medicine to ensure that any adverse effects of natural products are reduced to meet numerous safety standards (Yuan, 2016).

However, the improved usage and commercialization of medicinal plants may lead to over-harvesting and exploitation (Jäger and Van Staden, 2000; Joy et al., 2001). Thus, various research fields such as phytochemistry, pharmacology, micromorphology, and micropropagation should conduct simultaneous investigations. The collaborative studies will ensure that the specific medicinal properties of different medicinal plants are identified, as this will allow the efficient utilization of medicinal plants by small-scale communities (Debnath et al., 2006). These associations would eliminate the risks of overexploitation and extinction of many valuable medicinal species by promoting the enrichment of medicinal plants (Williams et al., 2000; Debnath et al., 2006).

1.2 Botanical description of *Tabernaemontana ventricosa* Hochst. ex A. DC

Tabernaemontana ventricosa (Omino, 1993) is an evergreen, small to medium-sized tree belonging to the Apocynaceae and genus *Tabernaemontana* (Schmelzer and Gurib-Fakim, 2008). Trees of *T. ventricosa* can grow up to 15 m tall (Schmelzer and Gurib-Fakim, 2008). It has a single slender, smooth grey-brown trunk and is dichotomously branched, as illustrated in Figure 1.1 A. The young branches appear soft and dark green, which turns a pale brown colour when mature. The leaves are opposite and simple, with a narrow elliptical blade, rounded base, and an acute or obtuse apex (Schmelzer and Gurib-Fakim, 2008). The leaf margins have a wavy and leathery texture (Schmelzer and Gurib-Fakim, 2008). The inflorescence displays a corymb pattern, that spans 5-23 cm (Schmelzer and Gurib-Fakim, 2008), as shown in Figure 1.1 B. The flowers are bisexual, salver-shaped (Schmelzer and Gurib-Fakim, 2008), whitish yellow (Figure 1.1 B), and exhibit a sweet-scent (Schmelzer and Gurib-Fakim, 2008). The flowers usually bloom from September to December in South Africa and Kenya (Schmelzer and Gurib-Fakim, 2008). The fruit comprises two separate obliquely ellipsoid follicles ranging from 6-7 cm in diameter (Schmelzer and Gurib-Fakim, 2008); these are illustrated in Figure 1.1 C.

This species is commonly known as the “Forest toad tree” or “Small-fruited toad tree” due to the green wart-like appearance of the skin on its fruit, as observed in Figure 1.1 C. The fruit appears dark-green and wrinkled with light-green speckles or markings showing two faint lateral ridges (Schmelzer and Gurib-Fakim, 2008). The fruit splits into two halves and displays a fleshy orange pulp containing several embedded seeds (Schmelzer and Gurib-Fakim, 2008). The seeds are obliquely ellipsoid, ranging from 11-23 mm long, with longitudinal grooves (Schmelzer and Gurib-Fakim, 2008). *Tabernaemontana ventricosa* species are largely distributed in eastern Nigeria, Ghana, the Democratic Republic of Congo, Kenya, and the northern and southern regions of Africa (Schmelzer and Gurib-Fakim, 2008). The geographic distribution of *T. ventricosa* is displayed in Figure 1.1 D. *Tabernaemontana ventricosa* species often occurs in open forests and thickets in woodlands, from sea levels to 1850 m in altitude (Schmelzer and Gurib-Fakim, 2008). The tree thrives in disturbed shady habitats and requires moderate water (Schmelzer and Gurib-Fakim, 2008).

In KwaZulu-Natal, all parts of *T. ventricosa* are frequently utilized in ethnomedicine to treat several ailments and diseases (Schmelzer and Gurib-Fakim, 2008). The stems and bark of *T. ventricosa* are often consumed in the form of a decoction to reduce elevated blood pressure and fever. Furthermore, the bark and stems are used to regenerate the nervous system (Schmelzer and Gurib-Fakim, 2008). According to Schmelzer and Gurib-Fakim (2008), the leaves contain high amoebic activity and are regularly used to reduce the growth of the amoeba protist. *Tabernaemontana ventricosa* contains a

rich source of latex shown in Figure 1.1 E, that is present in all parts of the species. Studies suggest that the chemical constituents found within the latex function to deter herbivores and microorganisms and may contain medicinal value (Schmelzer and Gurib-Fakim, 2008; Naidoo et al., 2009; Naidoo et al., 2020).

There is an excessive number of alkaloids within *T. ventricosa* (Schripsema et al., 1986). Schripsema et al. (1986) identified and reported a vital compound, conopharyngine, an indole alkaloid commonly used to heal wounds (Kokwaro, 1976). Additionally, large quantities of a rare compound identified as a strychnan alkaloid were observed within *T. ventricosa* crude extracts (Schripsema et al., 1986). Furthermore, several alkaloids such as 10-hydroxyheyneanine, 16-epi-isositsirikine, apparicine, tubotaiwine, norfluorocurarine, and akuammicine have been detected within this species (Schripsema et al., 1986). In addition, a recent study conducted by Andima et al. (2021) discovered many alkaloidal and non-alkaloidal compounds from the root bark, stem bark, and leaves (mixture) of *T. ventricosa*. These compounds included 3-ketopropylcoronadine, vobasine, ibogamine, voacristine, 10-hydroxycoronaridine, 10-hydroxyibogamine, stigmasterol, quebrachitol, and ursolic acid (Andima et al., 2021).

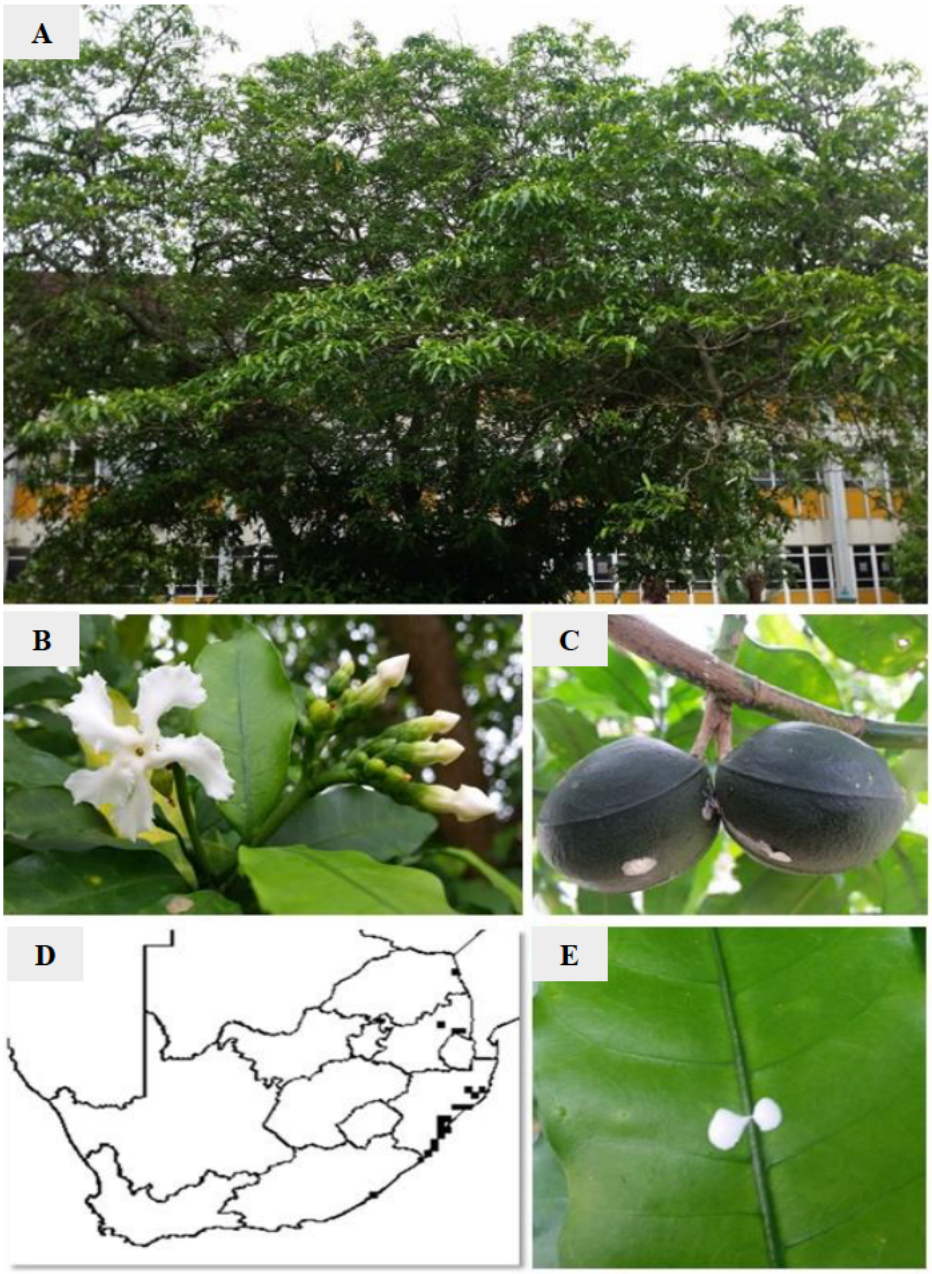

Figure 1.1: *Tabernaemontana ventricosa* captured at the University of KwaZulu-Natal (UKZN)-Westville campus, Durban, South Africa. Co-ordinates: 29˚49'03.3" S 30˚56'32.7˚E.

[A] Dichotomously branched tree.

[B] White salver-shaped flowers with faint yellow markings and distinct inflorescence.

[C] Obliquely ellipsoid follicle fruit joined at the base.

[D] Distribution of *T. ventricosa* in South Africa, Image adapted from SANBI RED LIST webpage (SANBI, 2018).

[E] Punctured leaf showing white latex exudate.

1.3 Ethnomedicinal uses of *Tabernaemontana* species

Many species within *Tabernaemontana* have several ethnomedicinal uses that range from decoctions to special pastes and are well-known to cure various illnesses and diseases (Van Beek et al., 1984; Munayi, 2016). The ethnomedicinal benefits of *Tabernaemontana* species in Africa are summarized in Table 1.1.

Table 1.1: Reported ethnomedicinal uses of *Tabernaemontana* species in Africa (Adapted from Munayi, 2016).

Plant	Plant part	Medicinal use	References
T. catharinensis	Rb, Sb, Le	Treats snake bites, eliminates warts, relieves a toothache, and obtains anti-inflammatory properties	Gomes et al., 2009; Rizo et al., 2013
T. corymbosa	Ls, Sb, Rb	Treats sores, orchitis, and hydrocele	Van Beek et al., 1984
T. crassa	Lx, Le, Sb, F	Treats ringworm infections, headaches, diarrhoea, and is used as a tonic and wound disinfectant	Irvine, 1961; Iwu, 1982; Van Beek et al., 1984
T. dichotoma	Se, Sb, Rb, Lx, F	Treats ulcers, snake bites, and reduces swelling	Van Beek et al., 1984
T. divaricata	Lx, Rb, Sb, Flo	Treats inflammation, sore eyes, headache, intestinal worms, vomiting, rabies, and fever	Van Beek et al., 1984; Sajem and Gosai, 2006; Jain et al., 2013
T. elegans	Rb	Treats pulmonary disease	Palgrave and Palgrave, 1957; Watt and Breyer-Brandwijk, 1962; Van Beek et al., 1984
T. orientalis	Rb, Lx, Le, Sb	Treats stomachache, sore nose, ulcers, sores, swelling, headaches, toothache, and induces abortion	Holdsworth, 1977; Van Beek et al., 1984
T. pachysiphon	Lx, Fs, Le, Rb	Treats sore eyes, wounds, headache, stomachache, constipation, and is used for hypnosis	Kokwaro, 1976; Van Beek et al., 1984; Omino and Kokwaro, 1993
T. stapfiana	Rb, Sb	Treats pneumonia and chest problems	Jeruto et al., 2008
T. ventricosa	Lx	Promotes wound healing, treats fever, reduces pressure, antiamoebic. Induces male/female infertility (Urethritis, Orchitis), and impotence	Kokwaro, 1976; Van Beek et al., 1984; Schmelzer and Gurib-Fakim, 2008

***Legend: Rb**-Rootbark; **Sb**-Stembark; **Se**-Seeds; **Ls**-Leaf sap; **Le**-leaves; **Lx**-Latex; **F**-Fruit; **Flo**-Flower; **Fs**-Fruit sap.*

1.4 Rationale

Medicinal plants are universally indispensable as they possess therapeutic properties and pharmacological effects (Shruthi et al., 2012). Biochemical compounds are usually extracted from whole plants or plant organs for traditional use or the manufacture of pharmaceutical drugs (Shruthi et al., 2012). Several species within *Tabernaemontana* are well known for their ethnomedicinal and pharmacological uses, thus indicating the bioactivity in *T. ventricosa* species. The presence of biologically active compounds within medicinal plants is linked to the production of secondary metabolites which correlates with one of the many functions of plant secretory organelles (Demarco et al., 2013). Specialized secretory cells recognized within *Tabernaemontana* are characterized as laticifers (Pickard, 2008). The primary purpose of laticifers is to produce secondary metabolites such as latex (Hagel et al., 2008). The function of latex remains unclear however, it has been suggested that the components found within this substance are responsible for wound healing and chemical defence against predators and pathogens (Pickard, 2008; Hagel et al., 2008; Castro and Demarco, 2008).

Phytochemical compounds such as triterpenes, fatty acids, phenolics, proteins, carbohydrates, cyanogenic glycosides, and alkaloids are major compounds present within *Tabernaemontana* (Munayi, 2016). These compounds are often considered chemotaxonomically necessary (Demarco and Castro, 2008; Hagel et al., 2008). The phytochemical analysis of many species within the *Tabernaemontana* genus has focused on various crude extracts, fractionations, chemical constituents, isolated compounds, and the discovery of novel compounds (Cardoso et al., 1998; Andima et al., 2021). However, despite the consistent usage of *Tabernaemontana* species in traditional medicine systems and the confirmation of their chemical constituents and biological activities, various species such as *T. ventricosa* are yet to be investigated for their morphological characteristics, chemical composition, and biological activities.

As mentioned previously in section 1.2, *T. ventricosa* is well known for a variety of monoterpene indole alkaloids that contain biological activity however, the literature regarding this species is outdated or very little knowledge is available therefore the current study was conducted to describe the ontogeny, morphology, and ultrastructure of secretory structures (laticifers) in embryos, seedlings, and adult plants (leaves and stems) of *T. ventricosa* using stereo, light, and electron microscopy. Additionally, studies on the chemical composition (Gas Chromatography-Mass Spectrometry) and biological activity (antioxidant, antibacterial, and cytotoxicity) were performed using crude extracts from the leaves and stems, and latex of *T. ventricosa*. Furthermore, due to the antibacterial properties of silver nanoparticles (AgNPs), additional research was conducted for the biological synthesis, characterization, and applications of AgNPs using various treatments. Once the

exact potential of this species is examined, it can be potentially used to formulate several relevant drugs in the medicinal sector.

1.5 Aims and objectives

The aims and objectives of the research chapters are as follows:

1.5.1 Chapter 3

Aim: To identify, characterize and describe the micromorphology, distribution, and chemical composition of laticifers in embryos, seedlings, and adult plants (leaves and stems) of *T. ventricosa*.

Objective 3.1: To identify, characterize, and describe the micromorphology of laticifers in embryos, seedlings, and adult plants (leaves and stems) of *T. ventricosa* using ontogeny studies and various microscopy techniques such as stereomicroscopy, light microscopy, and Scanning Electron Microscopy (SEM).

Objective 3.2: To determine the presence, location, and distribution of chemical compounds of the laticifers in leaves, stems, and latex of *T. ventricosa* using various histochemical assays.

Objective 3.3: To investigate the fluorescence features of the laticifers and latex in the leaves and stems of *T. ventricosa* using various histochemical stains.

Objective 3.4: To examine the ultrastructure of laticifers and latex by analyzing ultrathin sections using Transmission Electron Microscopy (TEM).

1.5.2 Chapter 4

Aim: To determine the organoleptic characters, phytochemical compositions, and antibacterial activities present in the leaves, stems, and latex extracts of *T. ventricosa*.

Objective 4.1: To extract phytochemical compounds present in the leaves and stems of *T. ventricosa* using a serial extraction (hexane, chloroform, and methanol) with increasing polarity.

Objective 4.2: To examine the organoleptic characters of the powdered leaf, stem, and latex of *T. ventricosa* using bright field and UV-fluorescence microscopy.

Objective 4.3: To determine the elemental composition of powdered leaf, stem, and latex of *T. ventricosa* using Energy-Dispersive X-ray (EDX) analysis.

Objective 4.4: To investigate the presence and composition of phytochemical compounds in the crude leaf and stem (hexane, chloroform, and methanol) and latex extracts of *T. ventricosa* using preliminary qualitative phytochemical tests and Thin-Layer Chromatography (TLC).

Objective 4.5: To identify the major chemical compounds in the crude leaf and stem (hexane, chloroform, and methanol), and latex extracts using Gas Chromatography-Mass Spectrometry (GC-MS).

Objective 4.6: To establish the antibacterial activity of the crude leaf and stem (hexane, chloroform, and methanol), and latex extracts against several gram-positive and gram-negative bacteria strains.

1.5.3 Chapter 5

Aim: To determine the antioxidant and cytotoxic potential of various crude leaf, stem, and latex extracts of *T. ventricosa* using multiple assays.

Objective 5.1: To assess the total phenolic and total flavonoid content in the crude leaf, stem, (hexane, chloroform, and methanol), and latex extracts using standard protocols such as the Folin-Ciolcalteu (total phenolics) and aluminum chloride colorimetric (total flavonoids) assays.

Objective 5.2: To evaluate the antioxidant activities present in the crude leaf and stem, (hexane, chloroform, and methanol), and latex extracts using the 2,2-diphenyl-1-picrylhydrazyl (DPPH), and Ferric Reducing Antioxidant Power (FRAP) assays.

Objective 5.3: To investigate the cytotoxic activity in the leaf and stem (hexane, chloroform, and methanol), and latex extracts of *T. ventricosa*, in selected mammalian cell lines; HEK293 (human embryonic kidney), HeLa (cervical carcinoma), and MCF-7 (breast adenocarcinoma), using the 3-(4,5-dimethylthiazol-2-yl)-2,5-diphenyl-2H-tetrazolium bromide (MTT) assay.

1.5.4 Chapter 6

Aim: To biologically synthesize, characterize and evaluate the bioactivity of silver nanoparticles (AgNPs) produced using extracts of the leaves and stems of *T. ventricosa*.

Objective 6.1: To determine the green synthesis of AgNPs using crude, fresh and powdered leaf, and stem extracts of *T. ventricosa*.

Objective 6.2: To characterize the synthesized AgNPs using ultraviolet (UV)-visible spectroscopy, Scanning Electron Microscopy (SEM), Energy-Dispersive X-ray (EDX) analysis, High-Resolution Transmission Electron Microscopy (HRTEM), Fourier-Transform Infrared (FTIR) spectroscopy, and Nanoparticle Tracking Analysis (NTA).

Objective 6.3: To evaluate the biological activities of the synthesized AgNPs using antibacterial and cytotoxicity assays.

1.5.5 Chapter 7

Aim: To biologically synthesize, characterize and evaluate the bioactivity of silver nanoparticles (AgNPs) produced using latex extracts of *T. ventricosa*.

Objective 7.1: To undertake the green synthesis of AgNPs using latex extracts of *T. ventricosa.*

Objective 7.2: To characterize the synthesized latex AgNPs using ultraviolet (UV)-visible spectroscopy, Scanning Electron Microscopy (SEM), Energy-Dispersive X-ray (EDX) analysis, High-Resolution Transmission Electron Microscopy (HRTEM), Fourier-Transform Infrared (FTIR) spectroscopy analysis, and Nanoparticle Tracking Analysis (NTA).

Objective 7.3: To examine the biological activities of the synthesized AgNPs using antibacterial and cytotoxicity assays.

1.6 Outline of the thesis

Chapter One highlights the background of the study and the lack of research associated with the research species, *T. ventricosa*. It emphasizes the aims and objectives of each chapter within the thesis. Furthermore, a brief outline of the thesis structure and overview of the methodology is mentioned. **Chapter Two** contains an extensive literature review. Firstly, the taxonomy, distribution, therapeutic uses of the family, and genus of the species are discussed. Secondly, secretory structures and exudates such as laticifers and latex and discussed. Lastly, phytochemical, pharmacological, and silver nanoparticle studies are considered. **Chapter Three** identifies the type, distribution, and histo-phytochemical compounds present in the laticifers and latex of *T. ventricosa*. **Chapter Four** identifies the organoleptic characters, fluorescence abilities, the chemical composition and evaluates the antibacterial activity of various plant extracts. **Chapter five** investigates the antioxidant activity and cytotoxicity of the plant extracts. **Chapter Six** and **Chapter Seven** outlines the synthesis, characterization, and biological activity of synthesized AgNPs using plant extracts and latex, respectively. Lastly, **Chapter Eight** concludes the study and highlights the important findings concerning the aims and objectives. The constraints of the study are also outlined. Lastly, recommendations for future research are discussed on enhancing the research fields of micromorphology, phytochemistry, pharmacology, and biological AgNPs synthesis.

1.7 Materials and methods overview

The comprehensive methodologies for each chapter are discussed accordingly in the respective chapters. A general overview of the research protocols for the present study is as follows:

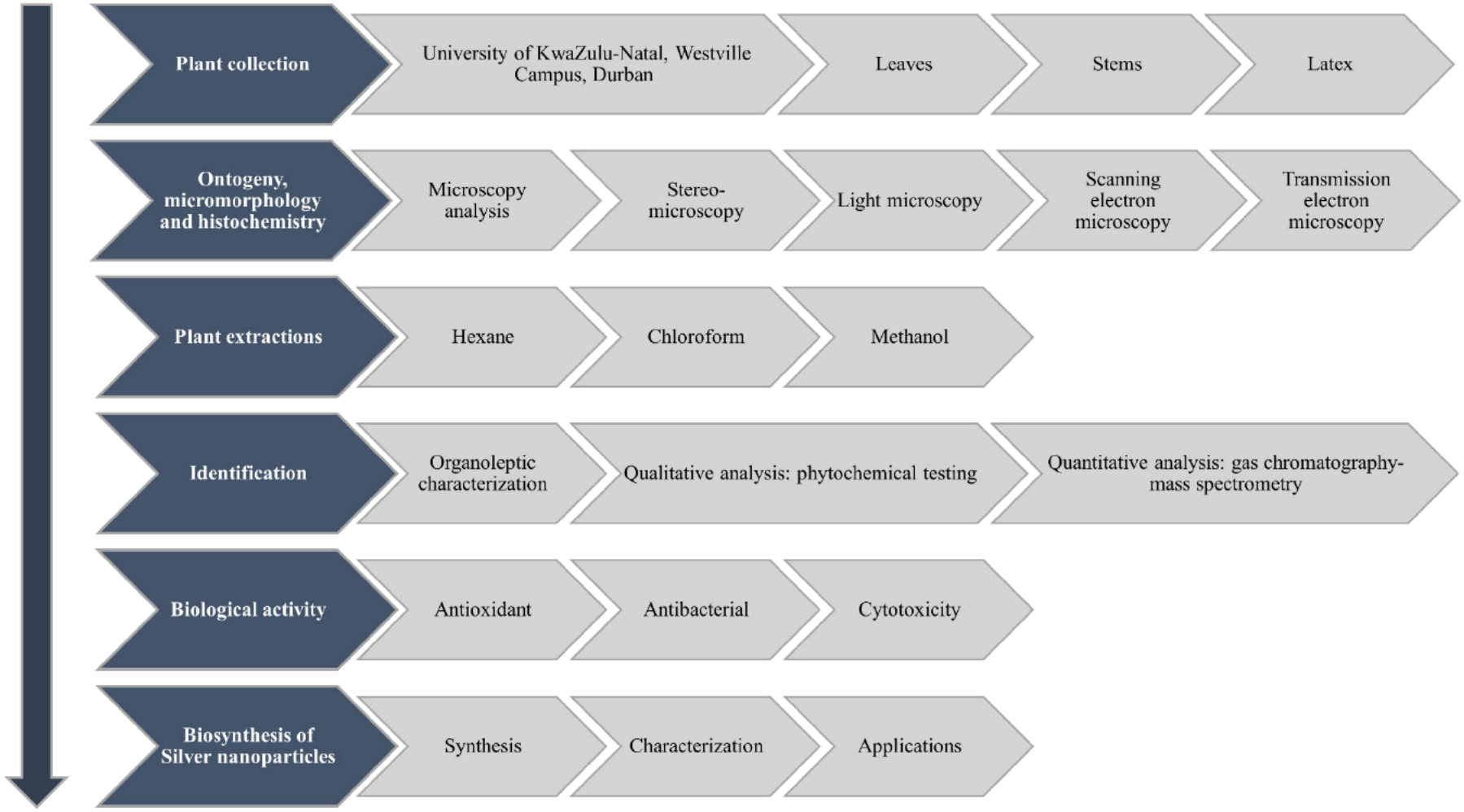

Figure 1.2: Flow diagram depicting the outlined methodology of the present study.

1.7 References

Abdullahi, A.A., 2011. Trends and challenges of traditional medicine in Africa. African Journal of Traditional, Complementary and Alternative Medicines 8, 115–123.

Andima, M., Ndakala, A., Derese, S., Biswajyoti, S., Hussain, A., Yang, L.J., Akoth, O.E., Coghi, P., Pal, C., Heydenreich, M., Wong, V.K.W., 2021. Antileishmanial and cytotoxic activity of secondary metabolites from *Taberneamontana ventricosa* and two aloe species. Natural Product Research, 1–5.

Boadu, A.A., Asase, A., 2017. Documentation of herbal medicines used for the treatment and management of human diseases by some communities in southern Ghana. Evidence–Based Complementary and Alternative Medicine. Article ID 3043061.

Cardoso, C.A., Vilegas, W., Honda, N.K., 1998. Qualitative determination of indole alkaloids, triterpenoids and steroids of *Tabernaemontana hilariana*. Journal of Chromatography 808, 264–268.

Castro, M.D., Demarco, D., 2008. Phenolic compounds produced by secretory structures in plants: A brief review. Natural Product Communications 3, 1273–1284.

Cragg, G.M., Newman, D.J., 2013. Natural products: A continuing source of novel drug leads. Biochimica et Biophysica Acta (BBA)–General Subjects 1830, 3670–3695.

Debnath, M., Malik, C.P., Bisen, P.S., 2006. Micropropagation: A tool for the production of high quality plant–based medicines. Current Pharmaceutical Biotechnology 7, 33–49.

Demarco, D., Castro, M.D., 2008. Laticíferos articulados anastomosados em espécies de Asclepiadeae (Asclepiadoideae, Apocynaceae) e suas implicações ecológicas. Brazilian Journal of Botany 31, 699–711.

Demarco, D., de Moraes Castro, M., Ascensão, L., 2013. Two laticifer systems in *Sapium haematospermum*—new records for Euphorbiaceae. Botany 91, 545–554.

Dias, D.A., Urban, S., Roessner, U., 2012. A historical overview of natural products in drug discovery. Metabolites 2, 303–336.

Drewes, S.E., 2012. Natural products research in South Africa: 1890–2010. South African Journal of Science 108, 17–24.

Erasto, P., Adebola, P.O., Grierson, D.S., Afolayan, A.J., 2005. An ethnobotanical study of plants used for the treatment of diabetes in the Eastern Cape Province, South Africa. African Journal of Biotechnology 4, 1458–1460.

Gomes, R.C., Neto, A.C., Melo, V.L., Fernandes, V.C., Dagrava, G., Santos, W.S., Beleboni, R.O., 2009. Ant–inociceptive and anti–inflammatory activities of *Tabernaemontana catharinensis*. Pharmaceutical Biology 47, 372–376.

Hagel, J.M., Yeung, E.C., Facchini, P.J. 2008. Got milk? The secret life of laticifers. Trends in Plant Science 13, 631–639.

Holdsworth, D.K., 1977. Medicinal plants of Papua New Guinea. Noumea: South Pacific Commission 123, 27.

Irvine, F.R., 1961. Woody plants of Ghana with special reference to their uses, revised ed. Oxford University Press, London.

Iwu, M.M., 1982. Perspective of Igbo tribal ethnomedicine. Ethnomedicine 7, 31–45.

Jäger, A.K., Van Staden, J., 2000. The need for cultivation of medicinal plants in Southern Africa. Outlook on Agriculture 29, 283–284.

Jain, S., Sharma, P., Ghule, S., Jain, A., Jain, N., 2013. *In vivo* anti–inflammatory activity of *Tabernaemontana divaricata* leaf extract on male albino mice. Chinese Journal of Natural Medicines 11, 0472−0476.

Joy, P.P., Thomas, J., Mathew, S., Skaria, B.P., 2001. Medicinal plants. Tropical Horiculture 2, 449−632.

Kinghorn, A.D., Pan, L., Fletcher, J.N., Chai, H., 2011. The relevance of higher plants in lead compound discovery programs. Journal of Natural Products 74, 1539–1555.

Kokwaro, J.O., 1976. Medicinal plants of East Africa, first ed. East African Literature. Kampala, Nairobi, Dar–es–Salaam.

Li, L., 2000. Opportunity and challenge of traditional Chinese medicine in face of the entrance to WTO (World Trade Organisation). China Information Traditional Chinese Medicine 7, 7–8.

Munayi, R.R., 2016. Phytochemical investigation of *Bridelia micrantha* and *Tabernaemontana ventricosa* for cytotoxic principles against drug sensitive leukemia cell lines (Doctoral dissertation, master's Thesis, University of Nairobi, Nairobi, Kenya.

Naidoo, C., Naidoo, Y., Dewir, Y.H., 2020. The secretory apparatus of *Tabernaemontana ventricosa* Hochst. ex A. DC. (Apocynaceae): Laticifer identification, characterization and distribution. Plants 9, 686–702.

Naidoo, G., Kaliamoorthy, S., Naidoo, Y., 2009. The secretory apparatus of *Xerophytaviscosa* (*Velloziaceae*): epidermis anatomy and chemical composition of the secretory product. Flora–Morphology, Distribution, Functional Ecology of Plants 204, 561–568.

Omino, E.A., Kokwaro, J.O., 1993. Ethnobotany of Apocynaceae Species in Kenya. Journal of Ethnopharmacology 40, 167–I80.

Palgrave, C., Palgrave, K.C., 1957. Trees of central Africa, National Publications Trust, Rhodesia and Nyasaland, 17–18.

Pan, S.Y., Pan, S., Yu, Z.L., Ma, D.L., Chen, S.B., Fong, W.F., Han, Y.F., Ko, K.M., 2010. New perspectives on innovative drug discovery: An overview. Journal of Pharmacy and Pharmaceutical Sciences 13, 450–471.

Pickard, W. F., 2008. Laticifers and secretory ducts: two other tube systems in plants. New Phytologist 177, 877–888.

Rios, J.L., Recio, M.C., 2005. Medicinal plants and anti–microbial activity. Journal of Ethnopharmacology 100, 80–84.

Rizo, W.F., Ferreira, L.E., Colnaghi, V., Martins, J.S., Franchi, L.P., Takahashi, C.S., Fachin, A.L., 2013. Cytotoxicity and genotoxicity of coronaridine from *Tabernaemontana catharinensis* A.D C in a human laryngeal epithelial carcinoma cell line (Hep–2). Genetics and Molecular Biology 36, 105–110.

Saito, H., 2000. Regulation of herbal medicines in Japan. Pharmacological Research 41, 515–519.

Sajem, A.L., Gosai, K., 2006. Traditional use of medicinal plants by the Jaintia Tribes in North Cachar Hills District of Assam, Northeast India. Journal of Ethnobiology and Ethnomedicine 2, 1–33.

SANBI: Red list of South African plants, http://redlist.sanbi.org/. Date last accessed: 10th August 2018.

Schmelzer, G.B., Gurib–Fakim, A., 2008. Medicinal Plants, first ed. Plant Resources of Tropical Africa 11,1. PROTA Foundation. Backhuys Publishers, Wageningen, Netherlands.

Schripsema, J., Hermans–Lokkerbol, A., Van der Heijden, R., Verpoorte, R., Svendsen, A.B., Van Beek, T.A., 1986. Alkaloids of *Tabernaemontana ventricosa*. Journal of Natural Products 49, 733–735.

Shakya, A.K., 2016. Medicinal plants: future source of new drugs. International Journal of Herbal Medicine 4, 59–64.

Shruthi, S.D., Rajeshwari, A., Govardhan Raju, K., Pavani, A., Vedamurthy, A.B., Ramachandra, Y.L., 2012. Phytochemical and anti–oxidant analysis of leaf extracts from *kirganelia reticulatabaill*. International Journal of Pharmacy and Pharmaceutical Sciences 4, 608–12.

Street, R.A., Prinsloo, G., 2012. Commercially important medicinal plants of South Africa: A review. Journal of Chemistry 2013, 1–16.

Thomas, S., Patil, D. A., Patil, A. G., 2009. Naresh Chandra: pharmacognostic evaluation and physicochemical analysis of *Averrhoa carambola* L. Fruit Journal of Herbal Medicine and Toxicology 2, 51–54.

Van Beek, T.A., Verpoorte, R., Svendsen, A.B., Leeuwenberg, A.J.M., Bisset, N.G., 1984. *Tabernaemontana* L. (Apocynaceae): A Review of its taxonomy, phytochemistry, ethnobotany and pharmacology. Journal of Ethnopharmacology 10, 1–156.

Van Vuuren, S.F., 2008. Anti–microbial activity of South African medicinal plants. Journal of Ethnopharmacology 119, 462–472.

Van Wyk, B.E., 2008. A broad review of commercially important southern African medicinal plants. Journal of Ethnopharmacology 119, 342–355.

Wadood, A., Ghufran, M., Jamal, S.B., Naeem, M., Khan, A., Ghaffar, R., 2013. Phytochemical analysis of medicinal plants occurring in local area of Mardan. Biochemistry and Analytical Biochemistry 2, 1–4.

Watt J. M., Breyer–Brandwijk, M.G., 1962. The Medicinal and poisonous plants of southern and eastern Africa, second ed. Livingstone, Edinburgh, London.

WHO. 2001. Legal status of traditional medicine and complementary/alternative medicine: a World–Wide Review. Geneva http://apps.who.int/iris/handle/10665/42452.

WHO., 2003. Fact Sheet., Traditional Medicine Geneva/ http://apps.who.int/gb/archive/pdf_files/WHA56/ea5618.pdf.

Williams, V.L., Balkwill, K., Witkowski, E.T.F., 2000. Unravelling the commercial market for medicinal plants and plant parts on the Witwatersrand, South Africa. Economic Botany 54, 310–327.

Yuan, H., Ma, Q., Ye, L., Piao, G., 2016. The traditional medicine and modern medicine from natural products. Molecules 21, 1−18.

CHAPTER 2:

REVIEW OF THE FAMILY APOCYNACEAE AND GENUS *TABERNAEMONTANA*: TAXONOMY, DISTRIBUTION, BIOLOGY, CHEMICAL COMPOSITION, AND BIOLOGICAL ACTIVITIES

Abstract

Several species belonging to the family Apocynaceae and genus *Tabernaemontana* have been well researched and utilized for their wide-ranging therapeutic properties. A few of the most prominent species include *Papaver somniferum*, *Calotropis gigantea* (L.) R. Br, *Alstonia scholaris* (L.) R. Br, *Alstonia macrophylla* Wall. ex G. Don. *Catharanthus roseus*, and *Tabernaemontana divaricata*. These species and many others within Apocynaceae often display pharmacological importance, that is habitually related to their chemical constituents. The current review aimed to extensively analyze, collate and describe an updated report of the current literature related to the taxonomy, distribution, biology, morphology, chemical composition, and pharmacognosy, and silver nanoparticle synthesis studies of the genus *Tabernaemontana*. The secondary metabolites within the genus have demonstrated immense medicinal potential for the treatment of diseases, infections, malaria, cancer, pain, fever, and injuries. Regardless of the indispensable reports and properties displayed by *Tabernaemontana* spp., there remains a wide variety of plants that are yet to be considered or examined. Thus, an additional inclusive study on species within this genus is essential.

Keywords: Alkaloids; Apocynaceae; Biological activity; Pharmacological properties; *Tabernaemontana.*

2.1 Introduction

The substantial appreciation of plants from primordial humanity has cemented a distinctive pathway towards traditional medicine's contemporary practice (Šantić et al., 2017). Traditional healers have exclusively and largely subsidized a range of health care necessities, including the preclusion of diseases, management, and treatment of non-communicable diseases, and psychological and gerontological well-being issues (Abdullahi, 2011). Numerous ailments and illnesses have been cured or treated by traditional healers due to the developments in herbal medicine (Shakya, 2016). The utilization of herbal remedies in various forms is generally preferred due to their effectiveness, affordability, and a reduced amount of side effects in contrast to conventional methods (Shakya, 2016).

Recently, the World health organization (WHO, 2018) has reported an exponential demand for traditional medicine in various regions such as Europe, Asia, America, and Western Pacific (Abdullahi, 2011). Approximately 40%-60% of people utilize curative plants to treat numerous sicknesses (Abdullahi, 2011). It has been noted that nearly 60% of the population in Hong Kong habitually depend on traditional health practitioners (Amzat and Abdullahi, 2008). In contrast, a substantial percentage of the inhabitants from Australia (46%), France (49%), and Canada (70%) frequently hinge on complementary and alternative medicine (Amzat and Abdullahi, 2008). Moreover, despite the deficiency and restrictions in modern medicine observed in African countries, only a single traditional healer is often allocated to treat approximately 500 people in stricken rural areas (Chatora, 2003).

However, despite the added approval towards conventional medicine, the continuous practice of traditional medical systems will systematically lead to the overexploitation of medicinal plants, especially in the plant family Apocynaceae (Dogbane) which is habitually used for its analgesic effects (Šantić et al., 2017). A prominent case within the Apocynaceae is the essential *Papaver somniferum*, commonly known as "Poppy" (Šantić et al., 2017). In 1806, Friedrich Sertumer directed the discovery of innovative compounds from opium poppy, as he successfully isolated morphine, an eminent palliative compound (Dutra, 2016). A few years later, Pierre-Jean Robiquet (1824) and George Merck Fraz effectively separated codeine and the alkaloid papaverine, respectively (Dutra, 2016).

Several members within Apocynaceae contribute primarily to the economy as they are crucial in the medicinal industry (Nazar et al., 2013). Distinctive features of the dogbane family include a

milky white substance characterized as “Latex” (Fahn, 1979; Pickard, 2008). Latex is present in a majority of Apocynaceae species and is often used for its healing properties and health benefits (Kumar et al., 2011). *Calotropis gigantea* (L.) R. Br, *Alstonia scholaris* (L.) R. Br. and *Alstonia macrophylla* Wall. ex G. Don are latex-bearing species that are well-known for their chemical constituents and therapeutic properties.

Calotropis gigantea (L.) R. Br, commonly known as the “Crown flower,” is a medium-sized woolly shrub that is native to Asia, China, India, Sri Lanka, Vietnam, Thailand, and Malaysia (Kadiyala et al., 2013). In traditional medicine, the entire plant is utilized to treat skin diseases, scabies, ringworm, pneumonia, and leprosy (Kirtikar and Basu, 1999; Kumar et al., 2011). In addition, the latex contains glycosides, more specifically “Giganteol,” which can be used for stings, toothaches, tumours, rheumatism, antiseptic, and purgative (Kadiyala et al., 2013). Furthermore, the biological assays conducted using the crude extracts of *C. gigantea* showed promising results for several pharmacological activities (Chitme et al., 2006; Wang et al., 2008; Mahatma et al., 2010; Bharathi et al., 2011; Rathod et al., 2011, Kadiyala et al., 2013).

The species *Alstonia scholaris* (L.) R. Br. and *Alstonia macrophylla* Wall. ex G. Don. are frequently used in traditional medicine in countries like India, Thailand, and China (Changwichit et al., 2011). Locally, these species are used to treat malaria, jaundice, gastrointestinal issues, and cancer (Khyade et al., 2014). Major chemical constituents responsible for the biological activity of the species include alkaloids, phenolics, steroids, iridoids, and terpenoids (Khyade et al., 2014). Similarly, the herb *Catharanthus roseus*, also known as “Madagascar periwinkle,” is a source of several indolomonoterpenic alkaloids (Pereira et al., 2010). Various parts of *C. roseus*, such as the leaves, stems, bark, and roots, contain an array of bioactive compounds (Pereira et al., 2010). A few of these compounds include vinblastine and vincristine and are utilized in modern medicine to treat Hodgkin’s disease, lymphocytic leukaemia, and neuroblastoma, respectively (Alan and Wilkes, 1964; Nazar et al., 2013).

Despite the essential properties displayed by the above species, there remains a variety of plants in Apocynaceae that are yet to be investigated. Regarding the recent information, this review concentrates on the primary and secondary studies that have examined the taxonomy, distribution, biology, chemical constituents, and biological activities of species belonging to Apocynaceae and the genus *Tabernaemontana*. The review explicitly elaborates on *Tabernaemontana* species, with emphasis on the pharmacological aspects that have been recently published.

2.2 Apocynaceae

The Apocynaceae (Dogbane family) belongs to the order Gentianales, that consists of five families, Apocynaceae, Gelseminaceae, Gentianaceae, Loganiaceae, and Rubiaceae (Endress, 2004; APG III, 2009; Rapini, 2012). Comprised of approximately 5100 species and 375 genera, the Apocynaceae is one of the ten largest angiosperm families (Rapini, 2012). Species within this family display variable habitable forms, from trees to vines and small herbs, also including a few succulents (Rapini, 2012). In addition, various species can be simply distinguished by the presence of latex, a bicarpelar gynoecium, or the synorganization of floral structures leading to the accumulation of pollinaria (Rapini et al., 2003). The accretion of pollinaria is a fundamental characteristic in the classification of the Apocynaceae (Rapini et al., 2003).

Apocynaceae was originally recognized by Anderson (1763), as "Apocyna" however, a few decades later, the Apocynaceae was formally confirmed as "Apocineae" by a French botanist Jussieu (1789) (Rapini, 2012). Later, a naturalist Robert Brown (1810) contributed to these classifications by the division of the group into two families based on the presence or absence of pollinaria (Endress, 2004; Rapini, 2012). Before the separation, Jussieu (1789) described "Apocyna" with 24 genera that were subdivided into three groups fundamentally distinguished by the gynoecium, fruit, and seed characteristics (Rapini, 2012; Nazar et al., 2013). According to Endress and Bruyns (2000), Apocynaceae consists of 5 sub-families, namely Rauvolfioideae (10 tribes, 83 genera), Apocynoideae (8 tribes, 80 genera), Periplocoideae (33 genera), Secamonoideae (8 genera), and Asclepiadoideae (4 tribes, 172 genera). The Rauvolfioideae and Apocynoideae families have descended from a common evolutionary ancestor however, they do not include all the descendant groups and therefore have a paraphyletic relationship. Conversely, the Periplocoideae, Secamonoideae, and Asclepiadoideae subfamilies have descended from a common evolutionary ancestor and are monophyletic (Rapini, 2012).

Rapini et al. (2007) observed the diversification of the Apocynaceae and subfamilies. As illustrated in Figure 2.1, the authors calibrated the Apocynaceae crown-group at 54 Mega-annum (ma) and showed the subfamily Asclepiadoideae to have emerged at 40 Ma, the Asclepiadeae at 35 Ma, and the Marsdenieae and Ceropegieae at 30 Ma. They suggested that the New World clade of Marsdenia would have appeared after 16 Ma and radiated at 9.9 Ma (Rapini et al., 2007).

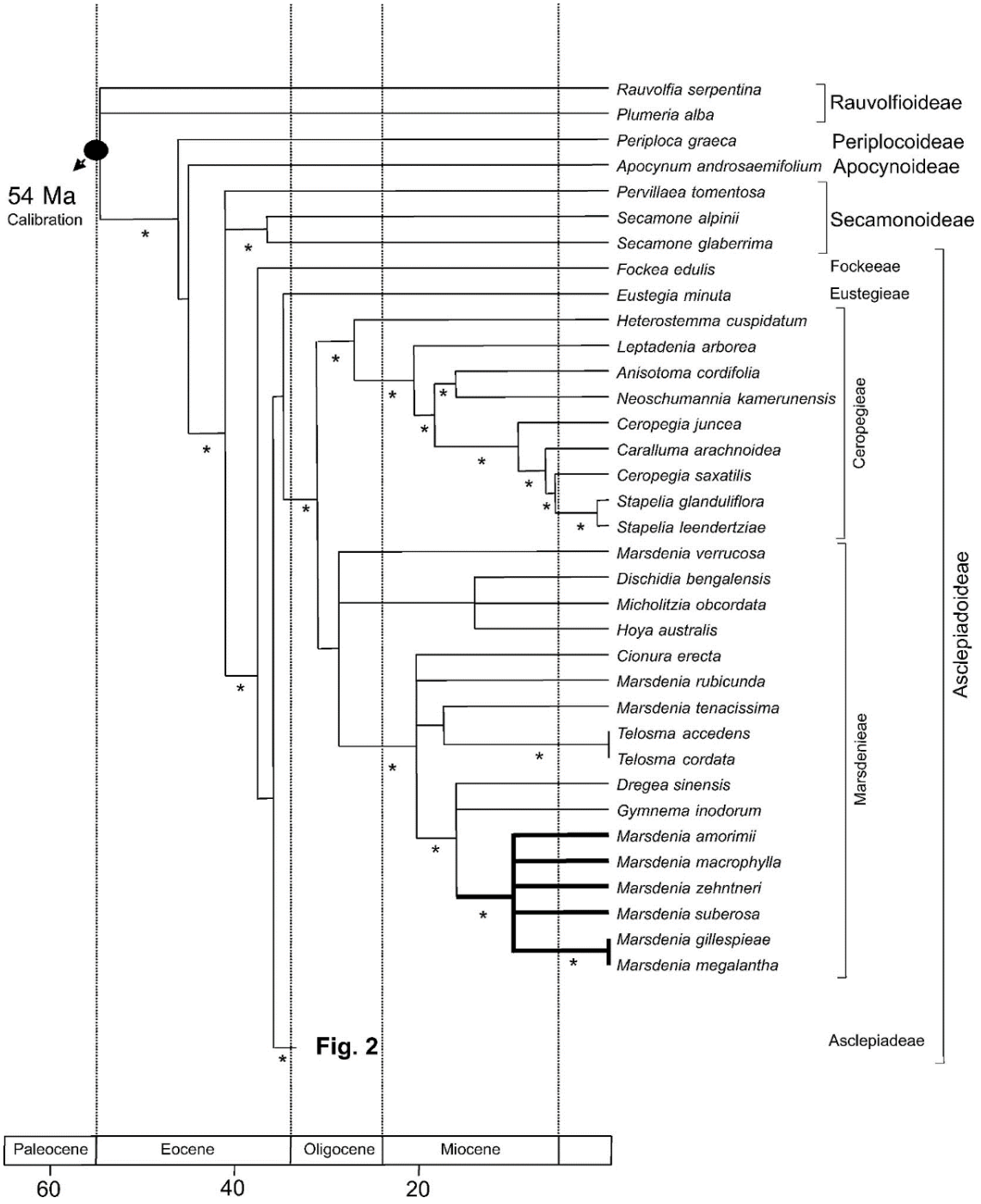

Figure 2.1: Chronogram showing the divergence times of the Apocynaceae and subfamilies. New world clades in bold lines. Asterisks (*) represent clades with a posterior probability greater than 94%. Scale units are millions of years ago (Rapini et al., 2007).

2.2.1 Distribution of Apocynaceae

Good (1947) was one of the first researchers to map the distribution of many taxa and subfamilies within Apocynaceae. As proposed by Good (1947), southern Africa and Madagascar are key distribution zones of diversity for these groups. As shown in Figure 2.2, the recent distribution of the Apocynaceae was found to be diverse in many parts of the world. There is an abundance of species that are soundly distributed throughout the humid pan-tropical and subtropical regions, that encompasses a portion of the temperate areas (Nazar et al., 2013). A large variety of species are often present in rainforests and swamps in the tropics of America, north of Australia, Africa and India, the Mediterranean region, and as well as the continental regions of southern Africa (Nazar et al., 2013), as observed in Figure 2.2.

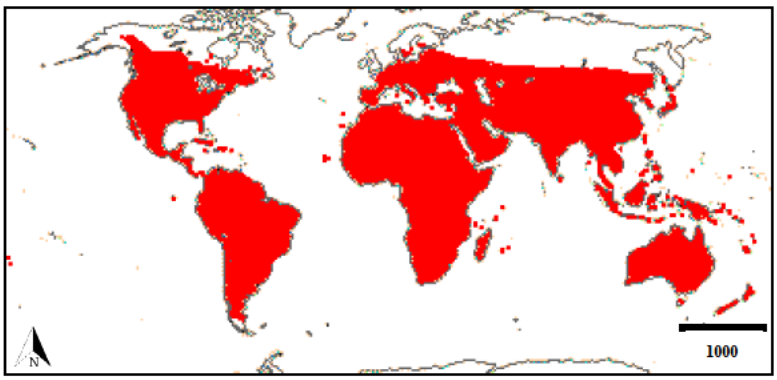

Figure 2.2: Worldwide distribution of Apocynaceae. Red regions represent populated areas (Angiosperm phylogeny website, 2018).

2.2.2 Apocynaceae systematics

As illustrated in Figure 2.3, Rapini (2012) observed the subfamily Rauvolfioideae as the basal grade of the family, whereas the subfamily Apocynoideae appears to be further derived from which Periplocoideae, Secamonoideae, and Asclepiadoideae arise. The subfamilies Secamonoideae and Asclepiadoideae form a clade, namely the Asclepiadaceae s.str. clade however, the position of the subfamily Periplocoideae remains uncertain (Rapini, 2012). The Periplocoideae subfamily has been present in various positions in the Apocynoideae, Periplocoideae, Secamonoideae, and Asclepiadoideae clade (APSA). Conversely, Sennblad and Bremer (2000) explained that the Periplocoideae subfamily is unlikely to be closely related to "Asclepiadaceae s.str." since both the subfamilies Secamonoideae and Asclepiadoideae displayed a closer relationship to the African tribe Baisseeae of Apocynoideae (Sennblad et al., 1998; Potgieter and Albert, 2001).

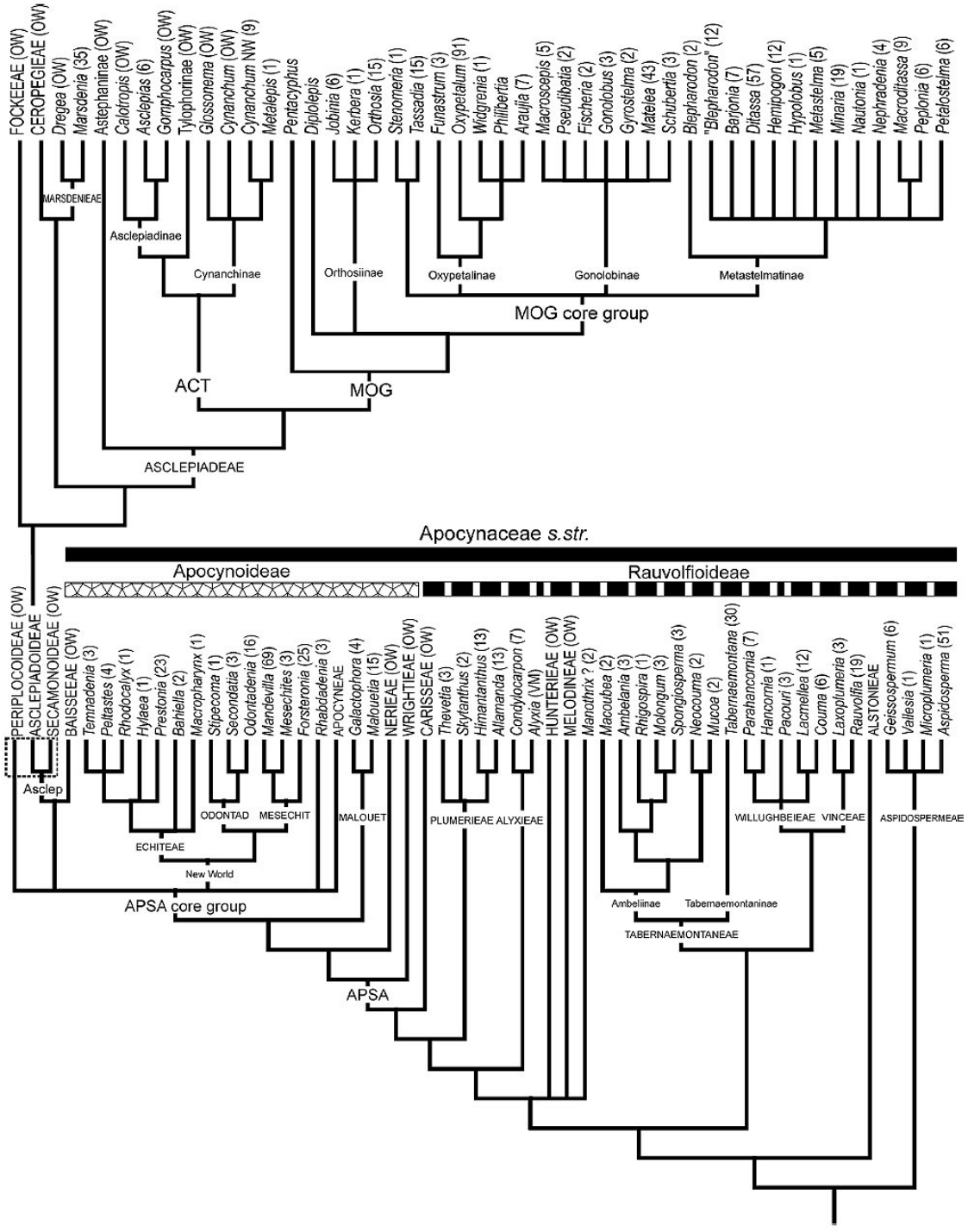

Figure 2.3: Reconstructed phylogenetic tree of the Apocynaceae. The traced rectangle shows the Asclepiadaceae *s.l.*; ACT (Asclepiadinae, Cynanchinae, and Tylophorinae), APSA (Apocynoideae, Periplocoideae, Secamonoideae, and Asclepiadoideae), Asclep (Asclepiadaceae *s.str.*), MALOUET (Malouetieae), MESECHIT (Mesechiteae), MOG (Metastelmatinae, Oxypetalinae, and Gonolobinae), ODONTAD (Odontadenieae), OW (Old World) (Rapini, 2012).

2.3 *Tabernaemontana* genus

The genus *Tabernaemontana* belonging to the family Apocynaceae was named by a German physician and botanist, J. Th. Muller (Van Beek et al., 1984a, b). As shown in Figure 2.4, at present approximately 100 species belonging to this genus have been distributed in tropical and subtropical regions around the world, including Africa, Asia, Oceania, and America (Silveira et al., 2017). *Tabernaemontana* species consists of flowering shrubs and small-medium-sized trees, that habitually grow in the savannahs, rocky outcrops, and forest understories (Marinho et al., 2016). Characteristics of the genus include tubular white flowers, follicular fruit with seeds embedded within a yellow to reddish aril, and a milky or watery latex exudate, that is often found in wounded species (Simões et al., 2010). Due to the latex content, plants within this genus are usually called "Milkweed" and are often used for their biological activities (Rapini et al., 2012; Silveira et al., 2017; Athipornchai, 2018).

Figure 2.4: Worldwide distribution of the genus *Tabernaemontana*. Green spots represent inhabited zones (iNaturalist, 2018).

In South Africa, the genus is represented by 2 species: *Tabernaemontana ventricosa* and *Tabernaemontana elegans* (Beentje et al., 1994; Munayi, 2016), that is shown in Figure 2.5 A and B.

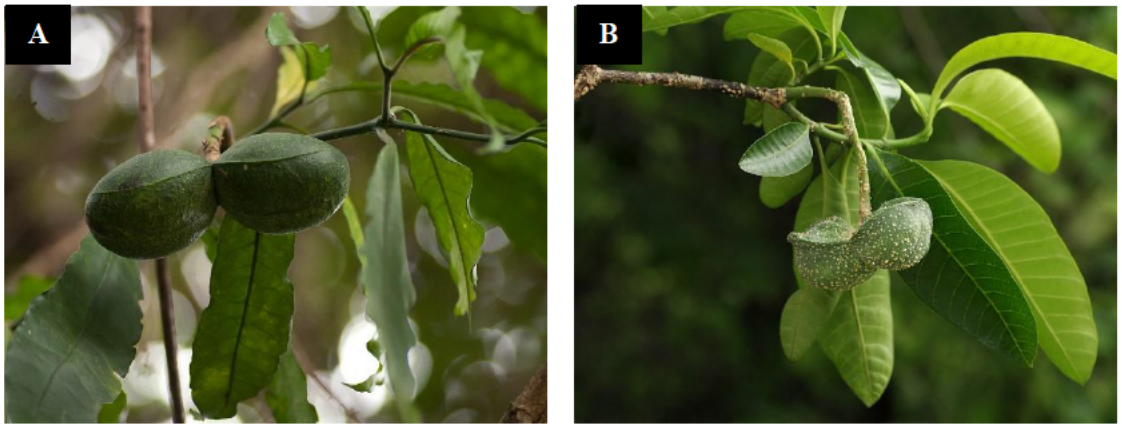

Figure 2.5: *Tabernaemontana* species in South Africa. [A] *Tabernaemontana ventricosa;* [B] *Tabernaemontana elegans*. Photo credit: Bart Wursten and Colin Weham (Flora of Zimbabwe, 2018).

Tabernaemontana ventricosa frequently termed the "Forest toad tree" and "Small-fruited toad-tree" is a small-medium sized tree that is native to Africa (Schmidt et al., 2002). All parts of the tree contain a white milky latex substance (Schmidt et al., 2002). Due to other better-known *Tabernaemontana* species, little or no research has been carried out on *T. ventricosa*. However, despite the lack of research *T. ventricosa* remains ethnomedicinally used in South Africa (Schmidt et al., 2002). The latex is used to promote the healing of wounds and is applied to sore eyes for pain relief (Schmelzer and Gurib-Fakim, 2008). Decoctions of the bark and stems are ingested for the treatment of high blood pressure and to reduce fever (Schmelzer and Gurib-Fakim, 2008). Additionally, the leaves reportedly contain high antiamoebic activity, that aids in the prevention of the amoeba protist (Schmelzer and Gurib-Fakim, 2008).

Tabernaemontana elegans, commonly called the "Toad tree" is a small tree found in river fringes and coastal scrub forests (Pallant et al., 2012). In Zimbabwe and Mozambique, the fruit is regularly eaten when ripe as it is deemed to contain medicinal properties (Van Beek et al., 1984a). The coagulated latex is used as a preventative measure for bleeding (Styptic) (Van Beek et al., 1984a). The VhaVenda and Zulu people digest root decoctions for pulmonary disease and chest pains (Arnold and Gulumian, 1984; Steenkamp et al., 2007). The seeds and stembark are used for the treatment of heart disease and cancer (Van Beek et al., 1984a). The root decoction may contain aphrodisiac properties (Neuwinger, 1666; Watt and Breyer-Brandwijk, 1962; Pallant et al., 2012).

Approximately 100 *Tabernaemontana* species from the subtropical and tropical regions of the world were screened for biological activity (Van Beek et al., 1984a). The authors reported on the antiamoebic, anticancer, antifertility, anti-inflammatory, antimicrobial, antioxidant, and antiviral properties for a range of *Tabernaemontana* species. A few of the most intensively studied species include the following:

Tabernaemontana divaricata, also known as the "Pinwheel flower" and "Crape Jasmine" is an evergreen shrub that occurs in the tropical regions of southern China, India, and Thailand (Basavaraj et al., 2011). Crape Jasmine is an intensively used medicinal plant, that is utilized as an aphrodisiac, tonic, and purgative (Basavaraj et al., 2011). According to Van Beek et al. (1984a), in western India, latex is used for inflammation and wound healing. In southern Africa, the plant juices are mixed with various oils and applied to the head and eyes to soothe pain (Van Beek et al., 1984a). In China, the juice of the leaves contains antihypertensive and diuretic effects and are used in the treatment of ulcers, sores, rabies, headaches, and fractures (Van Beek et al., 1984a; Dantu et al., 2012).

Tabernaemontana catharinensis usually referred to as "Snakeskin", is a small tree native to Brazil and is found in many surrounding countries (Nicola et al., 2013). This species is used frequently in traditional medicine for the removal of warts and as an antidote for snakebites (Boligan, 2012). Nicola et al. (2013) stated that the extracts of *T. catharinensis* are significantly important as they contain antimicrobial, antitumour, antioxidant, and anti-inflammatory activities. Recently, Marques et al. (2018) supported the use of *T. catharinensis* for the treatment of inflammatory disorders, as the hydroethanolic leaf extracts of this species exhibited suitable anti-inflammatory activity.

Tabernaemontana crassa, also known as "Adam's apple flower", occurs in Africa, DR Congo, and north of Angola (Van Beek et al., 1985). Several alkaloids have been identified in the stem, bark, root, and seeds of *T. crassa*, possibly suggesting the source of its medicinal properties (Van Beek et al., 1984a). This species has several traditional uses, which include, a local anaesthetic, treatment of malaria, wounds, sores, and abscesses (Van Beek et al., 1984a; Fonge et al., 2012). The latex is used often as a haemostatic and as a sedative to calm periods of insanity (Van Beek et al., 1984a).

Tabernaemontana corymbosa locally referred to as "Jelutong badak" or "Resting" is a wild shrub or small tree that primarily occurs in Indonesia, Laos, Thailand, Vietnam, Malaysia, and China (Abubakar and Loh, 2016). All parts of *T. corymbosa* are often used in ethnobotany for the treatment of syphilis, ulcerations, fever, sores, jaundice, tumours, and postnatal healing (Rahmatullah et al., 2010; Ong et al., 2011; Abubakar and Loh, 2016). This species comprises an array of indole alkaloids that display cytotoxicity against several human cell lines (Athipornchai, 2018). A study by Zhang et al. (2015a) successfully isolated and evaluated the cytotoxicity of *T. corymbosa* extracts. The results of the study showed that three vobasinyl-ibogan type bisindole alkaloids isolated from the twigs of *T. corymbosa* exhibited substantial cytotoxicity activity in comparison to a chemotherapy drug, cisplatin (Zhang et al., 2015a).

Tabernaemontana contorta, also known as "Pete Pete," in Nigeria displays a widespread distribution in the tropical and subtropical regions of the world (Ndongo et al., 2017). This species often grows in closed forest understories in areas including America, Africa, Asia, Oceania, and Australia (Leeuwenberg, 1991; Ndongo et al., 2017). The leaves of *T. contorta* are utilized for the prevention of keloids and used for their antiseptic properties (Burkill, 1985). Ndongo et al. (2017) investigated the chemopreventive activity of two isolated bisdoline alkaloids from the root methanolic extracts of *T. contorta*. In the study, the alkaloid contortarine A presented chemo preventive activity via quinone reductase, whereas the alkaloid compound 16-epi-pleiomutinine showed anticancer activity (Ndongo et al., 2017).

Tabernaemontana cymosa also referred to as "Grão-de-galo" or "Wild jasmine" is a small tree native to Columbia, Venezuela, Trinidad and Tobago, and Brazil (Marinho et al., 2016; Gómez-Calderón et al, 2017). According to Gómez-Calderón et al. (2017), the bioactivity of *T. cymosa* has been extensively studied as the species displays antimicrobial, antiparasitic, antitumour, antifebrile, and analgesic activities (Yang et al., 2005). However, due to an array of biological properties displayed by this species, Gómez-Calderón et al. (2017) considered the possible antiviral activity of *T. cymosa* seeds. According to the results of the study, the isolated compounds from *T. cymosa*, namely lupeol acetate and voacangine substantially reduced the infection of Dengue fever, thus displaying significant antiviral activity (Gómez-Calderón et al, 2017).

2.4 Secretory structures

Secretory structures or tissues are known as specialized single cells or differently shaped multicellular structures, that excrete specific substances (Fahn, 1979). These structures are classified based on their structure, location, secondary metabolites, and mode of secretion (Naidoo et al., 2009). Secretory structures that appear on the external surface of various plant organs are usually characterized as trichomes, salt glands, nectaries, and hydathodes, whereas structures that are found internally are classified as resin ducts, idioblasts, oil cells, and laticifers (Thomas, 1991). Secretory structures are well-known to contain secondary metabolites such as essential oils, resins, tannins, salts, and latex (Turner et al., 1998). It has been reported that the function of these plant metabolites is often linked to defence mechanisms against herbivores and microorganisms and is equally important in pharmacological and taxonomic studies (Fahn, 1988; Naidoo et al., 2009).

2.5 Laticifers

Laticifers are defined as highly specialized cells (or files of cells) that are comprised of a suspension of numerous tiny particles in the sap of unspecified composition with various refractive indices (Pickard, 2008). In 1884, De Bary initially described laticifers as "Laticiferous tubes" that continuously transverse the entire length of mature plant organs (Fahn, 1979). According to Van Die (1955), the distinct cytoplasm within laticifers identified as latex consists of several components, which may be divided into various groups such as polyisoprene hydrocarbons, triterphenols and sterols, fatty acids and aromatic acids (esterified), carotenes, phospholipids, proteins and inorganic constituents (Fahn, 1979). Moreover, Heinrich (1969) reported that the latex of certain plants may contain specific substances such as composite sugars, variously shaped starch grains, tannins, proteins, and alkaloids. Despite the common milky white colour often observed in many latex-bearing plants, the colour often varies in many plant species as it may appear yellow, orange, red, brown, or even colourless (Pickard, 2008).

Latex bearing plants have been found in approximately 12 500 species representing 22 families, that include monocotyledons and eudicotyledons (Evert, 2006). Although, studies have proposed estimates of 20 000 species in over 40 families (Lewinsohn, 1991). As observed in Figure 2.6, the schematic diagram displays the widespread distribution of the different types of laticifers, it has been suggested that these secretory structures are of polyphyletic origin as they are often found dispersed throughout generally unrelated plant orders (Keating, 2003).

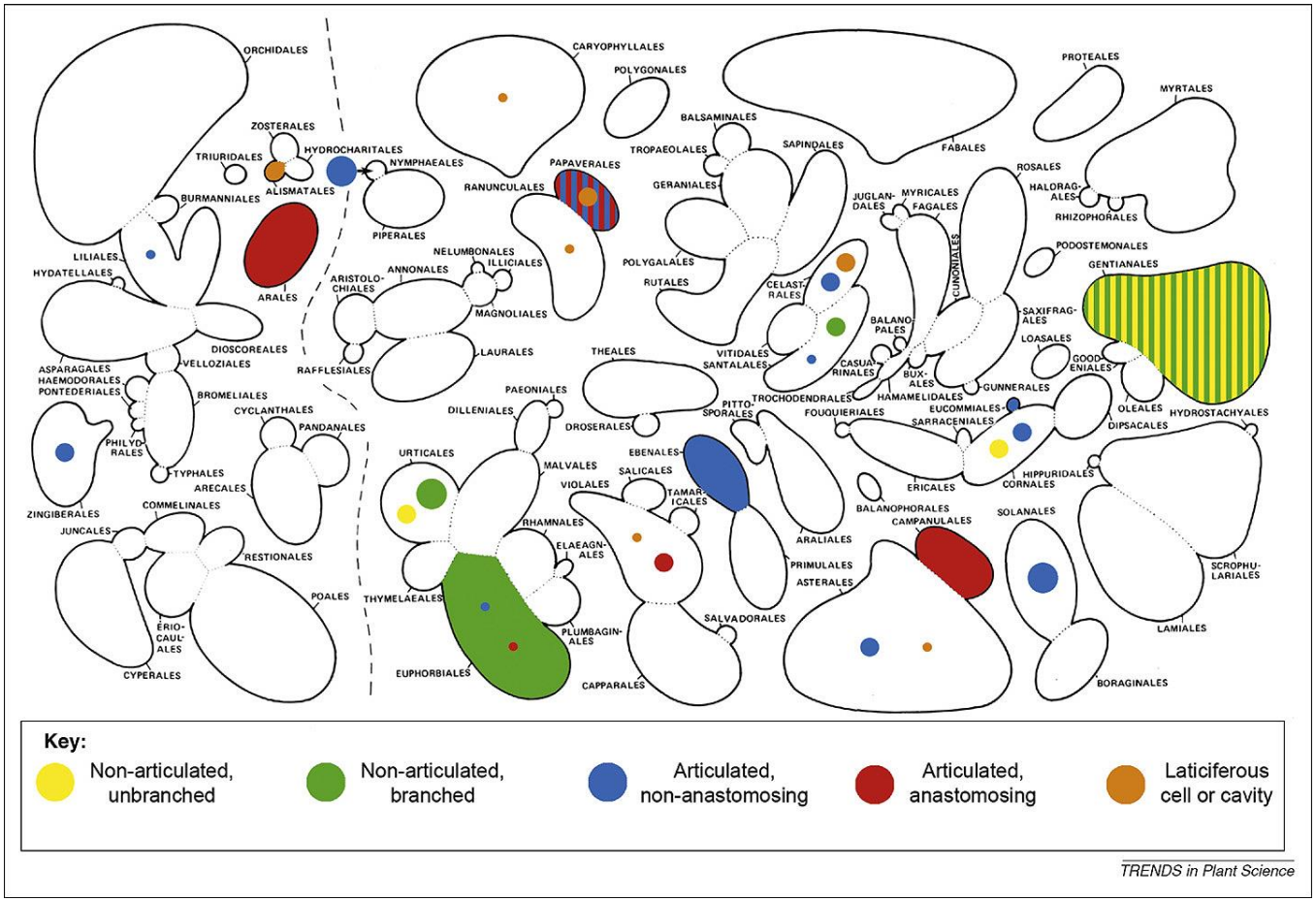

Figure 2.6: Schematic diagram representing the four major laticifer types of cavities in angiosperms. Each branch of the phylogenetic tree represents a different order in the classification. Branch thickness is proportional to the number of species in the order. The occurrence of various laticifers in each order is represented as follows: Small dots, <1% of genera; medium dots, 1-10% of genera; large dots, 10-50% of genera; filled, >50% of genera (Hagel et al., 2008).

.

2.5.1 Types of laticifers

Laticifers have been classified into two major categories such as the articulated and the non-articulated types (Hagel, 2008). The development of the four major categories of laticifers is illustrated in Figure 2.7. The classification of laticifers was established based on their mode of development and morphological characteristics (Fahn, 1979; Hagel, 2008). Articulated laticifers are present in both the primary and secondary bodies of a plant (Pickard, 2008; Castelblanque et al., 2017). They are comprised of multiple interconnected simple cells and may be either nonanastomosing (unbranched) or anastomosing (branched) (Fahn, 1979; Mahlberg, 1993; Pickard, 2008; Castelblanque et al., 2017). Whereas non-articulated laticifers usually arise in the primary system of the plant body, are multinucleate, and develop from a single coenocytic cell, that displays significant elongation during plant growth (Hagel et al., 2008; Pickard, 2008; Canaveze and Machado, 2016). These cells may exhibit one of two forms involving unbranched vessels or branched networks (Krishnamurthy et al., 2013). Intrusive growth is often linked with the expansion and differentiation of non-articulated laticifers, although it has been mentioned that both varieties of laticifers may exhibit this form of development (Evert, 2006). Several species within Apocynaceae are classified according to the characteristics of non-articulated laticifers, however, the laticifers of *Asclepias*, *Blepharodon*, *Matelea* spp., and many more do not exhibit these characteristics (Mahlberg, 1993). Due to these inconsistencies, it has been suggested that laticifer ontogeny should be critically examined for an accurate form of classification (Gama et al., 2017).

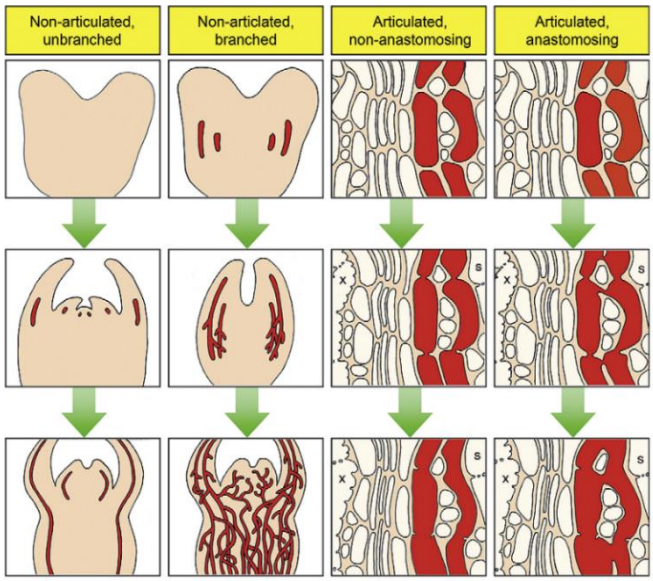

Figure 2.7: Development of the four major laticifer types. Laticifers and their initials are depicted in red. Abbreviations: s = sieve element; x = xylem vessel (Hagel, 2008).

2.5.2 Growth and development of laticifers

Mahlberg (1993) critically studied the ontogeny of non-articulated laticifers. The findings of the study suggest non-articulated, branched laticifers develop from single initials, that are evident within embryos (Hagel, 2008). Throughout the development of seedlings, laticifer initials tend to extend intrusively between neighbouring cells for the formation of coenocytic cells via karyokinesis without the development of a cell plate (Pickard, 2008; Castelblanque et al., 2016). The network of non-articulated branched laticifers is often a consequence of a set number of initials within embryos and interestingly have been found to vary within several species (Hagel, 2008). Table 2.1 displays a summary of the important features of major laticifer types during growth and development (Hagel, 2008). Mahlberg (1961) investigated the growth of laticifers in *Nerium oleander* species, where he observed 28 initials in immature embryos. By contrast, Mahlberg and Sabharwal (1968) studied the laticiferous network of *Euphobia engelmanni*, which gave rise to four initials. Initials of articulated laticifers have only been observed in a few species such as the rubber tree, where a sequence of initials are derived from meristematic regions including the apical meristem and cambium (Castelblanque et al., 2016). Adjacent cell walls within the meristematic regions usually undergo partial or complete perforation to ensure the formation of elongated cells that are joined via extensively perforated cell wells (Nessler and Mahlberg, 1981).

Table 2.1: Summary of the major features of different laticifer types (Hagel, 2008).

Feature	Non, articulated, unbranched	Non, articulated, branched	Articulated, non-anastomosing	Articulated, Anastomosing
Composition	Single coenocytic cell	Single coenocytic cell	A multicellular column with intact or perforated transverse walls	A multicellular column with perforated transverse and lateral walls
Initials	Post-embryonic	Embryonic	Protophloem and/or phloem	Protophloem and/or phloem
Multinucleate origin	Karyokinesis	Karyokinesis	Protoplast fusion	Protoplast fusion
Growth	Intrusive	Intrusive	Differentiation of phloem initials	Differentiation of phloem initials, some intrusive
Appearance at maturity	Long, tubular strands	Branched networks	Long, tubular strands	Branched networks

2.5.3 Defence systems: Laticifers, latex, and crystals

Since the discovery of laticifers, there have been plentiful suggestions regarding the functions of these highly specialized cells and their contents known as latex (Fahn, 1979; De Barry, 1877; Hagel, 2008). According to Fahn (1979), the most probable function of laticifers is protection. Several decades later, studies conducted by Hagel (2008) and Konno (2011) supported this assumption. These studies suggested that latex contains numerous specialized metabolites that are possibly cytotoxic. Furthermore, Konno (2011), stated that the compounds within latex-bearing plants are highly concentrated. The authors also investigated the alkaloidal content in mulberry (*Morus* spp), whereby the findings remarkably demonstrated that the concentrations of sugar-mimic alkaloids were approximately concentrated 100 times higher in latex compared to whole leaves. Herbivorous insects that feed on latex-bearing plants are often challenged by the high concentrations of defence substances within the latex, rather than the lower concentrations contained in leaves since relatively large droplets of latex often emerge at a site of puncture on plant organs (Konno, 2011). Figure 2.8 illustrates that these insects are often immediately trapped due to the stickiness of the latex and are shortly poisoned from the large dosages of secondary metabolites within the latex that accumulates at the point of plant tissue damage (Dussourd, 1995; Konno, 2011).

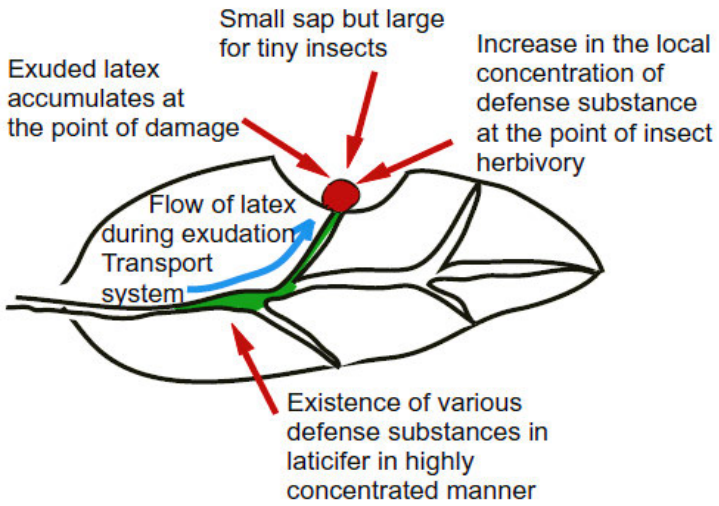

Figure 2.8: Schematic representation of latex-borne and canalicular insect defences. Latex with concentrated defence substances (region in green) prior to insect attack, and thereafter is concentrated at the point of damage (area shown in red) immediately after the plant tissue injury (Konno, 2011).

In addition to the high concentrations of latex consumed by insect-eating herbivores, these organisms are similarly faced by the occurrence of various calcium oxalate crystals (CaOx) that are observed in over 215 plant families (Nakata, 2003; Franceschi and Nakata, 2005). Calcium oxalate crystals are biologically formed from oxalic acid and usually develop within cell vacuoles recognized as crystal idioblasts (Foster, 1956; Franceschi and Nakata, 2005). The morphology of CaOx crystals often varies based on cell type, calcium availability, and several other environmental factors (Mazen et al., 2004; Franceschi and Nakata, 2005). Currently, there are 5 categories of CaOx crystals based on these factors comprising of crystal sand, raphide, druse, styloid, and prismatic (Figure 2.9) (Franceschi and Horner, 1980; Nakata, 2003; Franceschi and Nakata, 2005). Furthermore, various crystals display a variety of functions depending on the type of CaOx crystals such as calcium regulation, ion balance, plant protection, tissue support, detoxification, and light gathering and reflection (Nakata, 2003). Despite limited research on the proposed functions of CaOx crystals, there is solid evidence for the role of CaOx crystals in plant defence and protection (Franceschi and Nakata, 2005). Authors have reported an increased accretion of CaOx crystals of two species, *Sida rhombilfolia,* and Norway spruce in response to artificial herbivory or plant tissue cutting (Tillman-Sutela and Kauppi, 1999; Molano-Flores, 2001; Nakata, 2003).

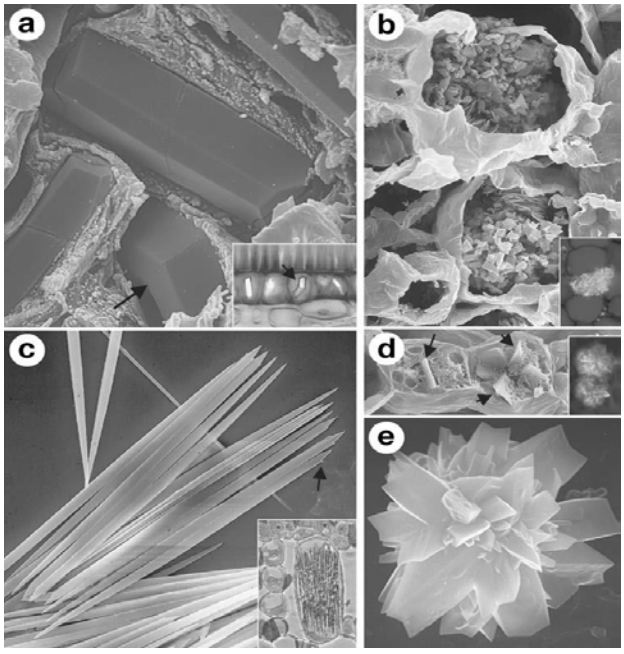

Figure 2.9: Morphology of CaOx crystals. (A) Prismatic crystals in bean seed coat. Arrows indicate kinked twin crystals; (B) Crystal sand in sugar beet leaf cells; (C) Raphide crystals from a ruptured *Pistia* raphide idioblast. Note barbs on one end of the crystals (arrows); (D) Developing druse crystals from *Pistia*. Only a few facets can be seen (arrows); (E) Isolated *Peperomia* druse crystal (Franceschi and Nakata, 2005).

2.6 Phytochemistry

Recently, there has been an increased awareness of medicinal plants, which may be attributed to their availability, cost-effectiveness, efficiency, and safety (Parekh and Chada, 2007; Shrestha et al., 2015; Bhadane et al., 2018). Phytochemicals obtained from plant sources are recognized as secondary metabolites and are usually synthesized in all parts of the plant body, including bark, leaves, stems, roots, flowers, seeds, and fruit (Nandagoapalan et al., 2016). The advancements in drug discovery of natural products have led to the establishment of representative bioactive constituents from medicinal plant species that include secondary metabolites such as steroids, glycosides, phenols, tannins, anthocyanins, flavonoids, terpenes, and alkaloids (Schmelzer and Gurib-Fakim, 2008).

Furthermore, the combination of the above-listed secondary metabolites contributes to the chemistry of essential oils (Boligon et al., 2013a, b). Essential oils are regarded as volatile compounds or oils and contain major components such as mono- and sesquiterpenoids, phenylpropanoids, and additional bioactive constituents (Gandhi et al., 2019). Approximately, 17 500 aromatic plant species produce essential oils, those of which mostly belong to angiosperm families such as Lamiaceae, Rutaceae, Myrtaceae, Zingiberaceae, Asteraceae, and Apocynaceae (Pavela et al., 2015). These aromatic oils often accumulate within plant secretory structures that include glandular trichomes, secretory cavities, resin ducts, and laticifers (Fahn, 2000). Naturally, essential oils are often characterized by a robust odour, flavour, or scent (Pavela et al., 2015). These aromatic components have several purposes for plants such as the attraction of pollinators and insects, protection from extreme climatic conditions (heat or cold), and defence mechanisms towards pests and microorganisms (Pavela et al, 2015).

The composition of essential oils plays a significant role in the accustomed usage of aromatic plants as several species are often used for different purposes (Bakkali et al., 2008). Similarly, various plant organs contain a type and varying quantity of essential oils and therefore exhibit a diverse range of biological and medicinal properties (Raut et al., 2014). The complex diversity of essential oils is habitually utilized for their bacterial, viricidal, antimicrobial, analgesic, sedative, anti-inflammatory, spasmolytic, and local anaesthesia properties (Bakkali et al., 2008). In addition, essential oils are also used in the perfumery, cosmetics, detergents, chemistry, and food product industries (Pavela et al., 2015). These industrial processes often require the extraction of essential oils via hydro distillation, steam distillation, dry distillation, or mechanical cold pressure, which gives rise to variable chemical compositions (Regnauult-Roger et al., 2012).

2.7 Major Bioactive Components of *Tabernaemontana* Species

Plants within the genus *Tabernaemontana* obtain a profusely high alkaloid content, usually displaying biological activity (Silveira et al., 2017). According to Van Beek et al. (1984a, b), alkaloids are organic nitrogenous compounds with the nitrogen being either in its primary, secondary, or tertiary form. Furthermore, monoterpene indole and bisindole alkaloids are the major classes of alkaloids within the *Tabernaemontana* genus, other compounds include terpenes, lactones, steroids, phenolics, and flavonoids (Van Beek et al., 1984a, b). Over 67 species have been investigated for indole alkaloids, of which 470 isolations of approximately 240 structurally different bases have been detected (Zhu et al., 1990; Marinho et al., 2016; Silveira et al., 2017).

The *Tabernaemontana* genus acquires a generous source of monoterpene indole alkaloids, which are derived from the aromatic acid tryptophan and the iridoid terpene secologanin (Athipornchai, 2018). The biosynthesis pathway of terpene indole alkaloids is illustrated in Figure 2.10 (Athipornchai, 2018). According to Hiraswa et al. (2009), monoterpene indole alkaloids have been found to exhibit numerous skeletal types, namely secotabersonine alkaloids, bis-vobtusine-type alkaloids, and bis-vosbsinyl-ibogan indole alkaloids. Currently, there are >1800 structurally diverse monoterpene-derived indole alkaloids that have been classified within *Tabernaemontana* (Marinho et al., 2016). Another major class of alkaloids identified in this genus is heterodimeric bis-indole alkaloids (Marinho et al., 2016). This compound has been characterized by the biosynthesis of dimeric structures from two independent-class alkaloids (Marinho et al., 2016).

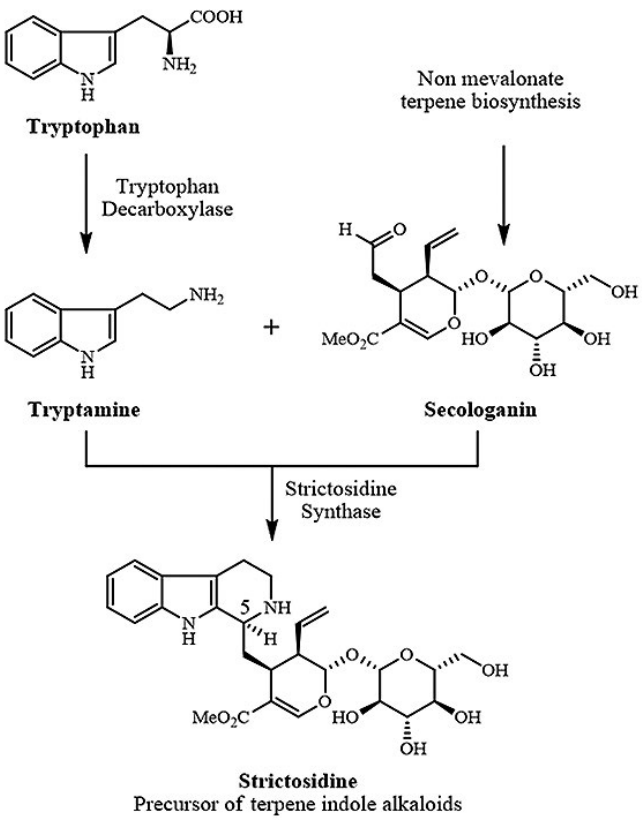

Figure 2.10: Biosynthesis pathway of terpene indole alkaloids (Athipornchai, 2018).

For centuries, several *Tabernaemontana* species, such as *T. divaricata, T. catharinensis, T. crassa,* and *T. elegans*, have been exploited in traditional and folk medicine for the treatment of illnesses and the prevention of diseases and ailments, such as sore throat, hypertension, abdominal pain, and pulmonary disease (Pratchayasakul et al., 2008; Pallant et al., 2012; Nicola et al., 2013; Basumatary et al., 2016; Garga and Das, 2017). A variety of chemical compounds extracted from many parts of *Tabernaemontana* species reportedly contain alkaloids, that exhibit biological activities, such as antimicrobial, antioxidant, anti-inflammatory, anticholinesterase, anti-neurodegenerative, anticancer, antidiabetic, antivenom, larvicidal, antihypertensive, wound healing, analgesic, and many other activities (Nicola et al., 2013; Marinho et al., 2016; Basumatary et al., 2016; Silveira et al., 2017; Garga and Das, 2017; Athipornchai, 2018). The details of the isolated compounds and respective pharmacological properties of a few *Tabernaemontana* species are summarized in the following paragraphs and displayed in Table 2.2.

The findings of Nicola et al. (2013) provide scientific support of the frequently used traditional medicinal plant *T. catharinensis*. The outcomes of the study revealed the presence of major alkaloids, such as 16-epi-affinine, coronaridine-hydroxyindolenine, voachalotine, voacristine-hydroxyindolenine, 12-methoxy-n-methyl-voachalotine, and a derivative of voacristine or voacangine (Table 2.2). It was suggested by Nicola et al. (2013) that these chemical constituents exhibited anticholinesterase activity and can be recommended for the future treatment of neurodegenerative disease.

According to Mairura (2006), a substantial amount of indole alkaloids has been detected and isolated from the stem bark, root bark, and seeds of *T. crassa*. Major alkaloids include those of the ibogan class, such as coronaridine, mono-and di-methoxy derivatives of isovoacangine, conopharyngine, and the aspidospermatan-class apparicine (Table 2.2). Mairura (2006) explained that the plant is highly toxic, as crude ethanolic extracts were found to be lethal to test subjects. Conversely, the study of Kuete et al. (2010) investigated the toxicity of hydro-ethanol stem-bark extracts and the results showed no toxicological activity, thus suggesting a novel source of naturally produced drugs.

Ingkaninan et al. (2006) investigated the phytochemical properties of the flowers, leaves, stems, and root extracts of *T. divaricata*. Additionally, four isolated compounds, namely 19,20-dihydrotabernamine, 19,20-dihydro-ervahanine A, conodurine, and tabernaelegantine A, were screened for biological activity (Ingkaninan et al., 2006). The findings revealed that the extracts and respective compounds displayed high antiacetylcholinesterase activity (Ingkaninan et al., 2006). In another study, Zhang et al. (2013) highlighted a few isolated compounds from *T. divaricata*, such as conophylline which was found to be effective against several cell lines.

Previous phytochemical research has shown *T. elegans* to contain several monoterpenoid indole alkaloids of which 24 were previously isolated (Danieli et al., 1980). The major indole alkaloidal components extracted from the whole plant and root bark of *T. elegans* were vobasine, dregamine, and tabernaemontaninol (Van der Heijden 1986; Beenjie et al., 1994; Athipornchai, 2018). A study by Pallant et al. (2012) reported the isolation and identification of alkaloids in the root extract of *T. elegans*. Major components observed were dregamine and voacangine, which exhibited significant antibacterial activity against gram-positive bacteria and *Mycobacterium* species.

Table 2.2: Major alkaloids isolated within the genus *Tabernaemontana*.

Species	Reported Alkaloids	References
T. angulata	Voacangine, voronaridine	De Assis et al., 2009
T. catharinensis	Isovoacangine, coronaridine, heyneanine, 16-epiaffinine, catharinensine, 16-decarbo-methoxyvoacamine, conodurine, ibogamine, tabernanthine, voacangine, 3-hydroxyvoacangine, 3-hydroxycoronaridine, 3-oxocoronaridine, catharanthine, voacangine hydroxyindolenine, rupicoline, coronaridinepseudoindoxyl, tetraphyllicine, olivacine, 6 N-hydroxyolivacine, 2-N-oxyolivacine, Nb-demethylvoacamine, voacamidine, tabersonine, 19-epivoacristine, 3-(2-oxopropyl) coronaridine, 12-methoxy-4-methylvoachalotine, voacristine, coronaridinehydroxyindolenine, voacristinehydroxyindolenine, vobasine, voachalotine	Araujo et al., 1984; Braga et al; 1984; Spitzer et al; 1995; Lemos et al., 1996; Cardoso et al., 1997; Cardoso et al., 1998; Cardoso and Vilegas, 1999; Batina et al., 2000; Pereira et al., 2008; Gonçalves et al., 2011; Santos et al., 2012
T. coriaceae	Taberpsychine, vincadifformine, minovincine, 3-oxominovincine, voacorine, epi-(20)-voacorine	Cava et al., 1968
T. corymbosa	Conoliferine, conodiparine A, conodiparine C, tronoharine, voastrictine, vobatricine, conodiparine E, conodirinine A, conodirinine B	Kam et al., 1995; Kam et al., 1999; Kam et al., 2000; Kam et al., 2002; Kam et al., 2003a; Kam et al., 2003b; Kam et al., 2003c
T. crassa	Conoduramine, 19-hydroxyconopharyngine, crassanine, ibogamine,coronaridine, isovoacangine, conopharyngine, apparicine	Van Beek et al., 1985; Cava et al., 1965; Cava et al., 1968; Kingston et al., 1977; Rastogi et al., 1980; Mairura et al., 2006
T. dichotoma	16,22-dihydro-16-hydroxyapparicine, dichomine, vallesamine, voacamine	Perera et al., 1983; Perera et al., 1984; Perera et al., 1985
T. divaricata	16-epi-affinine, coronaridine-hydroxyindolenine, voachalotine, voacristine-hydroxyindolenine, 12-methoxy-n-methyl-voachalotine, conofoline, conophyllidine, 3S-cyanocoronaridine, 5-hydroxy-6-oxocoronaridine, 5-oxocoronaridine, 6-oxocoronaridine, ibogamine, voacangine, 3-ethoxyvoacangine, voaharine, voalenine, coronaridine, heyneanine, voacristine, voacamine, decarbomethoxyvoacamine, 19,20-dihydroervahanine, 19,20-dihydrotabernamine, 19,20-dihydro-ervahanine A, conodurine, tabernaelegantine A	Cava et al., 1968; Arambewela and Ranatunge 1991; Kam et al., 1992; Kam et al., 1995; Henriques et al., 1996; Kingston et al., 1977; Rastogi et al., 1980; Kam et al., 2003c; Kam et al., 2004; Ingkaninan et al.,2006; Nicola et al., 2013
T. elegans	Apparicine, dregamine,vobasine, dregamine, tabernaemontaninol, voacangine	Danieli et al., 1980; Danieli and Palmisano, 1986; Van der Heijden, 1986; Pallant et al., 2012

Table 2.2: *Cont.*

T. heterophylla	Voacangine, coronaridine, 19-heyneanine, vobasine, affinisine, olivacine	Wolter Filho et al., 1983
T. hystrix	Ibogaine, iboxygaine, voacangine, coronaridine, voacristine, 19-epivoacristine, iboxygaine, hydroxyindolenine, montanine, vobasine, olivacine, ibogamine, affinine, hystrixnine, affinisine, Nb-methylaffinisine, coronaridine, 3-oxocoronaridine, 5-oxocoronaridine, ibogamine-5,6-dione, coronaridinehydroxyindolenine, vobasine, 12-methoxy-voachalotine	Hwang et al., 1969; Monnerat et al., 2005; De Souza et al., 2010
T. pachysiphon	Conodurine, 3-hydroxyconopharyngine,16-epiisositsirikine	Kingston et al., 1977; Van Beek et al., 1984a
T. laeta	Vobasine, affinine, normacusine B, geissoschizol, voacamine, conodurine, vobasine, affinine, akuammidine, affinisine, geissoschizol, voacamine, conodurine, coronaridine, conoduramine, voacangine, isovoacristine, Nb-methylvoachalotine, tabernamine, ibogamine, conopharyngine, voacangine hydroxyindolenine, voachalotine oxindole, normacusine B, pericyclivine, dehydrovoachalotine, Nb-methylvoachalotine, olivacine	Jahodář, et al., 1974; Voticky et al., 1977; You et al., 1994; Medeiros et al., 2001 Vieira et al., 2008
T. rupicola	Rupicoline, montanine	Niemann and Kessel, 1966
T.salzmannii	Voacangine, isovoacangine, (3S)-hydroxyisovoacangine, coronaridine, 3-oxo-coronaridine, (19S)-heyneanine, voachalotine, olivacine	Figueiredo et al., 2010
T.siphilitica	Isobonafousine	Damak et al., 1980
T. solanifolia	Voacangine, isovoacangine, coronaridine, heyneanine, isovoacristine, voacangine hydroxyindolenine, vobasine, voachalotine, 12-methoxy-Nb-methylvoachalotine, voacamine	Gower et al., 1986
T. stapfiana	Ibogamine	Cava et al., 1968; Kingston et al., 1977; Rastogi et al., 1980

2.8 Pharmacological properties of *Tabernaemontana* species

There are limited studies available on *T. ventricosa* (Schmelzer and Gurib-Fakim, 2008; Munayi, 2016). Moreover, the available information on the indole alkaloids and their biological activity is scarce (Schmelzer and Gurib-Fakim, 2008; Munayi, 2016; Mehrbod et al., 2018) A few studies have observed the bioactivity of certain chemical compounds (Van Beek et al., 1984a, b; Mehrbod et al., 2018). Van Beek et al. (1984a) reported that the alkaloid akuammincine, belonging to the strychnan class exhibited opioid activity in opiate receptor studies. The same group investigated the antibacterial, antifungal, and antimalarial activities of *T. ventricosa* extracts however, no activity was observed *in vitro*. Mehrbod et al. (2018) investigated the effect of *T. ventricosa* plant extracts against the influenza A virus. This investigation supported the study of Van Beek et al. (1984a), as the results concluded that the leaf extracts of *T. ventricosa* were ineffective against the influenza A virus. Due to the traditional uses of *T. ventricosa* being very similar to those of other well-known studied species, a few studies are conducted on *T. ventricosa*, thus it is necessary to evaluate the medicinal potential of this species to determine its probable pharmacology activity.

Considering the several medicinal uses of *Tabernaemontana* species in traditional medicine, many of their proposed biological activities have been confirmed, others invalidated, while countless species remain undefined (Silveira et al., 2007). Additionally, the improvements in science and medicine have allowed for the discovery of new properties of extracts, fractionations, and the identification and isolation of novel compounds (Silveira et al., 2007). Despite the presence of biologically active chemical compounds within the genus *Tabernaemontana*, multiple species lack chemical and biological evaluation however, many species have been previously investigated (Pratchayasakul et al., 2008). The details of the pharmacological properties of a few *Tabernaemontana* species are summarized in the following paragraphs.

2.8.1 Antioxidant Activity

Antioxidants are identified as molecules or compounds that regulate the process of autoxidation either by intersecting the movement of free radicals or directly constraining their formation (Fierascu et al., 2018; Toghueo and Boyom, 2019). Medicinal plants are often recognized for their rich source of antioxidants, that include phenolic acids, phenolic diterpenes, flavonoids, volatile oils, carotenoids, and anthocyanidins (Fierascu et al., 2018). These compounds target free radicals by quenching oxygen molecules, breaking antioxidant chains, donating hydrogen molecules, or acting as reducing agents (Figure 2.11) (Shori, 2015; Fierascu et al., 2018). Therefore, antioxidants are suggested to decrease oxidative stress, improve immune function, and increase healthy longevity (Tan et al., 2018). Several factors can alter the antioxidant capacity of a certain species, these include the rate of reaction between the samples and the reactive species and the concentration ratio between the antioxidant and the target (Silveira et al., 2017). According to Magalhães et al. (2008), there are multiple methods used to determine the antioxidant activity of plant species however, various methods may result in the variation of results. Many species within the *Tabernaemontana* genus have been investigated for their antioxidant activity using different techniques that include the inhibition and scavenging activity of Reactive Oxygen Species (ROS) and Reactive Nitrogen Species (RNS), reducing capacity, and metal-chelating capacity (Silveira et al., 2017).

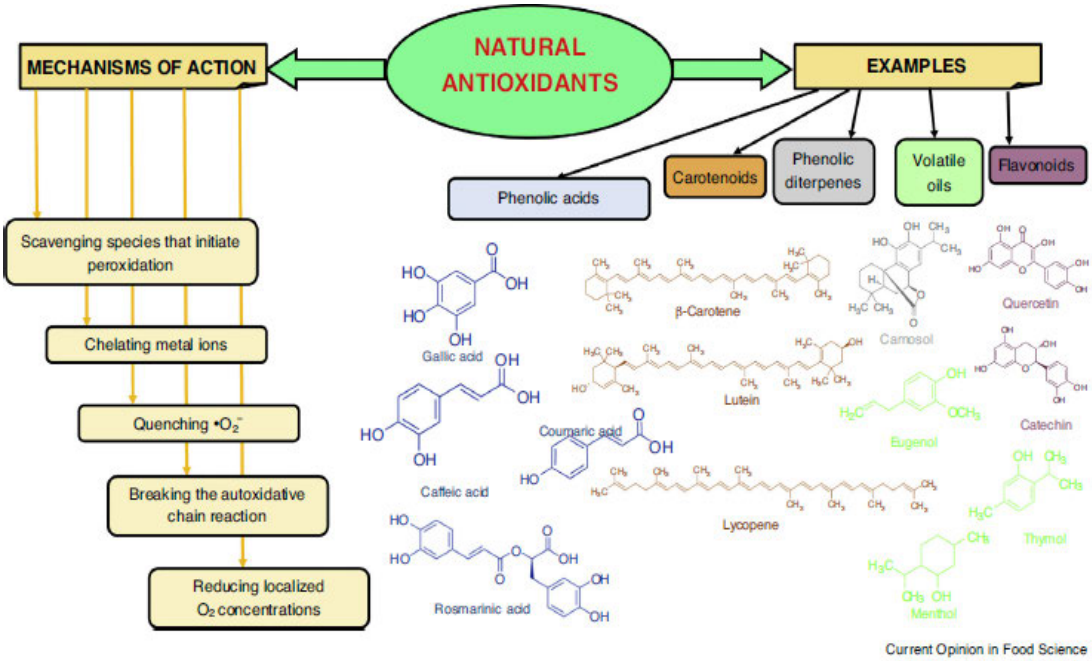

Figure 2.11: Examples of natural antioxidants and their modes of action (Fierascu et al., 2018).

The most frequently studied species within this genus is *T. catharinensis* (Nicola et al., 2013). Boligon et al. (2013a) investigated the crude leaf extracts and fractions of *T. catharinensis* by using the thiobarbituric acid reactive substances technique. Ethyl acetate and n-butanol fractions yielding half-maximal inhibitory concentration (IC_{50}) of 6.71 ± 0.19 μg/mL and 26.15 ± 0.08 μg/mL respectively displayed optimal results. Furthermore, Boligon et al. (2013a) also assessed the 1,1-diphenyl-2-picrylhydrazyl (DPPH) inhibition of *T. catharinensis* extracts, which exhibited good results with an IC_{50} value of 4.64 ± 1.25 mg/mL to 27.78 ± 0.93 mg/mL. In addition, Nicola et al. (2013) examined the antioxidant activity and the alkaloidal fraction in the branch and leaf ethanolic extracts of *T. catharinensis*. The findings of the study revealed significant antioxidant activity from the alkaloidal fraction, with an IC_{50} of 37.18 μg/mL. Table 2.3 summarizes the antioxidant properties of *Tabernaemontana* species.

Table 2.3: Antioxidant activities of extracts and compounds from *Tabernaemontana* species.

Species	Part/ Exudate	Extract/Compound	Models/Methods	References
T. alternifolia	Root and leaf	Methanol, chloroform, dichloromethane, and dichloroethane	2,2-Diphenyl-1-picrylhydrazyl (DPPH) method	Jain et al., 2010; Wasupongpun et al., 2010; Baskar et al., 2012; Satishkumar et al., 2012; Manasa et al., 2015; Shrikanth et al., 2015
T. catharinensis	Branch, leaf, root, stem, stem bark, and fruit	Supercritical fluid extraction, essential oils, ethanol, alkaloidal fractions, 16-epi-affinine, voacangine, voacristine hydroxy indolenine, ethyl acetate, hydroethanolic, and fractions	DPPH method, radical reduction-*in vitro*, ferric reducing antioxidant power (FRAP), 2,2-azino-bis-(3ethylbenzothiazoline-6-sulphonic acid (ABTS), coupled oxidation of carotene and linoleic acid assay-Male Wistar diabetic rats	Pereira et al., 2003; Santos et al., 2009; Boligon et al., 2012; Boligon et al., 2013a; Boligon et al., 2013b; Nicola et al., 2013; Boligon et al., 2014; Piana et al., 2014; Pergher et al., 2019; Sari et al., 2020
T. coronary	Flower	Petroleum ether, alcohol, and water	Hydroxyl and superoxide radicals *in vitro*, nitric oxide (NO) scavenging, and lipid peroxidationinhibition activity	Jolly et al., 2006; Gupta et al., 2010
T. corymbosa	Root, stem, and leaf	Petroleum ether, chloroform, methanol, and water	DPPH method, metal chelation, and reducing power methods - *in vitro*	Zulkefli et al., 2013
T. divaricata	Leaf, flower, stem, root, and latex	Methanol, aqueous, ethanol, petroleum ether, hexane, chloroform, ethyl acetate, ethyl-4-n-octyl benzoate, ethyl-4-n-decyl benzoate, and digalactosyldeconate	FRAP, DPPH method - *in vitro*, hydrogen peroxide (H_2O_2) free radicals, reducing power -*in vitro*, superoxide anion radical scavenging, NO, ABTS, H_2O_2 scavenging, and $A\beta_{25-35}$ peptide, novel object recognition test (NOR), crystal violet staining and lipid peroxidation	Jain et al., 2010; Wasupongpun et al., 2010; Choudhary et al., 2011; Khan, 2011; Rumzhum et al., 2012; Venkatacahlapathi et al., 2014; Mueller et al., 2015; Anbukkarasi et al., 2017; Khongsombat et al., 2018; Kalaimagal et al., 2019; Santhi et al., 2020
T. heyneana	Leaf, stem, bark, and trunk	Ethanol and sodium hypochlorite	Total phenolic content and DPPH method	Bhavana et al., 2020
T. recurva	Whole plant	Methanol	Total phenolic content	Banik, 2017

2.8.2 Anti-Inflammatory Activity

Inflammation is defined as a compound biological process that involves an adamant response of an organism to injury or damage of tissue (Elgorashi and McGaw, 2019). The development of inflammation is often induced by microbial infection, chemical injury, cell injury, and death (Calixto et al., 2003). The consequences of these inducers are primarily indicated by pain, redness, heat, and swelling, which arise due to the deviations in blood flow, capillary permeability, and afferent nerve fibers (Iwalewa et al., 2007; Rashid et al., 2018). Subsequently, these changes imitate the restoration of inflamed tissue and constrain additional damage to the organism (Elgorashi and McGaw, 2019).

Based on the characteristics of inflammation, this composite process is divided into acute and chronic inflammation (Garga and Das, 2017; Elgorashi and McGaw, 2019). Acute inflammation occurs almost instantly, or a few hours following injury, and usually displays symptoms of redness, heat, and edema (Garga and Das, 2017). These indicators often arise due to the migration of fluids, plasma proteins, and leukocytes into the injured area (Iwalewa et al., 2007; Garga and Das, 2017). Whereas, chronic inflammation occurs over an extended interval and is histologically characterized by the occurrence of lymphocytes and macrophages, which subsequently results in the development of fibrosis and necrosis tissue (Calixto, 2000). The rapid development of chronic inflammation leads to the advancements of several degenerative diseases such as rheumatoid arthritis, asthma, inflammatory bowel disease, and heart disease (Iwalewa et al., 2007; Garga and Das, 2017; Elgorashi and McGaw, 2019).

The standardized protocol for the evaluation of anti-inflammatory activity comprises *ex vivo* and *in vivo* experiments (Silveira et al., 2017). Many *Tabernaemontana* species have been assessed for anti-inflammatory activity. Table 2.4 summarizes the anti-inflammatory properties of *Tabernaemontana* species. Jolly et al. (2006) investigated the anti-inflammatory activity of ethanolic flower extracts obtained from *T. divaricata*. Mice models were subjected to acute carrageenan and chronic formalin. The results showed significant anti-inflammatory activity in both models at a dose of 100 mg/kg, in comparison to the standard reference drug diclofenac (25 mg/kg). Furthermore, Jain et al. (2013) examined the *in vivo* anti-inflammatory activity of *T. divaricata* leaves. In this study, hexane fractionations containing a profuse source of flavonoids were tested on male albino mice. The results revealed extensive anti-inflammatory activity, that displayed enhanced results in comparison to the positive drug indomethacin (Jain et al., 2013).

Table 2.4: Anti-inflammatory activities of extracts and compounds from *Tabernaemontana* species.

Species	Part/ exudate	Extract/Compound	Cell Lines/Models/ Methods	References
T. alternifolia	Root	Methanol	Lethal toxicity annulation murine models	Vineetha et al., 2020
T. bufalina	Aerial parts	Coronaridine and pandine	Reduction of lipopolysaccharide (LPS) – induced NO production	Zhang et al., 2015b
T. catharinensis	Stem bark and leaf	Ethanol, ethyl acetate, dichloromethane, n-butanol, and hydroethanolic	Carrageenan-induced rat paw edema in Wistar albino male rat models, irritant contact dermatitis models in mice, paw edema parameters in pain models involved with TRPA1 activation, and dermatitis models	Rates et al., 1993; Gomes et al., 2009; Marques et al., 2018; Brum et al., 2019; Camponogara et al., 2019a; Campongara et al., 2019b
T. divaricata	Flower, leaf, stem, and aerial parts	Ethanol, ethyl acetate, aqueous, methanol, and hexane fraction	Carrageenan and formalin-induced - mice models, reduction of interleukin (IL)-6 secretion and tumour necrosis factor (TNF)-α production, Wistar rat models and reduced croton oil-induced edema in mice models	Jolly et al., 2006; Kanthlal et al., 2011; Jain et al., 2013; Mueller et al., 2015; Anbukkarasi et al., 2019
T. pachysiphon	Leaf	Tubotaiwine and apparicine	Mouse abdominal constriction testing	Ingkaninan et al., 1999
T. pandacaqui	Stem	Ethanol and alkaloid fraction	Carrageenan-induced rat paw edema models	Taesotikul et al., 2003
T. pauciflora	Root	Voacangine, coronaridine, and 3-(2-oxopropyl)- coronaridine	Mice and Guinea pig models	Okuyuma et al., 1992

2.8.3. Antimicrobial Activity

Antimicrobials are defined as complex compounds that constrain the development of microorganisms at diminutive concentrations (Bhadane et al., 2018). These compounds are often described as secondary metabolites and are regularly produced and extracted from medicinal plants or microorganisms (Ncube et al., 2008). The efficiency of antimicrobial activity is dependent upon several factors such as various microbial strains, technique (*in vivo* or *in vitro* assay), and type of sample (Silveira et al., 2017). Studies have reported the evaluation of *Tabernaemontana* extracts as natural antibiotics that include various extraction techniques and microorganisms (Marinho et al., 2016). Monoterpenoid indole alkaloids such as voacamine type and 3-hydroxy-iboga are biologically active compounds and are reportedly used as antimicrobial agents, inhibiting the growth of bacteria, fungus, and parasites (Marinho et al., 2016).

2.8.3.1. Antifungal Activity

Singh et al. (2011) investigated the antifungal activity of a biologically active compound from *T. divaricata*. A major compound from the *Tabernaemontana* genus, coronaridine was identified and isolated from the ethanolic extract of *T. divaricata* (Singh et al., 2011), which displayed weak antifungal activity against *Penicillium chrysogenum*, comparable with nystatin [minimum inhibitory concentration (MIC) 9.8-14.0 mg/mL]. Conversely, Boligon et al. (2015) investigated the dichloromethane and n-butanol fractions of ethanolic leaf extracts from *T. catharinensis*. The dichloromethane fractions showed significant activity against the fungal strains *Candida albicans*, *Candida glabrata*, *Cryptococcus neoformans*, *Saccharomyces cerevisiae*, *Aspergillus flavus*, and *Aspergillus fumigatus* with MIC ranging from 31.25 to 1000 mg/mL. Table 2.5 summarizes the antifungal properties of *Tabernaemontana* species.

Table 2.5: Antifungal activities of extracts and compounds from *Tabernaemontana* species.

Species	Part/exudate	Extract/Compound	Cell Lines/Models/ Methods	References
T. alternifolia	Root and leaf	Methanol, chloroform, acetone, ethanol, aqueous, methanol with 9% of water and 1% of acetic acid	*Aspergillus terreus*, *Scopulariopsis* sp, *Aspergillus niger*, *Gibberella fujikuroi*, *P. chrysogenum*, *Candida albicans*, *Rhizopus mucor*, *Aspergillus parasiticus* and *Trichoderma viridians. (T. viride)*	Shrikanth et al., 2015; Jain et al., 2017
T. angulata	Aerial parts	Chloroform and methanol	*C. albicans* (American Type Tissue Culture Collection ATCC - 10231)	Suffredini et al., 2002
T. catharinensis	Aerial parts, leaf, root bark, root, and bark	Methanol, dichloromethane, n-butanol fractions of ethanol, ethanol, 12 methoxy – Nb – methylvoachalotine	*Microsporum canis*, *Microsporum gypseum*, *Trichophyton mentagrophytes*, Trichophyton *rubrum*, *Epidermophyton floccosum*, *C. albicans*, *Candida glabrata*, C*ryptococcus neoformans*, *Saccharomyces cerevisiae*, *Aspergillus flavus*, *Aspergillus fumigatus*, and *T. rubrum* strains	Henriques et al., 1996; Zacchino et al., 1998; Medeiros et al., 2011; Boligon et al., 2015
T. dichotoma	Root bark, stem bark, leaf, fruit, and seed	Ethanol and methanol	*A. niger* (ATCC 16904), *C. albicans* (ATCC 10235), *A. niger* (MTCC 281), *C. albicans* (ATCC 10231), *P. chrysogenum* (MTCC 2725), *Phanerochaete chrysosporium* (MTCC 787), and *Ralstonia entropha* (MTCC 1255)	Perera et al., 1984; Wankhede et al., 2013; Kumari et al., 2015
T. divaricata	Flower and leaf	Ethanol, methanol and water	*P. chrysogenum*, *Malassezia furfur* and Poisoned food technique *in vitro*	Ingkaninan et al., 2006; Kumari et al., 2015; Satapathy et al., 2018; Rakkimuthu et al., 2019
T. elegans	Root	Ethanol	*C. albicans* (ATCC 10231) and *C. albicans* (NHLS 255)	Pallant et al., 2009
T. pachysiphon	Root bark	Ethanol	*A. niger* and *C. albicans*	Uwumarongie et al., 2007; Uwumarongie et al., 2008
T. solanifolia	Leaf, bark, and root	Methanol	*C. albicans* B311 strain	Gower et al., 1986
T. stapfiana	Leaf, fruit, root, and stem bark	Methanol fractions -hexane, dichloromethane, and ethyl acetate	*C. albicans* (ATCC 90028), *C. neoformans* (ATCC 66031) and *M. gypseum* (KMR 101)	Ruttoh et al., 2009a

2.8.3.2. Antiviral Activity

Boligon et al. (2015) evaluated the dichloromethane, ethyl acetate, and n-butanol fractions from the ethanolic extracts of *T. catharinensis*. The extracts and fractions displayed substantial antiviral activity on herpes simplex virus type 1 (HSV-1) in contrast to acyclovir (IC_{50} 1.50 mg/mL) (Boligon et al., 2015). Furthermore, significant antiviral activity was observed from the dichloromethane and ethyl acetate fractions (Boligon et al., 2015). The dichloromethane and ethyl acetate fractions of the bark-stem fractions showed IC_{50} values of 2.62 µg/mL and 2.88 µg/mL, respectively, whereas the fractions of the leaves showed IC_{50} values of 0.60 µg/mL and 2.21 µg/mL, respectively (Boligon et al., 2015). It is suggested that biologically active compounds, such as steroids, terpenoids, and phenolics, present in the dichloromethane, ethyl acetate, and n-butanol fractions are accountable for the antiviral activity (Boligon et al., 2015; Silveira et al., 2017). Table 2.6 summarizes the antiviral properties of *Tabernaemontana* species.

Table 2.6: Antiviral activities of extracts and compounds from *Tabernaemontana* species.

Species	Part/ exudate	Extract/ Compound	Cell Lines/ Models/ Methods	References
T. catharinensis	Stem bark	Dichloromethane, ethyl acetate, and n-butanol fractions of ethanol	HSV-1	Boligon et al., 2015
T. cymosa	Bark and seed	Ethanol, lupeol acetate and voacangine	Dengue virus strains, DENV-2/NG, and DENV-2/16681 in cultured Vero or U937 cells, and Chikungunya Virus	Hernández-Castro et al., 2015; Gómez-Calderón et al., 2017
T. elegans	Leaf and stem	Ethanol	HSV-1	Twilley et al., 2017
T. laeta	Leaf, stem, and latex	Hydroethanol	HSV–1, vaccinia virus Western Reserve (VACV-WR), and encephalomyocarditis virus (EMCV)	Brandão et al., 2011
T. pachysiphon	Root and stem bark	Ethanol	HSV-1, poliovirus, and Semlicki Forest virus	Díaz Castillo et al., 2012
T. ventricosa	Leaf	Methanol	Influenza A virus (IAV)	Mehrbod et al., 2018

2.8.3.3. Antibacterial Activity

Over the past 50 years, extensive research has been conducted pertaining to the advancements in antibacterial medicines (Moghadamtousi et al., 2014). Moreover, due to the reoccurrence of multidrug-resistant bacteria, there is an excessive necessity for the development of novel and innovative antibacterial agents displaying multidrug resistance (Wise et al., 1998; Moghadamtousi et al., 2014). According to Malla et al. (2015), approximately 25% of modern medication has been established on the core basis of plant-related compounds. Thus, the active screening of medicinal plants is imperative for the discovery of new antibacterial compounds (Singh et al., 2016).

The indole alkaloids of *Tabernaemontana* exhibit a wide range of pharmacological activities, including antibacterial activity against gram-positive and gram-negative bacteria (Medeiros et al., 2011). Gindri et al. (2013) investigated the antibacterial activity of the ethanolic extract and its fractions from the leaves of *T. catharinensis*. The extracts and fractions were tested against multiple bacterial strains, such as *Staphylococcus aureus*, *Aeromonas* sp., *Micrococcus* sp., *Proteus mirabilis*, *Escherichia coli*, *Klebsiella pneumoniae*, *Enterococcus faecalis*, and *Pseudomonas aeruginosa*, that were compared against the antibiotic's ampicillin (MIC = 8.0 mg/mL), cefoperazone (MIC = 16.0 mg/mL), and imipenem (MIC = 0.06 mg/mL). The findings showed positive results against *Micrococcus* sp., *P. mirabilis*, and *P. aeruginosa* (MIC values of 31.3, 62.5, and 62.5 mg/mL, respectively) (Gindri et al., 2013). Table 2.7 summarizes the antibacterial properties of *Tabernaemontana* species.

Table 2.7: Antibacterial activities of extracts and compounds from *Tabernaemontana* species.

Species	Part/ Exudate	Extract/ Compound	Cell Lines/Models/Methods	References
T. alternifolia	Stem bark and root	Aqueous, petroleum ether, methanol, chloroform, acetone, ethanol, dichloromethane, dichloroethane, and ethyl acetate	*Methicillin-resistant S. aureus* (MRSA), vancomycin-resistant *S. aureus* (VRSA), *Bacillus subtilis* (ATCC 6633), *Staphylococcus aureus* (ATCC 6538P), *Staphylococcus epidermidis* (ATCC 12228), *Escherichia coli* (ATCC 8739), *S. aureus* (ATCC 43300), *P. aeruginosa* (DMH 1), *S. aureus* (DMH 2–DMH 8 and 10–DMH 14), *E. coli* (DMH 9), *Bacillus flexus, Proteus aureus, Salmonella typhi, Klebsiella pneumoniae, Bacillus cereus, S. aureus* (NCIM-2931), *Pseudomonas aeruginosa* (NCIM-2200), *Proteus vulgaris* (NCIM-2813), *E. coli* (NCIM-2931), *E. coli* (ATCC 8739), and MRSA (ATCC 43300)	Marathe et al., 2013; Manasa et al., 2015; Shrikanth et al., 2015
T. angulata	Aerial parts and stem	Chloroform, methanol, dichloromethane/methanol, and aqueous	*P. aeruginosa* (ATCC 90270), *S. aureus* (ATCC 6538), and *C. albicans*	Spitzer et al., 1995; Suffredini et al., 2002; De Assis et al., 2009
T. catherinensis	Thin branch, leaf root and, stem bark	Alkaloid fraction, ethanol, methanol alkaloids, dichloromethane, n-butanol fractions, 12-methoxy-Nb-methylvoachalotine, monogagaine and vobparicine	*Mycobacterium tuberculosis* H37Rv, *Mycobacterium avium, Mycobacterium kansasii, Mycobacterium malmoense Mycobacterium fortuitum, Mycobacterium smegmatis, Micrococcus* sp., *Enterococcus faecalis, Proteus mirabilis, S. aureus, Aeromonas* sp., *E. coli, K. pneumoniae, P. aeruginosa, B. subtilis* (ATCC 6633), *S. aureus* (ATCC 25923), *S. aureus* MR (ATCC 43300), *S. epidermidis* (ATCC1220228), *E. coli* (ATCC 35218), *Enterobacter cloacae* (ATCC 202), *P. aeruginosa* (ATCC 27853), *Streptococcus faecalis* (ATCC 29232), *K. pneumoniae* (ATCC 700603), *Salmonella enteritidis* (EB 1874/88), *Shigella flexneri* (2EB 7), *Acinetobacter lwoffii* strains, *T. rubrum, Enterococcus* sp., and *Citrobacter*	Van Beek et al., 1984a; Van Beek et al., 1984b; Henriques, et al., 1996; Guida et al., 2003; Pereira et al., 2003; Fonseca et al., 2008; Ramos et al., 2008; Froeder et al., 2012; Gindri et al., 2013; Boligon et al., 2015

Table 2.7: *Cont.*

T. citrifolia	Not indicated	Voacangine and ibogaine	*M. tuberculosis*, *M. avium*, and *M. kansasii*	Rastogi et al., 1998
T. coronaria	Leaf	Methanol	*M. tuberculosis* H37Rv (ATCC 2561)	Mohamad et al., 2011
T. corymbosa	Stem bark	Alkaloid fraction	*B. cereus* (ATCC 11778), *P. aeruginosa* (ATCC 27853), *S. aureus* (ATCC 25923), and *E. coli* (ATCC 35218)	Bakhtiar et al., 2011
T. dichotoma	Root bark, stem bark, stem, bark, leaf, and fruit	Monogagaine, acid aqueous, and ethanol	*B. subtilis*, *B. subtilis* (ATCC 6633), *S. aureus* (ATCC 6538), *P. aeruginosa* (ATCC 9027), and *E. coli* (ATCC 8739)	Van Beek et al.,1985; Henriques et al., 1996
T. divaricata	Leaf, bark, petal, flower, twig, and root	Ethanol, chloroform, petroleum ether, diethyl ether, methanol, aqueous, acetone, alkaloids, 5-oxocoronaridine, alkaloid fraction, dichloromethane, ethyl acetate, taberdivamines A and B	*K. pneumoniae*, *S. aureus*, *Staphylococcus saprophyticus*, *Streptococcus agalatiae*, *Streptococcus pyogenes*, *E. faecalis*, *S. typhi*, *E. coli*, *Shigella boydii*, *Shigella dysenteriae*, *P. aeruginosa*, *B. cereus*, *Klebsiella* sp., *Streptococcus uberis*, *E. coli* (ATCC 25922), *K. pneumoniae* (ATCC 35657), *Salmonella typhimurium* (MTCC 441), *S. flexneri* (ATCC 29508), *S. aureus* (ATCC25923), *Aeromonas hydrophila*, *S. epidermidis*, *Gardnerella vaginalis*, *Streptococcus agalactiae*, *Propionibacterium acnes*, *Corynebacterium macbinleyi*, *B. subtilis*, *S. faecalis*, *Bacillus megaterium*, *P. mirabilis*, *S. flexneri* (BCH 995), *S. boydii* (8), *Shigella sonnei* (NK 840), *S. dysenteriae* (1), *S. dysenteriae* (9), *Vibrio cholerae* (1023), *V. atherin* (1341), *V. cholerae* (575), *V. cholerae* (1311), *V. cholerae* (756), *E. coli* (RH 07/12), *E. coli* (18/9), *E. coli* (K88), *Enterobacter spp*., *Streptococcus suis*, *Salmonella* sp., *Corynebacterium diphtheriae* (AP596), *S. aureus* (ML 267), *S. aureus* (MTCC 96), *S. aureus* (ATCC 6538), *B. subtilis* (MTCC 441), *Bacillus pumilis* (8241*) P. aeruginosa* (AP585 NLF), *K. pneumoniae* strains, *Salmonella Paratyphi*, *Lacto bacillus*, *P.* vulgaris, and *Enterobacter aerogenes*	Arambewela et al., 1991; Ashikur et al., 2011; Gopinath et al., 2011; Pushpa et al., 2011; Singh et al., 2011; Shaker et al., 2012 Thombre et al., 2013; Venkatachalapathi, et al., 2014; Kumari et al., 2015; Mueller et al., 2015; Sumitha et al., 2015; Radhika et al., 2017; Raja et al., 2018; Zhu et al., 2020

Table 2.7: *Cont*.

T. elegans	Root	Ethanol, hexane, dichloromethane, and ethyl acetate	*Haemophilus influenzae* (ATCC 49217), *H. influenzae* (NHLS 609), *B. subtilis* (ATCC 6633), *E. faecalis* (ATCC 29212), S. *aureus* (ATCC 1200), *S. aureus* (ATCC 12600), *S. aureus* (NHLS 363), *S. aureus* (NHLS 284), *Streptococcus pneumoniae* (ATCC 49619), *S. pneumoniae* (NHLS 203), *S. pneumoniae* (NHLS 405), *M. tuberculosis* resistant (MRC 3366), *M. tuberculosis* H37RV (ATCC 25177), *M. smegmatis* (ATCC 14468*), E. coli* (ATCC 35218*), K. pneumoniae* (ATCC 13883), *P. aeruginosa* (ATCC 9027) and *M. tuberculosis* H37Rv	Pallant et al., 2009; Pallant et al., 2012; Luo et al., 2011
T. heterophylla	Stem	Dichloromethane	*M. tuberculosis*	Gramham et al., 2003
T. pachysiphon	Leaf, root, and stem bark	Ethanol, Ibogaine, 12 methoxy-ibogamine, 10-methoxyibogamine and 3-R/S-hydroxy-conopharyngine	*S. aureus, E. coli, B. subtilis, Agrobacterium tumefaciens, B. subtilis* (ATCC 6633), *S. aureus* (ATCC 6538), *P. aeruginosa* (ATCC 9027), and *E. coli* (ATCC 8739)	Van Beek et al., 1984a; Uwumarongie., et al., 2008; Duru et al., 2010
T. solanifolia	Leaf, bark, and root	Voacangine, isovoacangine, coronaridine, heyneanine, isovoacristine, voacangine hydroxyindolenine, vobasine, voachalotine, 12-methoxy-Nb-methylvoachalotine and voacamine	*C. albicans* (B311)	Gower et al., 1986
T. stapfiana	Root and stem	Methanol	*S. aureus*, MDRS, *E. faecalis, B. subtilis,* and *S. typhi*	Ruttoh et al., 2009b

2.8.3.4. Antiamoebic Activity

Parasitic infections are regarded as one of the most leading contributors to human health problems and are often distributed via contaminated food and water sources (Singh et al., 2009). Amoebiasis is a lethal disease that arises from the ingestion of pathogenic microorganisms and occurs predominantly in tropical areas including China, Mexico, the eastern portion of South America, south-east and west Africa, Asia, and the Indian subcontinent (Sharma and Sharma, 2001; Hayat et al., 2016). The protozoan parasite *Entamoeba histolytica* is dominant in these regions and affects approximately 12% of the world's population, whilst responsible for copious mortality rates, ranging from 40 000 to 110 000 deaths per year (Sharma and Sharma, 2001; Negi et al., 2018). Since there is no vaccine against *E. histolytica*, metronidazole (MNZ) is regularly used to treat infection against amoebiasis however, there are serious consequences of the drug, such as amoebic resistance and several side effects, including impaired physical and mental development (McGaw et al., 2000). Due to the serious side effects of MNZ, many infected people have opted for a more natural approach using traditional medicine (Sharma and Sharma, 2001).

Several *Tabernaemontana* species are often used in various parts of the world for their antimicrobial, antiparasitic, and antiamoebic action. Van Beek et al. (1984a) investigated a variety of *Tabernaemontana* species to establish their antiamoebic activity. In the study, approximately 15 *Tabernaemontana* species were tested against the protozoan *E. histolytica*. The study exhibited adequate results, as four extracts from three species showed promising activity below 0.5 mg/mL against the parasite protozoan *E. histolytica* (Van Beek et al., 1984a). Additionally, Uwumarongie et al. (2007) evaluated the antiamoebic activity of *T. pachysiphon* root and stem bark extracts. The findings of their study showed relatively high antiamoebic activity against *E. histolytica* (Uwumarongie et al., 2007). Table 2.8 summarizes the antiameobic properties of *Tabernaemontana* species.

Table 2.8: Antiamoebic activities of extracts and compounds from *Tabernaemontana* species.

Species	Part/Exudate	Extract	Cell Lines/Models/ Methods	References
T. aurantiaca	Leaf and twig	Ethanol	*E.histolytica*	Van Beek et al., 1984a
T. chippii	Leaf, root bark, and stem bark	Ethanol	*E. histolytica*	Van Beek et al., 1984a
T. contorta	Leaf and twig	Ethanol	*E. histolytica*	Van Beek et al., 1984a
T. crassa	Stem bark	Ethanol	*E. histolytica*	Van Beek et al., 1984a
T. dichotoma	Leaf	Ethanol	*E. histolytica*	Van Beek et al., 1984
T. glandulosa	Leaf and stem bark	Ethanol	*E. histolytica*	Van Beek et al., 1984a
T. heterophylla	Leaf and twig	Ethanol	*E. histolytica*	Van Beek et al., 1984a
T. longiflora	Leaf and twig	Ethanol	*E. histolytica*	Van Beek et al., 1984a
T. orientalis	Leaf and twig	Ethanol	*E. histolytica*	Van Beek et al., 1984a
T. pachysiphon	Root bark and stem bark	Ethanol	*E. histolytica*	Van Beek et al., 1984a; Gakuya et al., 2013; Uwumarongie et al., 2007
T. penduliflora	Stem bark	Ethanol	*E. histolytica*	Sumitha et al., 2015
T. psorocarpa	Leaf	Ethanol	*E. histolytica*	Sumitha et al., 2015
T. undulata	Stem bark	Ethanol	*E. histolytica*	Sumitha et al., 2015
T. ventricosa	Leaf and stem bark	Ethanol	*E. histolytica*	Sumitha et al., 2015
***Tabernaemontana* species**	Root	Not indicated	*E. histolytica*	Jamil et al., 2003

2.8.4 Anticancer and Cytotoxicity

The irrepressible division of cells habitually leads to the formation of cell masses, that are frequently termed as growths or tumours (Tamokou and Kuete, 2014). These masses are classified as malignant (cancerous) or benign (noncancerous) and are often influenced by several characteristics, such as an irregular diet, genetic factors, and ecological aspects (Reddy et al., 2003; Sudarshan et al., 2016). These negative influences give rise to an amplified rate of cancer since approximately 18.1 million people are expected to be diagnosed with cancer (WHO, 2018; Bray et al., 2018; Rosales et al., 2020a, b). However, with the consistent applications of effective cancer treatments, such as radiotherapy, surgery, immunotherapy, and chemotherapy, these values may subside (Gillet and Gottesman, 2010; Kuete et al., 2015). However, among these treatments, chemotherapy remains challenging due to the occurrence of multidrug resistance (MDR), which is defined by the resistance of tumours to chemotherapeutic agents (Ferreira and Paterna, 2019).

Considering the above, the constant discovery of anticancer agents using medicinal plants has displayed minimal side effects and act as modulators of MDR. Thus, recently, several medicinal plants, especially within the genus *Tabernaemontana*, have been screened to evaluate their potential effect on the growth and development of cancerous cells (Silveira, 2017). Pereira et al. (2008) investigated the isolation and structure of the chemical constituents present in the root bark of *T. catharinensis*. Twenty-seven compounds were detected in the ethanol and *n*-butanol extracts however, only 12 compounds were identified. Approximately three compounds, namely, ibogamine, 3-oxo-coronaridine, and 12-methoxy-4-methylvoachalotine (Table 2.9), showed substantial cytotoxicity in SKBR-3 breast adenocarcinoma and C-8161 human melanoma tumour cell lines (Pereira et al., 2008).

Thind et al. (2008) examined the cytotoxic properties of *T. divaricata*. In the study, various leaf extracts prepared in a range of solvents (chloroform, methanol, ethyl acetate, and hexane) were tested in the following cell lines: HCT-15 (colon), HT-29 (colon), MCF-7 (breast), and PC-3 (prostate) (Thind et al., 2008). Ethyl acetate extract was the most promising as it displayed significant cytotoxic activity against the colon cell line (502713) with a low dose of 10 µg/mL (Thind et al., 2008). Additionally, the chloroform extracts also showed considerable cytotoxicity against three colon cell lines with a slightly higher dosage of 30 µg/mL (Thind et al., 2008).

In another study, Rumzhum et al. (2012) screened the leaf extracts of *T. divaricata* using a brine shrimp bioassay. The results of the study revealed possible cytotoxicity (LC_{50} = 1 µg/mL) in comparison to the positive control, vincristine sulphate (LC_{50} = 0.3 µg/mL). Figueiredo et al. (2010) reported the cytotoxicity of *Tabernaemontana salzmannii* root and leaf extracts on human leukemia cells (THP-1). In this study, nine alkaloids were isolated; however, only two alkaloids, isovoacangine and voacangine (Table 2.2) displayed extensive cancer cell death, with an IC_{50} of 52.11 µM and 61.40 µM, respectively (Figueiredo et al., 2010). The above-isolated compounds from various *Tabernaemontana* species are frequently used to treat a range of cancer types, such as breast, renal, leukemia, lung, testicular, ovarian, germ, and colon cancer (Jordan et al., 1991; Ma et al., 2009; Nobili et al., 2009; Bhanot et al., 2011; Khazir et al., 2014; Munayi, 2016).

Recently, Rosales et al. (2019a) also evaluated the anticancer properties of indole alkaloids *of T. catharinensis*. In the study, six compounds were identified, namely, 16-*epi*affinine, 12-methoxy-*n*-methyl-voachalotine, affinisine, voachalotine, coronaridinehydroxyindoline, and ibogamine (Table 2.9) (Rosales et al., 2019a). The isolated indole alkaloids were tested *in vitro* against several cell lines, including tumour cells A375 (melanoma cell line) and A549 (adenocarcinoma human alveolar basal epithelial cells), and non-tumour Vero cells (African green monkey kidney epithelial cells) (Rosales et al., 2019a). *In vitro* toxicity showed the fractionation containing affinisine demonstrated toxicity against A375, with an IC_{50} of 11.73 µg/mL, and maybe a chemotherapeutic agent for A375 melanoma cells (Rosales et al., 2019a, b). Table 2.9 summarizes the anticancer properties of *Tabernaemontana* species.

Table 2.9: Anticancer activities of extracts and compounds from *Tabernaemontana* species.

Species	Part/ Exudate	Extract/Compound	Cell Lines/Models/Methods	References
T. angulata	Stem	Chloroform and methanol	Human breast adenocarcinoma (MCF-7), human prostate cancer (PC-3), human lung cancer (NCI-H460), human colon cancer (KM-12), human glioblastoma (SF-268), and myeloma (RPMI-8226)	De Assis et al., 2009
T. alternifolia	Stem bark and leaf	Aqueous, hexane, ethyl acetate, and methanol	Vero cell line, human gastric carcinoma (A-549, MCF-7, AGS), and human colon adenocarcinoma (COLO 320 DM and Vero cell lines)	Baskar et al., 2012; Marathe et al., 2013
T. bovina	Aerial parts	Taberdivarine C–F	Human cervical carcinoma (HeLa), human breast adenocarcinoma (MCF-7), and colon carcinoma (SW480)	Zhang et al., 2015c
T. bufalina	Aerial parts	3′-(2-oxopropyl)-19,20 dihydro-tabernamine, 3′-(2 oxopropyl) ervahanine B, 19,20 dihydrovobparicine, ibogamine, coronaridine, voacangine, hainanervatasine, 3-(2-oxopropyl) coronaridine, 3,3′-(oxopropyl) dicoronaridine, isotabernamine, taberdivarines C, taberdivarine D, tabernaelegantine B, tabernaelegantinine B, 19,20-dihydrotabernamine A, taberdivarine E, ervadivaricatine B, taberdivarine F tabernaecorymbosine A, tabernaelegantine C, tabernaelegantine A, and 19-(2-oxopropyl)-conoduine	Small cell lung carcinoma (A-549) and human breast adenocarcinoma (MCF-7)	Zhou et al., 2018
T. calcarea	Whole plant	Voacristine, isovoacristine, 19-epi-voacristine, hydroxytabernanthine,11-hydroxycoronaridine, 19-epi-heyneanine, 3(R/S)-19-epi-3-oxovoacristine, hydroxyindolenine, 10-methoxyibogamine (ibogaine), and 11-methoxyibogamine	Ovarian cancer (A2780)	Chaturvedula et al., 2003
T. catharinensis	Leaf, seed, root, bark, and stem	Coronaridine, tabersonine, olivacine, coronaridine-hydroxyindolenine,	Ehrlich's carcinoma, sarcoma 180, human breast carcinoma (SK-BR-3), melanoma	Gower et al., 1986; Rates et al., 1993; De

Table 2.9: *Cont.*

		catharinensine, decarbomethoxyvoacamine, tabernamine, aqueous, ethanol, and alkaloid fraction	tumour cells (SK-BR-3 and C-8161), laryngeal carcinoma (Hep-2 and normal 3 T3 cell lines), human melanoma cell lines (A375, WM1366, SK-MEL-28), normal skin cell line (CCD-1059Sk), adenocarcinomic human alveolar basal epithelial cells (A549), Vero cells (African green monkey kidney epithelial cells)	Almeida et al., 2004; Pereira et al., 2004; Pereira et al., 2008; Rizo et al., 2013; Rosales et al, 2019a; Rosales et al., 2019b
T. contorta	Root	Contortarine A, 16-epi-pleiomutinine and N4-chloromethyl-pleiomutinine	Quinone reductase induction (QR) and NF-kB inhibition assay	Ndongo et al., 2017
T. corymbosa	Stem bark, leaf, and twig	Alkaloid fraction, jerantinine A, jerantinine C, jerantinine B, jerantinine B acetate,jerantinine D, jerantinine E, jerantinine F, conodiparine A, oxoconodiparine A, conodiparine B,oxoconodiparineB,vobasidine A, vobasidine B, vobasidine C, vobasidine D, taipinisinetabernaemontanine, dreagamine, vobasine, 16-epivobasine, vobasenal, 16-epivobasenal, vincristine, 16-decarbomethoxy-voacaminepseudoindoxyl, conolutinine, lirofoline A, conoliferine, conomicidine A, conomicidineB, ibogamine, ibogaine, ibogaine-7-hydroxyindolenine, iboxygaine, iboluteine, coronaridine, heyneanine, 19-epi-heyneanine, 7(R)-geissoschizol oxindole, 7(S)-geissoschizol oxindole, 16(R),7(R)-19,20-eisositsirikine oxindole, affinisine, voachalotine, norfluorocurarine, antirhine, velbanamine, 20(S) hydroxy-1,2 dehydro- pseudo-aspi-dospermidine, tabercorines A–C, acetyl-tabernaecorymbosine A, tabernaricatine A, tabernaricatine B, tabernaricatine D, 16-decarbomethoxyvoacamine, conodurine,	Human non-small lung carcinoma (A549), human cervical carcinoma (C33A), human oral epidermoid carcinoma (vincristine resistant KB, vincristine-sensitive (KB/S), vincristine-resistant cells KB/VJ300), human colon colorectal (HCT-116 cells, HT-29), human breast adenocarcinoma (MDA-MB-231, MCF-7), human breast cancer (MDA-468), human hepatoma (Hep-G2 and SMMC-7721) cells, human leukemia (HL-60), hepatocarcinoma cell line (SMMC-7721), lung and colon carcinoma (SW480), human carcinoma (KB, P-glycoprotein over- expressing multi-drug resistant KB cells) and human carcinoma (KB, KB-VIN cells)	Kam et al., 1998; Lim et al., 2008; Bakhtiar et al., 2011; Frei et al., 2013; Ma et al., 2014a; Ma et al., 2014b; Raja et al., 2014; Sim et al., 2014; Lim et al., 2015; Zhang et al., 2015a; Yuan et al., 2017; Al-Hayali, 2018; Zhang et al., 2018

Table 2.9: *Cont.*

		tabernaecorymbosine,taburnaemines A−I, tabernaecorymbosine A, tabernaricatineC, tabernaricatine D, 16′-decarbo-methoxytabernaecorymbosine, tabercorymines, and conofolidine		
T. divaricata		Chloroform, petroleum ether, methanol, ethylacetate, hexane, ethanol, hydroalcohol, acetone, aqueous, dichloromethane, chloroform- 5-oxocoronaridine, 3- oxocoronaridine, coronaridine, ibogamine, tabernaemontamine, vobasine, voacamine, tabernaricatines A–F, bisindole alkaloids, 16-decarbo-methoxyvoacamine, tabernaecorymbosine A, isovoacangine, heyneanine, voacangine, 19acetonyliso-voacangine, vincadiffine, difforlemeine, voaphylline, hecubine, voacangine hydroxyindolenine, voacryptine, 19S-heyneanine, 19S-voacangarine, lo-methoxyeglandine-noxide lo-hydroxycoronaridine, heyneatine, O-acetyl vallesamine, pericalline, dihydrocondylocarpine, camptothecin, 9-methoxycamptothecin, conoduramine, and coronaridinehydroxyindolenine	Human colon carcinoma (HCT-15, HT-29, and 502713), human breast adenocarcinoma (MCF-7), human prostate cancer (PC-3), leukemia (HP-1), brine shrimp lethality, lung carcinoma large cell (COR-L23), laryngeal carcinoma (Hep-2), Vero cells, sarcoma 180, cloned Chinese hamster lung fibroblast (V_{79} cells), human colon cancer (HT-29), human small cell lung carcinoma (A-549), human hepatic cancer (HepG-2), human and rat normal skeletal muscle cell cultures (L6), renal cell carcinoma in Wistar rats, human myeloid leukemia (HL-60), hepatocellular carcinoma (SMMC-7721), colon cancer (SW480), human breast cancer (BC1), human oral epidermoid carcinoma (KB), and KB drug-resistant strain (KB-V1), human prostate cancer (LNCaP), human lung cancer (Lu1), murine, lymphocytic leukemia (P388), human glioma (U373), human epidermoid carcinoma (A431), human colon cancer (Col2), human fibrosarcoma (HT), human melanoma (Mel2), hormone-dependent breast cancer (ZR-75-1), Kl3-V1 cells, and human leukemia (MOLT4)	Gunasekera et al., 1980; Lee et al., 2005; Thind et al., 2008; Singh et al., 2011; Dantu et al., 2012; Rumzhum et al., 2012; Boa et al., 2013; Hullatti et al., 2013; Thombre et al., 2013; Poornima and Gopalakrishnan, 2014; Ohishi et al., 2015; Selvakumar and Kumar, 2015; Doshi et al., 2017
T. elegans	Whole plant and root	Ethanol, ethyl acetate,indole alkaloids, tabernaelegantinine B, tabernaelegantine C, dregamine, eleganine A, tabernine A-C, 16-epi-dregamine, and monomeric indole bisindole alkaloids	Human macrophages (THP-1 cells), cell viability screening (trypan blue dye exclusion assay), human hepatoma (HuH-7, HCT-116, and SW620 cells), human cervical epithelial carcinoma (HeLa), African green monkey kidney cells (Vero), and human embryonic kidney (HEK-293),	Mansoor et al., 2009; Luo et al., 2011; Mansoor et al., 2013; Zaima et al., 2013

Table 2.9: *Cont.*

T. hystrix	Root bark	Voacamine	Lymphoblastoid (CEM-WT), osteosarcoma (U-2 OS-WT), and drug-resistant cell lines (CEM-R and U-2 OS-R)	Meschini et al., 2003
T. laeta	Stem bark	Ethyl acetate	Human carcinoma (KB cells)	You et al., 1994
T. pandacaqui	Leaf	Ethanol	Human primary renal cell carcinoma (786-0), colon adenocarcinoma grade II (HT-29), ovarian carcinoma (OVCAR-3), melanoma (SK-MeI-28), glioblastoma (SNB-19), human breast adenocarcinoma (MCF-7), human prostate cancer (PC-3), and small cell lung carcinoma (A549)	Bradacs et al., 2010
T. solanifolia,	Leaf, bark, and root	12-methoxy-Nb-methyl-voachalotine	Leukemia (3PS31)	Gower et al., 1986
T. salzmannii,	Root bark	Voacangine	Monocytic leukemia (THP-1)	Figueiredo et al., 2010

2.8.5 Acetylcholinesterase Activity

Alzheimer's disease (AD) is defined as an advanced chronic and aggressive neurodegenerative disease, that is habitually accompanied by the severe disturbance of multiple cortical functions, including memory impairment, judgment, orientation, understanding, language learning capacity, and personality changes (Suganthy et al., 2009; Pereira et al., 2010; Chaiyana et al., 2013). Clinically, this cognitive disorder is often characterized by the occurrence of several amyloidal β-peptide plaques, neurofibrillary tangles, atrophy of basal forebrain cholinergic neurons, oxidative stress, and reduced neurotransmitter levels (Chattipakorn et al., 2007; Nicola et al., 2013; Rawa et al., 2019). According to Adewusi and Steenkamp (2011), AD is amongst the leading disorders worldwide as it is liable for approximately 50%-60% of dementia in elders. Moreover, a dramatic incline, possibly affecting 7%-10% of individuals over 65 and 40% of persons over 80 years is anticipated within the next 50 years, without the intervention of rehabilitation (Ingkaninan et al., 2003; Suganthy et al., 2009).

Popular methods for the treatment of AD are often based on the cholinergic hypothesis, which suggests that the impairment of memory is directly related to a reduction in the function of cholinergic in the brain (Ingkaninan et al., 2003). Thus, several approaches regarding the enhancement of acetylcholine levels using acetylcholinesterase (AChE) inhibitors are frequently investigated (Ingkaninan et al., 2003; Rawa et al., 2019). Currently, approved AChE inhibitors include tacrine, donepezil, rivastigmine, and galanthamine (Ingkaninan et al., 2003; Andrade et al., 2005; Chattipakorn et al., 2007). However, despite the beneficial effects on cognitive functioning, these inhibitors have displayed undesirable side effects, such as gastrointestinal issues, nausea, vomiting, and reduced bioavailability (Mukherjee et al., 2007; Ranjan and Kumari, 2017). Considering the latter, the discovery of alternative natural AChE inhibitors displaying minimal side effects is essential (Chattipakorn et al., 2007; Ranjan and Kumari, 2017; Rawa et al., 2019).

Therapeutic plants have been investigated for their complex compounds that contain natural and innovative AChE inhibitors (Ingkaninan et al., 2003; Andrade et al., 2005). Several *Tabernaemontana* species have been recognized and investigated for their monoterpene indole alkaloids, which have demonstrated AChE inhibitory activity (Athipornchai et al., 2020). Ingkaninan et al. (2003) investigated the AChE inhibitory activity of methanolic extracts of *T. divaricata*. In the study, extracts (0.1 mg/mL) were tested *in vivo* using rats as test models (Ingkaninan et al., 2003). The results were promising as approximately 90% of AChE activity was observed. Furthermore, most recently, Athipornchai et al. (2020) revealed the AChE inhibitory activity of the methanol, n-hexane, and ethyl acetate extracts of *Tabernaemonata pandacaqui* flowers. The results showed that the ethyl acetate extract displayed the strongest AChE inhibitory activity, with inhibition of 35.4% at 5 mg/mL (Athipornchai et al., 2020). Considering the latter, prior and recent studies have shown the potential of plant AChE inhibitors, which

should be further investigated. Table 2.10 summarizes the acetylcholinesterase activities of *Tabernaemontana* species.

Table 2.10: Antiacetylcholinesterase activities of extracts and compounds from *Tabernaemontana* species.

Species	Plant Organ/ Exudate	Extract/Compound	Methods	References
T. amygdalifolia	Latex	Ethanol and methanol	Ellman's method	Wijayabandara et al., 2008
T. australis	Stem and stalk	Ethanol	Ellman's method	Andrade et al., 2005
T. divaricata	Leaf, flower, root, stem, and latex	Methanol, ethanol, phosphate buffer, petroleum ether, dihydrotabernamine, 19,20-dihydro-ervahanine A conodurine, tabernaelegantine A, Taberhanine, voafinine, *N*-methylvoafinine, voafinidine, voalenine, conophyllinine, conophylline, and conofoline,	Ellman's method	Kam et al., 2003c; Ingkaninan et al., 2003; Ingkaninan et al., 2006; Chattipakkorn et al., 2007; Thind et al., 2008; Nakdook et al., 2010; Chaiyana et al., 2013; Singh et al., 2015
T. iboga	Root bark	Ibogaine and physostigmine	Ellman's method	Alper et al., 2012
T. laeta	Stalk and stem	Ethanol	Ellman's method	Vieira et al., 2008
T. pandacaqui	Flower	Methanol	Ellman's method	Athipornchai, 2020

2.9 Other biological activities

Khan (2011) investigated the gastrointestinal effects of the methanol extract from *T. divaricata* flowers. In the study, a rat pyloric ligation-induced gastric ulceration model was used to evaluate the potential effects, along with the standard drug omeprazole (8.0 mg/kg) (Khan, 2011). It was revealed that the extract reduced the amount of gastric juice, free and total acidities, ulcer index, and pH of gastric acid produced (Khan, 2011). The standard drug, omeprazole showed percentage protection of 89.8%, and the extract 79.5%, respectively (Khan, 2011). In another report, Khan et al. (2013) further examined the methanol extract from the flowers of *T. divaricata*, using a range of concentrations (125.0, 250.0, and 500.0 mg/kg). Some inducers, such as aspirin and ethanol, were tested against gastric ulcers (Khan et al., 2013). The standard positive control was misoprostol (Khan et al., 2013). Several parameters, such as catalase, superoxide dismutase, mucin, and total protein were measured and displayed a reduced index when treated with extracts. It has been suggested that the gastrointestinal effects of the extracts occur through an antioxidant pathway (Khan et al., 2013).

The antidiabetic activity of *T. divaricata* methanol extract was examined on alloxan-induced diabetic rats (Kanthal et al., 2014). The results displayed substantial antidiabetic activity, with an additional reduction in the effect of oxidative damage observed in rats (Kanthal et al., 2014). The extracts exhibited a similar mechanism in relation to the positive control, glibenclamide. The study of Kanthlal et al. (2014) recommends that the methanol extract may alert the insulin receptors, therefore triggering a stimulation or production of β-stem cells in the pancreas of the test subjects. In another study, the compound conophylline, displayed antidiabetic activity (Kojima et al., 2006). Furthermore, conophylline was efficient in inducing the activity of activin A in AR42J cells, which in turn stimulated modification in endocrine cells (Kojima et al., 2006). Fujii et al. (2009), investigated the same compound against diabetic rats. In the study, an increased plasma level in normal and streptozotocin-induced diabetic rats was observed along with a significant decrease in blood glucose levels, indicative of antidiabetic activity (Fujii et al., 2009). In rat pancreatic acinar carcinoma cells and cultured rat pancreatic tissues, the compound conophylline was found to rapidly-produce β-cell differentiation, thus inducing differentiation into insulin-producing cells (Fujii et al., 2009; Kuete et al., 2010).

Tabernaemontana catharinensis is often used for its antivenom properties (Silveira, 2017). De Almeida et al. (2004) examined its antivenom effects. The alkaloidal aqueous fractionation from the root bark of *T. catharinensis* was tested *in vivo* using *Crotalus durissus terrificus* (De Almeida et al., 2004). It was observed that the extracts were able to extensively defuse the poisonous action of the venom (De Almeida et al., 2004). Núñez et al. (2004), investigated the antivenom activity of *T. elegans*. The study showed potential inhibition against *Crotalus durissus cumanensis* venom (Núñez et al., 2004). The antivenom potential of *Tabernaemontana alternifolia* root extract was tested *in vitro* and *in vivo* against *Echis carinatus* venom (Vineetha et al., 2019). A range of pharmacological assays, including lethal toxicity determination, hemorrhagic, and neutralization studies, was carried out using chick embryo models (Vineetha et al., 2019). The extracts showed promising results, since fibrinogen degradation, hemorrhage, and venom-induced edema were significantly reduced in the models (Vineetha et al., 2019).

Recently, Vineetha and coauthors (2020) investigated the *in vitro* and *in vivo* inhibitory effects of *T. alternifolia* methanolic root extract against *Naja naja* venom. Similarly, in their previous study, the fibrinogenolytic, direct, and indirect hemolytic activities for the neutralization of the venom were observed (Vineetha et al., 2019; Vineetha et al., 2020). The results of the study by Vineetha et al., (2020) yet again showed a great potential, since fibrinogen and hemolytic were neutralized effectively, and the edema ratio was significantly reduced (Vineetha et al., 2019; Vineetha et al., 2020). The latex of several *Tabernaemontana* species is habitually utilized for its wound-healing effects (Silveira et al., 2017).

Subsequently, *T. catharinensis* is known for its many medicinal uses, including wound-healing effects (Silveira et al., 2017).

2.10 Silver Nanoparticles (AgNPs)

Recent trends in science have promoted the synthesis of AgNPs in the field of nanotechnology (Devaraj et al., 2014). Nanoparticles (NPs) are extremely small materials that exhibit nanoscale dimensions ranging from 1-100 nm (Lateef et al., 2018). Due to their nanoscale size, these particles display a large surface area to volume ratio (Chouhan et al., 2018). The properties of AgNPs, such as their size, shape, and morphology, have enhanced their activity and thus are used in an extensive range of applications, such as health, medicine, food, textiles, and agricultural sectors (Lateef et al., 2018). Many metals have been evaluated for the synthesis of NPs, such as gold (Au), copper (Cu), and silver (Ag) however, comparable to these metals, reports have shown that Ag is not considered a hazardous substance (Barberia-Rouque et al., 2018). Gorchev and Ozolins (2011) reported that minor amounts of Ag were absorbed in laboratory test subjects ranging between 0% and 10%.

The two main methods used to obtain NPs comprise a "Top-down" approach, which can be described as the process whereby NPs are reduced in size until they reach a suitable material; conversely, the "Bottom-down" approach involves the development of NPs from an elemental entity, such as atoms and molecules (Mittal et al., 2013). The top-down method consists of chemical and physical techniques that are often energy-consuming and produce imperfect NPs (Thakkar et al., 2010). Moreover, the bottom-down technique includes biological methods, which regularly produce colloidal dispersions of homogenous particles with fewer defects (Singh et al., 2016).

Current research has shown that the biological synthesis (i.e., the use of living organisms) of AgNPs has driven investigations towards a "Greener synthesis" approach, which is simple, cost-effective, environmentally friendly, and easily upscaled for large-scale synthesis (Devaraj et al., 2014; Sigamoney et al., 2016). According to Chouhan (2018), the method of biological synthesis using a greener approach is relatively simple, as it requires less time and energy comparable to physical and chemical methods. This approach involves incubating crude aqueous extracts obtained from various plants or plant organs with an aqueous solution comprised of a metal salt, such as silver nitrate ($AgNO_3$) (Mittal et al., 2013). The reaction between the metabolites in the plant extract then reduces the metal ions in solution, thus metal NPs are produced (Mittal et al., 2013). An illustration of the biological synthesis of AgNPs is shown in Figure 2.12. The use of environmentally friendly plant extracts was discovered to generate a considerable number of AgNPs using $AgNO_3$ as an inorganic metal (Chouhan et al., 2018). Reported studies have found that AgNPs exhibit significant antimicrobial activity and low toxicity to humans (Banerjee and Narendhirakannan, 2011; Safavi, 2012; Chouhan, 2018).

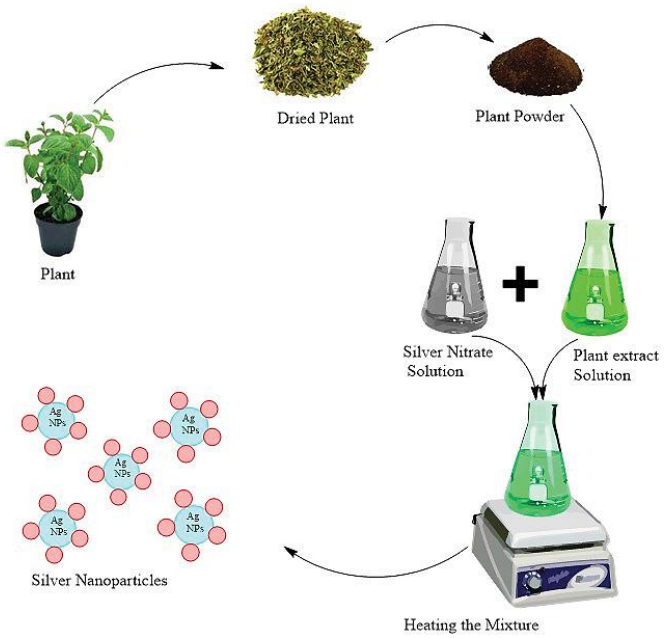

Figure 2.12: Schematic representation of the biological synthesis of AgNPs (Khan et al., 2017).

Recently, several AgNP investigations have been conducted using *Tabernaemontana* species, with *T. divaricata* being the most investigated species (Table 2.11). In the study by Devaraj et al. (2014), various *T. divaricata* extracts were used for biosynthesis, characterized, and assessed for cytotoxicity using MCF-7 cell lines. The analysis showed that the average particle size ranged from 22.85 nm and the biosynthesized NPs showed potential cytotoxicity in human breast cancer cells (MCF-7) (Devaraj et al., 2014). These NPs could probably be regularly used in various sectors, such as medical, cosmetic, and food applications (Devaraj et al., 2014). In another study conducted by Anbukkarasi et al. (2020), *T. divaricata* extracts were used for biosynthesizing NPs and the resulting biosynthesized NPs were tested *in vivo* to prevent the formation of cataracts in selenite-induced cataractogenesis in Wistar rat pups (Anbukkarasi et al., 2020). It was revealed that rats induced with AgNPs treatment displayed a reduction in lenticular alterations compared to plant extract-treated rats (Anbukkarasi et al., 2020). The results of the study recommend that biosynthesized AgNPs using *T. divaricata* extracts may provide limitations of selenite-induced cataractogenesis *in vivo*, while simultaneously sustaining standard lenticular calcium homeostasis by avoiding adjustments in important lenticular proteins (Anbukkarasi et al., 2020).

Table 2.11: Biological activity of synthesized AgNPs using extracts from *Tabernaemontana* species.

Species	Plant organ/ Exudate	Extract	Biological activity	References
T. divaricata	Leaf	Aqueous and ethanol	Cytotoxicity (Human breast cancer cell line-MCF-7), *in vitro* antioxidant, anticataractogenic, and *in vivo* anticataractogenic	Devaraj et al., 2014; Anbukkarasi, et al., 2017; Anbukkarasi et al., 2020

2.11 Conclusion

The current review established an inclusive assessment of the major alkaloidal compounds within species belonging to the genus *Tabernaemontana* and the family Apocynaceae, that demonstrated pharmacological potential. The various secondary metabolites derived from *Tabernaemontana* species, such as terpenes, lactones, steroids, phenolics, flavonoids, and alkaloids, are often utilized in ethnobotany for their curative effects. Furthermore, these bioactive components have displayed numerous biological activities, including antimicrobial, antioxidant, anti-inflammatory, anticholinesterase, antineurodegenerative, anticancer, antidiabetic, antivenom, larvicidal, antihypertensive action, wound healing, and analgesic properties. However, despite the presence of biologically active chemical compounds within the genus *Tabernaemontana*, many species lack chemical and biological evaluation. Thus, further research is crucial to gain insight into the bioactive compounds of this esteemed genus and their relative pharmacological activities.

2.12 References

Abdullahi, A.A., 2011. Trends and challenges of traditional medicine in Africa. African Journal of Traditional, Complementary and Alternative medicines 8, 115–123.

Abubakar, I.B., Loh, H.S., 2016. A review on ethnobotany, pharmacology and phytochemistry of *Tabernaemontana corymbosa*. Journal of Pharmacy and Pharmacology 68, 423–432.

Adewusi, E.A., Steenkamp, V., 2011. *In vitro* screening for acetylcholinesterase inhibition and antioxidant activity of medicinal plants from southern Africa. Asian Pacific Journal of Tropical Medicine 4, 829-835.

Alan, C.A., Wilkes, B., 1964. Studies on the suppression of immune responses by the periwinkle alkaloids vincristine and vinblastine. Journal of Clinical Investigation 43, 2394–2403.

Al-Hayali, M.Z.K. Characterisation of Anticancer Properties of a Novel and Naturally Isolated Bisindole Alkaloid, Conofolidine. Ph.D. Thesis, University of Nottingham, Nottinghamshire, UK, 2018.

Ali Khan, M.S., Jais, M., Manan, A., Afreen, A., 2013. Prostaglandin analogous and antioxidant activity mediated gastroprotective action of *Tabernaemontana divaricata* (L.) R. Br. Flower methanolic extract against chemically induced gastric ulcers in rats. BioMed Research International 2013, 1–18.

Alper, K., Reith, M.E.A., Sershen, H., 2012. Ibogaine and the inhibition of acetylcholinesterase. Journal of Ethnopharmacology 139, 879–882.

Amzat, J., Abdullahi, A.A., 2008. Roles of traditional healers in the fight against HIV/AIDS. Studies on Ethno-Medicine 2, 153–159.

Anbukkarasi, M., Sundararajan, M., Venkadeswaran, K., Ruban, V.V., Anand, T., Geraldine, P. 2019. Antihypercholesterolemic, antioxidative and anti-inflammatory potential of an extract of the plant *Tabernaemontana divaricata* in experimental rats fed an atherogenic diet. Biocatalysis and Agricultural Biotechnology 19, 101115.

Anbukkarasi, M., Thomas, P.A., Sheu, J.-R., Geraldine, P., 2017. *In vitro* antioxidant and anticataractogenic potential of silver nanoparticles biosynthesized using an ethanolic extract of *Tabernaemontana divaricata* leaves. Biomedicine and Pharmacotherapy 91, 467–475.

Anbukkarasi, M., Thomas, P.A., Teresa, P.A., Anand, T., Geraldine, P., 2020. Comparison of the efficacy of a *Tabernaemontana divaricata* extract and of biosynthesized silver nanoparticles in preventing cataract formation in an *in-vivo* system of selenite-induced cataractogenesis. Biocatalysis and Agricultural Biotechnology 23, 101475.

Andrade, M.T., Lima, J.A., Pinto, A.C., Rezende, C.M., Carvalho, M.P., Epifanio, R.A., 2005. Indole alkaloids from *Tabernaemontana australis* (Müell. Arg) Miers that inhibit acetylcholinesterase enzyme. Bioorganic & Medicinal Chemistry 13, 4092-4095.

Angiosperm Phylogeny Group, 2009. An update of the Angiosperm Phylogeny Group classification for the orders and families of flowering plants: APG III. Botanical Journal of the Linnean Society 161, 105–121.

Arambewela, L.S., Ranatunge, T., 1991. Indole alkaloids from *Tabernaemontana divaricata*. Phytochemistry 30, 1740–1741.

Araujo, A.R., Kascheres, C., Fujiwara, F., Marsaioli, A.J., 1984. Catharinensine, an oxindole alkaloid from *Peschiera catharinensis*. Phytochemistry 23, 2359–2363.

Arnold, H.J., Gulumian, M., 1984. Pharmacopoeia of traditional medicine in Venda. Journal of Ethnopharmacology 12, 35–74.

Ashikur, R.M., Hasanuzzaman, M., Mofizur, R.M., Zahan, S.I., Muhuri, R.S., 2011. Evaluation of antibacterial activity of study of leaves of *Tabernaemontana divaricata* (L.*)*. International Research Journal of Pharmacy 2, 123–127.

Athipornchai, A., 2018. A review on *Tabernaemontana* spp.: Multipotential medicinal plant. Asian Journal of Pharmaceutical and Clinical Research 11, 45–53.

Athipornchai, A., Ketpoo, P., Saeeng, R., 2020. Acetylcholinesterase Inhibitor from *Tabernaemontana pandacaqui* Flowers. Natural product communications 15, 1934578X20911488.

Bakhtiar, M., Izzati, M.N., Darnis, D. Cytotoxic and antimicrobial activities of alkaloids from *Tabernaemontana corymbose.* In Proceedings of the 5th AASP Conference, Bandung, Indonesia, 16–19 June 2011.

Bakkali, F., Averbeck, S., Averbeck, D., Idaomar, M., 2008. Biological effects of essential oils–a review. Food and Chemical Toxicology 46, 446–475.

Banerjee, J., Narendhirakannan, R.T., 2011. Biosynthesis of silver nanoparticles from *Syzygium cumini* (L.) seed extract and evaluation of their *in vitro* antioxidant activities. Digest Journal of Nanomater and Biostructures 6, 961–968.

Banik, S., 2017. Evaluation of thrombolytic, membrane stabilizing, and antioxidant activities of methanolic extract of *Tabernaemontana recurva* Roxb. Discovery Phytomedicine 4, 17.

Bao, M.F., Yan, J.M., Cheng, G.G., Li, X.Y., Liu, Y.P., Li, Y., Cai, X.H., Luo, X.D., 2013. Cytotoxic Indole Alkaloids from *Tabernaemontana divaricata*. Journal of Natural Products 76, 1406–1412.

Barberia-Roque, L., Gámez-Espinosa, E., Viera, M., Bellotti, N., 2018. Assessment of three plant extracts to obtain silver nanoparticles as alternative additives to control biodeterioration of coatings. International Biodeterioration and Biodegradation. In press: https://doi.org/10.1016/j.ibiod.2018.06.011.

Basavaraj, P., Shivakumar, B., Shivakumar, H., 2011. Anxiolytic activity *of Tabernaemontana divaricata* (Linn) R. Br. flowers extract in mice. International Journal of Pharma and Bio Sciences 2, 65–72.

Baskar, A.A., Numair, K.-S.A., AlSaif, M.-A., Ignacimuthu, S., 2012. *In vitro* antioxidant and antiproliferative potential of medicinal plants used in traditional Indian medicine to treat cancer. Redox Reports 17, 145–156.

Basumatary, A.R., 2016. Preliminary phytochemical screening of some compounds from plant stem bark extracts of *Tabernaemontana divaricata* Linn. used by Bodo Community at Kokrajhar District, Assam, India. Archives of Applied Science Research 8, 47–52.

Batina, M.D.F.C., Cintra, A.C.O., Veronese, E.L.G., Lavrador, M.A.S., Giglio, J.R., Pereira, P.S., Dias, D.A., França, S.C., Sampaio, S.V., 2000. Inhibition of the Lethal and Myotoxic Activities of *Crotalus durissus terrificus* Venom by *Tabernaemontana catharinensis*: Identification of One of the Active Components. Planta Medica 66, 424–428.

Beentje, H., Adamson, J., Bhanderi, D., 1994. Kenya trees, shrubs, and lianas. National Museums of Kenya: Nairobi, Kenya.

Bhadane, B.S., Patil, M.P., Maheshwari, V.L., Patil, R.H., 2018. Ethnopharmacology, phytochemistry, and biotechnological advances of family Apocynaceae: a review. Phytotherapy Research 32, 1181–1210.

Bhanot, A., Sharma R., Noolvi M. N., 2011. Natural Sources as Potential Anti-cancer Agents: A Review. International Journal of Phytomedicine 3, 09–26.

Bharathi, P., Thomas, A., Thomas, A., Krishnan, S., Ravi, T.K., 2011. Antibacterial activity of leaf extracts of *Calotropis gigantea* Linn. against certain gram negative and gram–positive bacteria. International Journal of Chemical Sciences 9, 919–923.

Bhavana, N.S., Prakash, H.S., Nalini, M.S., 2020. Fungal Endophytes from *Tabernaemontana heyneana* Wall. (Apocynaceae), their Molecular Characterization, L-asparaginase and Antioxidant Activities. Jordan Journal of Biological Sciences 13, 543–550.

Boligon, A.A., Athayde, M.L., 2012. Phytochemical investigation and cytotoxic properties of *Tabernaemontana catharinensis* A. DC. cultivated in Brazil. Research Journal of Phytochemistry 6, 127–131.

Boligon, A.A., de Freitas, R.B., de Brum, T.F., Piana, M., Belke, B.V., da Rocha, J.B.T., Athayde, M.L., 2013a. Phytochemical constituents and *in vitro* antioxidant capacity of *Tabernaemontana catharinensis* A. DC. Free Radicals and Antioxidants 3, 77–80.

Boligon, A.A., Piana, M., Kubiça, T.F., Mario, D.N., Dalmolin, T.V., Bonez, P.C., Weiblen, R., Lovato, L., Alves, S.H., Campos, M.M., Athayde, M.L., 2015. HPLC analysis and anti-microbial, anti-mycobacterial and anti-viral activities of *Tabernaemontana catharinensis* A. DC. Journal of Applied Biomedicine 13, 7–18.

Boligon, A.A., Piana, M., Schawnz, T.G., Pereira, R.P., Rocha, J.B.T., Athayde, M.L., 2014. Chromatographic Analysis and Antioxidant Capacity of *Tabernaemontana catharinensis*. Natural Product Communications 9, 61–4.

Boligon, A.A., Schwanz, T.G., Piana, M., Bandeira, R.V., Frohlich, J.K., Brum, T.F.D., Zadra, M., Athayde, M.L., 2013b. Chemical composition and antioxidant activity of the essential oil of *Tabernaemontana catharinensis* A. DC. leaves. Natural product research 27, 68–71.

Bradacs, G., Maes, L., Heilmann, J., 2010. *In vitro* cytotoxic, antiprotozoal and antimicrobial activities of medicinal plants from Vanuatu. Phytotherapy Research 24, 800–809.

Braga, R.M., Filho, H.F.L., Reis, F.A.M.,1984. 13C NMR analysis of alkaloids from *Peschiera fuchsiaefolia*. Phytochemistry 23, 175–178.

Brandão, G.C., Kroon, E.G., dos Santos, J.R., Stehmann, J.R., Lombardi, J.A., de Oliveira, A.B., 2011. Antiviral activity of plants occurring in the state of Minas Gerais (Brazil): Part III. Journal of Chemical and Pharmaceutical Research 3, 223–236.

Bray, F., Ferlay, J., Soerjomataram, I., Siegel, R.L., Torre, L.A., Jemal, A., 2018. Global cancer statistics 2018: GLOBOCAN estimates of incidence and mortality worldwide for 36 cancers in 185 countries. CA: A Cancer Journal for Clinicians 68, 394–424.

Brum, E.D.S., Becker, G., Fialho, M.F.P., Casoti, R., Trevisan, G., Oliveira, S.M., 2019. TRPA1 involvement in analgesia induced by *Tabernaemontana catharinensis* ethyl acetate fraction in mice. Phytomedicine 54, 248–258.

Burkill, H.M., 1985. The useful plants of West Tropical Africa, second edition, Families AD Royal Botanic Gardens.

Calixto, J.B., 2000. Efficacy, safety, quality control, marketing and regulatory guidelines for herbal medicines (phytotherapeutic agents). Brazilian Journal of medical and Biological Research 33, 179–189.

Calixto, J.B., Cabrini, D.A., Ferreira, J., Campos, M.M., 2000. Kinins in pain and inflammation. Pain 87, 1–5.

Calixto, J.B., Otuki, M.F., Santos, A.R., 2003. Anti-inflammatory compounds of plant origin. Part I. Action on arachidonic acid pathway, nitric oxide and nuclear factor κ B (NF-κB). Planta Medica 69, 973–983.

Camponogara, C., Casoti, R., Brusco, I., Piana, M., Boligon, A.A., Cabrini, D.A., Trevisan, G., Ferreira, J., Silva, C.R., Oliveira, S.M., 2019a. *Tabernaemontana catharinensis* leaves exhibit topical anti-inflammatory activity without causing toxicity. Journal of Ethnopharmacology 231, 205–216.

Camponogara, C., Casoti, R., Brusco, I., Piana, M., Boligon, A.A., Cabrini, D.A., Trevisan, G., Ferreira, J., Silva, C.R., Oliveira, S.M., 2019b. *Tabernaemontana catharinensis* leaves effectively reduce the irritant contact dermatitis by glucocorticoid receptor-dependent pathway in mice. Biomedicine and Pharmacotherapy 109, 646–657.

Canaveze, Y., Machado, S.R., 2016. The occurrence of intrusive growth associated with articulated laticifers in *Tabernaemontana catharinensis* A. DC., a new record for Apocynaceae. International Journal of Plant Sciences 177, 458–467.

Cardoso, C.A., Vilegas, W., Honda, N.K., 1998. Qualitative determination of indole alkaloids, triterpenoids and steroids of *Tabernaemontana hilariana*. Journal of Chromatography A 808, 264–268.

Cardoso, C.A., Vilegas, W., Pozetti, G.L.,1997. Gas chromatographic analysis of indole alkaloids from *Tabernaemontana hilariana*. Journal of Chromatography A 788, 204–206.

Cardoso, C.A.L., Vilegas, W., 1999. Droplet counter-current chromatography of indole alkaloids from *Tabernaemontana hilariana*. Phytochemical Analysis 10, 60–63.

Castelblanque, L., Balaguer, B., Martí, C., Rodríguez, J.J., Orozco, M., Vera, P., 2016. Novel insights into the organisation of laticifer cells: A cell comprising a unified whole system. Plant Physiology 172, 1032–1044.

Castelblanque, L., Balaguer, B., Martí, C., Rodríguez, J.J., Orozco, M., Vera, P., 2017. Multiple facets of laticifer cells. Plant Signaling and Behavior 12, 1–5.

Cava, M., Talapatra, S., Weisbach, J., Douglas, B., Raffauf, R., Beal, J., 1965. Gabunine: A natural dimeric indole derived from perivine. Tetrahedron Letters 6, 931–935.

Cava, M.P., Nomura, K., Talapatra, S.K., Mitchell, M.J., Schlessinger, R.H., Buck, K.T., Beal, J.L., Douglas, B., Raffauf, R.F., Weisback, J.A., 1968. Alkaloids of *Stephania glabra*. Direct chemical correlation of the absolute configuration of some Benzyltetrahydroisoquinoline, Proaporphine, and Aporphine Alkaloids. New protoberberine alkaloid. The Journal of Organic Chemistry 33, 2785–2789.

Chaiyana, W., Schripsema, J., Ingkaninan, K., Okonogi, S., 2013. 3′-R/S-Hydroxyvoacamine, a potent acetylcholinesterase inhibitor from *Tabernaemontana divaricata*. Phytomedicine 20, 543–548.

Changwichit, K., Khorana, N., Suwanborirux, K., Waranuch, N., Limpeanchob, N., Wisuitiprot, W., Suphrom, N., Ingkaninan, K., 2011. Bisindole alkaloids and secoiridoids from *Alstonia macrophylla* Wall. ex G. Don. Fitoterapia 82, 798–804.

Chatora, R., 2003. An overview of the traditional medicine situation in the African region. African Health Monitor 4, 4–7.

Chattipakorn, S., Pongpanparadorn, A., Pratchayasakul, W., Pongchaidacha, A., Ingkaninan, K., Chattipakorn, N., 2007. *Tabernaemontana divaricata* extract inhibits neuronal acetylcholinesterase activity in rats. Journal of Ethnopharmacology 110, 61–68.

Chaturvedula, V.S.P., Sprague, S., Schilling, J.K., Kingston, D.G.I., 2003. New Cytotoxic Indole Alkaloids from *Tabernaemontana calcarea* from the Madagascar Rainforest1. Journal of Natural Products 66, 528–531.

Chitme, H.R., Chandra, R., Kaushik, S., 2006. Evaluation of analgesic activities *of Calotropis gigantea* extract *in vivo*. Asia Pacific Journal of Pharmacology 16, 157–162.

Choudhary, R., Saroha, A.E., Swarnkar, P., 2011. Screening of endogenous antioxidants in some medicinal plants. Toxicology and Environmental Chemistry 93, 656–664.

Chouhan, N., 2018. Silver nanoparticles: Synthesis, characterization and applications. In: Silver nanoparticles-fabrication, characterization and applications. Editors: Maaz, K. IntechOpen.

Damak, M., Ahond, A., Potier, P., 1980. Bonafousine and isobonafousine, dimeric alkaloids from *Bonafousia tetrastachya* (Humboldt, Bonpland et Kunth) Markgraf (apocynaceae). Bulletin de la Société chimique de France 9, 490–495.

Danieli, B., Palmisano, G., 1986. Alkaloids from *Tabernaemontana*. In The alkaloids: Chemistry and pharmacology Academic Press 27, 1–130.

Danieli, B., Palmisano, G., Gabetta, B., Martinelli, E.M., 1980. Tabernaelegantinines C and D, two new bisindole alkaloids containing a cyano group from *Tabernaemontana elegans* Stapf. Part 2. Journal of Chemical Society 1, 601–606.

Dantu, A.S., Shankarguru, P., Ramya, D.D., Vedha, H.B., 2012. Evaluation of *in vitro* anti-cancer activity of hydroalcoholic extract of *Tabernaemontana divaricata*. Asian Journal of Pharmaceutical Clinical Research 5, 59–61.

de Almeida, L., Cintra, A.C., Veronese, E.L., Nomizo, A., Franco, J.J., Arantes, E.C., Giglio, J.R., Sampaio, S.V., 2004. Anticrotalic and antitumoral activities of gel filtration fractions of aqueous extract from *Tabernaemontana catharinensis* (Apocynaceae). Comparative Biochemistry and Physiology Part C: Toxicology and Pharmacology 137, 19–27.

De Assis, C.M., Moreno, P.R.H., Young, M.C.M., Campos, I.P.D.A., Suffredini, I.B.,2009. Isolamento e avaliação da atividade biológica dos alcalóides majoritários de *Tabernaemontana angulata* Mart. ex Müll. Arg., Apocynaceae. Revista Brasileira de Farmácia 19, 626–631.

De Barry, A., 1877. Vergleichende anatomie der vegetationsorgane der phanerogamen und farne., W. Engelmann, Leipzig.

De Souza, J.J., Mathias, L., Vieira, I.J.C., Braz-Filho, R., 2010. Two New Indole Alkaloids from *Tabernaemontana hystrix* Steud. (Apocynaceae). Helvetica Chimica Acta 93, 422–429.

Devaraj, P., Aarti, C., Kumari, P., 2014. Synthesis and characterisation of silver nanoparticles using *Tabernaemontana divaricata* and its cytotoxic activity against MCF7 cell line. International Journal of Pharmacology and Pharmaceutical Science 6, 86–90.

Díaz Castillo, F., Morelos Cardona, S.M., Carrascal Medina, M., Pájaro González, Y., Gómez Estrada, H., 2012. Actividad larvicida de extractosetanólicos de *Tabernaemontana cymosa* y *Trichiliahirta* sobrelarvas de estadio III y IV de *Aedes aegypti* (Diptera: Culicidae) Revista Cubana de Plantas Medicinales 17, 256–267.

Doshi, G.M., Kanad, P.P., Azad, N., Desai, A., Somani, R.R., Chaskar, P.K., 2017. *In vitro* Cytotoxicity Studies on *Tabernaemontana divaricata* leaves extracts by sulforhodamine B assay method. International Journal of Pharmaceutical Sciences Review and Research 45, 179–182.

Duru, C.M., Mbata, T.I., 2010. The antimicrobial activities and phytochemical screening of ethanolic leaf extracts of *Hedrantherabarteri* Hook and *Tabernaemontana pachysiphon* Stapf. Journal of Developmental Biology and Tissue Engineering 2, 1–4.

Dussourd, D.E., 1995. Entrapment of aphids and whiteflies in lettuce latex. Ecology and Population Biology 88, 163–172.

Dutra, R.C., Campos, M.M., Santos, A.R., Calixto, J.B., 2016. Medicinal plants in Brazil: Pharmacological studies, drug discovery, challenges and perspectives. Pharmacological research 112, 4–29.

Elgorashi, E., McGaw, L.J., 2019. African plants with *in vitro* anti-inflammatory activities: A review. South African Journal of Botany 126, 142–169.

Endress, M.E., 2004. Apocynaceae: brown and now. Telopea 10, 525–541.

Endress, M.E., Bruyns, P.V., 2000. A revised classification of the Apocynaceae sl. The Botanical Review 66, 1–56.

Evert, R.F., 2006. Esau's plant anatomy, third ed. New York, USA: Wiley-Inter science.

Fahn, A., 1979. Secretory tissues in plants. illustrated ed. Academic Press.

Fahn, A., 1988. Secretory tissues in vascular plants. New Phytologist 108, 229–257.

Fahn, A., 2000. Structure and function of secretory cells. Advances in botanical research 31, 37–76.

Ferreira, M.J.U., Paterna, A., 2019. Monoterpene indole alkaloids as leads for targeting multidrug resistant cancer cells from the African medicinal plant *Tabernaemontana elegans*. Phytochemistry Revisions 18, 971–987.

Fierascu, R.C., Ortan, A., Fierascu, I.C., Fierascu, I., 2018. *In vitro* and *in vivo* evaluation of antioxidant properties of wild-growing plants. A short review. Current Opinion in Food Science 24, 1–8.

Figueiredo, E.R., Vieira, I.J., de Souza, J.J., Braz Filho, R., Mathias, L., Kanashiro, M.M., Cortes, F.H., 2010. Isolation, identification and antileukemic activity of the monoterpene indole alkaloids from *Tabernaemontana salzmannii* (A. DC.), Apocynaceae. Revista Brasileira de Farmacognosia 20, 675–681.

Fonge, B.A., Egbe, E.A., Fongod, A.G.N., Focho, D.A., Tchetcha, D.J., Nkembi, L., Tacham, W.N., 2012. Ethnobotany survey and uses of plants in the Lewoh-Lebang communities in the Lebialem highlands, SouthWest Region, Cameroon. Journal of Medicinal Plants Research 6, 855–865.

Fonseca, T.L., Von Groll, A., Leitão, G.G., Scaini, C.J., Ramos, D.F., Silva, P.E.A., 2008. Antimycobacterial Vegetal Extracts against *Mycobacterium fortuitum* and *Mycobacterium malmoense*. Vittalle 20, 65–71.

Foster, A.S., 1956. Plant idioblasts: Remarkable examples of cell specialization. Protoplasma 46, 184–93.

Franceschi, V.R., Horner, H.T., 1980. Calcium oxalate crystals in plants. The Botanical Review, 46, 361–427.

Franceschi, V.R., Nakata, P.A., 2005. Calcium oxalate in plants: Formation and function. Annual of Review of Plant Biology 56, 41–71.

Frei, R., Staedler, D., Raja, A., Franke, R., Sasse, F., Gerber-Lemaire, S., Waser, J., 2013. Total Synthesis and Biological Evaluation of Jerantinine E. Angewandte Chemie International Edition 52, 13373–13376.

Froeder, A.L.F., Nunes, L., Pappis, L., Boligon, A.A., de Brum, T.F., Dalmolin, T.V., Bonez, P.C., Campos, M.M.A., Athayde, M.L., 2012. Atividad eantimicrobiana do extratobrutoefrações das folhas de *Tabernaemontana catharinensis* frente à *Mycobacterium tuberculosis.* Revista Fitoterapia 12, 176.

Fujii, M., Takei, I., Umezawa, K., 2009. Antidiabetic effect of plant extract containing conophylline by oral administration in streptozotocin-treated and Goto-Kakizaki rats. Biomedicine and Pharmacotherapy 63, 710–716.

Gakuya, D.W., Itonga, S., Mbaria, J., Muthee, J., Musau, J., 2013. Ethnobotanical survey of biopesticides and other medicinal plants traditionally used in Meru central district of Kenya. Journal of Ethnopharmacology 145, 547–553.

Gama, T.D.S.S., Rubiano, V.S., Demarco, D., 2017. Laticifer development and its growth mode in *Allamanda blanchetii* A. DC. (Apocynaceae). The Journal of the Torrey Botanical Society 144, 303–312.

Gandhi, G.R., Vasconcelos, A.B.S., Haran, G.H., da Silva Calisto, V.K., Jothi, G., Quintans, J.D.S.S., Cuevas, L.E., Narain, N., Júnior, L.J.Q., Cipolotti, R., Gurgel, R.Q., 2019. Essential oils and its bioactive compounds modulating cytokines: A systematic review on anti-asthmatic and immunomodulatory properties. Phytomedicine 152854, 1–9.

Garga, D., Das, T., 2017. Preliminary phytochemical screening and anti-inflammatory effect of the Aqueous extract of *Tabernaemontana divaricata* flower in wister rats. International Journal of Current Pharmaceutical Research 9, 9–12.

Gillet, J.P., Gottesman, M.M., 2010. Mechanisms of multidrug resistance in cancer. In Multi-drug resistance in cancer. Humana Press 4, 47–76.

Gindri, A.L., Boligon, A.A., Mario, D.N., Frohlich, J.K., de Brum, T.F., Alves, S.H., Athayde, M.L., 2013. Potencial anti-microbiano do extrato bruto e frações das folhas de *Tabernaemontana catharinensis* A. DC. Revista Contexto and Saúde 11, 1213–1216.

Gomes, R., Neto, A., Melo, V., Fernandes, V., Dagrava, G., Santos, W., Pereira, P.S., Couto, L., Beleboni, R.O., 2009. Antinociceptive and anti-inflammatory activities of *Tabernaemontana catharinensis*. Pharmaceutical Biology 47, 372–376.

Gómez-Calderón, C., Mesa-Castro, C., Robledo, S., Gómez, S., Bolivar-Avila, S., Diaz-Castillo, F., Martínez-Gutierrez, M., 2017. Antiviral effect of compounds derived from the seeds of *Mammea americana* and *Tabernaemontana cymosa* on Dengue and Chikungunya virus infections. BMC complementary and alternative medicine 17, 57–69.

Gonçalves, D., Araújo, J., Francisco, M., Coelho, M., Franco, J., 2011. Avaliação da atividade antimicrobiana *in vitro* do extrato de *Tabernaemontana catharinensis* A. DC. Revista brasileira de plantas medicinais 13, 197–202.

Good, R., 1947. The geography of the flowering plants. London: Longmans, Green and Co.

Gopinath, S.M., Suneetha, T.B., Mruganka, V.D., Ananda, S., 2011. Evaluation of antibacterial activity of *Tabernaemontana divaricata* (L.) leaves against the causative organisms of bovine mastitis. International Journal of Research in Phytochemistry and Pharmacology 1, 211–213.

Gorchev, H.G., Ozolins, G., 2011. WHO guidelines for drinking-water quality. WHO Chron 38, 104–108.

Gower, A.E., Pereira, B.D.S., Marsaioli, A.J., 1986. Indole alkaloids from *Peschiera campestris*. Phytochemistry 25, 2908–2910.

Graham, J., Pendland, S., Prause, J., Danzinger, L., Vigo, J.S., Cabieses, F., Farnsworth, N., 2003. Antimycobacterial evaluation of Peruvian plants. Phytomedicine 10, 528–535.

Guida, A., Battista, G.D., Bargardi, S., 2003. Actividad antibacteriana de alcaloides de *Tabernaemontana catharinensis* A. DC. ARS Pharmaceutica 44, 167–173.

Gunasekera, S.P., Cordell, G., Farnsworth, N.R., 1980. Anticancer indole alkaloids of *Ervatamia heyneana*. Phytochemistry 19, 1213–1218.

Gupta, M., Kanti, M.U., Gomathi, P., Sambath, K.R., 2010. Antioxidant and free radical scavenging activities of *Ervatamia coronaria* Stapf. leaves. Iranian Journal of Pharmaceutical Research 3, 119–126.

Hagel, J.M., Yeung, E.C., Facchini, P.J., 2008. Got milk? The secret life of laticifers. Trends in Plant Science 13, 631–639.

Hayat, F., Azam, A., Shin, D., 2016. Recent progress on the discovery of antiamoebic agents. Bioorganic and Medicinal Chemistry Letters 26, 5149–5159.

Heinrich, G., 1969. Elektronenmikroskopische beobachtungen zur entstehungsweise der exkretbehalter von *Ruta graveolens*, *Citrus limon* und *Poncirus trifolialiata*. Ost Botany Z117 3, 97–403.

Henriques, A., Melo, A., Moreno, P.R.H., Ene, L., Henriques, J., Schapoval, E.E.S., 1996. *Ervatamia coronaria*: Chemical constituents and some pharmacological activities. Journal of Ethnopharmacology 50, 19–25.

Hernández-Castro, C., Diaz-Castillo, F., Martinez-Gutierrez, M., 2015. Ethanol extracts of *Cassia grandis* and *Tabernaemontana cymosa* inhibit the *in vitro* replication of dengue virus serotype 2. Asian Pacific Journal of Tropical Diseases 5, 98–106.

Hirasawa, Y., Miyama, S., Hosoya, T., Koyama, K., Rahman, A., Kusumawati, I., Alasmontamine, A., 2009. A first tetrakis monoterpene indole alkaloid from *Tabernaemontana elegans*. Organic letters 11, 5718–21.

Hullatti, K., Pathade, N., Mandavkar, Y., Godavarthi, A., Biradi, M., 2013. Bioactivity-guided isolation of cytotoxic constituents from three medicinal plants. Pharmaceutical Biology 51, 601–606.

Hwang, B., Weisbach, J.A., Douglas, B., Raffauf, R.F., Cava, M.P., Bessho, K., 1966. Problems in chemotaxonomy. V. Alkaloids of *Peschiera lundii*. Isolation and structure elucidation of voacristine pseudoindoxyl and iboxygaine hydroxyindolenine. Journal of Organic Chemistry 34, 412–415.

iNaturalist., https://www.inaturalist.org/taxa/132896-T*abernaemontana*, Date accessed, 4th September 2018.

Ingkaninan, K., Changwijit, K., Suwanborirux, K., 2006. Vobasinyl-iboga bisindole alkaloids, potent acetylcholinesterase inhibitors from *Tabernaemontana divaricate* root. Journal of Pharmacy and Pharmacology 58, 847–852.

Ingkaninan, K., Ijzerman, A.P., Taesotikul, T., Verpoorte, R., 1999. Isolation of Opioid-active Compounds from *Tabernaemontana pachysiphon* leaves. Journal of Pharmacy and Pharmacology 51, 1441–1446.

Ingkaninan, K., Temkitthawon, P., Chuenchom, K., Yuyaem, T., Thongnoi, W., 2003. Screening for acetylcholinesterase inhibitory activity in plants used in Thai traditional rejuvenating and neurotonic remedies. Journal of Ethnopharmacology 89, 261–264.

Iwalewa, E.O., McGaw, L.J., Naidoo, V., Eloff, J.N., 2007. Inflammation: The foundation of diseases and disorders. A review of phytomedicines of South African origin used to treat pain and inflammatory conditions. African Journal of Biotechnology 6, 2868–2885.

Jahodář, L., Votický, Z., Cava, M.P., 1974. Geissoschizol in *Peschiera laeta*. Phytochemistry 13, 2880–288.

Jain, S., Jain, A., Jain, N., Jain, D., Balekar, N., 2010. Phytochemical investigation and evaluation of *in vitro* free radical scavenging activity of *Tabernaemontana divaricata* Linn. Natural Product. Research 24, 300–304.

Jain, S., Sharma, P., Ghule, S., Jain, A., Jain, N., 2013. *In vivo* anti-inflammatory activity of *Tabernaemontana divaricata* leaf extract on male albino mice. Chinese Journal of Natural Medicines 11, 472–476.

Jain, S.K., Sharma, P., Balekar, N., Jain, D.K., 2017.Antioxidant and antifungal activity of some medicinal plant extracts. Journal of Drug Delivery and Therapeutics 7, 189–191.

Jamil, S., Ahmad, S., Akhtar, J., Alam, K., 2003. Antiamoebic plants used in Unani System of Medicine. Natural. Product Radiance 2, 1–6.

Jolly, C., Thambi, P., Kuzhivelil, B., Sabu, M., 2006. Antioxidant and anti-inflammatory activities of the flowers of *Tabernaemontana coronaria* (L) R.Br. Indian Journal of Pharmaceutical Sciences 68, 352.

Jordan, M. A., Thrower, D., Wilson, L., 1991. Mechanism of Inhibition of Cell Proliferation by Vinca Alkaloids. Cancer Research 51, 2212–2222.

Kadiyala, M., Ponnusankar, S., Elango, K., 2013. *Calotropis gigantiea* (L.) R. Br (Apocynaceae): A phytochemical and pharmacological review. Journal of Ethnopharmacology 150, 32–50.

Kalaimagal, C., 2019. *In vitro* antioxidant activity in ethanolic leaf extract of *Tabernaemontana divaricata* (L.). International Journal of Bio-Pharma Research 8, 2602–2606.

Kam, T.S., Anuradha, S., 1995. Alkaloids from *Tabernaemontana divaricata*. Phytochemistry 40, 313–316.

Kam, T.S., Loh, K.Y., Lim, L.H., Loong, W.L., Chuak, C.H., Wei, C., 1992. New Alkaloids from the Leaves of *Tabernaemontana divaricata*. Tetrahedron Letters 33, 969–972.

Kam, T.-S., Pang, H.-S., Choo, Y.-M., Komiyama, K., 2004. Biologically Active Ibogan and Vallesamine Derivatives from *Tabernaemontana divaricata*. Chemistry and Biodiversity 1, 646–656.

Kam, T.-S., Pang, H.-S., Lim, T.-M., 2003c. Biologically active indole and bisindole alkaloids from *Tabernaemontana divaricata*. Organic and Biomolecular Chemistry 1, 1292–1297.

Kam, T.S., Sim, K.M., 2002. Five new iboga alkaloids from *Tabernaemontana corymbosa*. Journal of Natural Products 65, 669–672.

Kam, T.S., Sim, K.M., 2003b. Conodirinine A and B, novel vobasine-iboga bisindoles incorporating an additional tetrahydro-1,3-oxazine unit on the vobasinyl moiety. Helvetica Analytica Chimica Acta 86, 122–126.

Kam, T.-S., Sim, K.-M., Koyano, T., Toyoshima, M., Hayashi, M., Komiyama, K., 1998. Conodiparines A-D, new bisindoles from *Tabernaemontana*. Reversal of vincristine-resistance with cultured cells. Bioorganic Medicinal Chemistry Letters 8, 1693–1696.

Kam, T.S., Sim, K.M., Lim, T.M., 1999. Tronoharine, a novel hexacyclic indole alkaloid from a Malayan *Tabernaemontana*. Tetrahedron Letters 40, 5409–5412.

Kam, T.S., Sim, K.M., Lim, T.M., 2000. Voastrictine, a novel pentacyclic quinolinic alkaloid from *Tabernaemontana*. Tetrahedron Letters 42, 4721–4723.

Kam, T.S., Sim, K.M., Pang, H.S., 2003a. New Bisindole Alkaloids from *Tabernaemontana corymbosa*. Journal of Natural Products 66, 11–16.

Kanthlal, S.K., Kumar, B.A., Joseph, J., Aravind, R., Frank, P.R., 2014. Amelioration of oxidative stress by *Tabernamontana divaricata* on alloxan-induced diabetic rats. Ancient Science of Life 33, 222–228.

Kanthlal, S.K., Suresh, V., Arunachalam, G., Frank, P.R., Kameshwaran, S., 2011. *In vivo* Evaluation of Analgesic and Antipyretic activity of Aerial parts of *Tabernaemontana divaricata* in Experimental Animal models. Pharmacology online 3, 1127–1133.

Keating, R.C., 2003. Leaf anatomical characters and their value in understanding morphoclines in the Araceae. Botanical Review 68, 510–523.

Khan, M.S.A., 2011. Gastroprotective Effect of *Tabernaemontana divaricata* (Linn.) R.Br. Flower Methanolic Extract in Wistar Rats. British Journal of Pharmaceutical Research 1, 88–98.

Khan, Y., Numan, M., Ali, M., Khali, A.T., Abbas, N., Shinwar, Z.K., 2017. Bio-synthesized silver nanoparticles using different plant extracts as anti-cancer agent. Journal of Nanomedicine and Biotherapeutic Discovery 1, 1–7.

Khazir, J., Mir, B.A., Pilcher, L.A., Riley, D.L., 2014. Role of plants in anticancer drug discovery. Phytochemistry Letters 7, 173–181.

Khongsombat, O., Nakdook, W., Ingkaninan, K., 2018. Inhibitory effects of *Tabernaemontana divaricata* root extract on oxidative stress and neuronal loss induced by amyloid β25-35 peptide in mice. Journal of Traditional and Complementary Medicine 8, 184–189.

Khyade, M.S., Kasote, D.M., Vaikos, N.P., 2014. *Alstonia scholaris* (L.) R. Br. and *Alstonia macrophylla* Wall. ex G. Don: A comparative review on traditional uses, phytochemistry and pharmacology. Journal of Ethnopharmacology 153, 1–18.

Kingston, D.G.I., Li, B.T., Ionescu, F., 1977. Plant anti-cancer agents III: Isolation of indole and bis-indole alkaloids from *Tabernaemontana holstii* roots. Journal of Pharmaceutical Science 66, 1135–1138.

Kirtikar, K.R., Basu, B.D., 1999. Indian medicinal plants. Dehrandun: International book distributor 191–192, 420–422, 993–994, 2045–2047.

Kojima, I., Umezawa, K., 2006. Conophylline: A novel differentiation inducer for pancreatic β cells. The International Journal of Biochemistry and Cell Biology 38, 923–930.

Konno, K., 2011. Plant latex and other exudates as plant defense systems: Roles of various defence chemicals and proteins contained therein. Phytochemistry 72, 1510–1530.

Krishnamurthy, K.V., Venkatasubramanian, P., Lalitha, S., 2013. Laticifers of Jatropha. In Jatropha, Challenges for a New Energy. Springer, New York, 3–10.

Kuete, V., Manfouo, R.N. and Beng, V.P., 2010. Toxicological evaluation of the hydroethanol extract of *Tabernaemontana crassa* (Apocynaceae) stem bark. Journal of Ethnopharmacology 130, 470–476.

Kuete, V., Saeed, M.E., Kadioglu, O., Börtzler, J., Khalid, H., Greten, H.J., Efferth, T., 2015. Pharmacogenomic and molecular docking studies on the cytotoxicity of the natural steroid wortmannin against multidrug-resistant tumor cells. Phytomedicine 22, 120–127.

Kumar, G., Karthik, L., Rao, K.V.B., 2011. A review on pharmacological and phytochemical profile of *Calotropis gigantea* Linn. Pharmacology online 1, 1–8.

Kumari, S., Mazumder, A., Bhattacharya, S., 2015. Pharmacognostical and antimicrobial studies of the stem of *Tabernaemontana divaricata* Linn. International Journal of Pharmaceutical Sciences 7, 101–104.

Lateef, A., Folarin, B.I., Oladejo, S.M., Akinola, P.O., Beukes, L.S., Gueguim-Kana, E.B., 2018. Characterisation, anti-microbial, antioxidant, and anti-coagulant activities of silver nanoparticles synthesized from *Petiveria alliacea* L. leaf extract. Preparative Biochemistry and Biotechnology 48, 646–652.

Lee, C., Houghton, P., 2005. Cytotoxicity of plants from Malaysia and Thailand used traditionally to treat cancer. Journal of Ethnopharmacology 100, 237–243.

Leeuwenberg, A.J.M., 1991. A Revision of *Tabernaemontana*: The Old-World Species, second edition, Royal Botanic Gardens, Kew, United kingdom.

Lemos, T.L.G., Andrade, C.H.S., Guimarães, A.M., Wolter-Filho, W., Braz-Filho, R., 1996. 19-Epivoacristine, an Iboga Alkaloid Isolated from *Peschiera affinis*. Journal of Brazilian Chemical Society 7, 123–126.

Lewinsohn, T.M., 1991. The geographical distribution of plant latex. Chemo Ecology 2, 64–68.

Lim, K.-H., Hiraku, O., Komiyama, K., Kam, T.-S., 2008. Jerantinines A−G, Cytotoxic Aspidosperma Alkaloids from *Tabernaemontana corymbosa*. Journal of Natural Products 71, 1591–1594.

Lim, K.-H., Raja, V.J., Bradshaw, T.D., Lim, S.-H., Low, Y.-Y., Kam, T.-S., 2015. Ibogan, Tacaman, and Cytotoxic Bisindole Alkaloids from *Tabernaemontana*. Cononusine, an Iboga Alkaloid with Unusual Incorporation of a Pyrrolidone Moiety. Journal of Natural Products 78, 1129–1138.

Luo, X., Pires, D., Aínsa, J.A., Gracia, B., Mulhovo, S., Duarte, A., Anes, E., Ferreira, M.J.U., 2011. Antimycobacterial evaluation and preliminary phytochemical investigation of selected medicinal plants traditionally used in Mozambique. Journal of Ethnopharmacology 137, 114–120.

Ma, K., Wang, J.-S., Luo, J., Yang, M.-H., Kong, L., 2014a. Tabercarpamines A–J, Apoptosis-Inducing Indole Alkaloids from the Leaves of *Tabernaemontana corymbosa*. Journal of Natural Products 77, 1156–1163.

Ma, K., Wang, J.-S., Luo, J., Yang, M.-H., Yao, H., Sun, H.-B., Kong, L.-Y., 2014b. Bistabercarpamines A and B, first vobasinyl-chippiine-type bisindole alkaloid from *Tabernaemontana corymbosa*. Tetrahedron Letters 55, 101–104.

Ma, X. and Wang, Z., 2009. Anticancer Drug Discovery in the Future: An Evolutionary Perspective. Drug Discovery Today 14, 1136–1142.

Magalhães, L.M., Segundo, M.A., Reis, S., Lima, J.L., 2008. Methodological aspects about *in vitro* evaluation of antioxidant properties. Analytica Chimica Acta 613, 1–19.

Mahatma, O.P., Singhvi, I., Shirsat Mrunal, K., Dwivedi, J., Vaya, R., 2010. Anti inflammatory and antipyretic activities leaves *of Calotropis gigantea* (Linn). Journal of Global Pharma Technology 2, 75–78.

Mahlberg, P.G., 1961. Embryogeny and histogenesis in *Nerium oleander*. II. Origin and development of the non-articulated laticifer. American Journal of Botany 48, 90–99.

Mahlberg, P.G., 1993. Laticifers: An historical perspective. Botanical Review 59, 1–23.

Mahlberg, P.G., Sabharwal, P.S., 1968. Origin and early development of non-articulated laticifers in embryos of *Euphorbia marginata*. American Journal of Botany 55, 375–381.

Mairura, F., 2006. Medicinal plants: *Tabernaemontana crass* Benth. Prota 589–591.

Malla, B., Gauchan, D.P., Chhetri, R.B., 2015. An ethnobotanical study of medicinal plants used by ethnic people in Parbat district of western Nepal. Journal of Ethnopharmacology 165, 103–117.

Manasa, D.J., Chandrashekar, K.R., 2015. Antioxidant and antimicrobial activities of *Tabernaemontana heyneana* Wall. An endemic plant of Western Ghats. International Journal of Pharmaceutical Sciences 7, 311–315.

Mansoor, T.A., Borralho, P.M., Dewanjee, S., Mulhovo, S., Rodrigues, C.M., Ferreira, M.-J.U., 2013. Monoterpene bisindole alkaloids, from the African medicinal plant *Tabernaemontana elegans*, induce apoptosis in HCT116 human colon carcinoma cells. Journal of Ethnopharmacology 149, 463–470.

Mansoor, T.A., Ramalho, R.M., Mulhovo, S., Rodrigues, C.M.P., Ferreira, M.-J.U., 2009. Induction of apoptosis in HuH-7 cancer cells by monoterpene and β-carboline indole alkaloids isolated from the leaves of *Tabernaemontana elegans*. Bioorganic and Medicinal Chemistry Letters 19, 4255–4258.

Marathe, N., Rasane, M., Kumar, H., A Patwardhan, A., Shouche, Y.S., Diwanay, S.S., 2013. *In vitro* antibacterial activity of *Tabernaemontana alternifolia* (Roxb) stem bark aqueous extracts against clinical isolates of methicillin resistant *Staphylococcus aureus*. Annals of Clinical Microbiology and Antimicrobials 12, 26.

Marinho, F.F., Simões, A.O., Barcellos, T., Moura, S., 2016. Brazilian *Tabernaemontana* genus: Indole alkaloids and phytochemical activities. Fitoterapia 114, 127–137.

Marques, J.I., Alves, J.S.F., Torres-Rêgo, M., Furtado, A.A., Siqueira, E.M.D.S., Galinari, E., Araújo, D.F.D.S., Guerra, G.C.B., Azevedo, E.P.D., Fernandes-Pedrosa, M.D.F., Zucolotto, S.M., 2018. Phytochemical analysis by HPLC–HRESI-MS and anti-inflammatory activity of *Tabernaemontana catharinensis*. International Journal of Molecular Sciences 19, 1–19.

Mazen, A.M., Zhang, D., Franceschi, V.R., 2004. Calcium oxalate formation *in Lemna minor*: physiological and ultrastructural aspects of high-capacity calcium sequestration. New phytologist 161, 435–448.

McGaw, L.J., Jäger, A.K., Van Staden, J., 2000. Antibacterial, anthelmintic and anti-amoebic activity in South African medicinal plants. Journal of Ethnopharmacology 72, 247–263.

Medeiros, M.R.F., de Melo Prado, L.A., Fernandes, V.C., Figueiredo, S.S., Coppede, J., Martins, J., Fiori, G.M.L., Martinez-Rossi, N.M., Beleboni, R.O., Contini, S.H.T., Pereira, P.S., 2011. Antimicrobial activities of indole alkaloids from *Tabernaemontana catharinensis*. Natural product communications 6, 1934578X1100600209.

Medeiros, W.L.B., Vieira, I.J.C., Mathias, L., Braz-Filho, R., Schripsema, J., 2001. A new natural auaternary indole slkaloid isolated from *Tabernaemontana laeta* Mart. (Apocynaceae). Journal of the Brazilian Chemical Society 12, 368–372.

Mehrbod, P., Abdalla, M.A., Njoya, E.M., Ahmed, A.S., Fotouhi, F., Farahmand, B., Gado, D.A., Tabatabaian, M., Fasanmi, O.G., Eloff, J.N., McGaw, L.J., 2018. South African medicinal plant extracts active against influenza A virus. BMC Complementary and Alternative Medicine 18, 112–121.

Meschini, S., Marra, M., Calcabrini, A., Federici, E., Galeffi, C., Arancia, G., 2003. Voacamine, a bisindolic alkaloid from *Peschiera fuchsiaefolia*, enhances the cytotoxic effect of doxorubicin on multidrug-resistant tumor cells. International Journal of Oncology 23, 1505–1513.

Mittal, A.K., Chisti, Y., Banerjee, U.C., 2013. Synthesis of metallic nanoparticles using plant extracts. Biotechnological Advances 31, 346–356.

Moghadamtousi, Z.S., Kadir, A.H., Hassandarvish, P., Tajik, H., Abubakar, S., Zandi, K., 2014. A review on antibacterial, antiviral, and antifungal activity of curcumin. BioMed Research International 2014, 1–12.

Mohamad, S., Zin, N.M., Wahab, H.A., Ibrahim, P., Sulaiman, S.F., Zahariluddin, A.S.M., Noor, S.S.M., 2011. Antituberculosis potential of some ethnobotanically selected Malaysian plants. Journal of Ethnopharmacology 133, 1021–1026.

Molano-Flores, B., 2001. Herbivory and calcium concentrations affect calcium oxalate crystal formation in leaves of *Sida* (Malvaceae). Annals of Botany 88, 387–391.

Monnerat, C.S., De Souza, J.J., Mathias, L., Braz-Filho, R., Vieira, I.J.C, 2005. A new indole alkaloid isolated from *Tabernaemontana hystrix* steud (Apocynaceae). Journal of the Brazilian Chemical Society 16, 1331–1335.

Mueller, M.O., Janngeon, K., Puttipan, R.I., Unger, F.M., Viernstein, H., Okonogi, S.I., 2015. Anti-inflammatory, antibacterial and antioxidant activities of Thai medicinal plants. International Journal of Pharmacy and Pharmaceutical Sciences 7, 123–128.

Mukherjee, P.K., Kumar, V., Mal., Houghton, P.J., 2007. Acetylcholinesterase inhibitors from plants. Phytomedicine 14, 289-300.

Munayi, R.R., 2016. Phytochemical investigation of *Bridelia micrantha* and *Tabernaemontana ventricosa* for cytotoxic principles against drug sensitive leukemia cell ines (Doctoral dissertation, Master's Thesis, University of Nairobi, Nairobi, Kenya.

Naidoo, G., Kaliamoorthy, S., Naidoo, Y., 2009. The secretory apparatus of *Xerophytaviscosa* (*Velloziaceae*): Epidermis anatomy and chemical composition of the secretory product. Flora-Morphology, Distribution, Functional Ecology of Plants 204, 561–568.

Nakata, P.A., 2003. Advances in our understanding of calcium oxalate crystal formation and function in plants. Plant Science 164, 901–909.

Nakdook, W., Khongsombat, O., Taepavarapruk, P., Taepavarapruk, N., Ingkaninan, K., 2010. The effects of *Tabernaemontana divaricata* root extract on amyloid β-peptide 25–35 peptides induced cognitive deficits in mice. Journal of Ethnopharmacology 130, 122–126.

Nandagoapalan, V., Doss, A., Marimuthu, C., 2016. Phytochemical analysis of some traditional medicinal plants. Bioscience Discovery 7, 17–20.

Nazar, N., Goyder, D.J., Clarkson, J.J., Mahmood, T., Chase, M.W., 2013. The taxonomy and systematics of Apocynaceae: Where we stand in 2012. Botanical Journal of the Linnean Society 171, 482–490.

Ncube, N.S., Afolayan, A.J., Okoh, A.I., 2008. Assessment techniques of antimicrobial properties of natural compounds of plant origin: current methods and future trends. African Journal of Biotechnology 7, 1797–1806.

Ndongo, J.T., Mbing, J.N., Tala, M.F., Monteillier, A., Pegnyemb, D.E., Cuendet, M., Laatsch, H., 2017. Indoline alkaloids from *Tabernaemontana contorta* with cancer chemopreventive activity. Phytochemistry 144, 189–196.

Negi, B., Poonan, P., Ansari, M.F., Kumar, D., Aggarwal, S., Singh, R., Azam, A., Rawat, D.S., 2018. Synthesis, antiamoebic activity and docking studies of metronidazole-triazole-styryl hybrids. European Journal of Medicinal Chemistry 150, 633–641.

Nessler, C.L., Mahlberg, P.G., 1981. Cytochemical localisation of cellulase activity in articulated anastomosing laticifers of *Papaver somniferum* L. (Papaveraceae). American Journal of Botany 68, 730–732.

Neuwinger, H.D.,1666. African Traditional Medicine, first ed. Medpharm Scientific Publishers.

Nicola, C., Salvador, M., Escalona Gower, A., Moura, S., Echeverrigaray, S., 2013. Chemical constituent's antioxidant and anti-cholinesterasic activity of *Tabernaemontana catharinensis*. The Scientific World Journal 2013, 1–10.

Niemann, C., Kessel, J.W., 1996. The Isolation of Rupicoline and Montanine, Two Pseudoindoxyl Alkaloids of *Tabernaemontana Rupicola* Benth. Journal Organic Chemistry 31, 2265–2269.

Nobili, S., Lippi, D., Witort, E., Donnini, M., Bausi, L., Mini, E. and Capaccioli, S., 2009. Natural compounds for cancer treatment and prevention. Pharmacological Research 59, 365–378.

Núñez, V., Otero, R., Barona, J., Fonnegra, R., Jiménez, S., Osorio, R.G., Quintana, J.C., Díaz, A., 2004. Inhibition of the Toxic Effects of *Lachesis muta*, *Crotalus durissus cumanensis* and *Micrurus mipartitus* Snake Venoms by Plant Extracts. Pharmaceutical Biology 42, 49–54.

Ohishi, K., Toume, K., Arai, M.A., Sadhu, S.K., Ahmed, F., Ishibashi, M., 2015. Coronaridine, an iboga type alkaloid from *Tabernaemontana divaricata*, inhibits the Wnt signaling pathway by decreasing β-catenin mRNA expression. Bioorganic and Medicinal Chemistry Letters 25, 3937–3940.

Okuyama, E., Gao, L.-H., Yamazaki, M., 1992. Analgesic Components from Bornean Medicinal Plants, *Tabernaemontana pauciflora* Blume and *Tabernaemontana pandacaqui* POIR. Chemical and Pharmaceutical Bulletin 40, 2075–2079.

Ong, H.C., Chua, S., Milow, P., 2011. Ethno-medicinal plants used by the Temuan villagers in Kampung Jeram Kedah, Negeri Sembilan, Malaysia. Studies on Ethno-Medicine 5, 95–100.

Pallant, C., Steenkamp, V., 2009. *In-vitro* bioactivity of Venda medicinal plants used in the treatment of respiratory conditions. Human and Experimental Toxicology 27, 859–866.

Pallant, C.A., Cromarty, A.D., Steenkamp, V., 2012. Effect of an alkaloidal fraction of *Tabernaemontana elegans* (Stapf.) on selected micro-organisms. Journal of Ethnopharmacology 140, 398–404.

Parekh, J., Chanda, S., 2007. Anti-bacterial and phytochemical studies on twelve species of Indian medicinal plants. African Journal of Biomedical Research 10, 175–181.

Pavela, R., 2015. Essential oils for the development of eco-friendly mosquito larvicides: a review. Industrial crops and products 76, 174–187.

Pereira, C.G., Leal, P.F., Sato, D.N., Meireles, M.A. SFE of pharmacological compounds from *Tabernaemontana catharinensis*: Analysis of the antioxidant and antimycobacterial activities. In Proceedings of the 6th International Symposium on Supercritical Fluids, Versailles, France, 28–30 April 2003.

Pereira, C.G., Marques, M.O.M., Barreto, A.S., Siani, A.C., Fernandes, E.C., Meireles, M.A.A, 2004. Extraction of indole alkaloids from *Tabernaemontana catharinensis* using supercritical CO^{2+}ethanol: An evaluation of the process variables and the raw material origin. Journal of Supercritical Fluids 30, 51–61.

Pereira, D.M., Ferreres, F., Oliveira, J.M., Gaspar, L., Faria, J., Valentão, P., Sottomayor, M., Andrade, P.B., 2010. Pharmacological effects of *Catharanthus roseus* root alkaloids in acetylcholinesterase inhibition and cholinergic neurotransmission. Phytomedicine 17, 646–652.

Pereira, P.S., França, S.D.C., Oliveira, P.V.A.D., Breves, C.M.D.S., Pereira, S.I.V., Sampaio, S.V., Nomizo, A., Dias, D.A., 2008. Chemical constituents from *Tabernaemontana catharinensis* root bark: A brief NMR review of indole alkaloids and *in vitro* cytotoxicity. Química Nova 31, 20–24.

Perera, P., Kanjanapoothi, D., Sandberg, F., Verpoorte, R., 1984. Screening for biological activity of different plant parts of *Tabernaemontana dichotoma*, known as divi kaduru in Sri Lanka. Journal of Ethnopharmacology 11, 233–241.

Perera, P., Sandberg, F., Van Beek, T., Verpoorte, R., 1985. Alkaloids of stem and rootbark of *Tabernaemontana dichotoma*. Phytochemistry 24, 2097–2104.

Perera, P., Van Beek T. A., Verpoorte R., 1983. Dichomine, a novel type of iboga alkaloid. Planta Medica 49, 232–235.

Pergher, D., Picolotto, A., Rosales, P.F., Machado, K.G., Cerbaro, A.F., França, R.T., Salvador, M., Roesch-Ely, M., Tasso, L., Figueiredo, J.G., 2019. Antinociceptive and antioxidant effects of extract enriched with active indole alkaloids from leaves of *Tabernaemontana catharinensis* A. DC. Journal of Ethnopharmacology 239, 111863.

Piana, M., Boligon, A.A., De Brum, T.F., Zadra, M., Belke, B.V., Froeder, A.L., Frohlich, J.K., Nunes, L.T., Pappis, L., Boligon, A.A., 2014. Phytochemical analysis and antioxidant capacity of *Tabernaemontana catharinensis* A. DC. Fruits and branches. Anais da Academia Brasileira de Ciências 86, 881–888.

Pickard, W.F., 2008. Laticifers and secretory ducts: Two other tube systems in plants. New Phytologist 177, 877–888.

Poornima, K., Gopalakrishnan, V.K., 2014. Anticancer activity of *Tabernaemontana coronaria* against carcinogen induced clear cell renal cell carcinoma. Chinese Journal of Biology 2014, 1–8.

Potgieter, K., Albert, V.A., 2001. Phylogenetic relationships within Apocynaceae *s.l.* based on trnL intron and trnL-F spacer sequences and propagule characters. Annals of the Missouri Botanical Gardens 88, 523–549.

Pratchayasakul, W., Pongchaidecha, A., Chattipakorn, N., Chattipakorn, S., 2008. Ethnobotany & ethnopharmacology of *Tabernaemontana divaricata*. Indian Journal of Medical Research 127, 317–335.

Pushpa, B., Latha, K.P., Vaidya, V.P., Shruthi, A., Shweath, C., 2011. *In vitro* anthelmintic activity of leaves extracts of *Tabernaemontana coronaria*. International Journal of ChemTech. Research 3, 1788–1790.

Radhika, B., 2017. Comparitive study of soxhlation and maceration extracts of *Tabernaemontana divaricta* leaves for antibacterial activity. Journal of Natural Products and Plant Resources 7, 34–39.

Rahmatullah, M., Kabir, A.A.B.T., Rahman, M.M., Hossan, M.S., Khatun, Z., Khatun, M.A., Jahan, R., 2010. Ethnomedicinal practices among a minority group of Christians residing in Mirzapur village of Dinajpur District, Bangladesh. Advances in Natural and Applied Sciences 4, 45–51.

Raja, A., AshokKumar, S., Marthandam, R.P., Jayachandiran, J., Khatiwada, C.P., Kaviyarasu, K., Raman, R.G., Swaminathan, M., 2018. Eco-friendly preparation of zinc oxide nanoparticles using *Tabernaemontana divaricata* and its photocatalytic and antimicrobial activity. Journal of Photochemistry and Photobiology B Biology 181, 53–58.

Raja, V.J., Lim, K.-H., Leong, C.-O., Kam, T.-S., Bradshaw, T.D., 2014. Novel antitumour indole alkaloid, Jerantinine A, evokes potent G2/M cell cycle arrest targeting microtubules. Investigational New Drugs 32, 838–850.

Rakkimuthu, R., Nithiyakamatchi, R., Sathishkumar, P., Ananda Kumar, A.M., Sowmiya, D., 2019. *In vitro* antifungal activity of formulated floral extracts against *malassezia furfur*. International Journal of Analytical and Experimental Modal Analysis 6, 1–10.

Ramos, D.F., Leitão, G.G., Costa, F.D.N., Abreu, L., Villarreal, J.V., Leitão, S.G., Fernández, S.L.S.Y., Da Silva, P.E.A., 2008. Investigation of the antimycobacterial activity of 36 plant extracts from the brazilian Atlantic Forest Revista Brasileira de Ciências Farmacêuticas 44, 669–674.

Ranjan, N., Kumari, M., 2017.Acetylcholinesterase inhibition by medicinal plants: A Review. Annals of Plant Sciences 6, 1640–1644.

Rapini, A., 2012. Taxonomy" under construction": Advances in the systematics of Apocynaceae, with emphasis on the Brazilian Asclepiadoideae. Rodriguésia 63, 075–088.

Rapini, A., Chase, M.W., Goyder, D.J., Griffiths, J., 2003. Asclepiadeae classification: Evaluating the phylogenetic relationships of New World Asclepiadoideae (Apocynaceae). Taxon 52, 33–50.

Rapini, A., Van den Berg, C., Liede-Schumann, S., 2007. Diversification of Asclepiadoideae (Apocynaceae) in the new world 1. Annals of the Missouri Botanical Garden 94, 407–422.

Rashid, R., Sharma, M., Wani, M.H., 2018. Anti-inflammatory activity of medicinal plants native to Jammu and Kashmir: A review. Journal of Pharmaceutical Innovation 7, 279–281.

Rastogi K., Kapil R. S., Popli S. P., 1980. New alkaloids from *Tabernaemontana divaricata*. Phytochemistry 19, 1209–1212.

Rastogi, N., Abaul, J., Goh, K.S., Devallois, A., Philogène, E., Bourgeois, P., 1998. Antimycobacterial activity of chemically defined natural substances from the Caribbean flora in Guadeloupe. FEMS Immunology and Medical Microbiology 20, 267–273.

Rates, S.M.K., Schapoval, E.E.S., Souza, L., Henriques, A.T., 1993. Chemical constituents and pharmacological activities of *Peschieraaustralis*. International Journal of Pharmacognosy 31, 288–294.

Rathod, N.R., Chitme, H.R., Irchhaiya, R., Chandra, R., 2011. Hypoglycemic effect of *Calotropis gigantea* Linn. leaves and flowers in streptozotocin-induced diabetic rats. Oman Medical Journal 26, 104–108.

Raut, J.S., Karuppayil, S.M., 2014. A status review on the medicinal properties of essential oils. Industrial Crops and Products 62, 250–264.

Rawa, M.S.A., Hassan, Z., Murugaiyah, V., Nogawa, T., Wahab, H.A., 2019. Anti-cholinesterase potential of diverse botanical families from Malaysia: Evaluation of crude extracts and fractions from liquid-liquid extraction and acid-base fractionation. Journal of Ethnopharmacology 245, 1–17.

Reddy, L.A.L.I.N.I., Odhav, B., Bhoola, K.D., 2003. Natural products for cancer prevention: A global perspective. Pharmacology and therapeutics 99, 1–13.

Regnault-Roger, C., Vincent, C., Arnason, J.T., 2012. Essential oils in insect control: Low-risk products in a high-stakes world. Annual review of entomology 57, 405–424.

Rizo, W.F., Ferreira, L.E., Colnaghi, V., Martins, J.S., Franchi, L.P., Takahashi, C.S., Beleboni, R.O., Marins, M., Pereira, P.S., Fachin, A.L., 2013. Cytotoxicity and genotoxicity of coronaridine from *Tabernaemontana catharinensis* A.DC in a human laryngeal epithelial carcinoma cell line (Hep-2). Genetics and Molecular Biology 36, 105–110.

Rosales, P.F., Gower, A., Benitez, M.L.R., Pacheco, B.S., Segatto, N.V., Roesch-Ely, M., Collares, T., Seixas, F.K., Moura, S., 2019b. Extraction, isolation and *in vitro* evaluation of affinisine from *Tabernaemontana catharinensis* in human melanoma cells. Bioorganic Chemistry 90, 103079.

Rosales, P.F., Marinho, F.F., Gower, A., Chiarello, M., Canci, B., Roesch-Ely, M., Paula, F.R., Moura, S., 2019a. Bio-guided search of active indole alkaloids from *Tabernaemontana catharinensis*: Antitumour activity, toxicity in silico and molecular modelling studies. Bioorganic hemistry 85, 66–74.

Rumzhum, N.N., Rahman, M.M., Kazal, M.K., 2012. Antioxidant and cytotoxic potential of methanol extract of *Tabernaemontana divaricata* leaves. International Current Pharmaceutical Journal 1, 27–31.

Ruttoh, E., Tarus, P., Bii, C., Machocho, A., Karimi, L., Okemo, P., 2009b. Antibacterial activity of *Tabernaemontana stapfiana* Britten (apocynaceae) extracts. African Journal of Traditional and Complementary Alternative Medicine 6, 186.

Ruttoh, E.K., Bii, C., Tarus, P.K., Machocho, A., Karimi, L.K., Okemo, P., 2009a. Antifungal activity of *Tabernaemontana stapfiana* Britten (Apocynaceae) organic extracts. Pharmacognosy Research 1, 387.

Safavi, K., 2012. Evaluation of using nanomaterial in tissue culture media and biological activity. Second International Conference on Ecological, Environmental and Biological, Sciences. October 13–14.

Santhi, R., Annapurani, S., 2020. Preliminary evaluation of *In vitro* and *In vivo* antioxidative and antitumor activities of flavonoid extract of *Tabernaemontana divaricata* leaves in Ehrlich's lymphoma and Dalton's lymphoma ascites model. Journal of Cancer Research Therapy 16, 78–87.

Šantić, Ž., Pravdić, N., Bevanda, M., Galić, K., 2017. The historical use of medicinal plants in traditional and scientific medicine. Psychiatria Danubina 29, 787–792.

Santos, A.K., Magalhaes, T.S., Monte, F.J., Mattos, M.C., Oliveira, M.C., Almeida, M.M., Lemos, T.L., Braz-Filho, R., 2009. Iboga alkaloids from *Peschier aaffinis* (Apocynaceae)-unequivocal 1H and 13C chemical shift assignments: Antioxidant activity. Química Nova 32, 1834–1838.

Santos, A.K.L., Machado, L.L., Bizerra, A.M.C., Monte, F.J.Q., Santiago, G.M.P., Braz-Filho, R., Lemos, T.L.G., 2012. New Indole Alkaloid from *Peschiera affinis* (Apocynaceae). Natural Product Communications 7, 729–30.

Sari, R., Conterno, P., Da Silva, L.D., De Lima, V.A., Oldoni, T.L.C., Thomé, G.R., Carpes, S., 2020. Extraction of Phenolic Compounds from *Tabernaemontana catharinensis* Leaves and Their Effect on Oxidative Stress Markers in Diabetic Rats. Molecules 25, 2391.

Satapathy, R., Beura, S., 2018. Management of *Colletotrichum gloeosporioides* (Penz.) Causing Cashew Anthracnose through Botanicals. International Journal of Current Microbiology Applied Sciences 7, 3539–3543.

Sathishkumar, T., Baskar R., 2012. Evaluation of antioxidant properties of *Tabernaemontana heyneana* Wall. leaves. Indian Journal of Natural Product Resources 3, 197–207.

Schmelzer, G.B., Gurib-Fakim, A., 2008. Medicinal Plants, first ed. Plant Resources of Tropical Africa 11,1. PROTA Foundation. Backhuys Publishers, Wageningen, Netherlands.

Schmidt, E., Lotter, M., McCleland, W., 2002. Trees and Shrubs of Mpumalanga and Kruger National park. Jacana Media: Johannesburg, South Africa.

Selvakumar, S., Kumar, A., 2015. Antiproliferative efficacy of *Tabernaemontana divaricata* against HEP2 cell line and Vero cell line. Pharmacognosy Magazine 11, 46–52.

Sennblad, B., Bremer, B., 2000. Is there a justification for differential a priori weighting in coding sequences? A case study from rbcL and Apocynaceae. Systematic Biology 49, 101–113.

Sennblad, B., Endress, M.E., Bremer, B., 1998. Morphology and molecular data in phylogenetic fraternity the tribe Wrightieae (Apocynaceae) revisited. American Journal of Botany 85, 1143–1158.

Shaker, I.A., Inampudi, S., Rayapu, V., 2012. Antimicrobial activity assay of *Tabernaemontana coronaria*. International Journal of Bioassays (IJB) 1, 4–5.

Shakya, A.K., 2016. Medicinal plants: future source of new drugs. International Journal of Herbal Medicine 4, 59–64.

Sharma, P., Sharma, J.D., 2001. A review of plant species assessed *in vitro* for antiamoebic activity or both antiamoebic and antiplasmodial properties. Phytotherapy Research: An International Journal Devoted to Pharmacological and Toxicological Evaluation of Natural Product Derivatives 15, 1–17.

Shori, A.B., 2015. Screening of antidiabetic and antioxidant activities of medicinal plants. Journal of integrative medicine 13, 297–305.

Shrestha, P., Adhikari, S., Lamichhane, B., Shrestha, B.G., 2015. Phytochemical screening of the medicinal plants of Nepal. IOSR Journal of Environmental Science, Toxicology and Food Technology 1, 11–17.

Shrikanth, V.M., Janardhan, B., Dhananjaya, B.L., Muddapura, U.M., More, S.S., 2015. Antimicrobial and antioxidant activity of methanolic root extract of *Tabernaemontana alternifolia* L. International Journal of Pharmacy and Pharmaceutical Sciences 7, 66–69.

Sigamoney, M., Shaik, S., Govender, P., Krishna, S.B.N., 2016. African leafy vegetables as bio-factories for silver nanoparticles: A case study on *Amaranthus dubius* C Mart. Ex Thell. South African Journal of Botany 103, 230–240.

Silveira, D., de Melo, A.F., Magalhães, P.O., Fonseca-Bazzo, Y.M., 2017. *Tabernaemontana* Species: Promising sources of new useful drugs. Studies in Natural Products Chemistry. Elsevier 54, 227–289.

Sim, D.S.-Y., Chong, K.-W., Nge, C.-E., Low, Y.-Y., Sim, K.-S., Kam, T.-S., 2014. Cytotoxic vobasine, tacaman, and corynanthe-tryptamine bisindole alkaloids from *Tabernaemontana* and structure revision of tronoharine. Journal of Natural Products 77, 2504–2512.

Simões, A.O., Endress, M.E., Conti, E., 2010. Systematics and character evolution of *Tabernaemontaneae* (Apocynaceae, Rauvolfioideae) based on molecular and morphological evidence. Taxon 59,772–790.

Singh, A.K., 2016. Structure, synthesis, and application of nanoparticles engineered nanoparticles. Elsevier.

Singh, B., Sharma, A.R., Vyas, K.G., 2011. Anti-microbial, ant-ineoplastic and cytotoxic activities of indole alkaloids from *Tabernaemontana divaricata* (L.) R. Br. Current Pharmaceutical Analysis 7, 125–132.

Singh, M.K., Usha, R., Hithayshree, K.R., Sukumaran, B.O., 2015. Hemostatic potential of latex proteases from *Tabernaemontana divaricata* (L.) R. Br. ex. Roem. and Schult. and *Artocarpus altilis* (Parkinson ex. F.A. Zorn) Forsberg. Journal of Thrombosis and Thrombolysis 39, 43–49.

Singh, S., Bharti, N., Mohapatra, P.P., 2009. Chemistry and biology of synthetic and naturally occurring antiamoebic agents. Chemical reviews 109, 1900–1947.

Spitzer, V., Rates, S.M.K., Henriques, A.T., Marx, F., 1995. The Fatty Acid Composition of the Seed Oil of *Peschiera australis* (Apocynaceae). Fette Seifen Anstrichmittel 97, 334–335

Steenkamp, V., Fernandes, A.C., Van Rensburg, C.E.J., 2007. Screening of Venda medicinal plants for anti-fungal activity against *Candida albicans*. South African Journal of Botany 73, 256–258.

Sudarshan, V.K., Mookiah, M.R.K., Acharya, U.R., Chandran, V., Molinari, F., Fujita, H., Ng, K.H., 2016. Application of wavelet techniques for cancer diagnosis using ultrasound images: A review. Computers in biology and medicine 69, 97–111.

Suffredini, I.B., Bacchi, E.M., Sakuda, T.M.K., Ohara, M.T., Younes, R.N., Varella, A.D., 2002. Antibacterial activity of Apocynaceae extracts and MIC of *Tabernaemontana angulata* stem organic extract. Revista Brasileira de Ciências Farmacêuticas 38, 89–94.

Suganthy, N., Pandian, S.K., Devi, K.P., 2009. Cholinesterase inhibitors from plants: Possible treatment strategy for neurological disorders-a review. International Journal of Biomedicine and Pharmaceutical Sciences 3, 87-103.

Sumitha, J., Padmalatha, C., Singh, A.R., 2015. Antibacterial efficacy of *Moringa oleifera* and *Tabernaemontana divaricata* flower extracts on occular pathogens. International Journal of Current Microbiology and Applied Sciences 4, 203–216.

Taesotikul, T., Panthong, A., Kanjanapothi, D., Verpoorte, R., Scheffer, J.J.C., 2003. Anti-inflammatory, antipyretic and antinociceptive activities of *Tabernaemontana pandacaqui* Poir. Journal of Ethnopharmacology 84, 31–35.

Tamokou, J. D., Kuete, V., 2014. Mutagenicity and carcinogenicity of African medicinal plants. Toxicological Survey of African Medicinal Plants 1, 277–322.

Tan, B.L., Norhaizan, M.E., Liew, W.P.P., Sulaiman Rahman, H., 2018. Antioxidant and oxidative stress: A mutual interplay in age-related diseases. Frontiers in pharmacology 9, 1162.

Thakkar, K.N., Mhatre, S.S., Parikh, R.Y., 2010. Biological synthesis of metallic nanoparticles. Nanomedicine: Nanotechnology, Biology and Medicine 6, 257–262.

Thind, T.S., Agrawal, S.K., Saxena, A.K., Arora, S., 2008. Studies on cytotoxic, hydroxyl radical scavenging and topoisomerase inhibitory activities of extracts of *Tabernaemontana divaricata* (L.) R. Br. ex Roem. and Schult. Food and Chemical Toxicology 46, 2922–2927.

Thomas, V., 1991. Structural, functional and phylogenetic aspects of the colleter. Annals of Botany 68, 287–305.

Thombre, R., Jagtap, R., Patil, N., 2013. Evaluation of phytoconstituents, antibacterial, antioxidant and cytotoxic activity of *Vitex negundo* L. and *Tabernaemontana divaricata* L. International Journal of Pharma and Bio Sciences 4, 389–396.

Tillman-Sutela, E., Kauppi, A., 1999. Calcium oxalate crystals in the mature seeds of Norway spruce, *Picea abies* (L.) Karst. Trees 13, 131–137.

Toghueo, R.M.K., Boyom, F.F., 2019. Endophytes from ethno-pharmacological plants: Sources of novel antioxidants-A systematic review. Biocatalysis and Agricultural Biotechnology 101430, 1–50.

Turner, G.W., Berry, B.M., Gifford, E.M., 1998. Schizogenous secretory cavities of *Citrus limon* (L.) Burm. F. and a reevaluation of the lysigenous gland concept. International Journal of Plant Science 159, 75–88.

Twilley, D., Langhansová, L., Palaniswamy, D., Lall, N., 2017. Evaluation of traditionally used medicinal plants for anticancer, antioxidant, anti-inflammatory and anti-viral (HPV-1) activity. South African Journal of Botany 112, 494–500.

Uwumarongie, H.O., Onwukaeme, D.N., Bafor, E.E., 2008. Antiulcer effects and elements of *Tabernaemontana pachysiphon* stem bark. Nigerian Journal of Pharmaceutical Research 7, 69–75.

Uwumarongie, O.H., Onwukaeme, D.N., Obasuyi, O., 2007. Antimicrobial activity of the methanolic leaf extract of *Tabernaemontana pachysiphon* stapf (Apocynaceae). Nigerian Journal of Natural Products and Medicine 11, 23–25.

Van Beek, T., Deelder, A., Verpoorte, R., Svendsen, A., 1984a. Antimicrobial, antiamoebic and antiviral screening of some *Tabernaemontana* species. Planta Medica 50, 180–185.

Van Beek, T.A., De Smidt, C., Verpoorte, R., 1985. Phytochemical investigation of *Tabernaemontana crassa*. Journal of Ethnopharmacology 14, 315–318.

Van Beek, T.A., Verpoorte, R., Svendsen, A.B., Leeuwenberg, A.J.M., Bisset, N.G., 1984b. *Tabernaemontana* L. (Apocynaceae): A review of its taxonomy, phytochemistry, ethnobotany and pharmacology. Journal of Ethnopharmacology 10, 1–156.

Van der Heijden R, Brouwer RL, Verpoorte R.,1986. Indole alkaloids from *Tabernaemontana elegans*. Planta Medica 2, 144–7.

Van Die, J., 1955. A comparative study of the particle fractions from Apocynaceae latices. Annals of Botanic Gardens 2, 1–124.

Venkatachalapathi, S., Saranya, C., Ravi, S., 2014. Isolation and characterization of Bio active compounds from *Tabernaemontana divaricata* and a study of its antioxidant and antibacterial activity. Indo American Journal of Pharmaceutical Research 4, 2401–2406.

Vieira, I.J., Medeiros, W.L., Monnerat, C.S., Souza, J.J., Mathias, L., Braz-Filho, R., Pinto, A.C., Sousa, P.M., Rezende, C.M., Epifanio, R.D.A., 2008. Two fast screening methods (GC-MS and TLC-ChEI assay) for rapid evaluation of potential anticholinesterasic indole alkaloids in complex mixtures. Anais da Academia Brasileira de Ciências 80, 419–426.

Vineetha, M., Bhavya, J., Veena, S., Mirajkar, K.K., Muddapur, U., Ananthraju, K., Zameer, F., More, S.S., 2020. *In vitro* and *in vivo* inhibitory effects of *Tabernaemontana alternifolia* against *Naja naja* venom. Saudi Pharmaceutical Journal 28, 692–697.

Vineetha, M.S., Bhavya, J., More, S.S., 2019. Inhibition of pharmacological and toxic effects of *Echiscarinatus* venom by *Tabernaemontana alternifolia* root extract. Indian Journal of Natural Product Research 10, 48–58.

Voticky, Z., Jahodar, L., Cava, M.P.,1997. Alkaloids from *Peschiera laeta* MART. Collect. Czechoslov. Chemical Communications 42, 1403–1406.

Wang, M., Mei, W., Deng, Y., Liu, S., Wang, Z., Dai, H., 2008. Cytotoxic cardenolides from the roots of *Calotropis gigantea*. Modern Pharmaceutical Research 1, 4–9.

Wankhede, S.B., Routh, M.M., Rajput, S.B., Karuppayil, S.M., 2013. Antifungal properties of selected plants of Apocynaceae family against the human fungal pathogen *Candida albicans*. International Current Pharmaceutical Journal 2, 122–125.

Wasupongpun, W., Premkaisorn, P., 2010. Evaluation of antioxidant activity of eleven thai medicinal herbs. Science Journal 26, 29–38.

Watt, J.M., Breyer-Brandwijk, M.G., 1962. The medicinal and poisonous plants of Southern and Eastern Africa, second ed. London: Livingstone.

WHO, World Heath Organization, 2018.

Wijayabandara, M.D.J., Khan, S.N., Choudhary, M.I. Novel Alpha-Glucosidase Inhibitor from *Tabernaemontana dichotoma*. U.S. Patent Application No. 11/553,465, May 1, 2008.

Wise, R., Hart, T., Cars, O., Streulens, M., Helmuth, R., Huovinen, P., Sprenger, M., 1998. Antimicrobial resistance "Is a major threat to public health," British Medical Journal 317, 609–610.

Wolter Filho, W., Pinheiro, M.L.B., Rocha, A.I.,1983. Alcalóides de *Tabernaemontana heterophylla* Vahl (Apocynaceae). Acta Amazonica 13, 409–412.

World Heath Organization. Available online https://www.who.int/data/gho/data/themes/topics/topic-details/GHO/world-health-statistics (accessed on 17 September 2018).

Yang, H., Protiva, P., Gil, R.R., Jiang, B., Baggett, S., Basile, M.J., Reynertson, K.A., Weinstein, I.B., Kennelly, E.J., 2005. Antioxidant and cytotoxic isoprenylated coumarins from *Mammea americana*. Planta Medica 71, 852–860.

You, M., Ma, X., Mukherjee, R., Farnsworth, N.R., Cordell, G.A., Kinghorn, A.D., Pezzuto, J.M., 1994. Indole Alkaloids from *Peschiera laeta* That Enhance Vinblastine-Mediated Cytotoxicity with Multi-drug-Resistant Cells. Journal of Natural Products 57, 1517–1522.

Yuan, Y.-X., Zhang, Y., Guo, L.-L., Wang, Y.-H., Goto, M., Morris-Natschke, S.L., Lee, K.-H., Hao, X., 2017. Tabercorymines A and B, two vobasinyl–ibogan-type bisindole alkaloids from *Tabernaemontana corymbosa*. Organic Letters 19, 4964–4967.

Zacchino, S., Santecchia, C., Lopez, S., Gattuso, S., Muñoz, J.D.D., Cruañes, A., Vivot, E., Cruañes, M.D.C., Salinas, A., De Ruiz, R., 1998. *In vitro* antifungal evaluation and studies on mode of action of eight selected species from the Argentine flora. Phytomedicine 5, 389–395.

Zaima, K., Koga, I., Iwasawa, N., Hosoya, T., Hirasawa, Y., Kaneda, T., Ismail, I.S., Lajis, N.H., Morita, H., 2013. Vasorelaxant activity of indole alkaloids from *Tabernaemontana dichotoma*. Journal of Natural Medicine 67, 9–16.

Zhang, B.-J., Teng, X.-F., Bao, M.-F., Zhong, X.-H., Ni, L., Cai, X.-H., 2015c. Cytotoxic indole alkaloids from *Tabernaemontana officinalis*. Phytochemistry 120, 46–52.

Zhang, D.-B., Yu, D.-G., Sun, M., Zhu, X.-X., Yao, X.-J., Zhou, S.-Y., Chen, J.-J., Gao, K., 2015b. Ervatamines A–I, anti-inflammatory monoterpenoid indole alkaloids with diverse skeletons from *Ervatamia hainanensis*. Journal of Natural Products 78, 1253–1261.

Zhang, H.-R., Li, D., Cao, H., Lu, X., Chu, Y.-K., Bai, Y.-F., Jin, Y.-P., Peng, S., Dou, Z., Hua, J.-L., 2013. Conophylline promotes the proliferation of immortalized mesenchymal stem cells derived from fetal porcine pancreas (iPMSCs). Journal of Integrative Agriculture 12, 678–686.

Zhang, Y., Guo, L., Yang, G., Guo, F., Di, Y., Li, S., Chen, D., Hao, X.-J., 2015a. New vobasinyl-ibogan type bisindole alkaloids from *Tabernaemontana corymbosa*. Fitoterapia 100, 150–155.

Zhang, Y., Yuan, Y.-X., Goto, M., Guo, L.-L., Li, X.-N., Morris-Natschke, S.L., Lee, K.-H., Hao, X.-J., 2018. Taburnaemines A–I, Cytotoxic vobasinyl-iboga-type bisindole alkaloids from *Tabernaemontana corymbosa*. Journal of Natural Products 81, 562–571.

Zhou, S.Y., Zhou, T.L., Qiu, G., Huan, X., Miao, Z.H., Yang, S.P., Cao, S., Fan, F., Cai, Y.S., 2018. Three new cytotoxic monoterpenoid bisindole alkaloids from *Tabernaemontana bufalina*. Planta Medica 84, 1127–113.

Zhu, J.P., Guggisberg, A., Kalt-Hadamowsky, M., Hesse, M., 1990. Chemotaxonomic study of the genus *Tabernaemontana* (Apocynaceae) based on their indole alkaloid content. Plant Systematics and Evolution 172, 13–34.

Zhu, W.T., Zhao, Q., Huo, Z.-Q., Hao, X.J., Yang, M., Zhang, Y., 2020. Taberdivamines A and B, two new quaternary indole alkaloids from *Tabernaemontana divaricata*. Tetrahedron Letters 61, 152400.

Zulkefli, H.N., Mohamad, J., Abidin, N.Z., 2013. Antioxidant activity of methanol extract of *Tinospora crispa* and *Tabernaemontana corymbosa*. Sains Malaysiana 42, 697–706.

CHAPTER 3:

THE SECRETORY APPARATUS OF *TABERNAEMONTANA VENTRICOSA* HOCHST. EX A. DC. (APOCYNACEAE): LATICIFER IDENTIFICATION, CHARACTERIZATION AND DISTRIBUTION

Abstract

Due to the inconsistencies in the interpretation of laticifers within the Apocynaceae, the current study aimed to distinguish, for the first time, the type and distribution of the laticifers in the embryos, seedlings, and adult plants of *Tabernaemontana ventricosa* (Forest toad tree). The characterization and distribution of laticifers were determined using light and electron microscopy. The findings revealed the presence of articulated anastomosing laticifers. The laticifers were found to have originated from ground meristematic and procambium cells and were randomly distributed in all ground and vascular tissue, displaying complex branching conformations. The presence of chemical constituents within the laticifers and latex determined by histochemical analysis revealed the presence of alkaloids, phenolics, neutral lipids, terpenoids, mucilage, pectin, resin acids, carboxylated polysaccharides, lipophilic, and hydrophilic substances, and proteins. These secondary metabolites perform an indispensable role in preventing herbivory, hindering, and deterring microorganisms and may have medicinal importance. The outcomes of the present study outlined the first micromorphology, anatomy, ultrastructural and chemical analysis of the laticifers of *T. ventricosa*. In addition, this investigation similarly established the probable functions of latex and laticifers.

Keywords: Alkaloids; Anastomosing; Articulated; Latex; Laticifers.

3.1 Introduction

The occurrence of laticifers and latex has been observed in approximately 12 500 plant species representing 22 families (Evert, 2006; Castelblanque et al., 2016; Castelblanque et al, 2017). Latex is characterized as a sticky suspension of several particles containing sap of various plant metabolites (Dussourd et al., 1987; Bauer et al., 2014; Shih and Morgan, 2020). These naturally occurring secondary metabolites are formed from several constituents which are usually produced via primary and secondary metabolism (Tiwari et al., 2016; Shih and Morgan, 2020). Plant secondary metabolites can be divided into three chemically distinct groups: terpenoids, phenolics, and nitrogen/sulfur-containing compounds (Wink, 2010; Pott et al., 2019). These diverse secondary metabolites are essential for plant growth, development, interactions, and defence systems (Pott et al., 2019; Shih and Morgan, 2020).

Natural secondary products such as latex are comprised of a variety of composite chemical constituents which is often species dependent e.g., terpenoids (*Hevea brasiliensis*), alkaloids (*Papaver somniferum*), phenolic glucosides (*Cannabis sativa*), proteins (*Ficus callosa*), and tannins (*Musa*) (Esau, 1965). The occurrence of these chemical constituents could attribute to the appearance of latex as the colour varies in plant species and may appear milky white, yellow, orange, red, brown, or even colourless (Metcalfe, 1967; Pickard, 2008). Despite the extensive occurrence of latex-bearing plants in approximately 10% of flowering species, there remains insufficient information available concerning the characterization, distribution, and mechanisms of laticifers in numerous plants (Evert, 2006; Castelblanque et al., 2016; Castelblanque et al, 2017).

Laticifers are defined as highly specialized cells (or files of cells) and have been classified into two types: the articulated and non-articulated type (Fahn, 1979; Mahlberg, 1993; Hagel et al., 2008; Ramos et al., 2019). Articulated laticifers occur in both the primary and secondary bodies of a plant and are comprised of multiple interconnected simple cells (Fahn, 1979; Mahlberg, 1993; Hagel et al., 2008; Pickard, 2008; Ramos et al., 2019). These cells are distinguished as either nonanastomosing (unbranched) or anastomosing (branched) (Castelblanque et al., 2016; Castelblanque et al, 2017). Whereas non-articulated laticifers usually only arise in the primary bodies of plants, are multinucleate, and develop from a single coenocytic cell (Hagel et al., 2008; Pickard, 2008; Canaveze and Machado, 2016; Ramos et al., 2019). These cells may display one of two forms: unbranched vessels or branched networks (Krishnamurthy et al., 2013; Ramos et al., 2019).

It has been reported that non-articulated laticifers are an ancestral characteristic feature of Apocynaceae, which often occur in all vegetative and reproductive organs of the family however, articulated laticifers have also been observed in *Tabernaemontana catharinensis* (Demarco and Castro, 2008; Canaveze and Machado, 2015; Castelblanque et al., 2016; Castelblanque et al., 2017). *Tabernaemontana ventricosa*

Hochst. ex A. DC. (Leeuwenberg and Kupicha, 1985), belongs to the Apocynaceae and has a disjunctive geographical distribution in Eastern Nigeria, Ghana, the Democratic Republic of Congo, Kenya, and the northern and southern regions of South Africa (Schmelzer and Gurib-Fakim, 2008). The species occurs in open forests and thickets in woodlands and thrives in disturbed shady habitats (Schmidt et al., 2002). In KwaZulu-Natal, the bark stems and leaves of *T. ventricosa* are used in ethnomedicine to palliate fever, reduce high blood pressure, treat wounds, and heal sore eyes (Leeuwenberg and Kupicha, 1985; Schmelzer and Gurib-Fakim, 2008; Schmidt et al., 2002; Mehrbod et al., 2018). Limited studies are available on *T. ventricosa* (Leeuwenberg and Kupicha, 1985; Schmelzer and Gurib-Fakim, 2008; Schmidt et al., 2002; Mehrbod et al., 2018) and to our knowledge, there are no existing reports on the morphology, anatomy, histochemistry, and ultrastructure of the laticifers of this species.

Due to the challenging interpretation and uncertainties of laticifers in Apocynaeceae, this study was carried out to describe the type and distribution of laticifers in embryos, seedlings, and adult plants of *T. ventricosa*, as well as perform a chemical analysis of the laticifers and latex to identify its probable functions.

3.2 Materials and Methods

3.2.1 Collection of leaf and stem samples

Fully grown and adult *T. ventricosa* plants (~ 12-15 m) of wild origin were collected from the University of KwaZulu-Natal (Westville campus), South Africa (1). 29˚49′03.3″S 30˚56′32.7″E; (2). 29˚49'02.5"S30˚56'32.5"E; (3). 3.29˚49'04.6"S30˚56'43.9" E, from February 2017 through October 2018. Approximately 3 plants of *T. ventricosa* were sampled for analysis, with the leaves and stems sampled in triplicates, for each plant. The plant material was taxonomically identified, and a voucher specimen (18222) was deposited at the Ward herbarium, School of Life Sciences, University of KwaZulu-Natal.

The leaves were classified into three different developmental stages namely, emergent (<10 mm), young (10-60 mm), and mature (>60 mm). For the purpose of stem analysis, only young stems were used, as mature stems were hardy and problematic for further examination. In addition, mature embryos, and seedling stems of *T. ventricosa* were also studied. These specimens were acquired, by the collection of seeds from mature fruits of *T. ventricosa* growing in a sloped area (29˚49′03.3″S 30˚56′32.7″E) during 2017 and 2018.

Seeds (n = 32) of *T. ventricosa* were carefully nicked (0.1 cm) using a sterile blade and soaked for approximately 48 h in distilled water (Canaveze and Machado, 2016). Then, embryos were isolated from soaked seeds (n = 16). To obtain *T. ventricosa* seedlings, seeds (n = 16) were cultivated into trays containing vermiculite and maintained in a growth chamber under controlled light (12 h photoperiod)

and air temperature (24˚C). The trays were watered regularly till the seedling's emergence. After 20 days, the seedlings displayed two cotyledons, a stem (3 cm), and the main root (4 cm).

3.2.2 Stereomicroscopy

Fresh emergent, young, and mature leaf samples were used to analyze the adaxial and abaxial surfaces. Images were obtained using the Nikon AZ100 stereomicroscope equipped with a Nikon fiber Illuminator (Nikon, Japan).

3.2.3 Scanning Electron Microscopy (SEM)

3.2.3.1 Chemical fixation

Young and mature leaves and young stems of *T. ventricosa* were hand sectioned (± 5 mm²) and fixed for 24 h in 2.5% glutaraldehyde. The sections were washed with 0.1 M phosphate buffer (pH 7.2) and post-fixed in 0.5% osmium tetroxide for 2 h. Thereafter, the samples were washed with 0.1 M phosphate buffer and subjected to dehydration by graded concentrations of ethanol (30%, 50%, 75%, and 100%). The sections were mounted onto aluminum, stubs using double-sided adhesive carbon tape, and then critically point-dried using a Quorum K850 Critical Point Dryer, and sputter-coated with gold (*ca*. 25 nm) in a Quorum Q150 RES sputter coater. Samples were viewed with a scanning electron microscope Zeiss LEO 1450 (Zeiss, Germany) at a working distance of 14-17 mm (5.00 kV). Images were captured using SmartSEM image software.

3.2.3.2 Freeze-fracture

Fresh young leaves and stems were trimmed (± 5 mm²) and were quenched in liquid nitrogen slush (-210˚C), thereafter the sections were manually fractured using a blade. The fractured samples were freeze-dried in an Edward's Modulyo EPTD3 freeze-drier for 72 h. The freeze-dried samples were mounted onto aluminum stubs using carbon adhesive tape and the stubs were coated with gold (*ca*. 25 nm) in a Quorum 150 RES sputter coater. The samples were then analyzed using SmartSEM imaging software on the LEO 1450 (Zeiss, Germany) scanning electron microscope at a working distance of 14-17 mm (5.00 kV).

3.2.4 Transmission Electron Microscopy (TEM)

Fresh young leaf and stem sections (adult plants), embryos, and the seedling stems (± 2 mm^2) were fixed in 2.5% glutaraldehyde for 24 h. The sections were washed with 0.1 M phosphate buffer (pH 7.2), followed by post-fixation with 0.5% osmium tetroxide for 4 h. Thereafter, the samples were washed with 0.1 M phosphate buffer and dehydrated sequentially in 30%, 50%, 75%, and 100% acetone. The dehydrated samples were infiltrated with 25%, 50%, and 75% of a Spurr's resin and acetone mixture for 12 h, respectively. Thereafter, the samples were infiltrated in 100% resin for 24 h and then embedded in 100% resin using silicone moulds and polymerized at 70˚C in an oven for 8 h.

The resin block samples containing leaf and stem sections, embryos, and seedling stems were sectioned using the Leica EM UC7 ultra-microtome equipped with a glass knife that was processed using a Glass Knife Maker LKB 7801A. Serial survey sections (0.5-1 µM) containing leaf and stem sections, embryos, and seedling stems, respectively were placed onto slides, stained with Toluidine Blue, and imaged using the Nikon Eclipse 80i light compound microscope (Nikon, Japan). The areas of interest were observed using serial survey sections, thereafter, ultrathin leaf sections (100 nm) were cut and picked up using copper grids. Prior to viewing, the copper grids were stained by placing the sections on a large drop of 2.5% uranyl acetate. The sections were stained for 10 min at 23˚C and rinsed with fresh distilled water. The copper grids were then placed onto drops of lead citrate in a closed glass Petri dish with dry NaOH pellets (avoids the build-up of moisture which causes the stain to precipitate). The copper grids were stained for 10 min, rinsed with distilled water, and placed on filter paper to dry. The sections were analyzed, and images were captured using a 100 kV JEOL 1010 transmission electron microscope equipped with iTEM software (JEOL, USA).

3.2.5 Histochemistry

Fresh young and mature leaves, and young stems were used to obtain semi-thin sections (80-100 µM) for histochemical analysis. The material was sectioned using the Oxford® Vibratome sectioning system and the sections were stained with the following reagents to detect the presence and localization of chemical compounds. Toluidine Blue was used to test for the presence of carboxylated polysaccharides, phosphate groups, and polyphenols (O' Brien et al., 1964). The presence of lipids was detected with Sudan IV and Sudan Black B (Demarco, 2017). Lignin aldehydes and cuticle components were detected with Phloroglucinol (Demarco, 2017). Phenolic compounds and terpenoids were tested using Ferric chloride and Ferric trichoride (Johansen 1940; Demarco, 2017). Ruthenium red was used to test for the presence of mucilage and pectin (Demarco, 2017). Nile blue was used to detect neutral and acidic lipids (Demarco, 2017). Proteins, essential oils, and resin acids were tested using Mercuric bromophenol blue (Mazia et al., 1953) and NADI reagent (Demarco, 2017), respectively. Alkaloids were detected using

Wagner's and Dittmar's reagent (Furr and Mahlberg, 1981). Acidic components were detected using a double stain technique comprised of Safranin and Fast green (Periasamy, 1967). Each test was carried out in triplicates (3 leaves and stems were sectioned, and 3 sections were used from each sample), unstained sections served as the control and sections were imaged and captured on the Nikon Eclipse 80i light microscope (Nikon, Japan). The presence of phenolic compounds was also tested using autofluorescence (330 and 380 nm) (Ascensão and Pais, 1987).

3.2.6 Fluorescence microscopy

Semi-thin sections (80-100 μM) of young leaf and stem sections were viewed at various wavelengths and images were captured using the Nikon Eclipse 80i light microscope (Nikon, Japan). The sections were stained with Acridine orange and 0.01% Calcofluor white solution to detect the viability of cells and cellulose in cell walls, respectively (Demarco, 2017).

3.2.7 Whole-mount staining

Whole seedling leaves were fixed for 24 h at 4˚C in a solution of formalin, acetic acid, and ethanol (3.5:10:50). The samples were washed with 70% ethanol and stained with Sudan Black B (0.1%) in 70% ethanol for 3-4 h at 23˚C. The samples were rinsed with 70% ethanol, distilled water and thereafter placed in 2.5 M NaOH solution until the leaves were cleared (Demarco et al., 2013). The samples were mounted onto a slide and the entire leaf was examined using the NIS-Elements D imaging software. Images were captured on the Nikon Eclipse 80i light compound microscope (Nikon, Japan).

3.3 Results and Discussion

3.3.1 Leaf micromorphology

Stereomicrographs revealed that the leaves of *T. ventricosa* display glabrous, leathery, and shiny adaxial and abaxial leaf surfaces with no prominent structures (Figure 3.1 a-d). The analysis of the leaf morphology of *T. ventricosa* is consistent with previous botanical observations (Schmelzer and Gurib-Fakim, 2008). Interestingly, there were occurrences of mite mastication on the waxy surface layer of the emergent leaves (Figure 3.1 a-c).

Mites were observed to be embedded on the adaxial leaf surface of emergent and young leaves. There were no observations of mites being present on the adaxial surfaces of mature leaves however, the manifestation of mites embedded on emergent leaves resulted in the formation of depressions (imprints) on the adaxial leaf surface of mature leaves (Figure 3.1 d). According to these results, it is exceedingly probable that herbivory has a crucial effect on the development of vegetative organs and the chemical composition of *T. ventricosa* (Hanley et al., 2007; Schmelzer and Gurib-Fakim, 2008).

Moreover, it has been suggested that the chemical composition within leaves is altered by insect-herbivores such as mites which rapidly feeds off latex (Hanley et al., 2007; Hagel et al., 2008), which latex is effective against chewing herbivores (Hanley et al., 2007; Konno, 2011). Therefore, the mites may be possibly challenged by the high concentrations of latex defence substances present within mature leaves (Hanley et al., 2007; Agrawal and Konno, 2009; Konno, 2011). This chemical defence trait plays an essential role in protecting plants against herbivore attacks (Hanley et al., 2007; Hagel et al., 2008; Agrawal and Konno, 2009). The most probable function of laticifers is protection, (Fahn, 1979; Hanley et al., 2007; Hagel et al., 2008; Konno, 2011), and this is evident in our findings on the laticifers of *T. ventricosa*.

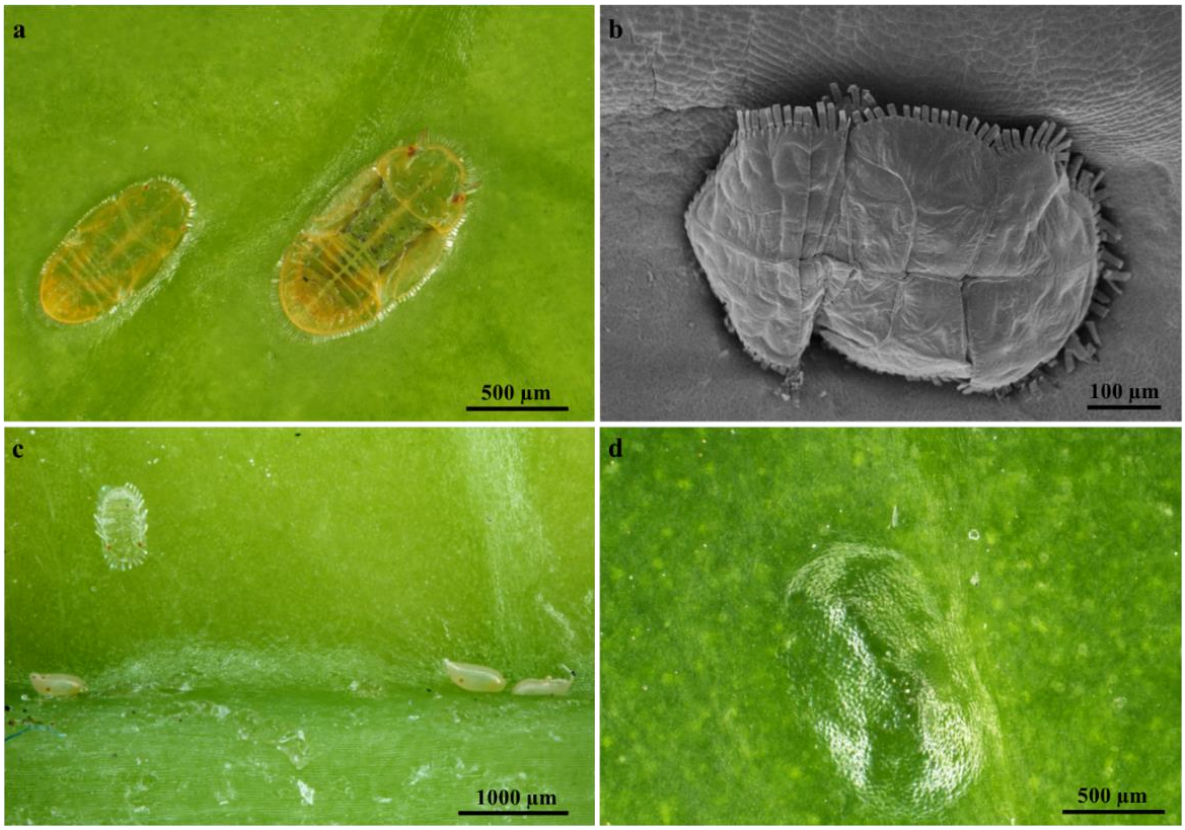

Figure 3.1: Micrographs showing insect-herbivore interactions on *T. ventricosa* adult plant leaves. (a) Mites appear embedded on the glabrous adaxial leaf surface of an emergent leaf. (b) Scanning Electron Microscopy micrograph showing a high-magnification image of an embedded mite on the adaxial leaf surface of an emergent leaf. (c) Stereomicrograph showing a waxy cuticle layer, an embedded mite and mite pupa on the shiny abaxial surface of a young leaf. (d) Sunken depression (imprint from mite) present on then leathery and shiny adaxial surface of a mature leaf.

3.3.2 Ontogeny and structure of laticifers

The laticifers of several species within Apocynaceae are often recognized as nonarticulated; however, articulated laticifers have been observed in a few species (Serpe et al., 2002; Demarco et al., 2008; Lopes et al., 2009; Gama et al., 2017; Pirolla-Souza et al., 2019). Articulated laticifers are described as multiple interconnected simple cells, with intact or perforated transverse and lateral walls (Hanley et al., 2007; Demarco et al., 2008; Hagel et al., 2008; Canaveze and Machado, 2016). By analogy, the present study reports for the first time the presence of articulated anastomosing laticifers in the embryos, seedlings, and adult plants of *T. ventricosa* (Figures 3.2-3.4). These results are relatively confounding with previous reports (Lopes et al., 2009; Pirolla-Souza et al., 2019) and simultaneously consistent with current reports that have described the presence of articulated anastomosing laticifers in Apocynaceae (Canaveze and Machado, 2016).

The prevalence of articulated anastomosing laticifers which is novel for *T. ventricosa* have been classified through rigorous analyses of mature embryos and seedlings, which is recognized as an essential technique to establish the development and characterization of laticifers (Demarco et al., 2013; Canaveze and Machado, 2016; Gama et al., 2017; Ramos et al., 2019). The analyses of embryos (Figure 3.2) and seedlings (Figure 3.3) showed that the laticifers of *T. ventricosa* were found to have originated from ground meristematic tissue and procambium cells. Whereas in the adult plants the laticifers were initiated from the vascular tissue (Figure 3.5 b), comparable to reports by Canaveze and Machado (2016), The progression of laticifers was observed to occur in the primary embryonic stages (Figure 3.2). These processes are simply notable due to distinctive characteristics such as thickened lateral walls, axial elongations, multinucleated spherical nucleus (Figure 3.2 d), terminal walls (Figures 3.2 b, d, and 3.3 b, c), and granular-filled protoplast (Figure 3.2 d). In the seedlings (Figure 3.3 c, d), lateral longitudinal laticifers are closely associated and were found to display an acute apex. According to Gama et al. (2017), these observations are the outcome of oblique sectioning of the laticifer apex. Besides, there is no consistent indication of intrusive growth around the surrounding tissues of the laticifer apex (Figure 3.3).

The laticifer system of *T. ventricosa* embryos are composed of straight and narrow laticifers (Figure 3.2), whereas sinuous and wide laticifers are observed in the seedling (Figure 3.3), the adult plant leaf blade, and young stem sections (Figure 3.4), which is similar to other studies (Demarco et al., 2013; Canaveze and Machado, 2015; Canaveze and Machado, 2016; Castelblanque et al., 2016; Castelblanque et al., 2017; Serpe et al., 2002; Gama et al., 2017). The continuous branching of laticifers usually results in the formation of a network comprised of multiple laticifers that expand and connect throughout the primary and secondary bodies of the plant (Serpe et al., 2002; Demarco et al., 2013; Gama et al., 2017). Laticifers are habitually accompanied by meristematic and adjacent cells that develop into an anastomosing complex system comprised of “Y,” “H,” or “U” conformations (Serpe et al., 2002; Demarco et al., 2013; Gama et al., 2017; Marinho and Teixeira., 2019). In Figure 3.4 a-f, distinctive branching conformations are seen, which indicate that the laticifer branching patterns in the adult leaves and stems of *T. ventricosa* are consistent with those observed in the genus (Canaveze and Machado, 2015; Canaveze and Machado, 2016).

3.3.3 Distribution of laticifers

Articulated anastomosing laticifers are present in all ground and vascular tissues and are closely associated with the phloem of young and mature leaf sections (Figure 3.5 a-c). In addition, laticifers were found scattered in the mesophyll region and often extend towards the leaf extremities (Figure 3.4 a, c, d, e, and Figure 3.7 a-c). These results confirm previous findings on growth mode and development of laticifers in *Tabernaemontana catharinensis* (Canaveze and Machado, 2015; Canaveze and Machado, 2016) and *Allamanda blanchetii* (Gama et al., 2017) In the stem, laticifers occur in the cambial region, cortical parenchyma, vascular tissue, and pith (Figure 3.6 a-d). In plants, laticifers often display extensive distribution patterns (Fineran et al., 1982; Rudall, 1994; Demarco et al., 2013). However, in some instances, the location may differ within vegetative organs, as it is assumed that the distribution patterns of laticiferous cells may be species-specific and might result as a valuable tool for classification at a taxonomic level (Demarco et al., 2013). These distribution patterns are relative to those seen in the genus *Tabernaemontana* (Serpe et al., 2002; Demarco et al., 2013; Canaveze and Machado, 2015; Canaveze and Machado, 2016; Castelblanque et al., 2016; Castelblanque et al., 2017; Gama et al., 2017).

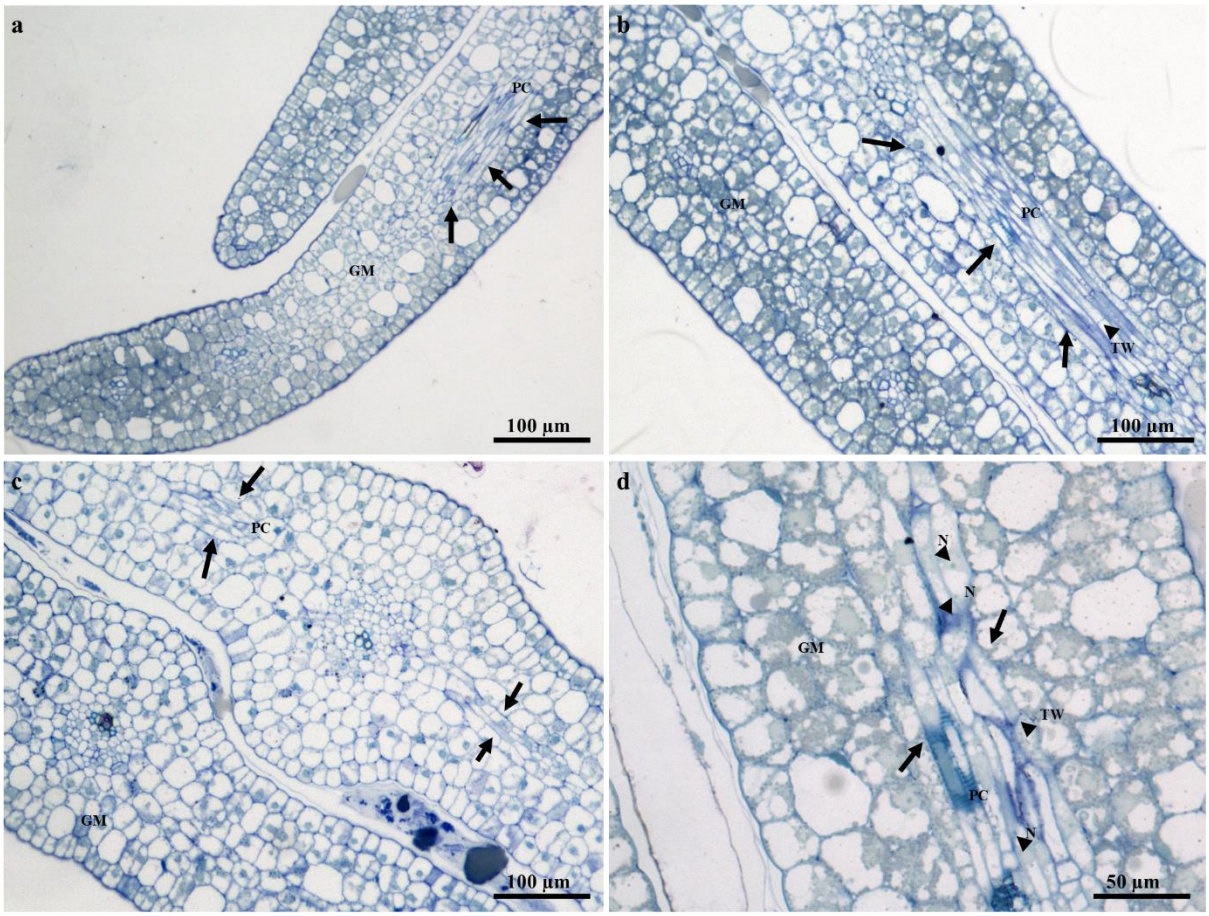

Figure 3.2: Light micrographs showing the anatomy of laticifers in the mature embryos of *T. ventricosa*. (a) A longitudinal section through the mature embryo displaying the formation of articulated laticifers in cotyledons. (b) A longitudinal section through the mature embryo depicts the arrangement of articulated laticifers in the vascular region. Note the terminal walls within the cell. (c) A transverse section through the embryo displaying the occurrence of laticifers in the hypocotyl region. (d) A transverse section showing a highly magnified region of vascular tissue and laticifers in the hypocotyl area. Note the occurrence of terminal walls, and multinucleated laticifers. Abbreviations: TW = Terminal wall, N = Nucleus, GM = Ground meristem, PC = Procambium. Arrows refer to laticifers.

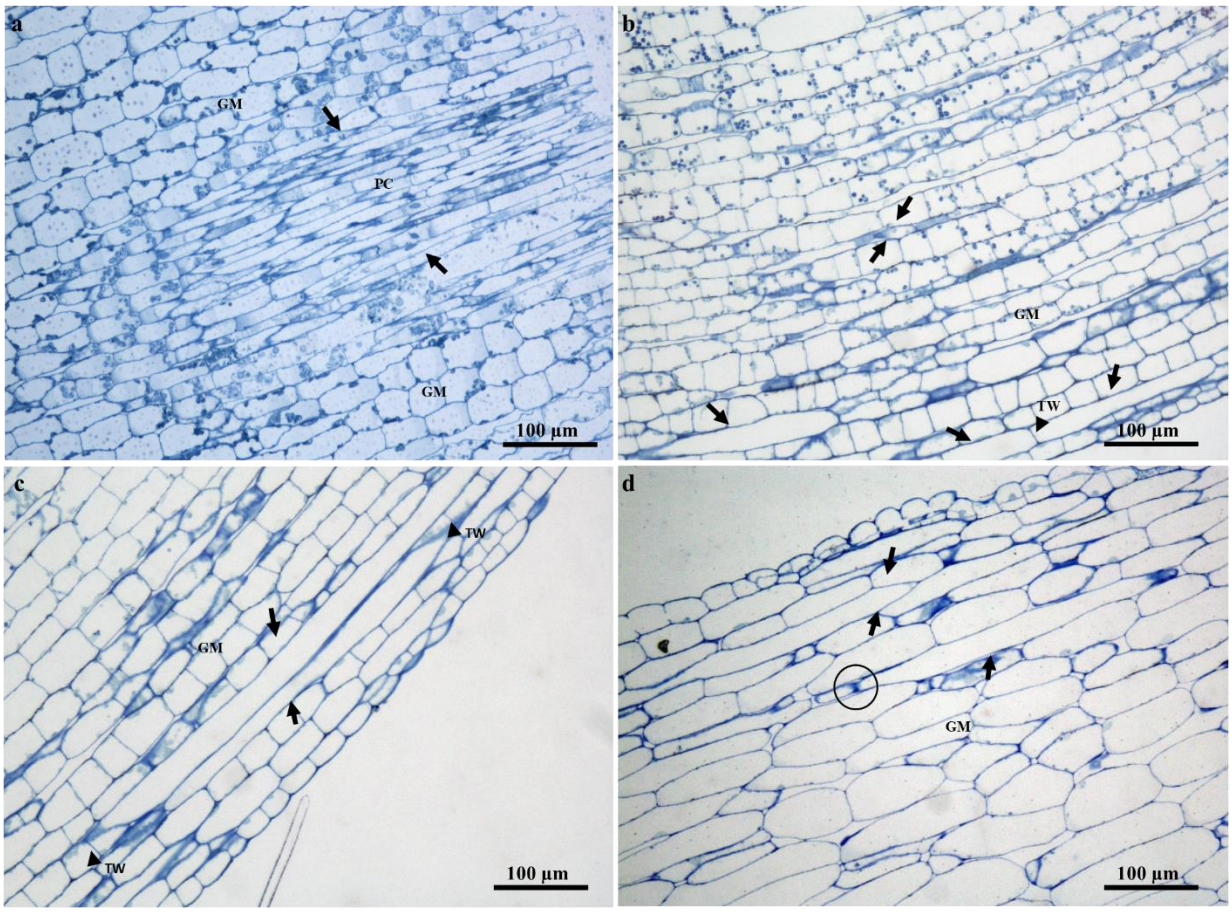

Figure 3.3: Light micrographs showing the anatomy of laticifers in the seedling stem of *T. ventricosa*. (a) A longitudinal section through a seedling stem displaying the occurrence of articulated anastomosing laticifers. (b) A longitudinal section through the stem of a seedling depicts the arrangement of articulated laticifers closely associated with the epidermal tissue. (c) A transverse section through the seedling stem displaying an elongated-tapered syncytia cell, with terminal walls at the lateral ends. (d) A transverse section through the seedling stem showing the arrangement of overlapping laticifers. Note the cell wall dissolution of terminal walls at the tapered regions. Abbreviations: TW = Terminal wall, GM = Ground meristem, PC = Procambium. Arrows refer to laticifers. Circle depicts cell wall dissolution.

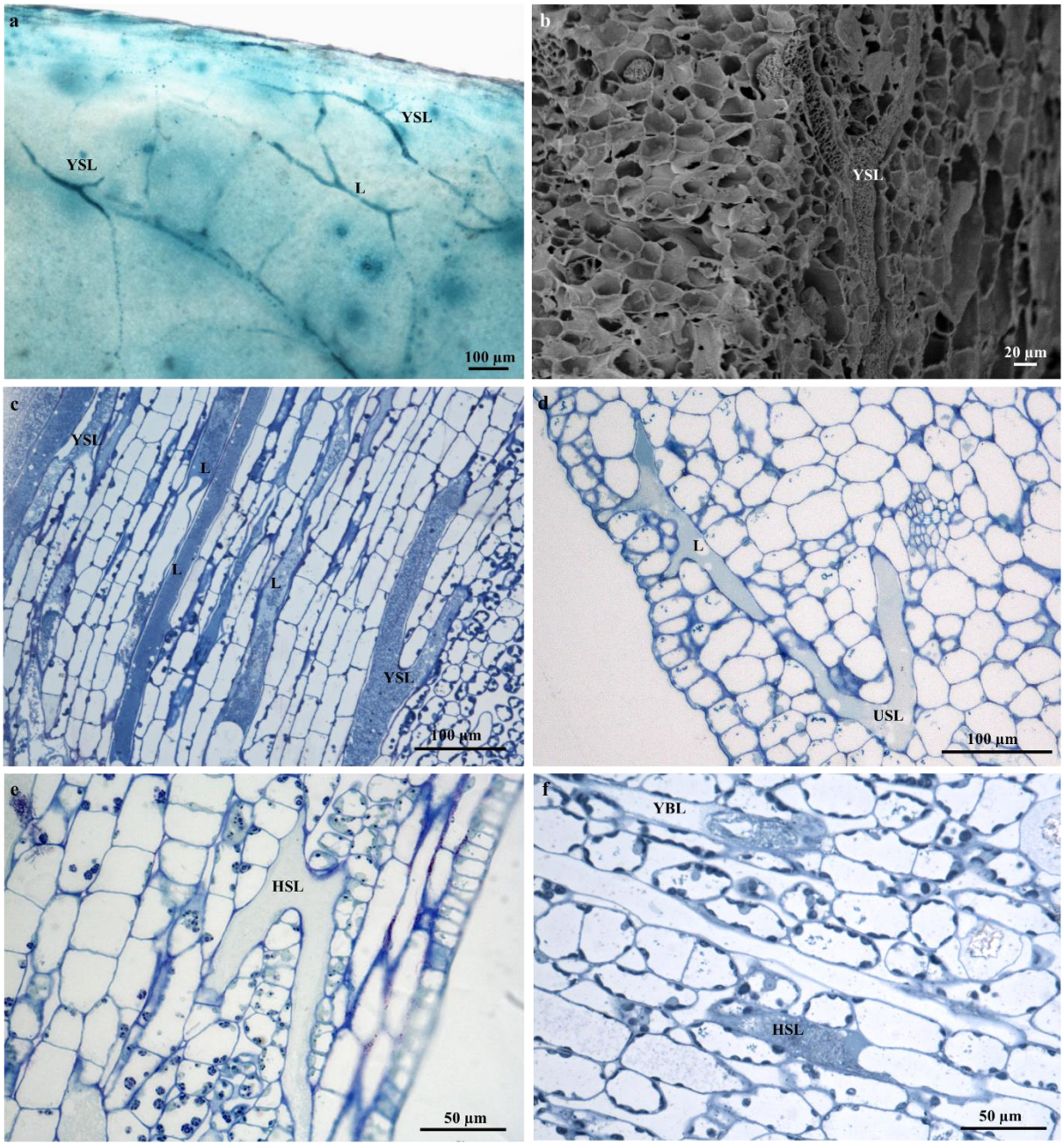

Figure 3.4: Articulated anastomosing laticifers of *T. ventricosa*. (a) Light micrograph of a whole stained seedling leaf showing a branched network of Y-shaped laticifers. (b) Scanning Electron Microscopy micrograph of a young stem fracture showing a single Y-shaped branched laticifer. (c) Light micrograph of sequential sectioned young leaf showing Y-shaped laticifers. (d) Light micrograph of an emergent leaf section showing a branching laticifer and a U-shaped branched laticifer. (e) Light micrograph of a young stem section displaying a branched H-shaped laticifer. (f) Light micrograph of a young stem section depicts branched Y- and H-shaped laticifers. Abbreviations: L = Laticifer, USL = U-shaped laticifer, YSL = Y-shaped laticifer, HSL = H-shaped laticifer.

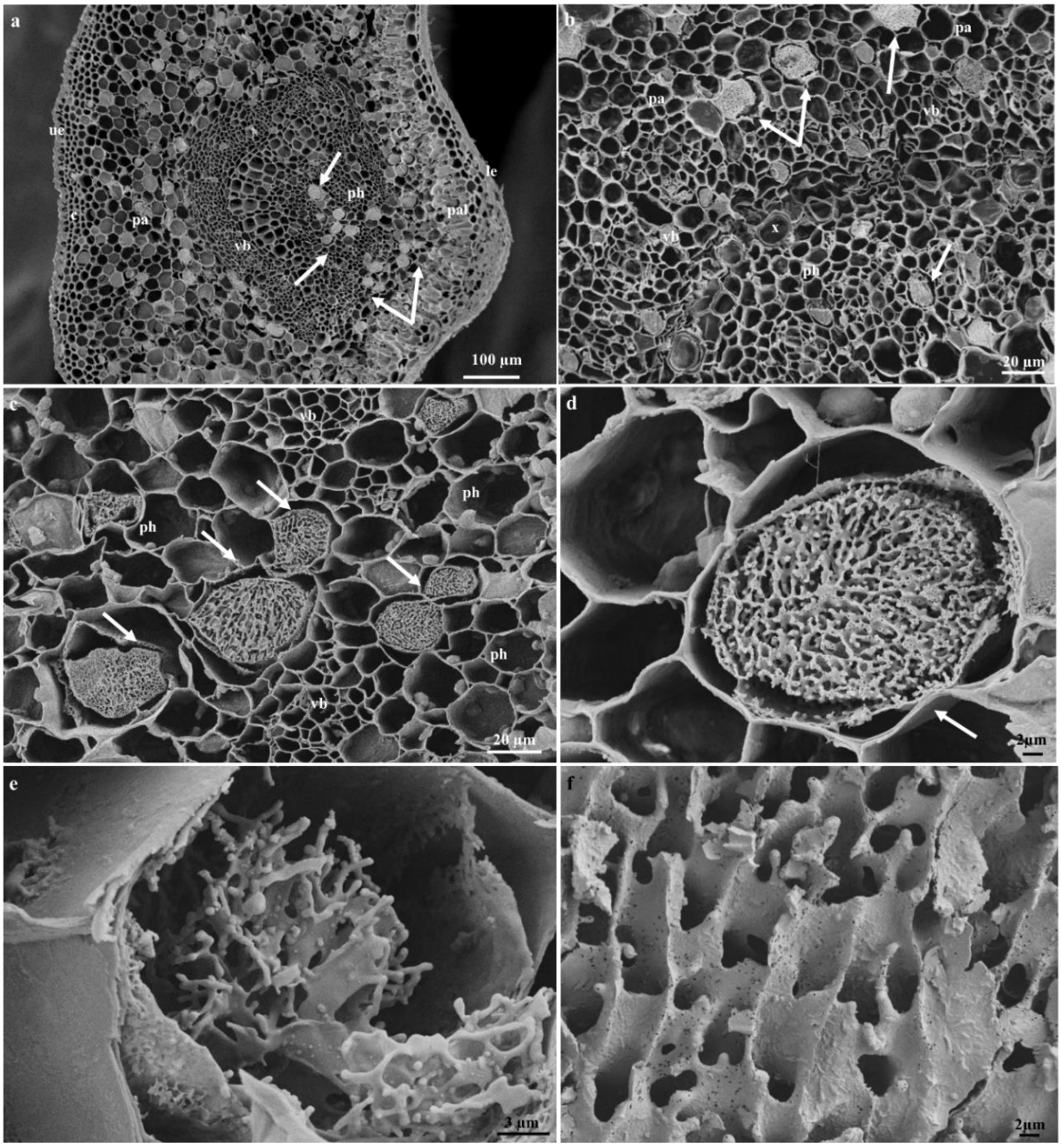

Figure 3.5: Scanning Electron Microscopy micrographs showing freeze-fractures of the adult leaves of *T. ventricosa*. (a) Low-magnification SEM micrograph showing a freeze-fracture of the midrib from a young leaf. (b) Freeze-fracture showing the distribution of laticiferous cells along the vascular bundles and phloem of a mature leaf midrib. (c) Laticifer cell distribution among vascular bundles of a young leaf midrib. (d) Laticifer cell showing latex exudate from a young leaf. (e) Latex exudate within laticifer cell from a young leaf. (f) High-magnification image showing the appearance of latex exudate from an emergent leaf. Abbreviations: ue = Upper epidermis, c = Collenchyma, pa = Parenchyma, vb = Vascular bundles, ph =Phloem, x = Xylem, pal = Palisade, le = Lower epidermis. Arrows refer to laticifer.

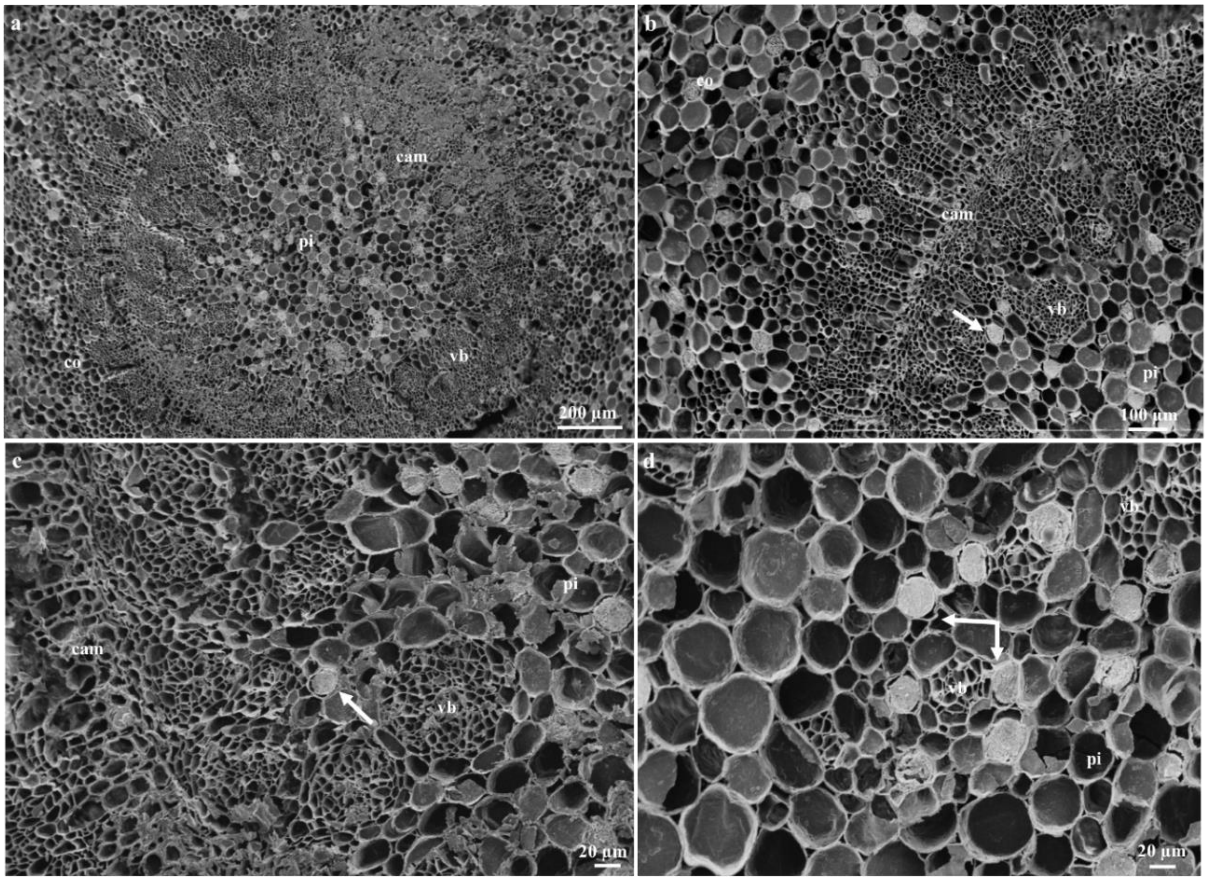

Figure 3.6: Scanning Electron Microscopy micrographs showing freeze-fractures of adult stems of *T. ventricosa.* (a) Low-magnification SEM micrograph showing the distribution of laticifers in a freeze-fracture of a young stem. (b) Freeze-fracture of a young stem depicts the arrangement of laticiferous cells along the vascular cambium. (c) Laticifer cell distribution among vascular bundles of a young stem. (d) High-magnification image showing appearance of laticifer and latex exudate from a young stem. Abbreviations vb = Vascular bundles, cam = Cambium, co = Cortex, pi = Pith. Arrows refer to laticifer.

3.3.4 Laticifer histochemical characterization

The milky white latex of *T. ventricosa* is a synapomorphy of the Apocynaceae (Rapini et al., 2003; Pickard, 2008; Kumar et al, 2011; Nazar et al., 2013). Considering the composite secretion of latex which is often comprised of a variety of specialized metabolites, several latex-bearing plants are well-known for their specific substances (Castro and Demarco, 2008; Lopes et al., 2009; Demarco et al., 2013; Gonçalves et al., 2018). The histochemical analysis of the laticifers and latex within the vegetative organs of *T. ventricosa* revealed for the first time in the species the presence of carboxylated polysaccharides (Figure 3.7 a and 3.8 a), lipophilic and hydrophilic substances (Figure 3.7 b and 3.8 b), proteins (Figure 3.7 i and 3.8 l), phenolics (Figure 3.7 e and 3.8 i), terpenoids (Figure 3.7 d and 3.8 d), neutral lipids (Figure 3.7 g and 3.8 h), alkaloids (Figure 3.7 j and 3.8 e), mucilage and pectin (Figure 3.7 k and 3.8 f), resin acids (Figure 3.7 f and 3.8 g) and acidic substances (Figure 3.7 l and Figure 3.8 j).

These findings are consistent with previous studies, as the compounds within the laticifers and latex were previously detected in species belonging to the genus *Tabernaemontana* and may be of therapeutic and pharmacological importance (Van Beek et al., 1984; Schripsema et al., 1986; Pallant et al., 2012; Marinho et al., 2016; Silveira et al., 2017; Athipornchai, 2018). Furthermore, regarding the chemical constituents detected within the leaf and stem sections of *T. ventricosa*, studies have shown a possible association between the secondary metabolites of latex and defence mechanisms against pathogens and herbivores (Fahn, 1979; Schripsema et al., 1986; Mahlberg et al., 1987; Farrell et al., 1991; Pickard, 2008; Hagel et al., 2008; Demarco and Castro, 2008; Konno, 2011; Demarco et al., 2013). The latex (Figure 3.5 d-f) found within the laticifers of *T. ventricosa* contains chemical compounds (Figure 3.7 a-l and 3.8 a-l), which may be lethal or function as a preventative towards herbivores and pathogens and most likely hinder microorganism proliferation (Schripsema et al., 1986; Hanley et al., 2007; Pickard, 2008; Hagel et al., 2008; Konno, 2011; Demarco et al., 2013).

A positive and intense colour reaction for alkaloids using Wagner's and Dittmar's reagents was observed in the laticifer protoplast of the vegetative organs (Figure 3.7 j and Figure 3.8 e). These results are consistent with the first phytochemical investigation performed on *T. ventricosa* as major alkaloidal components namely, 10-hydroxyheyneanine and akuammicine were detected and isolated from the leaves and stembark (Schripsema et al., 1986). According to the results of the current study, the traditional usage of the plant may be related to the high presence of alkaloids, which is often used for the treatment of various ailments such as high fever, pain, and exposed wounds (Schmelzer and Gurib-Fakim, 2008; Mehrbod et al., 2018). Moreover, previous reports on *Tabernaemontana* species showed that the alkaloids dregamine and voacangine isolated from *T. elegans* and indole alkaloids found in *T.*

catharinensis exhibited substantial antibacterial activity and have medicinal value (Pereira et al., 2004; Pallant et al., 2012).

It has been observed that plants within the genus *Tabernaemontan*a often obtain a profusely high alkaloid content, usually displaying biological activity (Silveira et al., 2017; Athipornchai, 2018). According to Van Beek et al. (1984), alkaloids are organic nitrogenous compounds with the nitrogen being either in its primary, secondary, or tertiary form (Van Beek et al., 1984). Additionally, monoterpene indole and bisindole alkaloids are the major classes of alkaloids within the *Tabernaemontana* genus, other compounds include terpenes, lactones, steroids, phenolics, and flavonoids (Van Beek et al., 1984; Marinho et al., 2016; Silveira et al., 2017; Athipornchai, 2018). A few of the latter compounds, namely alkaloids (Figures 3.7 j and 3.8 e), terpenoids (Figures 3.7 d and 3.8 d), and phenolics (Figures 3.7 e and 3.8 i) have been observed in the current study.

Preliminary observations with autofluorescence revealed the presence of plastids indicated by a red fluorescence and phenolics which displayed a high-intensity blue fluorescence colour within the laticifer cells (latex) of vegetative organs (Figure 3.9 a-b). Phenols have been reported to contain antioxidant, anti-inflammatory, and antibacterial properties (Thombre et al., 2013; Athipornchai, 2018). A few of the cell walls of laticifers stained with Acridine orange in leaf sections (Figure 3.9 c) displayed a yellow-green fluorescence however, many laticifer cell walls in the leaf and stem sections (Figure 3.9 c-d) also displayed a uniform red-orange colouration of high intensities. Lignified tissues are distinguished by a yellow-green fluorescence, whilst non-lignified tissue exhibits an orange-red fluorescence (Demarco, 2017). Calcofluor white staining depicted higher concentrations of cellulose in laticifer walls (Demarco, 2017), as these cells were observed to produce an intense blue colour (Figure 3.9 e, f). The composition of cell walls was examined in all histochemical and fluorescence tests to differentiate between neighbouring cells and laticifers. These observations were made using cell thickness and composition of laticifer cell walls as standard measures (Demarco, 2017).

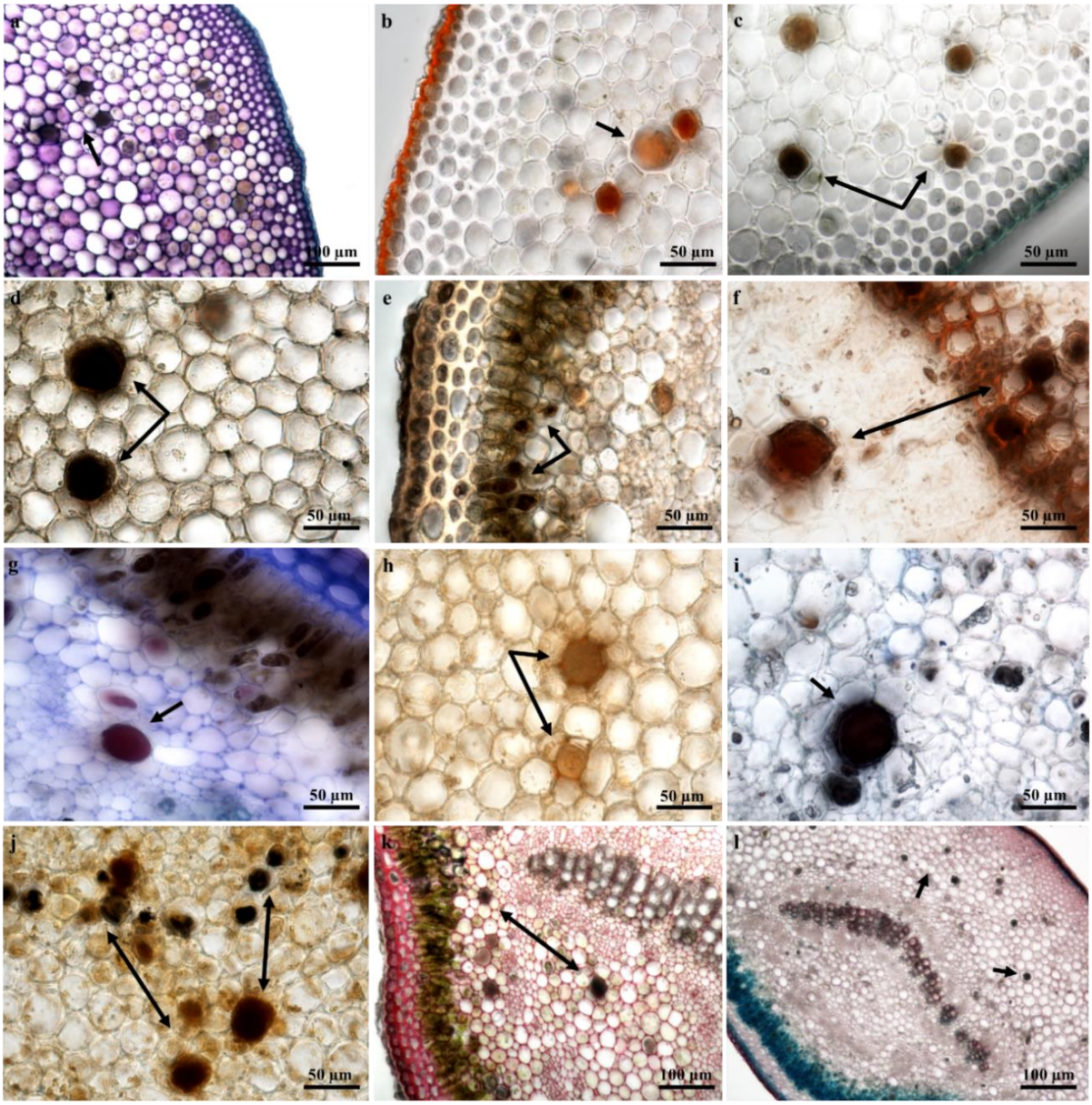

Figure 3.7: Histochemical observations of laticifers in young leaf midrib sections of *T. ventricosa*. (a) Presence of polysaccharides within laticifer cells stained using Toluidene Blue. (b) Positive staining of lipids within laticifers using Sudan IV. (c) Negative staining of lipids, cutin and suberised cell walls of laticifers using Sudan black B. (d) Ferric trichloride positively stained laticifers a dark-black colour. (e) Presence of phenolics within laticifer cells stained using Ferric chloride. (f) Intense staining of resin acids within laticifers using NADI reagent. (g) Intense staining of neutral lipids within laticifers using Nile blue. (h) Negative staining lignin aldehydes within laticifer and cell components stained using Phloroglucinol. (i) Intense blue-black staining of proteins in laticifers. (j) Intense staining of alkaloids within laticifers stained using Wagner's and Dittmar's reagent. (k) Positive staining of mucilage and pectin using Ruthenium red. (l) Presence of acidic substances in laticifers stained using Safranin and Fast Green. Arrows refer to laticifer.

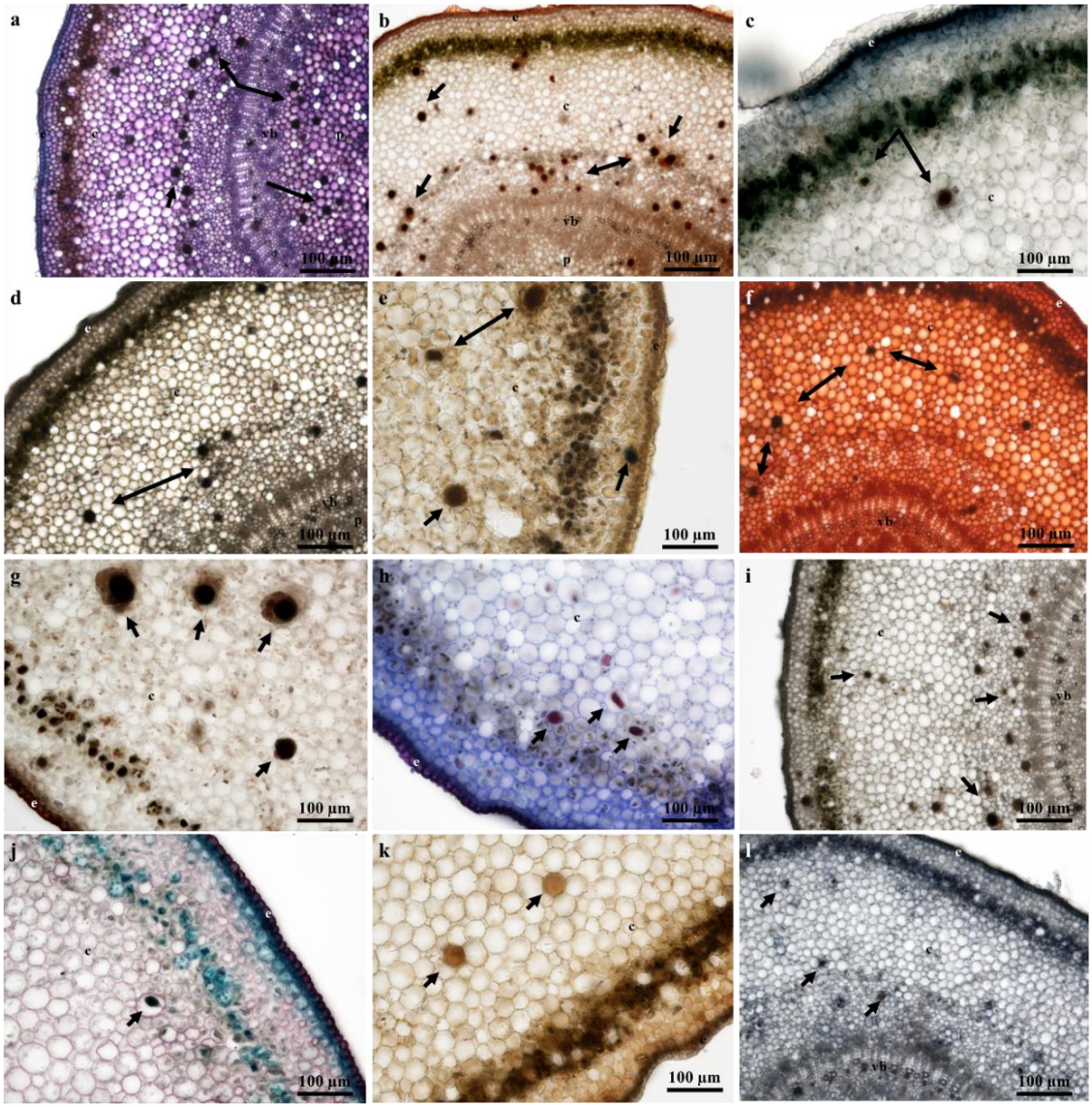

Figure 3.8: Histochemical observations of laticifers in young stem sections of *T. ventricosa*. (a) Presence of polysaccharides in laticifers stained using Toluidene Blue. (b) Lipids stained using Sudan IV. (c) Negative staining of lipids using Sudan Black B. (d) Ferric trichloride positively stained laticifers a dark black colour. (e) Alkaloids identified within laticifers using Wagner's and Dittmar's reagent. (f) Detection of mucilage and pectin using Ruthenium red. (g) Intense staining of resin acids in laticifers using NADI reagent. (h) Neutral lipids in laticifer identified using Nile blue. (i) Detection of phenolics within laticifer stained using Ferric chloride. (j) Presence of acidic substances within laticifers stained using Safranin and Fast Green. (k) Negative staining of lignin aldehydes using Phloroglucinol. (l) Proteins detected in laticifers. Arrows refer to laticifer.

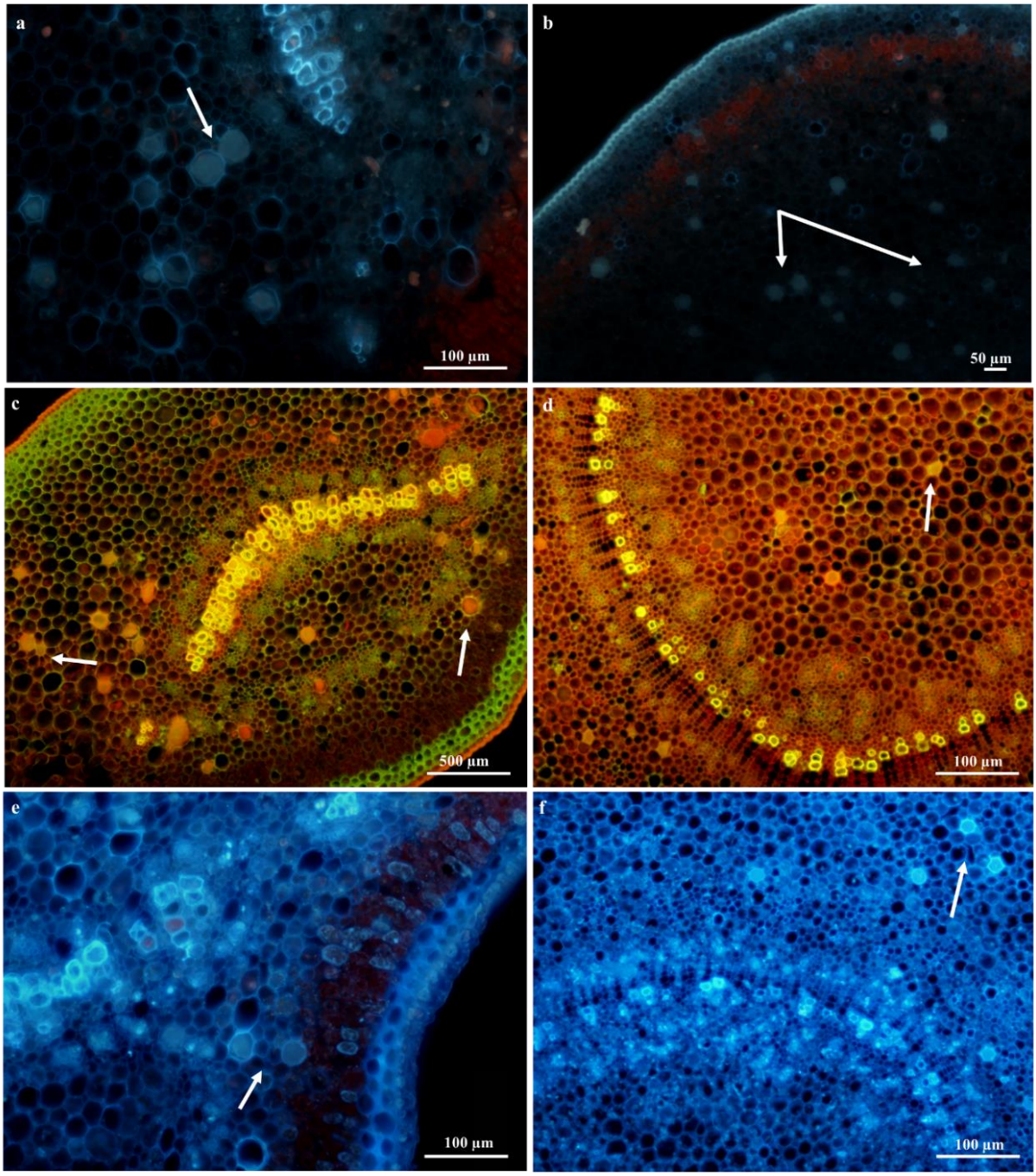

Figure 3.9: Fluorescence microscopy of young leaf midrib and young stem sections of *T. ventricosa*. (a) Auto-fluorescence of laticifer cell in leaf section showing intense blue fluorescence indicating the presence of phenolics. (b) Positive auto-fluorescence stain of stem section indicative of phenolics. (c-d) Leaf and stem sections stained orange-red using Acridine Orange indicating non-lignified laticifer contents. (e-f) Positive staining for cellulose using Calcofluor White on leaf and stem sections. Arrows refer to laticifer.

3.3.5 Laticifer ultrastructure of adult leaves

Due to the difficulty experienced in the ultrastructural analyses of embryos, seedlings, and adult stems, only young leaf material was used for ultrastructural investigations. The laticifer system in the young leaves of *T. ventricosa* was formed by the accumulation of new cells, accompanied by a rapid discontinuity of transverse cell walls, resulting in the combination of their protoplasts (Figure 3.10). These ultrastructural changes have been similarly observed in other latex-bearing species (Demarco et al., 2013; Canaveze and Machado, 2016; Gama et al, 2017). These cells were notable from surrounding ground and vascular tissue by contact with adjacent cells via cell wall dissolution (Figure 3.10 c), irregularly thickened cell walls (Figure 3.10 e), latex content (Figure 3.10 c and 3.11 c, d), and their lengthened form (Figure 3.11 a), similarly observed in other studies (Canaveze and Machado, 2016; Gama et al, 2017). Irregularly shaped laticifers displaying acuminate ends (acute apex) were found appressed to the middle lamella of adjacent cells indicative of an oblique section of the apical cell as observed in Figure 3.10 a. With the analyses of the terminal walls of laticifers, it is possible to observe the expansion of laticifers via the dissolution of its cell walls and the concurrent accumulation of new cells to the existing laticifers (Figure 3.10 a, c) which has been observed in *T. catharinensis* (Castro and Demarco, 2008; Canaveze and Machado, 2016). The rapid cell wall dissolution of laticifers usually occurs from the center towards the periphery (Figure 3.10 c) of the cell (Castro and Demarco, 2008). This process is achieved by small lytic vesicles formed from the peripheral endoplasmic reticulum (Castro and Demarco, 2008; Canaveze and Machado, 2016; Gama et al, 2017). Subsequently, the plasma membrane and tonoplast of both cells merge resulting in the formation of a continuous laticifer with one central vacuole (Castro and Demarco, 2008; Gama et al, 2017).

Golgi bodies and dictyosomes were observed embedded within the cell (Figure 3.10 e, f), with small vacuoles in proximity (Figure 3.11 a). It has been suggested that these smaller vacuoles are the initial forms of a central vacuole and possibly contribute to the abundance of vesicles (Wilson and Mahlberg, 1978; Canaveze and Machado, 2016; Gama et al., 2017). The formation of small vacuoles is due to the endoplasmic reticulum and electron-dense material observed in the cytoplasm (Figure 3.10 c). Initial subcellular alterations of the cytoplasm are due to the combination of tiny highly vacuolated cells (Figure 3.11 a-c), that result in the establishment of a large central vacuole within a cell (Castro and Demarco, 2008; Canaveze and Machado, 2016; Gama et al, 2017). The increased size of the central vacuole was found to compress the cytoplasm into a thin parietal layer, likewise to literature (Gama et al, 2017). At this stage of latex production, the contents of the cell are altered significantly (Canaveze and Machado, 2016; Gama et al, 2017), as an abundance of mitochondria (Figure 3.11 b, c), lipid bodies (Figure 3.10 b), osmiophilic bodies (Figures 3.10 b-d and 3.11 b), plastids and starch grains were observed (Figure 3.10 a, d). The occurrence of plentiful mitochondria is possibly associated with the supply and demand of energy required by the secretory process of the variable components of latex

(Wilson and Mahlberg, 1980; Gama et al., 2017). At the initiation of the secretory process, osmiophilic bodies are produced and relocated to the central vacuole. This process has been observed in *Calotropis gigantea* (Roy et al., 1992).

The latex that fills the laticier lumen is regarded as the protoplast of the laticifer (Castro and Demarco, 2008; Demarco, 2015) and contains an emulsion of latex-containing rubber particles within the parietal cytoplasm (Figure 3.11 d). Furthermore, a rupture (natural or induced) of the laticifer cell wall results in the release of its latex contents, which is often used as a protective mechanism by latex-bearing plants (Hanley et al., 2007; Konno, 2011).

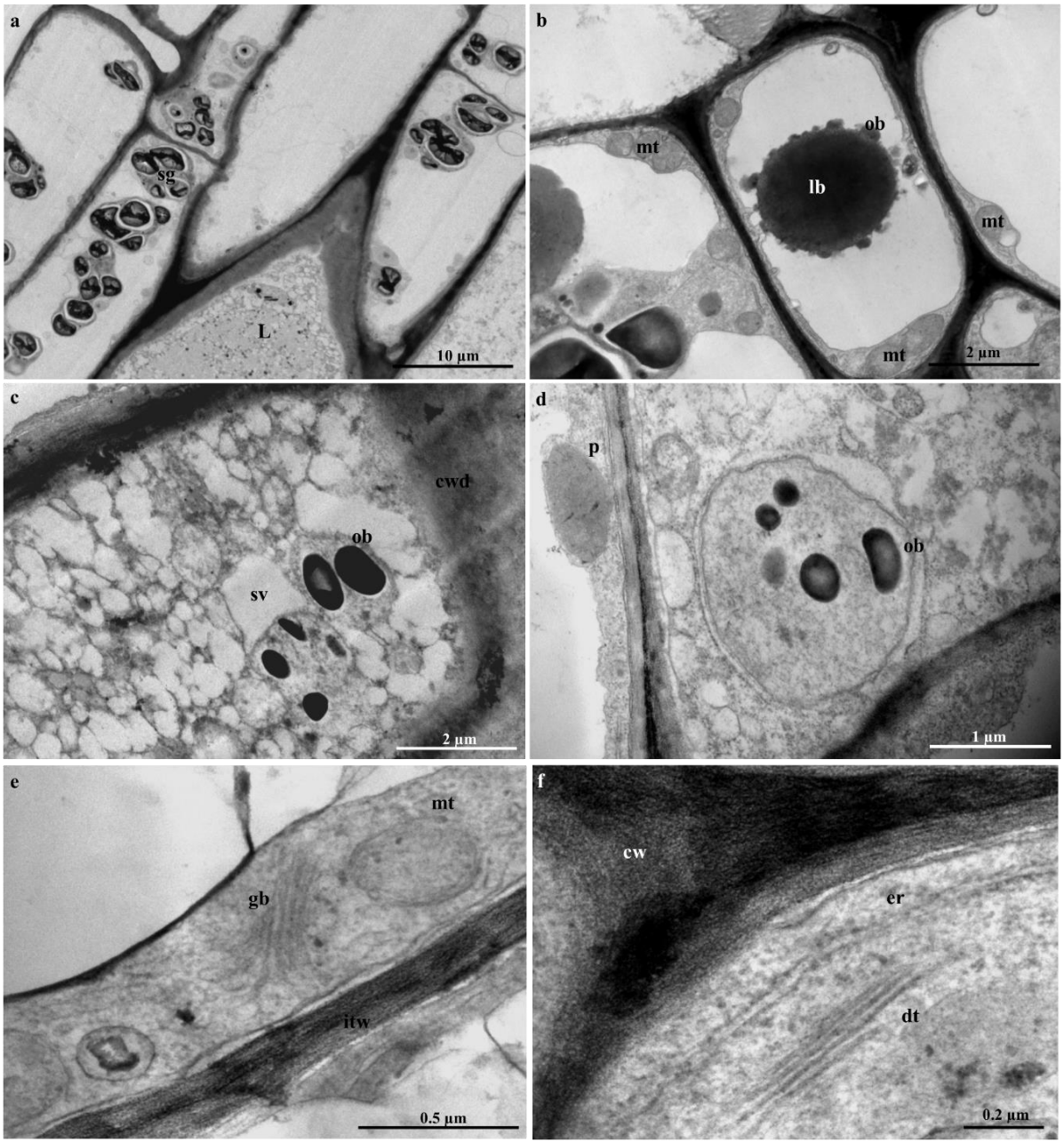

Figure 3.10: Ultrastructure of laticifers in the adult leaves of *T. ventricosa*. (a) Oblique section of a laticifer cell showing an acute apex and starch grains. (b) Lipid body closely associated with osmiophilic bodies. (c) Coalescence of small vacuole with granular laticifer cell content. (d) Osmiophilic bodies free in the cytosol and plastid with an electron-dense globule. (e) Presence of mitochondria, golgi body and irregular thickening of cell walls. (f) Expansion of endoplasmic reticulum and presence of dictyosomes nearby the cell wall. Abbreviations: L = Laticifer, sg = Starch grain, cwd = Cell wall dissolution, sv = Small vacuole, ob = Osmiophilic bodies, p = Plastid, gb = Golgi body, mt = Mitochondria, itw = Irregular thickened walls, er = Endoplasmic reticulum, dt = Dictyosomes, cw = Cell wall, lb = Lipid body.

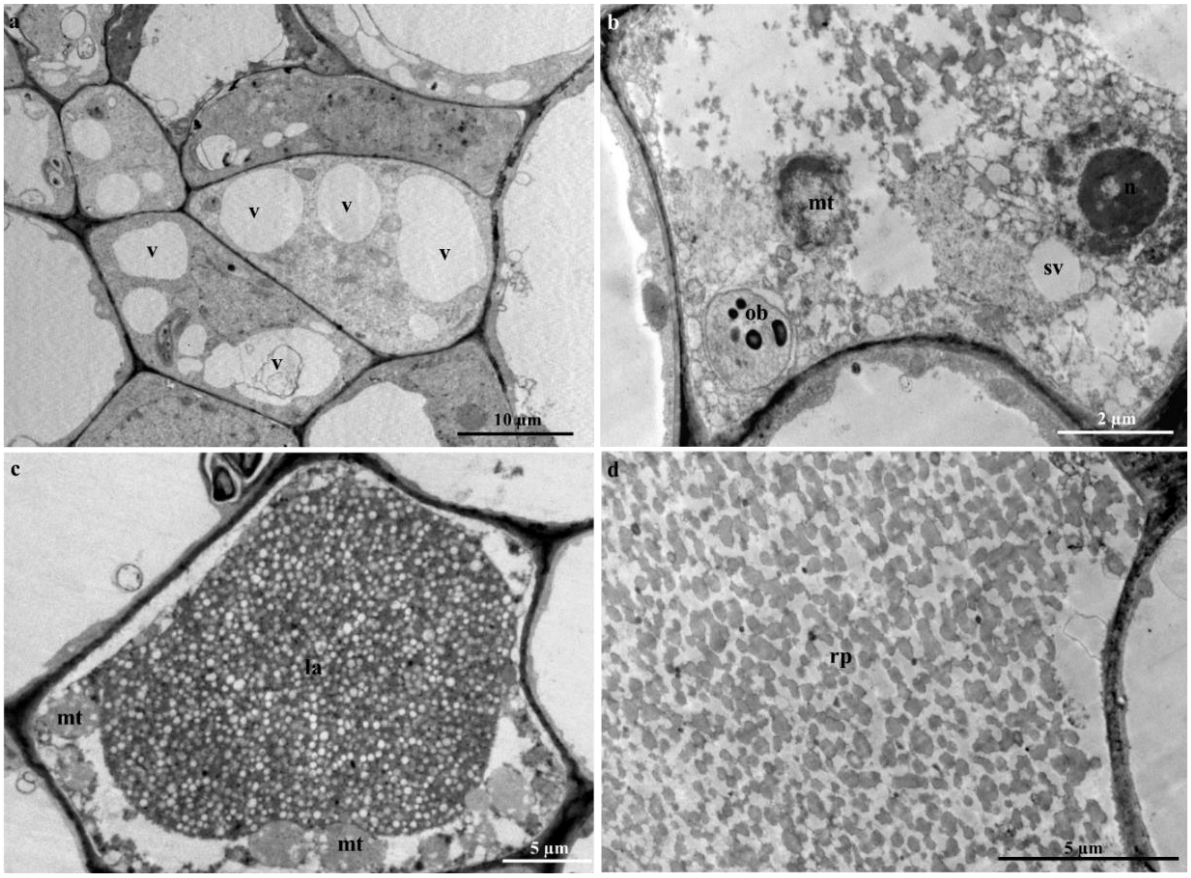

Figure 3.11: Latex production in adult leaves of *T. ventricosa*. (a) Highly vacuolated cytoplasm of young laticifer. (b) Initiation of secretory activity. (c) Latex metabolites forming an emulsion within the central vacuole of the laticifer cell. (d) Rubber particles within the latex emulsion. Abbreviations: v = Vacuole, ob = Osmiophilic bodies, mt = Mitochondria, n = Nucleus, sv = Small vacuole, la = Latex, rp = Rubber particles.

3.4 Conclusion

This study reports for the first time, the type and distribution of laticifers in the embryos, seedlings, and adult plants of *T. ventricosa*, and the plausible functions of laticifers and latex within this species. The ontogenetic studies of *T. ventricosa* confirmed the presence of articulated anastomosing laticifers. The laticifers were found to have originated from ground meristematic tissue and procambium cells, where they eventually disperse into all ground and vascular tissue. The complex branching patterns of laticifers usually develop into a composite system comprised of "Y," "H," or "U" conformations. The latter observations are consistent with the literature since recently majority of the laticifers belonging to the Apocynaceae have been classified as articulated. In addition, histochemical analyses revealed a variety of secondary metabolites including carboxylated polysaccharides, lipophilic and hydrophilic substances, proteins, phenolics, terpenoids, neutral lipids, alkaloids, mucilage, pectin, resin acids, and acidic substances present in the laticifers of *T. ventricosa*. Considering the chemical composition of the latex present in the lumen of laticifers, it is suggested that the latex is used as a protective mechanism against herbivory. Furthermore, the presence of alkaloids within the latex highlights its potential therapeutic value for the treatment of various ailments.

3.5 References

Agrawal, A.A., Konno, K., 2009. Latex: a model for understanding mechanisms, ecology, and evolution of plant defense against herbivory. Annual Review of Ecology, Evolution and Systematics 40, 311–331.

Ascensão, L., Pais, M.S.S., 1987. Glandular trichomes of *Artemisia campestris* (ssp. *Maritima*): Ontogeny and histochemistry of the secretory product. Botanical Gazette 148, 221–227.

Athipornchai, A., 2018. A Review on *Tabernaemontana* spp.: Multipotential medicinal plant. Asian Journal of Pharmaceutical and Clinical research 11, 45–53.

Bauer, G., Gorb, S.N., Klein, M.C., Nellesen, A., von Tapavicza, M., Speck, T., 2014. Comparative study on plant latex particles and latex coagulation in *Ficus benjamina*, *Campanula glomerata* and three Euphorbia species PloS One 9, 1–8.

Canaveze, Y., Machado, S.R., 2015. Leaf colleters in *Tabernaemontana catharinensis* (Apocynaceae, Rauvolfioideae): Structure, ontogenesis, and cellular secretion. Botany 93, 287–296.

Canaveze, Y., Machado, S.R., 2016. The occurrence of intrusive growth associated with articulated laticifers in *Tabernaemontana catharinensis* A.DC., a new record for Apocynaceae. International Journal of Plant Sciences 177, 458–467.

Castelblanque, L., Balaguer, B., Martí, C., Rodríguez, J.J., Orozco, M., Vera, P., 2016. Novel insights into the organisation of laticifer cells: A cell Comprising a unified whole system. Plant Physiology 172, 1032–1044.

Castelblanque, L., Balaguer, B., Martí, C., Rodríguez, J.J., Orozco, M., Vera, P., 2017. Multiple facets of laticifer cells. Plant Signaling and Behavior 12, 1–6.

Castro, M.D., Demarco, D., 2008. Phenolic compounds produced by secretory structures in plants: A brief review. Natural Product Communications 3, 1273–1284.

Demarco, D. 2015. Micromorfologı´a y histoquı´mica de los laticı´feros de ´organos vegetativos de especies de *Asclepiadoideae* (Apocynaceae). Acta Biológica Colombiana 20, 57–65.

Demarco, D., 2017. Histochemical analysis of plant secretory structures. In Histochemistry of Single Molecules. Humana Press, New York 31–330.

Demarco, D., Castro, M.D., 2008. Laticíferos articulados anastomosados em espécies de Asclepiadeae (Asclepiadoideae, Apocynaceae) e suas implicações ecológicas. Brazilian Journal of Botany 31, 699–711.

Demarco, D., de Moraes Castro, M., Ascensão, L., 2013. Two laticifer systems in *Sapium haematospermum*—new records for Euphorbiaceae. Botany 91, 545–554.

Dussourd, D.E., Eisner, T., 1987. Vein-cutting behavior: Insect counterploy to the latex defense of plants. Science 237, 898–901.

Esau, K., 1965. Plant Anatomy, second ed. McGraw-Hill, New York.

Evert, R.F., 2006. Esau's plant anatomy, third ed. Wiley-Interscience, New York.

Fahn, A., 1979. Secretory tissues in plants, illustrated ed. Academic Press, London.

Farrell, B.D., Dussourd, D.E., Mitter, C., 1991. Escalation of plant defense: Do latex and resin canals spur plant diversification? The American Naturalist 138, 881–900.

Fineran, B.A., 1982. Distribution and organisation of non-articulated laticifers in mature tissues of poinsettia (*Euphorbia pulcherrima* Willd.). Annals of Botany 50, 207– 220.

Furr, M., Mahlberg, P.G., 1981. Histochemical analyzes of laticifers and glandular trichomes in *Cannabis sativa*. Journal of Natural Products 44, 153–159.

Gama, T.S.S., Rubiano, V.S., Demarco, D., 2017. Laticifer development and its growth mode in *Allamanda blanchetii* A. DC. (Apocynaceae). The Journal of the Torrey Botanical Society 144, 303–312.

Gonçalves, M.P., Mercadante-Simões, M.O., Ribeiro, L.M., 2018. Ontogeny of anastomosed laticifers in the stem apex of *Hancornia speciosa* (Apocynaceae): A topographic approach. Protoplasma 255, 1713–1724.

Hagel, J.M., Yeung, E.C., Facchini, P.J., 2008. Got milk? The secret life of laticifers. Trends in Plant Science 13, 631–639.

Hanley, M.E., Lamont, B.B., Fairbanks, M.M., Rafferty, C.M., 2007. Plant structural traits and their role in anti-herbivore defence. Perspectives in Plant Ecology, Evolution and Systematics 8, 157–178.

Johansen, D. A., 1940. Plant Microtechnique, first ed. McGraw-Hill, New York.

Konno, K., 2011. Plant latex and other exudates as plant defense systems: Roles of various defense chemicals and proteins contained therein. Phytochemistry 72, 1510–1530.

Krishnamurthy, K.V., Venkatasubramanian, P., Lalitha, S., Bahadur, B., Sujatha, M., Carels, N., 2013. Laticifers of *Jatropha*. In *Jatropha*, Challenges for a New Energy. Springer, New York 3–10.

Kumar, G., Karthik, L., Rao, K.V.B., 2011. A review on pharmacological and phytochemical profile of *Calotropis gigantea Linn.* Pharmacologyonline 1, 1–8.

Leeuwenberg, A.J.M.; Kupicha, F.K. Apocynaceae; Launert, E., 1985. Ed.; Flora Zambesiana: London, UK, 395–503.

Lopes, K.L.B., Thadeo, M., Azevedo, A.A., Soares, A.A., Meira, R.M.S.A., 2009. Articulated laticifers in the vegetative organs of *Mandevilla atroviolacea* (Apocynaceae, Apocynoideae). Botany 87, 202–209.

Mahlberg, P.G., 1993. Laticifers: An historical perspective. Botanical Review 59,1–23.

Mahlberg, P.G., Davis, D.G., Galitz, D.S., Manners, G.D. 1987. Laticifers and the classification of *Euphorbia*: The chemotaxonomy of *Euphorbia esula* L. Botanical Journal of the Linnean Society 94 165–180.

Marinho, C.R., Teixeira, S.P., 2019. Novel reports of laticifers in *Moraceae and Urticaceae*: Revisiting synapomorphies. Plant Systematics and Evolution 305, 13–31.

Marinho, F.F., Simões, A.O., Barcellos, T., Moura, S., 2016. Brazilian *Tabernaemontana* genus: Indole alkaloids and phytochemical activities. Fitoterapia 114, 127–137.

Mazia, D., Brewer, P. A., Alfert, M., 1953. The cytochemical staining and measurement of protein with Mercuric Bromophenol blue. Marine Biological Laboratory 104, 57–67.

Mehrbod, P., Abdalla, M.A., Njoya, E.M., Ahmed, A.S., Fotouhi, F., Farahmand, B., Gado, D.A., Tabatabaian, M., Fasanmi, O.G., Eloff, J.N., McGaw, L.J., 2018. South African medicinal plant extracts active against influenza A virus. BMC Complementary and Alternative Medicine 18, 112–121.

Metcalfe, C.R., 1967. Distribution of latex in the plant kingdom. Economic Botany 21, 115–127.

Nazar, N., Goyder, D.J., Clarkson, J.J., Mahmood, T., Chase, M.W., 2013. The taxonomy and systematics of Apocynaceae: Where we stand in 2012. Botanical Journal of the Linnean Society 171, 482–490.

O' Brien, T.P., Feder, N., McCully, M.E., 1964. Polychromatic staining of plant cell walls by Toluidine Blue O. Protoplasma 59, 368–373.

Pallant, C.A., Cromarty, A.D., Steenkamp, V., 2012. Effect of an alkaloidal fraction of *Tabernaemontana elegans* (Stapf.) on selected micro-organisms. Journal of Ethnopharmacology 140, 398–404.

Pereira, C.G., Marques, M.O., Barreto, A.S., Siani, A.C., Fernandes, E.C., Meireles, M.A.A., 2004. Extraction of indole alkaloids from *Tabernaemontana catharinensis* using supercritical CO_2+ ethanol: An evaluation of the process variables and the raw material origin. The Journal of Supercritical Fluids 30, 51–61.

Periasamy, K., 1967. A technique of staining sections of paraffin-embedded plant materials without employing a graded ethanol series. Journal of Microscopy 87, 109–112.

Pickard, W.F., 2008. Laticifers and secretory ducts: Two other tube systems in plants. New Phytologist 177, 877–888.

Pirolla-Souza, A., Arruda, R.C.O., Pace, M.R., Farinaccio, M.A., 2019. Leaf anatomical characters of *Rhabdadenia* (Rhabdadenieae, Apocynaceae), their taxonomic implications, and notes on the presence of articulated laticifers in the genus. Plant Systematics and Evolution 305, 797–810.

Pott, D.M., Osorio, S., Vallarino, J.G., 2019. From central to specialized metabolism: An overview of some secondary compounds derived from the primary metabolism for their role in conferring nutritional and organoleptic characteristics to fruit. Frontiers in Plant Science 10, 1–19.

Ramos, M.V., Demarco, D., da Costa Souza, I.C., de Freitas, C.D.T., 2019. Laticifers, latex, and their role in plant defense. Trends in Plant Science 24, 553–567.

Rapini, A., Chase, M.W., Goyder, D.J., Griffiths, J., 2003. *Asclepiadeae* classification: Evaluating the phylogenetic relationships of New World *Asclepiadoideae* (Apocynaceae). Taxon 52, 33–50.

Roy, A. T., DE, D.N., 1992. Studies on differentiation of laticifers through light and electron microscopy in *Calotropis gigantea* (Linn.) R. Br. Annals of Botany 70, 443–449.

Rudall, P., 1994. Laticifers in Crotonoideae (Euphorbiaceae): Homology and evolution. Annals of Missouri Botanical Garden 81, 270–282.

Schmelzer, G.B., Gurib-Fakim, A., 2008. Medicinal Plants, first ed. Plant Resources of Tropical Africa 11, 1. PROTA Foundation. Backhuys Publishers, Wageningen, Netherlands.

Schmidt, E., Lotter, M., McCleland, W., 2002. Trees and shrubs of Mpumalanga and Kruger National park. Jacana.

Schripsema, J., Hermans-Lokkerbol, A., Van der Heijden, R., Verpoorte, R., Svendsen, A.B., Van Beek, T.A., 1986. Alkaloids of *Tabernaemontana ventricosa*. Journal of Natural Products 49, 733–735.

Serpe, M.D., Muir, A.J., Driouich, A., 2002. Immunolocalization of beta -D-glucans, pectins, and arabinogalactan-proteins during intrusive growth and elongation of non-articulated laticifers in *Asclepias speciosa* Torr Planta 215, 357–310

Shih, M.L., Morgan, J.A., 2020. Metabolic flux analysis of secondary metabolism in plants. Metabolic engineering communications 123, 1–7.

Silveira, D., de Melo, A.F., Magalhães, P.O., Fonseca-Bazzo, Y.M., 2017. *Tabernaemontana* Species: Promising sources of new useful drugs. In Studies in Natural Products Chemistry. Elsevier 54, 227–289.

Thombre, R., Jagtap, R., Patil, N., 2013. Evaluation of phytoconstituents, anti-bacterial, anti-oxidant and cytotoxic activity of *Vitex negundo* L. and *Tabernaemontana divaricata* L. International Journal of Pharmaceutical and Biological Sciences 4, 389–396.

Tiwari, P., Sangwan, R.S., Sangwan, N.S., 2016. Plant secondary metabolism linked glycosyltransferases: An update on expanding knowledge and scopes. Biotechnology advances 34, 714-739.

Van Beek, T.A., Verpoorte, R., Svendsen, A.B., Leeuwenberg, A.J.M., Bisset, N.G., 1984. *Tabernaemontana* L. (Apocynaceae): A review of its taxonomy, phytochemistry, ethnobotany and pharmacology. Journal of Ethnopharmacology 10, 1–156.

Wilson, K.J., Mahlberg, P.G., 1978. Ultrastructure of non-articulated laticifers in mature embryos and seedlings of *Asclepias syriaca* L (*Asclepiadaceae*). American Journal of Botany 65, 98–109.

Wilson, K.J., Mahlberg, P.G., 1980. Ultrastructure of developing and mature non-articulated laticifers in the milkweed *Asclepias syriaca* L. (Asclepiadaceae). American Journal of Botany 67, 1160–1170.

Wink, M., 2010. Introduction: Biochemistry, physiology and ecological functions of secondary metabolites. Annual plant reviews volume 40: Biochemistry of Plant Secondary Metabolism 40, 1–19.

CHAPTER 4:

PHYTOCHEMICAL COMPOSITION AND ANTIBACTERIAL EVALUATION OF *TABERNAEMONTANA VENTRICOSA* HOCHST. EX A. DC. LEAF, STEM, AND LATEX EXTRACTS

Abstract

The novel discoveries of biologically active compounds from medicinal plants have driven various research fields towards establishing essential sources of natural drug candidates. *Tabernaemontana ventricosa* Hochst. ex A. DC. (Apocynaceae) is a medicinal plant often used to palliate fever, treat wounds, and reduce blood pressure. The present study aimed to examine the organoleptic characters, elemental composition, phytochemical compounds and evaluate the antibacterial activity of the crude leaf, stem, and latex extracts of *T. ventricosa*. The microscopic analyses of the organoleptic characters, fluorescence analysis, and elemental composition revealed no harmful compounds. Qualitative phytochemical screening of the extracts detected alkaloids, flavonoids, saponins, sterols, steroids, phenols, fats, fixed oils, carbohydrates, and amino acids. These results correspond to the significant chemical classes observed within *Tabernaemontana*. The chemical composition of the crude leaf and stem, and latex extracts determined by Gas Chromatography-Mass Spectrometry (GC-MS) analysis showed alkaloids, terpenes, phytosterols, and fatty alcohols. Major identified compounds (>1%) in all extracts were α-linolenic acid, pentadecanoic acid, α-d-mannofuranoside, methyl, 13-docosenamide, (Z)-, 9,12-octadecadienoic acid (Z,Z)-, lup-20(29)-en-3-ol, acetate, (3β), 9,19-cyclolanost-24-en-3-ol, (3β) and β-amyrin. These compounds possess pharmacological effects such as antibacterial, anti-inflammatory, and anticancer properties. The antibacterial activity was evaluated using various extracts, with different concentrations against gram-positive and gram-negative bacterial strains. Substantial antibacterial activity of the methanolic extracts of the leaf and stem and latex extracts were observed against *Bacillus subtilis* (ATCC 6653), *Escherichia coli* (ATCC 25922), *Methicillin-resistant Staphylococcus aureus* (MRSA) (ATCC 43300), *Staphylococcus aureus* (ATCC 29213), and *Pseudomonas aeruginosa* (ATCC 27853) respectively. Leaf and stem hexane extracts showed considerable activity against *B. subtilis* and MRSA. Conversely, *E. coli*, MRSA, *S. aureus*, and *P. aeruginosa* displayed resistance or minimal activity at relatively low concentrations. These results suggest that the extracts of *T. ventricosa* have a substantial antibacterial activity that justifies its use in traditional medicine. Further studies should be considered to establish the full pharmacological potential of this species.

Keywords: Alkaloids; Antibacterial activity; Chemical composition; Extract; GC-MS.

4.1 Introduction

Natural compounds synthesized from medicinal plants are regularly used as an alternate source of medicine (Nicola et al., 2013; Silveira et al., 2017). Plant metabolites are categorized into primary and secondary metabolites based on their relative function (Figueiredo et al., 2008). Primary metabolites often contribute to the growth and development of plants whereas, secondary metabolites serve to deter herbivores, pathogens, and microbes, and most importantly, contain valuable therapeutic properties (Shakya, 2016). These curative benefits are habitually attributed to an array of molecules that act synergistically on targeted elements of complex cellular pathways and thus are more effective than modern allopathic medicine (Garga and Das, 2017). According to the World Health Organization (WHO) approximately 70%-80% of the world's population relies on non-conventional sources of traditional medicine. Since an estimate of 25% of modern medicine is derived from higher plants, screening medicinal plants to establish their chemical composition and evaluate prospective pharmacological activity is necessary (Akerele, 1993; Vijayan et al., 2007; Garga and Das, 2017;WHO, 2018).

Recently, the human population has been severely impacted by the rise of infectious diseases which has often been associated with the persistent resistance of antibiotic pathogens such as *Staphylococcus aureus, Micrococcus sp., Klebsiella pneumoniae, Pseudomonas aeruginosa, Proteus mirabilis, Enterococcus faecalis, Bacillus subtilis, Saccharomyces cerevisiae A, Candida albicans, Candida tropicalis* and several more (Marathe et al., 2013). Thus, various research fields such as phytochemistry and pharmacology must constantly discover and improve valuable sources of innovative biologically active compounds from medicinal species. These advancements in phytotherapeutic medicine are crucial in our dynamic world (Calixto, 2000; Marinho et al., 2016).

The species of Apocynaceae and genus *Tabernaemontana* have been extensively investigated due to their profuse source of alkaloids (Marathe et al., 2013; Silveira et al., 2017). According to Marinho et al. (2016), monoterpene indole and bisindole alkaloids are major alkaloids within the genus among other compounds such as terpenes, lactones, steroids, phenolics, and flavonoids. A few major bioactive compounds within the genus include vobasine, isovoacangine, voachalotine (*Tabernaemontana catharinensis*), 16-epi-affinine, coronaridine-hydroxyindolenine, voacristine, hydroxyindolenine (*Tabernaemontana divaricata*), and apparicine, dregamine, vobasine, dregamine (*Tabernaemontana elegans*) (Marinho et al., 2016; Silveira et al., 2017; Naidoo et al., 2021). Studies have shown that these chemical constituents possess a range of biological activity which include antimicrobial, antioxidant, anti-inflammatory, anticholinesterase, anticancer, antidiabetic, antivenom, larvicidal, antihypertensive

action, wound healing, and analgesic effects (Marinho et al., 2016; Silveira et al., 2017; Athipornchai et al., 2018; Naidoo et al., 2021).

Tabernaemontana ventricosa Hochst. ex A.DC., commonly known as the "Forest toad tree," is a medium-sized latex bearing tree (Schmidt et al., 2002), that is native to South Africa and displays a disjunct distribution in Nigeria, Ghana, and Kenya (Schmelzer and Gurib-Fakim, 2008). Traditionally, latex is often applied to wounds and sore eyes to promote healing, and reportedly cause male/female infertility (urethritis and orchitis), whereas decoctions using fresh or powdered leaf and stem material are consumed to reduce hypertension and fever (Kokwaro, 1976; Schmelzer and Gurib-Fakim, 2008; Mehrbod et al., 2018). Additionally, according to Van Beek et al. (1984), the latex and the leaves contain significant antiamoebic activity. Andima et al. (2021) have indicated that several isolated compounds from the root bark, stem bark, and leaves of *T. ventricosa* have displayed substantial antileishmanial and cytotoxic activity. However, despite the confirmation of several bioactive compounds within the genus, there remains a variety of under-studied species, such as *T. ventricosa* which is yet to be explored for its chemical composition and biological activity. Considering the inadequate and outdated studies associated with *T. ventricosa*, the present study investigated the organoleptic characters, elemental composition, phytochemical compounds, and antibacterial potential of the crude leaf, stem, and latex extracts of *T. ventricosa*.

4.2 Materials and Methods

4.2.1 Plant and exudate collection

The leaves, stems, and latex from fully grown *T. ventricosa* plants (~ 12-15 m in height) of wild origin were collected from the University of KwaZulu-Natal (Westville campus), South Africa, located at 29˚49′03.3″S 30˚56′32.7″E. A combination of emergent, young, and mature leaves and stems were collected for analysis. The plant material and exudate were taxonomically identified, and a voucher specimen (18222) was deposited at the Ward herbarium, School of Life Sciences, University of KwaZulu-Natal. The plant material was inspected for any signs of microbial and fungal contamination and the leaves and stems were separately air-dried for three months at 23˚C, and thereafter ground at high speed into a fine powder using a grinder (Mellerware, Model: 29105). The powdered material was kept in an airtight consol^{TM} glass jar, out of direct sunlight, at 23˚C, until further use. The latex exudate was aseptically collected by careful incisions in the soft stems of the plant with a sharp blade. The latex was diluted in distilled water (1:1; *v/v*), and the sample was centrifuged at 5000 rpm/ref for 10 min using an Eppendorf centrifuge (Model: 5415R, USA). The pellet was removed, and the supernatant was stored at -8˚C until further use.

4.2.2 Organoleptic evaluation

Organoleptic examinations were performed using powdered leaf, stem, and latex samples. The samples were evaluated using the following characters: state, appearance, colour, and odour.

4.2.3 Fluorescence analysis

Various reagents were used to determine the fluorescence activity of the powdered leaf, stem, and latex samples. For the analysis, approximately 0.1 g of powdered plant material was placed onto clean glass slides and combined with two drops of the respective reagents. The mixtures were allowed to stand for 3 min for absorption. Samples were viewed using NIS-Elements D imaging software, and images were captured on the Nikon Eclipse 80i light compound microscope (Nikon, Japan), equipped with a Nikon DS-Fi1 camera under brightfield light (visible) and ultraviolet illumination (UV-2A) ranging from 330-380 nm. The following reagents were used for analysis: Powder + water (H_20), powder + sulphuric acid (H_2SO_4), powder + acetic acid, powder + sodium hydroxide (NaOH), powder + hydrochloric acid (HCl), powder + ethanol (EtOH), powder + ethyl acetate, powder + hexane, powder + chloroform, powder + methanol, powder + petroleum ether, powder + diethyl ether and powder + acetone (Ankad et al., 2015; Azhagumadhavan et al., 2019).

4.2.4 Energy-Dispersive X-ray analysis (EDX)

Energy-Dispersive X-ray analysis was conducted on powdered leaf, stem, and latex samples harvested from *T. ventricosa*. The leaf and stem material were procured during phytochemistry, prior reflux extractions. Fresh latex samples were collected aseptically and subjected to liquid nitrogen slush (-210˚C) and freeze-dried in an Edward's Modulyo EPTD3 freeze-dryer for 72 h. The freeze-dried samples were crushed using a mortar and pestle. The fine powder was placed onto carbon tape and attached to aluminum stubs. The stubs containing samples were sputter-coated with gold (*ca*. 25 nm) in a Quorum 150 RES. Samples were analyzed using the Aztec Analysis Software (Oxford Instruments, UK) on Ultra Plus FEGSEM (Carl Zeiss, Germany) at 5 kV to determine the elemental composition.

4.2.5 Phytochemistry

The powdered material (leaves and stems) was extracted separately by a reflux extraction in hexane at a ratio of 10 g of plant material to 100 mL of solvent. A sequence of four extractions (3 h each) was performed using a heated mantle at approximately 60˚C. The extracts were filtered separately after each extraction using filter paper (Whatman No. 1). Fresh hexane was added to the apparatus (round bottom flasks) containing leaf and stem material, respectively, for additional extractions. The reflux extraction was repeated with chloroform and methanol.

4.2.5.1 Evaporation and concentration

Following extractions, the leaf and stem extracts and latex supernatants were entirely air-dried in a well-ventilated dark room (~23˚C) for approximately 30 days. The dried extracts were stored in airtight glass bottles at 4˚C. The percentage yield of the extracts was calculated as follows:

$$\text{Extract yield (\%)} = \frac{\text{Weight of dried extract (g)}}{\text{Weight of powdered material (g)}} \times 100 \quad \textbf{(4.1)}$$

4.2.6. Qualitative phytochemical analysis

Qualitative phytochemical analysis of the leaf, stem, and fresh latex extracts obtained from *T. ventricosa* were performed according to standard protocols (Tiwari et al., 2011; Tiwari and Husain, 2017).

4.2.6.1 Test for Carbohydrates

- **Molish's test**

  One drop of alcoholic α-naphthol solution was added to 1 mL of extract. The mixture was well-shaken, and a few drops of concentrated sulphuric acid was added. The formation of violet rings indicated the presence of carbohydrates.

- **Benedict's test**

  A few drops of the extract were combined with 1 mL of Benedict's reagents. The solutions were mixed and heated in a water bath at 60˚C for 2 min. A distinctive orange-red precipitate indicated the presence of reducing sugars.

- **Fehling's test**

  A few drops of Fehling's A and B solutions were added to 5 mL of the extracts and heated in a water bath at 60˚C. The formation of a red precipitate was indicative of reducing sugars.

4.2.6.2 Test for Amino acids

- **Ninhydrin test**

  One drop of Ninhydrin solution was added to 1 mL of extract. A purple colouration indicated the presence of amino acids.

4.2.6.3 Test for Alkaloids

- **Mayer's test**

Extracts (2 mL) were treated with a few drops of Mayer's reagents. The formation of a yellow-coloured precipitate confirmed the presence of alkaloids.

- **Wagner's test**

Extracts (2 mL) were treated with Wagner's reagent. A brown-reddish precipitate indicated the presence of alkaloids.

- **Dragendroff's test**

A few drops of extract (2 mL) were treated with Dragendroff's reagent. A red precipitate confirmed the presence of alkaloids.

4.2.6.4 Test for Flavonoids

- **Lead acetate test**

A few drops of 5% lead acetate solution were added to 5 mL of extract. A thick cloudy white precipitate indicated the presence of phenolic compounds.

4.2.6.5 Test for Saponins

- **Froth test**

A few drops of extract (2 mL) were diluted with distilled water and made up to 20 mL. The suspension was hand-shaken in a test tube for 15 min. The formation of a 1 cm layer of white foam indicated the presence of saponins.

- **Foam test**

The extract (1 mL) was vigorously shaken with 2 mL of water. The persistence of a white foamy layer for 10 min indicated the presence of saponins.

4.2.6.6 Test for Sterols

- **Sterol test**

Extracts (1 mL) were treated with 3 mL chloroform. A few drops of sulphuric acid were added to the side of the test tube. The mixture was shaken (10 min) and allowed to stand. The formation of red rings and a green fluorescence ring below indicated a positive test for cholesterol.

4.2.6.7 Test for Steroids

- **Chloroform test**

The extracts (1 mL) were treated with 2 mL chloroform and 3 mL concentrated sulphuric acid. The formation of a red colour layer indicated the presence of steroids.

4.2.6.8 Test for Phenols

- **Ferric chloride test**

Extracts (2 mL) were treated with four drops of ferric chloride. Distinctive green rings or the formation of a bluish-black precipitate indicated a positive test for phenols.

4.2.6.9 Fixed fats and oils

- **Filter paper test**

One drop of the extract was pressed between two pieces of filter paper (Whatman no. 1). The presence of oil stains indicated a positive test for fixed fats and oils.

4.2.7 Thin-Layer Chromatography (TLC)

Leaf and stem crude extracts were evaluated using TLC for the separation of chemical compounds. Separate beakers were used to resuspend 5 mg of leaf and stem concentrated crude extracts in 5 mL of hexane, chloroform, and methanol solvent, respectively. The dissolved crude extracts were separately filtered using Whatman No.1 filter paper. Glass capillaries were used to spot a drop of each of the sample solutions onto pre-coated silica gel 60 F_{254} TLC plates (Biolab, Merck). The plates were developed in a beaker containing a solvent system of 9.5 mL toluene, 0.7 mL ethyl acetate, and 0.3 mL formic acid. The solvent system was allowed to run up the plate (8.5 cm). The plates were viewed, and images were captured under UV light at wavelengths 254 nm and 366 nm. Subsequently, the plates were sprayed with an anisaldehyde-sulphuric acid solution and heated in an oven at 105˚C for 5 min. Images were taken in visible light. The retention factor (*Rf*) values were calculated as follows:

$$Rf = \frac{\text{Xsample}}{\text{Xsolvent}} \quad \textbf{(4.2)}$$

Where X_{sample} = distance travelled by substance

$X_{solvent}$ = distance travelled by solvent front.

4.2.8 Gas Chromatography-Mass Spectrometry (GC-MS)

Leaf and steam extracts dissolved in the respective analytical reagent (AR) solvents (hexane, chloroform, and methanol) and latex extracts were subjected to filtration using Whatman filter paper No. 4. For further filtration, the extracts were filtered through a 0.22 µM membrane filter. The analyses of the extracts were performed using a GC-MS (QP-2010 Ultra Shimadzu, Japan) instrument, equipped with a DB-5MS capillary column (0.25 µM internal diameter and 0.25 µM film thickness) with a dimension of 30 m in length. Helium was used as the carrier gas at 44.9 kPa, with a total flow rate of 4.9 mL/min and a linear velocity of 36.7 $cm.sec^{-1}$ at a purge flow rate of 3.0 mL/min. The injection volume ratio was 1:0. The injection port temperature was 250˚C, and the column temperature was programmed at 50˚C and held for 1 min, and thereafter set to rise to 310˚C. The running time of the sample was 10 min. An 8 µL injection volume was used in split-less injection mode. The compounds of interest were externally evaluated by comparison with previous literature and the mass spectral search program affiliated with the National Institute of Standards and Technology, USA (NIST 07) database.

4.2.9 Antibacterial assay

4.2.9.1 Sample preparation

Stock solutions of the plant crude extracts (hexane, chloroform, and methanol) from the leaves and stems were prepared by resuspending 1 mg of concentrated crude extract in 1 mL of 10% dimethylsulfoxide (DMSO), respectively. Previously collected and prepared latex was adjusted to 1 mg/mL. The various stock solutions (1 mg/mL) for respective treatments were homogenized using a vortex (Model:VM-1000, Taiwan). Thereafter, stock solutions of each plant extract were reconstituted in 10% DMSO to concentrations ranging from 3.125, 6.25,12.5, 25, 50, to 100 mg/mL.

4.2.9.2 Microorganisms

The extracts were screened for antibacterial activity against three gram-positive bacterial strains *Bacillus subtilis* (ATCC 6653), *Methicillin-resistant Staphylococcus aureus* (MRSA) (ATCC 43300), *Staphylococcus aureus* (ATCC 29213), and two gram-negative bacterial strains *Escherichia coli* (ATCC 25922) and *Pseudomonas aeruginosa* (ATCC 27853).

4.2.9.3 Antibacterial screening

In vitro antibacterial screening of the extracts was conducted using the agar disc diffusion technique as per the Clinical and Laboratory Standards Institute (CLSI) guidelines (2006). Sterile Whatman filter paper No. 1 discs were prepared (diameter 6 mm) and impregnated with 20 µL of the respective extract concentrations (3.125, 6.25,12.5, 25, 50,100 mg/mL) and dried at room temperature for 1 h before use (Marathe et al., 2013). Bacterial strains were aseptically cultured at 37˚C overnight on Mueller- Hinton (MH) agar media (Biolab, Merck). After 18-24 h a loopful of bacteria were resuspended in test tubes containing autoclaved (Model: HL-340, Temp.: 121-132˚C, Pres.: 127 kg/cm^2, Taiwan) distilled water and vortexed (Model:VM-1000, Taiwan) to ensure the solutions were standardized. An optical density (OD) of the bacterial strains equivalent to 0.5 McFarland turbidity standard (OD 0.08 - 0.1 at λ 625 nm) was assessed using a UV-vis spectrophotometer (Agilent Technologies Cary 60 spectrophotometer, USA). An ideal OD was archived after further dilution of the inoculum with sterile water.

Sterile cotton swabs were used to streak (4 quadrants) the inoculum over the entire surface of the agar. The prepared discs containing extracts were carefully placed onto the agar using sterile forceps. The plates were incubated at 37˚C and after 18-24 h, the zones of growth inhibition were examined to determine the antibacterial activity of the relative extracts. The screening was done in triplicate with streptomycin (gram-positive) and gentamicin (gram-negative) used as the standard antibacterial positive controls, and 10% DMSO without plant extracts was used as the negative control. The zones of inhibition were measured (mm), recorded, and averaged, and images of the plates were captured. The following criteria was used to assess the zone of inhibition or resistance to extracts, No activity = (0 mm); Slight activity = (1-6 mm); Moderate activity = (>7 or <9 mm); Significant activity = (>9mm). R = Resistant.

4.2.10 Statistical analyses

The results were presented as means ± standard deviation, n = 3. Statistical analyses were performed using R Statistical computing software of the R Core Team, 2020, version 3.6.3, followed by Tukey's honest significant difference range *post hoc* tests (*P <0.05).

4.3 Results and Discussion

4.3.1 Organoleptic characterization

The consistent usage of medicinal plants in experimental investigations has highlighted the importance of quality control in formulating natural products (Tatiya et al., 2012; Singh et al., 2014). During the quality control process, various parameters such as sample quality, purity, and authentication are examined however, there are several concerns related to the lack of stringent medicinal plant profiling techniques (Verma and Singh, 2008; Singh et al., 2014). Due to the underlying issues regarding quality control processes, these developments must undergo standardization to ensure a broad acceptance of medicinal plant-based products during clinical application (Patil et al., 2012; Akbar et al., 2014; Aslam and Afridi., 2018). The study examined the organoleptic characters of leaf, stem, and latex powders of *T. ventricosa* as a baseline to ensure the acceptance of the present species in modern medical systems. This procedure is basic, cost-effective, and provides the proper identity of plant material before in-depth chemical analyses (Patil et al., 2012). The organoleptic evaluation of all plant samples was performed using the following characters: state, texture, colour, and odour (Table 4.1). The leaf powder was dark green in colour, fine-textured, and emitted a slight odour. The stem powder displayed a pale yellow-green colouration, with a fibrous/rough texture and a slight odour. Whereas the latex powder exhibited a white-cream colour, with a grainy texture and aromatic odour. The results indicated that the plant material is safe for consumption and should not cause any adverse effects.

Table 4.1: Organoleptic characters of the powdered leaves, stems, and latex samples of *T. ventricosa.*

Plant samples	State	Texture	Colour	Odour
Leaves	Powder	Fine	Dark green	Characteristic
Stems	Powder	Fibrous	Yellow green	Characteristic
Latex	Powder	Grainy	Whitish cream	Characteristic

4.3.2. Fluorescence analysis

Fluorescence analysis using powdered plant material is another simple, affordable, and widely accepted method for pharmacognostic assessments (Zhao et al., 2011; Aslam and Afridi., 2018). The fluorescence features of the leaf, stem, and latex powder of *T. ventricosa* were analyzed using brightfield (visible) and UV-light (330-380 nm). A variety of reagents were used to determine the characteristic reactions of the various solvent properties (Table 4.2). The powdered plant material displayed different colour reactions when treated with specific reagents and observed using brightfield

or UV-light (Figure 4.1). These unique features are essential for evaluating possible plant-based drugs (Tatiya et al., 2012).

Table 4.2: Fluorescence analysis of the powdered leaves, stems, and latex samples of *T. ventricosa.*

Treatment	Plant sample					
	Leaves		Stems		Latex	
	Bright/visible light	**UV-light**	**Bright/visible light**	**UV-light**	**Bright/visible light**	**UV-light**
Powder only	Green and brown	Fluorescent blue, green, and reddish	Brown and green	Fluorescent blue and red	Light brown	Fluorescent blue
Powder + H_20	Dark green	Red and blue	Green	Fluorescent blue and red	Light grey	Fluorescent blue
Powder + H_2SO_4	Orange-red and black	Red and blue	Red and black	Fluorescent blue and red	Orange-red	Fluorescent blue and green
Powder + Acetic acid	Brown	Light Fluorescent blue-green	Greenish-yellow	Light blue fluorescent	Grey	Dark blue
Powder + Aqueous NaOH	Medium green	Fluorescent blue-green	Green and brown	Fluorescent blue and red	Brown	Fluorescent blue
Powder + HCl	Medium green	Greenish blue	Brown	Fluorescent blue	Creamy white	Blue
Powder + Ethanol	Dark green to black	Red, blue-green	Dark brown	Fluorescent blue and red	Greyish brown	Fluorescent blue
Powder + Ethyl acetate	Dark green to black	Red, blue, and green	Brownish-green	Fluorescent red and blue	Greyish brown	Fluorescent blue
Powder + Hexane	Dark green to black	Blue, red, and green	Greenish brown	Fluorescent blue, green, and red	Greyish brown	Fluorescent blue
Powder + Chloroform	Greenish black	Red, blue, and green	Brown	Fluorescent red, blue, and black	Greyish	Fluorescent blue
Powder + Methanol	Greenish black	Blue-green and red	Brown	Fluorescent blue and red	Brown	Cloudy fluorescent blue
Powder + Petroleum ether	Greenish brown	Blue-green and red	Brown	Fluorescent blue-green and red	Brown	Fluorescent blue
Powder + Diethyl ether	Dark green	Blue-green and red	Yellow-brown	Fluorescent blue and red	Greyish-brown	Cloudy fluorescent blue
Powder + Acetone	Dark green-black	Blue and green	Dark brown	Fluorescent red and blue	Dark-grey	Fluorescent blue

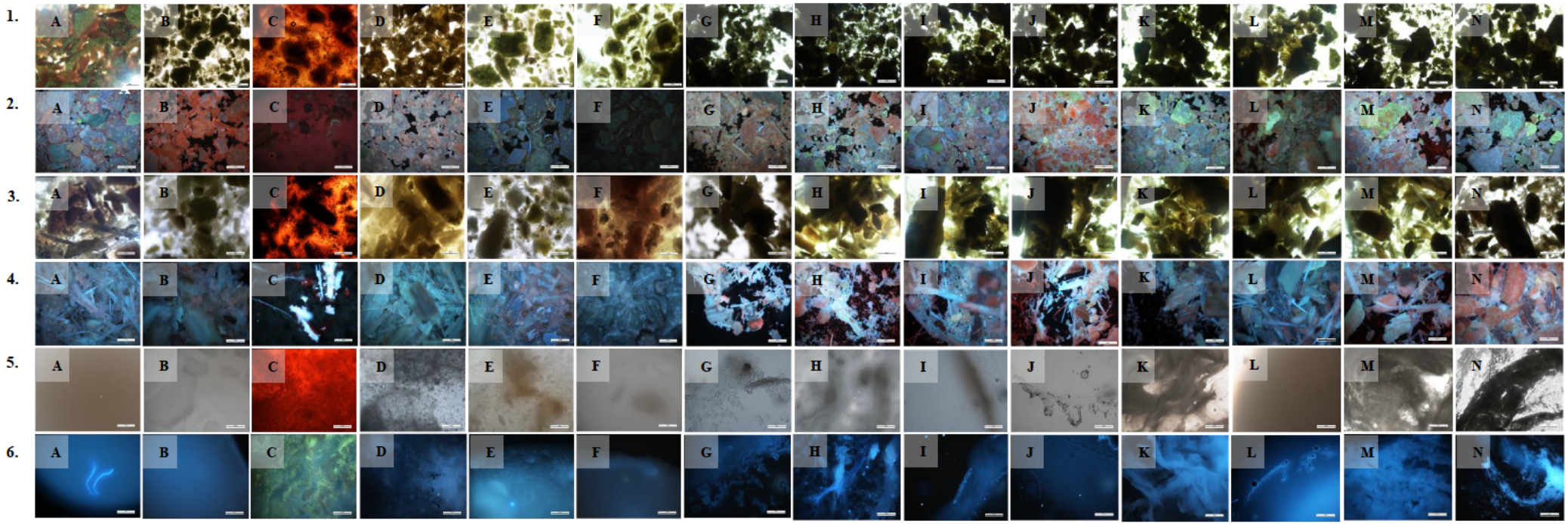

Figure 4.1: Fluorescence analysis using powdered leaf, stem and latex samples of *T. ventricosa* (n=3) (1) Leaves brightfield; (2) Leaves UV-light; (3) Stems brightfield; (4) Stems UV-light; (5) Latex brightfield; (6) Latex UV-light; (A) Powdered plant material only; (B) Powdered plant material + water (H_20); (C) Powdered plant material + sulphuric acid (H_2SO_4); (D) Powdered plant material + acetic acid; (E) Powdered plant material + sodium hydroxide (NaOH); (F) Powdered plant material + hydrochloric acid (HCl); (G) Powdered plant material + ethanol (EtOH); (H) Powdered plant material + ethyl acetate; (I) Powdered plant material + hexane; (J) Powdered plant material + chloroform; (K) Powdered plant material + methanol; (L) Powdered plant material + petroleum ether; (M) Powdered plant material + diethyl ether; (N) Powdered plant material + acetone.

4.3.3 Energy-Dispersive X-ray (EDX) analysis

The elemental composition of powdered leaf, stem, and freeze-dried latex was examined using EDX analysis. The results displayed in Table 4.3 and Figure 4.2 showed the variable elemental composition across the powdered leaf, stem, and freeze-dried latex of *T. ventricosa* . Minor amounts of sulfur (S), magnesium (Mg), copper (Cu) manganese (Mn), and oxygen (O_2) (usually <10% of relative element X-ray intensity of the sample) which are regarded as essential trace elements in plants (Pachauri et al., 2013) are displayed on Table 4.3. The slight intensity of potassium (K) (0.45%) in latex could be associated with the osmotic adjustments of the contents within laticiferous cells (Bouteau et al., 1993; Okubo and Utsunomiya, 1996; Mahouachi, 2009). The high intensities of calcium (Ca) shown in Table 4.3 and illustrated in Figure 4.2 could be attributed to the presence of calcium crystals within the plant and latex samples (Dassanayake and Larkin, 2017).

Table 4.3: Average percentage of the elemental composition of powdered leaf, stem, and freeze-dried latex of *T. ventricosa*.

Elements	**Elemental composition %**		
	Leaves	**Stems**	**Latex**
Carbon di-oxide	53.00 ± 7.93	73.21 ± 20.56	70.69 ± 5.51
Oxygen	35.71 ± 6.31	23.83 ± 16.77	21.34 ± 0.49
Magnesium	0.58 ± 0.10	0.25 ± 0.35	0.63 ± 0.08
Sulphur	0.81 ± 0.00	00.00 ± 0.00	2.39 ± 1.59
Potassium	0.80 ± 0.00	2.35 ± 3.15	0.45 ± 0.39
Calcium	7.57 ± 0.33	0.20 ± 0.28	3.49 ± 3.04
Manganese	0.00 ± 0.00	00.00 ± 0.00	0.49 ± 0.45
Copper	0.00 ± 0.00	0.67 ± 0.69	0.51 ± 0.53

Values represent mean ± SD (n = 3)

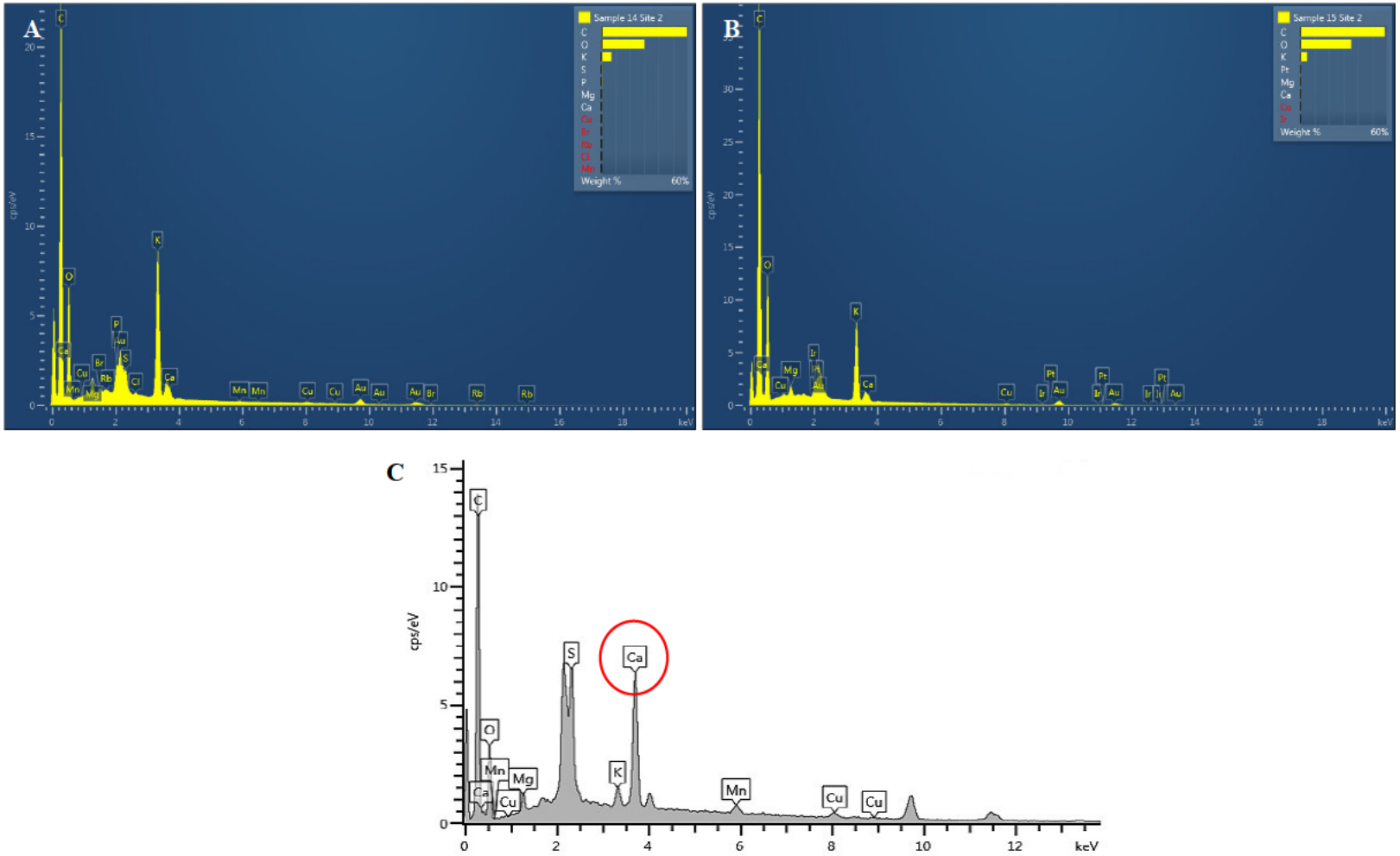

Figure 4.2: An EDX spectrum showing the elemental composition of powdered leaf, stem, and freeze-dried latex of *T. ventricosa*. (A) Powdered leaf; (B) Powdered stem; (C) Freeze-dried latex.

4.3.4 Extract yield

The methanol leaf extracts displayed the highest extract percentage yield, followed by the methanol stem extracts (Table 4.4). In contrast, the hexane stem and leaf extracts showed the lowest percentage yield, respectively. Overall, a higher percentage yield was observed in the crude extracts from the leaves compared to the stems (Table 4.4). Furthermore, the percentage yield of the latex extract was similarly high (15%). These observations suggest the presence of several polar compounds in the leaves and latex compared to the stems, specifically within the methanol extracts (Akwu et al., 2019).

Table 4.4: Percentage yield of the leaves, stems, and latex of *T. ventricosa*.

Crude extracts	**Leaves**	**Stems**	**Latex**	**Leaves**	**Stems**	**Latex**
	Dried extract yield (g)			**Yield (%)**		
Hexane	0.05	0.04	0.15	5.28	4.36	15.00
Chloroform	0.08	0.07		8.78	7.28	
Methanol	0.20	0.18		20.17	18.64	

4.3.5 Phytochemical Characterization

Tabernaemontana ventricosa is often used ethnomedicinally in South Africa to treat various ailments and has been reported to possess a variety of medicinal properties (Schmidt et al., 2002; Pratchayasakul et al., 2008; Mehrbod et al., 2018; Andima et al. 2021). In the current study, the extracts of *T. ventricosa* leaves, stems, and latex were screened to detect phytochemical constituents. Qualitative phytochemical screening confirmed the presence of various compound groups. Positive results were observed in the leaf and stem crude extracts for carbohydrates, amino acids, alkaloids, flavonoids, saponins, sterols, steroids, phenols and fats, and fixed oils (Table 4.5). In comparison, the latex extracts yielded negative reactions for sterols, steroids, and phenols (Table 4.5). Previous phytochemical investigations of *Tabernaemontana* species have detected triterpenes, steroids, sterols, flavonoids, phenyl propanoids, phenolics, and alkaloids (Cardoso et al., 1998; Mederios et al., 2001; Chattipakorn et al., 2007). Compared to the literature, the current phytochemical analysis of *T. ventricosa* crude extracts is similar to the chemical composition of other *Tabernaemontana* species (Van Beek et al., 1984; Basavaraj et al., 2011; Pallant et al., 2012; Marques et al., 2018).

According to Silveira et al. (2017), species within *Tabernaemontana* are popularly used for their high production of indole alkaloids that are often biologically active. The results presented in Table 4.5 display high-intensity reactions for most alkaloid tests using various crude leaf and stem, and latex extracts. The overall observations of the present phytochemical analysis correspond to the first phytochemical investigation on *T. ventricosa* (Schripsema et al., 1986). In a study by Schripsema et al. (1986), the ethanol extract of the stem bark yielded an extent of triterpenes in the first fractionations; however, latter fractionations showed several alkaloidal components. These compounds could be attributed to the traditional usage of the leaves, bark, stems, and latex to treat hypertension, fever, and lesions (Schmelzer and Gurib-Fakim, 2008).

As shown in Table 4.5, many of the extracts tested for saponins, sterols, and steroids showed relatively intense colour reactions. These compounds exhibit antimicrobial, antifungal, anti-inflammatory, antioxidant, and antitumour properties (Desai et al., 2009; Singh et al., 2012; Patel and Savjani, 2015). Furthermore, the phytochemical constituents such as flavonoids, phenols, fixed fats, and oils, did not display significantly intense reactions comparable to other compound groups. Despite their slightly positive reactions, studies have characterized these secondary metabolites as bioactive compounds that display anti-inflammatory, antimicrobial and antioxidant activities (Thombre et al., 2013; Tiwari and Husain., 2017; Athipornchai, 2018).

4.3.6 Thin Layer Chromatography

An effort was made to preliminarily analyze the separation of various phytochemical compound groups of *T. ventricosa*. The separation of bands is shown in Figure 4.3 A-C. The visualization of the various bands was done using UV-light at 366 nm and after exposure to anisaldehyde-sulphuric acid, thereafter they were viewed in visible light. The highest number of bands under UV-light at 366 nm was seen in stems extracted with hexane, followed by stems extracted with chloroform. The increased number of bands visible at various wavelengths suggests the ideal separation of phytochemical compounds (Francis and Sudha, 2017). Similarly, plates viewed using visible light showed a higher number of bands for stems extracts than leaf extracts (Figure 4.2 C). According to Pallant et al. (2012), there is significant scope for TLC data available on several *Tabernaemontana* species. From the results of the TLC profile of the crude extracts and *Rf* values (Table 4.6), the majority of the compounds observed in stem extracts were polar *Rf* <0.2, whereas many polar compounds *Rf* >0.2 are shown in leaf extracts. Due to the thermolability and low volatility of polar compounds, there are limitations in the analysis of these compounds using GC-MS analysis (Cardoso et al., 1988; Iwasaki et al., 2012).

Table 4.5: Qualitative phytochemical screening of various crude leaf, stem, and latex extracts of *T. ventricosa.*

Compound group	Phytochemical tests	Leaves			Stems			Latex
		Hexane	Chloroform	Methanol	Hexane	Chloroform	Methanol	
Carbohydrates	Molish's	++	++	+	++	+	+	++
	Benedict's	+	++	-	+	+	-	+
	Fehling's	-	++	++	-	++	++	+
Amino acids	Ninhydrin	-	-	++	-	-	++	+
Alkaloids	Mayer's	+	++	++	++	++	+	+
	Wagner's	++	++	++	++	++	+	++
	Dragendroff	++	++	+	++	++	+	+
Flavonoids	Lead acetate	-	-	++	-	-	++	++
Saponins	Froth	++	++	++	++	++	+	++
	Foam	++	++	++	++	++	+	+
Sterols	Sterol	++	++	+	++	++	-	-
Steroids	Chloroform	++	++	+	++	++	-	-
Phenols	Ferric chloride	+	+	+	-	+	+	-
Fixed fats and oils	Filter paper	++	-	+	++	-	+	++

Legend: Intense reaction = (++); *slight reaction* = (+); *no reaction* = (-), (n = 3).

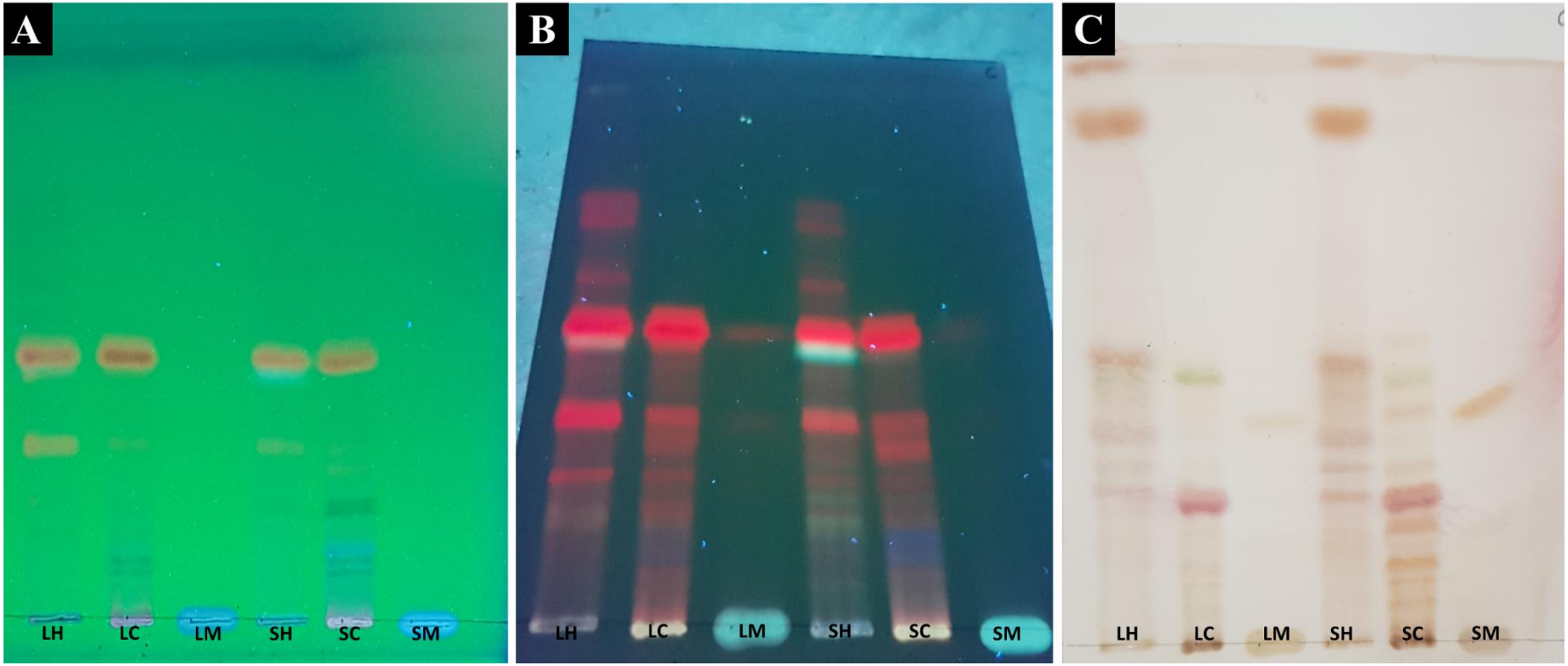

Figure 4.3: Thin Layer Chromatography (TLC) plates separating major phytochemical compound groups in hexane, chloroform, and methanolic leaf and stem crude extracts. Plate (A) Viewed at 254 nm; (B) Viewed at 366 nm; (C) Viewed after spraying with an anisaldehyde-sulphuric acid solution. Abbreviations: LH = Leaf hexane; LC = Leaf chloroform; LM = Leaf methanol; SH = Stem hexane; SC = Stem chloroform; SM = Stem methanol (SM).

Table 4.6: Thin layer chromatography profile of *T. ventricosa* leaf and stem crude extracts with *Rf* values.

	***Rf* values of crude extracts (mm)**					
	Leaves			**Stems**		
Bands	**Hexane**	**Chloroform**	**Methanol**	**Hexane**	**Chloroform**	**Methanol**
1	0.26	0.23	0.33	0.26	0.07	0.36
2	0.32	0.45	-	0.31	0.11	-
3	0.38	-	-	0.36	0.14	-
4	0.49	-	-	0.46	0.19	-
5	0.88	-	-	0.89	0.25	-
6	0.98	-	-	0.99	0.31	-
7	-	-	-	-	0.36	-
8	-	-	-	-	0.46	-

4.3.7 Gas Chromatography-Mass Spectrometry

Gas Chromatography-Mass Spectrometry analysis was performed to characterize the major components of the leaf, stem, and latex extracts of *T. ventricosa*, using various solvents (Appendix 1A). The identified compounds according to their retention time, molecular formula, molecular weight, and peak area percentage are presented in Tables 4.7-4.13. The total ion chromatogram of the various extracts is displayed in Figure 4.4. The results indicated the presence of 16, 16, and 6 significant compounds (>1%) in the leaf hexane (LH), leaf chloroform (LC), and leaf methanol (LM) crude extracts, respectively. In contrast, the number of major compounds (>1%) in the stem hexane (SH), stem chloroform (SC), and stem methanol (SM) crude extracts were 15, 16, and 12, respectively. Furthermore, 8 major compounds (>1%) were detected in the latex extracts. In total, approximately 89 major compounds (>1%) were observed in the crude leaf, stem, and latex extracts (Tables 4.7-4.13). The majority of these compounds were detected across all crude extracts. Overall, a more significant number of compounds were observed in the stem crude extracts (42 major compounds) than the leaf crude extracts (38 major compounds). However, the major compounds (>1%) identified from the leaf crude extracts accumulated to total area percentages of 76.11% (LH), 93.56% (LC), and 98.49% (LM), respectively whereas, the stems were marginally lower, displaying a total area percentage of 73.96% (SH), 94.23% (SC) and 98.66% (SM). Approximately 8 compounds were identified in the latex extracts, with a total area percentage of 96.98%.

Various bioactive compounds were identified during the GC-MS analysis. The most significant compounds include, α-linolenic acid (18.75%), 5H-3,5a-epoxynaphth[2,1-c]oxepin, dodecahydro-3,8,8,11a-tetramethyl-, [3Sx3α,5aα,7aα,11aβ,11bα)]- (12.07%) and pentadecanoic acid (9.71%) in the LH extracts (Table 4.7), pentadecanoic acid (20.05%), oxiraneoctanoic acid, 3-octyl-, cis- (14.32%) and 13-docosenamide, (Z)- (12.83%) in the LC extracts (Table 4.8) and α-d-mannofuranoside, methyl

(43.40%), 1,2,3,5-cyclohexanetetrol, (1α,2β,3α,5β)- (27.46%) and 13-docosenamide, (Z)- (12.62%) in the LM extracts (Table 4.9). In the stem extracts, the major compounds were 5H-3,5a-epoxynaphth[2,1-c]oxepin, dodecahydro-3,8,8,11a-tetramethyl-,[3S-(3α,5aα,7aα,11aβ,11bα)]-(18.18%), pentadecanoic acid (10.15%) and 9,12-octadecadienoic acid (Z,Z)- (9.17%) in the SH extracts (Table 4.10), pentadecanoic acid (21.59%), oxiraneoctanoic acid, 3-octyl-, cis- (18.80%) and 13-docosenamide, (Z)- (12.52%) in the SC extracts (Table 4.11) and quinic acid (31.13%), α-d-mannofuranoside, methyl (28.72%) and 3-*O*-methyl-d-glucose (14.99%) in the SM extracts (Table 4.12). In the latex extracts (Table 4.13), substantial compounds were lup-20(29)-en-3-ol, acetate, (3β)-(36.09%), 9,19-cyclolanost-24-en-3-ol, (3β)- (33.28%) and β-amyrin (7.85%). Many compounds were present across majority of the extracts therefore indicating bioactivity in both plant parts and latex.

The above-mentioned, naturally occurring bioactive compounds are likely responsible for the pharmacological activities of several *Tabernaemontana* species, including *T. ventricosa* (Marinho et al., 2016; Silveira et al., 2017; Athipornchai et al., 2018; Naidoo et al., 2021). In South Africa, *T. ventricosa* leaves are often consumed in the form of a decoction to reduce high blood pressure (Schmelzer and Gurib-Fakim, 2008). The antihypertension properties of the leaves of *T. ventricosa* could be attributed to the polysaturated fatty acid compound α-linolenic acid which was detected within the leaf hexane extracts (Pan et al., 2012; Ok et al., 2020). Fatty acids such as α-linolenic acids are crucial since they cannot be produced by the human body and may only be consumed via vegetable products (Barceló-Coblijn and Murphy, 2009; Pan et al., 2012; Ok et al., 2020). Furthermore, α-linolenic acid is known for its range of pharmacological properties, which include neuroprotective, anticarcinogenic, antidepressant, antioxidant, and antihypertension effects (Table 4.14) (Heuteaux et al., 2006; Hennessy et al., 2011; Blondeau et al., 2016; Olushola-Siedoks et al., 2019; Ok et al., 2020; Zhu et al., 2020).

The cyclic ether compound 5H-3,5a-epoxynaphth[2,1-c] oxepin, dodecahydro-3,8,8,11a-tetramethyl-, [3S-(3α,5aα,7aα,11aβ,11bα)] was present in large amounts throughout most extracts (Figure 4.4). This compound displays a clear to pale yellow colouration and radiates powerful amber notes with strong trigeminal effects (Surburg and Panten, 2016; Malik et al., 2016). Moreover, it is well-known for its antitermite and antifungal effects (Malik et al., 2016; Prayitno et al., 2020). The free fatty acid recognized as pentadecanoic acid is often used for its anticancer, antiasthmatic, antiabortive, antimicrobial, and antioxidant properties (Adachi et al., 1993; Patra et al., 2017; Ansarali et al., 2018; Rao et al., 2019). Other uses of pentadecanoic acid include treating male alopecia, heart issues, and a specialized agent for myocardial imaging (Coenen et al., 1981).

Interestingly, α-d-mannofuranoside methyl displayed an excessive potency concerning biological activity. Arora et al. (1994) investigated the deoxy disubstituted derivatives of α-d-mannofuranoside methyl where it displayed significant activity for the treatment of colon and melanoma cancer. In addition, the same study stated that a reduction in skin cell proliferation and an inhibition of the proliferative response of splenic T-lymphocytes were observed. Other properties include anti-inflammatory, antiallergic, antibiotic, antibacterial, and antimycotic activities, in addition to its use in autoimmune disorders, including rheumatoid arthritis, osteoarthritis, psoriasis, atopic dermatitis, scleroderma, and systemic lupus erythematosus, and the auto-immune deficiency (Sattigeri et al., 2009; Kamurthy et al., 2015).

Moreover, it has been reported that the compounds oxiraneoctanoic acid, 3-octyl-, cis-, 13-docosenamide, (Z)-, 9,12-octadecadienoic acid (Z, Z)-, quinic acid and 3-*O*-methyl-d-glucose have been utilized for their significant biological effects such as antimicrobial, antiangiogenic, antinociceptive, antiviral, antifungal, antitumour, antineuroactive, anti-inflammatory, antiacne, antidrogenic, hepatoprotective, antiarthritic, anticoronary, nematicide, insectifuge, antihistaminic, antieczemic, antioxidant, radioprotective, antidiabetic, astringent and glucose transport in normal/ischemic brains, metabolic stability, membrane transport, preservation of mouse sperm, improved desiccation tolerance of keratinocytes, reduced toxicity of streptozotocin and detector in imaging (Table 4.14) (Manilal et al., 2009; Gopalakrishnan et al., 2011; Sudha et al., 2013; Geng et al., 2014; Caprioli et al., 2015; Parthipan et al., 2015; Hussein et al., 2016; Shareef et al., 2016; Chen et al., 2018; ; Rao and Anisha, 2018; Rivlin and Navon, 2018; Liu et al., 2019; Thasneem et al., 2019; Hasan et al., 2019; Fernandes et al., 2019; Mahmoudi et al., 2021).

Furthermore, ibogamine-18-carboxylic acid (voacangine) is an important compound detected in many extracts and is reported to be cytotoxic to tumour cells (Chen et al., 2016). Moreover, other properties of this compound include the psychoactive, hallucinogenic, neurobiological, antiaddictive, cardiac, central nervous system, antidepression, drug detoxification, antitumour, anti-inflammatory, antinociceptive, anticonvulsant, tremorgenic antibacterial, and uterophic effects (Hamdiani et al., 2018; Corkery et al., 2018; Luzuriaga-Quichimbo et al., 2018). The extensive pharmacological effects displayed by compounds detected within the latex extracts demonstrate the importance of latex-bearing species in traditional and modern medicine.

The compounds lupan-3-ol acetate, 9,19-cyclolanost-24-en-3-ol, (3β)-, β-amyrin, and obtusifoliol were distinctively detected in the latex extracts of *T. ventricosa* (Table 4.13). Lupan-3-ol acetate is a triterpenoid and has a variety of uses such as antiprotozoal, antimicrobial, anti-inflammatory, antitumour, antidiabetic, antifungal, antiparasitic, antiviral and infertility effects (Rodeiro et al., 2009;

Murugan et al., 2012; Ogunwole et al., 2017; Rao and Anisha, 2018; Ighodaro et al, 2019). On the other hand, 9,19-cyclolanost-24-en-3-ol, (3β)- is often used for its antibacterial and antilisteria activity (Penduka et al., 2014; Kalita et al., 2018). Furthermore, the compound β-amyrin was found to display several pharmacological properties such as the inhibition of collagen-induced platelet aggregation, antidiabetic, antioxidant, cytotoxicity, anti-inflammatory, analgesic, gastroprotective, anti-Parkinson effects, antifibrotic and antihyperglycemic effects (Aragáo et al., 2006; Aragáo et al., 2015; Ching et al., 2010; Fernandes et al., 2011; Fabiyi et al., 2012; Wagh et al., 2012; Kapewangolo et al., 2017; da Silva Júnior et al., 2017; Nogueira et al., 2019; Kamaraj et al., 2019).

Additionally, the plant sterol compound obtusifoliol was identified in relatively large amounts in the latex extracts of *T. ventricosa*. A similar study conducted by Bailen et al. (2016) also reported obtusifoliol as a key component in the latex of extracts of *Euphorbia officinarum.* In that study, obtusifoliol displayed significant insecticidal, cytotoxic and antiparasitic activity (Bailen et al., 2016). Further uses of this compound include inhibitory effects on Epstein-Barr virus early antigen (EBA-EA) and growth arrest on *Cryptococcus neoformans* (Venkateswarlu, 1996; Tanaka et al., 2000; Aghaei et al., 2016; Bailen et al., 2016).

The results of the present study differ from the initial phytochemical investigation on *T. ventricosa* which was performed by Schripsema et al. (1986). The major alkaloidal components reported in the previous study were 10-hydroxyheyneanine, 16-epi-isositsirikine, apparicine, tubotaiwine, norfluorocurarine, and akuammicine. Furthermore, recently Andima et al. (2021) successfully isolated several compounds from the root bark, stem bark, and leaves of *T. ventricosa*. The identified alkaloidal compounds included 3-ketopropylcoronadine, vobasine, ibogamine, voacristine, 10-hydroxycoronaridine, and 10-hydroxy ibogamine, whereas, the non-alkaloidal compounds were comprised of stigmasterol, quebrachitol, and ursolic acid (Andima et al., 2021). However, in the present study, only the monoterpenoid alkaloids ibogamine, ibogamine-18-carboxylic acid (voacangine), and voaluteine were detected in most extracts (Tables 4.7-4.13). Nevertheless, a considerable amount of various other bioactive compounds was revealed in the GC-MS analysis of the crude stem, leaf, and latex extracts of *T. ventricosa*. According to the results presented in Table 4.14, the identified compounds have been reported to possess significant biological activity, which subsequently supported the ethnomedicinal usage of the latex bearing tree, *T. ventricosa.*

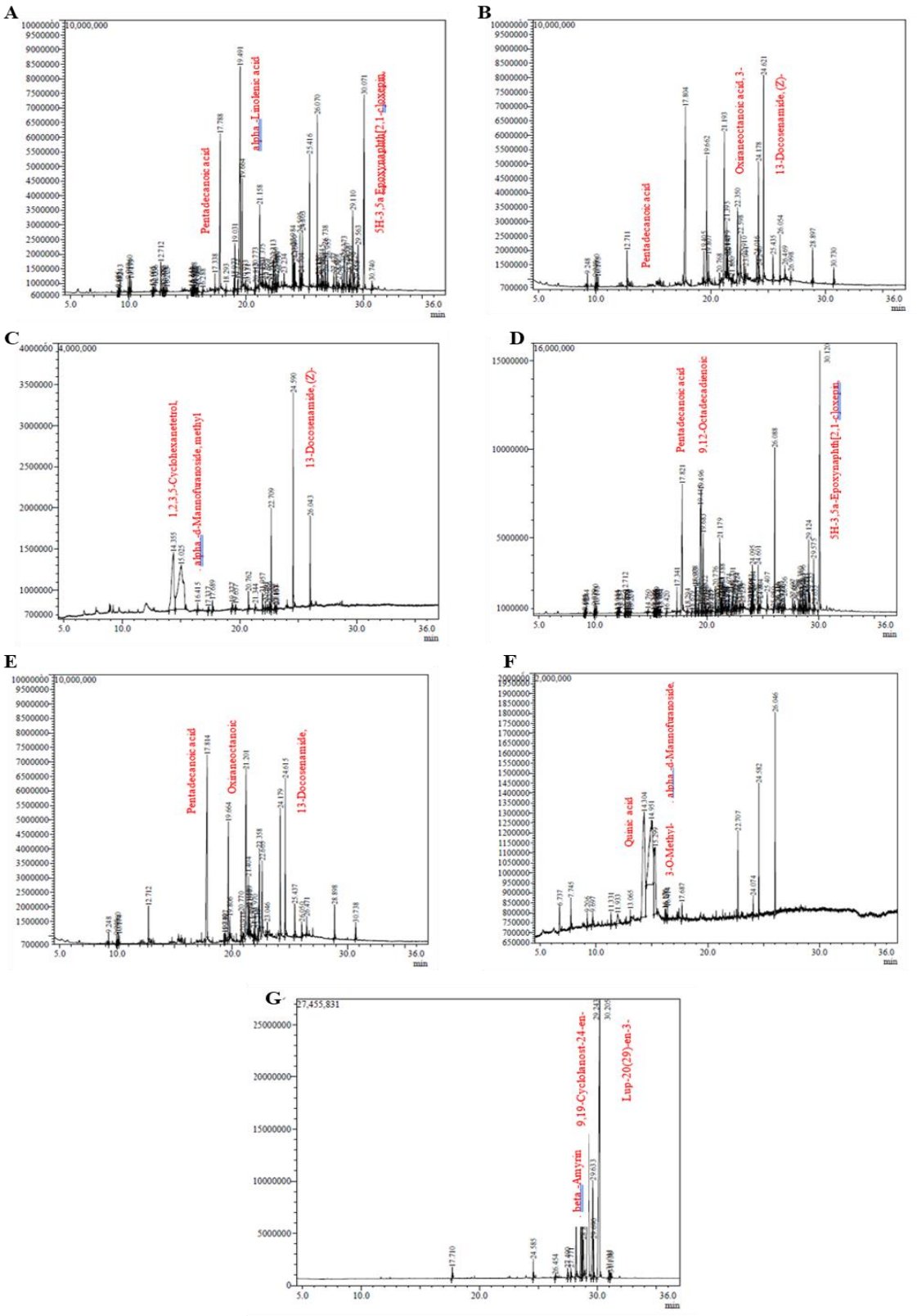

Figure 4.4: Total ion chromatogram of the extracts of *T. ventricosa*. (A) Leaf hexane; (B) Leaf chloroform; (C) Leaf methanol; (D) Stem hexane; (E) Stem chloroform; (F) Stem methanol; (G) Latex.

Table 4.7: Compounds identified in the leaf hexane extracts of *T. ventricosa* using GC-MS.

Peak	Total area %	Compound	Retention time	Molecular formula	Molecular weight	CAS NO.
24	**9.71**	**Pentadecanoic acid**	**17.788**	**$C_{15}H_{30}O_2$**	**242**	**1002-84-2**
27	1.34	Methyl (Z)-5,11,14,17-eicosatetraenoate	19.031	$C_{21}H_{34}O_2$	318	59149-01-8
29	**18.75**	**α-Linolenic acid**	**19.491**	**$C_{18}H_{30}O_2$**	**278**	**463-40-1**
30	4.76	Octadecanoic acid	19.664	$C_{18}H_{36}O_2$	284	57-11-4
35	3.89	cis-Vaccenic acid	21.158	$C_{18}H_{34}O_2$	282	506-17-2
41	1.24	8-Hexadecenal, 14-methyl-, (Z)-	22.313	$C_{17}H_{32}O$	252	60609-53-2
47	1.53	2-methylhexacosane	23.984	$C_{27}H_{56}$	380	0-00-0
48*	0.91	Ibogamine	24.050	$C_{19}H_{24}N_2$	280	481-87-8
50	1.70	13-Docosenamide, (Z)-	24.595	$C_{22}H_{43}NO$	337	112-84-5
52	1.73	Squalene	24.803	$C_{30}H_{50}$	410	111-02-4
53	5.65	Tetratetracontane	25.416	$C_{44}H_{90}$	618	7098-22-8
54	6.18	Ibogamine-18-carboxylic acid, 12-methoxy-, methyl ester	26.070	$C_{22}H_{28}N_2O_3$	368	510-22-5
58*	0.33	Voaluteine	26.580	$C_{22}H_{28}N_2O_4$	384	3306-58-9
61*	0.86	Vitamin E	26.955	$C_{29}H_{50}O_2$	430	59-02-9
66	1.38	β-Sitosterol	28.373	$C_{29}H_{50}O$	414	83-46-5
67	1.09	Lanosterol	28.587	$C_{30}H_{50}O$	426	79-63-0
70	4.03	9,19-Cyclolanost-24-en-3-ol, acetate, (3β)-	29.110	$C_{32}H_{52}O_2$	468	1259-10-5
71	1.06	Acetic acid, 3-hydroxy-7-isopropenyl-1,4a-dimethyl-2,3,4,4a,5,6,7,8-octahydronaphthalen-2-yl ester	29.229	$C_{17}H_{26}O_3$	478	0-00-0
74	**12.07**	**5H-3,5a-Epoxynaphth[2,1-c]oxepin, dodecahydro-3,8,8,11a-tetramethyl-, [3S-(3α,5aα,7aα,11aβ,11bα)]-**	**30.071**	**$C_{18}H_{30}O_2$**	**278**	**1153-34-0**

* Represents *essential* compounds <1% total area.

Table 4.8: Compounds identified in the leaf chloroform extracts of *T. ventricosa* using GC-MS.

Peak	Total area %	Compound	Retention time	Molecular formula	Molecular weight	CAS NO.
5	1.60	Phenol, 2,4-bis(1,1-dimethylethyl)-	12.711	$C_{14}H_{22}O$	206	96-76-4
6	**20.05**	**Pentadecanoic acid**	**17.804**	**$C_{15}H_{30}O_2$**	**242**	**1002-84-2**
7	1.49	cis,cis,cis-7,10,13-Hexadecatrienal	19.405	$C_{16}H_{26}O$	234	56797-43-4
8	9.80	Octadecanoic acid	19.662	$C_{18}H_{36}O_2$	284	57-11-4
9	1.71	Octadecanamide	19.807	$C_{18}H_{37}NO$	283	124-26-5
11	**14.32**	**Oxiraneoctanoic acid, 3-octyl-, cis-**	**21.193**	**$C_{18}H_{34}O_3$**	**298**	**24560-98-3**
12	5.57	9-Octadecenamide, (Z)-	21.395	$C_{18}H_{35}NO$	281	301-02-0
17	5.88	12-Methyl-E,E-2,13-octadecadien-1-ol	22.350	$C_{19}H_{36}O$	280	0-00-0
18	3.79	Hexadecanoic acid, 2-hydroxy-1-(hydroxymethyl)ethyl ester	22.598	$C_{19}H_{38}O_4$	330	23470-00-0
19	1.12	Octadecanoic acid, 9,10-epoxy-, isopropyl ester	22.910	$C_{21}H_{40}O_3$	340	95007-80-0
22	7.82	Octadecanoic acid, 2,3-dihydroxypropyl ester	24.178	$C_{21}H_{42}O_4$	358	123-94-4
24	**12.83**	**13-Docosenamide, (Z)-**	**24.621**	**$C_{22}H_{43}NO$**	**337**	**112-84-5**
25	1.46	7-Methyl-Z,Z-8,10-hexadecadien-1-ol acetate	25.435	$C_{19}H_{34}O_2$	294	0-00-0
26	2.37	Ibogamine-18-carboxylic acid, 12-methoxy-, methyl ester	26.054	$C_{22}H_{28}N_2O_3$	368	510-22-5
29	2.41	Silane, dimethyl(docosyloxy)butoxy-	28.897	$C_{28}H_{60}O_2Si$	456	0-00-0
30	1.34	1,3,5-Cycloheptatriene, 2,4-di-t-butyl-7,7-dimethyl-	30.730	$C_{17}H_{28}$	232	0-00-0

Table 4.9: Compounds identified in the leaf methanol extracts of *T. ventricosa* using GC-MS.

Peak	Total area %	Compound	Retention time	Molecular formula	Molecular weight	CAS NO.
1	**27.46**	**1,2,3,5-Cyclohexanetetrol, (1α,2β,3α,5β)-**	**14.355**	**$C_6H_{12}O_4$**	**148**	**53585-08-3**
2	**43.40**	**α-d-Mannofuranoside, methyl**	**15.025**	**$C_7H_{14}O_6$**	**194**	**4097-91-0**
14	5.31	Diisooctyl phthalate	22.709	$C_{24}H_{38}O_4$	390	131-20-4
18	**12.62**	**13-Docosenamide, (Z)-**	**24.590**	**$C_{22}H_{43}NO$**	**337**	**112-84-5**
19	4.31	1,4-Benzenedicarboxylic acid	24,900	$C_{24}H_{38}O_4$	390	6422-86-2
20	5.39	Ibogamine-18-carboxylic acid, 12-methoxy-, methyl ester	26.043	$C_{22}H_{28}N_2O_3$	368	510-22-5

Table 4.10: Compounds identified in the stem hexane extracts of *T. ventricosa* using GC-MS.

Peak	Total area %	Compound	Retention time	Molecular formula	Molecular weight	CAS NO.
27	**10.15**	**Pentadecanoic acid**	**17.821**	**$C_{15}H_{30}O_2$**	**242**	**1002-84-2**
34	**9.17**	**9,12-Octadecadienoic acid (Z,Z)-**	**19.445**	**$C_{18}H_{32}O_2$**	**280**	**60-33-3**
35	5.74	Dichloroacetic acid, tridec-2-ynyl ester	19.496	$C_{15}H_{24}C_{l2}O_2$	306	0-00-0
37	4.06	Octadecanoic acid	19.683	$C_{18}H_{36}O_2$	284	57-11-4
47	4.39	Oxiraneoctanoic acid, 3-octyl-, cis-	21.179	$C_{18}H_{34}O_3$	298	24560-98-3
59	1.51	13-Tetradecenal	22.331	$C_{14}H_{26}O$	210	85896-31-7
71	1.57	Ibogamine	24.095	$C_{19}H_{24}N_2$	280	481-87-8
74	1.56	13-Docosenamide, (Z)-	24.601	$C_{22}H_{43}NO$	337	112-84-5
79	6.68	Ibogamine-18-carboxylic acid, 12-methoxy-, methyl ester	26.088	$C_{22}H_{28}N_2O_3$	368	510-22-5
82*	0.23	Voaluteine	26.583	$C_{22}H_{28}N_2O_4$	384	3306-58-9
85*	0.43	Vitamin E	26.956	$C_{29}H_{50}O_2$	430	59-02-9
89	1.11	β-Sitosterol	28.380	$C_{29}H_{50}O$	414	83-46-5
91	1.18	Lanosterol	28.596	$C_{30}H_{50}O$	426	79-63-0
96	3.72	9,19-Cycloergost-24(28)-en-3-ol, 4,14-dimethyl-, acetate, (3β,4α,5α)-	29.124	$C_{32}H_{52}O_2$	468	10376-42-8
97	1.37	α-Amyrin	29.235	$C_{30}H_{50}O$	426	638-95-9
98	2.94	4,4,6a,6b,8a,11,11,14b-Octamethyl-1,4,4a,5,6,6a,6b,7,8,8a,9,10,11,12,12a,14,14a,14b-octadecahydro-2H-picen-3-one	29.575	$C_{30}H_{48}O$	424	0-00-0
100	**18.81**	**5H-3,5a-Epoxynaphth[2,1-c]oxepin, dodecahydro-3,8,8,11a-tetramethyl-, [3S-(3α,5aα,7aα,11aβ,11bα)]-**	**30.120**	**$C_{18}H_{30}O_2$**	**278**	**1153-34-0**

* Represents *essential* compounds <1% total area.

Table 4.11: Compounds identified in the stem chloroform extracts of *T. ventricosa* using GC-MS.

Peak	Total area %	Compound	Retention time	Molecular formula	Molecular weight	CAS NO.
5	1.57	Phenol, 2,4-bis(1,1-dimethylethyl)-	12.712	$C_{14}H_{22}O$	206	96-76-4
6	**21.59**	**Pentadecanoic acid**	**17.814**	**$C_{15}H_{30}O_2$**	**242**	**1 002-84-2**
9	9.47	Octadecanoic acid	19.664	$C_{18}H_{36}O_2$	284	57-11-4
10	1.20	Octadecanamide	19.806	$C_{18}H_{37}NO$	283	124-26-5
11	1.14	Oxiraneoctanoic acid, 3-octyl-, methyl ester, cis-	20.770	$C_{19}H_{36}O_3$	312	2566-91-8
13	**18.80**	**Oxiraneoctanoic acid, 3-octyl-, cis-**	**21.201**	**$C_{18}H_{34}O_3$**	**298**	**24560-98-3**
15	1.15	9-Octadecenamide, (Z)-	21.450	$C_{18}H_{35}NO$	281	301-02-0
19	1.05	7-Hexadecenoic acid, methyl ester, (Z)-	21.970	$C_{17}H_{32}O_2$	268	56875-67-3
21	6.26	12-Methyl-E,E-2,13-octadecadien-1-ol	22.358	$C_{19}H_{36}O$	280	0-00-0
22	5.30	Hexadecanoic acid, 2-hydroxy-1-(hydroxymethyl)ethyl ester	22.605	$C_{19}H_{38}O_4$	330	23470-00-0
24	7.60	Octadecanoic acid, 2,3-dihydroxypropyl ester	24.179	$C_{21}H_{42}O_4$	358	123-94-4
25	**12.52**	**13-Docosenamide, (Z)-**	**24.615**	**$C_{22}H_{43}NO$**	**337**	**112-84-5**
26	2.00	Octadecanoic acid, 9,10-epoxy-, isopropyl ester	25.437	$C_{21}H_{40}O_3$	340	95007-80-0
27*	0.75	Ibogamine-18-carboxylic acid, 12-methoxy-, methyl ester	26.050	$C_{22}H_{28}N_2O_3$	368	510-22-5
28	1.00	7-Methyl-Z,Z-8,10-hexadecadien-1-ol acetate	26.471	$C_{19}H_{34}O_2$	294	0-00-0
29	2.25	Silane, dimethyl(docosyloxy)butoxy-	28.898	$C_{28}H_{60}O_2Si$	456	0-00-0
30	1.33	1,4-Epoxynaphthalene-1(2H)-methanol,4,5,7-tris(1,1-dimethylethyl)-3,4-dihydro-	30.738	$C_{23}H_{36}O_2$	344	56771-86-9

* Represents *essential* compounds <1% total area.

Table 4.12: Compounds identified in the stem methanol extracts of *T. ventricosa* using GC-MS.

Peak	Total area %	Compound	Retention time	Molecular formula	Molecular weight	CAS NO.
1	1.67	Thymine	6.737	$C_5H_6N_2O_2$	126	65-71-4
2	1.51	4H-Pyran-4-one, 2,3-dihydro-3,5-dihydroxy-6-methyl-	7.745	$C_6H_8O_4$	144	28564-83-2
5*	0.54	Succinic acid, monoamide, N,N-di(2-ethylhexyl)-, ethyl ester	11.331	$C_{22}H_{43}NO_3$	369	0-00-0
6	1.93	n-Propyl heptyl ether	11.933	$C_{10}H_{22}O$	158	71112-89-5
8	**31.13**	**Quinic acid**	**14.304**	**$C_7H_{12}O_6$**	**192**	**77-95-2**
9	**28.72**	**α-d-Mannofuranoside, methyl**	**14.951**	**$C_7H_{14}O_6$**	**194**	**4097-91-0**
10	**14.99**	**3-O-Methyl-d-glucose**	**15.299**	**$C_7H_{14}O_6$**	**194**	**0-00-0**
11	3.21	4-Dodecanol	15.351	$C_{14}H_{28}O_2$	228	60826-25-7
12	0.61	IS,14S-Bicyclo	15.445	$C_{16}H_3O_8$	350	136982-939
13	1.04	A-d-6,3-Furanose	15.731	$C_7H_{12}O_6$	192	0-00-0
15	2.70	Diisooctyl phthalate	22.707	$C_{24}H_{38}O_4$	390	131-20-4
17	4.38	13-Docosenamide, (Z)-	24.582	$C_{22}H_{43}NO$	337	112-84-5
18	7.38	Ibogamine-18-carboxylic acid, 12-methoxy-, methyl ester	26.046	$C_{22}H_{28}N_2O_3$	368	510-22-5

* Represents *essential* compounds <1% total area.

Table 4.13: Compounds identified in the latex extracts of *T. ventricosa* using GC-MS.

Peak	Total area %	Compound	Retention time	Molecular formula	Molecular weight	CAS NO.
6	4.42	Obtusifoliol	28.221	$C_{30}H_{50}O$	426	16910-32-0
7	7.17	Lanosterol	28.634	$C_{30}H_{50}O$	426	79-63-0
8	3.19	9,19-Cycloergost-24(28)-en-3-ol, 4,14-dimethyl-, acetate, (3β,4α,5α)-	28.754	$C_{32}H_{52}O_2$	468	10376-42-8
9	2.89	9,19-Cyclolanost-24-en-3-ol, acetate, (3β)-	28.818	$C_{32}H_{52}O_2$	468	1259-10-5
10	**33.28**	**9,19-Cyclolanost-24-en-3-ol, (3β)-**	**29.243**	**$C_{30}H_{50}O$**	**426**	**469-38-5**
11	**7.85**	**β-Amyrin**	**29.633**	**$C_{30}H_{50}O$**	**426**	**559-70-6**
12	2.09	9,19-Cyclolanostan-3-ol, 24-methylene-, (3β)-	29.690	$C_{31}H_{52}O$	440	1449-09-8
13	**36.09**	**Lup-20(29)-en-3-ol, acetate, (3β)-**	**30.205**	**$C_{32}H_{52}O_2$**	**468**	**1617-68-1**

Table 4.14: Biological properties associated with the chemical compounds with a peak area % >1 in leaf, stem, and latex extracts of *T. ventricosa*.

Compound	Properties	References
Pentadecanoic acid	Treatment of male alopecia, heart agent, agent for myocardial imaging, anticancer, antiasthmatic, antiabortive, antimicrobial, antioxidant	Coenen et al., 1981; Adachi et al., 1993; Patra et al., 2017; Ansarali et al., 2018; Rao et al., 2019
Methyl (Z)-5,11,14,17-eicosatetraenoate	Antimicrobial, dysentery, diarrhoea, plant growth stimulator, antifungal, anticancer, antioxidant, and antidiabetic	Sridevi et al., 2014; Bagewadi et al., 2019
α-Linolenic acid	Neuroprotective effects, stroke prevention, anti-inflammatory, immunomodulatory, antiobese, anticarcinogenic, improves cardiovascular health, antidepressant, stroke prevention, nutraceutical, antioxidant, hypertension and protection of lipopolysaccharide-induced acute lung injury	Heuteaux et al., 2006; Hennessy et al., 2011; Nguemeni et al., 2013; Blondeau et al., 2016; Olushola-Siedoks et al., 2019; Ok et al., 2020; Zhu et al., 2020
Octadecanoic acid	Osteosarcoma therapy, anticancer, antioxidant, anti-inflammatory, antimicrobial, insecticidal, soap, and cosmetics	Ong et al., 2016; Manivannan et al., 2017; Xi et al., 2019; Warra, 2019.
cis-Vaccenic acid	Coronary heart disease, heart failure, colon cancer, sickle cell anemia, antibacterial, hypolipidemic and anticarcinogenic	Semwal et al., 2018; Oyedeji et al., 2018; Olushola-Siedoks et al., 2019; Mohammed and Ali, 2020
8-Hexadecenal, 14-methyl-, (Z)-	Pheromone	Levinson et al., 1978
2-methylhexacosane	Sexual dimorphism in flies, pheromone, anti-microbial and lowers blood cholesterol	Mutis et al., 2009, Spikes et al., 2010; Khatua et al., 2016; Taiwo et al., 2018
Ibogamine	Psychoactive, hallucinogenic effects, neurobiological effects, antiaddictive, cardiac effects, seizures, central nervous system effects, antidepression, anticancer, drug detoxification, antitumour, anti-inflammatory, antinociceptive, anticonvulsant, tremorgenic	Harini et al., 2016; Chen and Huang, 2017; Corkery et al., 2018; Luzuriaga-Quichimbo et al., 2018
13-Docosenamide, (Z)-	Indicator of benign prostatic hypertrophy, treatment, prevention to disturbances of the secretory system, antimicrobial, angiogenic effect, antinociceptive, antiviral, neuroactive compound, antifungal and antitumour	Geng et al., 2014; Shareef et al., 2016; Chen et al., 2018; Thasneem et al., 2019; Hasan et al., 2019; Prasher, 2019
Squalene	Carcinogenic treatment, antioxidant, antitumour, skin treatment, reduce cholesterol, detoxification of xenobiotics, cosmetics, immunologic	Huang et al., 2009; Sumi et al., 2018; Lozano-Grande et al., 2018;

Table 4.14: *Cont.*

	adjuvant in vaccines, improve immunity, anticancer, antisenescence, improves cardiovascular health, antimicrobial, antibiotics, supplements, drug delivery, anti-inflammatory, antiatherosclerotic and antineoplastic	Martínez-Beamonte et al., 2020; Ibrahim et al., 2020
Tetratetracontane	Anti-inflammatory, antibacterial, antiulcer, antioxidant, cytoprotective, anticandidal, antimicrobial and anti-Alzheimer	Ko et al., 2017; Jayalakshmi et al., 2018; Amudha et al., 2018
Ibogamine-18-carboxylic acid, 12-methoxy-, methyl ester	Antibacterial, bio-impact, uterophic effect	Hamdiani et al., 2018
Voaluteine	Psychoactive agent, antidiarrheal and bacteriostatic activity	Macabeo et al., 2009; Hussain et al., 2012
Vitamin E	Antioxidant, cosmetics, treat cognitive impairment, Alzheimer's, photoprotective, vibration disease, epidermolysis bullosa, cancer prevention, claudication, cutaneous ulcers, collagen synthesis, wound healing, atherosclerotic heart disease, anti-inflammatory, immune function, cellular signalling, lower cholesterol, cardiovascular disease, neurogenerative disease, prevents muscular degeneration, anticancer	Thiele et al., 2005; Duncan and Suzuki, 2017; Browne et al., 2019
β-Sitosterol	Anticancer, reduce cholesterol, anti-inflammatory, immunomodulator, anti-neoplastic, antipyretic, antibacterial, hepatoprotective, antioxidant, rheumatoid arthritis, colon cancer, benign prostatic hypertrophy, breast cancer, weight loss, antidiabetic, antiulcer, antinociceptive, sedative, central nervous system effects, and wound healing	Chai et al., 2008; Duarte et al., 2016; Kulkarni et al., 2016; Moustafa and Thabet, 2017; Paniagua-Pérez et al., 2017; Nweze et al., 2019
Lanosterol	Antioxidant, anti-diabetic, mitigates cytotoxicity, preventative of cataract formation, regulates human rhinovirus, neuroprotective, Parkinson disease	Lim et al., 2012; Upadhyay et al., 2018; Shen et al., 2018; McCrae et al., 2018; Hua et al., 2019
9,19-Cyclolanost-24-en-3-ol, acetate, (3β)-	Antibacterial, anticancer, antidiabetics and pesticides	Kalita et al., 2018; Ravi et al., 2018; Hage-Hülsmann et al., 2019; Nair et al., 2020
Acetic acid, 3-hydroxy-7-isopropenyl-1,4a-dimethyl-2,3,4,4a,5,6,7,8-octahydronaphthalen-2-yl ester	Wound healing, antibacterial, pseudomonal infections, and insulin resistance	Nagoba et al., 2008
5H-3,5a-Epoxynaphth[2,1-c]oxepin, dodecahydro-3,8,8,11a-tetramethyl-, [3S-(3α,5aα,7aα,11aβ,11bα)]-	Antitermite, antifungi, and fragrance agent	Surburg and Panten, 2016; Malik et al., 2016; Prayitno et al., 2020

Table 4.14: *Cont.*

9,12-Octadecadienoic acid (Z,Z)-	Cytotoxicity, antimicrobial, soap, reduce cholesterol, promotes cell structure, cosmetics, anti-inflammatory, antiacne, S-α reductase inhibitor, hypocholesterolemic, anticancer, antiandrogenic, hepatoprotective, antiarthritic, anticoronary, nematicide, insectifuge, antihistaminic and antieczemic and antioxidant	Manilal et al., 2009; Gopalakrishnan et al., 2011; Sudha and Mohan et al., 2013; Sharma et al., 2015; Parthipan et al., 2015
Dichloroacetic acid, tridec-2-ynyl ester	Cosmetics, tropical medication, genital warts, an inhibitor of pyruvate dehydrogenase kinase (enzyme), and brain cancer	Roy et al., 2019
Oxiraneoctanoic acid, 3-octyl-, cis-	Antibacterial	Hussein et al., 2016
13-Tetradecenal	Antioxidant, antiepileptic, antibacterial, pesticide, antimicrobial and antifungal	Sathya et al., 2016; Jackson, 2018
9,19-Cycloergost-24(28)-en-3-ol,4,14-dimethyl-,acetate, (3β,4α,5α)-	Antioxidant	Srinivasan and Priya, 2019
α-Amyrin	Immunosuppressive, inhibition of collagen-induced platelet aggregation and platelet activation factor, antimicrobial, antifungal, anti-inflammatory, antiviral, anticancer, antinociceptive, antiulcer, analgesic, antioxidant, antisedative, antipyretic, anticonvulsant, antierectile, antihyperglycemic, larvicidal, cytotoxic, antispasmodic, antihepatotoxic, epilepsy, neuroprotective and antimalarial	Appiah et al., 2017; Sushma et al., 2017; Arana-Argáez, 2017; Abdullahhi et al., 2018; Rao and Anisha, 2018; Kosasih et al., 2020
4,4,6a,6b,8a,11,11,14b-Octamethyl-1,4,4a,5,6,6a,6b,7,8,8a,9,10,11,12,12a,14,14a,14b-octadecahydro-2H-picen-3-one	Antibacterial, antioxidant, antitumour, and antineoplastic	Sharma et al., 2019; Helal et al., 2019; Awonyemi et al., 2020
Phenol, 2,4-bis(1,1-dimethylethyl)-	Antilarval, endocrinal regulation, antimicrobial, herbicide, food addictive, cancer drugs, pesticide, antioxidant, anti-inflammatory, antiviral, antifungal, sores, rheumatism and antiphytopathogenic	Choi et al., 2013; Daben and Dashak, 2017; Ren et al., 2019; Nguyen, 2020; Zhao et al., 2020
cis,cis,cis-7,10,13-Hexadecatrienal	Antioxidant and larvicidal	Bonilla and Sabral, 2019; Andrade et al., 2019
Octadecanamide	Potential biomarker, industrial interest, hypolipidemic, cardiovascular activity, antidepressant, and reduced cholesterol	Nizioł et al., 2016; Rocha et al., 2020
9-Octadecenamide, (Z)-	Anti-inflammatory, antibacterial, antioxidant, chemical additive/modifier, enhances pheromones, hepatoprotective, antimicrobial, and analgesic	Hase et al., 2017; Hameed et al., 2018; Naik et al., 2018; Olaoluwa et al., 2018

Table 4.14: *Cont.*

12-Methyl-E,E-2,13-octadecadien-1-ol	Antibacterial, anticonvulsant, aesthetic, antibacterial, antihistaminic, antioxidant, allergenic, analgesic, antiseptic, antisalmonella and antidiabetic	Chunsriimyatav et al., 2013; Adeyemi et al., 2017; Ahmadi et al., 2017; Alrabie et al., 2019
Hexadecanoic acid, 2-hydroxy-1-(hydroxymethyl)ethyl ester	Antioxidant, antimicrobial, anticancer, hemolytic, pesticide, antioxidant, anti-inflammatory, antihelminthic, analgesic, antibacterial, anticholinesterase, antimalarial, antipyretic, hypotensive, arachidonic acid inhibitor, aromatic amino acid decarboxylase activity, inhibits quorum sensing and biofilm formation in *chromobacterium violaceum*	Jiji and Subin, 2017; Hasan et al., 2019; Kim 2020; Sivakumaran et al., 2019; Venkatramanan et al., 2020
Octadecanoic acid, 9,10-epoxy-, isopropyl ester	Signature molecule of Pneumocystis carinii to determine phylogenetic affinities and biosurfactant	Kaneshiro et al., 1996; Muthukamalam et al., 2017
Octadecanoic acid, 2,3-dihydroxypropyl ester	Antimicrobial, anti-inflammatory, antioxidant, hepatoprotective, antihistaminic, hypocholesterolemic, anticancer, skin ailments, acid inhibitor, nematocidal activity, antiarthritic, antiasthma, and diuretic	Arora, 2017; Kumari et al, 2019; Tadigiri et al., 2020
7-Methyl-Z,Z-8,10-hexadecadien-1-ol acetate	Unknown	Unknown
Silane, dimethyl(docosyloxy)butoxy-	Precursor silicone polymer	Sathya et al., 2016
1,3,5-Cycloheptatriene, 2,4-di-t-butyl-7,7-dimethyl-	Antibacterial	Trust and Bartlett, 1975
Oxiraneoctanoic acid, 3-octyl-, methyl ester, cis-	Antibacterial	Hussein et al., 2016
7-Hexadecenoic acid, methyl ester, (Z)-	Antibacterial, antifungal, cosmetics, antioxidant, hypocholesterolaemia, an androgenic, hemolytic, and α-reductase inhibitor	Abubaker and Majinda, 2016; Khan and Bhadauria, 2017
1,4-Epoxynaphthalene-1(2H)-methanol, 4,5,7-tris(1,1-dimethylethyl)-3,4-dihydro-	Anti-inflammatory and tissue degrader	Hemalatha et al., 2018
1,2,3,5-Cyclohexanetetrol, (1α,2bet,3α,5β)-	Unknown	Unknown
α-d-Mannofuranoside, methyl	Antiallergic, antiinflammatory, antibiotic, antibacterial, and antimycotic	Kamurthy et al., 2015
Diisooctyl phthalate	Antimicrobial, inhibiting melanogenesis, pesticides, antiandrogenic effects, addictive's, plasticizers and inhibits the growth of foodborne harmful bacteria	Muszkat and Raucher, 1997; Kondo and Okumura, 2010; Yang et al., 2020; Nguyen et al., 2020
1,4-Benzenedicarboxylic acid	Antibacterial, antifungal, and neonatal septic infection	Aly et al., 2012; Fan et al., 2020

Table 4.14: *Cont.*

Thymine	An indicator of UV-light damage and stabilizes nucleic structures by binding with adenine	Degani et al., 1980; Kushwaha et al., 2019
4H-Pyran-4-one, 2,3-dihydro-3,5-dihydroxy-6-methyl-	Mutagen antimicrobial, anti-inflammatory, antioxidant, antiproliferative, automatic nerve activity, ameliorative effects, antibiotic effect, antidiabetic, antifungal, thermal degradative pathway and reduces harm from tobacco usage	Kumar et al., 2010; Hameed et al., 2015; Rao and Naika, 2018; Olaniyan et al., 2018
Succinic acid, monoamide, N,N-di(2-ethylhexyl)-, ethyl ester	Anti-microbial, control blood glucose levels, regulating lipid abnormalities, acylating agents, detergents, surfactant, ion chelator, flavoring agent, antibiotics, vitamin production, antibacterial and a prognostic indicator of physiological changes to colorectal cancer stem cells (CCSCS) induced by FxOH treatment	Feng et al., 2010; Terasaki et al., 2018; Liu et al., 2019
n-Propyl heptyl ether1	Unknown	Unknown
Quinic acid	Antioxidant, antitumour, antimutagenic, anticarcinogenic, neuroprotective, radioprotective, antidiabetic, antineuroinflammatory, astringent, hepatoprotective, and anti-inflammatory	Jadhav et al., 2014; Caprioli et al., 2015; Fernandes et al., 2019; Mahmoudi et al., 2021
3-*O*-Methyl-d-glucose	Glucose transport in normal/ischemic brains, metabolic stability, minimize neuropathological consequences of ischemic damage, membrane transport, preservation of mouse sperm, improves desiccation tolerance of keratinocytes and reduced toxicity of streptozotocin, a marker for glucose transport and breast cancer detection in imaging	Jay et al., 1990; Liu et al., 2012; Jin et al., 2018; Rao and Anisha, 2018; Rivlin and Navon, 2018
4-Dodecanol	Unknown	Unknown
IS,14S-Bicyclo	Alzheimer's	Beck et al., 2004
A-d-6,3-Furanose	Unknown	Unknown
Obtusifoliol	Cell growth inhibition, Apoptotic effects on breast cancer cells (MCF-7 and MDA-MB231), inhibitory effects on Epstein-Barr virus early antigen (EBA-EA), induction in a preliminary screening of their potential antitumour promoting activities, and growth arrest on *cryptococcus neoformans*	Venkateswarlu, 1996; Aghaei et al., 2016; Bailen et al., 2016

Table 4.14: *Cont.*

9,19-Cyclolanost-24-en-3-ol, (3β)-	Antibacterial and antilisteria activity	Penduka et al., 2014; Kalita et al., 2018
β-Amyrin	Inhibits collagen-induced platelet aggregation, aspirin, antidiabetic, antioxidant, cytotoxicity, anti-inflammatory, analgesic, gastroprotective, prevents hepatic lesions, antinociceptive properties, sedative, antidepressant, anticholinesterase. hepatoprotective, anti-pruritic, anticancer against hepatocellular carcinoma, anti-Parkinson effects, anti-fibrotic, antihyperglycemic, hypolipidemic, and atherosclerosis treatment	Aragáo et al., 2006; Aragáo et al., 2015; Ching et al., 2010; Fernandes et al., 2011; Fabiyi et al., 2012; Wagh et al., 2012; Wei et al., 2017; da Silva Júnior et al., 2017; Nogueira et al., 2019; Kamraj et al., 2019
9,19-Cyclolanostan-3-ol, 24-methylene-, (3β)-	Preventative of the human immunodeficiency virus (HIV), antimicrobial and antilisteria	Penduka et al., 2014; Arora et al., 2017; Ibrahim et al., 2018; Ameachi et al., 2018
Lup-20(29)-en-3-ol, acetate, (3β)-	Anti-protozoal, anti-microbial, anti-inflammatory, anti-tumour, anti-prostate cancer, anti-infertility effects, antidiabetic, larvicidal activity, antifungal, antibacterial, antiparasitic, antiviral, and lupus generating	Rodeiro et al., 2009; Murugan et al., 2012; Ogunwole et al., 2017; Rao and Anisha, 2018; Ighodaro et al, 2019

4.3.8 Antibacterial activity

The eminent alkaloids detected within the genus *Tabernaemontana* have motivated researchers to evaluate various species to develop new and improved antimicrobials (Naidoo et al., 2021). Although plenty of species within this genus display antibacterial activity, some notable species include *T. catharinensis* and *T. divaricata.* Recently, these species have been examined for their potential antibacterial activity against various bacterial strains (Radhika et al., 2017; Richard et al., 2021). *Tabernaemontana catharinensis* latex extracts displayed significant antibacterial activity against *Alicyclobacillus* (Richard et al., 2021), whereas *T. divaricata* showed substantial activity against *Proteus vulgaris* (ZOI-22mm) and *Staphylococcus aureus* (ZOI-17) (Radhika et al., 2017). Due to the evident antibacterial activities displayed by *Tabernaemontana* species, researchers must continue to screen medicinal plants to discover innovative antimicrobial drugs (Marathe et al., 2013; Sendeku et al., 2015). Thus, the present study aimed to screen the leaf, stem, and latex extracts of *T. ventricosa* using the agar disc diffusion technique. The antibacterial potential of these extracts was assessed using six different concentrations (3.125, 6.25,12.5, 25, 50, 100 mg/mL.) against five pathogenic bacterial strains, three gram-positive: *Bacillus subtilis* (ATCC 6653), *Methicillin-resistant Staphylococcus aureus* (MRSA) (ATCC 43300), *Staphylococcus aureus* (ATCC 29213), and two gram-negative bacterial strains: *Escherichia coli* (ATCC 25922) and *Pseudomonas aeruginosa* (ATCC 27853) (Appendix 2A).

The different extracts and concentrations displayed a variable degree of bacterial growth in the zone of inhibition (mm) against various bacterial strains (Table 4.15). The study showed that the leaf methanol, stem methanol, and the latex extracts of *T. ventricosa* displayed significant activity against *B. subtilis*, *E. coli*, MRSA, *S. aureus*, and *P. aeruginosa*. Additionally, the leaf and stem hexane extracts showed substantial activity against *B. subtilis* and MRSA. Conversely, *E. coli*, MRSA, *S. aureus*, and *P. aeruginosa* displayed resistance or minimal activity at relatively low concentrations (3.125, 6.25,12.5 mg/mL). Overall, across all bacterial strains, the mean zone of inhibition (mm) of the reference antibiotics was between 8.00 ± 1.00 mm and 14.00 ± 2.00 mm, which was moderately greater compared to the extracts, which ranged from 6.00 ± 0.00 mm to 12.67 ± 0.58 mm. Most notably, significant differences were observed for the antibacterial activity of the different extract types and concentrations within each bacterial strain (P <0.05), except for MRSA, which did not display any significant difference across the various extracts (P >0.05).

In 1984, Van Beek et al. performed a complex investigation on the antimicrobial, antiamoebic, and antiviral screening of various *Tabernaemontana* species. In that study, *T. ventricosa* species were collected from the Netherlands, and the flowers, leaves, and stembark were used for antibacterial, antiyeast, and antifungal activity (Van Beek et al., 1984). The findings of Van Beek et al. (1984) revealed the resistance of *B. subtilis*, *S. aureus*, and *E. coli* against all extracts, apart from the flower extracts (50 mg/mL), which displayed moderate inhibition (11 mm) against *B. subtilis*. Similarly, Mehrbod et al. (2018) studied the effect of *T. ventricosa* plant extracts against the influenza A virus. This investigation supported the study of Van Beek et al. (1984), as the results concluded that the leaf extracts of *T. ventricosa* were ineffective using *in vitro* studies. However, the findings of the current study display contrasting results since moderate to substantial antibacterial activity of the leaf, stem, and latex extracts were observed (Table 4.15). The positive results in the current study could be attributed to the location of collected plant material, different extracts (plant material and solvents), various extraction preparation and techniques, the broad range of treatment concentrations, and the variety of bacterial strains. In both the studies, similar bacterial strains were used as test organisms, with the major contrast between the studies being the site of plant collection (South Africa), extract type (hexane, chloroform, and methanol), and concentration of extracts (3.125, 6.25,12.5, 25, 50, 100 mg/mL). The variations applied in the current study are possibly responsible for the inhibition of bacterial growth.

Furthermore, we propose that the antibacterial activity of *T. ventricosa* is likely due to the various compounds detected during GC-MS analysis. According to the antibacterial results, considerable activity was observed for the following extracts: leaf and stem hexane, leaf and stem methanol, and latex extracts. Interestingly, many of these extracts contained chemical compounds (Tables 4.7-4.4.13), that are reportedly biologically active (Table 4.14), and have been found to display antimicrobial activity in various species. Major components such as α-linolenic acid, pentadecanoic acid, α-d-mannofuranoside, methyl, 13-docosenamide, (Z)-, 9,12-octadecadienoic acid (Z,Z)-, lup-20(29)-en-3-ol, acetate, (3β), 9,19-cyclolanost-24-en-3-ol, (3β) and β-amyrin have been reported for their antimicrobial activity and may attribute to the positive antibacterial activity observed in the present study (Wagh et al., 2012; Parthipan et al., 2015; Rao and Anisha, 2018; Bagewadi et al., 2019; Rao et al., 2019). However, further studies are necessary to confirm the specific compounds responsible for the substantial antibacterial activity.

Table 4.15: Zones of inhibition (mm) of various leaf, stem, and latex extracts of *T. ventricosa* against gram-positive and gram-negative bacterial strains.

Bacterial strains	Concentration (mg/mL)	Treatments/extracts							Positive control (10 ug/mL)		
		Leaf hexane	Leaf chloroform	Leaf methanol	Stem hexane	Stem chloroform	Stem methanol	Latex	Leaf	Stem	Latex
BS	**3.125**	R	6.33 ± 0.58	6.33 ± 0.58	R	6.33 ±0.58	R	R	**14.00 ± 2.00***	**9.00 ± 1.00***	**10.33 ± 1.53***
	6.25	6.33 ± 0.58	6.33 ± 0.58	6.67 ± 0.58	6.67 ± 0.58	6.33 ± 0.58	7.00 ± 3.79	R			
	12.5	7.00 ± 0.58	6.33 ± 0.58	6.67 ± 0.58	6.67 ± 0.58	6.67 ± 0.58	7.33 ± 0.00	6.67 ± 0.58			
	25	9.33 ± 0.00	6.33 ± 0.58	8.33 ± 0.58	8.33 ± 0.58	7.00 ± 1.00	7.33 ± 0.58	7.33 ± 1.16			
	50	10.67 ± 0.58	7.33 ± 0.58	9.33 ± 0.58	8.00 ± 0.00	7.33 ± 1.16	8.33 ± 0.58	12.00 ± 2.65			
	100	11.67 ± 0.58	7.33 ± 1.16	9.67 ± 0.78	12.67 ± 0.58	8.67 ± 0.58	9.33 ± 1.53	12.33 ± 2.08			
EC	**3.125**	R	R	R	R	R	R	R	**8.67 ± 1.53**	**8.67 ± 0.58**	**9.67 ± 1.53**
	6.25	R	R	R	R	R	R	R			
	12.5	R	R	7.00 ± 0.00	R	7.00 ± 0.00	7.00 ± 000	R			
	25	R	7.00 ± 0.00	7.00 ± 0.00	R	7.67 ± 0.58	7.00 ± 0.00	R			
	50	6.00 ± 0.00	7.67 ± 2.89	7.67 ± 0.58	6.00 ± 0.00	8.00 ± 1.00	8.67 ± 0.58	8.33 ± 0.58			
	100	6.67 ± 0.58	7.67 ± 0.58	9.00 ± 1.00	6.67 ± 0.58	8.33 ± 0.58	10.33 ± 2.52	9.33 ± 0.58			
MRSA	**3.125**	R	R	R	R	R	R	R	**8.00 ± 1.00***	**9.33 ± 0.58***	**9.6 ± 2.52***
	6.25	R	R	R	R	R	R	R			
	12.5	7.67 ± 1.16	7.33 ± 0.58	7.33 ± 0.58	6.67 ± 0.58	6.67 ± 0.58	6.67 ± 0.58	7.00 ± 0.00			
	25	7.67 ± 0.58	7.33 ± 0.58	7.33 ± 0.58	8.00 ± 1.73	8.00 ± 1.00	7.00 ± 0.00	7.00 ± 0.00			
	50	8.00 ± 1.00	7.33 ± 0.58	8.00 ± 1.73	9.00 ± 1.73	8.33 ± 1.16	7.33 ± 0.58	7.33 ± 0.58			
	100	8.00 ± 1.00	7.33 ± 1.16	9.67 ± 1.16	9.33 ± 0.58	8.67 ± 0.58	8.67 ± 0.58	8.33 ± 0.58			
SA	**3.125**	R	R	R	R	R	R	R	**8.00 ± 1.00***	**9.67 ± 0.58***	**10.33 ± 1.16***
	6.25	R	6.67 ± 0.58	6.67 ± 0.58	R	R	R	R			
	12.5	R	6.67 ± 0.58	6.67 ± 0.58	R	6.67 ± 0.58	6.67 ± 0.58	R			
	25	R	7.00 ± 0.00	7.33 ± 0.58	R	7.00 ± 0.00	7.00 ± 0.00	7.33 ± 0.58			
	50	R	7.67 ± 0.58	7.67 ± 0.58	6.67 ± 0.58	7.00 ± 0.00	7.00 ± 0.00	7.67 ± 0.58			
	100	R	8.67 ± 0.58	9.00 ± 1.00	6.67 ± 0.58	7.00 ± 0.00	9.33 ± 2.08	8.00 ± 0.00			
PA	**3.125**	R	R	R	R	R	R	R	**8.00 ± 1.73**	**9.33 ± 0.58**	**9.33 ± 1.53**
	6.25	R	R	R	R	6.00 ± 0.00	R	R			
	12.5	R	6.33 ± 0.58	R	R	6.33 ± 0.58	6.67 ± 0.58	R			
	25	R	6.67 ± 0.58	6.67 ± 0.58	R	7.00 ± 1.00	7.33 ± 0.58	R			
	50	6.33 ± 0.58	7.00 ± 0.00	7.00 ± 0.00	6.67 ± 0.58	7.33 ± 0.58	7.67 ± 1.16	8.33 ± 0.58			
	100	6.33 ± 0.58	7.00 ± 0.00	10.33 ± 1.16	7.33 ± 0.58	7.33 ± 0.58	9.67 ± 1.53	9.00 ± 1.00			

NB: mm (In length). No activity = (**0 mm**); Slight activity = (**1-6 mm**); Moderate activity = (**>7 or <9 mm**); Significant activity = (**>9mm**). **R** = Resistant, **BS** = *Bacillus subtilis* (ATCC 6653), **EC** = *Escherichia coli* (ATCC 25922), **MRSA** = *Methicillin Resistant Staphylococcus aureus* (ATCC 43300), **SA** = *Staphylococcus aureus* (ATCC 29213), **PA** = *Pseudomonas aeruginosa* (ATCC 27853), Positive controls (Gentamicin 10 µg/mL, Streptomycin 10 µg/mL*) and (n = 3).

4.4 Conclusion

This study highlighted that the organoleptic and fluorescence analysis techniques are simple, cost-effective, and essential pharmacological assessments. These results indicated that the plant material is safe and may be utilized during drug evaluation studies. The EDX analysis detected various elements which are essential for plant growth and development. Moreover, the high composition of calcium is possibly related to many calcium crystals present within the latex. The phytochemical characterization of the leaf, stem, and latex extracts detected various chemical classes such as carbohydrates, amino acids, alkaloids, flavonoids, saponins, sterols, steroids, phenols, and fixed fats and oils, which is comparable to similar species within the genus. The TLC analysis displayed exceptional separation of the various phytochemical compound groups however, despite the considerable scope of TLC data within the genus, further investigations regarding this aspect should be undertaken to expand our knowledge on the specific bioactive compounds within the species. The GC-MS analysis of *T. ventricosa* identified several biologically active compounds. The results revealed a higher number of compounds in the stems compared to the leaves. However, the quantity of compounds in terms of area percentage was higher in the leaves. Similar compounds were identified in all extracts, with major compounds being α-linolenic acid, pentadecanoic acid, α-d-mannofuranoside, methyl, 13-docosenamide, (Z)-, 9,12-octadecadienoic acid (Z,Z)-, lup-20(29)-en-3-ol, acetate, (3β), 9,19-cyclolanost-24-en-3-ol, (3β) and β-amyrin. The compounds mentioned above were possibly responsible for the antibacterial activity observed in the leaf and stem hexane, leaf and stem methanol, and latex extracts. Many studies have reported that these above-mentioned compounds contain a range of pharmacological properties such as antimicrobial, anti-inflammatory, chemoprotective, genotoxicity, antioxidant, neuroprotection, and antidiabetic. Considering the potential applications of the leaf, stem, and latex extracts of *T. ventricosa* and their chemical composition, further research should be conducted on the isolation, purification, and elucidation of compounds detected from different parts of the plant. This information could be used to establish their pharmacological properties and possibly produce novel drug leads and herbal remedies for the treatment and prevention of certain diseases and ailments.

4.6 References

Abdullahi, M.N., Ilyas, N., Hajara, I., Kabir, Y.M., 2018. Isolation and Characterisation of an Alpha-amyrin Acetate Isolated from the Leaves of *Microtrichia perotitii* DC (Asteraceae). Drugs 1, 3–4.

Abubakar, M.N., Majinda, R.R., 2016. GC-MS analysis and preliminary antimicrobial activity of *Albizia adianthifolia* (Schumach) and *Pterocarpus angolensis* (DC). Medicines 3, 3.

Adachi, K., Yokoyama, D., Tamai, H., Sadai, M., Oba, K., 1993. Effect of the glyceride of pentadecanoic acid on energy metabolism in hair follicles. International Journal of Cosmetic science 15, 125–131.

Adeyemi, M.A., Ekunseitan, D.A., Abiola, S.S., Dipeolu, M.A., Egbeyale, L.T., Sogunle, O.M., 2017. Phytochemical analysis and GC-MS determination of *Lagenaria breviflora* R. fruit. International Journal of Pharmacognosy and Phytochemical Research 9, 1045–1050.

Aghaei, M., Yazdiniapour, Z., Ghanadian, M., Zolfaghari, B., Lanzotti, V., Mirsafaee, V., 2016. Obtusifoliol related steroids from *Euphorbia sogdiana* with cell growth inhibitory activity and apoptotic effects on breast cancer cells (MCF-7 and MDA-MB231). Steroids 115, 90–97.

Ahmadi, A., Khalili, M., Mashaee, F., Nahri-Niknafs, B., 2017. The effects of solvent polarity on hypoglycemic and hypolipidemic activities of *Vaccinium arctostaphylos* L. Unripe fruits. Pharmaceutical Chemistry Journal 50, 746–752.

Akbar, S., Hanif, U., Ali, J., Ishtiaq, S., 2014. Pharmacognostic studies of stem, roots and leaves of *Malva parviflora* L. Asian Pacific Journal of Tropical Biomedicine 4, 410–415.

Akerele, O., 1993. Nature's medicinal bounty: Don't throw it away. World Health Forum 14, 390–395.

Akwu, N.A., Naidoo, Y., Singh, M., Nundkumar, N., Lin, J., 2019. Phytochemical screening, *in vitro* evaluation of the antimicrobial, antioxidant and cytotoxicity potentials of *Grewia lasiocarpa* E. Mey. ex Harv. South African Journal of Botany 123, 180–192.

Alrabie, A., Al-Qadsy, I., Farooqui, M., 2019. GC-MS analysis, HPTLC fingerprint profile and DPPH free radical scavenging assay of methanol extract of *martynia annua* linn seeds. International Journal of Pharmacy and Pharmaceutical Sciences 11, 16–22.

Aly, A.A., Ghandour, M., Alfakeh, M.S., 2012. Synthesis and characterization of transition metal coordination polymers derived from 1, 4-benzenedicarboxylate and certain azoles. Turkish Journal of Chemistry 36, 69–79.

Ameachi, N.C., Chijioke, C.L., 2018. Evaluation of bioactive compounds in *Pseudarenthemum tunicatum* leaves using gas chromatography-mass spectrometry. Evaluation 18, 53–60.

Amudha, P., Jayalakshmi, M., Pushpabharathi, N., Vanitha, V., 2018. Identification of bioactive components in *Enhalus acoroides* seagrass extract by gas chromatography–mass spectrometry. Asian Journal of Pharmaceutical and Clinical Research 11, 131–137.

Andima, M., Ndakala, A., Derese, S., Biswajyoti, S., Hussain, A., Yang, L.J., Akoth, O.E., Coghi, P., Pal, C., Heydenreich, M., Wong, V.K.W., 2021. Antileishmanial and cytotoxic activity of secondary metabolites from *Taberneamontana ventricosa* and two aloe species. Natural Product Research 1–5.

Andrade, H.G., Ordaz, A.K.E., Gurrola, G.T., Rodríguez, Y.M.G., García, F.J.E.,Vargas, L.M.T., 2019. Identificación de nuevos metabolitos secundarios en *Persea americana* Miller variedad *Drymifolia*. Revista Mexicana De Ciencias Agrícolas 23, 253–265.

Ankad, G.M., Pai, S.R., Upadhya, V., Hurkadale, P.J.,Hegde, H.V., 2015. Pharmacognostic evaluation of *Achyranthes coynei*: Leaf. Egyptian Journal of Basic and Applied Sciences 2, 25–31.

Ansarali, S., 2018. Identification of biological components from potential bone healer medicinal plants. Journal of Drug Delivery and Therapeutics 8, 32–41.

Appiah, K.S., Mardani, H.K., Osivand, A., Kpabitey, S., Amoatey, C.A., Oikawa, Y., Fujii, Y., 2017. Exploring alternative use of medicinal plants for sustainable weed management. Sustainability 9, 1468.

Aragão, G.F., Carneiro, L.M., Júnior, A.P., Bandeira, P.N., Lemos, T.L., Viana, G.S.D.B., 2007. Antiplatelet Activity of α.-and β.-Amyrin, Isomeric Mixture from *Protium heptaphyllum*. Pharmaceutical Biology 45, 343–349.

Aragão, G.F., Carneiro, L.M.V., Junior, A.P.F., Vieira, L.C., Bandeira, P.N., Lemos, T.L.G., Viana, G.D.B., 2006. A possible mechanism for anxiolytic and antidepressant effects of alpha-and β-amyrin from *Protium heptaphyllum* (Aubl.) March. Pharmacology Biochemistry and Behavior 85, 827–834.

Aragão, G.F., Carneiro, L.M.V., Rota-Junior, A.P., Bandeira, P.N., Lemos, T.L.G.D., Viana, G.S.D.B., 2015. Alterations in brain amino acid metabolism and inhibitory effects on PKC are possibly correlated with anticonvulsant effects of the isomeric mixture of α-and β-amyrin from *Protium heptaphyllum.* Pharmaceutical biology 53, 407–413.

Arana-Argáez, V.E., Chan-Zapata, I., Canul-Canche, J., Fernández-Martín, K., Martín-Quintal, Z., Torres-Romero, J.C., Coral-Martínez, T.I., Lara-Riegos, J.C.,Ramírez-Camacho, M.A., 2017. Immunosuppresive effects of the methanolic extract of *Chrysophyllum cainito* leaves on macrophage functions. African Journal of Traditional Complementary and Alternative Medicines 14, 179–186.

Arora, S., Kumar, G., Meena, S., 2017. GC-MS analysis of bioactive compounds from the whole plant hexane extract of *cenchrus setigerus* vahl. Pharma Science Monitor 8, 137–146.

Arora, S.K., 1994. D-substituted and deoxy disubstituted derivatives of o-d-mannofuranosides and b-l-gulofuranosides having anti-inflammatory and anti-proliferative activity. United States registered patent 45, 1–22.

Aslam, I., Afridi, M.S.K., 2018. Pharmacognostic characterization of *Beaumontia grandiflora* (Roxb.) Wall. leaf for taxonomic identification for quality control of a drug. Journal of Applied Research on Medicinal and Aromatic plants 8, 53–59.

Athipornchai, A., 2018. A review on *Tabernaemontana* spp.: Multipotential medicinal Plant. Asian Journal of Pharmaceutical and Clinical Research 11, 45–53.

Awonyemi, I., Abegunde, M.S., Olabiran, T.E., 2020. Analysis of bioactive compounds from *Raphia taedigera* using gas chromatography–mass spectrometry. Eurasian Chemical Communications 2, 938–944.

Azhagumadhavan, S., Senthilkumar, S., Padma, M., Sasikala, P., Jayaseelan, T., Ganesan, S., 2019. A study on establishment of phytochemical analysis of quality parameters and fluorescence analysis of *Costus spicatus*-rhizome extract medicinal plants a well-known tropical folklore medicine. Journal of Drug Delivery and Therapeutics 9, 240–243.

Bagewadi, Z.K., Muddapur, U.M., Madiwal, S.S., Mulla, S.I., Khan, A., 2019. Biochemical and enzyme inhibitory attributes of methanolic leaf extract of *Datura inoxia* Mill. Environmental Sustainability 2, 75–87.

Bailen, M., Khamlichi, M.D., Benharref, A., Martinez-Diaz, R.A, Gonzalez-Coloma, A., 2016. New bioactive semisynthetic derivatives of 31-norlanostenol and obtusifoliol from *Euphorbia officinarum.* Natural Product Communications 11, 1934578X1601100609.

Barceló-Coblijn, G., Murphy, E.J., 2009. Alpha-linolenic acid and its conversion to longer chain n− 3 fatty acids: Benefits for human health and a role in maintaining tissue n− 3 fatty acid levels. Progress in Lipid Research 48, 355–374.

Basavaraj, P., Shivakumar, B., Shivakumar, H., 2011. Anxiolytic activity of *Tabernaemontana divaricata* (Linn) R. Br. flowers extract in mice. International Journal of Pharmaceutical and Biological Sciences 2, 65–72.

Beck, J., Pharmacia., Upjohn CO., 2004. Use of bicyclo compounds for treating alzheimer's disease. U.S. Patent Application 10/482,098.

Blondeau, N., 2016. The nutraceutical potential of omega-3 alpha-linolenic acid in reducing the consequences of stroke. Biochimie 120, 49–55.

Bonilla, J., Sobral, P.J., 2019. Gelatin-chitosan edible film activated with Boldo extract for improving microbiological and antioxidant stability of sliced Prato cheese. International Journal of Food Science and Technology 54, 1617–1624.

Bouteau, F., Perino, C., Cornel, D., Rona, J.P., 1993. Sugar absorption and potassium channels in protoplasts of *Hevea brasiliensis* laticiferous vessels. Bioelectrochemistry and Bioenergetics 31, 215–228.

Browne, D., McGuinness, B., Woodside, J.V., McKay, G.J., 2019. Vitamin E and Alzheimer's disease: What do we know so far?. Clinical Interventions in Aging 14, 1303.

Calixto, J.B., 2000. Efficacy, safety, quality control, marketing and regulatory guidelines for herbal medicines (phytotherapeutic agents). Brazilian Journal of Medical and Biological Research 33, 179–89.

Caprioli, G., Cortese, M., Sagratini, G., Vittori, S., 2015. The influence of different types of preparation (espresso and brew) on coffee aroma and main bioactive constituents. International Journal of Food Sciences and Nutrition 66, 505–513.

Cardoso, C.A., Vilegas, W., Honda, N.K., 1998. Qualitative determination of indole alkaloids, triterpenoids and steroids of *Tabernaemontana hilariana*. Journal of Chromatography 808, 264–268.

Chai, J.W., Kuppusamy, U.R., Kanthimathi, M.S., 2008. Beta-sitosterol induces apoptosis in MCF-7 cells. Malaysian Journal of Biochemistry and Molecular Biology 16, 28–30.

Chattipakorn, S., Pongpanparadorn, A., Pratchayasakul, W., Pongchaidacha, A., Ingkaninan, K., Chattipakorn, N., 2007. *Tabernaemontana divaricata* extract inhibits neuronal acetylcholinesterase activity in rats. Journal of Ethnopharmacology 110, 61–68.

Chen, C., Zhu, J., Jia, S., Mi, S., Tong, Z., Li, Z., Li, M., Zhang, Y., Hu, Y., Huang, Z., 2018. Effect of ethanol on Mulberry bark hydrothermal liquefaction and bio-oil chemical compositions. Energy 162, 460–475.

Chen, H.M., Yang, Y.T., Li, H.X., Cao, Z.X., Dan, X.M., Mei, L., Guo, D.L., Song, C.X., Dai, Y., Hu, J., Deng, Y., 2016. Cytotoxic monoterpenoid indole alkaloids isolated from the barks of *Voacanga africana* Staph. Natural Product Research 30, 1144–1149.

Chen, J., Huang, Y., 2017. Phosphine-catalyzed sequential [4+ 3] domino annulation/allylic alkylation reaction of MBH carbonates: Efficient construction of seven-membered heterocycles. Organic letters 19, 5609–5612.

Ching, J., Chua, T.K., Chin, L.C., Lau, A.J., Pang, Y.K., Jaya, J.M., Tan, C.H., Koh, H.L., 2010. Beta-amyrin from *Ardisia elliptica* Thunb. is more potent than aspirin in inhibiting collagen-induced platelet aggregation. Indian Journal of Experimental Biology 48, 275–279.

Choi, S.J., Kim, J.K., Kim, H.K., Harris, K., Kim, C.J., Park, G.G., Park, C.S., Shin, D.H., 2013. 2, 4-Di-tert-butylphenol from sweet potato protects against oxidative stress in PC12 cells and in mice. Journal of Medicinal Food 16, 977–983.

Chunsriimyatav, G., Dumaa, M., Regdel, D., Gerelt-Od, Y., Selenge, D., 2013. GC-MS analysis of some bioactive volatile constituents from aerial parts of *Polygonatum odoratum* (Mill. Druce). International Journal of Current Science 7, 142–145.

Clinical and Laboratory Standards Institute., 2006. Performance Standards for Antimicrobial Disk Susceptibility Tests, Approved standard-Ninth Edition (M2-A9). Wayne, PA: (CLSI) Philadelphia.

Coenen, H.H., Harmand, M.F., Kloster, G., Stöcklin, G., 1981. 15-(p-[75Br] bromophenyl) pentadecanoic Acid: Pharmacokinetics and Potential as Heart Agent. Journal of Nuclear Medicine 22, 891–896.

Corkery, J.M., 2018. Ibogaine as a treatment for substance misuse: Potential benefits and practical dangers. Progress in Brain Research 242, 217–257.

da Silva Júnior, W.F., de Oliveira Pinheiro, J.G., de França Almeida, C.D.L., Rüdiger, A.L., Barbosa, E.G., Lima, E.S., da Veiga Júnior, V.F., da Silva Júnior, A.A., Aragão, C.F.S., de Lima, Á.A.N., 2017. Thermal behavior and thermal degradation kinetic parameters of triterpene α, β amyrin. Journal of Thermal Analysis and Calorimetry 127, 1757–1766.

Daben, J.M., Dashak, D.A., 2017. Extraction, isolation and mass spectral analysis of *Crinum zeylanicum* (beautiful crinum) bulbs. Ewemen Journal of Herbal Chemistry and Pharmacology Research 3, 52–58.

Dassanayake, M., Larkin, J.C., 2017. Making plants break a sweat: the structure, function, and evolution of plant salt glands. Frontiers in Plant Science 8, 1–20.

Degani, N., Ben-Hur, E., Riklis, E., 1980. DNA damage and repair: Induction and removal of thymine dimers in ultraviolet light irradiated intact water plants. Photochemistry and Photobiology 31, 31–36.

Desai, S.D., Desai, D.G., Kaur, H., 2009. Saponins and their biological activities. Pharma Times 41, 13–16.

Duarte, P.F., Chaves, M.A., Borges, C.D., Mendonça, C.R.B., 2016. Avocado: Characteristics, health benefits and uses. Ciência Rural 46, 747–754.

Duncan, K.R., Suzuki, Y.J., 2017. Vitamin E nicotinate. Antioxidants 6, 20–34

Fabiyi, O.A., Atolani, O., Adeyemi, O.S., Olatunji, G.A., 2012. Antioxidant and cytotoxicity of β-amyrin acetate fraction from *Bridelia ferruginea* leaves. Asian Pacific Journal of Tropical Biomedicine 2, 981–984.

Fan, T., Ye, L., Jiang, H., Wang, H., He, D., Zhang, J., Liu, C., 2020. Two mixed-ligand Cu (II) coordination polymers: treatment on neonatal septic infections by reducing the serum procalcitonin production. Inorganic and Nano-Metal Chemistry 51, 434–441.

Feng, S., Zeng, W., Luo, F., Zhao, J., Yang, Z., Sun, Q., 2010. Antibacterial activity of organic acids in aqueous extracts from pine needles (*Pinus massoniana Lamb*.). Food Science and Biotechnology 19, 35–41.

Fernandes, C.P., Correa, A.L., Cruz, R.A., Botas, G.D.S., Silva-Filho, M.V., Santos, M.G., de Brito, M.A., Rocha, L., de Produtos Naturais, L.D.T., 2011. Anticholinesterasic activity of *Manilkara subsericea* (Mart.) Dubard triterpenes. Latin American Journal of Pharmacy 30, 1631–1634.

Fernandes, F., Pereira, E., Círić, A., Soković, M., Calhelha, R.C., Barros, L., Ferreira, I.C., 2019. *Ocimum basilicum* var. purpurascens leaves (red rubin basil): A source of bioactive compounds and natural pigments for the food industry. Food and function 10, 3161–3171.

Figueiredo, A.C., Barroso, J.G., Pedro, L.G., Scheffer, J.J., 2008. Factors affecting secondary metabolite production in plants: Volatile components and essential oils. Flavour and Fragrance Journal 23, 213–226.

Francis, B.T., Sudha, S., 2017. Preliminary phytochemical screening and thin layer chromatography of polyherbal anti-diabetic extracts. International Journal of Pharmaceutical and Biological Sciences 8, 108–112.

Garga, D., Das, T., 2017. Preliminary phytochemical screening and anti-inflammatory effect of the aqueous extract of *Tabernaemontana divaricata* flower in wister rats. International Journal of Current Pharmaceutical Research 9, 9–12.

Geng, Y., Sun, F., Ma, Y., Deng, L., Lü, J., Li, T., Wang, C., 2014. Serum metabolomics analysis on benign prostate hyperplasia in mice based on liquid chromatography-mass spectrometry. *Se pu*= Chinese Journal of Chromatography 32, 1301–1305.

Gopalakrishnan, S., Saroja, K., Elizabeth, J.D., 2011. GC-MS analysis of the methanolic extract of the leaves of *Dipteracanthus patulus* (Jacq.) Nees. Journal and Chemical and Pharmaceutical Research 3, 477–480.

Hage-Hülsmann, J., Metzger, S., Wewer, V., Buechel, F., Troost, K., Thies, S., Loeschcke, A., Jaeger, K.E., Drepper, T., 2019. Biosynthesis of cycloartenol by expression of plant and bacterial oxidosqualene cyclases in engineered *Rhodobacter capsulatus*. Journal of Biotechnology: X 4, 100014.

Hamdiani, S., Al-As' ari, M., Satriani, A.R., Hadi, S., 2018, October. Alkaloids from Pulai (*Alstonia scholaris* (L.) R. Br.) leaves of Lombok Island on the basis of GC-MS analysis. In AIP Conference Proceedings 2023, 020091

Hameed, I.H., Hussein, H.J., Kareem, M.A., Hamad, N.S., 2015. Identification of five newly described bioactive chemical compounds in methanolic extract of *Mentha viridis* by using gas chromatography-mass spectrometry (GC-MS). Journal of Pharmacognosy and Phytotherapy 7, 107–125.

Hameed, R.H., Hussein, H.M., Hameed, I.H., 2018. Analysis of Bioactive Chemical Compounds of Methanolic Seed Extract of *Annona cherimola* (Graviolla) Using Gas Chromatography-Mass Spectrum Technique. Indian Journal of Public Health 9, 471.

Harini, R.S., Saivikashini, A., Keerthana, G., Kumaresan, K., Murugesan, S., Senthilkumar, N., 2016. Profiling metabolites of *Carica papaya* Linn. variety CO7 through GC-MS analysis. Journal of Pharmacognosy and Phytochemistry 5, 200.

Hasan, M.M., Al Mahmud, M.R., Islam, M.G., 2019. GC-MS analysis of bio-active compounds in ethanol extract of *Putranjiva roxburghii* Wall. fruit peel. Pharmacognosy Journal 11, 146–149.

Hase, G.J., Deshmukh, K.K., Pokharkar, R.D., Gaje, T.R., Phatanagre, N.D., 2017. Phytochemical Studies on *Nerium oleander* L. using GC-MS. International Journal of Pharmacognosy and Phytochemical Research 9, 885–891.

Helal, N.M., Ibrahim, N., Khattab, H., 2019. Phytochemical analysis and antifungal bioactivity of *Pulicaria undulata* (L.) methanolic extract and essential oil. Egyptian Journal of Botany 59, 827–844.

Hemalatha, D., Prabhu, S., Rani, W.B., Anandham, R., 2018. Isolation and characterization of toxins from *Xenorhabdus nematophilus* against *Ferrisia virgata* (Ckll.) on tuberose, *Polianthes tuberosa*. Toxicon 146, 42–49.

Hennessy, A.A., Ross, R.P., Devery, R., Stanton, C., 2011. The health promoting properties of the conjugated isomers of α-linolenic acid. Lipids 46, 105–119.

Heurteaux, C., Laigle, C., Blondeau, N., Jarretou, G., Lazdunski, M., 2006. Alpha-linolenic acid and riluzole treatment confer cerebral protection and improve survival after focal brain ischemia. Neuroscience 137, 241–251.

Hua, H., Yang, T., Huang, L., Chen, R., Li, M., Zou, Z., Wang, N., Yang, D., Liu, Y., 2019. Protective effects of lanosterol synthase up-regulation in UV-B-induced oxidative stress. Frontiers in Pharmacology 10, 947.

Huang, Z.R., Lin, Y.K., Fang, J.Y., 2009. Biological and pharmacological activities of squalene and related compounds: Potential uses in cosmetic dermatology. Molecules 14, 540-554.

Hussain, H., Hussain, J., Al-Harrasi, A., Green, I.R., 2012. Chemistry and biology of the genus *Voacanga*. Pharmaceutical Biology 50, 1183–1193.

Hussein, H.J., Hadi, M.Y., Hameed, I.H., 2016. Study of chemical composition of *Foeniculum vulgare* using Fourier transform infrared spectrophotometer and gas chromatography-mass spectrometry. Journal of Pharmacognosy and Phytotherapy 8, 60–89.

Ibrahim, N., Zakaria, A.J., Ismail, Z., Ahmad, Y., Mohd, K.S., 2018. Application of GCMS and FTIR fingerprinting in discriminating two species of Malaysian stingless bees propolis. International Journal of Engineering and Technology 7, 106–112.

Ibrahim, N.I., Fairus, S., Zulfarina, M.S., Naina Mohamed, I., 2020. The efficacy of squalene in cardiovascular disease risk-a systematic review. Nutrients 12, 414.

Ighodaro, O.M., Asejeje, F.O., Adeosun, A.M., Ujomu, T., Bakre, S.R., 2019. Anti-diabetic potential and gas chromatography mass spectroscopy (GC-MS) profile of a formulated polyherbal drug (FPD). The Journal of Phytopharmacology 8, 129–134.

Iwasaki, Y., Sawada, T., Hatayama, K., Ohyagi, A., Tsukuda, Y., Namekawa, K., Ito, R., Saito, K., Nakazawa, H., 2012. Separation technique for the determination of highly polar metabolites in biological samples. Metabolites 2, 496–515.

Jackson, H., 2018. Respiratory risk associated with indoor air pollutants in the form of settled house dust. Journal of Environmental Science and Engineering B 6 2017, 231–293.

Jadhav, V., Kalase, V., Patil, P., 2014. GC-MS analysis of bioactive compounds in methanolic extract of *Holigarna grahamii* (wight) Kurz. International Journal of Health and Medicine 35, 35–9.

Jay, T.M., Dienel, G.A., Cruz, N.F., Mori, K., Nelson, T., Sokoloff, L., 1990. Metabolic stability of 3-O-methyl-D-glucose in brain and other tissues. Journal of Neurochemistry 55, 989–1000.

Jayalakshmi, M., Vanitha, V., Sangeetha, R., 2018. Determination of phytocomponents in ethanol extract of *brassica oleracea*-using gas chromatography–mass spectroscopy technique. Asian Journal of Pharmaceutical Clinical Research 11, 133–136.

Jiji, P.G., Subin, M.P., 2017. Qualitative phytochemical screening and GC-MS analysis in the leaf methanolic extracts of *Kamettia caryophyllata* (Roxb.) Nicolson and Suresh. Paripex Indian Journal Research 6, 470–479.

Jin, T., Mehrens, H., Wang, P., Kim, S.G., 2018. Chemical exchange-sensitive spin-lock MRI of glucose analog 3-O-methyl-d-glucose in normal and ischemic brain. Journal of Cerebral Blood Flow and Metabolism 38, 869–880.

Kalita, B.C., Gupta, D.D., Das, A.K., Hui, P.K., Tag, H., 2018. Gas Chromatography-Mass Spectrometry of Methanol Extract of *Urtica dioica* L. from Arunachal Pradesh, India. Journal of Clinical Trial and Case Reports 1, 52000111.

Kamaraj, M.C., Olikkavi, K., Vennila, L., Bose, S.S., Raj, S.M., 2019. In Silico Docking and Anti-Cancer activity of the isolated Compounds (Alpha and Beta Amyrin) from methanolic bark extract of *Shorea robusta*. International Journal of Pure Medical Research 4, 11–15.

Kamurthy, H., Dontha, S., Vedula, A., 2015. Phytochemical screening of isolated compounds from *Nymphaea nouchali* Burm. f. flowers. European Journal of Medicinal Plants 9, 1–12.

Kaneshiro, E.S., Ellis, J.E., Guo, Z., Jayasimhulu, K., Maiorano, J.N., Kallam, K.A., 1996. Characterizations of neutral lipid fatty acids and cis-9, 10-epoxy octadecanoic acid in *Pneumocystis carinii carinii*. Infection and Immunity 64, 4105–4114.

Kapewangolo, P., Omolo, J.J., Fonteh, P., Kandawa-Schulz, M., Meyer, D., 2017. Triterpenoids from *Ocimum labiatum* activates latent HIV-1 expression *in vitro*: Potential for use in adjuvant therapy. Molecules 22, 1703.

Khan, A.M., Bhadauria, S., 2017. Isolation of some potential phytocompounds from *Adhatoda vasica* through Gas Chromatography-Mass Spectroscopy analysis. Asian Journal of Pharmaceutical Clinical Research 10, 328–332.

Khatua, S., Pandey, A., Biswas, S.J., 2016. Phytochemical evaluation and antimicrobial properties of *Trichosanthes dioica* root extract. Journal of Pharmacognosy and Phytochemistry 5, 410.

Kim, B.R., Kim, H.M., Jin, C.H., Kang, S.Y., Kim, J.B., Jeon, Y.G., Park, K.Y., Lee, I.S., Han, A.R., 2020. Composition and antioxidant activities of volatile organic compounds in radiation-bred *Coreopsis cultivars*. Plants 9, 717.

Ko, E.Y., Cho, S.H., Kang, K., Kim, G., Lee, J.H., Jeon, Y.J., Kim, D., Ahn, G., Kim, K.N., 2017. Anti-inflammatory activity of hydrosols from *Tetragonia tetragonoides* in LPS-induced RAW 264.7 cells. EXCLI Journal 16, 521.

Kokwaro, J.O., 1976. Medicinal plants of East Africa, first ed. East African Literature. Kampala, Nairobi, Dar-es-Salaam.

Kondo, F., Okumura, M., Oka, H., Nakazawa, H., Izumi, S.I., Makino, T., 2010. Determination of phthalates in diet and bedding for experimental animals using gas chromatography-mass spectrometry. Bulletin of Environmental Contamination and Toxicology 84, 212–216.

Kosasih, K., Sumaryono, W., Supriyono, A., Mudhakir, D., 2020. Possible cytotoxic activity analysis of diethyl ether extract of *Vaccinium varingiaefolium* (Blume) Miq. leaves by GC-MS method. Journal of Pharmaceutical Sciences and Research 12, 840–847.

Kulkarni, S.S., Lanjewar, R.B., Gadegone, S.M., 2016. A review on levodopa and beta-sitosterol and its pharmacological actions in *Bauhinia racemosa*, *Canavalia gladiata*, *Vigna vexillata* medicinal plants. Journal of Medicinal Plants 4, 259–264.

Kumar, P.P., Kumaravel, S., Lalitha, C., 2010. Screening of antioxidant activity, total phenolics and GC-MS study of *Vitex negundo*. African Journal of Biochemistry Research 4, 191–195.

Kumari, N., Menghani, E., Mithal, R., 2019. GCMS analysis & assessment of antimicrobial potential of rhizospheric Actinomycetes of AIA3 isolate. Indian Journal of Traditional Knowledge (IJTK) 19, 111–119.

Kushwaha, P., Yadav, S.S., Singh, V., Dwivedi, L.K., 2019. GC-MS analysis of bio-active compounds in methanolic extract of *Ziziphus mauritiana* fruit. International Journal of Pharmaceutical Science Research 10, 2911–2916.

Levinson, A.R., Levinson, H.Z., Schwaiger, H., Cassidy, R.F., Silverstein, R.M., 1978. Olfactory behavior and receptor potentials of the khapra beetle *Trogoderma granarium* (Coleoptera: Dermestidae) induced by the major components of its sex pheromone, certain analogues, and fatty acid esters. Journal of Chemical Ecology 4, 95–108.

Lim, L., Jackson-Lewis, V., Wong, L.C., Shui, G.H., Goh, A.X.H., Kesavapany, S., Jenner, A.M., Fivaz, M., Przedborski, S., Wenk, M.R., 2012. Lanosterol induces mitochondrial uncoupling and protects dopaminergic neurons from cell death in a model for Parkinson's disease. Cell Death & Differentiation 19, 416–427.

Liu, H., Fan, J., Wang, C., Li, C., Zhou, X., 2019. Enhanced β-amyrin synthesis in *Saccharomyces cerevisiae* by coupling an optimal acetyl-CoA supply pathway. Journal of Agricultural and Food Chemistry 67, 3723–3732.

Liu, J., Lee, G.Y., Lawitts, J.A., Toner, M., Biggers, J.D., 2012. Preservation of mouse sperm by convective drying and storing in 3-O-methyl-D-glucose. PLoS One 7, 29924.

Liu, Q., Tang, G.Y., Zhao, C.N., Gan, R.Y., Li, H.B., 2019. Antioxidant activities, phenolic profiles, and organic acid contents of fruit vinegars. Antioxidants 8, 78.

Lozano-Grande, M.A., Gorinstein, S., Espitia-Rangel, E., Dávila-Ortiz, G., Martínez-Ayala, A.L., 2018. Plant sources, extraction methods, and uses of squalene. International Journal of Agronomy 2018, 1–13.

Luzuriaga-Quichimbo, C.X., Ruiz Téllez, T., Blanco Salas, J., Cerón Martínez, C.E., 2018. Scientific validation of the traditional knowledge of Sikta (*Tabernaemontana sananho*, Apocynaceae) in the Canelo-Kichwa Amazonian community. Mediterranean Botany 39, 183–191.

Macabeo, A.P., Alejandro, G.J., Hallare, A., Vidar, W., Villaflores, O., 2009. Phytochemical survey and pharmacological activities of the indole alkaloids in the genus *Voacanga Thouars* (Apocynaceae)-an update. Pharmacognosy Reviews 3, 143.

Mahmoudi, M., Abdellaoui, R., Boughalleb, F., Yahia, B., Mabrouk, M., Nasri, N., 2021. Characterization of lipids, proteins, and bioactive compounds in the seeds of three *Astragalus* species. Food Chemistry 339, 127824.

Mahouachi, J., 2009. Changes in nutrient concentrations and leaf gas exchange parameters in banana plantlets under gradual soil moisture depletion. Scientia Horticulturae 120, 460–466.

Malik, B., Pirzadah, T.B., Tahir, I., Abdin, M.Z., Rehman, R.U., 2016. Phytochemical studies on *Cichorium intybus* L.(chicory) from Kashmir Himalaya using GC-MS. Journal of Pharmacy Research 10, 715–726.

Manilal, A., Sujith, S., Kiran, G.S., Selvin, J., Shakir, C., 2009. Cytotoxic potentials of red alga, *laurencia brandenii* collected from the Indian coast. Global Journal of Pharmacology 3, 90–94.

Manivannan, P., Muralitharan, G., Balaji, N.P., 2017. Prediction aided *in vitro* analysis of octa-decanoic acid from *Cyanobacterium Lyngbya* sp. as a proapoptotic factor in eliciting anti-inflammatory properties. Bioinformation 13, 301.

Marathe, N.P., Rasane, M.H., Kumar, H., Patwardhan, A.A., Shouche, Y.S., Diwanay, S.S., 2013. *In vitro* antibacterial activity of *Tabernaemontana alternifolia* (Roxb) stem bark aqueous extracts against clinical isolates of methicillin resistant *Staphylococcus aureus*. Annals of Clinical Microbiology and Antimicrobials 12, 1–8.

Marinho, F.F., Simões, A.O., Barcellos, T., Moura, S., 2016. Brazilian *Tabernaemontana* genus: Indole alkaloids and phytochemical activities. Fitoterapia 114, 127–137.

Marques, J.I., Alves, J.S.F., Torres-Rêgo, M., Furtado, A.A., Siqueira, E.M.D.S., Galinari, E., Araújo, D.F.D.S., Guerra, G.C.B., Azevedo, E.P.D., Fernandes-Pedrosa, M.D.F., Zucolotto, S.M., 2018.

Phytochemical analysis by HPLC–HRESI-MS and anti-inflammatory activity of *Tabernaemontana catharinensis*. International Journal of Molecular Sciences 19, 1–19.

Martínez-Beamonte, R., Sanclemente, T., Surra, J.C., Osada, J., 2020. Could squalene be an added value to use olive by-products?. Journal of the Science of Food and Agriculture 100, 915–925.

McCrae, C., Dzgoev, A., Ståhlman, M., Horndahl, J., Svärd, R., Große, A., Großkopf, T., Skujat, M.A., Williams, N., Schubert, S., Echeverri, C., 2018. Lanosterol synthase regulates human rhinovirus replication in human bronchial epithelial cells. American Journal of Respiratory Cell and Molecular Biology 59, 713–722.

Medeiros, W.L., Vieira, I.J.C., Mathias, L., Braz-Filho, R., Schripsema, J., 2001. A new natural auaternary indole alkaloid isolated from *Tabernaemontana laeta* Mart. (Apocynaceae). Journal of the Brazilian Chemical Society 12, 368–372.

Mehrbod, P., Abdalla, M.A., Njoya, E.M., Ahmed, A.S., Fotouhi, F., Farahmand, B., Gado, D.A., Tabatabaian, M., Fasanmi, O.G., Eloff, J.N., McGaw, L.J., 2018. South African medicinal plant extracts active against influenza A virus. BMC Complementary and Alternative Medicine 18, 112–121.

Mohammed, M.J., Ali, O.A., 2020. Isolation, characterization, and biological activity of some fatty acids and volatile oils from *iraqi eucalyptus microtheca* plant. International Journal of Pharmaceutical Quality Assurance 11, 136–140.

Moustafa, E.M., Thabet, N.M., 2017. Beta-sitosterol upregulated paraoxonase-1 via peroxisome proliferator-activated receptor-γ in irradiated rats. Canadian Journal of Physiology and Pharmacology 95, 661–666.

Murugan, R., Arunachalam, K., Parimelazhagan, T., 2012. Antioxidant, anti-inflammatory activity, and phytochemical constituents of *Ficus* (*Ficus amplissima* Smith) Bark. Food Science and Biotechnology 21, 59–67.

Muszkat, L., Bir, L., Raucher, D., 1997. Identification of mixed O-phenyl alkyl phthalate esters in an agricultural land. Bulletin of Environmental Contamination and Toxicology 58, 348–355.

Muthukamalam, S., Sivagangavathi, S., Dhrishya, D., Sudha-Rani, S., 2017. Characterization of dioxygenases and biosurfactants produced by crude oil degrading soil bacteria. Brazilian Journal of Microbiology 48, 637–647.

Mutis, A., Parra, L., Palma, R., Pardo, F., Perich, F., Quiroz, A., 2009. Evidence of contact pheromone use in mating behavior of the raspberry weevil (Coleoptera: *Curculionidae*). Environmental Entomology 38, 192–197.

Nagoba, B., Wadher, B., Kulkarni, P., Kolhe, S., 2008. Acetic acid treatment of pseudomonal wound infections. European Journal of General Medicine 5, 104–106.

Naidoo, C.M., Naidoo, Y., Dewir, Y.H., Murthy, H.N., El-Hendawy, S., Al-Suhaibani, N., 2021. Major Bioactive Alkaloids and Biological Activities of *Tabernaemontana* Species (Apocynaceae). Plants 10, 313.

Naik, S.K., Gurushanthaiah, M., Raju, N.G., Johnson, W.M.S., Mahesh, G.M., 2018. Extraction of Bio-active compounds of *Eclipta Alba* through GC-MS Analysis. Research Journal of Pharmaceutical Biological and Chemical Sciences 9, 297–302.

Nair, A.N.S., Nair, R.V.R., Nair, A.P.R., Nair, A.S., Thyagarajan, S., Johnson, A.J., Baby, S., 2020. Antidiabetes constituents, cycloartenol and 24-methylenecycloartanol, from *Ficus krishnae*. PloS One 15, 0235221.

Nguemeni, C., Gouix, E., Bourourou, M., Heurteaux, C., Blondeau, N., 2013. Alpha-linolenic acid: A promising nutraceutical for the prevention of stroke. Pharma Nutrition 1, 1–8.

Nguyen, N.H., Nguyen, T.T., Ma, P.C., Ta, Q.T.H., Duong, T.H., Vo, V.G., 2020. Potential antimicrobial and anticancer activities of an ethanol extract from *bouea macrophylla*. Molecules 25, 1996.

Nicola, C., Salvador, M., Escalona Gower, A., Moura, S., Echeverrigaray, S., 2013. Chemical constituent's anti-oxidant and anti-cholinesterasic activity of *Tabernaemontana catharinensis*. The Scientific World Journal 2013, 1–10.

Nizioł, J., Ossoliński, K., Ossoliński, T., Ossolińska, A., Bonifay, V., Sekuła, J., Dobrowolski, Z., Sunner, J., Beech, I., Ruman, T., 2016. Surface-transfer mass spectrometry imaging of renal tissue on gold nanoparticle enhanced target. Analytical Chemistry 88, 7365–7371.

Nogueira, A.O., Oliveira, Y.I.S., Adjafre, B.L., de Moraes, M.E.A., Aragao, G.F., 2019. Pharmacological effects of the isomeric mixture of alpha and beta amyrin *from Protium heptaphyllum*: A literature review. Fundamental and Clinical Pharmacology 33, 4–12.

Nweze, C., Ibrahim, H., Ndukwe, G.I., 2019. Beta-sitosterol with antimicrobial property from the stem bark of pomegranate (*Punica granatum* Linn). Journal of Applied Sciences and Environmental Management 23, 1045–1049.

Ogunwole, E., Kunle-Alabi, O.T., Akindele, O.O.,Raji, Y., 2017. Adverse Effects of *Saccharum officinarum* Molasses on Rat Testicular Cells. Advances in Toxicology and Toxic Effects 3, 001–008.

Ok, F., Kaplan, H.M., Kizilgok, B.,Demir, E., 2020. Protective effect of Alpha-Linolenic acid on Lipopolysaccharide-Induced Orchitis in mice. Andrologia 52, 13667.

Okubo, M., Utsunomiya, N., 1996. Effects of sodium chloride on growth, gas exchange and ion concentration in latex of Fig (*Ficus carica* L.). Environmental Control in Biology 34, 259–65.

Olaniyan, O.T., Kunle-Alabi, O.T., Raji, Y., 2018. Protective effects of methanol extract of *Plukenetia conophora* seeds and 4H-Pyran-4-One 2, 3-Dihydro-3, 5-Dihydroxy-6-Methyl on the reproductive function of male Wistar rats treated with cadmium chloride. JBRA Assisted Reproduction 22, 289.

Olaoluwa, O., Moronkola, D., Taiwo, O., Iganboh, P., 2018. Volatile oil composition, antioxidant and antimicrobial properties of *Boerhavia erecta* L. and *Euphorbia hirta* L. Trends in Phytochemical Research 2, 171–178.

Olushola-Siedoks, A.A., Igbo, U.E., Asieba, G.O., Ojo, B.I., Akinola, T.O., Igwe, C.C., 2019. Preliminary investigations on the health benefits of *Citrullus colocynthis* (L.) schrad seeds. European Journal of Nutrition and Food Safety 10, 187–198.

Ong, M.G., Mat Yusuf, S.N.A., Lim, V., 2016. Pharmacognostic and antioxidant properties of *Dracaena sanderiana* leaves. Antioxidants 5, 28.

Oyedeji, F.O., Erazua, E.A., Adeleke, B.B., 2018. GC-Mass spectroscopic chemical characterization and physico-chemical properties of oil from seed kernels of four cultivars of *Magnifera Indica*. European Journal of Pure and Applied Chemistry 5, 1–11.

Pachauri, T., Singla, V., Satsangi, A., Lakhani, A., Kumari, K.M., 2013. SEM-EDX characterization of individual coarse particles in Agra, India. Aerosol and Air Quality Research 13, 523–536.

Pallant, C.A., Cromarty, A.D., Steenkamp, V., 2012. Effect of an alkaloidal fraction of *Tabernaemontana elegans* (Stapf.) on selected micro-organisms. Journal of Ethnopharmacology 140, 398–404.

Pan, H., Hu, X.Z., Jacobowitz, D.M., Chen, C., McDonough, J., Van Shura, K., Lyman, M., Marini, A.M., 2012. Alpha-linolenic acid is a potent neuroprotective agent against soman-induced neuropathology. Neurotoxicology 33, 1219–1229.

Paniagua-Pérez, R., Flores-Mondragón, G., Reyes-Legorreta, C., Herrera-López, B., Cervantes-Hernández, I., Madrigal-Santillán, O., Morales-González, J.A., Álvarez-González, I., Madrigal-Bujaidar, E., 2017. Evaluation of the anti-inflammatory capacity of beta-sitosterol in rodent assays. African Journal of Traditional, Complementary and Alternative Medicines 14, 123–130.

Parthipan, B., Suky, M.G.T., Mohan, V.R., 2015. GC-MS analysis of phytocomponents in *Pleiospermium alatum* (Wall. ex Wight & Arn.) Swingle, (Rutaceae). Journal of Pharmacognosy and Phytochemistry 4, 216–222.

Patel, S.S., Savjani, J.K., 2015. Systematic review of plant steroids as potential anti-inflammatory agents: Current status and future perspectives. The Journal of Phytopharmacology 4, 121–125.

Patil, P.S., Venkatanarayanan, R., Argade, P.D., Shinde, P.R., 2012. Assessment of pharmacognostic and phytochemical standards of *Thespesia populnea* (L.) root. Asian Pacific Journal of Tropical Biomedicine 2, 1212–1216.

Patra, J.K., Lee, S.W., Park, J.G., Baek, K.H., 2017. Antioxidant and antibacterial properties of essential oil extracted from an edible seaweed *Undaria pinnatifida*. Journal of Food Biochemistry 41, 12278.

Penduka, D., Buwa, L., Mayekiso, B., Basson, A.K., Okoh, A.I., 2014. Identification of the antilisterial constituents in partially purified column chromatography fractions of *Garcinia kola* seeds and their interactions with standard antibiotics. Evidence-Based Complementary and Alternative Medicine 2014, 1–8.

Prasher, I.B., 2019. Screening of *Peniophora nuda* (a white rot fungus) for the presence of commercially important bioactive metabolites. Vegetos, 32, 307–315.

Pratchayasakul, W., Pongchaidecha, A., Chattipakorn, N., Chattipakorn, S., 2008. Ethnobotany & Ethnopharmacology of *Tabernaemontana divaricata*. Indian Journal of Medical Research 127, 317–355.

Prayitno, T.A., Widyorini, R., Lukmandaru, G., 2020. Chemical variation of five natural extracts by non-polar solvent. Maderas: Ciencia y tecnología 22, 15–33.

Radhika, B., 2017. Comparitive Study of Soxhlation and Maceration Extracts of *Tabernaemontana divaricta* Leaves for Antibacterial Activity. Journal of Natural Products and Plant Resources 7, 34–39.

Rao, A., Naika, R., 2018. Antioxidant and cytotoxic properties of *Pavetta crassicaulis* Bremek. leaf crude extract and its isolated pure compound. Indian Journal of Natural Products and Resources (IJNPR) [Formerly Natural Product Radiance (NPR)] 8, 335–350.

Rao, M.R., Anisha, G., 2018. Preliminary phytochemical and GC MS study of one medicinal plant *Carissa spinarum*. Indo American Journal of Pharmaceutical Research 8, 414–21.

Rao, M.R.K., Anisha, G., Prabhu, K., Shil, S., Vijayalakshmi, N., 2019. Preliminary Phytochemical and Gas Chromatography-Mass Spectrometry study of one medicinal plant *Carissa carandas*. Drug Invitation Today 12, 1629–1630.

Ravi, R., Husna Zulkrnin, N.S., Rozhan, N.N., Nik Yusoff, N.R., Mat Rasat, M.S., Ahmad, M.I., Hamzah, Z., Ishak, I.H., Mohd Amin, M.F., 2018. Evaluation of two different solvents for *Azolla pinnata* extracts on chemical compositions and larvicidal activity against *Aedes albopictus* (Diptera: *Culicidae*). Journal of Chemistry 2018, 1–8.

Ren, J., Wang, J., Karthikeyan, S., Liu, H., Cai, J., 2019. Natural anti-phytopathogenic fungi compound phenol, 2, 4-bis (1, 1-dimethylethyl) from TL-1. *Pseudomonas fluorescens* Indian Journal of Biochemistry and Biophysics (IJBB) 56, 162–168.

Richard, F., dos Anjos Szczerepa, M.M., Mucellini, K.L., Zanqueta, É.B., Lancheros, C.A.C., Nakamura, T.U., Nakamura, C.V., Endo, E.H., Junior, M.M., Mikcha, J.M.G., Gonçalves, R.A.C., 2021. Antibacterial activity of crude extract of *Tabernaemontana catharinensis* latex (A. DC) against *Alicyclobacillus* spp. Research, Society and Development 10, 16310917907-e16310917907.

Rivlin, M., Navon, G., 2018. CEST MRI of 3-O-methyl-D-glucose on different breast cancer models. Magnetic Resonance in Medicine 79, 1061–1069.

Rocha, K.C., Alonso, C.G., Leal, W.G.O., Schultz, E.L., Andrade, L.A., Ostroski, I.C., 2020. Slow pyrolysis of *Spirulina platensis* for the production of nitrogenous compounds and potential routes for their separation. Bioresource Technology 313, 123709.

Rodeiro, I., Donato, M.T., Jimenez, N., Garrido, G., Molina-Torres, J., Menendez, R., Castell, J.V., Gómez-Lechón, M.J., 2009. Inhibition of human P450 enzymes by natural extracts used in traditional medicine. Phytotherapy Research: An International Journal Devoted to Pharmacological and Toxicological Evaluation of Natural Product Derivatives 23, 279–282.

Roy, S.J., Baruah, P.S., Lahkar, L., Gurung, L., Saikia, D., Tanti, B., 2019. Phytochemical analysis and antioxidant activities of *Homalomena aromatic* Schott. Journal of Pharmacognosy and Phytochemistry 8, 1379–1385.

Sathya, S., Lakshmi, S., Nakkeeran, S., 2016. Combined effect of biopriming and polymer coating on chemical constituents of root exudation in chilli (*Capsicum annuum* L.) cv. K 2 seedlings. Journal of Applied and Natural Science 8, 2141–2154.

Sattigeri, V.J., Arora, S.K., Salman, M., Princeton, N.J., Palle, V.P., Nagarajan, M., Shirumala, H.R., Aulakh, G.K., Ray, A., 2009. Derivatives of pentose monosaccharides as anti-inflammatory compounds. United States registered patent 41, 1–53.

Schmelzer, G.B., Gurib-Fakim, A., 2008. Medicinal Plants, first ed. Plant Resources of Tropical Africa 11,1. PROTA Foundation. Backhuys Publishers, Wageningen, Netherlands, Volume 1, pp. 597–598.

Schmidt, E., Lotter, M., McCleland, W., 2002. Trees and Shrubs of Mpumalanga and Kruger National Park. Jacana.

Schripsema, J., Hermans-Lokkerbol, A., Van der Heijden, R., Verpoorte, R., Svendsen, A.B., Van Beek, T.A., 1986. Alkaloids of *Tabernaemontana ventricosa*. Journal of Natural Products 49, 733–735.

Semwal, P., Painuli, S., Badoni, H., Bacheti, R.K., 2018. Screening of phytoconstituents and antibacterial activity of leaves and bark of *Quercus leucotrichophora* A. Camus from Uttarakhand Himalaya. Clinical Phytoscience 4, 1–6.

Sendeku, W., Alefew, B., Mengiste, D., Seifu, K., Girma, S., Wondimu, E., Bekuma, G., Verma, D., Berhane, N., 2015. Antibacterial activity of *Croton macrostachyus* against some selected pathogenic bacteria. Biotechnology International 8, 11–20.

Shakya, A.K., 2016. Medicinal plants: Future source of new drugs. International Journal of Herbal Medicine 4, 59–64.

Shareef, H.K., Muhammed, H.J., Hussein, H.M., Hameed, I.H., 2016. Antibacterial effect of ginger (*Zingiber officinale*) roscoe and bioactive chemical analysis using gas chromatography mass spectrum. Oriental Journal of Chemistry 32, 20–40.

Sharma, A., Kumar, V., Kohli, S.K., Thukral, A.K., Bhardwaj, R., 2015. Phytochemicals in *Brassica juncea* L. seedlings under imidacloprid-epibrassinolide treatment using GC-MS. Journal of Chemical and Pharmaceutical Research 7, 708–711.

Sharma, R., Zimik, M. and Arumugam, N., 2019. Isolation and GCMS characterization of certain non-polar compounds from *spilanthes ciliata*. International Journal of Pharmacy and Biological Sciences 8, 889–903.

Shen, X., Zhu, M., Kang, L., Tu, Y., Li, L., Zhang, R., Qin, B., Yang, M., Guan, H., 2018. Lanosterol synthase pathway alleviates lens opacity in age-related cortical cataract. Journal of Ophthalmology 2018, 1–9.

Silveira, D., de Melo, A.F., Magalhães, P.O., Fonseca-Bazzo, Y.M., 2017. *Tabernaemontana* Species: Promising sources of new useful drugs. In Studies in Natural Products Chemistry, Atta-U-Rahman (Ed.) Elsevier 54, 227–289.

Singh, G., Kumar, P., Jindal, A., 2012. Antibacterial potential of sterols of some medicinal plants. International Journal of Pharmacy and Pharmaceutical Science 4, 159–3162.

Singh, P., Khosa, R.L., Srivastava, S., Mishra, G., Jha, K.K., Srivastava, S., Verma, R.K., Tahseen, M.A., 2014. Pharmacognostical study and establishment of quality parameters of aerial parts of *Costus speciosus*–a well-known tropical folklore medicine. Asian Pacific Journal of Tropical Biomedicine 4, 486–491.

Sivakumaran, G., Prabhu, K., Rao, M.R., Jones, S., Sundaram, R.L., Ulhas, V.R., Vijayalakshmi, N., 2019. Gas chromatography-mass spectrometry analysis of one Ayurvedic oil, *Ksheerabala Thailam*. Drug Invent Today 11, 2661–5.

Spikes, A.E., Paschen, M.A., Millar, J.G., Moreira, J.A., Hamel, P.B., Schiff, N.M., Ginzel, M.D., 2010. First contact pheromone identified for a longhorned beetle (Coleoptera: *Cerambycidae*) in the subfamily Prioninae. Journal of Chemical Ecology 36, 943–954.

Sridevi, G., Prema, S., Sekar, S., Sembulingam, K., 2014. Phytochemical analysis of *Pergularia daemia* for its bioactive components through gas chromatographic mass spectrometry (GCMS). IOSR Journal of Pharmacy 4, 41–46.

Srinivasan, S., Priya, V., 2019. Phytochemical screening and GC-MS analysis of *Cyperus dubius, Rottb*. (Cyperaceae). Journal of Medicinal Plants 7, 89–98.

Sudha, T., Chidambarampillai, S., Mohan, V.R., 2013. GC-MS analysis of bioactive components of aerial parts of *Fluggea leucopyrus* Willd. (Euphorbiaceae). Journal of Applied Pharmaceutical Science 3, 126.

Sumi, E.R., Anandan, R., Rajesh, R., Ravishankar, C.N., Mathew, S., 2018. Nutraceutical and therapeutic applications of squalene. Fishery Technology 55, 229–237.

Surburg, H., Panten, J., 2016. Common fragrance and flavor materials: Preparation, properties and uses, Sixth ed. John Wiley & Sons.

Sushma, V., Pal, S.M., Viney, C., 2017. GC-MS Analysis of Phytocomponents in the Various Extracts of *Shorea robusta Gaertn* F. International Journal of Pharmacognosy and Phytochemical Research 9, 783–788.

Tadigiri, S., Das, D., Allen, R.C., Vishnu, V.R., Veena, S.S, Karthikeyan, S., 2020. Isolation and characterization of chemical constituents from B. *amyloliquefaciens* and their nematicidal activity. Mortality 8, 2062–2066.

Taiwo, O.M., Mbachu, K.A., Olaoluwa, O., Prabodh, S., 2018. Essential oil compositions of *Basella alba linnaeus* and *Cnidoscolus aconitifolius* (mill.) Johnson, World Journal of Pharmacy and Pharmaceutical Sciences 7, 285-295.

Tanaka, R., Kasubuchi, K., Kita, S., Tokuda, H., Nishino, H., Matsunaga, S., 2000. Bioactive steroids from the whole herb of *Euphorbia chamaesyce*. Journal of Natural Products 63, 99–103.

Tatiya, A., Surana, S., Bhavsar, S., Patil, D., Patil, Y., 2012. Pharmacognostic and preliminary phytochemical investigation of *Eulophia herbacea* Lindl. Tubers (Orchidaceae). Asian Pacific Journal of Tropical Disease 2, 50–55.

Terasaki, M., Mima, M., Kudoh, S., Endo, T., Maeda, H., Hamada, J., Osada, K., Miyashita, K., Mutoh, M., 2018. Glycine and succinic acid are effective indicators of the suppression of epithelial-

mesenchymal transition by fucoxanthinol in colorectal cancer stem-like cells. Oncology reports 40, 414–424.

Thasneem, Z.A., Aravindh, K., Fencia, M.J.M., Kumar, C.N., Pavithra, T., Rajkumar, K., Surendran, S., Vidhya, M., Mahesh, R., Ramalakshmi, S., 2019. GC-MS analysis of yellow pigmented *Macrococcus equipercicus* isolated from alfalfa rhizosphere soil fields of Coimbatore. Journal of Applied and Natural Science 11, 645–649.

Thiele, J.J., Hsieh, S.N., Ekanayake-Mudiyanselage, S., 2005. Vitamin E: Critical review of its current use in cosmetic and clinical dermatology. Dermatologic Surgery, 805–813.

Thombre, R., Jagtap, R., Patil, N., 2013. Evaluation of phytoconstituents, antibacterial, anti-oxidant and cytotoxic activity of *Vitex negundo* L. and *Tabernaemontana divaricata* L. International Journal of Pharmaceutical and Biological Sciences 4, 389–396.

Tiwari, P., Kumar, B., Kaur, M., Kaur, G., Kaur, H., 2011. Phytochemical screening and extraction: A review. Internationale Pharmaceutica Sciencia 1, 98–106.

Tiwari, S.C., Husain, N., 2017. Biological activities and role of flavonoids in human health. Indian Journal of Science and Research 12, 193–196.

Trust, T.J., Bartlett, K.H., 1975. Antibacterial activity of tropilidine and tropone. Antimicrobial agents and Chemotherapy 8, 381–383.

Upadhyay, A., Amanullah, A., Mishra, R., Kumar, A., Mishra, A., 2018. Lanosterol suppresses the aggregation and cytotoxicity of misfolded proteins linked with neurodegenerative diseases. Molecular Neurobiology 55, 1169–1182.

Van Beek, T.A., Deelder, A.M., Verpoorte, R. and Svendsen, A.B., 1984. Antimicrobial, antiamoebic and antiviral screening of some *Tabernaemontana species*. Planta Medica 50, 180–185.

Venkateswarlu, K., Kelly, S.L., 1996. Biochemical characterisation of ketoconazole inhibitory action on *Aspergillus fumigatus*. FEMS Immunology and Medical Microbiology 16, 11–20.

Venkatramanan, M., Sankar Ganesh, P., Senthil, R., Akshay, J., Veera Ravi, A., Langeswaran, K., Vadivelu, J., Nagarajan, S., Rajendran, K., Shankar, E.M., 2020. Inhibition of quorum sensing and biofilm formation in *Chromobacterium violaceum* by fruit extracts of *Passiflora edulis*. ACS omega 5, 25605–25616.

Verma, S., Singh, S.P., 2008. Current and future status of herbal medicines. Veterinary World 1, 347.

Vijayan, A., John, J.V., Parthipan, B., Renuka, C., 2007. Traditional remedies of Kani tribes of Kottoor reserve forest. Journal of Traditional Knowledge 6, 589–594.

Wagh, S.J., Gujar, J.G., Gaikar, V.G., 2012. Experimental and modeling studies on extraction of amyrins from latex of mandar (*Calotropis gigantea*). Indian Journal of Chemical Technology 19, 427–433.

Warra, A.A., 2019. Analyzing Physicochemical Properties of Wild Grapes (Lannea Microcarpa) Seed Oil. Indonesian Journal of Computing, Engineering and Design (IJoCED) 1, 37–43.

Wei, C.C., Chang, C.H., Liao, V.H.C., 2017. Anti-Parkinsonian effects of β-amyrin are regulated via LGG-1 involved autophagy pathway in *Caenorhabditis elegans*. Phytomedicine 36, 118–125.

Xi, Y., Jiang, T., Yu, Y., Yu, J., Xue, M., Xu, N., Wen, J., Wang, W., He, H., Shen, Y., Chen, D., 2019. Dual targeting curcumin loaded alendronate-hyaluronan-octadecanoic acid micelles for improving osteosarcoma therapy. International Journal of Nanomedicine 14, 6425.

Yang, M.T., Kuo, T.F., Chung, K.F., Liang, Y.C., Yang, C.W., Lin, C.Y., Feng, C.S., Chen, Z.W., Lee, T.H., Hsiao, C.L., Yang, W.C., 2020. Authentication, phytochemical characterization and antibacterial activity of two Artemisia species. Food Chemistry 333, 127458.

Zhao, F., Wang, P., Lucardi, R.D., Su, Z., Li, S., 2020. Natural sources and bioactivities of 2, 4-di-tert-butylphenol and its analogs. Toxins 12, 35.

Zhao, Z., Liang, Z., Ping, G., 2011. Macroscopic identification of Chinese medicinal materials: traditional experiences and modern understanding. Journal of Ethnopharmacology 134, 556–564.

Zhu, X., Wang, B., Zhang, X., Chen, X., Zhu, J., Zou, Y., Li, J., 2020. Alpha-linolenic acid protects against lipopolysaccharide-induced acute lung injury through anti-inflammatory and anti-oxidative pathways. Microbial Pathogenesis 142, 104077.

CHAPTER 5:

IN VITRO INVESTIGATION OF THE ANTIOXIDANT AND CYTOTOXIC POTENTIAL OF *TABERNAEMONTANA VENTRICOSA* HOCHST. EX A. DC. LEAF, STEM, AND LATEX EXTRACTS

Abstract

Tabernaemontana ventricosa (Apocynaceae) is a latex-bearing plant that is used in traditional medicine systems for its therapeutic benefits such as reducing fever and hypertension and wound healing. However due to the limited information on the pharmacological activities of this species, the present study aimed to investigate the antioxidant potential of the leaf, stem, and latex extracts of *T. ventricosa*, using the Folin-Ciolcalteu (total phenolics), aluminum chloride colorimetric (total flavonoids), 2,2-diphenyl-1-picrylhydrazyl (DPPH), and Ferric Reducing Antioxidant Power (FRAP) assays. The cytotoxic activity was evaluated in the human cell lines; HEK293 (embryonic kidney), HeLa (cervical carcinoma), and MCF-7 (breast adenocarcinoma) using the MTT assay. The latex extracts possessed highest total phenolic content (115.36 ± 2.89 mg GAE/g), the stem hexane extracts (21.33 ± 0.42 mg GAE/g), followed by the chloroform leaf (7.89 ± 0.87 mg GAE/g) and chloroform stem (4.69 ± 0.21 mg GAE/g) extracts exhibiting moderate phenolic content. The flavonoid content was substantially high ranging from 946.92 ± 6.29 mg QE/g in the stem hexane, 768.96 ± 5.43 mg QE/g in the latex, 693.24 ± 4.12 mg QE/g in the stem chloroform, and 662.20 ± 1.00 mg QE/g in the leaf hexane extracts. The DPPH and FRAP assays showed varying amounts of antioxidant potential. For the DPPH assays, at 240 µg/mL, the stem hexane (70.10%), stem methanol (65.24%), and stem chloroform (60.26%) showed the highest percentage of inhibition, with IC_{50} values of 6.19 µg/mL (stem methanol), 16.26 µg/mL (stem hexane) and 22.56 µg/mL (stem chloroform). In contrast, the FRAP assays displayed minimal percentage inhibition ranging from 4.73% to 14.40 %, except for the latex extracts which displayed moderate inhibition at 15 µg/mL (21.82%) and substantial inhibition at 240 µg/mL (98.48%). For the cytotoxicity analysis, the HeLa and MCF-7 cell lines were the most sensitive to the extracts, with the hexane, chloroform, and methanol leaf and stem, and latex extracts affecting the percentage cell survival considerably. This study concludes that the various parts of *T. ventricosa* exhibited strong antioxidant activity that correlates to the cytotoxic potential of this species. Hence, further analysis should focus on the isolation of specific antioxidant compounds that could be investigated for their anticancer potential.

Keywords: Antioxidant; Cytotoxicity; DPPH; Flavonoids; FRAP; Phenols.

5.1. Introduction

Cancer is a composite terminal disease whereby irregular cells rapidly divide and often attack several tissues or migrate into various other locations (Munayi, 2016). There are three significant and common causes of cancer, which include improper diet (Key et al., 2002), genetic character (Migliore and Coppedè, 2002), and ecological factors (Boffetta and Nyberg, 2003) such as ultraviolet (UV)-light, infectious agents, and pollution (Soerjomataram, 2018). The hasty incline in the critical contributors to this disease has directly increased cancer rates over the last decade (WHO, 2018; Herzallah et al., 2019; Rosales et al., 2019). According to the global cancer statistics in 2018, approximately 18.1 million people are likely to be diagnosed with cancer, and an additional 10 million cancer-related deaths were anticipated in 2020 (WHO, 2018, Bray et al., 2018; Ferlay et al., 2019; de Martel et al., 2020). Global cancer statistics have revealed that lung cancer is the foremost cause of cancer mortality (18.4%), closely followed by breast cancer (11.6%), stomach cancer (8.2%), liver cancer (8.2%), prostate cancer (7.1%) and colorectal cancer (6.1%) (Bray et al., 2018). According to Made et al. (2017), nearly 38 000 (8%) of the total deaths in South Africa in 2014 were associated with cancer. Regardless of the widespread usage of chemotherapy, radiation therapy, and immunotherapy, these treatments introduce significant consequences ranging from multidrug resistance (MDR), exhaustive side effects, and the generation of Reactive Oxygen Species (ROS), which ultimately induce detrimental effects to DNA (deoxyribonucleic acid) and cellular signalling pathways (Hussain et al., 2003; Glebova et al., 2015; Thyagarajan and Sahu, 2018).

Recently, the discovery of novel compounds from medicinal plant extracts has been considered for the treatment of cancer (Majolo et al., 2019; Rosales et al., 2019; Singh et al., 2019). These compounds are often preferred over conventional techniques since natural compounds display minimal side effects and act as a modulator of MDR (Silveria, 2017; Kumar and Jaitak, 2019; Hamed et al., 2019). Approximately 60% of anticancer agents are often generated from plant-based compounds (Newman and Cragg, 2007; Gezici and Şekeroğlu, 2019; Morsy, 2019; Priya and Satheeshkumar, 2020). The most common plant-derived anticancer products include vinca alkaloids, combretastatin, taxanes, camptothecin, and epipodophyllotoxin (Wall and Wani, 1996; Imbert, 1998; Da Rocha et al., 2001; Khazir et al., 2014). Additionally, phenolics, flavonoids, and volatile essential oils are often utilized in cancer research due to their rich source of antioxidants (Fierascu et al., 2018; Sammar et al., 2019; Alfa and Arroo, 2019). These compounds are exploited to combat ROS, resulting in the reduction of oxidative stress, improvement of immune function, and an increase in longevity (Shori, 2015; Fierascu et al., 2018; Tan et al., 2018). According to Kam et al. (2004), several species belonging to the genus *Tabernaemontana* contain indole alkaloids, which may suppress the growth and development of tumour cells.

Tabernaemontana ventricosa Hochst. ex A. DC. (Forest toad tree) is a latex-bearing plant belonging to the Apocynaceae and a genus consisting of medium-sized flowering trees within *Tabernaemontana* (Schmidt et al., 2002). This species emits a pungent sweet scent from tubular salver-shaped whitish-yellow flowers (Schmelzer and Gurib-Fakim, 2008). Approximately 100 species of the *Tabernaemontana* genus are primarily distributed in tropical and subtropical regions of the world, including Africa, Asia, and America (Schmelzer and Gurib-Fakim, 2008; Silveira et al., 2017). The species *T. ventricosa* and *T. elegans* are the two species reported to occur in South Africa (Beentje et al., 1994; Schmelzer and Gurib-Fakim, 2008; Munayi, 2016). Previous phytochemical analysis on *T. ventricosa* indicated the presence of major alkaloidal components and large quantities of triterpenes (Schripsema, 1986). Parts of *T. ventricosa* are reportedly used in traditional medicine systems in KwaZulu-Natal to palliate fever, reduce blood pressure, treat wounds, and heal sore eyes (Schmelzer and Gurib-Fakim, 2008; Mehrbod et al., 2018). Insufficient research is available on *T. ventricosa*, although a few studies have investigated the biological activity of certain chemical compounds. Van Beek et al. (1984) reported on the alkaloidal compounds conopharyngine and akuammincine, which showed healing and opioid activity, respectively.

Considering the scarcity of information available on the pharmacological activities of *T. ventricosa* and the crucial discoveries of curative agents from innovative plant-based products, the current investigation aimed to determine the antioxidant activities of the hexane, chloroform, and methanol leaf and stem, and latex extracts of *T. ventricosa* using various protocols such as the Folin-Ciocalteu for total phenolics content, aluminum chloride colorimetric for total flavonoids content, 2,2-diphenyl-1-picrylhydrazyl (DPPH), and Ferric Reducing Antioxidant Power (FRAP) assays. The cytotoxic activities of all extracts was also evaluated in the human cell lines; HEK293 (human embryonic kidney cells), HeLa (cervical carcinoma), and MCF-7 (breast adenocarcinoma) using the 3-(4,5-dimethylthiazol-2-yl)-2,5-diphenyl-2H-tetrazolium bromide (MTT) assay.

5.2. Materials and Methods

5.2.1 Plant and exudate collection

Leaves, stems, and latex exudate from fully grown *T. ventricosa* plants (~ 12-15 m in height) of wild origin were collected from the University of KwaZulu-Natal (Westville campus), South Africa (29˚49′03.3″S 30˚56′32.7″E). A combination of emergent, young, and mature leaves and stems were collected for analysis. The plant material and exudate were taxonomically identified, and a voucher specimen (18222) was deposited at the Ward herbarium, School of Life Sciences, University of KwaZulu-Natal. The plant material was inspected for any signs of microbial and fungal contamination. Thereafter the leaves and stems were separately air-dried for three months at 23˚C and ground at high speed into a fine powder using a grinder (Mellerware, Model: 29105). The powdered material was kept in an airtight consol™ glass jar, out of direct sunlight, at 23˚C, until further use. The latex exudate was aseptically collected by careful incisions in the soft stems of the plant with a sharp blade. The latex was diluted in distilled water (1:1; *v*/*v*), and the sample was centrifuged at 5000 rpm/ref for 10 min using an Eppendorf centrifuge (Model: 5415R, USA). The pellet was removed, and the supernatant was stored and at -8˚C until further use.

5.2.2 Extraction

Powdered samples of leaves (10 g) and stems (10 g) were separately and sequentially extracted by reflux extraction with 100 mL of hexane. A sequence of four extractions (3 h each) was performed for each solvent, using a heated mantle at approximately 60˚C. The extracts were filtered separately after each extraction using filter paper (Whatman No. 1). Additional hexane was added for extractions. The reflux extraction was repeated with chloroform and methanol. The resulting leaf and stem extracts for each solvent were stored separately in sterilized consol™ glass jars, in a dark room.

5.2.3 Evaporation and concentration

Following extractions, the leaf and stem extracts, and latex supernatants were entirely air-dried in a well-ventilated dark room (~23˚C) for approximately 30 days. The dried extracts were stored in airtight glass bottles at 4˚C. The percentage yield of the extracts was calculated as in equation 5.1.

$$\text{Extract yield (\%)} = \frac{\text{Weight of dried extract (g)}}{\text{Weight of powdered material (g)}} \times 100 \quad \textbf{(5.1)}$$

5.2.4 Quantification of total phenolics, total flavonoids, and antioxidant assays

5.2.4.1. Preparation of stock solutions

Various stock solutions such as leaf hexane (LH); leaf chloroform (LC); leaf methanol (LM); stem hexane (SH); stem chloroform (SC) and stem methanol (SM) were prepared by resuspending 1 mg of dried crude extracts (i.e., hexane, chloroform, and methanol) in 1 mL of methanol solvent respectively. Previously collected and prepared latex (LX) supernatants were adjusted to 1 mg/mL. All the stock solutions (1 mg/mL) were homogenized using a vortex (Model:VM-1000, Taiwan), and various concentrations (15, 30, 60, 120, and 240 µg/mL) were prepared for total phenolics, total flavonoids, and antioxidant assays.

5.2.4.2. Total phenolic content: Folin-Ciocalteu method

The Folin-Ciocalteu method was used to determine the total phenolic content of the respective extracts (Liu and Yao, 2007). Approximately 150 µL of diluted Folin-Ciocalteu reagent (10%) and 0.7 M of sodium carbonate (Na_2CO_3) was added to 30 µL sample extracts. The mixtures were incubated at 23˚C (room temperature), in the dark for 30 min. Thereafter, the absorbance (Abs) of the samples was measured at 765 nm using a Synergy HTX Multi-mode reader (BioTek Instruments Inc., USA). The results were expressed as milligrams of gallic acid equivalents (GAE) per gram of dry weight using the equation:

$$\mathrm{Ctp} = \mathrm{C} * \frac{\mathrm{V}}{\mathrm{M}} \qquad \textbf{(5.2)}$$

Where Ctp = Total phenolic content (mg/g) in GAE (gallic acid) equivalent
C = Concentration of gallic acid obtained from calibration curve in mg/mL
V = Volume of extract in mL
M = Mass of extract in gram

5.2.4.3. Total flavonoid content: The aluminum chloride colorimetric assay

The aluminum chloride colorimetric assay was used to determine the total flavonoid content of the respective extracts, the protocol of Arruda et al. (2018), with slight modifications was employed. Diluted extracts (25 µL) were mixed with 100 µL ultrapure millipore water (Milli *Q* water) and 7.5 µL of 5% $NaNO_2$. After 5 min, approximately 7.5 µL mL of 10% $AlCl_3$ was added to the reaction and left undisturbed for a further 6 min. Thereafter, 50 µL of 1M NaOH and 60 µL of ultrapure millipore water (Milli *Q* water) was added respectively. The solutions were mixed, and the absorbance of samples were measured at 510 nm using a Synergy HTX Multi-mode reader (BioTek Instruments Inc., USA). Ethanol was used as a blank and the total flavonoid content was expressed as mg quercetin equivalents (QE/per gram of dry weight) using the equation:

$$\mathrm{Ctf} = \mathrm{C} * \frac{\mathrm{V}}{\mathrm{M}} \qquad \textbf{(5.3)}$$

Where Ctf = Total flavonoid content (mg/g) in QE (quercetin) equivalent
C = Concentration of quercetin obtained from calibration curve in mg/mL
V = Volume of extract in mL
M = Mass of extract in gram.

5.2.4.4. The 2,2′-diphenyl-1- picrylhydrazyl (DPPH) scavenging activity

The free radical scavenging activity of *T. ventricosa* extracts was examined using DPPH, with adjustments of the method described by Akwu et al. (2019). Ascorbic acid was served as the positive control at different concentrations in methanol (15, 30, 60, 120, and 240 µg/mL). The DPPH solution (0.3 mM) was prepared in 99% methanol. Briefly, 50 µL of 0.3 mM DPPH was added to 100 µL of each extract. The solutions were mixed well and incubated in the dark at 23˚C for 30 min. The colorimetric observation from purple to yellow indicated the scavenging potential of the extracts. The absorbance was measured at 517 nm using a Synergy HTX Multi-mode reader (BioTek Instruments Inc., USA) against a blank (no sample/standard). The IC_{50} was determined using the inhibition curves. The scavenging activity of the extracts was established using the following equation:

$$\text{DPPH Scavenging activity \%} = \left[\frac{(\text{Abs control} - \text{Abs sample})}{\text{Abs control}}\right] * 100 \quad \textbf{(5.4)}$$

Where Abs control is the absorbance of the DPPH and methanol, while
Abs sample is the absorbance of DPPH radical in the presence of the sample or standard.
The percentage obtained of the scavenging extracts was compared with the positive control.

5.2.4.5. Ferric (Fe^{3+}) reducing antioxidant power (FRAP) assay

The FRAP activity of the extracts was determined using the method described by Akwu et al. (2019). Briefly, 25 µL of each extract (15, 30, 60,120 and 240 µg/mL) was mixed with 25 µL of 0.2 M sodium phosphate buffer (pH 6.6). Thereafter, 50 µL of 1% potassium ferricyanide was added to the mixture, which was incubated in an oven at 50˚C for 30 min. The reaction was halted with the addition of 25 µL of 10% trichloroacetic acid, 25 µL of ultrapure millipore water (Milli *Q* water), and 5 µL of 0.1% iron (III) chloride ($FeCl_3$). This was then mixed and incubated at 23˚C for 10 min, and the absorbance was measured at 700 nm using a Synergy HTX Multi-mode reader (BioTek Instruments Inc., USA). The results were expressed as a percentage of the absorbance of the extracts of gallic acid (standard) using the formula:

$$\text{\% Inhibition} = \left[\frac{\text{Abs of sample}}{\text{Abs of gallic acid}}\right] * 100 \quad \textbf{(5.5)}$$

5.2.5. MTT cytotoxicity assay

Three human cell lines viz., embryonic kidney (HEK293), breast adenocarcinoma (MCF-7), and cervical carcinoma (HeLa) were procured from the ATCC, Manassas, USA. For use in the cytotoxicity assays, all three cell lines were grown to confluency in 25 cm^2 tissue culture flasks using Eagle's Minimum Essential Medium (EMEM), containing 10% (*v/v*) gamma-irradiated FBS and 1% antibiotics (100 units/mL penicillin, 100 µg/mL streptomycin) in a HEPA Class 100 Steri-Cult CO_2 incubator (Thermo-electron Corporation, USA), at 37˚C in 5% CO_2. Upon confluency, the cells were trypsinized and seeded into clear 96-well plates and incubated at 37˚C overnight. The cells were then prepared by replenishing the growth medium with a fresh complete medium (EMEM + 10% FBS + 1% antibiotics). Thereafter, 100 µL of the seven extracts with varying concentrations ranging from 15 to 240 µg/mL were added to the cells and incubated at 37˚C for 36 h. The cells (100 µL) without treatment (extract) were used as the positive control (*c.a* 100% viability). All assays were conducted in triplicate.

The methods briefly described by Mosmann (1983) and Daniels and Singh (2019), were used to evaluate the cytotoxic potential activity of the extracts from the leaves, stems, and latex of *T. ventricosa* in the three cell lines. Following 48 h of incubation at 37˚C, the growth medium was aspirated and replaced with 100 µL of medium containing 10 µL MTT solution (5 mg/mL in PBS), and the cells containing the treatment and negative control were incubated for a further 4 h at 37˚ C in 5% CO_2. The medium-MTT mixture was then removed and replaced with 100 µL dimethylsulphoxide (DMSO). The absorbances were then measured at 570 nm using a Mindray MR-96A microplate reader (Vacutec, Germany). Graphs were used to determine the concentration at which there was an inhibition of 50% in cell growth (IC_{50}). The viability of the cell lines was directly related to the absorbance. Percentage cell survival was calculated using equation 5.6 :

$$\% \text{ cell survival} = \frac{(\text{Average optical density of control cells only})}{\text{Average optical density of treated cells}} \times 100 \quad \textbf{(5.6)}$$

5.2.6 Statistical analyses

The results were presented as means ± standard deviation, n = 3. Statistical analyses were performed using R Statistical computing software of the R Core Team, 2020, version 3.6.3, followed by Tukey's honest significant difference range *post hoc* tests (*P <0.05).

5.3 Results and Discussion

5.3.1 Quantification of plant extracts

The highest percentage yield was obtained from the methanol extracts of leaves (20.17%) and stems (18.64%) respectively (Table 5.1). Overall, the metabolite yield detected throughout the crude extracts was higher in the leaves comparable to the stems. Moreover, the latex extract displayed a substantial percentage yield of 15%. Akwu et al. (2019) suggested that the leaves and latex of *T. ventricosa* may contain a larger variety and quantity of polar compounds when compared to the stems.

Table 5.1: Percentage yield of the extracts of the leaves, stems, and latex of *T. ventricosa*.

Crude extracts	Leaves	Stems	Latex	Leaves	Stems	Latex
	Dried extract yield (g)			Yield (%)		
Hexane	0.05	0.04	0.15	5.28	4.36	15.00
Chloroform	0.08	0.07		8.78	7.28	
Methanol	0.20	0.18		20.17	18.64	

5.3.2 Total phenolic content

Phenolic compounds are essential as they are responsible for the absorption and neutralization of free radicals, the quenching of singlet and triplet oxygen molecules, or the decomposition of peroxides (Thombre et al., 2013; Dutta and Ray, 2020). The phenolic compounds present within plants often aids in several biological properties such as antimicrobial, antiviral, antiallergic, anti-inflammatory, and anticancer activity (Thombre et al., 2013; Dutta and Ray, 2020). The present study assessed the total phenolic content using the Folin-Ciolcalteu method which ranged from weak to significant phenolic content (Table 5.2). The highest total phenolic content was observed for the latex extracts (115.36 ± 2.89 mg GAE/g), followed by the stem hexane extracts (21.33 ± 0.42 mg GAE/g), with the chloroform leaf (7.89 ± 0.87 mg GAE/g) and chloroform stem (4.69 ± 0.21 mg GAE/g) extracts exhibiting moderate phenolic content, whereas the lowest levels of phenolics were in found in the leaf hexane and methanol extracts (Table 5.2). A similar report by Banik et al. (2017), investigated the antioxidant potential of *Tabernaemontana recurva* whole plant extracts. The total phenolic assay revealed a moderate number of phenols (5.89 ± 0.29 mg GAE/g). In another study, Sari et al. (2020) evaluated the total phenolic content of *Tabernaemontana catharinensis* extracts which presented a value of 23.34 mg GAE/g. However, in comparison to Boligon et al. (2014) significant differences were observed for the same species, *T. catharinensis* which ranged from 135.57 to 562.780 mg GAE/g. The total phenolic content of other *Tabernaemontana* species was much higher than that observed in the present study,

except for the latex extracts. Thus, it is highly likely that these differences could be due to the variation in plant material used (Raju and Rao, 2021).

Table 5.2: Total phenolic content of the leaf, stem, and latex extracts of *T. ventricosa*.

Crude extracts	Total phenols (mg GAE/g)		
	Leaves	**Stems**	**Latex (only)**
Hexane	1.01 ± 0.82	21.33 ± 0.42	115.36 ± 2.89
Chloroform	7.89 ± 0.87	4.69 ± 0.21	
Methanol	1.75 ± 0.13	0.99 ± 0.16	

Data displayed as mean ± SD of triplicates (n = 3).

5.3.3 Total flavonoid content

Flavonoids are classified as a group of phenolics and are strong antioxidants that are often used to prevent the occurrence of cardiovascular and liver diseases (Thombre et al., 2013; Dutta and Ray, 2020). The total flavonoid content in the current study showed significant values ranging from 152.22 ± 0.76 to 946.92 ± 6.29 mg QE/g. The highest number of flavonoids were observed for the stem hexane (946.92 ± 6.29 mg QE/g), latex (768.96 ± 5.43 mg QE/g), stem chloroform (693.24 ± 4.12 mg QE/g), and leaf hexane (662.20 ± 1.00 mg QE/g) extracts respectively whereas the lowest amount was observed for the leaf and stem methanol extracts (Table 5.3). The total flavonoid content of *T. ventricosa* extracts showed contrasting results compared to studies by Sathishkumar and Baskar (2012). In their study, the total flavonoid content in the fresh leaves of *Tabernaemontana heyneana* was much lower with a value of 4.4 ± 0.17 mg QE/g. However, it has been reported that the accumulation of flavonoids is often associated with drought-tolerant plants, such as the *Arabidopsis* species (Nakabayashi et al., 2014).

Table 5.3: Total flavonoid content of the leaf, stem, and latex extracts of *T. ventricosa.*

Crude extracts	Total flavonoids (mg QE/g)		
	Leaves	**Stems**	**Latex (only)**
Hexane	662.20 ± 1.00	946.92 ± 6.29	768.96 ± 5.43
Chloroform	332.83 ± 0.96	693.24 ± 4.12	
Methanol	152.22 ± 0.76	262.19 ± 2.36	

Data displayed as mean ± SD of triplicates (n = 3).

5.3.4 Antioxidant activity

Several studies investigated the antioxidant potential of *Tabernaemontana* species using many techniques, thus a great variation in results has been observed in the literature (Boligon et al., 2013; Nicola et al., 2013; Silveira et al., 2017; Naidoo et al., 2021; Raju and Rao, 2021). Herein, the antioxidant potential of the hexane, chloroform, and methanol extracts from the leaf and stem, and latex of *T. ventricosa* were investigated at various concentrations (15, 30, 60, 120 to 240 µg/mL) using DPPH scavenging activity FRAP assays. These assays are commonly used to determine the inhibition, generation, or scavenging ability against ROS (Silveira et al., 2017).

The results for the DPPH and FRAP assays were variable (Figure 5.1 and Figure 5.2). However, the % inhibition for all extracts was dose-dependent across both assays. For the DPPH assays, the stem methanol (54.28%), stem hexane (50.83%), and stem chloroform (49.08%) displayed the highest % inhibition at the lowest concentration (15 µg/mL), whereas at the higher concentrations (240 µg/mL), stem hexane (70.10%), stem methanol (65.24%), and stem chloroform (60.26%) showed the highest % inhibition (Figure 5.1). In comparison to the control (ascorbic acid), the values of the stem extracts were within range, however, the leaf extracts displayed very weak inhibition (Figure 5.1). Overall, for the DPPH assays, the stem crude extracts revealed a better % inhibition compared to the leaf and latex extracts. The IC_{50} values of the extracts were significantly larger than the positive control ascorbic acid (3.11 µg/mL) (Table 5.4). However, the stem extracts displayed better IC_{50} values compared to the leaf extracts, with the stem methanol (6.19 µg/mL), stem hexane (16.26 µg/mL), and stem chloroform (22.56 µg/mL) displaying moderate activity (Table 5.4).

Studies have shown that *T. catharinensis* is amongst one of the most intensively studied species within the genus (Silveira et al., 2017). The results of the current study are similar to those reported by Santos et al. (2009). In their study, the root ethanolic crude extracts and several isolated alkaloidal compounds from *T. catharinensis* were evaluated using the DPPH assay, which displayed significant inhibition ranging from 50% to 82%. Boligon et al. (2013), investigated the leaf crude extracts and fractions of *T. catharinensis* using several antioxidant techniques. The DPPH results revealed substantial IC_{50} values ranging from 4.64 ± 1.25 mg/mL to 27.78 ± 0.93 mg/mL, which are consistent with the values exhibited by the stem extracts herein. Additional reports by Nicola et al. (2013), indicated good antioxidant potential of *T. catharinensis* branches, leaves, and fractions. The most significant value was obtained by the alkaloid fraction which displayed an IC_{50} value of 37.18 ug/mL. Raju and Rao (2021) investigated the antioxidant potential using *Tabernaemontana divaricata* latex. In their study, the latex extracts showed moderate inhibition (28 ± 3.0%). However, in the present study very poor antioxidant values were observed for the latex extracts.

While moderate to significant results were observed for the DPPH assays, the FRAP assay displayed minimal % inhibition across extracts and concentrations ranging from 4.73% to 14.40 %, except for the latex extracts which displayed moderate inhibition at 15 µg/mL (21.82%) and substantial inhibition at 240 µg/mL (98.48%), comparable with the control which displayed a percentage inhibition of 26.30% (15 µg/mL) and 99.64% (240 µg/mL) (Figure 5.2). The % inhibition of the latex extracts was very similar to that of the control (gallic acid) (Figure 5.2). Raju and Rao (2021), likewise observed antioxidant activity in the latex extracts, thus indicating a significant quantity of antioxidant molecules. The results further revealed that the ferric ion reducing power of the extracts is consistent with the low quantity of phenolic compounds observed in Table 5.2, except for the latex extracts. Previous reports have revealed that *T. divaricata* ethanolic, hexane, and ethyl acetate stem extracts exhibited weak ferric reducing antioxidant capacities when compared to butylated hydroxytoluene (BHT) (Mueller et al., 2015), which are very similar to the current FRAP results. However, Sari et al. (2020) reported high levels of antioxidant activity in *T. catharinensis* using many techniques such as DPPH, FRAP, and many more. The IC_{50} values for the FRAP assay were very weak (>1000 µg/mL), with all extracts besides the latex extracts (42.22 µg/mL) which showed moderate activity when compared to the control gallic acid (29.44 µg/mL) (Table 5.4). Comparatively, the DPPH and FRAP assays showed similar results, which indicated that the stem extracts exhibited a better antioxidant potential rather than the leaf extracts.

The differences in the antioxidant capacity in the present study are highly likely due to the variation in environmental conditions (soil and climate) of the plant sample/type of plant organ used (Sari et al., 2020; Raju and Rao, 2021). Furthermore, according to Dutta and Ray (2020) extracts often display a variation in their antioxidant potential, which is regularly associated with the usage of various base solvents and several extraction methods, that usually alters the composition of phytochemical compounds and therefore scavenges free radicals differently based on their polarity. Reports have shown that antioxidants are optimally extracted using polar solvents (Gonzalez-Gurvara et al., 2004). A study by Dutta and Ray (2020) confirmed that leaf methanolic extracts using fractions of *Manilkara hexandra* displayed significant antioxidant potential. Furthermore, due to the complex mechanisms of the oxidation process, the comparison of the antioxidant potentials of the extracts, fractions, and isolated compounds of certain species and across species are very challenging since various methods are often utilized, and this often leads to a large variation in the antioxidant capacity of many species (Silveira et al., 2017).

Overall, significant differences (P <0.05 and P <0.01) were observed for the extracts and concentrations for both the DPPH and FRAP assays. However, despite the variation among antioxidant techniques leading to the differences in antioxidant potential the results of the present study indicate

that the leaf, stem, and latex extracts of *T. ventricosa* contain varying degrees of antioxidant potential and is therefore suggested as a natural source of antioxidants due to its probable oxidizing agents.

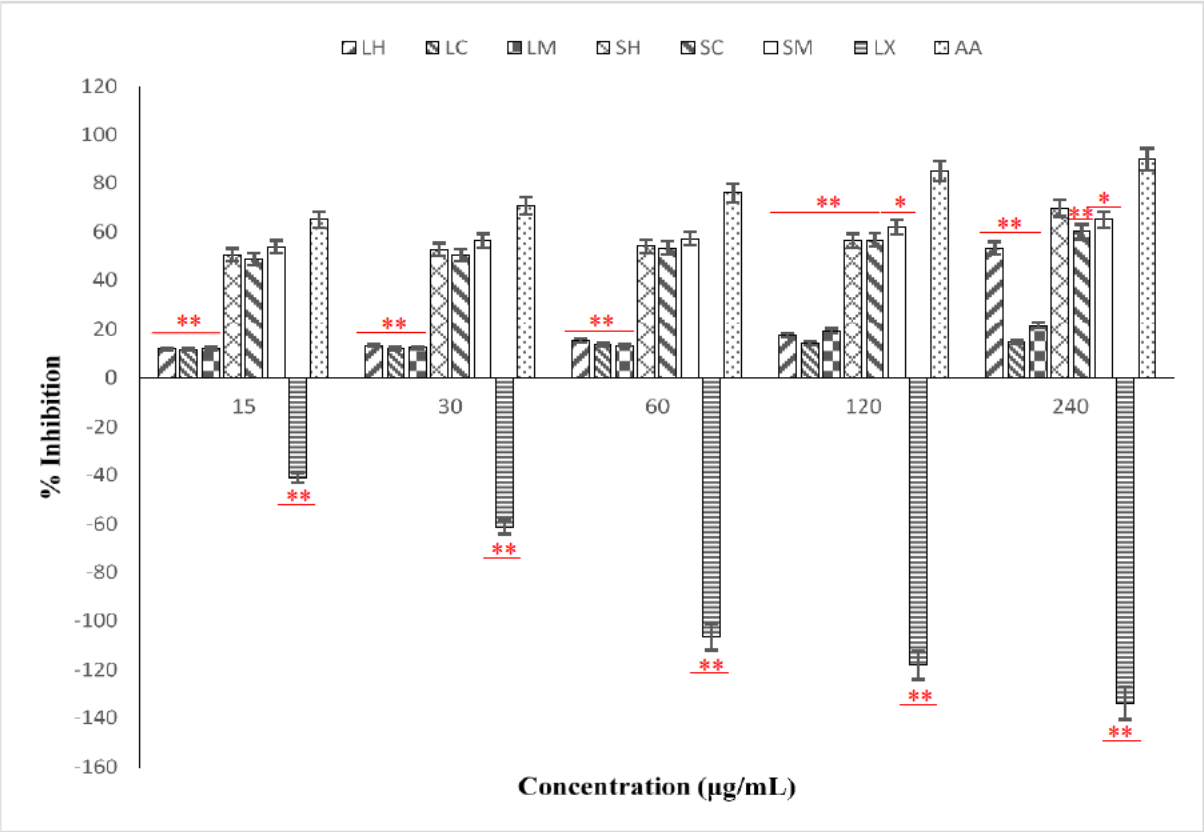

Figure 5.1: *In vitro* antioxidant activity (% inhibition_DPPH) using leaf hexane (LH); leaf chloroform (LC); leaf methanol (LM); stem hexane (SH); stem chloroform (SC); stem methanol (SM) and latex (LX) extracts of *T. ventricosa*. Standard = Ascorbic acid (AA). **P* <0.05 and ***P* <0.01 are considered significant.

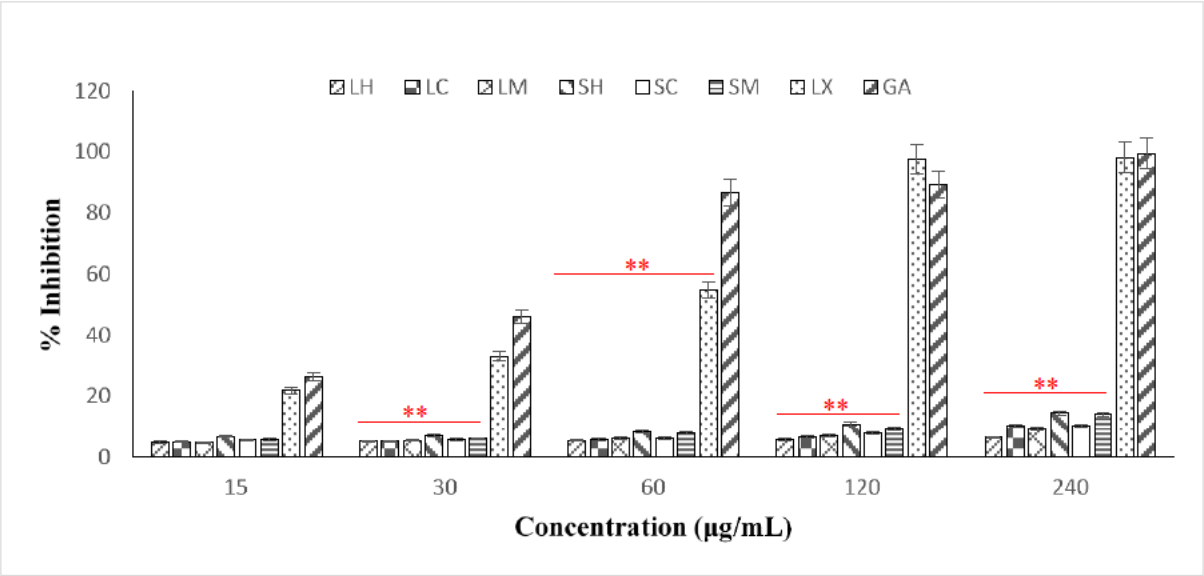

Figure 5.2: *In vitro* antioxidant activity (% inhibition_FRAP) using leaf hexane (LH); leaf chloroform (LC); leaf methanol (LM); stem hexane (SH); stem chloroform (SC); stem methanol (SM) and latex (LX) extracts of *T. ventricosa*. Standard = Gallic acid (GA). **P* <0.05 and ***P* <0.01 are considered significant.

Table 5.4: IC_{50} values of the antioxidant activities of the various extracts from leaves, stems, and latex of *T. ventricosa*.

Crude extract	DPPH (µg/mL)	FRAP (µg/mL)
Leaf hexane	538.66	>1000
Leaf chloroform	>1000	>1000
Leaf methanol	>1000	>1000
Stem hexane	19.26	>1000
Stem chloroform	22.56	>1000
Stem methanol	6.19	>1000
Latex	ND	42.22
Ascorbic acid	3.11	29.44*

Data presented as mean, (n = 3). *GA = Gallic acid; ND = Not determined.

5.3.5 MTT cytotoxicity activity

Despite the advancements in contemporary medicine and sciences, we are frequently challenged by the complications of major side effects and many other factors which are often associated with ordinary cancer treatments such as surgery (removal of tumours), chemotherapy, radiotherapy, and immunotherapy (Majolo et al., 2019). Thus, researchers are determined on screening several medicinal plants to discover novel natural anticancer agents (Majolo et al., 2019; Rosales et al., 2019; Singh et al., 2019; Naidoo et al., 2021). The family Apocynaceae and genus *Tabernaemontana* are well known for their medicinal and pharmacological properties such as cytotoxic and anticancer activities (Silveira, 2017). A prominent example includes the compound vincristine (Oncovin®) found in *Tabernaemontana* which is an antitumour agent that is often used for oncology treatments and subsequently halts the process of metaphase which results in the prevention of rapidly dividing cancerous cells (Ferreira and Paterna, 2019; Pergher et al., 2019; Yu et al., 2020). Due to the significant anticancer and cytotoxic potentials of *Tabernaemontana* species, the present study aimed to evaluate the cytotoxicity of the leaf, stem, and latex extracts of an unstudied species, *T. ventricosa*. For the MTT assays, various extracts with a range of concentrations (15, 30, 60, 120 to 240 µg/mL) were screened in 3 human cell lines, HEK293 (embryonic kidney), MCF-7 (breast adenocarcinoma), and HeLa (cervical carcinoma).

The cytotoxic potentials of all extracts of the leaves, stems, and latex of *T. ventricosa* on the various cell lines are displayed in Figure 5.3. All extracts showed moderate activity at the lowest concentrations, whereas at higher concentrations substantial cytotoxicity in the cells were observed. Thus, this is suggestive of a dose-dependent relationship for all extracts. The results of the current study revealed that at the lowest concentrations (15 µg/mL), HeLa cells treated with stem hexane extracts showed the most sensitivity (61.29%), while at the highest concentrations (240 µg/mL), HeLa cells treated with latex extracts showed substantial cell sensitivity (30.27%) (Figure 5.3). Overall, it appears that cell lines HeLa and MCF-7 were most sensitive to the extracts, with the hexane, chloroform, and methanol leaf and stem, and latex extracts affecting the percentage cell survival considerably, and therefore contains effective cytotoxic activity (Figure 5.3). Furthermore, it was noted that significant differences were observed for the cytotoxic analyses of all extracts within each concentration and across all cell lines ($P < 0.01$ and/or $P < 0.05$).

Similarly, Thind et al. (2008), investigated the cytotoxic activity of the leaves of *T. divaricata* using various solvents such as hexane, chloroform, methanol, and ethyl acetate. In their study, a range of concentrations were used (10 to 100 µg/mL) against several cell lines such as: HCT-15 (colon), HT-29 (colon), 502713 (colon), MCF-7 (breast) and PC-3 (prostate). Their results showed that hexane extracts did not display any cytotoxicity unlike the present study however, the methanol extracts displayed 71%

and 76% of cell inhibition in 502713 and HT-29 colon cancer cell lines, respectively. Moreover, the chloroform extracts also showed inhibition in HCT-15 (72%) and HT-29 (71%) cancer cell lines. Likewise, in the present study, these extracts also showed moderate to significant activity in the cell lines. Furthermore, recently Rosales et al. (2019), investigated the isolated compounds from *T. catharinensis*. The results showed that the isolated compound affinisine displayed selective cytotoxic activity in A375 cells (melanoma), with survival rates above 50%, which are in line with the results of the current study (Rosales et al., 2019).

The extracts of *T. ventricosa* displayed a range of cytotoxicities, showing low (IC_{50} >100), moderate (IC_{50} >50-100), and substantial (IC_{50} <50) proliferative effects. Significant cytotoxic effects were displayed by the latex extracts (17.20 µg/mL) in the MCF-7 cell line, whereas moderate activity was observed for the leaf hexane extracts (54.81 µg/mL) in the HeLa cell line, and the stem hexane extracts (83.33 µg/mL) for the HEK293 cell line (Table 5.5). However, weak IC_{50} values showing low proliferative effects were noted for the stem chloroform extracts in MCF-7 (1402.88 µg/mL), latex extracts (231.10 µg/mL) in HEK293, and stem methanol extracts (164.66 µg/mL) against HeLa cell lines (Table 5.5).

According to Pallant et al. (2012), previous research relating to the cytotoxic activity of *Tabernaemontana* species has been variable. These values do however correspond with previous reports. Earlier studies of the *Tabernaemontana* species have displayed significant cytotoxicity. A study by Kingston et al. (1978) investigated the cytotoxicity of *Tabernaemontana arborea* extracts in P-388 cells (murine lymphocytic leukemia) which revealed a substantial IC_{50} value of 8 µg/mL. However, reports by Pallant et al. (2012), which investigated the aqueous extracts of *Tabernaemontana elegans*, a sister species of *T. ventricosa* revealed weak toxicity of human lymphocytes with IC_{50} values ranging from 80 to 160 µg/mL, similar to the present study. However, most recently Andima et al. (2021), investigated the cytotoxic activity of isolated compounds voacristine and vobasine from *T. ventricosa* stembark, roots, twigs, and leaves extracts (mixture). The study confirmed low proliferative (>100) effects for isolated compounds, except for voacristine (23.00 µg/mL) which displayed significant cytotoxic activity in the HepG2 (human liver cancer cells). It is highly likely, that voacristine is responsible for the cytotoxic activity displayed by the extracts in the present study however, the variations may be due to the concentration of various alkaloids within the species, environmental factors, type of plant material used, method of extraction and solvent type (Pereira et al., 2004; Pallant et al., 2012). However, despite these factors, previous studies have indicated that the *Tabernaemontana* species have shown promising cytotoxic activity, with IC_{50} values below 20 µg/mL, suggesting the strong potential of these species (Pallant et al., 2012).

According to the literature, phenolic compounds possess several biological properties which include anticancer properties furthermore, flavonoids are well known for their detoxifying effects which are associated with the inhibition of the transcription factors that are responsible for the activation of tumour promoters (Mathivanan et al., 2010; Sathishkumar and Baskar, 2012; Rumzhum and Rahman, 2012). The cytotoxic potential displayed predominantly by the leaf and stem hexane extracts, and latex extracts correlate with the antioxidant assays, which also revealed antioxidant activity for these extracts. Moreover, due to the moderate phenolic content, substantial flavonoid content, strong antioxidant potential (DPPH and FRAP), and several indole alkaloidal compounds present in the extracts of *T. ventricosa*, the phytochemical compound types within this species are likely to be responsible for the moderate to significant cytotoxic activity revealed herein (Pallant et al., 2012; Silveira et al., 2017 Andima et al., 2021).

A.

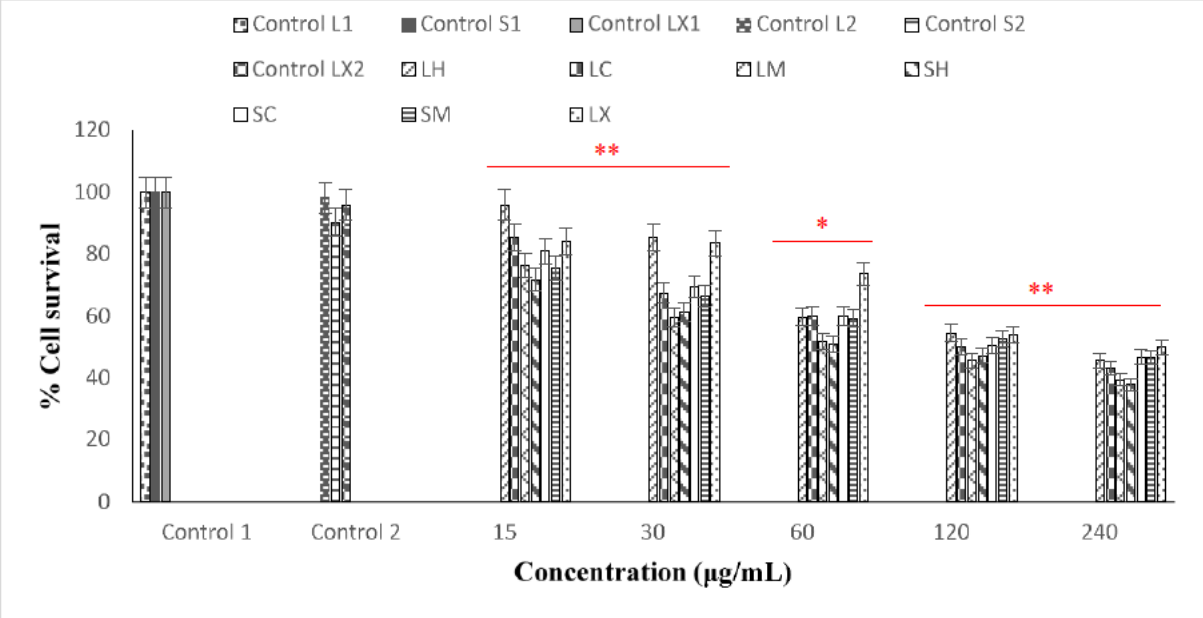

B.

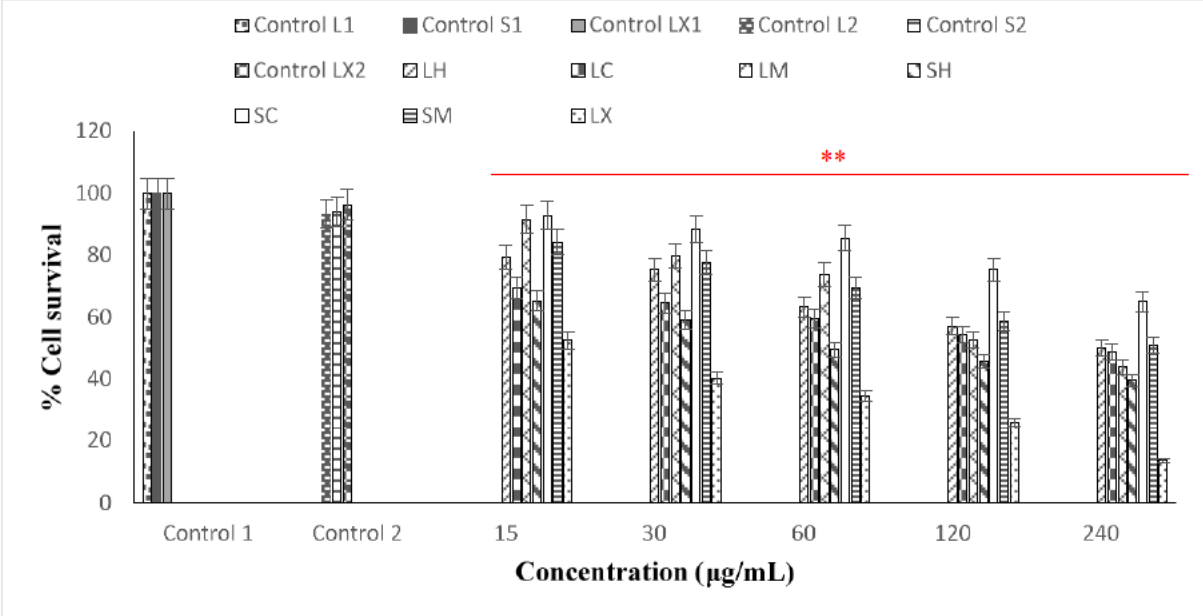

C.

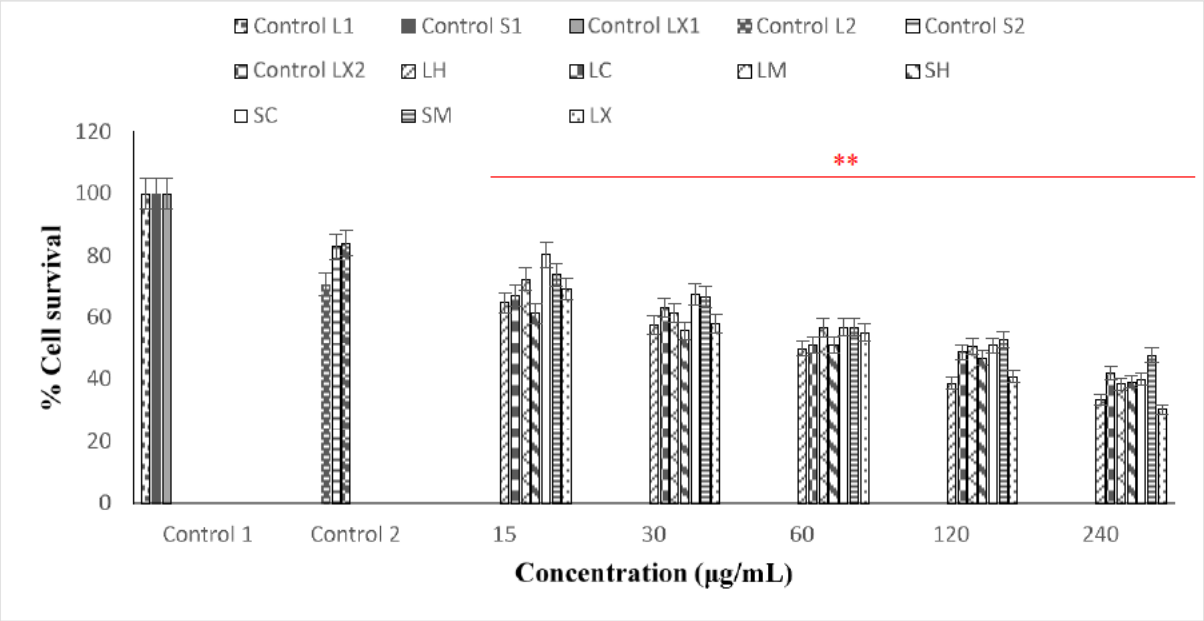

Figure 5.3: *In vitro* cytotoxicity (% cell survival) of leaf hexane (LH); leaf chloroform (LC); leaf methanol (LM); stem hexane (SH); stem chloroform (SC); stem methanol (SM) and latex (LX) extracts of *T. ventricosa*. Control 1 = cells only; Control 2 = cells + DMSO. (A) HEK293; (B) MCF-7 and (C) HeLa cell lines. **P* <0.05 and ***P* <0.01 are considered significant.

Table 5.5: IC_{50} values of the cytotoxic activity of the crude leaf and stem, and latex extracts of *T. ventricosa*.

Crude extracts	Cell lines		
	HEK293	MCF-7	HeLa
	Concentration µg/mL		
Leaf hexane	156.90	232.13	54.81
Leaf chloroform	129.39	208.54	97.60
Leaf methanol	86.23	168.24	101.82
Stem hexane	83.33	73.20	67.63
Stem chloroform	150.75	1402.88	115.86
Stem methanol	161.01	260.70	164.66
Latex	231.1	17.20	63.50

Data presented as mean, (n = 3).

5.4 Conclusion

The present study indicated that the leaf, stem, and latex extracts of *T. ventricosa* contain significant cytotoxic and antioxidant potentials. Overall, the stem and latex extracts showed higher antioxidant and cytotoxic potential as compared to the leaf extracts. Furthermore, the total phenolic and flavonoid content, and % inhibition of antioxidants (DPPH and FRAP assays) displayed by the extracts could be attributed to several phytochemical compounds, more specifically indole alkaloids. Moreover, it can be suggested that these compounds contribute to the strong antioxidant potential of this species, which in turn promote the cytotoxic activity of *T. ventricosa* extracts. The current study revealed a substantial connection between the antioxidant activity of the leaf and stem hexane and latex extracts and their cytotoxic activity. However, further studies should focus on the elucidation of the compounds and their respective antioxidant and cytotoxic properties to determine the specific correlation involved in these processes. This study constitutes the first report on the *in vitro* antioxidant and cytotoxic potential of the extracts of *Tabernaemontana ventricosa*.

5.5 References

Akwu, N.A., Naidoo, Y., Singh, M., 2019. Cytogenotoxic and biological evaluation of the aqueous extracts of *Grewia lasiocarpa*: An *Allium* cepa assay. South African Journal of Botany 125, 371–380.

Alfa, H.H., Arroo, R.R., 2019. Over 3 decades of research on dietary flavonoid antioxidants and cancer prevention: What have we achieved? Phytochemistry Reviews 18, 989–1004.

Ames, B.N., Gold, L.S., Willett, W.C., 1995. The causes and prevention of cancer. Proceedings of the National Academy of Sciences 92, 5258–5265.

Andima, M., Ndakala, A., Derese, S., Biswajyoti, S., Hussain, A., Yang, L.J., Akoth, O.E., Coghi, P., Pal, C., Heydenreich, M., Wong, V.K.W., 2021. Antileishmanial and cytotoxic activity of secondary metabolites from *Taberneamontana ventricosa* and two aloe species. Natural Product Research, 1–5.

Arruda, H.S., Pereira, G.A., de Morais, D.R., Eberlin, M.N., Pastore, G.M., 2018. Determination of free, esterified, glycosylated and insoluble-bound phenolics composition in the edible part of *araticum* fruit (*Annona crassiflora* Mart.) and its by-products by HPLC-ESI-MS/MS. Food chemistry 245,738-749.

Banik, S., Hury, G.A., Hussain, M.S., Chen, U., Chowdhury, M.R.A., 2017. Evaluation of thrombolytic, membrane stabilizing, and antioxidant activities of methanolic extract of *Tabernaemontana recurva* Roxb. Discovery Phytomedicine 4, 17–20.

Beentje, H., Adamson, J., Bhanderi, D., 1994. Kenya trees, shrubs, and lianas. National Museums of Kenya.

Boffetta, P., Nyberg, F., 2003. Contribution of environmental factors to cancer risk. British Medical Bulletin. 68, 71–94.

Boligon, A.A., de Freitas, R.B., de Brum, T.F., Piana, M., Belke, B.V., da Rocha, J.B.T., Athayde, M.L., 2013. Phytochemical constituents and *in vitro* antioxidant capacity of *Tabernaemontana catharinensis* A. DC. Free Radicals and Antioxidants 3, 77–80.

Boligon, A.A., Piana, M., Schawnz, T.G., Pereira, R.P., Rocha, J.B., Athayde, M.L., 2014. Chromatographic analysis and antioxidant capacity of *Tabernaemontana catharinensis*. Natural Product Communications 9, 1934578X1400900119.

Bray, F., Ferlay, J., Soerjomataram, I., Siegel, R.L., Torre, L.A., Jemal, A., 2018. Global cancer statistics 2018: GLOBOCAN estimates of incidence and mortality worldwide for 36 cancers in 185 countries. CA: A Cancer Journal for Clinicians 68, 394–424.

Da Rocha, A. B., Lopes, R. M., Schwartsmann, G., 2001. Natural Products in Anticancer Therapy. Current Opinion in Pharmacology 1, 364–369.

Daniels, A.N., Singh, M., 2019. Sterically stabilized siRNA: Gold nanocomplexes enhance c-MYC silencing in a breast cancer cell model. Nanomedicine 14, 1387–1401.

de Martel, C., Georges, D., Bray, F., Ferlay, J., Clifford, G.M., 2020. Global burden of cancer attributable to infections in 2018: A worldwide incidence analysis. The Lancet Global Health 8, 180–190.

Dutta, S., Ray, S., 2020. Comparative assessment of total phenolic content and *in vitro* antioxidant activities of bark and leaf methanolic extracts of *Manilkara hexandra* (Roxb.) Dubard. Journal of King Saud University-Science 32, 643–647.

Ferlay, J., Colombet, M., Soerjomataram, I., Mathers, C., Parkin, D.M., Piñeros, M., Znaor, A., Bray, F., 2019. Estimating the global cancer incidence and mortality in 2018: GLOBOCAN sources and methods. International Journal of Cancer 144, 1941–1953.

Ferreira, M.J.U., Paterna, A., 2019. Monoterpene indole alkaloids as leads for targeting multidrug resistant cancer cells from the African medicinal plant *Tabernaemontana elegans*. Phytochemistry Reviews 18, 971–987.

Fierascu, R.C., Ortan, A., Fierascu, I.C., Fierascu, I., 2018. *In vitro* and *in vivo* evaluation of antioxidant properties of wild-growing plants. A short review. Current Opinion in Food Science 24, 1–8.

Gezici, S., Şekeroğlu, N., 2019. Current perspectives in the application of medicinal plants against cancer: Novel therapeutic agents. Anti-Cancer Agents in Medicinal Chemistry (Formerly Current Medicinal Chemistry-Anti-Cancer Agents) 19, 101–111.

Glebova K, Veiko N, Kostyuk S, Izhevskaya V, Baranova A., 2015. Oxidized extracellular DNA as a stress signal that may modify response to anticancer therapy. Cancer Letters 356, 22–33.

Gonzalez-Guevara, J.L., Gonzalez-Lavaut, J.A., Pino-Rodriguez, S., Garcia-Torres, M., Carballo-Gonzalez, M.T., Echemendia-Arana, O.A., Molina-Torres, J., Prieto-Gonzalez, S., 2004. Phytochemical screening and *in vitro* antiherpetic activity of four *Erythtroxylum* species. Acta Farmaceut Bonaer 23, 506–509.

Hamed, A.R., Abdel-Azim, N.S., Shams, K.A., Hammouda, F.M., 2019. Targeting multidrug resistance in cancer by natural chemosensitizers. Bulletin of the National Research Centre 43, 1–14.

Herzallah, H.K., Antonisamy, B.R., Shafee, M.H., Al-Otaibi, S.T., 2019. Temporal trends in the incidence and demographics of cancers, communicable diseases, and non-communicable diseases in Saudi Arabia over the last decade. Saudi Medical Journal 40, 277–268.

Hussain, S.P., Hofseth, L.J., Harris, C.C., 2003. Radical causes of cancer. Nature Reviews Cancer 3, 276–285.

Imbert, T. F., 1998. Discovery of podophyllotoxins. Biochimie 80, 207–222.

Kam, T.S., Pang, H.S., Choo, Y.M., Komiyama, K., 2004. Biologically active ibogan and vallesamine derivatives from *Tabernaemontana divaricata*. Chemistry and Biodiversity 1, 646–656.

Key, T.J., Allen, N.E., Spencer, E.A., Travis, R.C., 2002. The effect of diet on risk of cancer. The Lancet 360, 861–868.

Khazir, J., Mir, B. A., Pilcher, L., Riley, D. L., 2014. Role of Plants in Anticancer Drug Discovery. Phytochemistry Letters 7, 173–181.

Kingston, D.G., Gerhart, B.B., Ionescu, F., Mangino, M.M., Sami, S.M., 1978. Plant anticancer agents V: New bisindole alkaloids from *Tabernaemontana johnstonii* stem bark. Journal of Pharmaceutical Sciences 67, 249–251.

Kumar, A., Jaitak, V., 2019. Natural products as multidrug resistance modulators in cancer. European Journal of Medicinal Chemistry 176, 268–291.

Liu, Q., Yao, H., 2007. Antioxidant activities of barley seeds extracts. Food chemistry 102, 732–737.

Made, F., Wilson, K., Jina, R., Tlotleng, N., Jack, S., Ntlebi, V., Kootbodien, T., 2017. Distribution of cancer mortality rates by province in South Africa. Cancer Epidemiology 51, 56–61.

Majolo, F., Delwing, L.K.D.O.B., Marmitt, D.J., Bustamante-Filho, I.C., Goettert, M.I., 2019. Medicinal plants and bioactive natural compounds for cancer treatment: Important advances for drug discovery. Phytochemistry Letters 31,196–207.

Mathivanan, T., Govindarajan, M., Elumalai, K., Krishnappa, K., Ananthan, A., 2010. Mosquito larvicidal and phytochemical properties of *Ervatamia coronaria* Stapf. (Family: Apocynaceae). Journal of Vector Borne Diseases 47, 178–180.

Mehrbod, P., Abdalla, M.A., Njoya, E.M., Ahmed, A.S., Fotouhi, F., Farahmand, B., Gado, D.A., Tabatabaian, M., Fasanmi, O.G., Eloff, J.N., McGaw, L.J., 2018. South African medicinal plant extracts active against influenza A virus. BMC Complementary and Alternative Medicine 18, 112–121.

Migliore, L., Coppedè, F., 2002. Genetic and environmental factors in cancer and neurodegenerative diseases. Mutation Research/Reviews in Mutation Research 512, 135–153.

Morsy, N., 2019. Anticancer agents from plants. Main Group Chemistry 18, 169–191.

Mosmann, T., 1983. Rapid colorimetric assay for cellular growth and survival: Application to proliferation and cytotoxicity assays. Journal of Immunological Methods 65, 55–63.

Mueller, M.O.N.I.K.A., Janngeon, K., Puttipan, R.I.N.R.A.M.P.A.I., Unger, F.M., Viernstein, H., Okonogi, S.I.R.I.P.O.R.N., 2015. Anti-inflammatory, antibacterial and antioxidant activities of Thai medicinal plants. International Journal of Pharmacy and Pharmaceutical Sciences 7, 123–128.

Munayi, R.R., 2016. Phytochemical investigation of *Bridelia micrantha* and *Tabernaemontana ventricosa* for cytotoxic principles against drug sensitive leukemia cell ines (Doctoral dissertation, Master's Thesis, University of Nairobi, Nairobi, Kenya.

Naidoo, C.M., Naidoo, Y., Dewir, Y.H., Murthy, H.N., El-Hendawy, S., Al-Suhaibani, N., 2021. Major Bioactive Alkaloids and Biological Activities of *Tabernaemontana* Species (Apocynaceae). Plants 10, 313.

Nakabayashi, R., Yonekura-Sakakibara, K., Urano, K., Suzuki, M., Yamada, Y., Nishizawa, T., Matsuda, F., Kojima, M., Sakakibara, H., Shinozaki, K., Michael, A.J., 2014. Enhancement of oxidative and drought tolerance in *Arabidopsis* by overaccumulation of antioxidant flavonoids. The Plant Journal 77, 367–379.

Newman, D. J., Cragg, G. M., 2007. Natural Products as Sources of New Drugs over the Last 25 Years. Journal of Natural Products 70, 461–477.

Nicola, C., Salvador, M., Escalona Gower, A., Moura, S., Echeverrigaray, S., 2013. Chemical constituents' antioxidant and anticholinesterasic activity of *Tabernaemontana catharinensis*. The Scientific World Journal 2013, 1–10.

Pallant, C.A., Cromarty, A.D., Steenkamp, V., 2012. Effect of an alkaloidal fraction of *Tabernaemontana elegans* (Stapf.) on selected micro-organisms. Journal of Ethnopharmacology 140, 398–404.

Pereira, C.G., Marques, M.O., Barreto, A.S., Siani, A.C., Fernandes, E.C., Meireles, M.A.A., 2004. Extraction of indole alkaloids from *Tabernaemontana catharinensis* using supercritical CO_2+ ethanol: an evaluation of the process variables and the raw material origin. The Journal of Supercritical Fluids 30, 51–61.

Pergher, D., Picolotto, A., Rosales, P.F., Machado, K.G., Cerbaro, A.F., França, R.T., Salvador, M., Roesch-Ely, M., Tasso, L., Figueiredo, J.G., Moura, S., 2019. Antinociceptive and antioxidant effects of extract enriched with active indole alkaloids from leaves of *Tabernaemontana catharinensis* A. DC. Journal of Ethnopharmacology 239, 1–12.

Priya, S., Satheeshkumar, P.K., 2020. Natural products from plants: Recent developments in phytochemicals, phytopharmaceuticals, and plant-based neutraceuticals as anticancer agents. In Functional and Preservative Properties of Phytochemicals 5, 145–163.

Raju, M., Rao, Y.V., 2021. Study of Catalase, Protease, Antioxidant and Antimicrobial Activities of *Tabernaemontana divaricata* Latex. Journal of Medicinal plants and By-product 10, 61–68.

Rosales, P.F., Marinho, F.F., Gower, A., Chiarello, M., Canci, B., Roesch-Ely, M., Paula, F.R., Moura, S., 2019. Bio-guided search of active indole alkaloids from *Tabernaemontana catharinensis*: Antitumour activity, toxicity in silico and molecular modelling studies. Bioorganic Chemistry 85, 66–74.

Rumzhum, N.N., Rahman, M.M., Kazal, M.K., 2012. Antioxidant and cytotoxic potential of methanol extract of *Tabernaemontana divaricata* leaves. International Current Pharmaceutical Journal 1, 27–31.

Sammar, M., Abu-Farich, B., Rayan, I., Falah, M., Rayan, A., 2019. Correlation between cytotoxicity in cancer cells and free radical-scavenging activity: *In vitro* evaluation of 57 medicinal and edible plant extracts. Oncology Letters 18, 6563–6571.

Santos, A.K.L., Magalhães, T.S., Monte, F.J.Q., Mattos, M.C.D., Oliveira, M.C.F.D., Almeida, M.M.B., Lemos, T.L., Braz-Filho, R., 2009. Alcaloides iboga de Peschiera affinis (Apocynaceae)-Atribuição inequívoca dos deslocamentos químicos dos átomos de hidrogênio e carbono: atividade antioxidante. *Química Nova 32*, 1834–1838.

Sari, R., Conterno, P., da Silva, L.D., de Lima, V.A., Oldoni, T.L.C., Thomé, G.R., Carpes, S.T., 2020. Extraction of phenolic compounds from *Tabernaemontana catharinensis* leaves and their effect on oxidative stress markers in diabetic rats. Molecules 25, 2391.

Sathishkumar, T., Baskar, R., 2012. Evaluation of antioxidant properties of *Tabernaemontana heyneana* Wall. leaves. Indian Journal of Natural Products and Resources 3, 197–207.

Schmelzer, G.B., Gurib-Fakim, A., 2008. Medicinal Plants, first ed. Plant Resources of Tropical Africa 11, 1. PROTA Foundation. Backhuys Publishers, Wageningen, Netherlands.

Schmidt, E., Lotter, M., McCleland, W., 2002. Trees and Shrubs of Mpumalanga and Kruger National Park. Jacana.

Schripsema, J., Hermans-Lokkerbol, A., Van der Heijden, R., Verpoorte, R., Svendsen, A.B., Van Beek, T.A., 1986. Alkaloids of *Tabernaemontana ventricosa*. Journal of Natural Products 49, 733–735.

Shori, A.B., 2015. Screening of antidiabetic and antioxidant activities of medicinal plants. Journal of Integrative Medicine 13, 297–305.

Silveira, D., de Melo, A.F., Magalhães, P.O., Fonseca-Bazzo, Y.M., 2017. *Tabernaemontana* Species: Promising Sources of new useful drugs. In: Studies in natural products chemistry. Elsevier 54, 227–289.

Singh, A., Masoodi, M., Nabi, N., Ashraf, I., 2019. Medicinal Plants as Combating Strategy Against Cancer: A Review. Cancer 7, 1–20.

Soerjomataram, I., Shield, K., Marant-Micallef, C., Vignat, J., Hill, C., Rogel, A., Menvielle, G., Dossus, L., Ormsby, J.N., Rehm, J., Rushton, L., 2018. Cancers related to lifestyle and environmental factors in France in 2015. European Journal of Cancer 105, 103–113.

Tan, B.L., Norhaizan, M.E., Liew, W.P.P., Sulaiman Rahman, H., 2018. Antioxidant and oxidative stress: A mutual interplay in age-related diseases. Frontiers in Pharmacology 9, 1–28.

Thind, T.S., Agrawal, S.K., Saxena, A.K., Arora, S., 2008. Studies on cytotoxic, hydroxyl radical scavenging and topoisomerase inhibitory activities of extracts of *Tabernaemontana divaricata* (L.) R. Br. ex Roem. and Schult. Food and Chemical Toxicology 46, 2922–2927.

Thombre, R., Jagtap, R., Patil, N., 2013. Evaluation of phytoconstituents, antibacterial, antioxidant and cytotoxic activity of *Vitex negundo* L. and *Tabernaemontana divaricata* L. The International Journal of Pharma and Bio Sciences 4, 389–396.

Thyagarajan, A., Sahu, R.P., 2018. Potential contributions of antioxidants to cancer therapy: Immunomodulation and radiosensitization. Integrative Cancer Therapies 17, 210–216.

Van Beek, T.A., Verpoorte, R., Svendsen, A.B., Leeuwenberg, A.J.M., Bisset, N.G., 1984. *Tabernaemontana* L. (Apocynaceae): A review of its taxonomy, phytochemistry, ethnobotany and pharmacology. Journal of Ethnopharmacology 10, 1–156.

Wall, M. E., Wani C. M., 1996. Camptothecin and Taxol: from Discovery to Clinic. Journal of Ethnopharmacology 51, 239–254.

WHO, World Health Organization, 2018.

Yu, Y., Zhao, S.M., Bao, M.F., Cai, X.H., 2020. An Aspidosperma-type alkaloid dimer from *Tabernaemontana bovina* as a candidate for the inhibition of microglial activation. Organic Chemistry Frontiers 7, 1365–1373.

CHAPTER 6:

SYNTHESIS, CHARACTERIZATION, AND BIOACTIVITY OF SILVER NANOPARTICLES (AGNPS) USING METHANOLIC, FRESH, AND POWDERED LEAF AND STEM EXTRACTS OF *TABERNAEMONTANA VENTRICOSA* HOCHST. EX A. DC

Abstract

Recent trends in nanoscience have indicated an increased demand for the synthesis of silver nanoparticles (AgNPs) due to their frequent application in the health, medicine, chemistry, food, textiles, agriculture, and energy sectors. The study aimed to biologically synthesize AgNPs using leaf and stem extracts (methanol, fresh and powdered) of *Tabernaemontana ventricosa*. The synthesized AgNPs were characterized using UV-visible spectroscopy, Scanning Electron Microscopy (SEM), High-Resolution Transmission Electron Microscopy (HRTEM), Energy-Dispersive X-ray (EDX) analysis, Fourier Transform Infrared (FTIR) spectral analysis, and Nanoparticle Tracking Analysis (NTA). The antibacterial activity of the synthesized AgNPs was assessed, along with their cytotoxic potential. The AgNPs were successfully synthesized using the *T. ventricosa* leaf and stem extracts. However, the synthesis of the AgNPs was more efficient using the leaf extracts rather than the stem extracts. The EDX showed that the elemental silver (Ag) content was much higher using leaf extracts compared to the stem extracts. The AgNPs synthesized using both leaf and stem extracts produced spherical, ovate, triangular-shaped nanoparticles (NPs). The AgNPs synthesized using the different extracts varied in particle size ranging from 16.06 ± 6.81 nm to 80.26 ± 24.93 nm across all treatments. However, NTA analyses displayed much larger particle sizes, which ranged from 63.9 ± 63.9 nm to 147.4 ± 7.4 nm. These differences are expected due to the variation in both techniques. The FTIR analysis suggested that the presence of functional groups such as alcohols, phenolic compounds, aldehydes, alkanes, esters, amines, and carboxylic acids may be responsible for the capping and stability of NPs. Additionally, the AgNPs synthesized using powdered and fresh leaf extracts displayed the most antibacterial inhibition against *Bacillus subtilis, Escherichia coli*, *Methicillin-resistant Staphylococcus aureus* (MRSA), *Staphylococcus aureus*, and *Pseudomonas aeruginosa*. The AgNPs synthesized using fresh leaf extracts showed significant cytotoxic potential (IC_{50} value 0.39 µg/mL) in the human cervical carcinoma (HeLa) cell line. Considering the potential of the various extracts to produce AgNPs, *T. ventricosa* extracts are recommended as bio-factories for the effective economical production of AgNPs.

Keywords: Antibacterial activity; Biosynthesis; Cytotoxicity; Nanoscience; *Tabernaemontana*.

6.1 Introduction

Contemporary trends in nanoscience have prompted the frequent synthesis and applications of silver nanoparticles (AgNPs) (Devaraj et al., 2014). Nanoparticles (NPs) are often described as extremely tiny materials that exhibit nanoscale dimensions ranging from 1-100 nm (Lateef et al., 2018). The specific features of AgNPs such as their large surface-area-to-volume ratio, size, shape, and morphology have optimized their activity in a variety of applications, which include health, medicine, chemistry, food, textiles, and agricultural sectors (Safavi, 2012; Mittal et al., 2013; Lateef et al., 2018). The production of NPs has been reported using chemical and physical methods, however, current research has revealed that the biological synthesis (i.e., use of living organisms) of AgNPs has driven research towards a "Green synthesis" approach (Devaraj et al., 2014; Khan et al., 2017). Biological methods are considered simplistic, cost-effective, environmentally friendly, and easily upscaled for large-scale synthesis (Devaraj et al., 2014; Sigamoney et al., 2016; Chandra et al., 2020).

Biosynthetic methods are categorized into two approaches. Firstly, the "Bottom-down" approach involves the synthesis of NPs from an elemental entity such as atoms and molecules (Mittal et al., 2013). This technique often produces colloidal dispersions of homogenous particles with fewer defects (Singh, 2016). Secondly, the "Top-down" approach is a process whereby NPs are reduced in size until it reaches a suitable material (Mittal et al., 2013). This method consists of chemical and physical techniques that are often energy-consuming and produce imperfect NPs (Thakkar et al., 2010). According to Chouhan (2018), biosynthetic synthesis using a greener approach is often preferred over conventional techniques, since it is relatively simple, requires less time and energy, and does not involve the use of toxic chemicals.

The synthesis of NPs utilizing whole plants, or their respective extracts has received more attention than the many biological techniques (Akhtar et al., 2015). As such there have been several reports of AgNPs synthesized using medicinal plant extracts such as *Ceratonia silique* (Awwad et al., 2013), *Ocimum sanctum* (Mallikkarjuna et al., 2011), *Coleus aromaticus* (Vanaja and Annadurai, 2012), *Jatropha curcas* (Bar et al., 2009), *Litchi chinensi*s (Tehri et al., 2020) and *Tabernaemontana divaricata* (Devaraj et al., 2014; Attri et al., 2021). The current study investigated the use of *Tabernaemontana ventricosa*, a medium-sized latex bearing plant belonging to Apocynaceae for the synthesis of AgNPs (Schmidt et al., 2002). This species is randomly distributed in Nigeria, Ghana, Kenya, and South Africa (Schmelzer and Gurib-Fakim, 2008). All parts of *T. ventricosa* are often used in traditional medicine to treat fever, wounds, and sore eyes (Mehrbod et al., 2018). The leaves and latex are rich in alkaloids and have been reported to contain antiamoebic activity (Schmelzer and Gurib-Fakim, 2008).

A considerable amount of AgNPs has been synthesized using several medicinal plant species (Devaraj et al., 2014). Hence, the current study aimed to biologically synthesize AgNPs using various leaf and stem extracts (methanolic, fresh and powdered) of *T. ventricosa*. Additionally, the study aimed to determine whether the differences in organ type influenced the morphology (particle size and shape), chemical nature, and antibacterial and cytotoxic activity of the synthesized AgNPs. The characterization and bioactivity of the AgNPs from *T. ventricosa* extracts were evaluated in this study.

6.2 Materials and Methods

6.2.1 Plant collection

Leaves and stems from fully grown *T. ventricosa* plants (~ 12-15 m in height) of wild origin were collected from the University of KwaZulu-Natal (Westville campus), South Africa, located at 29˚49′03.3″S 30˚56′32.7″E. A combination of emergent, young, and mature leaves and stems were collected for analysis. The plant material was taxonomically identified, and a voucher specimen (18222) was deposited at the Ward herbarium, School of Life Sciences, University of KwaZulu-Natal.

6.2.2. Preparation of plant extracts

The collected plant material was inspected for any signs of microbial and fungal contamination and the leaves and stems were separately air-dried for three months at 23˚C, and thereafter ground at high speed into a fine powder using a grinder (Mellerware, Model: 29105). The powdered material was kept in an airtight consol™ glass jar, out of direct sunlight, at 23˚C, until further use.

6.2.2.1 Reflux extraction

Crude methanolic leaf and stem extracts were prepared by reflux extraction using Analytical grade (AR) methanol at a ratio of 10 g powdered material to 100 mL solvent. A round-bottom flask was heated (60˚C) by a reflux extraction and the extraction proceeded for 3 h. The solutions were filtered (Whatman No. 1), the extract was retained, and the procedure was repeated twice. The resulting leaf and stem extracts for each solvent were stored separately in air-tight sterilized consol™ glass jars and kept in a dark room, at 4˚C until further use.

6.2.2.2 Fresh extract

Freshly collected leaf and stem material were thoroughly washed using sterile distilled water, dried with tissue paper, and thereafter cut into fine pieces. The leaf and stem pieces were weighed (35 g) and extracted with 100 mL sterile distilled water using an oven at 60˚C for 30 min. The fresh extracts were cooled, filtered using Whatman No. 1 filter paper, stored separately in air-tight sterilized consol^{TM} glass jars, and kept in a dark room, at 4˚C until further use.

6.2.2.3 Powder extract

Powdered leaf and stem material (10 g) was extracted with 200 mL of sterile distilled water in an oven at 60˚C for 60 min. Following extraction, the extracts were cooled and separately filtered using Whatman No. 1 filter paper. The powdered leaf and stem extracts were stored in air-tight sterilized consol^{TM} glass jars and kept in a dark room, at 4˚C until further use.

6.2.3 Synthesis of AgNPs

The AgNPs were synthesized according to the protocols of Devaraj et al. (2014) and Akwu et al. (2021), with modifications. A 1 mM aqueous solution of silver nitrate ($AgNO_3$) (Biolab, Merck) was prepared with sterile deionized water and used for the experimental analysis. For AgNPs synthesis, 10 mL of each extract was added to 90 mL of $AgNO_3$ solution for the reduction into Ag ions from $AgNO_3$. The solution was stirred and heated in a water bath at 80˚C for 3 h. The colour transformation of the solution from a colourless to a yellowish-brownish colour indicated the synthesis of AgNPs (Devaraj et al., 2014). Once the colouration of the solutions reached a maximum intensity, the flasks were removed from the water bath to avoid agglomeration of the NPs. For the negative control, 10 mL of distilled water was added to 90 mL of $AgNO_3$ and incubated at 80˚C for 3 h in a water bath. The negative control displayed no colour change, indicating that the process of AgNPs production was extract dependant. All analyses were conducted in triplicates (n = 3).

6.2.4 UV-visible spectral analysis

The confirmation of AgNP formation was determined by UV-vis spectral analysis. Approximately 1 mL of synthesized solutions were used for analyses, using $AgNO_3$ solution as a blank. The synthesized AgNPs solutions and controls were concurrently analyzed, and the absorbance was scanned (medium speed) from 200-800 nm using a UV-vis spectrophotometer (SHIMADZU UV-1800, Germany), and the corresponding peaks were recorded.

6.2.5 Preparation, purification, and quantification of samples

Subsequently, the six synthesized AgNP solutions: leaf methanol (LM), fresh leaf (FL), powdered leaf (PL), stem methanol (SM), fresh stem (FS), and powdered stem (PS) were subjected to centrifugation (BECKMAN COULTER, Avanti®J-E, USA) thrice at 10 000 rpm for 30 min each at 4˚C. Following centrifugation, the supernatants were discarded, and the pellet was rinsed using 20 mL of distilled water for the removal of additional residues such as contaminating plant material, solution biomolecules, and cellular metabolites. The wash step was repeated thrice, and the resultant suspensions were subjected to drying using an oven at 50˚C. After approximately 7 days, the yield (dry mass) of the synthesized AgNPs was determined using the equation 6.1. For further analyses, the dried AgNPS were reconstituted using sterile distilled water.

$$\text{Extract yield } (\%) = \frac{\text{Weight of dried extract (g)}}{\text{Weight of plant material (g)}} \times 100 \quad \textbf{(6.1)}$$

6.2.6 Characterization of AgNPs

6.2.6.1 Scanning Electron Microscopy (SEM) and Energy-Dispersive X-ray (EDX) analysis

Synthesized NP solutions were sonicated (SONICLEAN, England) for 20 min, and one drop of each sample was placed directly onto separate aluminum stubs and dried using a mercury lamp for 60 min. The stubs containing the dried samples were sputter-coated with a thin layer (*ca*. 25 nm) of gold in a Quorum module sputter coater (Q150 R ES, UK). The samples were coated twice for approximately 10 min each to avoid charging. Thereafter, the samples were analyzed and viewed at different magnifications, using an Ultra Plus FEGSEM (Carl Zeiss, Germany), at 5 kV. During analyses, the NP size, shape, and distribution were determined using SmartSEM version 5 software (Carl Zeiss, Germany). Simultaneous EDX analyses were performed using the Zeiss Ultra Plus X-ray spectrometer, equipped with an Astronomical Thermal Emission Camera (Aztec) version 1.2 at 20 kV. Samples were analyzed using the Aztec Analysis Software (Oxford Instruments, UK) to determine the elemental composition of synthesized AgNP samples.

6.2.6.2 High-Resolution Transmission Electron Microscopy (HRTEM)

High-Resolution Transmission Electron Microscopy was used to determine the morphology and size of the synthesized AgNPs. Previously sonicated samples (for even distribution of AgNPs) was for used for analyses. Carbon-coated (Quorum Q150 TE, UK) formvar grids (200 mesh) were dipped into each solution and placed under a mercury lamp for 30 min to ensure sample evaporation. The samples were viewed using the HRTEM JEM 2100 (JOEL, Japan), equipped with Gatan software, at a voltage of 200 kV. The morphology and size of the AgNPs were accomplished using ImageJ software for analyses (Java 1.8.0) (n = 5).

6.2.6.4 Fourier Transform Infrared (FTIR) spectral analysis

Dried AgNPs samples produced using various extracts were analyzed using a FTIR spectrometer (Agilent Cary 60) with Agilent MicroLab PC software (version 5.1.22) for the detection and characterization of the surface chemistry and functional groups of capping agents. The data was collected using ATR Diamond-1 Bounce with 30 background and samples were scanned in the range 4000-650cm$^{\wedge-1}$, with a resolution of 4 cm$^{\wedge-1}$. The various stretching and bending of bonds and peaks were interpreted using ResolutionPro software version 5.0.0.395.

6.2.6.5 Nanoparticle Tracking Analysis (NTA)

The particle size distribution and zeta potential of all biosynthesized NPs and nanocomplexes were measured by NTA (Nanosight NS500, UK). Approximately, 1 mL of 1:100 dilutions (in 18 MOhm water-ultrapure millipore) for each sample was prepared, vortexed (Model:VM-1000, Taiwan) for 30 sec, and sonicated (SONICLEAN, England) for 20 min prior analyses. Measurements were conducted at 25˚C at 24 V and images were captured and analyzed using the NTA version 3.2 analytical software.

6.2.7 Biological assessment of synthesized AgNPs

6.2.7.1 Sample preparation

Stock solutions of the synthesized AgNPs, leaf methanol (LM), fresh leaf (FL), powdered leaf (PL), stem methanol (SM), fresh stem (FS), and powdered stem (PS), were prepared by resuspending 1 mg of the dried AgNP powder in 1 mL of sterile distilled water. The various stock solutions (1 mg/mL) for the respective treatments were homogenized using a vortex (Model:VM-1000, Taiwan). Thereafter, stock solutions of each solution were reconstituted in distilled water to provide a variety of concentrations ranging from 3.125, 6.25,12.5, 25, 50, to 100 mg/mL.

6.2.7.2 Antibacterial screening

The various solutions of the synthesized AgNPs were screened for antibacterial activity against three gram-positive bacterial strains *Bacillus subtilis* (ATCC 6653), *Methicillin-resistant Staphylococcus aureus* (MRSA) (ATCC 43300), *Staphylococcus aureus* (ATCC 29213), and two gram-negative bacterial strains *Escherichia coli* (ATCC 25922) and *Pseudomonas aeruginosa* (ATCC 27853). *In vitro* antibacterial screening of each synthesized AgNPs solution was conducted using the agar disc diffusion technique as per the Clinical and Laboratory Standards Institute (CLSI, 2006). Sterile Whatman filter paper No. 1 discs were prepared (diameter 6 mm) and impregnated with 20 µL of the respective AgNPs solution at concentrations of 3.125, 6.25,12.5, 25, 50, and 100 mg/mL and dried at room temperature for 1 h before use (Marathe et al., 2013). Bacterial strains were aseptically cultured at 37˚C overnight on Mueller-Hinton (MH) agar media (Biolab, Merck). After 18-24 h a loopful of bacteria were resuspended in test tubes containing autoclaved (Model: HL-340, Temp.: 121-132˚C, Pres.: 127 kg/cm^2, Taiwan) distilled water and vortexed (Model:VM-1000, Taiwan) to ensure that the solutions were standardized. The optical density (OD) of the bacterial strains equivalent to 0.5 McFarland turbidity standard (OD 0.08-0.1 at λ 625 nm) was assessed using a UV-vis spectrophotometer (Agilent Technologies Cary 60 spectrophotometer, USA), and the desirable OD was obtained by further dilution of the inoculum with additional sterile water.

Sterile cotton swabs were used to streak (4 quadrants) the inoculum over the entire surface of the agar. The prepared discs containing AgNPs solutions were carefully placed onto the agar using sterile forceps. The plates were incubated at 37˚C, and after 18-24 h, the zones of growth inhibition were examined to determine the antibacterial activity of the relative synthesized AgNPs. The screening was done in triplicates and streptomycin (gram-positive), and gentamicin (gram-negative) was used as the standard antibacterial positive controls, and sterile distilled water was used as the negative control. The silver nitrate solution (1 mM) was also tested. The zones of inhibition were measured (mm), recorded, and averaged, and images of the plates were captured. The following criteria was used to assess the zone of inhibition or resistance to synthesized AgNPs; No activity = (0 mm); Slight activity = (1-6 mm); Moderate activity = (>7 or <9 mm); Significant activity = (>9mm). R = Resistant.

6.2.8 MTT cytotoxicity assay

Three cell lines viz., human embryonic kidney (HEK293), breast adenocarcinoma (MCF-7), and cervical carcinoma (HeLa) cells were procured from the ATCC, Manassas, USA. All three cell lines were grown to confluency in 25 cm^2 tissue culture flasks using Eagle's Minimum Essential Medium (EMEM) containing 10% (*v*/*v*) gamma-irradiated FBS and 1% antibiotics (100 units/mL penicillin, 100 µg/mL streptomycin) in a HEPA Class 100 Steri-Cult CO_2 incubator (Thermo-electron Corporation, USA), at 37˚C and 5% CO_2. Upon confluency, the cells were trypsinized and seeded into clear 96-well plates and incubated at 37˚C overnight to allow cell adhesion. The cells were prepared by replenishing the growth medium with a fresh complete medium (EMEM + 10% FBS + 1% antibiotics). Thereafter, approximately 100 µL of the six synthesized AgNPs solutions at various concentrations ranging from 15, 30, 60, 120 to 240 µg/mL were added to the cells and incubated for 37˚C for 36 h. Control cells only (without treatment) were used as the positive control (*c.a* 100% viability). All assays were conducted in triplicate (n = 3).

The methods described by Mosmann (1983) and Daniels and Singh (2019), were used to evaluate the cytotoxic potential activity of the synthesized AgNPs from the leaves and stems of *T. ventricosa* on three cell lines. Following 48 h of incubation at 37˚C, the growth medium was aspirated and replaced with 100 µL of medium containing 10 µL of MTT solution (5 mg/mL in PBS), and the cells containing the treatment and negative control were incubated for a further 4 h at 37˚C in 5% CO_2 atmosphere. The medium-MTT mixture was then removed and replaced with 100 µL dimethylsulphoxide (DMSO). The absorbances were then measured at 570 nm using a Mindray MR-96A microplate reader (Vacutec, Germany). The graphs were used to determine the concentration at which 50% cell growth inhibition (IC_{50}) occurred. The viability of the cell lines was directly related to the absorbance. Percentage cell survival was calculated using equation 6.2:

$$\%\ \text{cell survival} = \frac{(\text{Average optical density of control cells only})}{\text{Average optical density of treated cells}} \times 100 \quad \textbf{(6.2)}$$

6.2.9 Statistical analyses

The results were presented as means ± standard deviation, (n = 3). Statistical analyses were performed using R Statistical computing software of the R Core Team, 2020, version 3.6.3, followed by Tukey's honest significant difference range *post hoc* tests (**P* <0.05; ***P* <0.01). Graphs were generated using Microsoft Excel, 2019.

6.3 Results and Discussion

6.3.1 Visual inspection of synthesized AgNPs

The visual confirmation of synthesized AgNPs using leaf methanol (LM), stem methanol (SM), fresh leaf (FL), fresh stem (FS), powdered leaf (PL), and powdered stem (PS) extracts of *T. ventricosa* was visually evident in terms of a colour variation of the reaction solutions. The methanol suspensions of *T. ventricosa* displayed a greenish solution for the leaves and a murky yellow colouration for the stems (Figure 6.1-1 A). The fresh suspensions for the leaves appeared pale yellow and the stem solution was colourless (Figure 6.1-1 B). While the powdered leaf and stem suspensions both displayed a bright yellow colour (Figure 6.1-1 C). However, after the addition of the $AgNO_3$, all the solutions revealed a colour change, except for the synthesized AgNPs using fresh stem extracts. The synthesized AgNPs using leaf and stem methanolic extracts turned deep brown/ ruby brown (Figure 6.1-2 A). Interestingly, the synthesized AgNPs using fresh stem extracts did not display any prominent colour changes and appeared extremely pale-yellow in colouration (Figure 6.1-2 B), however, the fresh leaf extracts appeared murky brown. The synthesized AgNPs using powdered leaf and stem extracts both appeared dark brown and golden brown respectively (Figure 6.1-2 C).

The subsequent colour changes of the above-mentioned solutions confirmed the synthesis of AgNPs since the brown colouration is a characteristic indication of the formation of AgNPs (Mallikarjuna et al., 2011; Vanaja and Annadurai, 2012; Netai et al., 2017). According to Shanker et al. (2004), the observed colour changes occurred due to the excitation of surface plasmon vibrations with AgNPs. Moreover, studies have shown AgNPs synthesized using medicinal plant extracts often displayed extreme colour changes following incubation (Sigamoney et al., 2016; Saddal et al., 2018). The current study exhibited variable colouration among the leaf and stem extracts following incubation (Figure 6.1). The most notable colour variation (slight visual change) was observed using fresh stem extracts for the synthesis of AgNPs. It has been suggested that these variations occur due to the use of various plant extracts (methanol, fresh, and powder) from different plant organs since each part of the plant (leaves, stems, bark, root, and flowers) may vary in the type, concentration and grouping of organic reducing agents, which are responsible for the capping of AgNPs (Kumar et al., 2010; Sigamoney et al., 2016; Lee et al., 2020).

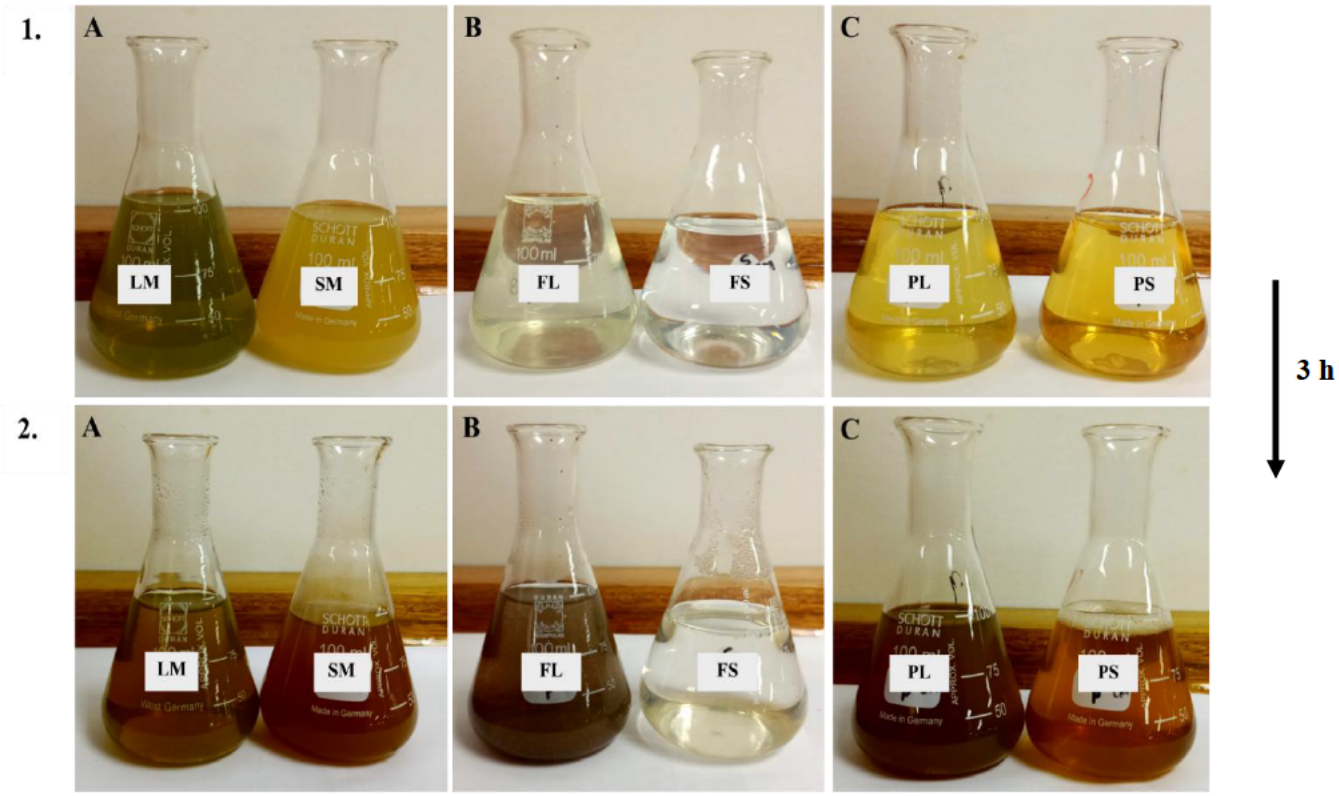

Figure 6.1: (1) A representative image displaying various extracts + $AgNO_3$ prior Ag nanoparticle synthesis (incubation); (2) Synthesised Ag nanoparticles (various extracts) after incubation with $AgNO_3$ for 3 h at 80˚C. (A) Leaf methanol (LM) and stem methanol (SM); (B) Fresh leaf (FL) and fresh stem (FS); (C) Powdered leaf (PL) and powdered stem (PS).

6.3.2 UV-visible spectroscopy

UV-visible absorption spectra are often used to confirm and characterize (formation, distribution, and stability) of synthesized AgNPs in a solution (Khanra et al., 2016; Daniels and Singh, 2019). In the present study, the production of biologically synthesized AgNPs using the various leaf and stem extracts (methanol, fresh, and powder) of *T. ventricosa* was followed by determining the surface plasmon resonance (SPR) of the various solutions at a wavelength ranging from 200-800 nm. Characteristic SPR bands for silver (Ag) are usually detected around 400-460 nm (Zargar, 2011; Sigamoney et al., 2016). The UV absorption spectra of the synthesized AgNPs are displayed in Figure 6.2. Variable absorption bands were observed for all AgNPs. The results of the current study observed strong SPR bands at 418, 418, 478, 364, 446, and 414 nm for synthesized AgNPs using leaf methanol (LM), stem methanol (SM), fresh leaf (FL), fresh stem (FS), powdered leaf (PL) and powdered stem (PS), respectively. The synthesized AgNPs produced using leaf extracts displayed maximum absorbances of 1.824 (LM), 0.521 (FL), and 1,036 (PL) compared to the stems which showed lower absorbance values of 1.599 (SM), 0.123 (FS), and 0.832 (PS) respectively. The wavelength of all synthesized AgNPs except fresh leaves

fell within the category of SPR bands for AgNPs. Previous studies using extracts of *T. divaricata* for the synthesis of AgNPs showed contrasting results as these extracts resulted in peaks at 420 nm (Devaraj et al., 2014), compared to the current study, which observed various other peaks (Figure 6.2). Moreover, the nature of lengthy tails as displayed in Figure 6.2 suggests deviations in the size distribution of the synthesized NPs (Mathew et al., 2020). Devaraj et al. (2014) observed broad peaks indicative of well-dispersed particles in the solutions.

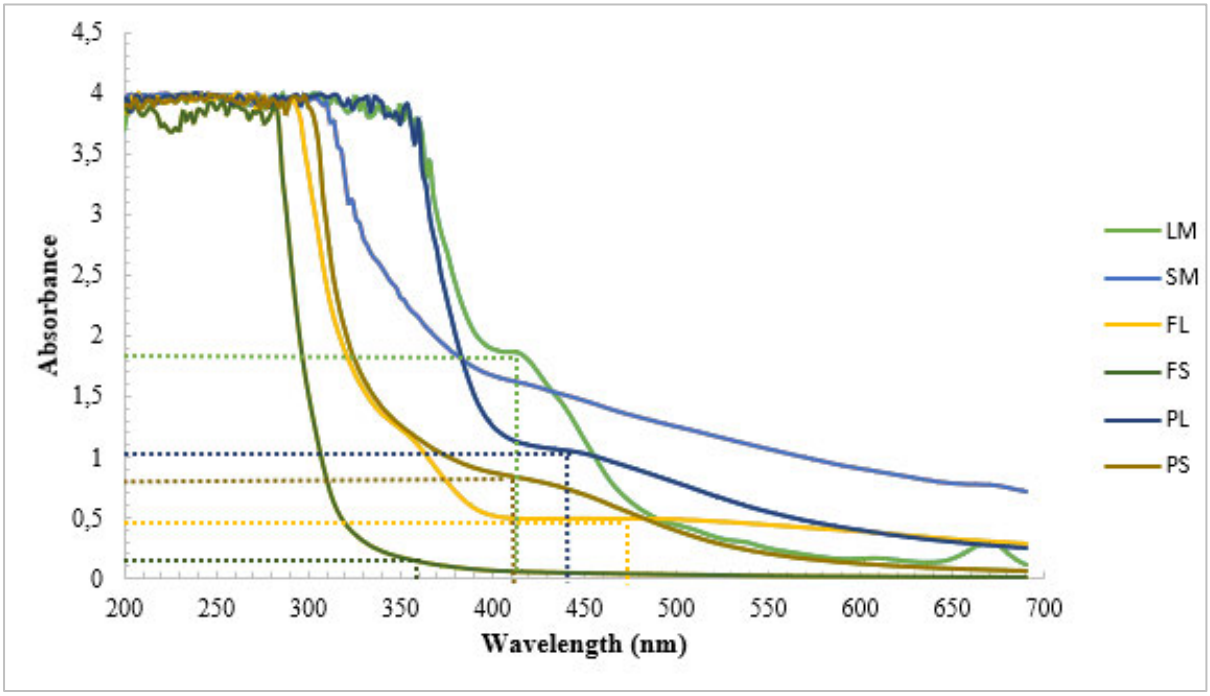

Figure 6.2: UV-vis spectra of AgNPs synthesized using leaf and stem extracts (methanolic, fresh and powdered) of *T. ventricosa*. Leaf methanol (LM); stem methanol (SM); fresh leaf (FL); fresh stem (FS); powdered leaf (PL); powdered stem (PS).

6.3.3 Quantification of synthesized AgNPs

The yield for synthesized AgNPs using leaf and stem extracts (methanol, fresh, and powder) of *T. ventricosa* was extremely low (Table 6.1). The highest percentage yield was observed for AgNPs synthesized using powdered leaf extracts (1.638%), followed by powdered stem extracts (1.190%). The AgNPs synthesized using methanol stem (0.737%) and methanol leaf extracts (0.659%) displayed the second-highest percentage yield, respectively, whereas the AgNPs synthesized using fresh leaves (0.023%) and fresh stems extracts (0.027%) showed the lowest percentage yield. The variable percentage yield for the synthesized AgNPs using various extracts could be attributed to several factors such as the plant organ used, preparation of plant material (dehydration), quantity and type of bioactive compounds present within extracts, temperature, and incubation time (Akula et al., 2011; Sigamoney et al., 2016; Hu and Hsieh, 2016).

Table 6.1: Percentage yield of the synthesized AgNPs using various extracts from the leaves and stems of *T. ventricosa*.

Extracts	Leaves	Stems	Leaves	Stems
	Dried extract yield (g)		Yield (%)	
Methanol extract	0.065	0.073	0.659	0.737
Fresh extract	0.007	0.009	0.023	0.027
Powdered extract	0.163	0.119	1.638	1.190

6.3.4 Scanning Electron Microscopy (SEM)

The morphology and general particle size of the synthesized AgNPs using the various extracts of *T. ventricosa* were characterized and confirmed using SEM. The SEM images illustrated in Figure 6.3 A-F substantiate the synthesis and particle size (<100 nm) of the AgNPs. The formation of AgNPs was predominantly spherical, uniform in terms of shape, and displayed extreme agglomeration. In a similar study, Devaraj et al. (2014) characterized the AgNPs synthesized using *T. divaricata* extracts. The SEM analysis showed that the synthesized AgNPs also displayed consistent spherical shaped NPs which ranged from 29-68 nm (<100 nm), however, the synthesized particles were well distributed compared to the current study which showed high agglomeration (Devaraj et al., 2014). It is suggested that agglomeration occurs as a result of dehydration/drying of the synthesized solutions (Sigamoney et al., 2016; Valenti and Giacomelli, 2017). Moreover, studies have shown that the degree of agglomeration and average particle size of AgNPs are often influenced by variations in reaction temperature, extract concentration, and $AgNO_3$ concentration (Song et al., 2009; Yaqoob et al., 2020).

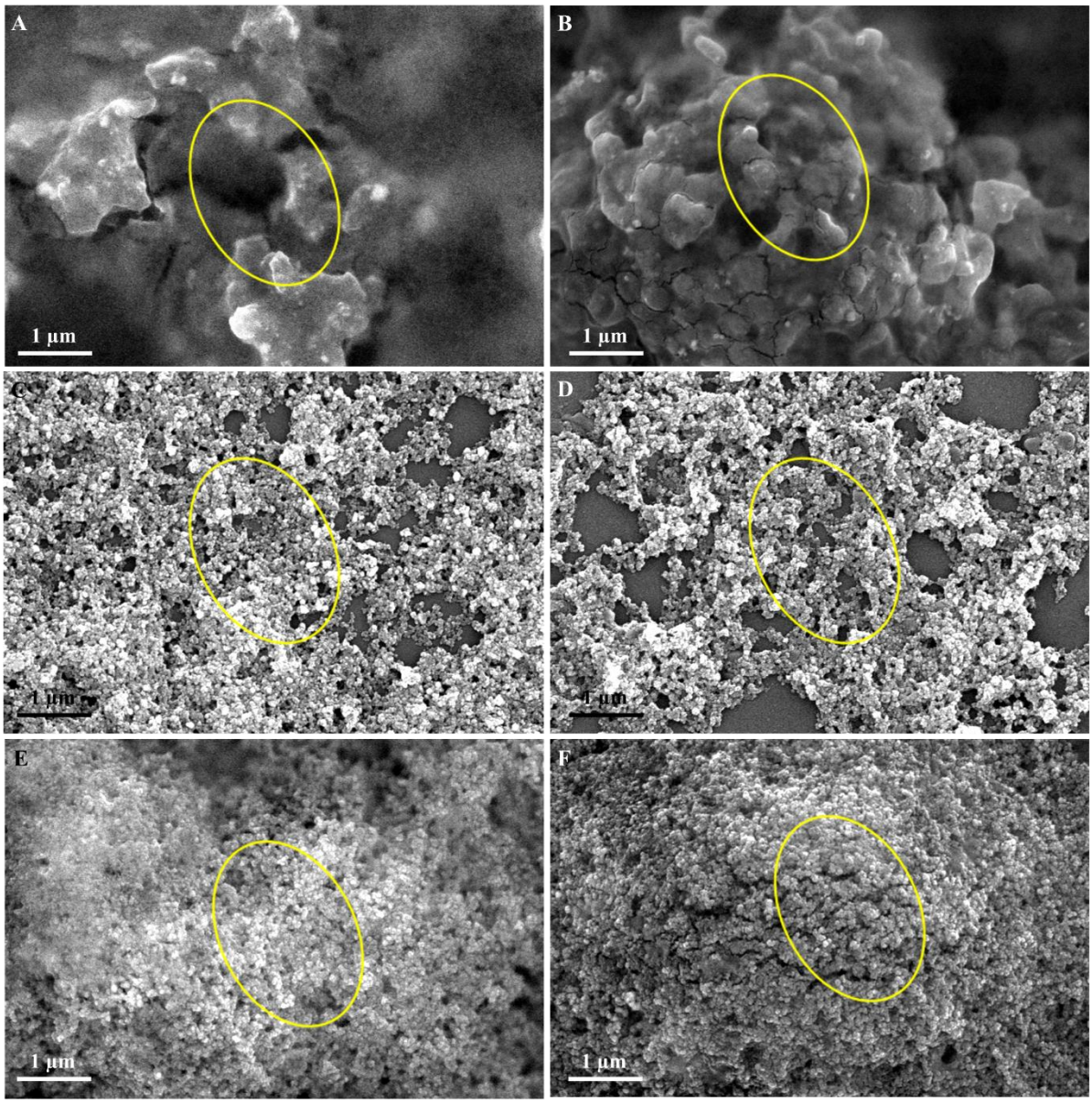

Figure 6.3: Scanning Electron micrographs of AgNPs synthesized using methanolic, fresh and powdered, leaf and stem extracts from *T. ventricosa.* (A) Leaf methanol (LM); (B) Stem methanol (SM); (C) Fresh leaf (FL); (D) Fresh stem (FS); (D) Powdered leaf (PL); (F) Powdered stem (PS). Circles indicate agglomeration of AgNPs.

6.3.5 Energy-Dispersive X-ray (EDX) analysis

The EDX analysis confirmed the presence of elemental Ag in all synthesized AgNPs using leaf and stem extracts (methanolic, fresh, and powder) of *T. ventricosa* (Table 6.2). All synthesized samples displayed characteristic elemental Ag peaks at 3 KeV (Figure 6.4), thus indicating the successful production of metallic AgNPs (Heemasager et al., 2014). The leaf extracts displayed significantly higher percentages of elemental Ag using leaf methanol (8.78%), fresh leaf (14.10%), and powdered leaf (37.00%) compared to the stem methanol, fresh stem, and powder stem which displayed slightly lower Ag compositions of 7.33%, 7.10% and 15.14% respectively (Table 6.2). The highest Ag signals were observed for synthesized AgNPs using powdered leaf extracts (Figure 6.4 E), whereas the lowest Ag signal was detected for synthesized AgNPs using fresh stem extracts (Figure 6.4 E).

It was suggested that the differences in the Ag composition detected within the various samples may be related to the variation of biochemical components found within the different plant organs (Kumar et al., 2010; Yaqoob et al., 2020). The differences in the type and combinations of bioactive compounds may affect the synthesis, yield, shape, size, and composition of AgNPs (Kumar et al., 2010). Previous phytochemical observations of *T. ventricosa* extracts (Schripsema et al., 1986), have observed differences between the chemical constituents found within the leaf and stem extracts, suggesting variations in elemental Ag observed in the AgNPs solutions. Studies suggest that phytochemical compounds such as saponins and tannins may increase the formation of metallic NPs during the reduction process of metal ions, thus resulting in an excessive accumulation of AgNPs (Kumar et al., 2010).

Moreover, these EDX results are in line with other species within *Tabernaemontana*. Attri et al. (2021), investigated the AgNPs from *T. divaricate* leaf extract that displayed an elemental composition of 46.96%, which was fairly similar to the composition detected by the synthesized AgNPs using powdered extracts in the current study. Furthermore, the EDX analysis detected strong peaks for carbon (C), oxygen (O_2), and potassium (K), and various other elements (Figure 6.4). It is highly likely that these elements are responsible for biomolecule capping and stabilization by the plant extracts and could also possibly be related to the elements detected within plant proteins (Song et al., 2009; Sigamoney et al., 2016). The latter elements correspond to the elemental mapping observed in the study by Attri et al. (2021).

Table 6.2: Average percentage of elemental Ag synthesized from extracts of *T. ventricosa*.

Extracts	Elemental silver (%)
Leaf methanol	8.78 ± 1.32
Stem methanol	7.33 ± 3.23
Fresh leaf	14.10 ± 12.08
Fresh stem	7.10 ± 5.66
Powdered leaf	37.00 ± 2.04
Powdered stem	15.14 ± 3.34

Values represent mean ± SD (n = 3).

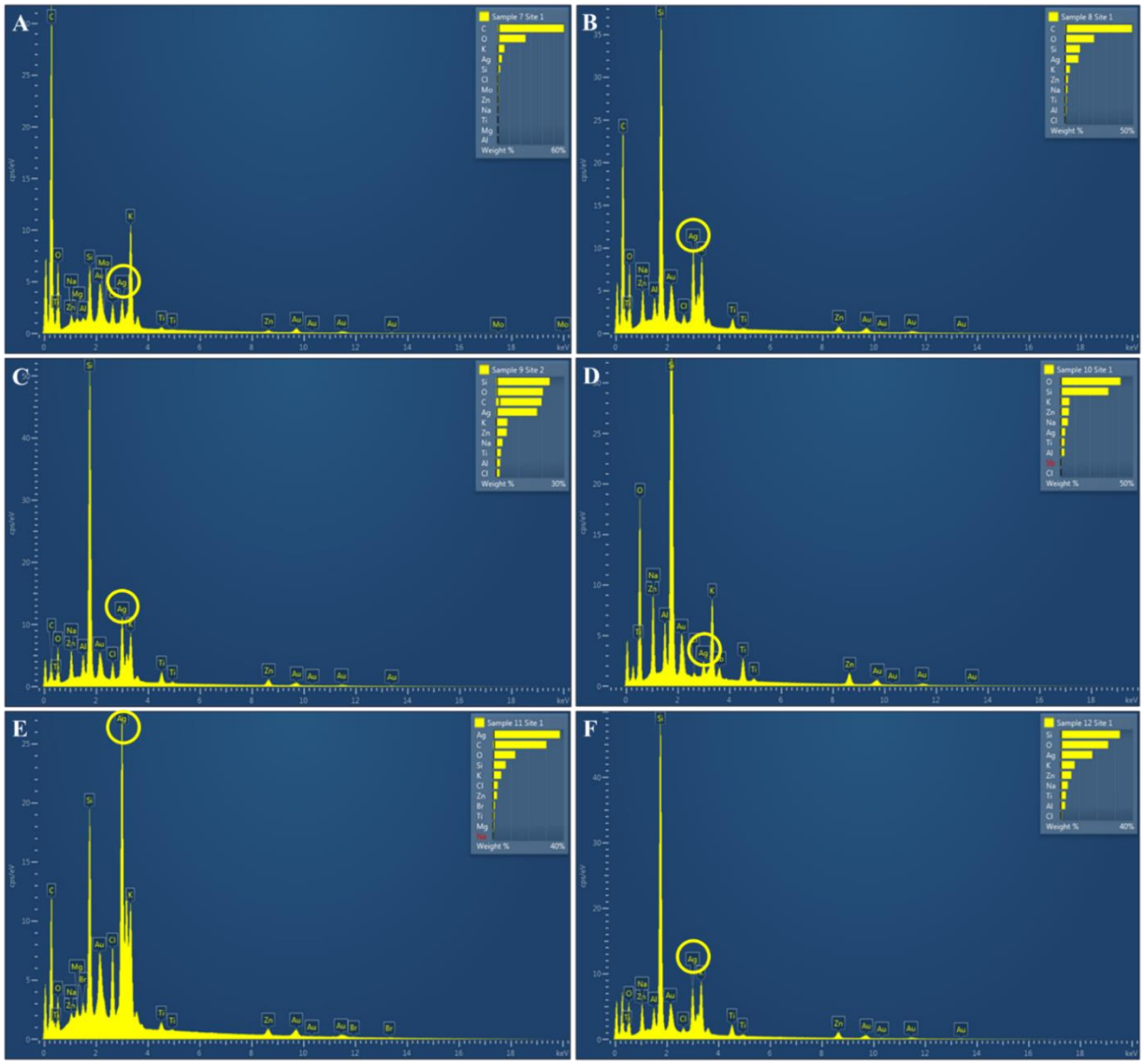

Figure 6.4: An EDX spectra of AgNPs synthesized using methanolic, fresh and powdered, leaf and stem extracts from *T. ventricosa.* (A) Leaf methanol (LM); (B) Stem methanol (SM); (C) Fresh leaf (FL); (D) Fresh stem (FS); (E) Powdered leaf (PL); (F) Powdered stem (PS). Circles indicate Ag.

6.3.6 High-Resolution Transmission Electron Microscopy (HRTEM) analyses

High-Resolution Transmission Electron Microscopy was used to characterize particle shape, size, and morphological distribution of synthesized AgNPs from *T. ventricosa* leaf and stem extracts (methanolic, fresh, and powder). The HRTEM micrographs displayed in Figure 6.5, showed similarities in the particle shape of synthesized AgNPs across all extracts, and the majority of the particles were spherical and ovate. Interestingly, the images also displayed hexagonal (Figure 6.5 A-C) and triangular-shaped (Figure 6.5 A-B, E) particles, which appeared randomly distributed across a few samples. However, the triangular-shaped particles were particularly distinguishable within the powdered leaf AgNPs samples (Figure 6.5 E). The particle shapes observed in the present study are comparable to reports by Devaraj et al. (2014) and Attri et al. (2021). In both these studies, the researchers investigated the particle shape of synthesized AgNPs using *T. divaricate* leaf extracts, which exhibited spherical-shaped particles and similarly highlighted infrequent appearances of triangular-shaped particles (Devaraj et al., 2014; Attri et al., 2021).

The average particle size of the synthesized AgNPs ranged from 16.09 ± 6.81 nm to 80.26 ± 24.93 nm and differed among all samples (Figure 6.6). The larger average particle sizes were observed for both fresh leaf (64.01 nm) and powder stem (80.26 nm) extracts, respectively, whereas smaller particle sizes were observed predominately in the leaf (18.80 nm) and stem methanol (23.86 nm) extracts followed by the fresh stem (23.02 nm) and powder leaf extracts (16.09 nm). Overall, the synthesized AgNPs varied significantly in particle size among the different extracts since the methanol extracts produced much smaller AgNPs followed by the fresh extracts and the powder extracts (Figure 6.6). Studies suggest that the average particle size of AgNPs could be related to the highly variable morphology of NPs that is often influenced by the various plant organs and extract types used during synthesis (Devaraj et al., 2014; Sigamoney et al., 2016). The size of the AgNPs appears to be following other reports within the genus since previous studies using *T. divaricate* leaf extracts observed an average AgNP size that ranged from 10 nm to 30 nm (Devaraj et al., 2014; Attri et al., 2021). The morphological distribution of the AgNPs appeared slightly agglomerated however, the majority of the AgNPs were well-separated (not in direct contact) and monodispersed (Figure 6.5) suggestive of the stabilization of the NPs by its respective capping agents (Annadurai et al., 2012; Devaraj et al., 2014). Moreover, the HRTEM images revealed a slight film surrounding the AgNPs produced using both plant organs. According to Mallikarjuna et al. (2011), the observed films are possibly functional groups that serve as capping agents of the synthesized AgNPs. Additionally, it is suggested that the capping of functional groups may offer extra stability to the AgNPs in solution (Mittal et al., 2013).

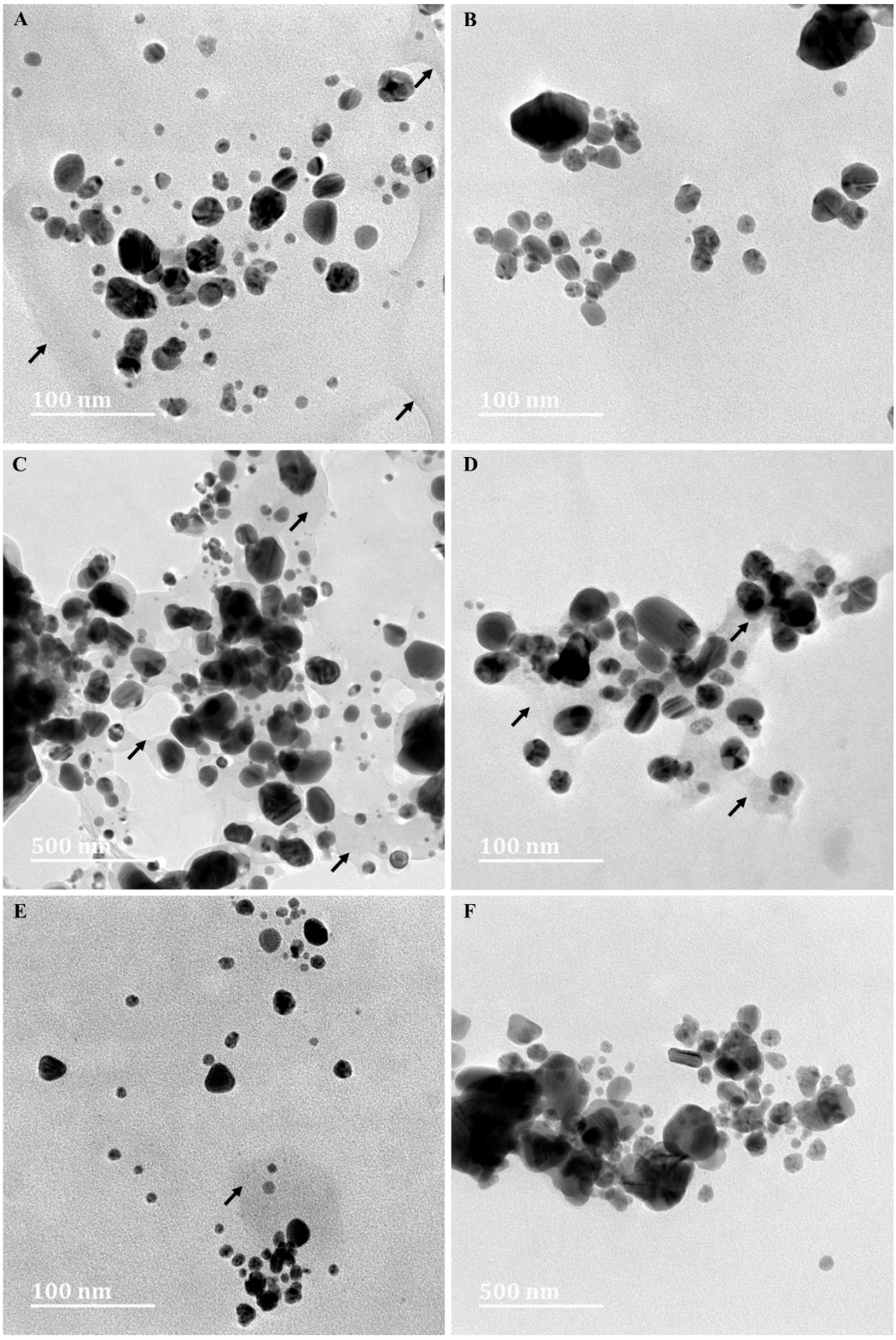

Figure 6.5: High-Resolution Transmission Electron Microscopy images of Ag nanoparticles synthesized using methanolic, fresh and powdered, leaf and stem extracts from *T. ventricosa*. (A) Leaf methanol (LM); (B) Stem methanol (SM); (C) Fresh leaf (FL); (D) Fresh stem (FS); (E) Powdered leaf (PL); (F) Powdered stem (PS). Arrows indicate film surrounding AgNPs.

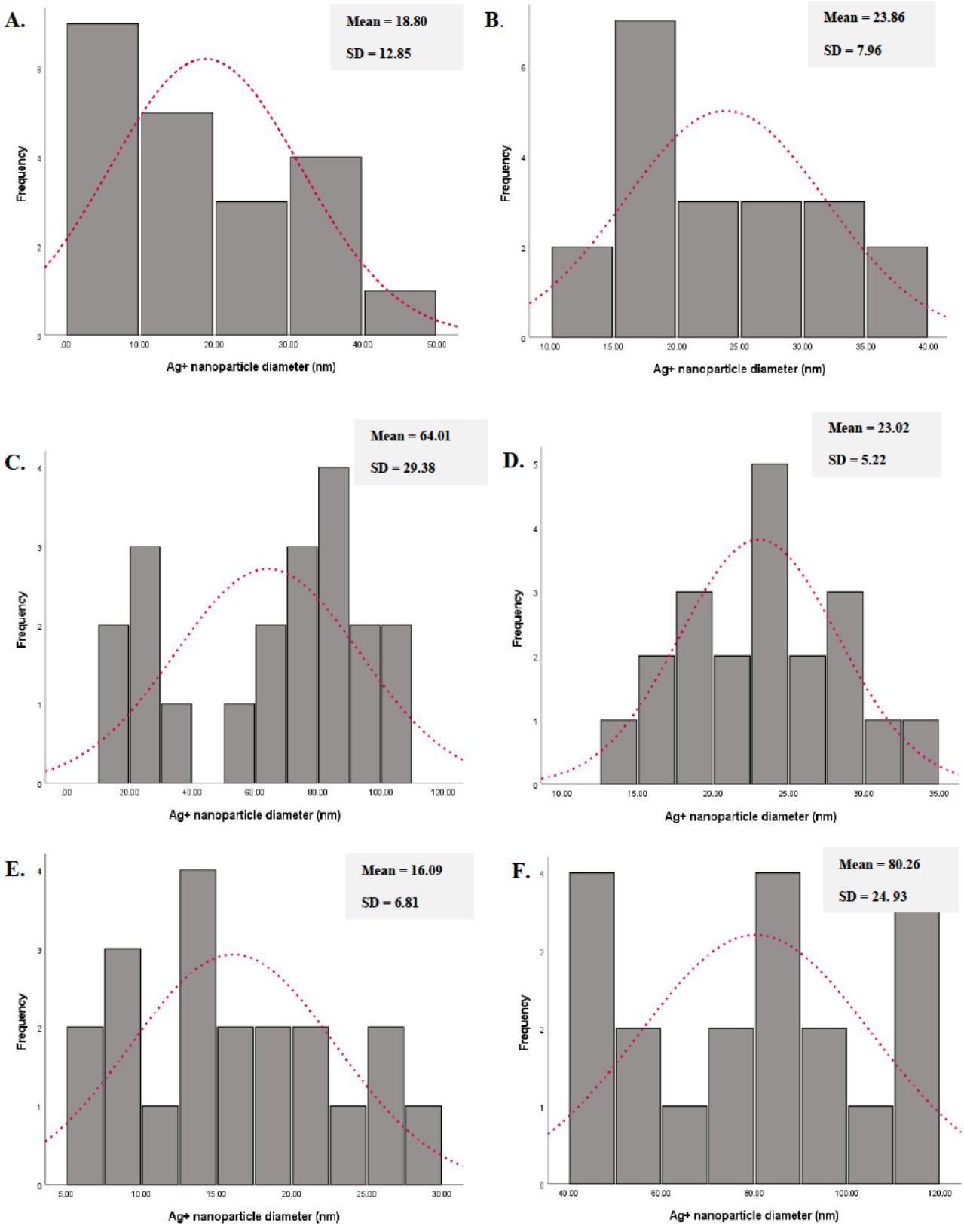

Figure 6.6: Particle size (nm) of synthesized AgNPs using methanolic, fresh and powdered, leaf and stem extracts from *T. ventricosa.* (A) Leaf methanol (LM); (B) Stem methanol (SM); (C) Fresh leaf (FL); (D) Fresh stem (FS); (E) Powdered leaf (PL); (F) Powdered stem (PS). n = 5.

6.3.7 Nanoparticle Tracking Analysis (NTA) and zeta potential

Nanoparticle Tracking Analysis is a valuable parameter that is often utilized by researchers in nanoscience for effective detection of NP size, distribution, surface stability of colloidal particles, and zeta potential (Patel and Agarwal, 2011; Joshi et al., 2019). In the present study, the NTA analyses were conducted on the various synthesized AgNPs (Appendix 3A). The hydrodynamic diameter (nm) of the AgNPs was 80.9 ± 8.8 nm, 70.2 ± 6.1 nm, 125.0 ± 41.8 nm, 63.9 ± 63.9 nm, 120.5 ± 36.2 nm, and 147.4 ± 7.4 nm using leaf methanol (LM), stem methanol (SM), fresh leaf (FL), fresh stem (FS), powdered leaf (PL), and powdered stem (PS), respectively (Table 6.3). Overall, the synthesized AgNPs sizes diameter from the NTA analysis ranged from 63.9 ± 63.9 nm to 147.4 ± 7.4 nm. However, the particle sizes measured using HRTEM and Image J analyses displayed a range from 16.09 nm to 80.26 nm. Although there is a large variation between the particle sizes using different techniques, these values correspond with each other to an extent. It has been reported that the variable differences observed between particles using HRTEM and NTA analyses may be attributed to the differences involved in sample preparation (Daniels and Singh, 2019). While HRTEM measures particles in a dried state, NTA measures particles in an aqueous medium that is closer to that expected in an *in vivo* system (Akinyelu and Singh, 2019; Oladimeji et al., 2021).

A common trend recognized in both analyses is the larger particle sizes of the AgNPs synthesized using fresh leaf and powdered stem extracts. However, despite these inconsistencies, the results obtained using NTA are often preferred over HRTEM due to the hydrodynamic environment of the NTA process (Preetam et al., 2016). The above-mentioned nanoparticle diameters (nm) observed in the current study are similar to those reported by Anbukkarasi et al. (2017), which ranged from 15 nm to 50 nm using TEM analyses and from 100 nm to 500 nm using NTA.

In addition to the particle size, the zeta potential of particles in the solution was also measured to determine the surface charges (Table 6.3). The measurement of the surface charges is a crucial indicator of the colloidal stability of NPs (Patel and Agrawal., 2011; Joshi et al., 2019). The zeta potential for NPs is often categorized into an acceptable range of greater than 25 mV or less than -30 mV since these values usually indicate improved stability, increased mobility, enhanced electrostatic repulsion, and reduced agglomeration (Daniels and Singh, 2019). The synthesized AgNPs across all extracts displayed low zeta potentials, except for AgNPs synthesized using stem methanol extracts (-30.3 ± 0.1 mV), suggestive of good colloidal stability. However, this value was significantly lower compared to reports by Anbukkarasi et al. (2017), where a large negative zeta potential value of the AgNPs synthesized using ethanolic leaf extracts of *T. divaricata* was observed.

Table 6.3: Average nanoparticle diameter (nm) and zeta potential (mV) of the synthesized AgNPs using the leaf and stem extracts (methanolic, fresh, and powdered) of *T. ventricosa*.

Extracts	Nanoparticle diameter (nm)	Zeta potential (mV)
Leaf methanol	80.9 ± 8.8	-3.5 ± 5.1
Stem methanol	70.2 ± 6.1	-30.3 ± 0.1
Fresh leaf	125.0 ± 41.8	15.6 ± 5.6
Fresh stem aqueous	63.9 ± 63.9	7.2 ± 7.2
Powdered leaf	120.5 ± 36.2	3.5 ± 0.1
Powdered stem	147.4 ± 7.4	5.9 ± 0.0

Mean ± standard error (n=3).

6.3.8 Fourier Transform Infrared (FTIR) spectroscopy

The FTIR spectroscopy measurements were undertaken to determine the biomolecules that are likely responsible for the reduction of Ag ions and the capping of the bio-reduced AgNPs produced by the leaf and stem extracts of *T. ventricosa*. The FTIR spectra displayed different stretches and bending of bonds at various peaks for all synthesized AgNPS using leaf methanol (LM), stem methanol (SM), fresh leaf (FL), fresh stem (FS), powdered leaf (PL), and powdered stem (PS) extracts, respectively (Table 6.4). However, the observed peak patterns were very similar across all AgNPs produced, with a few significant differences in peaks observed for certain AgNPs (Figure 6.7).

The FTIR spectra exhibited prominent peaks at 3295.32, 3273.38, 2924.68, 2394.69, 2105.80, 1623.91, 1336.46, 1050.28 and 802.05 cm^{-1} for LM extracts (Figure 6.7 A), 3304.50, 3261.97, 2922.18, 2340.00, 2110.75, 1601.17, 1334.31, 1043.12, 989.51, 922.32 and 822.50 cm^{-1} for SM extracts (Figure 6.7 B), 3260.11, 2933.85, 2395.37, 2346.05, 2095.91, 1599.57, 1319.11, 1044.99 and 820.01 cm^{-1} for FL extracts (Figure 6.7 C), 3274.20, 2936.60, 2395.51, 2353.80, 2117.48, 2091.37, 1862.28, 1605.68, 1335.16, 1054.95 and 821.96 cm^{-1} for FS extracts (Figure 6.7 D), 3223.35, 2930.02, 2342.72, 2112.99, 1859.66, 1588.93, 1383.96, 1050.83, 817.51 and 769.33 cm^{-1} for PL extracts (Figure 6.7 E), 3256.75, 3237.75, 2930.54, 2339.50, 2102.08, 1592.84, 1368.53, 1050.52, 819.44 and 769.03 cm^{-1} for PS extracts (Figure 6.7 F).

The FTIR spectra displayed strong intensity peaks between 3200 cm^{-1} and 3400 cm^{-1} for all AgNP solutions (Figure 6.7). These peaks correspond to the strong broad O–H stretch of alcohols, C–H stretch of alkynes, C=O, C–O, O–H stretching of carboxylic acids, and H–bonded to phenols (Devaraj et al., 2014; Fatima et al., 2020; Attri et al., 2021), whereas the bands observed between 2922 cm^{-1} and 2936 cm^{-1} correspond to the medium C–H stretch of alkanes and the strong broad N–H stretch of amine salts (Fatima et al., 2020). Strong peaks displayed by bands from regions between 2339 cm^{-1} and 2395 cm^{-1} resemble O=C=O carbon dioxide stretching however, bands in the 2100 cm^{-1} to 2140 cm^{-1} region represent weak C≡C alkyne stretching (Devaraj et al., 2014; Fatima et al., 2020; Attri et al., 2021).

Interestingly, the compound group isothiocyanate N=C=S showed strong stretching at 2095.91 cm^{-1} (FL) and 2091.37 cm^{-1} (FS) in fresh extracts only (Devaraj et al., 2014; Preetam et al., 2016). The sharp peaks from 1588.93 cm^{-1} to 1623.91 cm^{-1} indicate C=C, C–O, and N–H stretching to alkenes and amines. The C–H plane bends to alkanes and aldehydes, C–O and O–H medium/strong stretches and bending of alcohols and phenols respectively, CO–O–CO strong broad stretching of anhydrides, and strong S=O stretches of sulfoxide, sulfonate/ sulfonamide all correspond to the 1043 cm^{-1}-1384 cm^{-1} region (Devaraj et al., 2014; Fatima et al., 2020; Attri et al., 2021). The medium peaks at 690 cm^{-1}-895 cm^{-1} correspond to medium C=C bending of alkenes and strong C–Br and C–l halo compounds (Preetam et al., 2016).

The observed FTIR spectra indicated the presence of a variety of functional groups at varying positions. The results suggest that the capping of the NPs may contain phenolic and terpenoid compounds, with functional groups of carboxylic acids, alcohols, alkanes, and esters which may have reduced $AgNO_3$ to AgNPs (Patel, 2013). Furthermore, the occurrence of medium intensity peaks in the amide region, more specifically the amide I (one) area, also suggests proteins/enzymes are likely responsible for the reduction of Ag ions for the synthesis of AgNPs (Shanker et al., 2004; Devaraj et al., 2014). According to the results of this study, the occurrence of proteins may be accountable for the formation of a thin film (cap) surrounding the AgNPs (Patel, 2013). Studies have confirmed that amino acid residues and peptides of proteins usually coat AgNPs to prevent the agglomeration of particles, allowing the stability of NPs in solution (Firdhouse and Lalitha, 2012; Annadurai et al., 2012; Nandiyanto and Ragadhita, 2019).

Table 6.4: FTIR spectral assignments of the synthesized AgNPs using various extracts of *T. ventricosa*.

Plant extract	Absorption frequency (cm^{-1})	Types of absorption/ vibration	Appearance	Interference/ functional group	Compound class
Leaf methanol	3295.32	Stretch	Strong broad	O–H	Alcohol
	3273.38	Stretch	Strong broad	O–H	Alcohol
	2924.68	Stretch	Medium	C–H	Alkane
	2394.69	Stretch	Strong	O=C=O	Carbon dioxide
	2105.80	Stretch	Weak	C≡C	Alkyne
	1623.91	Stretch	Medium	C=C	Conjugated alkene
	1336.46	Bending	Medium	O–H	Alcohol
	1050.28	Stretch	Strong	C–O	Primary alcohol
	802.05	Bending	Medium	C=C	Alkene

Table 6.4: *Cont.*

Stem methanol	3304.50	Stretch	Medium	N–H	Aliphatic primary amine
	3261.97	Stretch	Strong broad	O–H	Alcohol
	2922.18	Stretch	Strong broad	N–H	amine salt
	2340.00	Stretch	Strong	O=C=O	Carbon dioxide
	2110.75	Stretch	Weak	C≡C	Alkyne
	1601.17	Stretch	Medium	C=C	Conjugated alkene
	1334.31	Bending	Medium	O–H	Alcohol
	1043.12	Stretch	Strong broad	CO–O–CO	anhydride
	989.51	Bending	Strong	C=C	alkene
	922.32	Bending	Strong	C=C	alkene
	822.50	Bending	Medium	C=C	alkene
Fresh leaf	3260.11	Stretch	Strong broad	O–H	Alcohol
	2933.85	Stretch	Strong broad	N–H	amine salt
	2395.37	Stretch	Strong	O=C=O	Carbon dioxide
	2346.05	Stretch	Strong	O=C=O	Carbon dioxide
	2095.91	Stretch	Strong	N=C=S	Isothiocyanate
	1599.57	Stretch	Strong	N–O	Nitro compound
	1319.11	Bending	Medium	O–H	Phenol
	1044.99	Stretch	Strong broad	S=O	sulfoxide
	820.01	Bending	Medium	C=C	alkene
Fresh stem	3274.20	Stretch	Strong broad	O–H	Alcohol
	2936.60	Stretch	Strong broad	N–H	amine salt
	2395.51	Stretch	Strong	O=C=O	Carbon dioxide
	2353.80	Stretch	Strong	O=C=O	Carbon dioxide
	2117.48	Stretch	Weak	C≡C	Alkyne
	2091.37	Stretch	Strong	N=C=S	Isothiocyanate
	1862.28	Bending	Weak	C–H	Aromatic compound
	1605.68	Stretch	Medium	C=C	Conjugated alkene
	1335.16	Stretch	Strong	S=O	Sulfonate/ sulfonamide
	1054.95	Stretch	Strong	C–O	Primary alcohol
	821.96	Bending	Medium	C=C	Alkene

Table 6.4: *Cont.*

Powder leaf	3223.35	Stretch	Strong broad	O–H	Alcohol
	2930.02	Stretch	Strong broad	N–H	Amine salt
	2342.72	Stretch	Strong	O=C=O	Carbon dioxide
	2112.99	Stretch	Weak	C≡C	Alkyne
	1859.66	Bending	Weak	C–H	Aromatic compound
	1588.93	Bending	Medium	N–H	Amine
	1383.96	Bending	Medium	C–H	Aldehyde
	1050.83	Stretch	Strong	C–O	Primary alcohol
	817.51	Bending	Medium	C=C	Alkene
	769.33	Stretch	Strong	C–Cl	Halo compound
Powder stem	3256.75	Stretch	Strong broad	O–H	Alcohol
	3237.75	Stretch	Strong broad	O–H	Alcohol
	2930.54	Stretch	Strong broad	N–H	Amine salt
	2339.50	Stretch	Strong	O=C=O	Carbon dioxide
	2102.08	Stretch	Weak	C≡C	Alkyne
	1592.84	Bending	Medium	N–H	Amine
	1368.53	Bending	Medium	O–H	Alcohol
	1050.52	Stretch	Strong	C–O	Primary alcohol
	819.44	Bending	Medium	C=C	alkene
	769.03	Stretch	Strong	C–Cl	Halo compound

A.

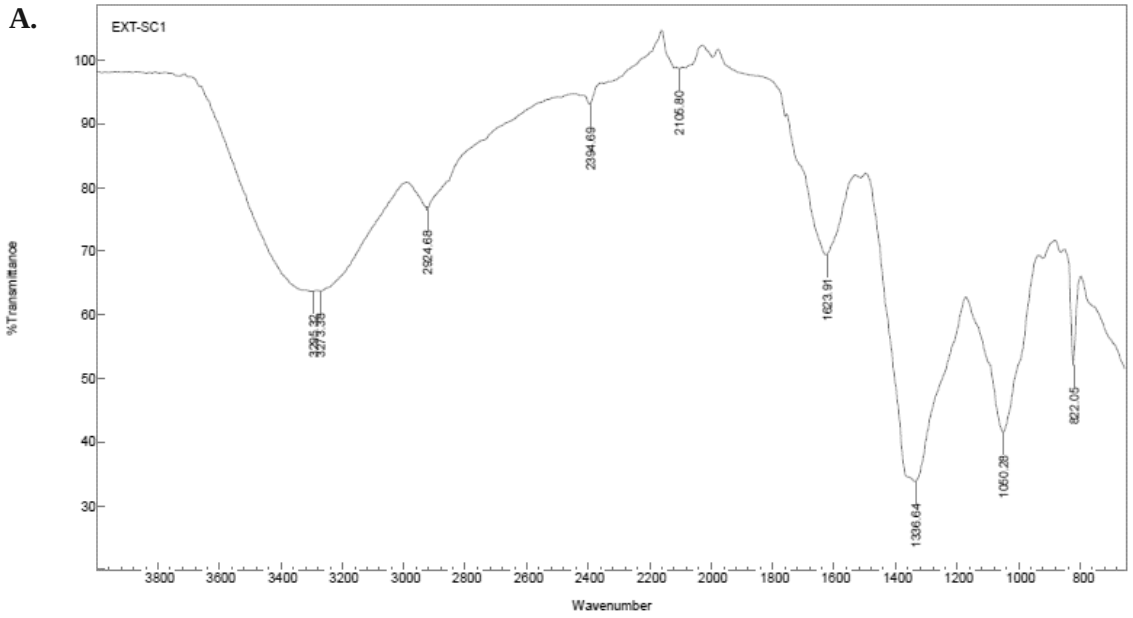
EXT-SC1
%Transmittance
Wavenumber
2924.68
2394.69
2105.80
1623.91
1396.64
1050.28
822.05

B.

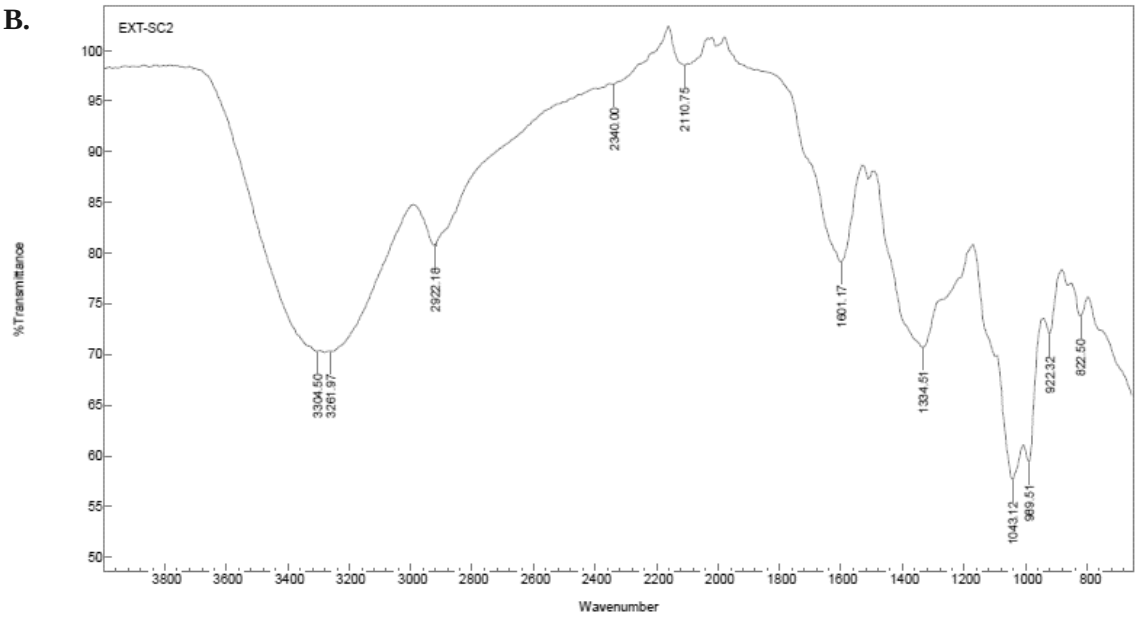
EXT-SC2
%Transmittance
Wavenumber
3304.50
3261.97
2922.18
2340.00
2110.75
1601.17
1334.51
1043.12
989.51
922.32
822.50

C.

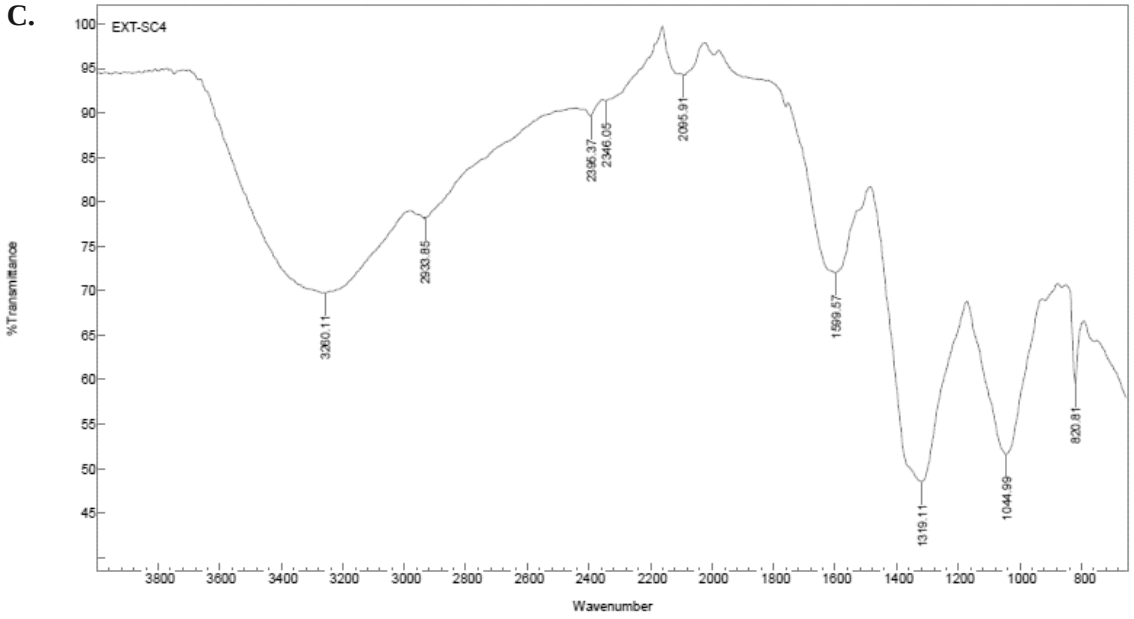
EXT-SC4
%Transmittance
Wavenumber
3260.11
2933.85
2396.37
2346.05
2095.91
1599.57
1319.11
1044.99
820.81

D.

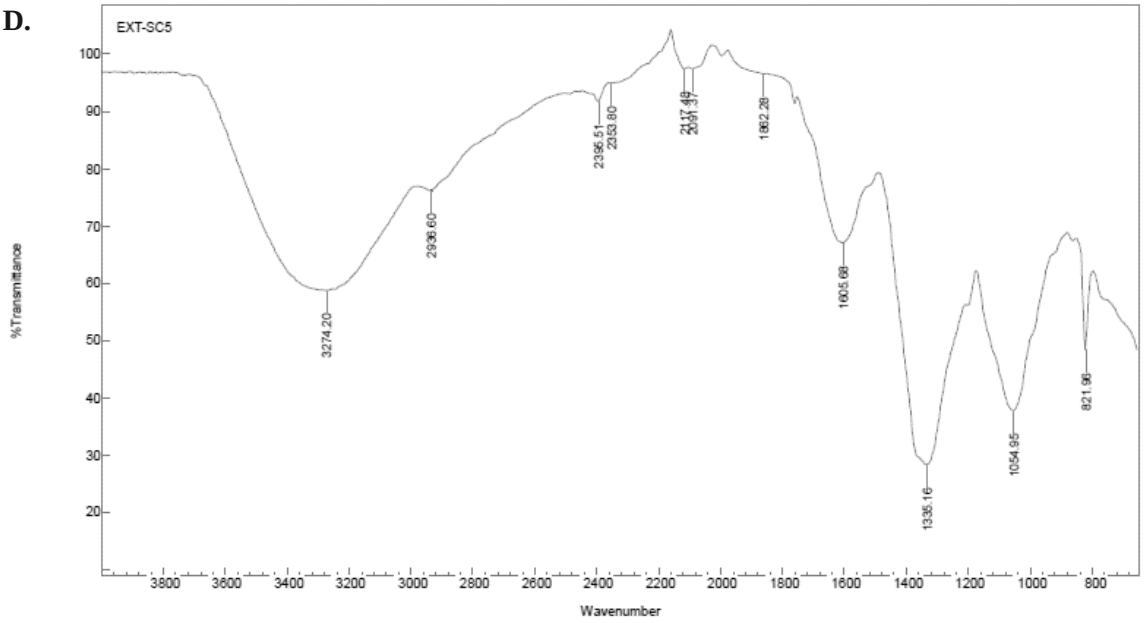
EXT-SC5
%Transmittance
Wavenumber
3274.20
2936.60
2396.51
2353.80
2117.48
2091.37
1862.28
1605.68
1335.16
1054.95
821.96

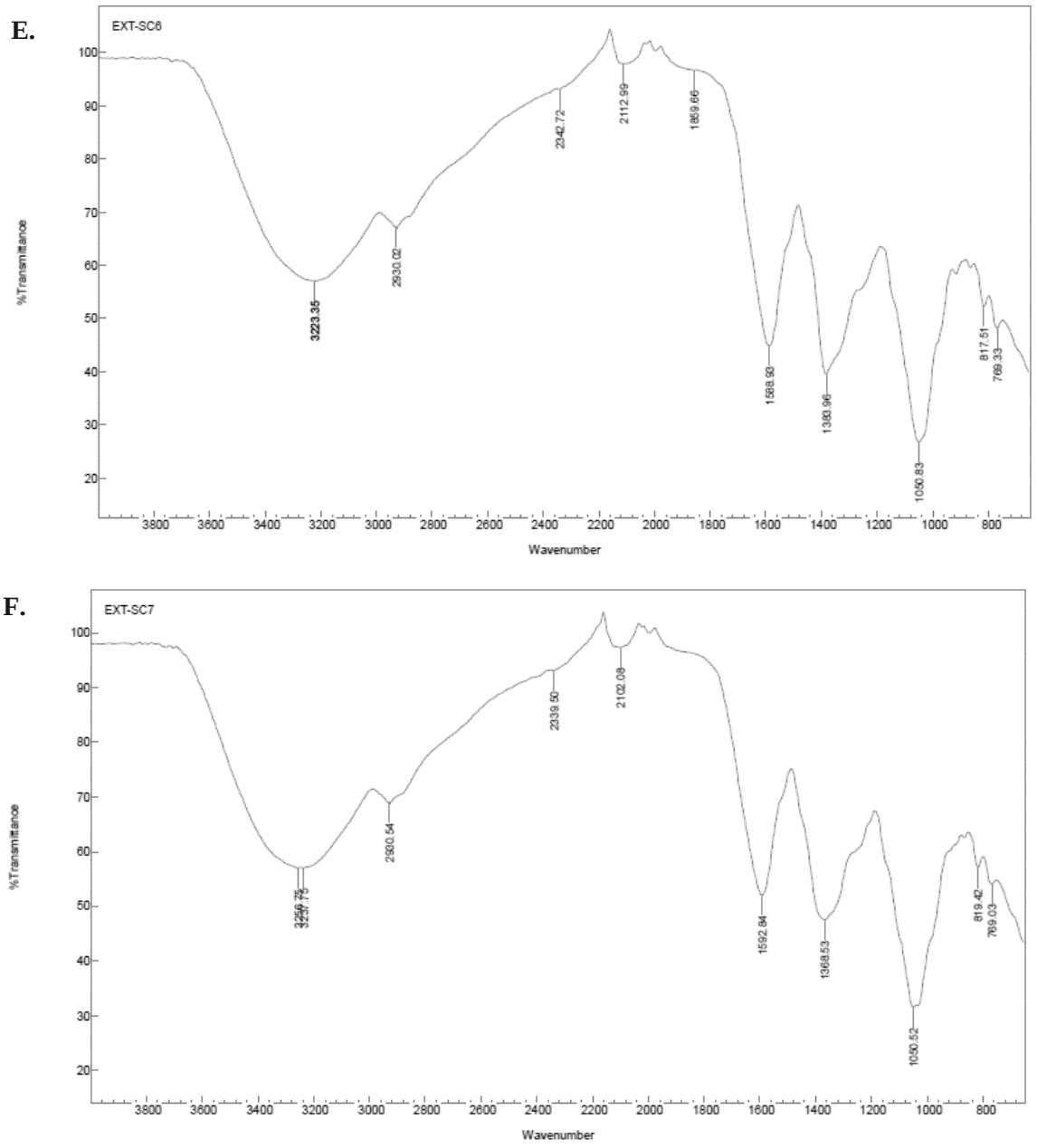

Figure 6.7: The FTIR spectra of AgNPs synthesized using leaf and stem (methanolic, fresh, and powdered) extracts of *T. ventricosa* (A) Leaf methanol extract; (B) Stem methanol extract; (C)Fresh leaf extract; (D) Fresh stem extract; (E) Leaf powder extract; (F) Stem powder extract.

6.3.9 Antibacterial assay

Recently, AgNPs synthesized using plant extracts have been extensively utilized in biological applications due to their broad range of bioactivities that include antioxidant, antimicrobial, cytotoxic, antiplasmodial, and anticancer properties (Anbukkarasi et al., 2017). There have been several reports of the potential antibacterial properties of various types of NPs synthesized using *Tabernaemontana* species such as *T. divaricata* (Sivaraj et al., 2014; Preetam et al., 2016; Anbukkarasi et al., 2017; Raja et al., 2018; Anbukkarasi et al., 2020; Attri et al., 2021) and *T. heyneana* (Manasa et al., 2021). However, despite the availability of several reports, the current literature seems to be focused on one species, namely *T. divaricata*. Therefore, due to the limited or lack of research available on other *Tabernaemontana* species, the current study aimed to evaluate the antibacterial potential of synthesized leaf and stem AgNPs of *T. ventricosa* using the agar disc diffusion method (Appendix 2A). During the antibacterial analyses, six concentrations ranging from 3.125 to 100 mg/mL were tested against five pathogenic bacterial strains, three gram-positive: *B. subtilis* (ATCC 6653), MRSA (ATCC 43300), *S. aureus* (ATCC 29213), and two gram-negative bacterial strains: *E. coli* (ATCC 25922) and *P. aeruginosa* (ATCC 27853).

The zones of inhibition of various AgNPs synthesized using extracts against several strains are presented in Table 6.5 The results revealed that the synthesized AgNPs using methanol stem, powdered leaf, fresh leaf extracts displayed noteworthy antibacterial activity against *B. subtilis, E. coli*, MRSA, *S. aureus, and P. aeruginosa*, whereas AgNPs synthesized using methanol leaves, powdered stems, and fresh stem extracts showed substantial to moderate antibacterial inhibition against all three-gram positive, and both gram-negative strains. Additionally, all AgNPs synthesized using various extracts showed slight inhibition against all bacterial strains at the lower concentrations (3.125, 6.25,12.5 mg/mL), except for AgNPs synthesized using methanol leaves and fresh stem, which displayed no activity against *P. aeruginosa* at the lowest concentrations. The results of the current study showed no major differences between AgNPs synthesized using leaf and stem extracts since both types of extracts demonstrated similar levels of inhibition against all bacterial strains.

The general trend of the results highlighted that the zone of inhibition of the reference antibiotics ranged from 8.67 ± 0.58 mm to 13.00 ± 2.00 mm, which was slightly lower compared to the AgNPs synthesized using various extracts with ranged from 0.00 ± 0.00 mm (no activity) to 15.33 ± 0.58 mm. At the lowest concentrations, the AgNPs synthesized using extracts showed very little activity compared to the antibiotics however, at higher concentrations, the AgNPs synthesized using methanol stems showed substantial activity (higher than the antibiotics) when tested against *B. subtilis.* Overall, significant differences were noted for the antibacterial analyses of AgNPs across all extract types and concentrations within each bacterial strain (P <0.05).

Recently, Attri, et al. (2021), investigated the AgNPs synthesized using leaf ethanolic extracts of *T. divaricate*, which showed good inhibition against *E. coli* and *B. subtilis* respectively. It has been suggested that the antibacterial activity of AgNPs using *T. divaricate* extracts is possibly attributed to the readily available free radicals within the bio-extracts, which reportedly increase antibacterial activity (Attri et al., 2021). Considering the similarities recorded in both *Tabernaemontana* species, it is highly likely that the free radicals present within *T. ventricosa* likewise influenced the antibacterial activities of the AgNPs in the present study. Moreover, it has been reported that the properties of AgNPs such as size (<100 nm) and shape (spherical, ovate, and triangular) are well-suited for their effectiveness against biological processes within microorganisms (Safavi, 2012). Studies have confirmed that AgNPs can modify the cell structure and function of bacterial cell walls by a process of denaturation, which leads to the prevention of bacterial respiration, destabilization of the outer membrane, induced depletion of intercellular adenosine triphosphate (ATP), and ultimately bacterial cell death (Vivekanandhan et al., 2011; Heemasager et al., 2014; Raja et al., 2018; Attri et al., 2021). The AgNPs synthesized using various leaf and stem extracts of *T. ventricosa* may positively attribute to the inhibition of bacteria.

Table 6.5: Zones of inhibition (mm) of synthesized AgNPs using various extracts of *T. ventricosa* against gram-positive and negative bacterial strains.

Bacterial strains	Concentration (mg/mL)	Synthesized AgNPs using various extracts						Positive control (10 ug/mL	
		Leaf methanol	Stem methanol	Fresh leaf	Fresh stem	Powder leaf	Powder stem	Leaf	Stem
BS	**3.125**	6.33 ± 0.58	6.33 ± 0.58	6.33 ± 0.58	6.00 ± 0.00	6.00 ± 0.00	6.00 ± 0.00		
	6.25	7.00 ± 0.00	7.00 ± 0.00	7.00 ± 0.00	7.00 ± 0.00	7.00 ± 0.00	6.67 ± 0.58		
	12.5	7.33 ± 0.58	6.33 ± 0.58	6.67 ± 0.58	8.67 ± 1.15	7.33 ± 0.58	7.33 ± 0.58	**13.00 ± 2.00***	**8.67 ± 0.58***
	25	8.67 ± 1.15	8.33 ± 0.58	8.00 ± 0.00	9.33 ± 0.58	9.33 ± 1.53	8.00 ± 0.00		
	50	9.33 ± 0.58	10.33 ± 0.58	9.33 ± 0.58	11.33 ± 1.15	11.33 ± 1.15	10.67 ± 0.58		
	100	10.33 ± 0.58	15.33 ± 0.58	10.33 ± 2.08	11.67 ± 0.58	13.67 ± 0.58	12.33 ± 0.58		
EC	**3.125**	8.33 ± 0.58	9.00 ± 1.00	9.00 ± 1.00	7.67 ± 0.58	8.67 ± 0.58	9.33 ± 0.58		
	6.25	9.67 ± 0.58	9.33 ± 0.58	9.33 ± 2.08	8.67 ± 0.58	9.67 ± 0.58	9.67 ± 2.52		
	12.5	10.33 ± 0.58	9.67 ± 0.58	9.67 ± 0.58	9.00 ± 1.00	10.33 ± 0.58	10.33 ± 0.58	**9.33 ± 0.58**	**9.00 ± 1.00**
	25	11.00 ± 1.00	10.33 ± 1.15	11.33 ± 0.58	9.67 ± 0.58	10.67 ± 0.58	10.67 ± 1.53		
	50	11.33 ± 0.58	12.33 ± 0.58	12.00 ± 1.00	11.33 ± 0.58	12.67 ± 1.15	12.67 ± 1.15		
	100	15.00 ± 2.00	13.67 ± 3.79	12.67 ± 2.08	12.33 ± 0.58	13.00 ± 1.00	13.00 ± 1.00		
MRSA	**3.125**	6.67 ± 0.58	6.67 ± 0.58	7.00 ± 0.00	7.33 ± 0.58	7.00 ± 1.00	7.33 ± 0.58		
	6.25	7.33 ± 0.58	7.33 ± 0.58	7.33 ± 0.58	8.00 ± 1.00	8.67 ± 1.15	7.33 ± 0.58		
	12.5	8.00 ± 1.00	8.00 ± 1.00	7.67 ± 0.58	8.33 ± 0.58	9.00 ± 01.00	7.67 ± 1.15	**9.00 ± 1.00***	**9.33 ± 0.58***
	25	9.33 ± 0.58	9.00 ± 1.00	10.00 ± 1.00	8.67 ± 0.58	9.67 ± 0.58	8.67 ± 0.58		
	50	10.00 ± 0.00	10.67 ± 0.58	12.67 ± 0.58	11.00 ± 1.00	13.00 ± 1.00	10.67 ± 1.15		
	100	11.67 ± 0.58	11.67 ± 0.58	13.00 ±1.73	11.67 ± 0.58	13.67 ± 0.58	11.00 ± 1.00		
SA	**3.125**	7.33 ± 0.58	9.33 ± 0.58	9.00 ± 1.00	10.00 ± 1.00	8.33 ± 0.58	8.33 ± 0.58		
	6.25	9.00 ± 0.58	10.00 ± 0.58	10.67 ± 0.69	10.33 ± 0.38	9.33 ± 0.51	10.33 ± 0.51		
	12.5	9.00 ± 1.00	10.33 ± 0.58	11.00 ± 1.00	10.33 ± 0.58	10.67 ± 0.58	10.67 ± 0.58	**9.00 ± 1.00***	**9.33 ± 0.58***
	25	10.00 ± 0.00	11.00 ± 1.00	11.67 ± 0.58	10.33 ± 0.58	11.00 ± 1.00	11.00 ± 1.00		
	50	10.67 ± 0.58	11.67 ± 0.58	12.33 ± 0.58	10.67 ± 0.58	11.33 ± 0.58	11.33 ± 0.58		
	100	11.67 ± 0.58	13.00 ± 1.00	14.33 ± 0.58	12.00 ± 0.58	12.33 ± 0.58	12.00 ± 1.00		
PA	**3.125**	0.00 ± 0.00	7.67 ± 0.58	8.33 ± 1.15	0.00 ± 0.00	8.00 ± 1.00	8.00 ± 1.00		
	6.25	8.00 ± 0.00	9.33 ± 1.15	8.67 ± 0.58	8.00 ± 0.00	8.33 ± 0.58	8.67 ± 0.58		
	12.5	8.33 ± 0.58	10.00 ± 1.00	9.00 ± 1.00	8.33 ± 0.58	8.33 ± 1.15	9.33 ± 0.58	**9.67 ± 1.53**	**9.00 ± 1.00**
	25	9.67 ± 0.58	10.33 ± 0.58	11.00 ± 1.00	10.33 ± 0.58	10.67 ± 0.58	9.67 ± 0.58		
	50	10.67 ± 0.58	11.67 ± 0.58	11.33 ± 1.53	10.67 ± 0.58	11.00 ± 1.00	10.33 ± 0.58		
	100	11.33 ± 0.58	13.00 ± 1.00	13.00 ± 1.00	12.00 ± 1.00	12.67 ± 0.58	11.00 ± 1.00		

No activity = (**0 mm**); Slight activity = (**1-6 mm**); Moderate activity = (**>7 or <9 mm**); Significant activity = (**>9mm**). **R** = Resistant, **BS** = *Bacillus subtilis* (ATCC 6653), **EC** = *Escherichia coli* (ATCC 25922), **MRSA** = *Methicillin Resistant Staphylococcus aureus* (ATCC 43300), **SA** = *Staphylococcus aureus* (ATCC 29213), **PA** = *Pseudomonas aeruginosa* (ATCC 27853), Positive controls (Gentamicin 10 µg/mL, Streptomycin 10 µg/mL*) and (n = 3).

6.3.10 Cytotoxicity assay

As mentioned previously, due to the increased demand for AgNPs in a variety of applications, these NPs must be evaluated for their potential cytotoxicity (Safavi, 2012; Mittal et al., 2013; Devarj et al., 2014; Lateef et al., 2018). The cytotoxic screening of various plant extracts, isolated chemical compounds, novel drugs, and synthesized NPs are often assessed using the MTT assay, that was developed by Mosmann (1983). Previous reports have demonstrated a substantial cytotoxic potential using synthesized NPs of *Tabernaemontana* species (Devaraj et al., 2014; Sivaraj et al., 2014; Preetam et al., 2016; Attri et al., 2021). In the current study, the cytotoxicity of synthesized AgNPs using various extracts of *T. ventricosa* at different concentrations (15, 30, 60, 120 to 240 µg/mL) was conducted using the MTT cell viability assay. One human non-cancerous cell line, HEK293 (human embryonic kidney), and two cancerous cell lines namely, MCF-7 (human breast adenocarcinoma) and HeLa (human cervical carcinoma) were utilized for the study.

As observed in Figure 6.8, control 1(cells only) were viable, and control 2 (cells + 0.1% DMSO) was reduced (72.56%-93.12%). The present investigation indicated that all AgNPs synthesized using various extracts of *T. ventricosa* showed significant cytotoxicity across all cell lines, including the normal cell line, HEK293. This suggests that AgNPs do not possess any selectivity between noncancerous and cancerous cell lines (Gichumbi et al., 2018). However, most recognized anticancer drugs such as 5-Fluorouracil are known for their antiproliferative effects against both cell types (normal or cancerous) (Gichumbi et al., 2018). The results further revealed that the synthesized AgNPs using fresh leaf and stem extracts displayed remarkable cytotoxic activity (lowest percentage cell survival) across three cell lines at 15 µg/mL and 240 µg/mL, respectively (Figure 6.8), with the exception of AgNPs synthesized using fresh stem extracts at 15 µg/mL for the MCF-7 cell line which showed a relatively high percentage cell survival compared to other treatments (Figure 6.8). Silver nanoparticles synthesized using leaf methanol and powdered stems showed moderately high cell survival across cell lines (Figure 6.8). These results confirm previous findings by Devaraj et al. (2014) and Sivaraj et al. (2014) since the leaf extracts of *T. divaricata* in both studies successfully inhibited the growth of cells by more the 90%. Overall, significant differences were observed for the cytotoxic analyses of AgNPs across all concentrations within each extract type ($P < 0.05$).

Most significantly an evident relationship between the AgNPs concentrations and percentage cell survival was noted, suggestive of dose-dependent cytotoxicity. These results correspond with reports by Devaraj et al. (2014), where *T. divaricata* leaf extracts were evaluated for its cytotoxic activity which similarly displayed dose-dependent cytotoxicity on MCF-7 cells. Likewise, Preetam et al. (2016), investigated the anticancer activity of gold NPs synthesized using *T. divarcata* extracts which also demonstrated a good dose-dependent association. Furthermore, Manasa et al. (2021) evaluated the

cytotoxicity of zinc oxide NPs using A549 cell lines, which likewise displayed dose-dependent cytotoxicity.

The IC_{50} values of AgNPs synthesized using various extracts of *T. ventricosa* showed moderate (IC_{50} >50-100) to significant (IC_{50} <50) cytotoxic activity, with none of the extracts displaying low antiproliferative activity (IC_{50} >100). AgNPs synthesized using fresh leaf extracts exhibited significant activity with IC_{50} values of 1.40 µg/mL, 6.50 µg/mL, and 0.30 µg/mL for cell lines HEK293, MCF-7, and HeLa, respectively. The weakest IC_{50} values were observed for AgNPs synthesized using powdered leaf (66.00 µg/mL), powdered stems (60.60 µg/mL), and leaf methanol (50.10 µg/mL) extracts respectively, across all cell lines. Overall, the most significant IC_{50} value was observed for AgNPs synthesized using fresh leaf extracts (0.39 µg/mL). The IC_{50} values reported in the present study are similar to those reported by Sivaraj et al. (2014), who observed a moderate IC_{50} value of 30.65 µg/mL for zinc oxide NPs using *T. divaricata* leaf extracts. Similarly, Devaraj et al. (2014) reported a significant IC_{50} value at 20 µL/mL however, Manasa et al. (2021), investigated the synthesis of zinc oxide particles from *T. heyneana* which showed a weak IC_{50} value between 89.47 and 185.80 µg/mL. These variations are possible due to the different types of NPs synthesized.

A.

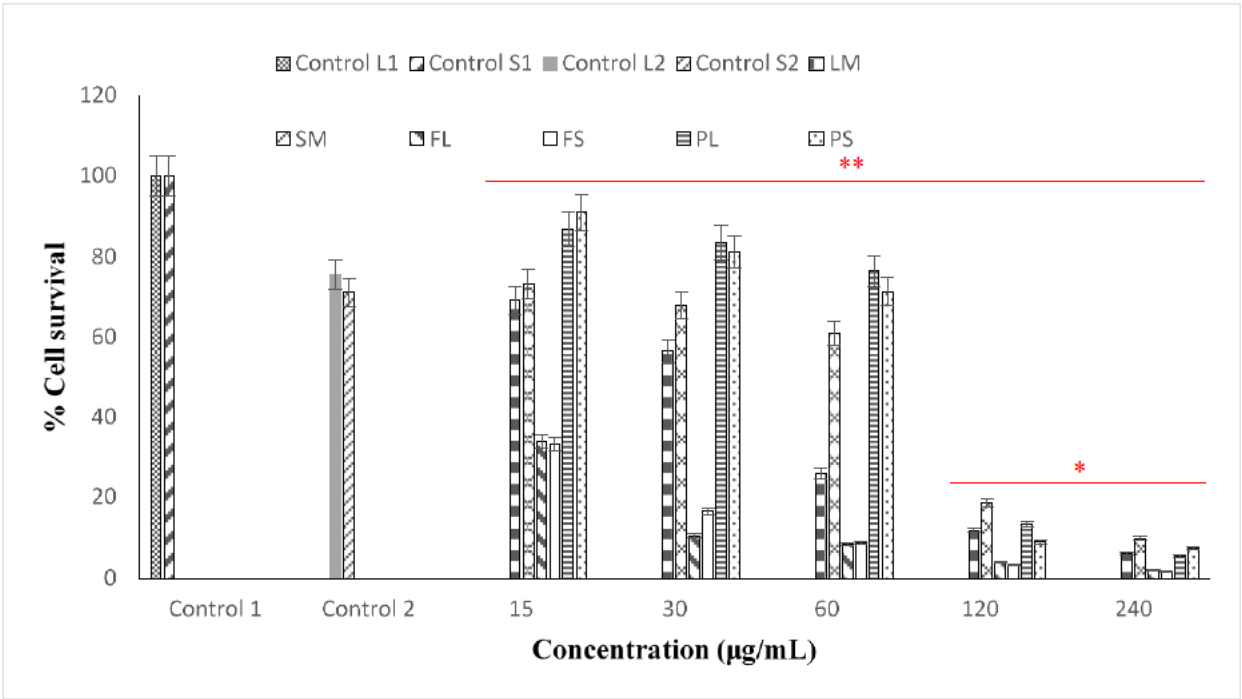

B.

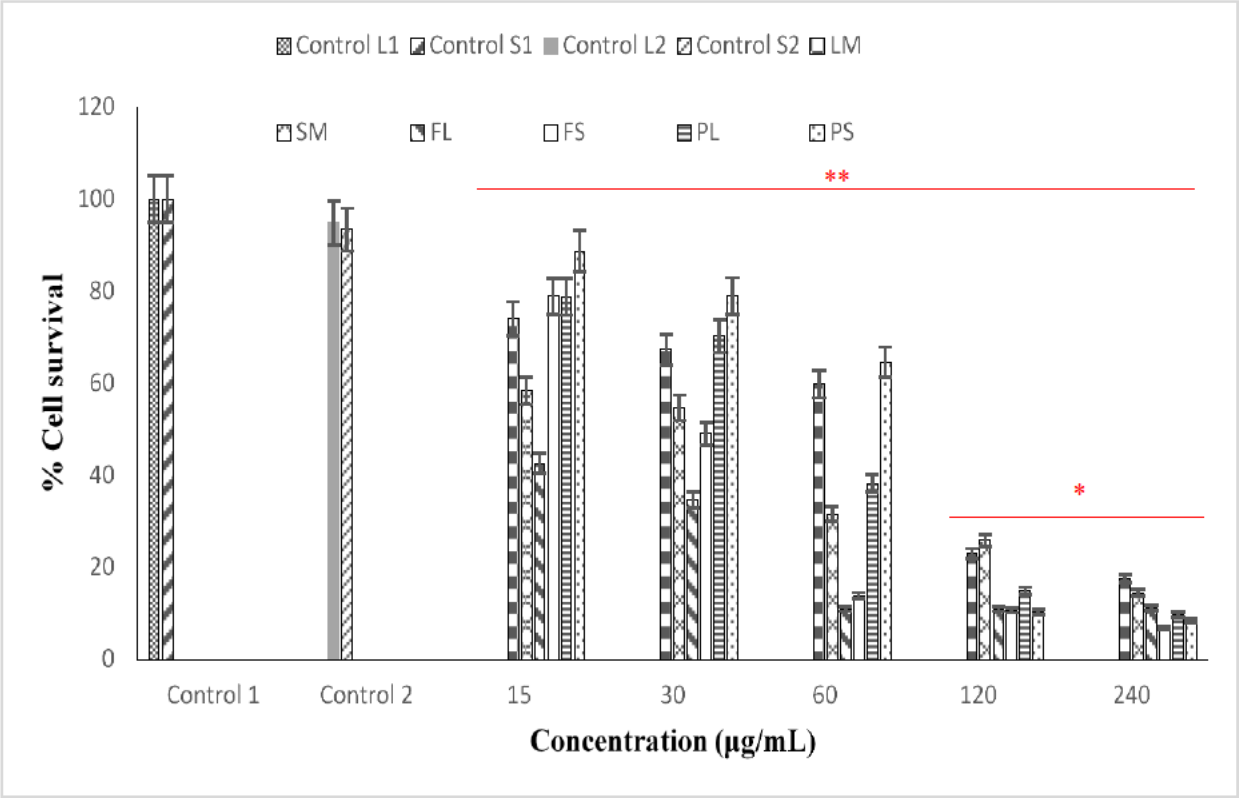

C.

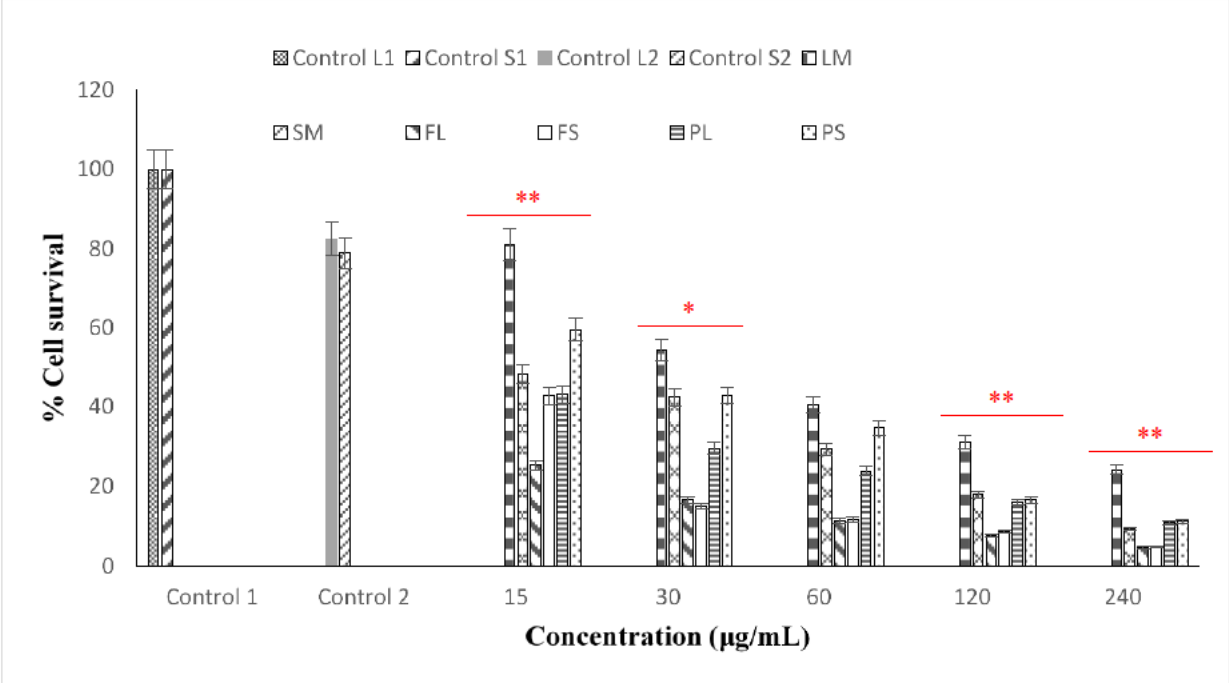

Figure 6.8: *In vitro* cytotoxicity activity of synthesised AgNPs using leaf methanol (LM); stem methanol; fresh leaf (FL); fresh stem (FS); powdered leaf (PL); powdered stem (PS) extracts from *T. ventricosa*. Control 1 = cells only; Control 2 = cells + DMSO. Percentage cell survival of (A) HEK293;(B) MCF-7 and (C) HeLa cell lines. **P* <0.05 and ***P* <0.01 are considered significant.

Table 6.6: IC_{50} values of the cytotoxic activity of the synthesized AgNPs using the leaf and stem extracts (methanolic, fresh, and powdered) of *T. ventricosa*.

Extracts	Cell lines		
	HEK293	**MCF-7**	**HeLa**
	Concentration µg/mL		
Leaf methanol	31.40	56.00	50.10
Stem methanol	51.70	27.80	15.24
Fresh leaf	1.40	6.50	0.39
Fresh stem	2.10	30.30	3.74
Powdered leaf	66.00	45.80	6.48
Powdered stem	63.80	60.60	23.28

6.4 Conclusion

The present study revealed the effective biosynthesis of AgNPs using various *T. ventricosa* leaf and stem extracts, which displayed differences in terms of colour change, elemental Ag composition, and size of the synthesized AgNPs. Overall, the AgNP yield was generally low, which could have been influenced by several variables. Synthesized AgNPs using various extracts of *T. ventricosa* produced spherical to ovate-shaped and triangular-shaped NPs, which ranged from 16.06 nm to 80.26 nm from HRTEM but were much larger when observed during NTA analyses, possibly due to its hydrodynamic environment. According to the EDX analyses, AgNPs synthesized using leaf extracts (LM, FL, and PL) were more efficient compared to stem extracts (SM, FS, and PS) in terms of AgNPs synthesis, as the elemental Ag content was much larger. The observed FTIR spectra suggested that the functional groups of the biochemical constituents found in the leaf and stem extracts may be responsible for the capping and stability of the synthesized Ag ions in the solution. These groups include alcohols, phenolics, aldehydes, alkanes, amines, and aromatic compounds, which have been reported in similar studies. Greater inhibition of bacterial growth was observed using leaf AgNPs extracts, such as the powdered leaf and fresh leaf extracts, which demonstrated substantial antibacterial activity against *B. subtilis*, *E. coli*, MRSA, *S. aureus, and P. aeruginosa*. There was a considerable cytotoxic activity observed in the present study with significant IC_{50} values displayed using fresh leaf extracts (0.39 µg/mL). Considering the potential of the various leaf and stem extracts for the production of AgNPs, further research should be undertaken using various ratios of $AgNO_3$ to establish an optimal protocol for AgNP synthesis. This is the first investigation of the production, characterization, and biological applications of the AgNPs of *T. ventricosa*. Based on these findings, *T. ventricosa* extracts are recommended as bio-factories for an efficient production of AgNPs.

6.5 References

Akhtar, M., Swamy, M.K., Umar, A., Al Sahli, A.A., 2015. Biosynthesis and characterization of silver nanoparticles from methanol leaf extract of *Cassia didymobotyra* and assessment of their antioxidant and antibacterial activities. Journal of Nanoscience and Nanotechnology 15, 9818–9823.

Akinyelu, J., Singh, M., 2019. Folate-tagged chitosan functionalized gold nanoparticles for enhanced delivery of 5-fluorouracil to cancer cells. Applied Nanoscience 9 ,7–17.

Akula, R., Ravishankar, G.A., 2011. Influence of abiotic stress signals on secondary metabolites in plants. Plant Signal Behaviour 6, 1720–1731.

Akwu, N.A., Naidoo, Y., Singh, M., Nundkumar, N., Daniels, A., Lin, J., 2021. Two Temperatures Biogenic Synthesis of Silver Nanoparticles from *Grewia lasiocarpa* E. Mey. ex Harv. Leaf and Stem Bark Extracts: Characterization and Applications. BioNanoScience 11, 142–158.

Anbukkarasi, M., Thomas, P.A., Sheu, J.R., Geraldine, P., 2017. *In vitro* antioxidant and anticataractogenic potential of silver nanoparticles biosynthesized using an ethanolic extract of *Tabernaemontana divaricata* leaves. Biomedicine & Pharmacotherapy 91, 467–475.

Anbukkarasi, M., Thomas, P.A., Teresa, P.A., Anand, T., Geraldine, P., 2020. Comparison of the efficacy of a *Tabernaemontana divaricata* extract and of biosynthesized silver nanoparticles in preventing cataract formation in an *in-vivo* system of selenite-induced cataractogenesis. Biocatalysis and Agricultural Biotechnology 23, 101475.

Annadurai, G., Gnanajobitha, G., Kannan, C., 2012. Green synthesis of silver nanoparticle using E*lettaria cardamomom* and assessment of its anti-microbial activity. International Journal of Pharmaceutical Sciences and Research 3, 323–30.

Attri, P., Garg, S., Ratan, J.K., Giri, A.S., 2021. Silver Nanoparticles from *Tabernaemontana Divaricate* leaf extract: Mechanism of action and Bio-application for photo degradation of 4-Aminopyridine. Research Square 1–31.

Awwad, A.M., Salem, N.M., Abdeen, A.O., 2013. Green synthesis of silver nanoparticles using *carob* leaf extract and its antibacterial activity. International Journal of Industrial Chemistry 4, 1–6.

Bar, H., Bhui, D. Kr, Sahoo, G.P., Sarkar, P., De, P.S., Misra, A., 2009. Green synthesis of silver nanoparticles using latex of *Jatropha curcas*. Colloids Surface. A Physicochemical and Engineering Aspects 339, 134–139.

Chandra, H., Kumari, P., Bontempi, E., Yadav, S., 2020. Medicinal plants: Treasure trove for green synthesis of metallic nanoparticles and their biomedical applications. Biocatalysis and Agricultural Biotechnology 24, 101518.

Chouhan, N., 2018. Silver Nanoparticles: Synthesis, characterization, and applications. In silver nanoparticles-fabrication, characterization and applications. Editors: Maaz, K. IntechOpen.

Clinical and Laboratory Standards Institute (2006) Performance Standards for Antimicrobial Disk Susceptibility Tests, Approved standard-Ninth Edition (M2-A9). Wayne, PA: (CLSI) Philadelphia.

Daniels, A.N and Singh, M., 2019. Sterically stabilized siRNA: gold nanocomplexes enhance c-MYC silencing in a breast cancer cell model. Nanomedicine 14, 1387–1401.

Devaraj, P., Aarti, C., Kumari, P., 2014. Synthesis and characterization of silver nanoparticles using *Tabernaemontana divaricata* and its cytotoxic activity against MCF7 cell line. International Journal of Pharmacology and Pharmaceutical Science 6, 86–90.

Fatima, K., Mahmud, S., Yasin, H., Asif, R., Qadeer, K., Ahmad, I., 2020. Authentication of various commercially available crude drugs using different quality control testing parameters. Pakistan Journal of Pharmaceutical Sciences 33, 1–17.

Firdhouse, M.J., Lalitha, P., 2012. Phyto-assisted synthesis and characterization of silver nanoparticles from *Amaranthus dubius*. International Journal of Applied Biology and Pharmaceutical Technology 3, 96–101.

Gichumbi, J.M., Friedrich, H.B., Omondi, B., Naicker, K., Singh, M., Chenia, H.Y., 2018. Synthesis, characterization, antiproliferative, and antimicrobial activity of osmium (II) half-sandwich complexes. Journal of Coordination Chemistry 71, 342–354.

Heemasagar, D., Jeeva, K., Sureshkumar, M., 2014. Enhanced anti-microbial activity of honey with green synthesized AgNPs by using *Tabernaemontana Coronaria* (JACQ.) wild flower extract. American Journal of PharmaTech Research 4, 1–12.

Hu, S., Hsieh, Y.L., 2016. Silver nanoparticle synthesis using lignin as reducing and capping agents: a kinetic and mechanistic study. International Journal of Biological Macromolecules 82, 856–862.

Joshi, A., Sharma, A., Bachheti, R.K., Husen, A.,Mishra, V.K., 2019. Plant-mediated synthesis of copper oxide nanoparticles and their biological applications. In Nanomaterials and Plant Potential. Springer, Cham 221–237.

Khan, Y., Numan, M., Ali, M., Khali, A.T., Abbas, N., Shinwar, Z.K., 2017. Bio-synthesized silver nanoparticles using different plant extracts as anti-cancer agent. Journal of Nanomedicine and Biotherapeutic Discovery 1, 1–7.

Khanra, K., Panja, S., Choudhuri, I., Chakraborty, A., Bhattacharyya, N., 2016. Antimicrobial and cytotoxicity effect of silver nanoparticle synthesized by *Croton bonplandianum* Baill. leaves. Nanomedicine Journal 3, 15–22.

Kumar, V., Yadav, S.C., Yadav, S.K., 2010. *Syzygium cumini* leaf and seed extract mediated biosynthesis of silver nanoparticles and their characterization. Journal of Chemical Technology and Biotechnology 85, 1301–1309.

Lateef, A., Folarin, B.I., Oladejo, S.M., Akinola, P.O., Beukes, L.S., Gueguim-Kana, E.B., 2018. Characterization, anti-microbial, anti-oxidant, and anti-coagulant activities of silver nanoparticles synthesized from *Petiveria alliacea* L. leaf extract. Preparative Biochemistry and Biotechnology, 1–7.

Lee, K.X., Shameli, K., Yew, Y.P., Teow, S.Y., Jahangirian, H., Rafiee-Moghaddam, R., Webster, T.J., 2020. Recent developments in the facile bio-synthesis of gold nanoparticles (AuNPs) and their biomedical applications. International Journal of Nanomedicine 15, 275.

Mallikarjuna, K., Narasimha, G., Dillip, G.R., Praveen, B., Shreedhar, B., Shree Lakshmi, C., Reddy, B.V.S., Deva Prasad Raju, B., 2011. Green synthesis of silver nanoparticles using *Ocimim* leaf extract and their characterization. Digest Journal of Nanomaterials and Biostructures 6, 181–186.

Manasa, D.J., Chandrashekar, K.R., Kumar, P., Suresh, D., Madhu Kumar, D.J., Ravikumar, C.R., Bhattacharya, T., Murthy, H.C., 2021. Proficient Synthesis of Zinc Oxide Nanoparticles from *Tabernaemontana Heyneana* Wall. Via Green Combustion Method: Antioxidant, Anti-Inflammatory, Antidiabetic, Anticancer and Photocatalytic Activities.. Results in Chemistry 3, 100178.

Marathe, N.P., Rasane, M.H., Kumar, H., Patwardhan, A.A., Shouche, Y.S., Diwanay, S.S., 2013. *In vitro* antibacterial activity of *Tabernaemontana alternifolia* (Roxb) stem bark aqueous extracts against clinical isolates of methicillin resistant *Staphylococcus aureus*. Annals of Clinical Microbiology and Antimicrobials 12, 1–8.

Mathew, S., Victorio, C.P., Sidhi, J., BH, B.T., 2020. Biosynthesis of silver nanoparticle using flowers of *Calotropis gigantea* (L.) WT Aiton and activity against pathogenic bacteria. Arabian Journal of Chemistry 13, 9139–9144.

Mehrbod, P., Abdalla, M.A., Njoya, E.M., Ahmed, A.S., Fotouhi, F., Farahmand, B., Gado, D.A., Tabatabaian, M., Fasanmi, O.G., Eloff, J.N., McGaw, L.J., 2018. South African medicinal plant extracts active against influenza A virus. BMC Complementary and Alternative Medicine 18, 112–121.

Mittal, A.K., Chisti, Y., Banerjee, U.C., 2013. Synthesis of metallic nanoparticles using plant extracts. Biotechnological Advances 31, 346–356.

Mosmann, T., 1983. Rapid colorimetric assay for cellular growth and survival: Application to proliferation and cytotoxicity assays. Journal of Immunological Methods 65, 55–63.

Nandiyanto, A.B.D., Oktiani, R., Ragadhita, R., 2019. How to read and interpret FTIR spectroscope of organic material. Indonesian Journal of Science and Technology 4, 97–118.

Netai, M.M., Stephen, N., Musekiwa, C., 2017. Synthesis of silver nanoparticles using *wild Cucumis anguria*: Characterization and antibacterial activity. African Journal of Biotechnology 16, 1911–1921.

Oladimeji, O., Akinyelu, J., Daniels, A., Singh, M., 2021. Modified Gold Nanoparticles for efficient Delivery of Betulinic Acid to Cancer Cell Mitochondria. International Journal of Molecular Sciences 22, 5072.

Patel, N., 2013. Biosynthesis and anti-bacterial activity of silver and gold nanoparticles from the leaf and callus extracts of *Amaranthus dubius*, *Gunnera perpensa*, *Ceratotheca triloba* and *Catharanthus roseus*. MSc thesis, Durban University of Technology, South Africa.

Patel, V.R., Agrawal, Y.K., 2011. Nanosuspension: An approach to enhance solubility of drugs. Journal of Advanced Pharmaceutical Technology & Research 2, 81.

Preetam Raj, J.P., Purushothaman, M., Ameer, K., Panicker, S.G., 2016. *In-vitro* anticancer and antioxidant activity of gold nanoparticles conjugate with *Tabernaemontana divaricata* flower SMs against MCF-7 breast cancer cells. Korean Chemical Engineering Research 54, 5–80.

Raja, A., Ashokkumar, S., Marthandam, R.P., Jayachandiran, J., Khatiwada, C.P., Kaviyarasu, K., Raman, R.G., Swaminathan, M., 2018. Eco-friendly preparation of zinc oxide nanoparticles using *Tabernaemontana divaricata* and its photocatalytic and antimicrobial activity. Journal of Photochemistry and Photobiology B: Biology 181, 53–58.

Saddal, S.K., Telang, T., Bhange, V.P., Kopulwar, A.P., Santra, S.R., Soni, M., 2018. Green synthesis of silver nanoparticles using stem extract of *Berberis aristata* and to study its characterization and antimicrobial activity. Journal of Pharmacy Research 12, 840.

Safavi, K., 2012. Evaluation of using nanomaterial in tissue culture media and biological activity. Second International Conference on Ecological, Environmental and Biological, Sciences. October 13–14.

Schmelzer, G.B., Gurib-Fakim, A., 2008. Medicinal Plants, first ed. Plant Resources of Tropical Africa 11,1. PROTA Foundation. Backhuys Publishers, Wageningen, Netherlands.

Schmidt, E., Lotter, M., McCleland, W., 2002. Trees and Shrubs of Mpumalanga and Kruger National park. Jacana.

Schripsema, J., Hermans-Lokkerbol, A., Van der Heijden, R., Verpoorte, R., Svendsen, A.B., Van Beek, T.A., 1986. Alkaloids of *Tabernaemontana ventricosa.* Journal of Natural Products 49, 733–735.

Shankar, S.S., Rai, A., Ahmad, A., Sastry, M., 2004. Rapid synthesis of Au, Ag, and bimetallic Au core–Ag shell nanoparticles using Neem (*Azadirachta indica*) leaf broth. Journal of Colloid and Interface Science 275, 496–502.

Sigamoney, M., Shaik, S., Govender, P., Krishna, S.B.N., 2016. African leafy vegetables as bio-factories for silver nanoparticles: a case study on *Amaranthus dubius* C Mart. Ex Thell. South African Journal of Botany 103, 230–240.

Singh, A.K., 2016. Structure, synthesis, and application of nanoparticles, engineered nanoparticles. Elsevier. Academic Press.

Sivaraj, R., Rahman, P., Rajiv, P., Venckatesh, R., 2014. Biogenic zinc oxide nanoparticles synthesis using *Tabernaemontana Divaricate* leaf extract and its anticancer activity against MCF-7 breast cancer cell Lines. In International Conference on Advances in Agricultural, Biological & Environmental Sciences, (AABES-2014) Oct 15-16, 2014 Dubai (UAE), 1–3.

Song, J.Y., Jang, H.K., Kim, B.S., 2009. Biological synthesis of gold nanoparticles using *Magnolia kobus* and *Diopyros kaki* leaf extracts. Process Biochemistry 44, 1133–1138.

Tehri, N., Kaur, R., Maity, M., Chauhan, A., Hooda, V., Vashishth, A., Kumar, G., 2020. Biosynthesis, characterization, bactericidal and sporicidal activity of silver nanoparticles using the leaves extract of *Litchi chinensis*. Preparative Biochemistry & Biotechnology 50, 865–873.

Thakkar, K.N., Mhatre, S.S., Parikh, R.Y., 2010. Biological synthesis of metallic nanoparticles. Nanomedicine Nanotechnology. Biology and Medicine 6, 257–262.

Valenti, L.E. and Giacomelli, C.E., 2017. Stability of silver nanoparticles: Agglomeration and oxidation in biological relevant conditions. Journal of Nanoparticle Research 19, 156.

Vanaja, M., Annadurai, G., 2012. *Coleus aromaticus* leaf extract mediated synthesis of silver nanoparticles and its bactericidal activity. Applied Nanoscience 9, 1–7.

Vivekanandhan, S., Christensen, L., Misra, M., Mohanty, A.K., 2011. Biosynthesis of silver nanoparticles using *murraya koenigii* (curry leaf): an investigation on the effect of broth concentration in reduction mechanism and particle size. Advanced Materials Letters 2, 429–434.

Yaqoob, A.A., Umar, K., Ibrahim, M.N.M., 2020. Silver nanoparticles: Various methods of synthesis, size affecting factors and their potential applications–a review. Applied Nanoscience 10, 1369–1378.

Zargar, M., Hamid, A.A., Bakar, F.A., Shamsudin, M.N., Shameli, K., Jahanshiri, F., Farahani, F., 2011. Green synthesis and anti-bacterial effect of silver nanoparticles using *Vitex negundo* L. Molecules 16, 6667–6676.

CHAPTER 7:

ANTIBACTERIAL AND CYTOTOXIC ACTIVITY OF BIOLOGICALLY SYNTHESIZED SILVER NANOPARTICLES (AGNPS) USING LATEX EXTRACTS OF *TABERNAEMONTANA VENTRICOSA* HOCHST. EX A. DC

Abstract

Silver nanoparticles (AgNPs) were biologically synthesized using latex extracts from *Tabernaemontana ventricosa*, characterized, and their respective biological activities were assessed. The synthesized AgNPs were characterized using UV-visible spectroscopy, Fourier Transform Infrared (FTIR) spectral analysis, Scanning Electron Microscopy (SEM), High-Resolution Transmission Electron Microscopy (HRTEM), Energy-Dispersive X-ray (EDX) analysis, and Nanoparticle Tracking Analysis (NTA). The antibacterial activity of the synthesized AgNPs was assessed against various gram-negative and gram-positive bacterial strains, and the cytotoxic potential was assessed in human cell lines, namely embryonic kidney (HEK293), breast adenocarcinoma (MCF-7), and cervical carcinoma (HeLa). The AgNPs were successfully biosynthesized using latex extracts. The AgNPs displayed a pale colour change, with prominent silver (Ag) peaks at 410 nm using UV-vis spectroscopy and the EDX data confirmed the elemental percentage composition of the AgNPs, while SEM and HRTEM revealed that synthesized AgNPs were spherical, ovate, and triangular, with diameters ranging from 5 nm-17.50 nm however, NTA measurements revealed larger hydrodynamic diameters. The FTIR spectra results displayed several peaks of bending and stretching associated with various functional groups such as alcohols, alkanes, amines, proteins, enzymes, and other biomolecules possibly responsible for the capping, reduction, and functionalization of AgNPs. The AgNPs showed substantial antibacterial activity (zone of inhibition) against *Escherichia coli* (12.67 ± 1.15 mm), *Staphylococcus aureus* (11.67 ± 0.58 mm), and *Pseudomonas aeruginosa* (11.33 ± 0.58 mm), with significant cytotoxic activity noted in the HeLa cells (10.52 µg/mL). The study confirmed the successful production of AgNPs using latex extracts of *T. ventricosa* and suggests that these latex extracts may be effective capping agents of nanoparticles (NPs).

Keywords: AgNPs; Biosynthesis; Antibacterial activity; Cytotoxicity; Latex; *Tabernaemontana*.

7.1 Introduction

Nanotechnology is an emerging trend in several fields such as physics, chemistry, material science, biology, and medicine (Mittal et al., 2013; Yusuf, 2020; Manasa et al., 2021). Nanoparticles (NPs) are often preferred for certain applications due to their ideal specifications such as tiny particle size (<100 nm), high surface area to volume ratio, complex electronic, optical, magnetic, chemical, and physical properties (Yusuf, 2020). Studies have indicated that silver nanoparticles (AgNPs) were usually synthesized using chemical approaches which are often expensive, time-consuming, and involve the use of toxic chemicals (Bar et al., 2009; de Matos et al., 2011; Chandrasekaran et al., 2016). Due to the several limitations associated with the chemical production of AgNPs, researchers are largely focused on the developments of the "Biological or green synthesis" of NPs. The production of biosynthesized AgNPs is favoured due to their simplicity, effectiveness, reduced cost, and eco-friendly properties (Bar et al., 2009; Kalaiselvi et al., 2019; Yusuf, 2020).

The efficient production of AgNPs using various biological methods, which include the utilization of microorganisms, plant extracts, or plant biomasses has been intensively explored (Bar et al., 2009; Rajkuberan et al., 2017; Kalaiselvi et al., 2019). However, it was noted that plant extracts are easily maintained since they do not require intra/extracellular synthesis, purification, or maintenance of cell cultures (Mittal et al., 2013; Rajkuberan et al., 2017). Many reports have recently highlighted the biosynthesis of AgNPs using multiple plant extracts such as *Cymbopogon citratus* (Masurkar et al., 2011), *Tabernaemontana divaricata* (Anbukkarasi et al., 2017; Anbukkarasi et al., 2020), and *Tabernaemontana heyneana* Wall. (Manasa et al., 2021). Most recently, latex extracts have been studied due to the presence of natural polymers which act as a stabilizer for NPs (Anbukkarasi et al., 2020). Studies have been reported for, *Jatropha curcas* (Bar et al., 2009), *Ficus sycomorus* (Salem et al., 2014), *Euphorbia nivulia* L. (Valodkar et al., 2011), *Hevea brasiliensis* L. (Guidelli et al., 2011), *Calotropis gigantea* L. (Rajkuberan et al., 2015), and *Euphorbia tirucalli* (Kalaiselvi et al., 2019).

The tree *Tabernaemontana ventricosa* Hochst. ex A. DC. commonly known as the "Forest toad tree", is a latex-bearing species belonging to Apocynaceae (Schmidt et al., 2002). This species displays a disjunct distribution in Nigeria, Ghana, Kenya, and South Africa (Schmelzer and Gurib-Fakim, 2008). Traditionally, the leaves, stems, and latex of *T. ventricosa* are often used to reduce fever and hypertension, treat wounds, and heal sore eyes (Mehrbod et al., 2018). Pharmacological properties of this plant include antiamoebic, antibacterial, antileishmanial, and cytotoxic activities (Van Beek et al., 1984; Schmelzer and Gurib-Fakim, 2008; Andima et al., 2021). The latex of *T. ventricosa* contains an abundant source of alkaloids, phenolics, and proteins that may be responsible for the medicinal value of this species and the capping and stability of NPs (Schripsema et al., 1986).

The continuous developments in the identification of novel plant bioactive compounds have driven researchers towards the application of latex extracts and their respective compounds for the synthesis of AgNPs (Mittal et al., 2013; Ambu et al., 2020; Chandra et al., 2020). Currently, there are several reports on the "Green synthesis" of AgNPs using various *Tabernaemontana* species, such as *T. divaricata* (Anbukkarasi et al., 2017; Anbukkarasi et al., 2020) and *T. heyneana* Wall. (Manasa et al., 2021). To the best of our knowledge, there are no existing reports on the synthesis of AgNPs using latex from the *Tabernaemontana* species. Considering the importance surrounding the synthesis of AgNPs using latex extracts, especially within the genus *Tabernaemontana*, the current investigation aimed to biologically synthesize, characterize, and evaluate the antibacterial and cytotoxicity of these green synthesized AgNPs using latex from *T. ventricosa*.

7.2 Materials and Methods

7.2.1 Latex collection and preparation

Tabernaemontana ventricosa plants were obtained from the University of KwaZulu-Natal (Westville campus), South Africa, located at 29˚49′03.3″S 30˚56′32.7″E. Fresh milky white latex exudates were aseptically collected by cutting the soft green stems and were stored in sterile tubes. Subsequently, 1 mL of the latex was diluted to 100 mL (1%) using sterile distilled water and stored at -8˚C until further use.

7.2.2 Synthesis of AgNPs

The AgNPs were synthesized according to the methods by Salem et al. (2014) with modifications. For the experimental analysis, approximately 90 mL of a 1 mM aqueous solution of silver nitrate ($AgNO_3$) (Biolab, Merck) was gradually added to 10 mL latex (Lx) extract. The solution was stirred and heated at 80˚C for 3 h. The negative control containing 10 mL of distilled water and 90 mL of $AgNO_3$ was treated the same way. All analyses were conducted in triplicates (n = 3).

7.2.3 UV-visible spectral analysis

The production of AgNPs using latex extracts was confirmed by UV-vis spectroscopy (SHIMADZU UV-1800, Germany) in a range of 200-800 nm. Approximately 1 mL of AgNP solution was used for analyses, using $AgNO_3$ solution as a blank. The synthesized AgNP solution and control were simultaneously analyzed, and the corresponding optical densities (OD) were noted.

7.2.4 Preparation, purification, and quantification of samples

Following confirmation of the synthesis of the AgNPs, the solutions were subjected to centrifugation, purification, and quantification. The synthesized solutions were centrifuged (BECKMAN COULTER, Avanti®J-E, USA) at 10 000 rpm for 30 min each at 4˚C, the supernatants were discarded, and the remaining pellet was rinsed with 20 mL of distilled water. The centrifugation and wash processes were conducted thrice to ensure the elimination of additional residues. The final solutions were dried in an oven set at 50˚C for 7 days, and the yield (dry mass) was determined using the equation 7.1. For further analyses, the dried AgNPs were reconstituted using sterile distilled water.

$$\text{Extract yield (\%)} = \frac{\text{Weight of dried extract (g)}}{\text{Weight of plant material (g)}} \times 100 \quad \textbf{(7.1)}$$

7.2.5 Characterization of AgNPs

7.2.5.1 Scanning Electron Microscopy (SEM) and Energy-Dispersive X-ray (EDX) analysis

Scanning Electron Microscopy and Energy Dispersive X-ray analysis were used for the initial characterization of synthesized AgNPs using latex extracts. Prior to analyses, the samples were sonicated (SONICLEAN, England) for 20 min, placed directly onto separate aluminum stubs, and dried for 60 min using a mercury lamp. The stubs were sputter-coated with a thin layer (*ca*. 25 nm) of gold using a sputter coater (Quorum 150 R ES, UK), which was loaded, and viewed using an Ultra Plus FEGSEM (Carl Zeiss, Germany), at 5 kV. During analyses, the NP size, shape, and distribution were determined using SmartSEM version 5 software (Carl Zeiss, Germany). Simultaneous EDX analyses were performed using the Zeiss Ultra Plus X-ray spectrometer, equipped with an Astronomical Thermal Emission Camera (Aztec) version 1.2 at 20 kV. Samples were analyzed using the Aztec Analysis Software (Oxford Instruments, UK) to determine the elemental composition of synthesized AgNPs samples.

7.2.5.2 High- Resolution Transmission Electron Microscopy (HRTEM)

High-Resolution Transmission Electron Microscopy was used to obtain highly magnified images of the morphology and size of the synthesized AgNPs. Prior to the analyses, carbon-coated (Quorum Q150 TE, UK) formvar grids (200 mesh) were dipped into previously sonicated AgNP latex samples and dried under a mercury lamp for 30 min. Thereafter, the samples were viewed using the HRTEM JEM 2100 (JEOL, Japan), equipped with Gatan software, at a voltage of 200 kV. The morphology and size of the AgNPs were determined using ImageJ software (Java version 1.8.0) (n = 5).

7.2.5.3 Fourier Transform Infrared (FTIR) spectral analysis

Fourier transform infrared spectroscopy of synthesized AgNPs using latex was conducted using an Agilent Cary 60 spectrometer equipped with Agilent MicroLab PC version 5.1.22 software for the detection and characterization of the surface chemistry and functional groups of the capping agents. The data was collected using ATR Diamond-1 Bounce with 30 background and sampling scans in the 4000-650cm^{-1}, range with a resolution of 4 cm^{-1}. The various stretching and bending of bonds and peaks were interpreted using ResolutionPro version 5.0.0.395.

7.2.5.4 Nanoparticle Tracking Analysis (NTA)

The size distribution and zeta potential of the AgNPs were determined by NTA (Nanosight NS500, UK). Approximately, 1 mL of 1:100 dilutions (in 18 MOhm water) of the sample was prepared, vortexed (Model:VM-1000, Taiwan) for 30 sec, and sonicated (SONICLEAN, England) for 20 min prior analyses. Measurements were conducted at 25˚C at 24 V and images were captured and analyzed using the NTA version 3.2 analytical software.

7.2.6 Biological assessment of synthesized AgNPs

7.2.6.1 Sample preparation

Stock solutions of the latex extract synthesized AgNPs using latex were prepared by resuspending 1 mg of the dried AgNP powder in 1 mL of sterile distilled water. The various stock solutions (1 mg/mL) for the respective treatments were homogenized using a vortex (Model:VM-1000, Taiwan). Thereafter, stock solutions of each solution were reconstituted in distilled water to provide concentrations ranging from 3.125, 6.25,12.5, 25, 50, to 100 mg/mL.

7.2.7.2 Antibacterial screening

Various concentrations of the synthesized AgNPs using latex extracts were screened for antibacterial activity against three gram-positive bacterial strains *Bacillus subtilis* (ATCC 6653), *Methicillin-resistant Staphylococcus aureus* (MRSA) (ATCC 43300), *Staphylococcus aureus* (ATCC 29213), and two gram-negative bacterial strains *Escherichia coli* (ATCC 25922) and *Pseudomonas aeruginosa* (ATCC 27853).

In vitro antibacterial screening of latex, AgNPs samples were conducted using the agar disc diffusion technique as per the Clinical and Laboratory Standards Institute (CLSI), (2006). Sterile Whatman filter paper No. 1 discs (diameter 6 mm) were prepared and impregnated with 20 µL of the respective AgNPs concentrations (3.125, 6.25,12.5, 25, 50,100 mg/mL) and dried at room temperature for 1 h before use (Marathe et al., 2013). Bacterial strains were aseptically cultured at 37˚C overnight on Mueller- Hinton (MH) agar media (Biolab, Merck). After 18-24 h a loopful of bacteria were resuspended in test tubes containing autoclaved (Model: HL-340, Temp.: 121-132˚C, Pres.: 127 kg/cm^2, Taiwan) distilled water and vortexed (Model:VM-1000, Taiwan) for 5 min to ensure the solutions were standardized. The optical density (OD) of the bacterial strains equivalent to 0.5 McFarland turbidity standard (OD 0.08-0.1 at λ 625 nm) was determined using a UV-vis spectrophotometer (Agilent Technologies Cary 60 spectrophotometer, USA). The desired OD was obtained by further dilution of the inoculum with additional sterile water.

Sterile cotton swabs were used to streak (four quadrants) the inoculum over the entire surface of the agar. The prepared discs containing latex AgNPs samples were carefully placed onto the agar using sterile forceps. The plates were incubated at 37˚C, and after 18-24 h, the zones of growth inhibition were examined to determine the antibacterial activity of the AgNPs using latex extracts. The screening was done in triplicates and streptomycin (gram-positive), and gentamicin (gram-negative) was used as the standard antibacterial positive controls, and sterile distilled water was used as the negative control. The $AgNO_3$ solution (1mM) was also tested. The zones of inhibition were measured (mm), recorded, and averaged, and images of the plates were captured. The following criteria was used to assess the zone of inhibition or resistance to synthesized AgNPs, No activity = (0 mm); Slight activity = (1-6 mm); Moderate activity = (>7 or <9 mm); Significant activity = (>9mm). R = Resistant.

7.2.7 MTT cytotoxicity assay

Three human cell lines viz., embryonic kidney (HEK293), breast adenocarcinoma (MCF-7), and cervical carcinoma (HeLa) were procured from the ATCC, Manassas, USA. All three cell lines were grown to confluency in 25 cm^2 tissue culture flasks using Eagle's Minimum Essential Medium (EMEM) containing 10% (*v*/*v*) gamma-irradiated FBS and 1% antibiotics (100 units/mL penicillin, 100 µg/mL streptomycin) in a HEPA Class 100 Steri-Cult CO_2 incubator (Thermo-electron Corporation, USA), at 37˚C in 5% CO_2. Upon confluency, the cells were trypsinized and seeded into clear 96-well plates and incubated at 37°C overnight to allow for cell adhesion. The cells were prepared by replenishing the growth medium with a fresh complete medium (EMEM + 10% FBS + 1% antibiotics). Thereafter, approximately 100 µL of the various concentrations of latex AgNP samples (15, 30, 60, 120 to 240 µg/mL) were added to the cells and incubated for 37˚C for 48 h. Control cells only (without treatment) were used as the positive control (*c.a* 100% viability). All assays were conducted in triplicates.

The methods briefly described by Mosmann (1983) and Daniels and Singh (2019), were used to evaluate the cytotoxic potential activity of the latex synthesized AgNPS on the three cell lines. Following 48 h of incubation at 37˚C, the growth medium was aspirated and replaced with 100 µL of medium containing 10 µL of MTT solution (5 mg/mL in PBS), and the cells containing the treatment and negative control were incubated for a further 4 h at 37˚C in 5% CO_2. The medium-MTT mixture was then removed and replaced with 100 µL dimethylsulphoxide (DMSO). The absorbances were then measured at 570 nm using a Mindray MR-96A microplate reader (Vacutec, Germany). Graphs were used to determine the concentration at which 50% cell growth inhibition (IC_{50}) occurred. The viability of the cell lines was directly related to the absorbance. Percentage cell survival was calculated following by following this equation .

$$\% \text{ cell survival} = \frac{(\text{Average optical density of control cells only})}{\text{Average optical density of treated cells}} \times 100 \quad \textbf{(7.2)}$$

7.2.8 Statistical analyses

The results were presented as means ± standard deviation, (n = 3). Statistical analyses were performed using R Statistical computing software of the R Core Team, 2020, version 3.6.3, followed by Tukey's honest significant difference range *post hoc* tests (**P* <0.05; ***P* <0.01). Graphs were generated using Microsoft Excel, 2019.

7.3 Results and Discussion

7.3.1 Visual inspection, UV-visible spectroscopy, and quantification of synthesized AgNPs

The synthesis of AgNPs using 1% latex extract was indicated by a slight colour change. Initially, the mixture (1% latex + $AgNO_3$) appeared white (Figure 7.1 A) however, following the incubation period, a light greyish colour was observed (Figure 7.1 B). Rathnayake et al. (2013), reported a similar colour change for the green synthesis of AgNPs inside centrifuged natural rubber latex. These visible colour changes are usually related to the reduction of silver (Ag) ions by the capping of biomolecules present within the respective extracts (Chandrasekaran et al., 2016; Rajkuberan et al., 2017). Moreover, literature has often associated a rapid and extreme colour change with the production of AgNPs however, this may vary based on several factors such as plant organ type, solvent/extract, concentration, duration of incubation, and presence of reducing agents (Kumar at al., 2010; Lee et al., 2020). Moreover, according to studies, it appears that the concentration (%) of the latex largely influences the production of AgNPs, since Bar et al. (2009) reported that 2% latex solution was insufficient for AgNPs synthesis compared to a 3% latex solution which displayed optimal results during the green synthesis.

Coupled with the visual assessment, the formation, distribution, and stability of the synthesized AgNPs using latex was further confirmed using UV-visible spectroscopy. The analysis showed prominent silver surface plasmon resonance (SPR) bands at 410 nm with an absorbance of 0.947 (Figure 7.2). The wavelength of the AgNPs fell within the accepted range, which is often detected between 400 nm and 460 nm (Zargar, 2011). Similarly, Chandrasekaran et al. (2016), displayed broad SPR peaks at 410 nm due to the collective oscillations of electrons however, the absorbances were much higher possibly related to the longer reaction times (72 h).

The yield of synthesized AgNPs using latex extracts amounted to 14.80%, which is a moderate quantity of AgNPs (Table 7.1). It was noted that several studies used higher concentrations of latex, increased temperature, and incubation times, and most importantly, each latex bearing species contained a variable chemical composition comparable to the current study (Bar et al., 2009; Akula et al., 2011; Sigamoney et al., 2016; Hu and Hsieh, 2016; Almeida et al., 2019; Akwu et al., 2021). Several of the above-mentioned variables may likely influence the quantification of AgNPs.

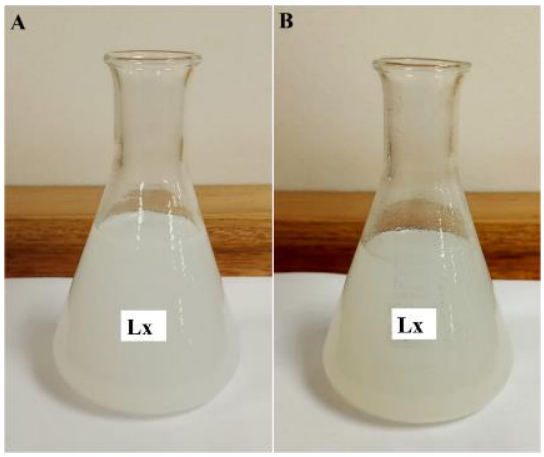

Figure 7.1: (A) Visual representation of latex extract + $AgNO_3$ prior Ag nanoparticle synthesis (incubation); (B) Synthesised Ag nanoparticles using latex extracts after incubation with $AgNO_3$ for 3 h at 80˚C.

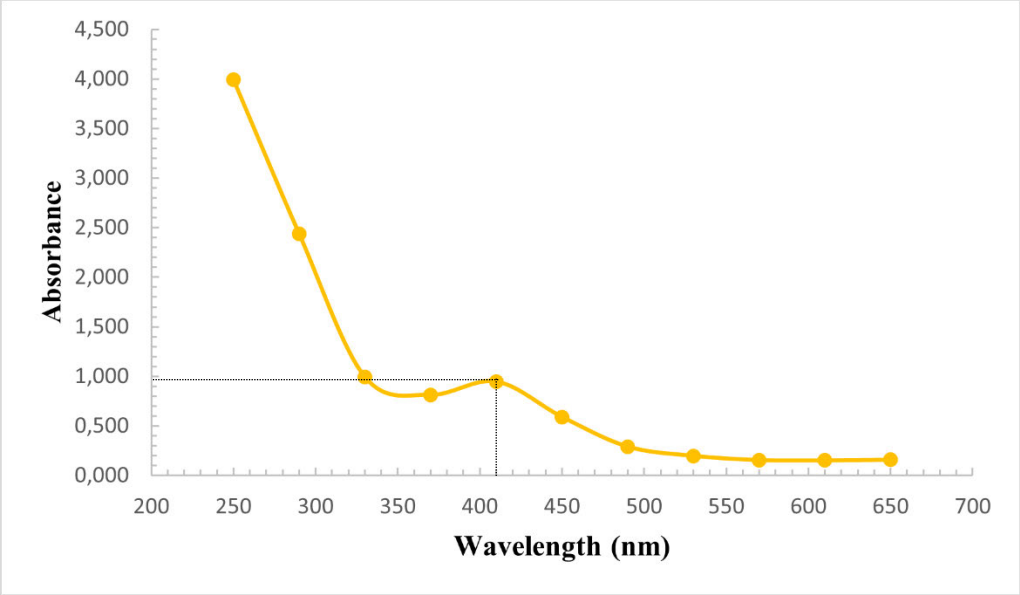

Figure 7.2: UV-vis spectra of AgNPs synthesized using latex extracts of *T. ventricosa.*

Table 7.1: Percentage yield of the synthesized AgNPs using latex extracts from *T. ventricosa.*

Extract	**Latex**
Dried extract yield (g)	0.15
Yield (%)	14.80

7.3.2 Scanning Electron Microscopy (SEM) and Energy-Dispersive X-ray (EDX) analysis

Scanning Electron Microscopy is often employed to deduce the size and morphology of NPs, whereas the detection, confirmation, and composition of AgNPs are conducted using EDX analysis (Sathishkumar et al., 2009; Patil et al., 2012; Borase et al., 2013). The SEM analysis in the present study revealed that AgNPs produced using latex extracts from *T. ventricosa* appeared <100 nm in size, mostly spherical and extremely agglomerated as displayed in Figure 7.3 A. These results are consistent with Borase et al. (2013). In their study *Ficus carica* latex extracts were similarly used to produce AgNPs, which were mainly spherical, and ranged from 50 to 200 nm, however, no occurrences of agglomeration were noted (Borase et al., 2013). The various types of microscopy (SEM vs ESEM) and the sample preparation techniques before SEM analyses differ, which may account for these observable differences. Moreover, additional reports have shown that the variation in agglomeration may be dependent upon several other aspects such as variations in reaction temperature, extract concentration, and $AgNO_3$ concentration (Song et al., 2009; Yaqoob et al., 2020). Furthermore, Durgawale et al. (2015), observed that the various interactions between hydrogen bonds and electrostatic forces of the bio-organic capping molecules may also influence the accumulation of smaller particle sizes, thus leading to an increased agglomeration of AgNPs.

The elemental analysis (Figure 7.3 B) indicated the presence of elemental Ag in AgNPs synthesized using latex. The EDX spectra showed a moderate Ag peak at 3 KeV (Figure 7.3 B), which is often associated with the optical absorption peaks of surface plasmon resonance for Ag (Bar et al., 2009; Magudapathy et al., 2001). Furthermore, these AgNPs displayed a percentage of elemental Ag of 3.89 ± 0.16% (Figure 7.3). Although the composition of elemental Ag does not appear high, the EDX analysis does confirm adequate Ag production. It has been proposed by several researchers, that the observable differences in the percentage composition of AgNPs are primarily affected by the chemical composition of the bioactive compounds of various extracts (Kumar et al., 2010; Sigamoney et al., 2016; Yaqoob et al., 2020). Furthermore, it is apparent that the lower concentration of latex (1%) used in the current study may be a contributing factor, since other studies have used higher concentrations of latex for the synthesis of AgNPs (Salem et al., 2014; Almeida et al., 2019; Kalaiselvi et al., 2019). Salem et al. (2014), utilized 3% latex solutions from *Ficus sycomorus* for the synthesis of AgNPs, and their results revealed a yield of 98.49%, which was significantly larger compared to the current study. The occurrences of other elemental signals such as oxygen (O_2), sodium (Na), potassium (K), and various other elements (Figure 7.3 B), are possibly due to the presence of several enzymes and proteins detected within the latex of *T. ventricosa* (Bar et al., 2009; Song et al., 2009; Salem et al., 2014; Sigamoney et al., 2016).

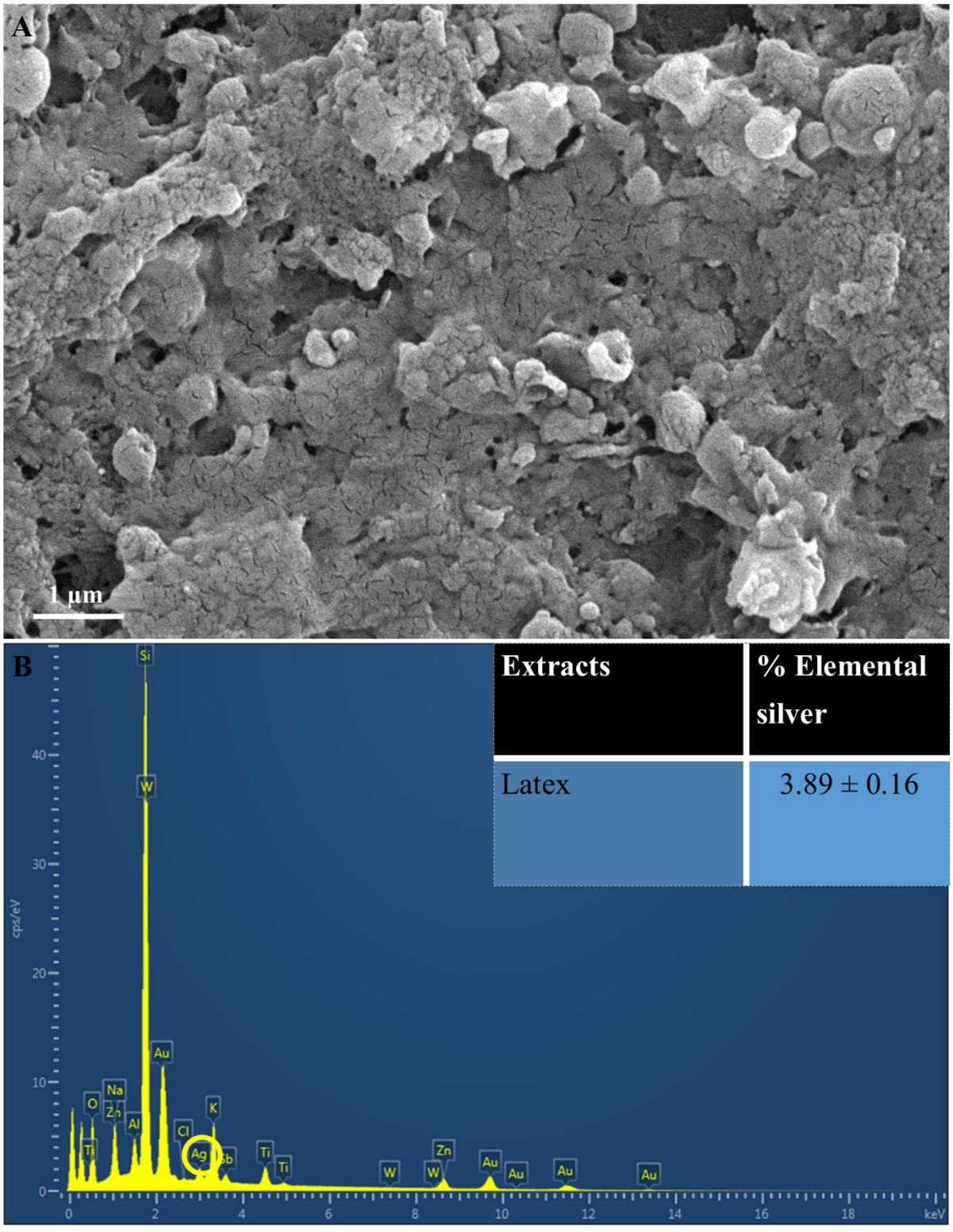

Figure 7.3: (A) Scanning Electron Microscopy images of AgNPs synthesized using latex extracts of *T. ventricosa*. Distinctive agglomeration within the image. (B) An EDX spectra and average elemental composition (%) of Ag in latex extracts. Circle indicated Ag.

7.3.3 High-Resolution Transmission Electron Microscopy (HRTEM)

The HRTEM images of AgNPs synthesized using latex extracts of *T. ventricosa* are displayed in Figure 7.4 A, whereas the particle size distribution is shown in Figure 7.4 B. The morphological distribution of the AgNPs is highlighted in Figure 7.4 A, reveals the absence of agglomeration, which is indicative that the synthesized AgNPs had good stability and were well dispersed (monodispersed) in the solution (Annadurai et al., 2012; Devaraj et al., 2014; Almeida et al., 2019). The thin matrix layer observed around the NPs is most likely due to the presence of biomolecules from *T. ventricosa* latex during the synthesis of the AgNPs, which provided further stability and prevented the formation of aggregates in the solution (Mittal et al., 2013; Chandrasekaran et al., 2016). The particles appeared spherical and ovate and some triangular (Figure 7.4 A). According to Bakar et al. (2007), characteristic features of natural rubber AgNPs are comprised of spherical to ovate shapes. However, Duragawale et al. (2015), investigated the AgNPs using latex of *Syandenium grantii* Hook F. and reported various morphologies of NPs such as spherical triangles, truncate triangles, and decahedral shapes. Many researchers have observed that NPs synthesized using latex extracts are often spherical (Raheman et al., 2011; Banu and Rathod, 2011; Mohamed et al., 2014; Mohamed et al., 2019). The HRTEM analysis in the present study (Figure 7.4 A) is consistent with these reports.

The diameter of the AgNPs ranged from 5 nm to 17.50 nm, with an average particle diameter of 11.68 ± 3.96 nm (Figure 7.4 B). It is apparent, that two broad size distribution of the particles are present, with one displaying smaller diameters ranging from 5 nm to 7.50 nm, whereas the other particles with larger diameters, ranges from 15 nm to 17.50 nm. This has also been observed by Bar et al. (2009) however, in their study, the presence of these broad peaks was associated with UV-vis spectra analyses which displayed two Ag peaks (425 nm and 464 nm), unlike the present study where only one Ag peak was observed at 410 nm. However, the differences in the composition and concentration of extracts may be accountable for these variations (Devaraj et al., 2014; Salem et al., 2014; Almeida et al., 2019; Kalaiselvi et al., 2019). Despite, these differences, the diameters of the AgNPs observed in the present study, are similar to those of Bar et al. (2009), Guidelli et al. (2011), and Almeida et al. (2019).

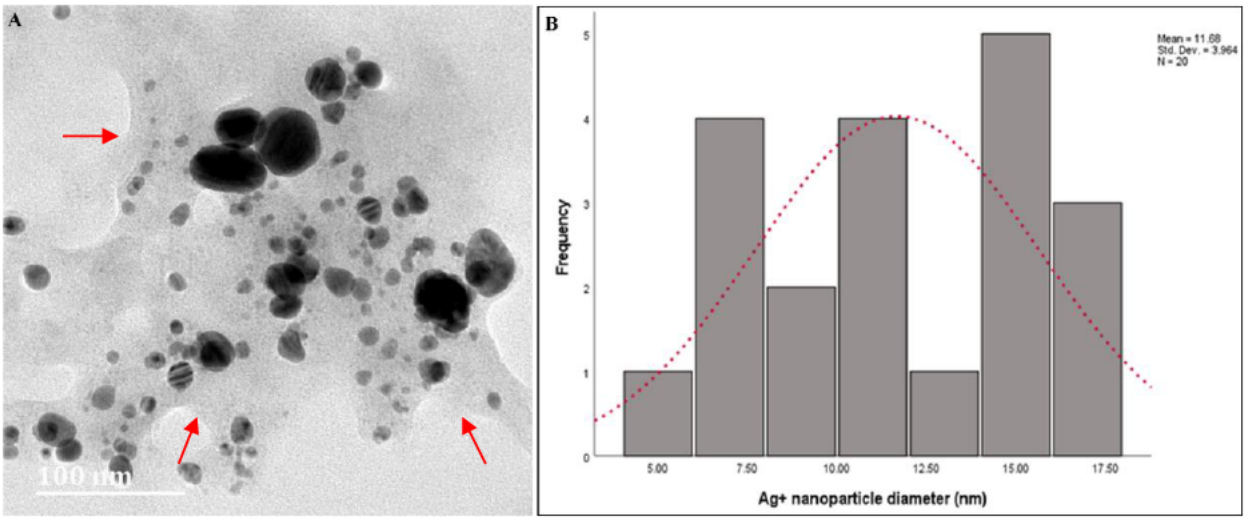

Figure 7.4: (A) High-Resolution Transmission Electron Microscopy micrographs of AgNPs synthesized using latex extracts from *T. ventricosa*. Arrows indicate film surrounding NPs. (B) Particle size (nm) of AgNPs synthesized using latex extracts from *T. ventricosa*. n = 20.

7.3.4 Nanoparticle Tracking Analysis (NTA) and zeta potential

The NTA analysis (Appendix 3A) revealed an average diameter of 57.2 ± 57.2 nm for AgNPs synthesized using latex extracts (Table 7.2). Although this value may seem large, it is relatively smaller in comparison to studies where the size of particles ranged from 32 nm to 220 nm in diameter (Patil et al., 2012; Borase et al., 2013). Furthermore, it was observed that the average diameter of particles observed using NTA analysis was much larger in comparison to HRTEM studies. It is suggested that the various techniques involved before or during analyses may influence the particle size differently. The measurement of particle size using NTA analyses in a hydrodynamic environment is often preferred, since it is closely associated with an *in vivo* system, unlike HRTEM samples which are in a dehydrated or powdered state (Akinyelu and Singh, 2019; Oladimeji et al., 2021).

The zeta potential value is often used to measure the surface charges of particles to ensure their stability within colloidal solutions (Borase et al., 2013). The zeta potential value herein was low (12.3 ± 12.3 mV); with the preferred range being greater than 25 mV or less than -30 mV (Daniels and Singh, 2019). These results indicated that the latex AgNPs of *T. ventricosa* displayed poor stability, low mobility, and reduced electrostatic repulsion. Borase et al. (2013), observed a zeta potential of -19.3 mV, thus suggesting moderate stability of the NPs, whereas Patil et al. (2012), revealed a zeta potential of -25. 2 mV. Kumar and Yadav (2009), suggested that proteins, polyphenols, and carbohydrates largely influence the synthesis of NPs, which may affect the zeta potential.

Table 7.2: Average nanoparticle diameter (nm) and zeta potential (mV) of the synthesized AgNPs using latex extracts of *T. ventricosa*.

Extracts	Nanoparticle diameter (nm)	Zeta potential (mV)
Fresh latex extract	57.2 ± 57.2	12.3 ± 12.3

Mean ± standard error (n=3).

7.3.5 Fourier Transform Infrared (FTIR) spectroscopy

Fourier transform infrared spectroscopy measurements were calculated for AgNPs synthesized from *T. ventricosa* latex extracts to examine the interactions between the biomolecules (capping agents) within the sample extract and the synthesized NPs. The spectral assignments of AgNPs using latex extracts are displayed in Table 7.3, whereas the absorption peaks displaying various stretching and bending are shown in Figure 7.5.

Table 7.3: FTIR spectral assignments of synthesized AgNPs using latex extracts of *T. ventricosa*.

Absorption Frequency (cm^{-1})	Types of absorption/ vibration	Appearance	Interference/ functional group	Compound class
3338.07	Stretch	Strong broad	O–H	Alcohol
3283.60	Stretch	Strong broad	O–H	Alcohol
2924.93	Stretch	Medium	C–H	Alkane
2330.92	Stretch	Strong	O=C=O	Carbon dioxide
2116.69	Stretch	Weak	C≡C	Alkyne
2087.22	Stretch	Strong	N=C=S	Isothiocyanate
1892.32	Bending	Weak	C–H	Aromatic compound
1732.58	Stretch	Strong	C=O	Aldehyde
1634.27	Bending	Medium	C=C	Alkene
1539.09	Stretch	Strong	N–O	Nitro compound
1361.45	Bending	Medium	O–H	Phenol
1336.41	Stretch	Strong	S=O	Sulfonate
1242.12	Stretch	Strong	C–O	Alkyl aryl ether
1147.68	Stretch	Strong	C–O	Tertiary alcohol
1095.34	Stretch	Strong	C–O	Secondary alcohol
1024.62	Stretch	Medium	C–N	Amine
823.30	Bending	Strong	C–H	1,2,3-trisubstituted

Prominent peaks located at 3338.07 cm^{-1} and 3283.60 cm^{-1} are assigned to alcohols (Barker et al., 2007; Fatima et al., 2020). Whereas peaks 2924.93 cm^{-1}, 2330.92 cm^{-1}, and 2116.69 cm^{-1} were due to alkanes, carbon dioxide, and alkynes, respectively (Kalaselvi et al., 2019; Fatima et al., 2020). Remarkably, the compound classes isothiocyanate (N=C=S) and aromatic compounds (C–H) were linked to the peaks 2087.22 cm^{-1} and 1892.32 cm^{-1} (Devaraj et al., 2014; Preetam et al., 2016). While strong stretching of C=O groups and medium bending of C=O groups assigned to aldehydes and alkenes were associated with peaks 1732.58 cm^{-1} and 1634.27 cm^{-1} respectively (Barker et al., 2007). Peaks 1539.09 cm^{-1}, 1361.45 cm^{-1}, 1336.41 cm^{-1} arise due to strong and medium bending and stretching of nitro compounds, phenols, and sulfonates (Borase et al., 2013; Fatima et al., 2020). Strong C–O stretching of peaks 1242.12 cm^{-1}, 1147.68 cm^{-1}, 1095.34 cm^{-1} were assigned to alkyl aryl ether, tertiary alcohols, and secondary alcohols, while peaks 1024.62 cm^{-1} and 823.30 cm^{-1} was due to the presence of amines (proteins/enzymes) and 1,2,3-trisubstituted compounds (Fatima et al., 2020; Attri et al., 2021). These results confirm the presence of several functional groups present in the latex extracts and indicate that the proteins, enzymes, and other biomolecules detected within the latex allow for the capping, reduction, and functionalization of AgNPs (Durgawale et al., 2015; Chandrasekaran et al., 2016).

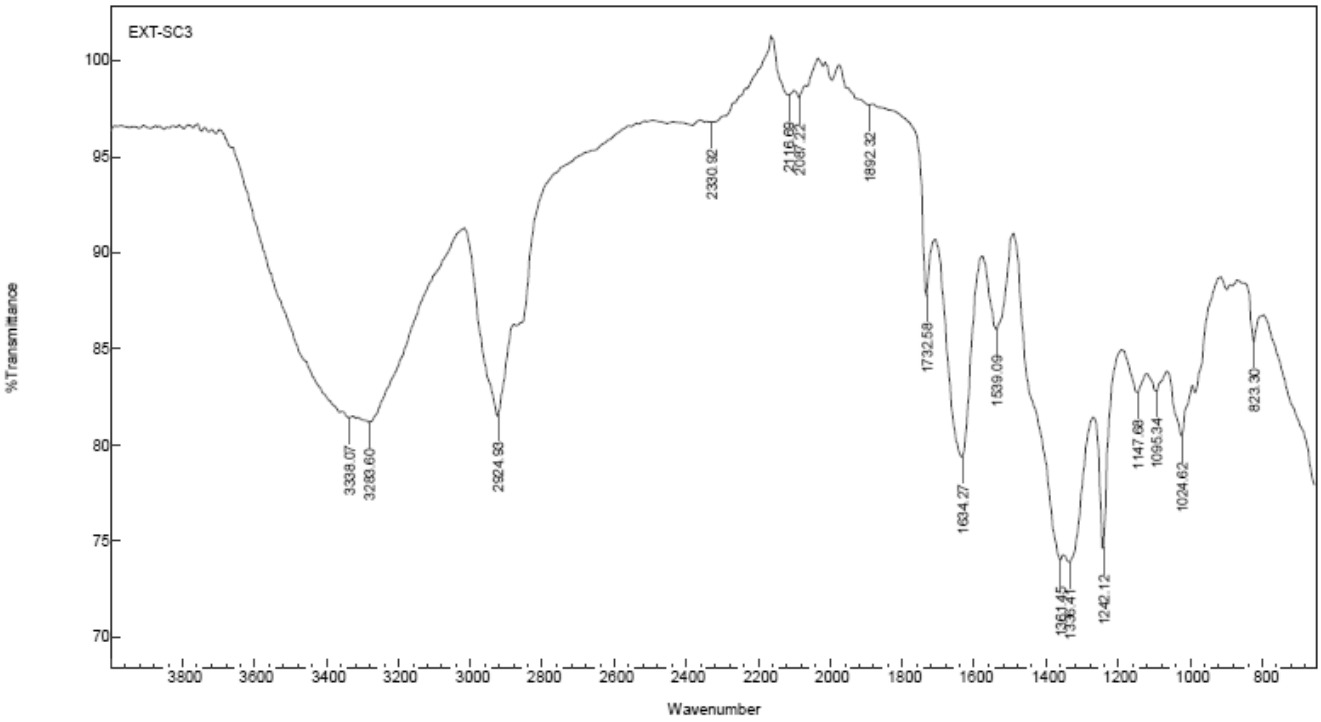

Figure 7.5: The FTIR spectra of AgNPs synthesized using latex extracts of *T. ventricosa*.

7.3.6 Antibacterial assay

The latex of several medicinal plants has often been utilized due to their antibacterial activities (de Matos et al., 2011; Borase et al., 2013; Kalaiselvi et al., 2019), coupled with the antibacterial properties of NPs we would expect remarkable antibacterial activity for these synthesized AgNPs using latex. Chandrasekaran et al. (2016), investigated the efficiency of AgNPs using latex from *Carica papaya*, which showed significant activity against *B. subtilis, Enterococcus faecalis, E. coli, Vibrio cholerae, Klebsiella pneumoniae, and Proteus mirabilis*. However, despite these significant results, there appears to be a lack of interest surrounding the synthesis and antibacterial applications of AgNPs synthesized using latex extracts. Thus, one of the aims of the present study was to evaluate the antibacterial activity of latex AgNPs using agar disk diffusion (Appendix 2B). The antibacterial activity of latex AgNPs was assessed against five pathogenic bacterial strains, three gram-positive: *B. subtilis* (ATCC 6653), MRSA (ATCC 43300), *S. aureus* (ATCC 29213), and two gram-negative bacterial strains: *E. coli* (ATCC 25922) and *P. aeruginosa* (ATCC 27853), using a range of concentrations (3.125 to 100 mg/mL) (Table 7.4).

The results displayed in Table 7.4 revealed that at the lowest concentrations (3.125 mg/mL) AgNPs synthesized using latex extracts displayed moderate antibacterial activity against MRSA (9.67 ± 0.58 mm), *S. aureus* (9.00 ± 1.00 mm), *E. coli* (8.67 ± 0.58 mm), *P. aeruginosa* (8.67 ± 1.15 mm) and *B. subtilis* (6.33 ± 0.58 mm), respectively. Whereas, at higher concentrations (100 mg/mL), substantial antibacterial activity was observed against *E. coli* (12.67 ± 1.15 mm), *S. aureus* (11.67 ± 0.58 mm), MRSA (11.33 ± 0.58 mm), *P. aeruginosa* (11.33 ± 0.58 mm), and *B. subtilis* (9.33 ± 0.58 mm), respectively. It was noted that the increased concentrations of latex AgNPs influenced the zones of inhibition (inhibition of bacterial growth) progressively, similar results were reported by Chandrasekaran et al. (2016). Furthermore, the results showed a substantial difference between the inhibition of bacterial growth using antibiotics which was much lower and ranged from 10.00 ± 1.00 mm to 10.67 ± 1.15 mm compared to the AgNPs synthesized using latex, which ranged from 10.33 ± 0.58 mm to 12.67 ± 1.15 mm, at the highest concentration (100 mg/mL). Overall, significant differences were noted ($P < 0.05$) for bacterial strains *E. coli*, MRSA, and *S. aureus* vs. *B. subtilis*, and all latex AgNPs concentrations except 12.5 and 25 mg/mL.

Previous reports have indicated that gram-positive bacteria are usually more resistant to AgNPs due to the presence of a peptidoglycan layer that often acts as a preventive barrier for NP entry (Chandrasekaran et al., 2016), compared to gram-negative bacteria which lacks this special layer and contains a negatively charged surface area which attracts Ag ions, thus are more susceptible to cell membrane damage by AgNPs (Shrivastava et al., 2007). Similar results were observed in the present study only for the gram-negative bacteria *E. coli*, and gram-positive bacteria *B. subtilis* and MRSA, whereas the other bacterial strains were not consistent with previous studies (Shrivastava et al., 2007; Chandrasekaran et al., 2016). Moreover, it was revealed that the properties of AgNPs can penetrate the cell wall of bacterial cells, thus causing damage/ destabilization of the outer membrane, which causes a cascade of denaturation events followed by inadequate bacterial respiration, reduced intracellular ATP, and eventually cell death (Vivekanandhan et al., 2011; Chandrasekaran et al., 2016; Raja et al., 2018; Attri et al., 2021).

Table 7.4: Zones of inhibition (mm) of synthesized AgNPs using latex extracts of *T. ventricosa* against gram-positive and gram-negative bacterial strains.

Concentration (mg/mL)		**Bacterial strains**				
		BS	**EC**	**MRSA**	**SA**	**PA**
Latex AgNPs	**3.125**	6.33 ± 0.58	8.67 ± 0.58	9.67 ± 0.58	9.00 ± 1.00	8.67 ± 1.15
	6.25	7.00 ± 0.00	9.00 ± 1.00	10.33 ± 0.58	10.00 ± 1.00	9.00 ± 1.00
	12.5	8.67 ± 0.58	10.67 ± 1.15	10.67 ± 1.15	10.33 ± 0.58	9.33 ± 1.15
	25	8.67 ± 0.58	11.00 ± 0.00	11.00 ± 1.00	10.67 ± 0.58	10.67 ± 0.58
	50	9.33 ± 0.58	12.33 ± 0.58	11.00 ± 1.00	11.33 ± 0.58	11.33 ± 0.58
	100	10.33 ± 0.58	12.67 ± 1.15	11.33 ± 0.58	11.67 ± 0.58	11.33 ± 1.15
Positive control (10 ug/mL)		**9.67 ± 1.53***	**9.67 ± 0.58**	**9.33 ± 1.53***	**10.67 ± 1.15***	**9.00 ± 1.00**

No activity = (**0 mm**); Slight activity = (**1-6 mm**); Moderate activity = (**>7 or <9 mm**); Significant activity = (**>9mm**). **R**= Resistant, **BS** = *Bacillus subtilis* (ATCC 6653), **EC** = *Escherichia coli* (ATCC 25922), **MRSA** = *Methicillin Resistant Staphylococcus aureus* (ATCC 43300), **SA** = *Staphylococcus aureus* (ATCC 29213), **PA** = *Pseudomonas aeruginosa* (ATCC 27853), Positive controls (Gentamicin 10 µg/mL, Streptomycin 10 µg/mL*) and (n = 3).

7.3.7 Cytotoxicity assay

Over the years researchers have examined the cytotoxic effects of AgNPs using various plant extracts and discovered that "Green" synthesized particles exhibited inhibitory effects at low concentrations, thus considering them safe in a variety of applications (Mohamed et al., 2014; Rajkuberan et al., 2015; Hassan et al., 2017). In the present study, the cytotoxicity of the AgNPs using latex extracts of *T. ventricosa* was evaluated in three human cell lines, HEK293 (embryonic kidney), MCF-7 (breast adenocarcinoma), and HeLa (cervical carcinoma). For the MTT cell viability assay (Mosmann, 1983), various concentrations of the AgNPs ranging from 15, 30, 60, 120 to 240 µg/mL were tested.

As observed in Figure 7.6, in the positive control 1 (cells only) and control 2 (cells + 0.1% DMSO) a reduction in viability (72.56%-93.12%) was noted whereas the percentage cell survival of all cell lines was significantly reduced by biosynthesized AgNPs. As the concentration of the AgNPs increased (15, 30, 60, 120, 240 µg/mL), the percentage of cell survival in all cell lines gradually decreased, suggesting a dose-dependent relationship. Likewise, Rajkuberan et al. (2017), investigated the AgNPs using latex extracts of *Euphorbia antiquorum* L, and further assessed the *in vitro* cytotoxicity of the AgNPs which similarly showed increasing anticancer activity against HeLa cells at increased concentrations. Furthermore, the results of the present study noted that at the lowest concentrations (15 µg/mL), HeLa, MCF-7, and HEK293 cells displayed moderate cytotoxicity, with HeLa cells (46.19%) displaying the most sensitivity (lowest cell survival), followed by MCF-7 (51.61%) and HEK293 (59.69%). Whereas, at the highest concentration (240 µg/mL), it was apparent that HeLa cells were once again most sensitive displaying significant cytotoxicity, with cell viabilities of 2.40%, followed by HEK293 (5.13%) and MCF (12.48%). Moreover, significant differences were observed for the cytotoxic analyses of latex AgNPs for all concentrations within each cell line ($P < 0.05$).

The IC_{50} values of latex AgNPs tested in HEK293, HeLa and MCF-7 were 13.70 µg/mL, 10.52 µg/mL, and 20.60 µg/mL, respectively (Table 7.5). All IC_{50} values were suggestive of noteworthy cytotoxic activity ($IC_{50} < 50$). Across all cell lines, the most significant IC_{50} was observed for the HeLa cells. Similarly, Rajkuberan et al. (2017), observed a substantial IC_{50} value (28 µg/mL) of AgNPs synthesized using *Euphorbia antiquorum* latex in the HeLa cell lines. Another report by Rajkuberan et al. (2015), evaluated the biosynthesized AgNPS using *Calotropis gigantea* latex against HeLa cell lines which displayed a moderate IC_{50} of 91.30 µg/mL. These variations in the observed IC_{50} values of AgNPs synthesized using latex, are possibly due to the presence of different capping compounds such as proteins and enzymes within the latex extracts (Durgawale et al., 2015; Chandrasekaran et al., 2016; Rajkuberan et al., 2017).

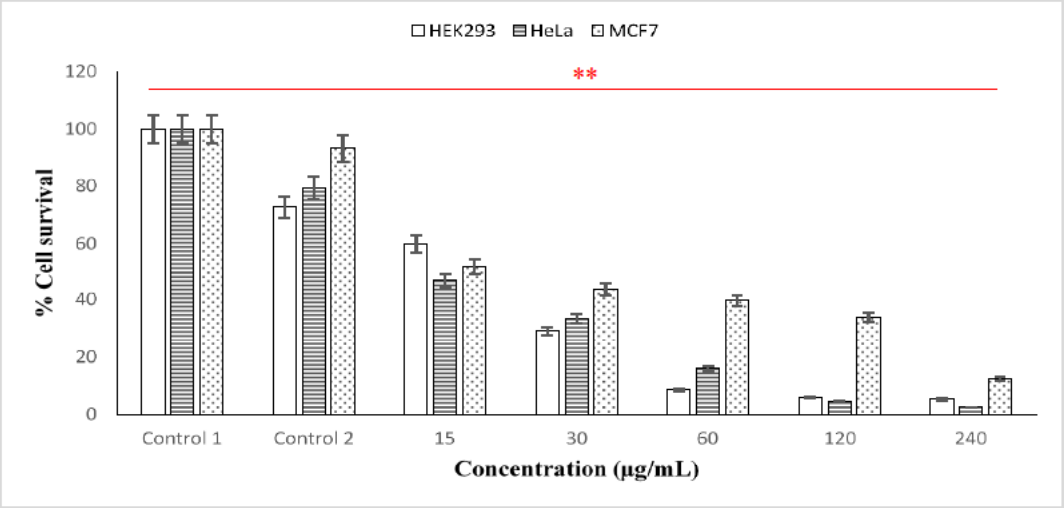

Figure 7.6: *In vitro* cytotoxicity activity of synthesised AgNPs using latex extracts from *T. ventricosa*. Control 1 = cells only; Control 2 = cells + DMSO. Percentage cell survival of HEK293; MCF-7 and HeLa cell lines. *P <0.05 and ** P <0.01 are considered significant.

Table 7.5: IC_{50} values of the cytotoxic activity of the AgNPs synthesized from the fresh latex extracts of *T. ventricosa*.

Extract	Cell lines		
	HEK293	HeLa	MCF-7
	Concentration µg/mL		
Latex	13.70	10.52	20.60

7.4 Conclusion

This study presented an efficient biological synthesis of AgNPs using latex extracts from *T. ventricosa*. During the characterization of synthesized AgNPs using latex, a pale colour change was observed, with prominent Ag peaks visible during UV-SPEC and EDX analyses. Furthermore, spherical, ovate, and triangular-shaped latex AgNPs (<100 nm) were visible during SEM and HRTEM studies. The FTIR results detected various functional groups within latex AgNPs, such as alcohols, alkanes, amines, proteins, enzymes, and other biomolecules possibly responsible for the capping, reduction, and functionalization of AgNPs. The antibacterial and cytotoxic evaluation of AgNPs using the latex of *T. ventricosa* displayed significant activity thus suggestive of the potential importance of these AgNPS in biomedical applications. To the best of our knowledge, this is the first report of the effective synthesis, characterization, and antibacterial and cytotoxic evaluation of AgNPs using latex of *T. ventricosa*.

7.5 References

Akinyelu, J., Singh, M., 2019. Folate-tagged chitosan functionalized gold nanoparticles for enhanced delivery of 5-fluorouracil to cancer cells. Applied Nanoscience 9, 7–17.

Akula, R., Ravishankar, G.A., 2011. Influence of abiotic stress signals on secondary metabolites in plants. Plant Signal Behaviour 6, 1720–1731.

Akwu, N.A., Naidoo, Y., Singh, M., Nundkumar, N., Daniels, A., Lin, J., 2021. Two Temperatures Biogenic Synthesis of Silver Nanoparticles from *Grewia lasiocarpa* E. Mey. ex Harv. Leaf and Stem Bark Extracts: Characterization and Applications. BioNanoScience 11, 142–158.

Almeida, L.M., Magno, L.N., Pereira, A.C., Guidelli, É.J., Baffa Filho, O., Kinoshita, A., Goncalves, P.J., 2019. Toxicity of silver nanoparticles released by *Hancornia speciosa* (*Mangabeira*) Biomembrane. Spectrochimica Acta Part A: Molecular and Biomolecular Spectroscopy 210, 329–334.

Ambu, G., Chaudhary, R.P., Mariotti, M., Cornara, L., 2020. Traditional uses of medicinal plants by ethnic people in the Kavrepalanchok district, Central Nepal. Plants 9, 759.

Anbukkarasi, M., Thomas, P.A., Sheu, J.R., Geraldine, P., 2017. *In vitro* antioxidant and anticataractogenic potential of silver nanoparticles biosynthesized using an ethanolic extract of *Tabernaemontana divaricata* leaves. Biomedicine & Pharmacotherapy 91, 467–475.

Anbukkarasi, M., Thomas, P.A., Teresa, P.A., Anand, T., Geraldine, P., 2020. Comparison of the efficacy of a *Tabernaemontana divaricata* extract and of biosynthesized silver nanoparticles in preventing cataract formation in an *in-vivo* system of selenite-induced cataractogenesis. Biocatalysis and Agricultural Biotechnology 23, 101475.

Andima, M., Ndakala, A., Derese, S., Biswajyoti, S., Hussain, A., Yang, L.J., Akoth, O.E., Coghi, P., Pal, C., Heydenreich, M., Wong, V.K.W., 2021. Antileishmanial and cytotoxic activity of secondary metabolites from *Taberneamontana ventricosa* and two aloe species. Natural Product Research 1–5.

Annadurai, G., Gnanajobitha, G., Kannan, C., 2012. Green synthesis of silver nanoparticle using *Elettaria cardamomom* and assessment of its anti-microbial activity. International Journal of Pharmaceutical Sciences and Research 3, 323–30.

Attri, P., Garg, S., Ratan, J.K., Giri, A.S., 2021. Silver Nanoparticles from *Tabernaemontana Divaricate* leaf extract: Mechanism of action and Bio-application for photo degradation of 4-Aminopyridine. Research Square 1–31.

Bakar, N.A., Ismail, J., Bakar, M.A., 2007. Synthesis and characterization of silver nanoparticles in natural rubber. Materials Chemistry and Physics 104, 276–283.

Banu, A., Rathod, V., 2011. Synthesis and characterization of silver nanoparticles by *Rhizopus stolonier*. International Journal of Biomedical and Advance Research 2, 148–58.

Bar, H., Bhui, D. Kr, Sahoo, G.P., Sarkar, P., De, P.S., Misra, A., 2009. Green synthesis of silver nanoparticles using latex of *Jatropha curcas*. Colloids Surface. A Physicochemical and Engineering Aspects 339, 134–139.

Borase, H.P., Patil, C.D., Suryawanshi, R.K., Patil, S.V., 2013. *Ficus carica* latex-mediated synthesis of silver nanoparticles and its application as a chemophotoprotective agent. Applied Biochemistry and Biotechnology 171, 676–688.

Chandra, H., Kumari, P., Bontempi, E., Yadav, S., 2020. Medicinal plants: Treasure trove for green synthesis of metallic nanoparticles and their biomedical applications. Biocatalysis and Agricultural Biotechnology 24, 101518.

Chandrasekaran, R., Gnanasekar, S., Seetharaman, P., Keppanan, R., Arockiaswamy, W., Sivaperumal, S., 2016. Formulation of *Carica papaya* latex-functionalized silver nanoparticles for its improved antibacterial and anticancer applications. Journal of Molecular Liquids 219, 232–238.

Clinical and Laboratory Standards Institute (2006) Performance Standards for Antimicrobial Disk Susceptibility Tests, Approved standard-Ninth Edition (M2-A9). Wayne, PA: (CLSI) Philadelphia.

Daniels, A.N., Singh, M., 2019. Sterically stabilized siRNA: gold nanocomplexes enhance c-MYC silencing in a breast cancer cell model. Nanomedicine 14, 1387–1401.

de Matos, R.A., da Silva Cordeiro, T., Samad, R.E., Vieira Jr, N.D., Courrol, L.C., 2011. Green synthesis of stable silver nanoparticles using *Euphorbia milii* latex. Colloids and Surfaces A: Physicochemical and Engineering Aspects 389, 134–137.

Devaraj, P., Aarti, C., Kumari, P., 2014. Synthesis and characterization of silver nanoparticles using *Tabernaemontana divaricata* and its cytotoxic activity against MCF7 cell line. International Journal of Pharmacology and Pharmaceutical Science 6, 86–90.

Durgawale, P.P., Phatak, R.S., Hendre, A.S., 2015. Biosynthesis of silver nanoparticles using latex of *Syandenium grantii* Hook f and its assessment of antibacterial activities. Digest Journal of Nanomaterials and Biostructures 10, 847.

Fatima, K., Mahmud, S., Yasin, H., Asif, R., Qadeer, K., Ahmad, I., 2020. Authentication of various commercially available crude drugs using different quality control testing parameters. Pakistan Journal of Pharmaceutical Sciences 33, 1–17.

Guidelli, E.J., Ramos, A.P., Zaniquelli, M.E.D., Baffa, O., 2011. Green synthesis of colloidal silver nanoparticles using natural rubber latex extracted from *Hevea brasiliensis*. Spectrochimica Acta Part A: Molecular and Biomolecular Spectroscopy 82, 140–145.

Hassan, M.H., Ismail, M.A., Moharram, A.M., Shoreit, A.A., 2017. Phytochemical and antimicrobial of latex serum of *Calotropis procera* and its silver nanoparticles against some reference pathogenic strains. Journal of Ecology Health and Environment 5, 65–75.

Hu, S., Hsieh, Y.L., 2016. Silver nanoparticle synthesis using lignin as reducing and capping agents: A kinetic and mechanistic study. International Journal of Biological Macromolecules 82, 856–862.

Kalaiselvi, D., Mohankumar, A., Shanmugam, G., Nivitha, S., Sundararaj, P., 2019. Green synthesis of silver nanoparticles using latex extract of *Euphorbia tirucalli*: A novel approach for the management of root knot nematode, *Meloidogyne incognita*. Crop Protection 117, 108–114.

Kumar, V., Yadav, S.C., Yadav, S.K., 2010. *Syzygium cumini* leaf and seed extract mediated biosynthesis of silver nanoparticles and their characterization. Journal of Chemical Technology & Biotechnology 85, 1301–1309.

Kumar, V., Yadav, S.K., 2009. Plant-mediated synthesis of silver and gold nanoparticles and their applications. Journal of Chemical Technology & Biotechnology: International Research in Process, Environmental & Clean Technology 84, 151–157.

Lee, K.X., Shameli, K., Yew, Y.P., Teow, S.Y., Jahangirian, H., Rafiee-Moghaddam, R., Webster, T.J., 2020. Recent developments in the facile bio-synthesis of gold nanoparticles (AuNPs) and their biomedical applications. International Journal of Nanomedicine 15, 275.

Magudapathy, P., Gangopadhyay, P., Panigrahi, B.K., Nair, K.G.M., Dhara, S., 2001. Electrical transport studies of Ag nanoclusters embedded in glass matrix. Physica B*:* Condensed Matter 299, 142–146.

Manasa, D.J., Chandrashekar, K.R., Kumar, P., Suresh, D., Madhu Kumar, D.J., Ravikumar, C.R., Bhattacharya, T., Murthy, H.C., 2021. Proficient Synthesis of Zinc Oxide Nanoparticles from *Tabernaemontana Heyneana* Wall. Via Green Combustion Method: Antioxidant, Anti-Inflammatory, Antidiabetic, Anticancer and Photocatalytic Activities. Results in Chemistry 3, 100178.

Marathe, N., Rasane, M., Kumar, H., A Patwardhan, A., Shouche, Y.S., Diwanay, S.S., 2013. *In vitro* antibacterial activity of *Tabernaemontana alternifolia* (Roxb) stem bark aqueous extracts against clinical isolates of methicillin resistant *Staphylococcus aureus*. Annals of Clinical Microbiology and Antimicrobials 12, 26.

Masurkar, S.A., Chaudhari, P.R., Shidore, V.B., Kamble, S.P., 2011. Rapid biosynthesis of silver nanoparticles using *Cymbopogan citratus* (lemongrass) and its antimicrobial activity. Nano-Micro Letters 3, 189–194.

Mehrbod, P., Abdalla, M.A., Njoya, E.M., Ahmed, A.S., Fotouhi, F., Farahmand, B., Gado, D.A., Tabatabaian, M., Fasanmi, O.G., Eloff, J.N., McGaw, L.J., 2018. South African medicinal plant extracts active against influenza A virus. BMC Complementary and Alternative Medicine 18, 112–121.

Mittal, A.K., Chisti, Y., Banerjee, U.C., 2013. Synthesis of metallic nanoparticles using plant extracts. Biotechnological Advances 31, 346–356.

Mohamed, N.H., Ismail, M.A., Abdel-Mageed, W.M., Shoreit, A.A.M., 2014. Antimicrobial activity of latex silver nanoparticles using *Calotropis procera*. Asian Pacific Journal of Tropical Biomedicine 4, 876–883.

Mohamed, N.H., Ismail, M.A., Abdel-Mageed, W.M., Shoreit, A.A.M., 2019. Antimicrobial activity of green silver nanoparticles from endophytic fungi isolated from *Calotropis procera* (Ait) latex. Microbiology 165, 967–975.

Mosmann, T., 1983. Rapid colorimetric assay for cellular growth and survival: Application to proliferation and cytotoxicity assays. Journal of Immunological Methods 65, 55–63.

Oladimeji, O., Akinyelu, J., Daniels, A., Singh, M., 2021. Modified Gold Nanoparticles for efficient Delivery of Betulinic Acid to Cancer Cell Mitochondria. International Journal of Molecular Sciences 22, 5072.

Patil, C.D., Borase, H.P., Patil, S.V., Salunkhe, R.B., Salunke, B.K., 2012. Larvicidal activity of silver nanoparticles synthesized using *Pergularia daemia* plant latex against *Aedes aegypti* and *Anopheles stephensi* and nontarget fish *Poecillia reticulata*. Parasitology Research 111, 555–562.

Preetam Raj, J.P., Purushothaman, M., Ameer, K., Panicker, S.G., 2016. *In-vitro* anticancer and antioxidant activity of gold nanoparticles conjugate with *Tabernaemontana divaricata* flower SMs against MCF-7 breast cancer cells. Korean Chemical Engineering Research 54, 5–80.

Raheman, F., Deshmukh, S., Ingle, A., Gade, A., Rai, M., 2011. Silver nanoparticles: Novel antimicrobial agent synthesized from an endophytic fungus *Pestalotia* sp. isolated from leaves of *Syzygium cumini* (L). Nano Biomedicine and Engineering 3, 174–178.

Raja, A., Ashokkumar, S., Marthandam, R.P., Jayachandiran, J., Khatiwada, C.P., Kaviyarasu, K., Raman, R.G., Swaminathan, M., 2018. Eco-friendly preparation of zinc oxide nanoparticles using *Tabernaemontana divaricata* and its photocatalytic and antimicrobial activity. Journal of Photochemistry and Photobiology B: Biology 181, 53–58.

Rajkuberan, C., Prabukumar, S., Sathishkumar, G., Wilson, A., Ravindran, K., Sivaramakrishnan, S., 2017. Facile synthesis of silver nanoparticles using *Euphorbia antiquorum* L. latex extract and evaluation of their biomedical perspectives as anticancer agents. Journal of Saudi Chemical Society 21, 911–919.

Rajkuberan, C., Sudha, K., Sathishkumar, G., Sivaramakrishnan, S., 2015. Antibacterial and cytotoxic potential of silver nanoparticles synthesized using latex of *Calotropis gigantea* L. Spectrochimica Acta Part A: Molecular and Biomolecular Spectroscopy 136, 924–930.

Rathnayake, I., Ismail, H., Azahari, B., De Silva, C., Darsanasiri, N., 2014. Imparting antimicrobial properties to natural rubber latex foam via green synthesized silver nanoparticles. Journal of Applied Polymer Science 131, 1–10.

Salem, W.M., Haridy, M., Sayed, W.F., Hassan, N.H., 2014. Antibacterial activity of silver nanoparticles synthesized from latex and leaf extract of *Ficus sycomorus*. Industrial Crops and Products 62, 228–234.

Sathishkumar, M., Sneha, K., Won, S.W., Cho, C.W., Kim, S., Yun, Y.S., 2009. *Cinnamon zeylanicum* bark extract and powder mediated green synthesis of nano-crystalline silver particles and its bactericidal activity. Colloids and Surfaces B: Biointerfaces 73, 332–338.

Schmelzer, G.B., Gurib-Fakim, A., 2008. Medicinal Plants, first ed. Plant Resources of Tropical Africa 11,1. PROTA Foundation. Backhuys Publishers, Wageningen, Netherlands.

Schmidt, E., Lotter, M., McCleland, W., 2002. Trees and Shrubs of Mpumalanga and Kruger National Park. Jacana.

Schripsema, J., Hermans-Lokkerbol, A., Van der Heijden, R., Verpoorte, R., Svendsen, A.B., Van Beek, T.A., 1986. Alkaloids of *Tabernaemontana ventricosa*. Journal of Natural Products 49, 733–735.

Shrivastava, S., Bera, T., Roy, A., Singh, G., Ramachandrarao, P., Dash, D., 2007. Characterization of enhanced antibacterial effects of novel silver nanoparticles. Nanotechnology 18, 225103.

Sigamoney, M., Shaik, S., Govender, P., Krishna, S.B.N., 2016. African leafy vegetables as bio-factories for silver nanoparticles: A case study on *Amaranthus dubius* C Mart. Ex Thell. South African Journal of Botany 103, 230–240.

Song, J.Y., Jang, H.K., Kim, B.S., 2009. Biological synthesis of gold nanoparticles using *Magnolia kobus* and *Diopyros kaki* leaf extracts. Process Biochemistry 44, 1133–1138.

Valodkar, M., Jadeja, R.N., Thounaojam, M.C., Devkar, R.V., Thakore, S., 2011. *In vitro* toxicity study of plant latex capped silver nanoparticles in human lung carcinoma cells. Materials Science and Engineering 31, 1723–1728.

Van Beek, T.A., Deelder, A.M., Verpoorte, R., Svendsen, A.B., 1984. Antimicrobial, antiamoebic and antiviral screening of some *Tabernaemontana s*pecies. Planta medica 50, 180–185.

Vivekanandhan, S., Christensen, L., Misra, M., Mohanty, A.K., 2011. Biosynthesis of silver nanoparticles using *murraya koenigii* (curry leaf): an investigation on the effect of broth concentration in reduction mechanism and particle size. Advanced Materials Letters 2, 429–434.

Yaqoob, A.A., Umar, K., Ibrahim, M.N.M., 2020. Silver nanoparticles: various methods of synthesis, size affecting factors and their potential applications–a review. Applied Nanoscience 10, 1369–1378.

Yusuf, M., 2020. Silver nanoparticles: Synthesis and applications, eds. Springer Nature, Switzerland

Zargar, M., Hamid, A.A., Bakar, F.A., Shamsudin, M.N., Shameli, K., Jahanshiri, F., Farahani, F., 2011. Green synthesis and anti-bacterial effect of silver nanoparticles using *Vitex negundo* L. Molecules 16, 6667–667.

CHAPTER 8:

CONCLUSIONS, CHALLENGES, AND RECOMMENDATIONS FOR FUTURE RESEARCH

8.1 Aims

The principal aim of this study was to characterize the type and distribution of laticiferous cells, examine the presence and location of histo-phytochemical compounds, determine the chemical composition, and lastly to evaluate the antibacterial, antioxidant, cytotoxic, and silver nanoparticle potential of the leaf, stem, and latex extracts of *Tabernaemontana ventricosa* Hochst. ex A. DC.

8.2 Major findings

This study presents the first report on the type and distribution of laticifers in the embryos, seedlings, and mature *T. ventricosa* plants. Moreover, the location and distribution of chemical constituents within the vegetative organs of *T. ventricosa,* along with the plausible functions of laticifers and latex were investigated (**Chapter 3**). Ontological studies revealed that *T. ventricosa* species are composed of articulated anastomosing laticifers. The origin of the laticifers emerged from the ground meristematic and procambium cells and deviated into the ground and vascular tissue systems. Laticifers displayed variable branching forms ranging from "Y," "H" or "U" conformations. Major chemical constituents such as carboxylated polysaccharides, lipophilic and hydrophilic substances, proteins, phenolics, terpenoids, lignin aldehydes, neutral lipids, alkaloids, mucilage, pectin, resin acids, and acidic substances displayed intense reactions within the lumen of laticifer cells. It is suggested that the latex of *T. ventricosa* is comprised of chemical compounds that are used as a protective mechanism by latex-bearing plants against herbivores and microorganisms, and possibly contain compounds of medicinal value.

The organoleptic characters, elemental analysis, chemical composition, and antibacterial activity of the leaf, stem, and latex extracts of *T. ventricosa* were investigated in **Chapter 4**. Overall, the results revealed that no harmful compounds were present. In addition, major phytochemical groups such as alkaloids, flavonoids, saponins, sterols, steroids, phenols, fixed fats and oils, carbohydrates, and amino acids were detected. Gas Chromatography-Mass Spectrometry (GC-MS) analysis showed the presence of several biologically active compounds which included α-linolenic acid, pentadecanoic acid, α-d-mannofuranoside, methyl, 13-docosenamide, (Z)-, 9,12-octadecadienoic acid (Z,Z)-, lup-20(29)-en-3-ol, acetate, (3β), 9,19-cyclolanost-24-en-3-ol, (3β), and β-amyrin. These compounds have been reported to contain a variety of pharmacological effects ranging from antimicrobial, anti-inflammatory,

chemoprotective, genotoxicity, antioxidant, neuroprotection, and antidiabetic properties Lastly, substantial antibacterial activity was observed by the leaf methanol, stem methanol, and latex extracts against several bacterial strains. Thus, this study supports the utilization of *T. ventricosa* extracts in traditional medicine systems.

The study also investigated the antioxidant and cytotoxic potential of the leaf, stem, and latex extracts of *T. ventricosa,* which showcased substantial activity (**Chapter 5**). Overall, the results revealed that strong antioxidant activity was present within the latex extracts, as confirmed by the total phenolics assay, whereas the stem hexane extracts displayed a large number of total flavonoids. In contrast, the DPPH and FRAP assays showed a variable degree of antioxidant activity across extracts however, the stem and latex extracts showed consistent antioxidant activity. Cytotoxic analysis revealed that the cell lines, HeLa and MCF-7 were the most sensitive to the extracts, with the hexane, chloroform, and methanol leaf and stem, and latex extracts, affecting the percentage cell survival significantly. Interestingly, there was a strong correlation between the antioxidant and cytotoxic activity, using the stem and latex extracts. The compounds within these extracts are probably responsible for the strong antioxidant potential of this species, which also contributes to the substantial cytotoxicity. However, further research is required to understand this complex relationship.

Chapter 6 and **Chapter 7** focused on the synthesis, characterization, and bioactivity (antibacterial and cytotoxic properties) of the AgNPs produced using various treatments (leaf methanol, fresh leaf, powdered leaf, stem methanol, fresh stem, and powdered stem), (**Chapter 6**) and latex extracts (**Chapter 7**) of *T. ventricosa*. **In Chapters 6 and 7**, an efficient biosynthesis of AgNPs using various treatments was observed by a visible colour change, a high silver (Ag) elemental composition, and favourable nanoparticle size. Overall, there were variable differences in these characterization methods which may be influenced by many variables. The shape of the AgNPs was spherical, ovate, and triangular. These variously shaped AgNPs were <100 nm in both AgNPs studies (**Chapters 6 and 7**). The NTA analysis showed much larger particle sizes, which was a result of its hydrodynamic environment. The elemental analysis showed that the leaf extracts effectively produced AgNPs with a higher composition of Ag compared to the stems (**Chapter 6**), whereas in **Chapter 7** the Ag elemental composition was very low. The FTIR analysis for both AgNPs studies (**Chapters 6 and 7**), showed a variety of functional groups such as alcohols, alkanes, amines, proteins, enzymes, and other biomolecules which are highly likely for the capping, reduction, and functionalization of AgNPs. In addition, the various functional groups responsible for the capping of AgNPs may also be accountable for the substantial antibacterial and cytotoxic activity (**Chapters 6 and 7**), since the chemical constituents may differ between treatments. However, the results of these studies highlight the potential usage of *T. ventricosa* extracts for the synthesis of AgNPs.

8.3 Challenges

The greatest challenge in the study was associated with microscopy techniques (**Chapter 3**). The characterization of laticiferous cells was a major task to ensure the preservation of the plant material without subjecting it to the possible collapse of internal cellular structures. This challenge was overcome by employing several treatments. In addition, the sectioning of fresh leaves for histochemical analysis was often difficult due to the rapid flow of latex exudate from the punctured leaf sections.

Regarding the antibacterial, antioxidant and cytotoxic activities observed in this study (**Chapters 4, 5, 6, and 7**), the inability to determine the chemical constituents solely responsible for respective activities was challenging. This was due to the combination of compounds present within the crude leaf and stem, and latex extracts. Each compound may likely cause a biologically specific effect.

An additional limitation observed in this study was the use of only one ratio of $AgNO_3$ for the synthesis of AgNPs (**Chapters 6 and 7**). The preparation of a single ratio of $AgNO_3$ did not provide a basis for an optimized protocol for the synthesis of AgNPs. Furthermore, the utilization of various temperatures (higher or lower) may also influence the synthesis and stability of AgNPs. It is possible that a greater quantity of AgNPs may have been synthesized using various ratios and temperatures.

In general, several constraints severely impacted my doctoral research. For instance, in December 2018, a fire occurred on the 5th floor of the Life Sciences Building, University of KwaZulu-Natal (Westville campus), which resulted in the loss of my research laboratory, general office space, research equipment, chemicals and reagents, plant samples and various other resources. Unfortunately, the construction of the damaged areas began in late February 2019 and is currently still under construction (delayed due to the COVID-19 pandemic). Consequently, the procurement of new chemicals and equipment and laboratory space was also delayed.

Moreover, my research was further delayed due to protest action during 2019/2020 and the subsequent closure of the University (16th March 2020) due to the COVID-19 pandemic which resulted in the added delay of experimental work. Upon my return to campus during COVID-19 (July 2020), I faced several added constraints due to COVID-19 protocols and restrictions, these included limited access to shared research spaces, equipment, and strict access to various departments. In addition, a portion of my research was supposed to be conducted at the UKZN-Microscopy and Microanalysis Unit however, due to the persistent failure of equipment, I have experienced consistent delays for the past two years.

8.4 Future perspectives

There are several possibilities for future research based on micromorphology, chemical analysis, biological activity, and AgNPs synthesis using *T. ventricosa*. In terms of micromorphological studies, the floral biology and laticifers within the reproductive organs of *T. ventricosa* should be investigated. This recommendation may be used to determine the existing taxonomic inconsistencies for subfamilies belonging to Apocynaceae. Furthermore, an in-depth phytochemical analysis based on the chemical composition should be conducted, as this will allow the isolation, purification, and elucidation of compounds detected from all parts of the plant. This information can be utilized to establish the specific pharmacological properties of various compounds and may lead to drug discovery systems. Additionally, the synthesis of AgNPs should be conducted by the manipulation of several variables such as different ratios and temperatures which may improve the production and stability of AgNPs synthesis and ensure a well-optimized AgNPs synthesis protocol.

8.5 Final comments

Tabernaemontana ventricosa is an important ethnomedicinal plant that is often utilized for the treatment of various diseases and ailments. The research of the current study validates the presence of several biologically active compounds within the leaf, stem, and latex extracts of *T. ventricosa*. The occurrence of these compounds is suggestive of the pharmacological properties displayed by the plant extracts which may be subjected to plant-based drug development.

Micromorphological analysis of the leaves and stems revealed the occurrence of articulated anastomosing laticifers. These laticiferous cells have been reported for the first time in *T. ventricosa*. The phytochemical, chemical composition, antibacterial, antioxidant, and cytotoxic potential of the extracts were also determined for the first time or re-evaluated after several years.

Lastly, AgNPs were synthesized for the first time using the leaf, stem, and latex extracts of *T. ventricosa* and have shown efficient production. Moreover, the synthesized AgNPs using various extracts displayed sufficient antibacterial and cytotoxic activity against a variety of bacterial strains and cell lines, thus suggesting the application of *T. ventricosa* extracts for the rapid, profitable, and eco-friendly method of producing AgNPs could be utilized in the field of health and medical research, such as drug delivery systems.

APPENDIX

Appendix 1A

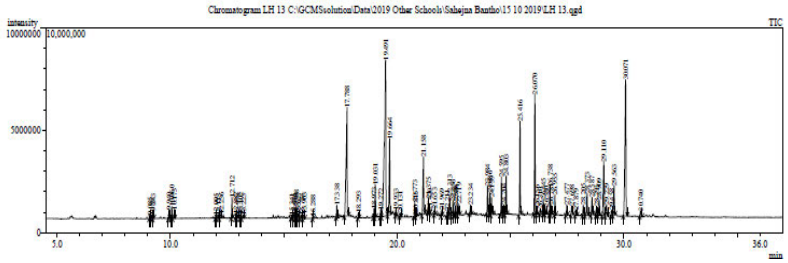

Peak Report TIC

Peak#	R.Time	I.Time	F.Time	Area	Area%	Height	Height%	A/H	Mark	Name
1	9.085	9.060	9.115	253302	0.14	175460	0.23	1.44		Octane, 2,3,6,7-tetramethyl-
2	9.183	9.135	9.210	217705	0.12	135687	0.18	1.60		Hexadecane, 4-methyl-
3	9.243	9.210	9.280	637293	0.35	392708	0.53	1.62		Benzene, 1,3-bis(1,1-dimethylethyl)-
4	9.940	9.905	9.970	610999	0.34	449093	0.60	1.36		11-Methyldodecanol
5	10.060	10.015	10.090	892133	0.49	587087	0.79	1.52		1-Undecene, 7-methyl-
6	10.173	10.090	10.205	638152	0.35	447675	0.60	1.43	V	2-Isopropyl-5-methyl-1-heptanol
7	12.005	11.975	12.030	245551	0.13	186534	0.25	1.32		Dodecane, 4-methyl-
8	12.113	12.030	12.145	351265	0.19	178902	0.24	1.96	V	Tridecanol, 2-ethyl-2-methyl-
9	12.236	12.145	12.270	323559	0.18	232366	0.31	1.39	V	Dodecane, 2,6,11-trimethyl-
10	12.712	12.675	12.745	1406939	0.77	1012464	1.36	1.39		Phenol, 2,4-bis(1,1-dimethylethyl)-
11	12.882	12.855	12.910	326014	0.18	213568	0.29	1.53		2-Isopropyl-5-methyl-1-heptanol
12	12.978	12.910	13.015	371414	0.20	174218	0.23	2.13	V	2-Isopropyl-5-methyl-1-heptanol
13	13.102	13.070	13.130	403716	0.22	239230	0.32	1.69		6-Tridecanol, 3,9-diethyl-
14	13.223	13.130	13.255	238793	0.13	158081	0.21	1.51	V	1-Hexadecanesulfonyl chloride
15	15.341	15.310	15.370	294833	0.16	157052	0.21	1.88		Trichloroacetic acid, hexadecyl ester
16	15.445	15.370	15.470	571058	0.31	181890	0.24	3.14	V	Trifluoroacetic acid, pentadecyl ester
17	15.500	15.480	15.530	332541	0.18	147387	0.20	2.26		2-Isopropyl-5-methyl-1-heptanol
18	15.558	15.530	15.595	683925	0.38	348580	0.47	1.96	V	Triacontyl trifluoroacetate
19	15.627	15.595	15.690	767791	0.42	245917	0.33	3.12	V	Octadecanoic acid
20	15.784	15.690	15.815	345485	0.19	186618	0.25	1.85	V	1-Hexadecanesulfonyl chloride
21	15.903	15.815	15.935	375293	0.21	229796	0.31	1.63	V	2-Isopropyl-5-methyl-1-heptanol
22	16.288	16.260	16.315	161938	0.09	119928	0.16	1.35		Isopropyl myristate
23	17.338	17.300	17.375	895691	0.49	603928	0.81	1.48		Hexadecanoic acid, methyl ester
24	17.788	17.665	17.860	17692139	9.71	5300568	7.10	3.34		Pentadecanoic acid
25	18.293	18.260	18.330	397921	0.22	274117	0.37	1.45		i-Propyl 14-methyl-pentadecanoate
26	18.973	18.940	18.995	656337	0.36	429593	0.58	1.53		9,12-Octadecadienoic acid, methyl ester
27	19.031	18.995	19.065	2438260	1.34	1622299	2.17	1.50	V	Methyl (Z)-5,11,14,17-eicosatetraenoate
28	19.272	19.245	19.300	496017	0.27	361835	0.48	1.37		Heptadecanoic acid, 16-methyl-, methyl este
29	19.491	19.300	19.570	34169338	18.75	7614529	10.19	4.49		cis,cis,cis-7,10,13-Hexadecatrienal
30	19.664	19.570	19.730	8663246	4.76	3725946	4.99	2.33	V	Octadecanoic acid
31	19.933	19.910	19.960	379793	0.21	263409	0.35	1.44		Sulfurous acid, 2-propyl tridecyl ester
32	20.131	20.090	20.170	319241	0.18	204692	0.27	1.56		1-Dodecanol, 2-hexyl-
33	20.773	20.725	20.795	1162559	0.64	759180	1.02	1.53		Oxiraneoctanoic acid, 3-octyl-, methyl ester,
34	20.815	20.795	20.845	354505	0.19	225894	0.30	1.57	V	2-Bromotetradecane
35	21.158	21.085	21.225	7081685	3.89	2795760	3.74	2.53		Oxiraneoctanoic acid, 3-octyl-, cis-
36	21.375	21.345	21.405	1023803	0.56	683325	0.91	1.50		13-Docosenamide, (Z)-
37	21.420	21.405	21.445	201859	0.11	169303	0.23	1.19	V	8-Methyl-6-nonenamide
38	21.653	21.620	21.675	388870	0.21	258194	0.35	1.51		Eicosane
39	21.969	21.925	21.995	438060	0.24	284941	0.38	1.54		7-Hexadecenoic acid, methyl ester, (Z)-
40	22.211	22.180	22.250	368342	0.20	259515	0.35	1.42		Methyl 12-oxo-9-dodecenoate
41	22.313	22.250	22.365	2251932	1.24	983175	1.32	2.29	V	8-Hexadecenal, 14-methyl-, (Z)-
42	22.456	22.365	22.485	1439297	0.79	712330	0.95	2.02	V	Tetratetracontane
43	22.546	22.485	22.560	607668	0.33	364263	0.49	1.67	V	8-Hexadecenal, 14-methyl-, (Z)-
44	22.586	22.560	22.645	1006374	0.55	473066	0.63	2.13	V	Hexadecanoic acid, 2-hydroxy-1-(hydroxym
45	22.719	22.645	22.765	945028	0.52	527991	0.71	1.79	V	Diisooctyl phthalate
46	23.234	23.180	23.285	890640	0.49	433370	0.58	2.06		Eicosane
47	23.984	23.930	24.050	2791142	1.53	1364309	1.83	2.05		2-methylhexacosane
48	24.086	24.050	24.120	1664042	0.91	1052264	1.41	1.58		Ibogamine
49	24.159	24.120	24.230	1615905	0.89	826483	1.11	1.96		Octadecanoic acid, 2,3-dihydroxypropyl este

Peak#	R.Time	I.Time	F.Time	Area	Area%	Height	Height%	A/H	Mark	Name
50	24.595	24.535	24.640	3094393	1.70	1842109	2.47	1.68		13-Docosenamide, (Z)-
51	24.704	24.640	24.735	989917	0.54	464995	0.62	2.13	V	Tetratetracontane
52	24.803	24.735	24.850	3151078	1.73	1871629	2.51	1.68		Squalene
53	25.416	25.355	25.465	8044325	4.42	4554181	6.10	1.77		Tetratetracontane
54	26.070	26.010	26.120	11257631	6.18	5866110	7.85	1.92		Ibogamine-18-carboxylic acid, 12-methoxy-,
55	26.156	26.120	26.190	633975	0.35	377446	0.51	1.68	V	Octacosyl acetate
56	26.310	26.275	26.420	481652	0.26	253927	0.34	1.90		Spiro[2H-indole-2,8'(7'H)-[3,7]methano[2H]
57	26.445	26.420	26.490	1175843	0.65	720418	0.96	1.63	V	.gamma.-Tocopherol
58	26.580	26.490	26.625	609957	0.33	366277	0.49	1.67	V	Voluteine
59	26.738	26.700	26.760	2233529	1.23	1418027	1.90	1.58		Tetratetracontane
60	26.781	26.760	26.835	834447	0.46	483961	0.65	1.72	V	n-Nonadecanol-1
61	26.955	26.920	27.000	1571142	0.86	982786	1.32	1.60		Vitamin E
62	27.477	27.430	27.525	956184	0.52	499543	0.67	1.91		Heptacosyl acetate
63	27.698	27.645	27.765	1101697	0.60	438268	0.59	2.51		Ergost-5-en-3-ol, (3.beta.)-
64	27.879	27.835	27.940	572374	0.31	268496	0.36	2.13		Stigmasterol
65	28.205	28.160	28.270	1209418	0.66	514905	0.69	2.35		Lanost-7-en-3-one, (9.beta.,13.alpha.,14.beta
66	28.373	28.270	28.440	2509494	1.38	1098045	1.47	2.29	V	.beta.-Sitosterol
67	28.587	28.530	28.645	1989332	1.09	844132	1.13	2.36		Lanosterol
68	28.795	28.755	28.835	1043546	0.57	456991	0.61	2.28		Acetic acid, 3-hydroxy-7-isopropenyl-1,4a-d
69	28.909	28.835	28.955	1603250	0.88	748957	1.00	2.14	V	Silane, dimethyl(docosyloxy)butoxy-
70	29.110	29.025	29.155	7338368	4.03	2659551	3.56	2.76		9,19-Cyclolanost-24-en-3-ol, acetate, (3.beta
71	29.229	29.155	29.290	1940200	1.06	557983	0.75	3.48	V	Acetic acid, 3-hydroxy-7-isopropenyl-1,4a-d
72	29.458	29.415	29.500	576007	0.32	260168	0.35	2.21		Hexadecanal
73	29.563	29.500	29.610	3650467	2.00	1443300	1.93	2.53	V	4,4,6a,6b,8a,11,11,14b-Octamethyl-1,4,4a,5,
74	30.071	29.965	30.150	21996078	12.07	6631609	8.88	3.32		5H-3,5a-Epoxynaphth[2,1-c]oxepin, dodecal
75	30.740	30.685	30.805	836112	0.46	293683	0.39	2.85		1,4-Epoxynaphthalene-1(2H)-methanol, 4,5,
				182190209	100.00	74692017	100.00			

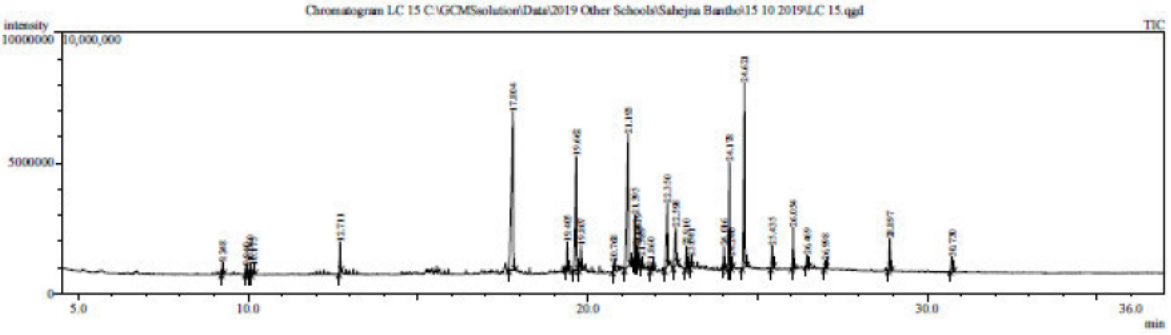

Peak Report TIC

Peak#	R.Time	I.Time	F.Time	Area	Area%	Height	Height%	A/H	Mark	Name
1	9.248	9.220	9.285	645980	0.56	432517	0.91	1.49		Benzene, 1,3-bis(1,1-dimethylethyl)-
2	9.940	9.915	9.975	470897	0.41	351308	0.74	1.34		1-Undecene, 7-methyl-
3	10.060	10.010	10.095	696696	0.61	453306	0.96	1.54		2-Isopropyl-5-methyl-1-heptanol
4	10.175	10.095	10.205	509054	0.45	354245	0.75	1.44	V	11-Methyldodecanol
5	12.711	12.680	12.745	1825653	1.60	1188669	2.51	1.54		Phenol, 2,4-bis(1,1-dimethylethyl)-
6	17.804	17.675	17.865	22928060	20.05	6094424	12.89	3.76		Pentadecanoic acid
7	19.405	19.370	19.450	1709137	1.49	1068794	2.26	1.60		cis,cis,cis-7,10,13-Hexadecatrienal
8	19.662	19.575	19.725	11199981	9.80	4381949	9.27	2.56		Octadecanoic acid
9	19.807	19.735	19.855	1956058	1.71	927707	1.96	2.11		Octadecanamide
10	20.768	20.735	20.790	496949	0.43	338285	0.72	1.47		Oxiraneoctanoic acid, 3-octyl-, methyl ester,
11	21.193	21.080	21.265	16378804	14.32	5089683	10.77	3.22		Oxiraneoctanoic acid, 3-octyl-, cis-
12	21.395	21.355	21.420	3461855	3.03	1833162	3.88	1.89		9-Octadecenamide, (Z)-
13	21.443	21.420	21.460	1268806	1.11	657372	1.39	1.93	V	9-Octadecenamide, (Z)-
14	21.479	21.460	21.510	1320730	1.16	854356	1.81	1.55	V	9-Octadecenamide, (Z)-
15	21.589	21.560	21.625	563610	0.49	397862	0.84	1.42		Tetradecanamide
16	21.860	21.840	21.950	476114	0.42	206451	0.44	2.31		9-Octadecenoic acid, 1,2,3-propanetriyl este
17	22.350	22.265	22.385	6722475	5.88	2428485	5.14	2.77		12-Methyl-E,E-2,13-octadecadien-1-ol
18	22.598	22.525	22.650	4332256	3.79	1463481	3.10	2.96		Hexadecanoic acid, 2-hydroxy-1-(hydroxym
19	22.910	22.875	22.940	1275455	1.12	838718	1.77	1.52		Octadecanoic acid, 9,10-epoxy-, isopropyl e
20	23.041	23.015	23.065	628467	0.55	431201	0.91	1.46		13-Docosenamide, (Z)-
21	24.016	23.990	24.050	1133908	0.99	803726	1.70	1.41		Ethyl stearate, 9,12-dioxoxy
22	24.178	24.125	24.225	8944139	7.82	4126566	8.73	2.17		Octadecanoic acid, 2,3-dihydroxypropyl este
23	24.240	24.225	24.270	616319	0.54	474940	1.00	1.30	V	Oxiraneoctanoic acid, 3-octyl-, cis-
24	24.621	24.550	24.685	14665525	12.83	7074899	14.97	2.07		13-Docosenamide, (Z)-
25	25.435	25.395	25.485	1669047	1.46	878339	1.86	1.90		7-Methyl-Z,Z-8,10-hexadecadien-1-ol acetat
26	26.054	26.010	26.090	2712007	2.37	1590587	3.36	1.71		Ibogamine-18-carboxylic acid, 12-methoxy-,
27	26.469	26.435	26.520	875470	0.77	441252	0.93	1.98		7-Methyl-Z,Z-8,10-hexadecadien-1-ol acetat
28	26.998	26.965	27.035	567389	0.50	303046	0.64	1.87		4,4'-Dimethylbenzoin
29	28.897	28.850	28.950	2751477	2.41	1216652	2.57	2.26		Silane, dimethyl(docosyloxy)butoxy-
30	30.730	30.680	30.790	1536667	1.34	567638	1.20	2.71		1,3,5-Cycloheptatriene, 2,4-di-t-butyl-7,7-di
				114338985	100.00	47269520	100.00			

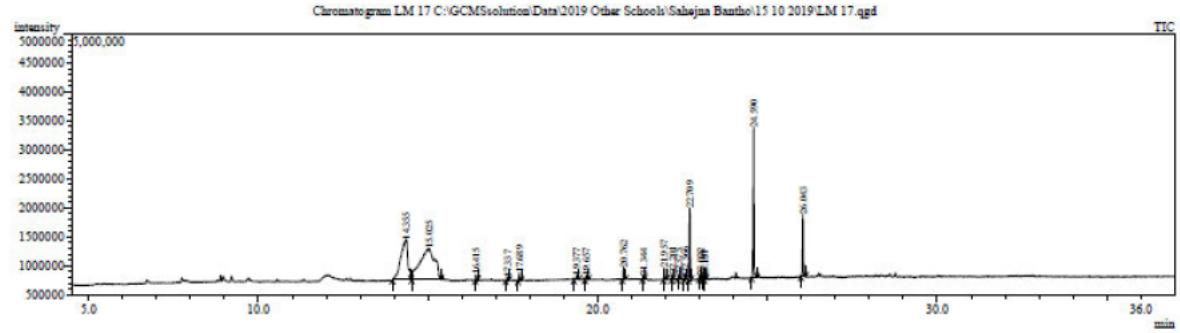

Peak Report TIC

Peak#	R.Time	I.Time	F.Time	Area	Area%	Height	Height%	A/H	Mark	Name
1	14.355	13.955	14.500	10078604	27.46	702715	9.35	14.34	MI	1,2,3,5-Cyclohexanetetrol, (1.alpha.,2.beta.,3
2	15.025	14.520	15.385	15933308	43.40	541205	7.20	29.44	MI	.alpha.-d-Mannofuranoside, methyl
3	16.415	16.395	16.465	129921	0.35	97828	1.30	1.33	MI	Phytol, acetate
4	17.337	17.290	17.385	67198	0.18	49703	0.66	1.35	MI	Pentanoic acid, 4-methyl-, methyl ester
5	17.689	17.645	17.750	300500	0.82	136843	1.82	2.20	MI	n-Hexadecanoic acid
6	19.377	19.295	19.450	239356	0.65	91918	1.22	2.60	MI	cis,cis,cis-7,10,13-Hexadecatrienal
7	19.657	19.620	19.730	89757	0.24	67468	0.90	1.33	MI	Decanedioic acid, dibutyl ester
8	20.762	20.720	20.820	331905	0.90	221993	2.95	1.50	MI	Oxiraneoctanoic acid, 3-octyl-, methyl ester,
9	21.344	21.320	21.380	89984	0.25	68850	0.92	1.31	MI	8-Methyl-6-nonenamide
10	21.957	21.935	22.035	315926	0.86	202412	2.69	1.56	MI	7-Hexadecenoic acid, methyl ester, (Z)-
11	22.201	22.175	22.215	141430	0.39	97057	1.29	1.46	MI	7-Hydroxy-3-(1,1-dimethylprop-2-enyl)coum
12	22.375	22.355	22.440	56548	0.15	51392	0.68	1.10	MI	Octadecanoic acid, 9,10-dihydroxy-, methyl
13	22.566	22.540	22.595	145392	0.40	90108	1.20	1.61	MI	Hexadecanoic acid, 2-hydroxy-1-(hydroxym
14	22.709	22.670	22.755	1950909	5.31	1238899	16.49	1.57	MI	Diisooctyl phthalate
15	23.022	22.990	23.045	80447	0.22	64036	0.85	1.26	MI	cis-9,10-Epoxyoctadecanamide
16	23.101	23.085	23.135	58059	0.16	40793	0.54	1.42	MI	Oxiranepentanoic acid, 3-undecyl-, methyl e
17	23.157	23.130	23.190	86771	0.24	53281	0.71	1.63	MI	Z-3-Methyl-2-hexenoic acid
18	24.590	24.530	24.680	4633856	12.62	2604450	34.67	1.78	MI	13-Docosenamide, (Z)-
19	26.043	25.990	26.125	1979126	5.39	1092189	14.54	1.81	MI	Ibogamine-18-carboxylic acid, 12-methoxy-,
				36708997	100.00	7513140	100.00			

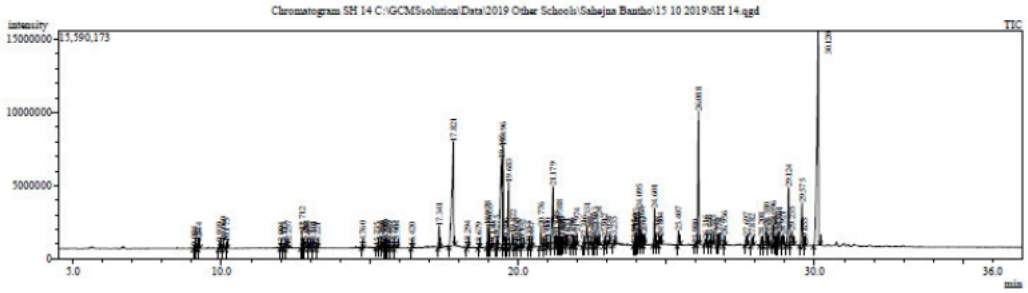

Peak Report TIC

Peak#	R.Time	I.Time	F.Time	Area	Area%	Height	Height%	A/H	Mark	Name
1	9.084	9.055	9.120	247465	0.09	166366	0.15	1.49		Decane, 4-methyl-
2	9.182	9.120	9.210	209485	0.07	125263	0.12	1.67		Decane, 2,3,4-trimethyl-
3	9.244	9.210	9.285	662688	0.24	433857	0.40	1.53	V	Benzene, 1,3-bis(1,1-dimethylethyl)-
4	9.939	9.905	9.970	601694	0.21	444476	0.41	1.35		1-Undecene, 7-methyl-
5	10.060	10.010	10.095	878043	0.31	569387	0.53	1.54		11-Methyldodecanol
6	10.173	10.145	10.210	609615	0.22	429748	0.40	1.42		2-Isopropyl-5-methyl-1-heptanol
7	12.004	11.975	12.035	237088	0.08	168887	0.16	1.40		Dodecane, 4-methyl-
8	12.113	12.055	12.150	351507	0.13	194205	0.18	1.81		10-Methylnonadecane
9	12.237	12.150	12.275	345003	0.12	230899	0.21	1.49	V	Decane, 2,3,5,8-tetramethyl-
10	12.712	12.675	12.740	1633126	0.58	1189640	1.10	1.37		Phenol, 2,4-bis(1,1-dimethylethyl)-
11	12.765	12.740	12.790	216518	0.08	149992	0.14	1.44	V	2-Isopropyl-5-methyl-1-heptanol
12	12.884	12.790	12.915	395244	0.14	245313	0.23	1.61	V	1-Dodecanol, 3,7,11-trimethyl-
13	12.977	12.940	13.010	350759	0.13	181292	0.17	1.93		2-Isopropyl-5-methyl-1-heptanol
14	13.101	13.060	13.135	405083	0.14	255048	0.24	1.59		Heptadecyl heptafluorobutyrate
15	13.221	13.190	13.250	225779	0.08	164014	0.15	1.38		2-Isopropyl-5-methyl-1-heptanol
16	14.760	14.730	14.795	317765	0.11	175728	0.16	1.81		Ethyl hydrogen sebacate
17	15.235	15.210	15.320	176237	0.06	105232	0.10	1.67		Henicosyl trifluoroacetate
18	15.344	15.320	15.370	313430	0.11	176940	0.16	1.77	V	Trifluoroacetic acid, pentadecyl ester
19	15.440	15.370	15.475	587832	0.21	239303	0.22	2.46	V	Octacosyl trifluoroacetate
20	15.500	15.475	15.530	372029	0.13	170870	0.16	2.18		Trifluoroacetoxy hexadecane
21	15.559	15.530	15.590	758239	0.27	374515	0.35	2.02	V	Trichloroacetic acid, hexadecyl ester
22	15.649	15.590	15.690	731573	0.26	247440	0.23	2.96	V	Nonadecyl pentafluoropropionate
23	15.785	15.690	15.815	367954	0.13	216027	0.20	1.70	V	Docosyl trifluoroacetate
24	15.904	15.815	15.940	407973	0.15	257179	0.24	1.59	V	2-Isopropyl-5-methyl-1-heptanol
25	16.420	16.395	16.450	194174	0.07	138809	0.13	1.40		Phytol, acetate
26	17.341	17.300	17.375	2114234	0.75	1447729	1.34	1.46		Hexadecanoic acid, methyl ester
27	17.821	17.670	17.875	28475934	10.15	7132850	6.60	3.99		Pentadecanoic acid
28	18.294	18.265	18.320	342643	0.12	247699	0.23	1.38		i-Propyl 14-methyl-pentadecanoate
29	18.679	18.650	18.715	177210	0.06	113304	0.10	1.56		Octadecanoic acid
30	18.978	18.940	19.005	2270868	0.81	1517944	1.41	1.50		9,12-Octadecadienoic acid, methyl ester
31	19.035	19.005	19.065	2106877	0.75	1396348	1.29	1.51	V	8,11,14-Docosatrienoic acid, methyl ester
32	19.130	19.065	19.155	270456	0.10	94313	0.09	2.87	V	Phytol
33	19.275	19.240	19.305	773604	0.28	536844	0.50	1.44		Methyl stearate
34	19.445	19.305	19.465	25710538	9.17	6062910	5.61	4.24	V	9,12-Octadecadienoic acid (Z,Z)-
35	19.496	19.465	19.565	16094867	5.74	6903962	6.39	2.33	V	Dichloroacetic acid, tridec-2-ynyl ester
36	19.596	19.565	19.620	973104	0.35	396592	0.37	2.45	V	E,E,Z-1,3,12-Nonadecatriene-5,14-diol
37	19.683	19.620	19.735	11373149	4.06	4453005	4.12	2.55	V	Octadecanoic acid
38	19.822	19.735	19.870	2767091	0.99	970520	0.90	2.85	V	Hexadecanoic acid, butyl ester
39	19.938	19.870	19.965	1131088	0.40	383187	0.35	2.95	V	Sulfurous acid, 2-propyl tetradecyl ester
40	20.025	19.965	20.110	606547	0.22	160635	0.15	3.78	V	Trifluoroacetoxy hexadecane
41	20.132	20.110	20.170	457424	0.16	269046	0.25	1.70	V	Octatriacontyl trifluoroacetate
42	20.353	20.325	20.385	205145	0.07	136263	0.13	1.51		Tributyl acetylcitrate
43	20.447	20.420	20.470	182006	0.06	137821	0.13	1.32		Tetratriacontyl heptafluorobutyrate
44	20.776	20.735	20.845	2610242	0.93	1434969	1.33	1.82		Oxirane,octanoic acid, 3-octyl-, methyl ester,
45	20.915	20.845	20.970	515933	0.18	148824	0.14	3.47	V	9-Eicosyne
46	21.000	20.970	21.085	1293442	0.46	293277	0.27	4.41	V	Cyclopentadecanone, 2-hydroxy-
47	21.179	21.085	21.240	12317980	4.39	4099325	3.80	3.00	V	Oxirane,octanoic acid, 3-octyl-, cis-
48	21.283	21.240	21.310	1444322	0.51	716549	0.66	2.02	V	Butyl 9,12-octadecadienoate
49	21.343	21.310	21.360	1303658	0.46	695356	0.64	1.87	V	Trichloroacetic acid, tridec-2-ynyl ester

Peak#	R.Time	I.Time	F.Time	Area	Area%	Height	Height%	A/H	Mark	Name
50	21.388	21.360	21.415	2698875	0.96	1488005	1.38	1.81	V	13-Docosenamide, (Z)-
51	21.440	21.415	21.455	687266	0.25	302123	0.28	2.27	V	3-Cyclohexylpropionamide
52	21.476	21.455	21.515	684086	0.24	341478	0.32	2.00	V	13-Docosenamide, (Z)-
53	21.540	21.515	21.630	576876	0.21	142736	0.13	4.04	V	Octadecanoic acid, butyl ester
54	21.651	21.630	21.675	249539	0.09	168997	0.16	1.48	V	Eicosane
55	21.786	21.760	21.835	485584	0.17	250642	0.23	1.94		2-Methyl-Z-7,8-epoxyhexadecane
56	21.878	21.845	21.915	351732	0.13	172403	0.16	2.04		Nonadecyl pentafluoropropionate
57	21.974	21.935	22.000	1295767	0.46	932294	0.86	1.39		7-Hexadecenoic acid, methyl ester, (Z)-
58	22.216	22.180	22.240	732104	0.26	489358	0.45	1.50		7-Hexadecenoic acid, methyl ester, (Z)-
59	22.331	22.240	22.385	4230407	1.51	1341015	1.24	3.15	V	12-Methyl-E,E-2,13-octadecadien-1-ol
60	22.457	22.385	22.490	1093449	0.39	379974	0.35	2.88	V	Eicosane
61	22.557	22.525	22.570	850812	0.30	545087	0.50	1.56	V	7-Methyl-Z,Z-8,10-hexadecadien-1-ol acetat
62	22.593	22.570	22.670	2066962	0.74	974158	0.90	2.12	V	Hexadecanoic acid, 2-hydroxy-1-(hydroxym
63	22.724	22.670	22.775	1748763	0.62	969358	0.90	1.80	V	Diisooctyl phthalate
64	22.912	22.880	22.945	846523	0.30	519080	0.48	1.63		Octadecanoic acid, 9,10-epoxy-, isopropyl e
65	23.038	23.015	23.065	456418	0.16	307757	0.28	1.48	V	13-Docosenamide, (Z)-
66	23.235	23.195	23.275	577283	0.21	312837	0.29	1.85		Tetratetracontane
67	23.915	23.890	23.930	241599	0.09	141114	0.13	1.71		1,1,3,6-tetramethyl-2-(3,6,10,13,14-pentame
68	23.950	23.930	23.965	840816	0.30	489403	0.45	1.72	V	Methyl 5,11,14-eicosatrienoate
69	23.983	23.965	24.005	1583305	0.56	879972	0.81	1.80	V	Eicosane
70	24.015	24.005	24.050	970760	0.35	656714	0.61	1.48	V	Tricyclo[20.8.0.0(7,16)]triacontane, 1(22),7(
71	24.095	24.050	24.125	4394896	1.57	2515136	2.33	1.75	V	Ibogamine
72	24.164	24.125	24.215	2182973	0.78	1037223	0.96	2.10	V	Octadecanoic acid, 2,3-dihydroxypropyl este
73	24.236	24.215	24.265	282438	0.10	176241	0.16	1.60	V	Ethyl stearate, 9,12-diepoxy
74	24.601	24.550	24.640	4374449	1.56	2508712	2.32	1.74		13-Docosenamide, (Z)-
75	24.708	24.640	24.735	723509	0.26	284950	0.26	2.54	V	5,5,7,7-Tetraethylundecane
76	24.804	24.735	24.840	962819	0.34	569764	0.53	1.69		Squalene
77	25.407	25.365	25.470	1860163	0.66	975815	0.90	1.91		Eicosane
78	25.980	25.955	26.020	230328	0.08	105897	0.10	2.18		Ibogamine-18-carboxylic acid, 12-methoxy-,
79	26.088	26.020	26.115	18742963	6.68	9087584	8.41	2.06	V	Ibogamine-18-carboxylic acid, 12-methoxy-,
80	26.316	26.280	26.365	588230	0.21	352509	0.33	1.67		Spiro[2H-indole-2,8'(7'H)-[3.7]methano[2H]
81	26.446	26.415	26.500	670555	0.24	350284	0.32	1.91		gamma.-Tocopherol
82	26.583	26.500	26.615	657911	0.23	418010	0.39	1.57	V	Voalkuteine
83	26.732	26.705	26.760	326198	0.12	212245	0.20	1.55		Eicosane
84	26.778	26.760	26.805	248044	0.09	171276	0.16	1.45	V	Carbonic acid, octadecyl 2,2,2-trichloroethyl
85	26.956	26.920	26.990	1200878	0.43	739028	0.68	1.62		Vitamin E
86	27.697	27.655	27.735	1211869	0.43	562050	0.52	2.16		Campesterol
87	27.882	27.845	27.945	1041729	0.37	501753	0.46	2.08		Stigmasterol
88	28.208	28.155	28.260	1515076	0.54	604307	0.56	2.51		Obtusifoliol
89	28.380	28.260	28.425	3116977	1.11	1310034	1.21	2.38	V	.beta.-Sitosterol
90	28.435	28.425	28.470	217836	0.08	185406	0.17	1.17	V	Silane, [[(3.beta.)-lanosta-8,24-dien-3-yl]oxy
91	28.596	28.545	28.625	3315867	1.18	1382146	1.28	2.40		Lanosterol
92	28.644	28.625	28.690	1215588	0.43	615671	0.57	1.97	V	1-Cycloheptene, 1,4-dimethyl-3-(2-methyl-1
93	28.723	28.690	28.755	474819	0.17	208966	0.19	2.27	V	9,19-Cycloergost-24(28)-en-3-ol, 4,14-dimet
94	28.801	28.755	28.865	2675800	0.95	984583	0.91	2.72	V	4,4,6a,6b,8a,11,11,14b-Octamethyl-1,4,4a,5,
95	28.921	28.865	28.975	1775144	0.63	766844	0.71	2.31	V	Silane, dimethyl(docosyloxy)butoxy-
96	29.124	29.040	29.160	10435688	3.72	3946588	3.65	2.64		9,19-Cycloergost-24(28)-en-3-ol, 4,14-dimet
97	29.235	29.160	29.305	3833513	1.37	979863	0.91	3.91	V	.alpha.-Amyrin
98	29.575	29.495	29.620	8249685	2.94	2906146	2.69	2.84		4,4,6a,6b,8a,11,11,14b-Octamethyl-1,4,4a,5,
99	29.655	29.620	29.705	789549	0.28	290309	0.27	2.72	V	9,19-Cyclolanostan-3-ol, 24-methylene-, (3.l
100	30.120	29.960	30.190	52765706	18.81	14656857	13.57	3.60		5H-3,5a-Epoxynaphth[2,1-c]oxepin, dodecal
				280466813	100.00	108010704	100.00			

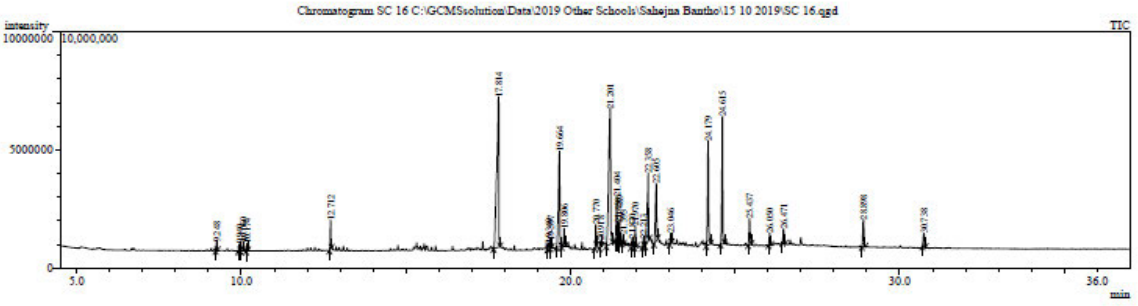

Peak Report TIC

Peak#	R.Time	I.Time	F.Time	Area	Area%	Height	Height%	A/H	Mark	Name
1	9.248	9.220	9.280	529211	0.43	367132	0.79	1.44		Benzene, 1,3-bis(1,1-dimethylethyl)-
2	9.940	9.910	9.970	428252	0.35	305540	0.65	1.40		1-Heptanol, 2,4-diethyl-
3	10.060	9.970	10.095	614272	0.50	404450	0.87	1.52	V	11-Methyldodecanol
4	10.174	10.145	10.205	437323	0.36	319648	0.68	1.37		11-Methyldodecanol
5	12.712	12.675	12.745	1939023	1.57	1233140	2.64	1.57		Phenol, 2,4-bis(1,1-dimethylethyl)-
6	17.814	17.665	17.860	26594816	21.59	6363720	13.63	4.18		Pentadecanoic acid
7	19.340	19.300	19.375	477425	0.39	261006	0.56	1.83		9,12-Octadecadienoic acid (Z,Z)-
8	19.397	19.375	19.430	568535	0.46	344762	0.74	1.65	V	Dichloroacetic acid, tridec-2-ynyl ester
9	19.664	19.570	19.730	11666519	9.47	4055758	8.69	2.88		Octadecanoic acid
10	19.806	19.730	19.850	1471966	1.20	762200	1.63	1.93		Octadecanamide
11	20.770	20.735	20.795	1402842	1.14	946765	2.03	1.48		Oxiraneoctanoic acid, 3-octyl-, methyl ester,
12	20.918	20.880	20.950	519236	0.42	265830	0.57	1.95		13-Tetradecenal
13	21.201	21.085	21.285	23156597	18.80	5731520	12.28	4.04		Oxiraneoctanoic acid, 3-octyl-, cis-
14	21.404	21.355	21.430	3885730	3.15	1930197	4.14	2.01		13-Docosenamide, (Z)-
15	21.450	21.430	21.465	1411345	1.15	832550	1.78	1.70	V	9-Octadecenamide, (Z)-
16	21.489	21.465	21.535	1717580	1.39	964428	2.07	1.78	V	13-Docosenamide, (Z)-
17	21.593	21.565	21.620	586171	0.48	400712	0.86	1.46		Octadecanamide
18	21.870	21.835	21.915	753411	0.61	386425	0.83	1.95		Cyclooctane, (methoxymethoxy)-
19	21.970	21.935	22.010	1292345	1.05	874080	1.87	1.48		7-Hexadecenoic acid, methyl ester, (Z)-
20	22.213	22.185	22.235	495401	0.40	346215	0.74	1.43		7-Hexadecenoic acid, methyl ester, (Z)-
21	22.358	22.270	22.390	7716408	6.26	2873668	6.16	2.69		12-Methyl-E,E-2,13-octadecadien-1-ol
22	22.605	22.535	22.655	6522703	5.30	2432994	5.21	2.68		Hexadecanoic acid, 2-hydroxy-1-(hydroxyme
23	23.046	23.015	23.070	610811	0.50	434917	0.93	1.40		8-Methyl-6-nonenamide
24	24.179	24.120	24.265	9366457	7.60	4422593	9.48	2.12		Octadecanoic acid, 2,3-dihydroxypropyl este
25	24.615	24.555	24.680	9987946	8.11	5423613	11.62	1.84		13-Docosenamide, (Z)-
26	25.437	25.395	25.500	2465543	2.00	1114309	2.39	2.21		Octadecanoic acid, 9,10-epoxy-, isopropyl e
27	26.050	26.015	26.090	929739	0.75	519372	1.11	1.79		Ibogamine-18-carboxylic acid, 12-methoxy-,
28	26.471	26.435	26.525	1227700	1.00	617558	1.32	1.99		7-Methyl-Z,Z-8,10-hexadecadien-1-ol acetat
29	28.898	28.850	28.955	2765332	2.25	1174090	2.52	2.36		Silane, dimethyl(docosyloxy)butoxy-
30	30.738	30.690	30.790	1632320	1.33	565476	1.21	2.89		1,4-Epoxynaphthalene-1(2H)-methanol, 4,5,
				123172959	100.00	46674668	100.00			

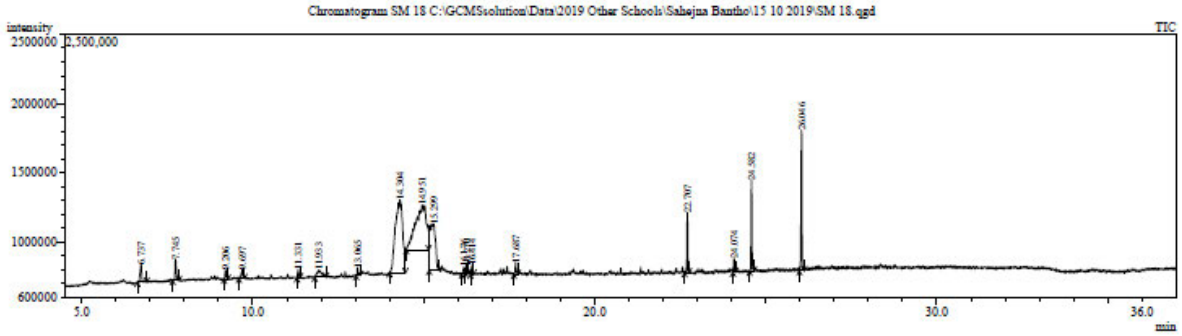

Peak Report TIC

Peak#	R.Time	I.Time	F.Time	Area	Area%	Height	Height%	A/H	Mark	Name
1	14.355	13.955	14.500	10078604	27.46	702715	9.35	14.34	MI	1,2,3,5-Cyclohexanetetrol, (1.alpha.,2.beta.,3
2	15.025	14.520	15.385	15933308	43.40	541205	7.20	29.44	MI	.alpha.-d-Mannofuranoside, methyl
3	16.415	16.395	16.465	129921	0.35	97828	1.30	1.33	MI	Phytol, acetate
4	17.337	17.290	17.385	67198	0.18	49703	0.66	1.35	MI	Pentanoic acid, 4-methyl-, methyl ester
5	17.689	17.645	17.750	300500	0.82	136843	1.82	2.20	MI	n-Hexadecanoic acid
6	19.377	19.295	19.450	239356	0.65	91918	1.22	2.60	MI	cis,cis,cis-7,10,13-Hexadecatrienal
7	19.657	19.620	19.730	89757	0.24	67468	0.90	1.33	MI	Decanedioic acid, dibutyl ester
8	20.762	20.720	20.820	331905	0.90	221993	2.95	1.50	MI	Oxiraneoctanoic acid, 3-octyl-, methyl ester,
9	21.344	21.320	21.380	89984	0.25	68850	0.92	1.31	MI	8-Methyl-6-nonenamide
10	21.957	21.935	22.035	315926	0.86	202412	2.69	1.56	MI	7-Hexadecenoic acid, methyl ester, (Z)-
11	22.201	22.175	22.215	141430	0.39	97057	1.29	1.46	MI	7-Hydroxy-3-(1,1-dimethylprop-2-enyl)coum
12	22.375	22.355	22.440	56548	0.15	51392	0.68	1.10	MI	Octadecanoic acid, 9,10-dihydroxy-, methyl
13	22.566	22.540	22.595	145392	0.40	90108	1.20	1.61	MI	Hexadecanoic acid, 2-hydroxy-1-(hydroxyme
14	22.709	22.670	22.755	1950909	5.31	1238899	16.49	1.57	MI	Diisooctyl phthalate
15	23.022	22.990	23.045	80447	0.22	64036	0.85	1.26	MI	cis-9,10-Epoxyoctadecanamide
16	23.101	23.085	23.135	58059	0.16	40793	0.54	1.42	MI	Oxiranepentanoic acid, 3-undecyl-, methyl e
17	23.157	23.130	23.190	86771	0.24	53281	0.71	1.63	MI	Z-3-Methyl-2-hexenoic acid
18	24.590	24.530	24.680	4633856	12.62	2604450	34.67	1.78	MI	13-Docosenamide, (Z)-
19	26.043	25.990	26.125	1979126	5.39	1092189	14.54	1.81	MI	Ibogamine-18-carboxylic acid, 12-methoxy-,
				36708997	100.00	7513140	100.00			

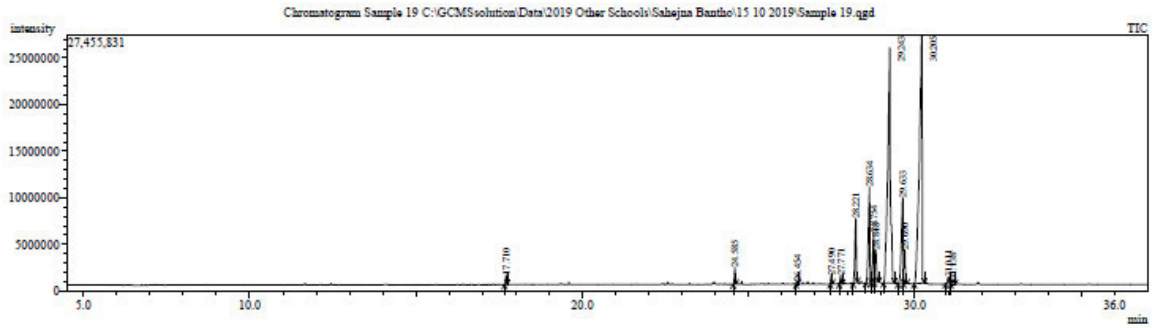

Peak Report TIC

Peak#	R.Time	I.Time	F.Time	Area	Area%	Height	Height%	A/H	Mark	Name
1	17.710	17.660	17.745	1765340	0.41	1073054	1.11	1.65		Pentadecanoic acid
2	24.585	24.540	24.625	2819805	0.66	1794505	1.85	1.57		13-Docosenamide, (Z)-
3	26.454	26.425	26.490	490088	0.11	315878	0.33	1.55		1,6,10,14,18,22-Tetracosahexaen-3-ol, 2,6,1
4	27.490	27.455	27.525	1486753	0.35	887629	0.91	1.67		Longifolenaldehyde
5	27.771	27.725	27.820	1864939	0.44	917590	0.94	2.03		14.alpha.-Methyl-5.alpha.-ergosta-8,24(28)-
6	28.221	28.140	28.275	18851982	4.42	6862123	7.07	2.75		Obtusifoliol
7	28.634	28.525	28.685	30557418	7.17	10268935	10.57	2.98		Lanosterol
8	28.754	28.685	28.780	13613971	3.19	5471039	5.63	2.49		9,19-Cyclosergost-24(28)-en-3-ol, 4,14-dimet
9	28.818	28.780	28.920	12334176	2.89	3479203	3.58	3.55	V	9,19-Cyclolanost-24-en-3-ol, acetate, (3.beta
10	29.243	29.055	29.380	141835850	33.28	25273236	26.03	5.61		9,19-Cyclolanost-24-en-3-ol, (3.beta.)-
11	29.633	29.490	29.660	33477359	7.85	9303888	9.58	3.60		.beta.-Amyrin
12	29.690	29.660	29.760	8927836	2.09	3673117	3.78	2.43	V	9,19-Cyclolanostan-3-ol, 24-methylene-, (3.l
13	30.205	29.975	30.285	153830206	36.09	26512087	27.30	5.80		Lup-20(29)-en-3-ol, acetate, (3.beta.)-
14	31.011	30.915	31.075	2611185	0.61	741534	0.76	3.52		Lupan-3-ol, acetate
15	31.138	31.075	31.215	1770707	0.42	533207	0.55	3.32		Lup-20(29)-en-3-ol, acetate, (3.beta.)-
				426237615	100.00	97107025	100.00			

APPENDIX 2A

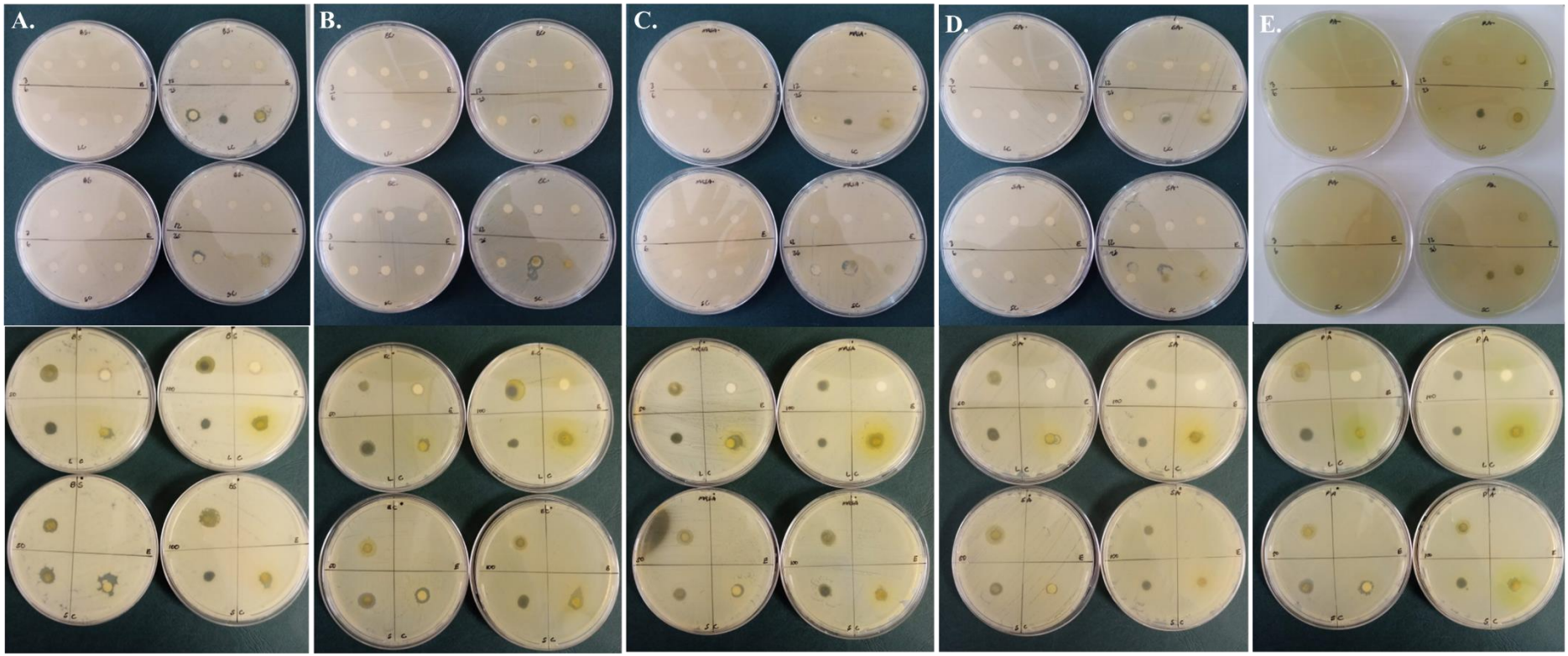

Figure 1: Zones of inhibition (mm) of various leaf, stem, and latex extracts (hexane, chloroform, and methanol) of *T. ventricosa* against gram-positive-negative bacterial strains (n = 3). (A) *B. subtilis* (BS); (B) *E. coli* (EC); (C) *Methicillin-resistant Staphylococcus aureus* (MRSA)*;*(D) *S. aureus* (SA); € *P. aeruginosa* (PA).

APPENDIX 2B

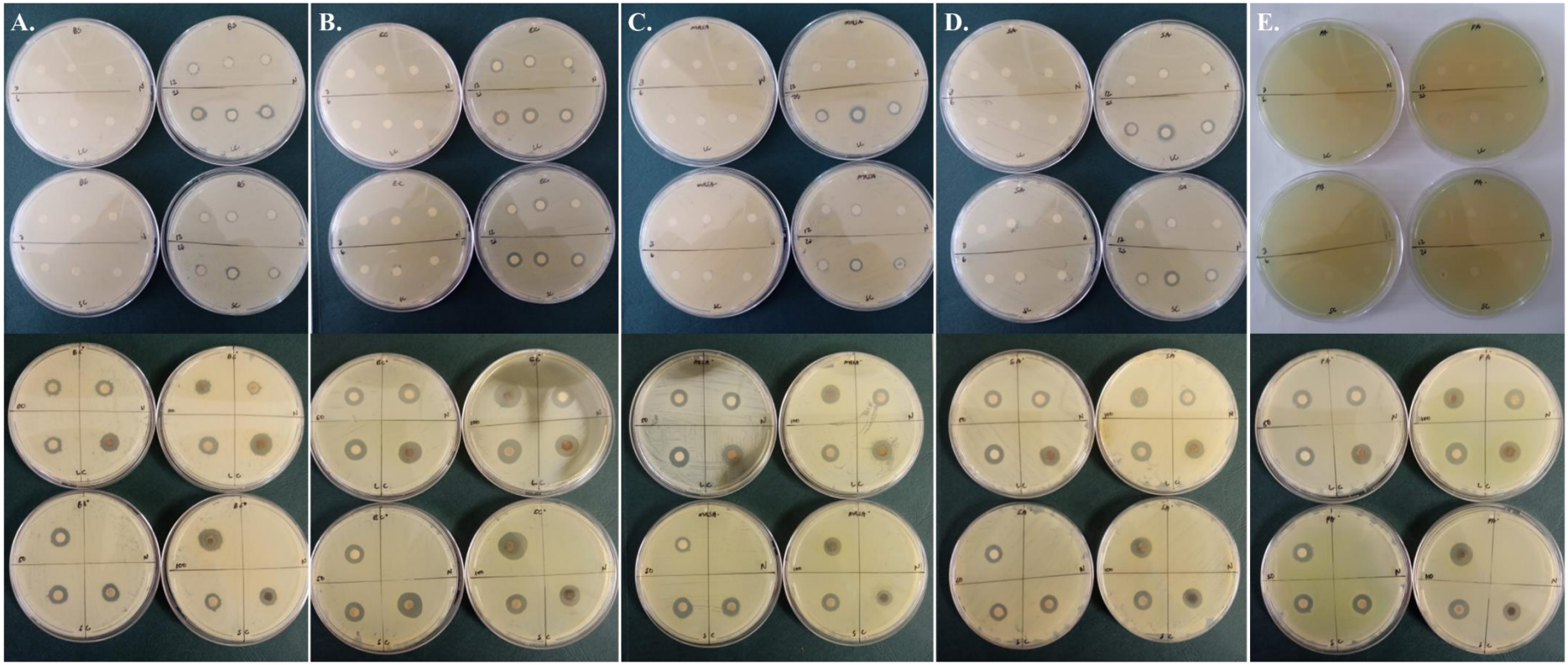

Figure 2: Zones of inhibition (mm) of various AgNPs synthesized using leaf, stem, and latex extracts of *T. ventricosa* against gram-positive-negative bacterial strains (n=3). (A) *B. subtilis* (BS); (B) *E. coli* (EC); (C) *Methicillin-resistant Staphylococcus aureus* (MRSA)*;*(D) *S. aureus* (SA); (E) *P. aeruginosa* (PA).

APPENDIX 3A

NANOSIGHT

SC1 2021-05-19 11-22-40

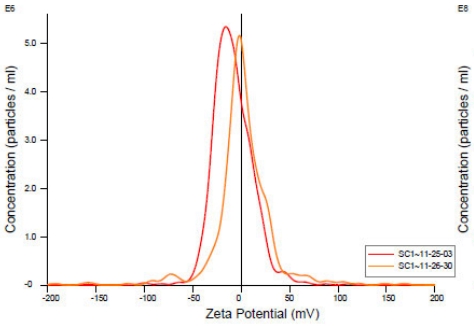

Concentration / Zeta Potential graph for Experiment:
SC1 2021-05-19 11-22-40

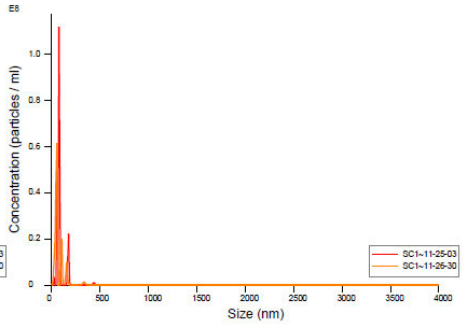

FTLA Concentration / Size graph for Experiment:
SC1 2021-05-19 11-22-40

Included Files

SC1 2021-05-19 11-25-03
SC1 2021-05-19 11-26-30

Details

NTA Version:	NTA 3.2 Dev Build 3.2.16
Script Used:	SC1.txt
Time Captured:	11:22:40 19/05/2021
Operator:	Aliscia
Pre-treatment:	
Sample Name:	SC1
Diluent:	Water
Remarks:	

Capture Settings

Camera Type:	sCMOS
Laser Type:	Blue405
Camera Level:	9
Slider Shutter:	607
Slider Gain:	15
FPS	25.0
Number of Frames:	1498
Temperature:	25.0 - 25.0 ºC
Viscosity:	(Water) 0.9 cP
Dilution factor:	Dilution not recorded

Analysis Settings

Detect Threshold:	7
Blur Size:	Auto
Max Jump Distance:	Auto: 14.0 - 22.3 pix

Results

Stats: Mean +/- Standard Error

Mean:	80.9 +/- 8.8 nm
Mode:	64.0 +/- 12.0 nm
SD:	52.4 +/- 0.3 nm
D10:	33.8 +/- 10.5 nm
D50:	54.7 +/- 11.3 nm
D90:	148.5 +/- 12.4 nm
Concentration:	2.22e+008 +/- 2.11e+007 particles/ml
	11.2 +/- 1.1 particles/frame
	35.3 +/- 15.3 centres/frame

Zeta Settings and Results

Parabola fit complete (poor quality fit)
Adjusted r-square: 0.90

Applied Voltage	24.0 V
Dielectric Constant:	80.00
Average Current	3.03 - 3.08 µA

Stats: Mean +/- Standard Error

Mean:	-3.5 +/- 5.1 mV
Mode:	-8.9 +/- 7.0 mV
SD:	26.1 +/- 5.4 mV
D10:	-28.6 +/- 3.6 mV
D50:	-6.0 +/- 5.6 mV
D90:	22.3 +/- 6.4 mV

NANOSIGHT

SC1 2021-05-19 11-22-40

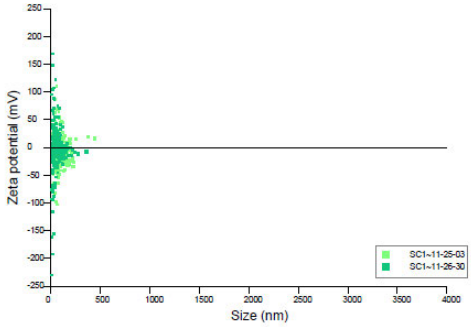

Zeta Potential / Size graph for Experiment:
SC1 2021-05-19 11-22-40

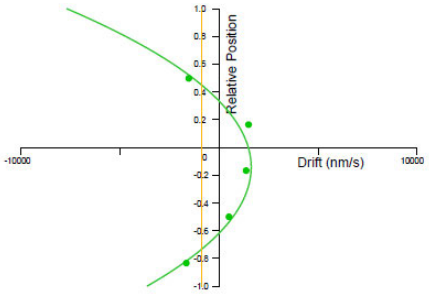

Flow profile for Experiment:
SC1 2021-05-19 11-22-40

NANOSIGHT

SC2 2021-05-19 12-22-41

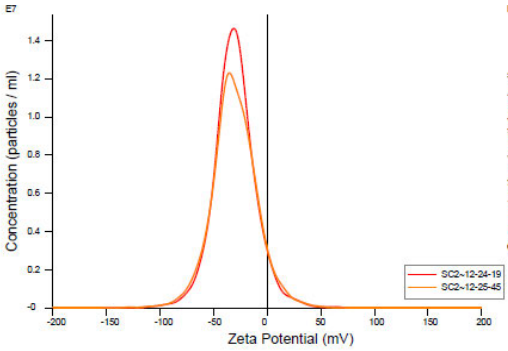

Concentration / Zeta Potential graph for Experiment:
SC2 2021-05-19 12-22-41

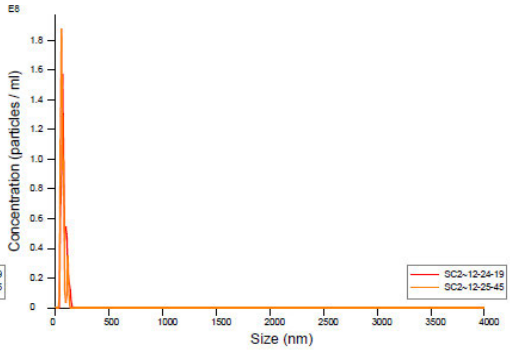

FTLA Concentration / Size graph for Experiment:
SC2 2021-05-19 12-22-41

Included Files

SC2 2021-05-19 12-24-19
SC2 2021-05-19 12-25-45

Details

NTA Version:	NTA 3.2 Dev Build 3.2.16
Script Used:	SC2.txt
Time Captured:	12:22:41 19/05/2021
Operator:	Aliscia
Pre-treatment:	
Sample Name:	SC2
Diluent:	Water
Remarks:	

Capture Settings

Camera Type:	sCMOS
Laser Type:	Blue405
Camera Level:	11
Slider Shutter:	890
Slider Gain:	146
FPS	25.0
Number of Frames:	1498
Temperature:	25.0 ºC
Viscosity:	(Water) 0.9 cP
Dilution factor:	Dilution not recorded

Analysis Settings

Detect Threshold:	7
Blur Size:	Auto
Max Jump Distance:	Auto: 18.1 - 19.4 pix

Results

Stats: Mean +/- Standard Error

Mean:	70.2 +/- 6.1 nm
Mode:	59.8 +/- 5.7 nm
SD:	21.5 +/- 1.8 nm
D10:	36.8 +/- 2.6 nm
D50:	54.3 +/- 5.7 nm
D90:	89.2 +/- 10.4 nm
Concentration:	5.95e+008 +/- 1.99e+007 particles/ml
	30.2 +/- 1.0 particles/frame
	38.2 +/- 1.2 centres/frame

Zeta Settings and Results

Parabola fit complete

Adjusted r-square:	1.00
Applied Voltage	24.0 V
Dielectric Constant:	80.00
Average Current	0.42 - 0.42 µA

Stats: Mean +/- Standard Error

Mean:	-30.3 +/- 0.1 mV
Mode:	-33.2 +/- 2.1 mV
SD:	20.8 +/- 0.7 mV
D10:	-55.5 +/- 1.3 mV
D50:	-31.9 +/- 0.1 mV
D90:	-6.2 +/- 0.9 mV

NANOSIGHT

SC2 2021-05-19 12-22-41

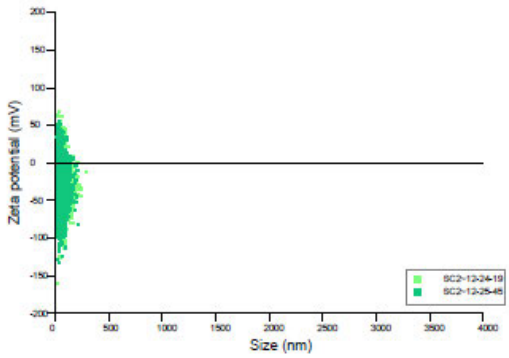

Zeta Potential / Size graph for Experiment:
SC2 2021-05-19 12-22-41

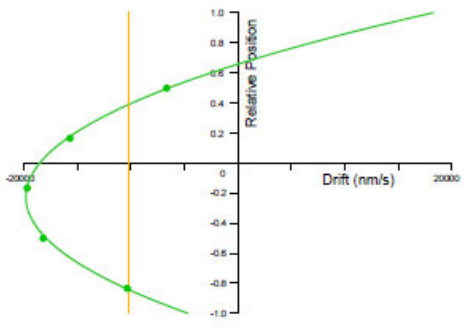

Flow profile for Experiment:
SC2 2021-05-19 12-22-41

NANOSIGHT

SC3 2021-05-20 10-20-36

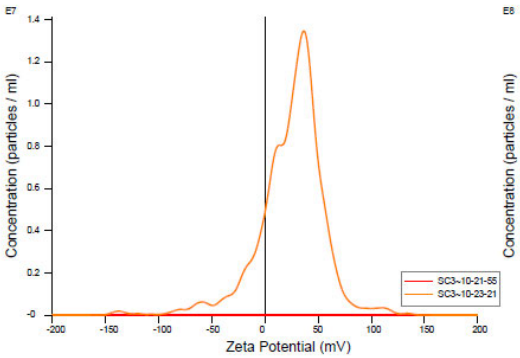

Concentration / Zeta Potential graph for Experiment:
SC3 2021-05-20 10-20-36

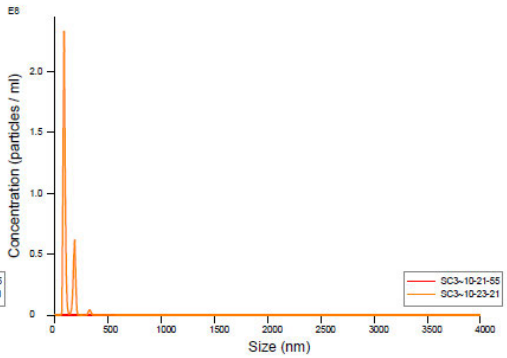

FTLA Concentration / Size graph for Experiment:
SC3 2021-05-20 10-20-36

Included Files

SC3 2021-05-20 10-21-55
SC3 2021-05-20 10-23-21

Details

NTA Version:	NTA 3.2 Dev Build 3.2.16
Script Used:	SC3.txt
Time Captured:	10:20:36 20/05/2021
Operator:	Aliscia
Pre-treatment:	
Sample Name:	SC3
Diluent:	Water
Remarks:	

Capture Settings

Camera Type:	sCMOS
Laser Type:	Blue405
Camera Level:	11
Slider Shutter:	890
Slider Gain:	146
FPS	25.0
Number of Frames:	1498
Temperature:	25.0 °C
Viscosity:	(Water) 0.9 cP
Dilution factor:	Dilution not recorded

Analysis Settings

Detect Threshold:	7
Blur Size:	Auto
Max Jump Distance:	Auto: 3.1 - 10.7 pix

Results

Stats: Mean +/- Standard Error	
Mean:	57.2 +/- 57.2 nm
Mode:	42.4 +/- 42.4 nm
SD:	26.8 +/- 26.8 nm
D10:	32.7 +/- 32.7 nm
D50:	39.8 +/- 39.8 nm
D90:	88.3 +/- 88.3 nm
Concentration:	5.31e+008 +/- 1.66e+008 particles/ml
	27.0 +/- 8.4 particles/frame
	77.5 +/- 8.9 centres/frame

Zeta Settings and Results

Parabola fit complete (poor quality fit)

Adjusted r-square:	0.87
Applied Voltage	24.0 V
Dielectric Constant:	80.00
Average Current	1.15 - 1.18 µA

Stats: Mean +/- Standard Error	
Mean:	12.3 +/- 12.3 mV
Mode:	18.3 +/- 18.3 mV
SD:	16.0 +/- 16.0 mV
D10:	-6.4 +/- 6.4 mV
D50:	14.1 +/- 14.1 mV
D90:	27.6 +/- 27.6 mV

NANOSIGHT

SC3 2021-05-20 10-20-36

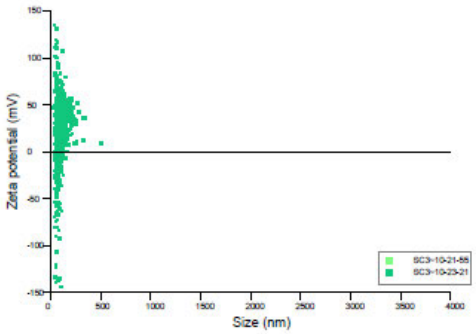

Zeta Potential / Size graph for Experiment:
SC3 2021-05-20 10-20-36

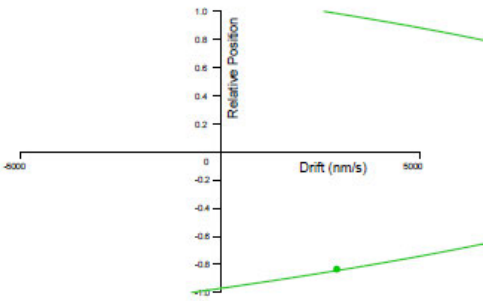

Flow profile for Experiment:
SC3 2021-05-20 10-20-36

NANOSIGHT

SC4 2021-05-20 10-55-22

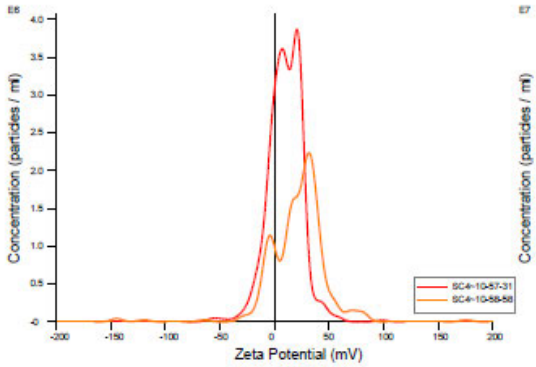

Concentration / Zeta Potential graph for Experiment:
SC4 2021-05-20 10-55-22

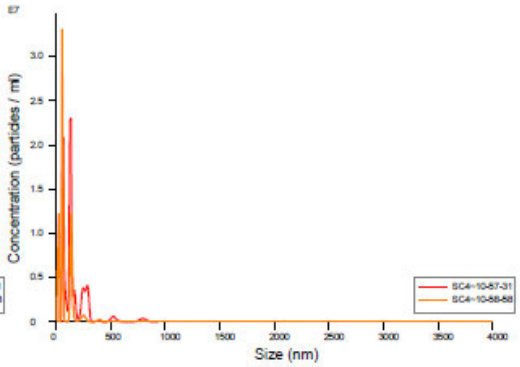

FTLA Concentration / Size graph for Experiment:
SC4 2021-05-20 10-55-22

Included Files

SC4 2021-05-20 10-57-31
SC4 2021-05-20 10-58-58

Details

NTA Version:	NTA 3.2 Dev Build 3.2.16
Script Used:	SC4.txt
Time Captured:	10:55:22 20/05/2021
Operator:	Aliscia
Pre-treatment:	
Sample Name:	SC4
Diluent:	Water
Remarks:	

Capture Settings

Camera Type:	sCMOS
Laser Type:	Blue405
Camera Level:	9
Slider Shutter:	607
Slider Gain:	15
FPS	25.0
Number of Frames:	1498
Temperature:	25.0 °C
Viscosity:	(Water) 0.9 cP
Dilution factor:	Dilution not recorded

Analysis Settings

Detect Threshold:	7
Blur Size:	Auto
Max Jump Distance:	Auto: 14.0 - 28.8 pix

Results

Stats: Mean +/- Standard Error	
Mean:	125.0 +/- 41.8 nm
Mode:	92.7 +/- 37.5 nm
SD:	97.4 +/- 30.8 nm
D10:	32.2 +/- 21.0 nm
D50:	84.4 +/- 37.5 nm
D90:	206.2 +/- 68.1 nm
Concentration:	1.18e+008 +/- 2.39e+007 particles/ml
	6.0 +/- 1.2 particles/frame
	17.3 +/- 1.6 centres/frame

Zeta Settings and Results

Parabola fit complete	
Adjusted r-square:	0.99
Applied Voltage	24.0 V
Dielectric Constant:	80.00
Average Current	1.33 - 1.33 µA
Stats: Mean +/- Standard Error	
Mean:	15.6 +/- 5.6 mV
Mode:	26.1 +/- 5.5 mV
SD:	21.8 +/- 5.8 mV
D10:	-8.8 +/- 0.9 mV
D50:	16.2 +/- 6.7 mV
D90:	35.2 +/- 9.2 mV

NANOSIGHT

SC4 2021-05-20 10-55-22

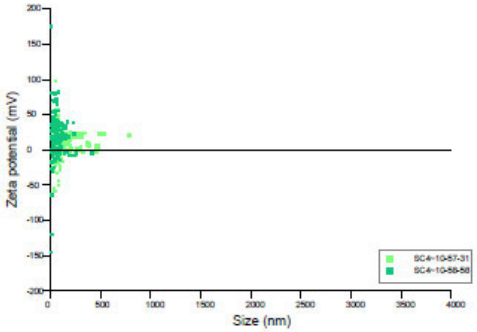

Zeta Potential / Size graph for Experiment:
SC4 2021-05-20 10-55-22

NANOSIGHT

SC5 2021-05-20 11-31-33

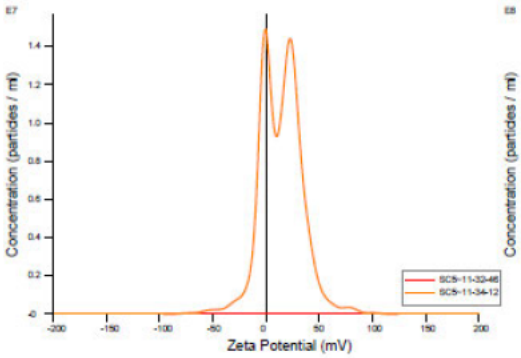

Concentration / Zeta Potential graph for Experiment:
SC5 2021-05-20 11-31-33

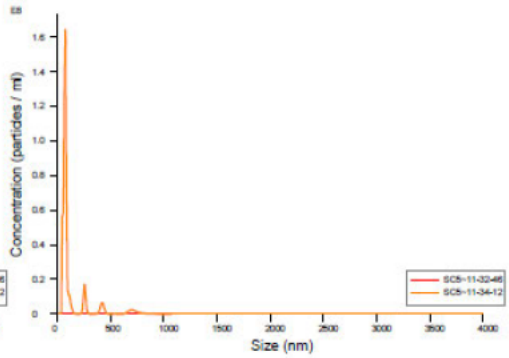

FTLA Concentration / Size graph for Experiment:
SC5 2021-05-20 11-31-33

Included Files

SC5 2021-05-20 11-32-46
SC5 2021-05-20 11-34-12

Details

NTA Version:	NTA 3.2 Dev Build 3.2.16
Script Used:	SC5.txt
Time Captured:	11:31:33 20/05/2021
Operator:	Aliscia
Pre-treatment:	
Sample Name:	SC5
Diluent:	Water
Remarks:	

Capture Settings

Camera Type:	sCMOS
Laser Type:	Blue405
Camera Level:	10
Slider Shutter:	696
Slider Gain:	73
FPS	25.0
Number of Frames:	1498
Temperature:	25.0 - 25.0 °C
Viscosity:	(Water) 0.9 cP
Dilution factor:	Dilution not recorded

Analysis Settings

Detect Threshold:	7
Blur Size:	Auto
Max Jump Distance:	Auto: 1.9 - 16.5 pix

Results

Stats: Mean +/- Standard Error

Mean:	63.9 +/- 63.9 nm
Mode:	36.3 +/- 36.3 nm
SD:	75.7 +/- 75.7 nm
D10:	20.5 +/- 20.5 nm
D50:	32.1 +/- 32.1 nm
D90:	127.8 +/- 127.8 nm
Concentration:	3.82e+008 +/- 2.55e+008 particles/ml
	19.4 +/- 12.9 particles/frame
	44.9 +/- 0.8 centres/frame

Zeta Settings and Results

Parabola fit complete (poor quality fit)

Adjusted r-square:	0.70
Applied Voltage	24.0 V
Dielectric Constant:	80.00
Average Current	0.91 - 0.93 µA

Stats: Mean +/- Standard Error

Mean:	7.2 +/- 7.2 mV
Mode:	-0.3 +/- 0.3 mV
SD:	9.9 +/- 9.9 mV
D10:	-4.1 +/- 4.1 mV
D50:	6.9 +/- 6.9 mV
D90:	18.2 +/- 18.2 mV

NANOSIGHT

SC5 2021-05-20 11-31-33

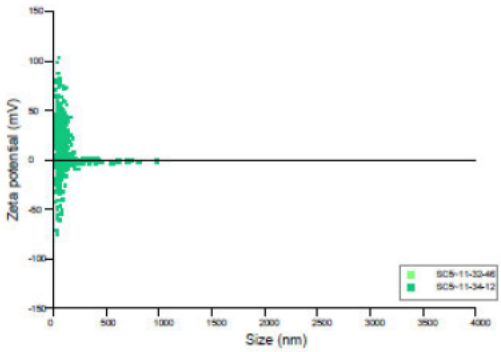

Zeta Potential / Size graph for Experiment:
SC5 2021-05-20 11-31-33

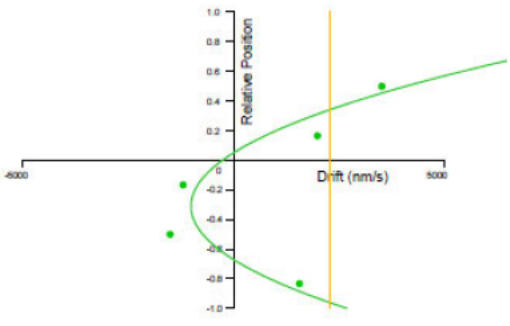

Flow profile for Experiment:
SC5 2021-05-20 11-31-33

NANOSIGHT

SC6 2021-05-20 12-03-27

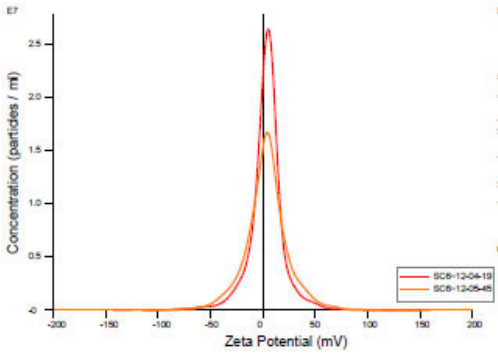

Concentration / Zeta Potential graph for Experiment:
SC6 2021-05-20 12-03-27

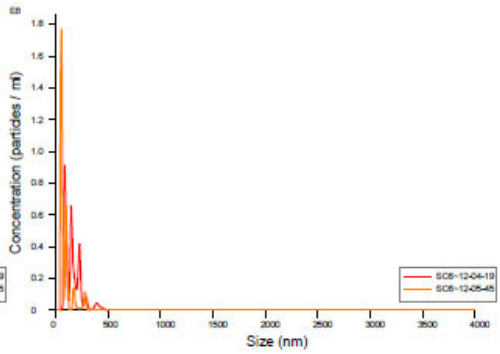

FTLA Concentration / Size graph for Experiment:
SC6 2021-05-20 12-03-27

Included Files

SC6 2021-05-20 12-04-19
SC6 2021-05-20 12-05-45

Details

NTA Version:	NTA 3.2 Dev Build 3.2.16
Script Used:	SC6.txt
Time Captured:	12:03:27 20/05/2021
Operator:	Aliscia
Pre-treatment:	
Sample Name:	SC6
Diluent:	Water
Remarks:	

Capture Settings

Camera Type:	sCMOS
Laser Type:	Blue405
Camera Level:	9 - 10
Slider Shutter:	607 - 696
Slider Gain:	15 - 73
FPS	25.0
Number of Frames:	1498
Temperature:	25.0 - 25.0 ºC
Viscosity:	(Water) 0.9 cP
Dilution factor:	Dilution not recorded

Analysis Settings

Detect Threshold:	7
Blur Size:	Auto
Max Jump Distance:	Auto: 11.6 - 17.3 pix

Results

Stats: Mean +/- Standard Error

Mean:	120.5 +/- 36.2 nm
Mode:	67.7 +/- 15.7 nm
SD:	68.3 +/- 10.4 nm
D10:	51.3 +/- 17.2 nm
D50:	92.2 +/- 43.2 nm
D90:	194.2 +/- 35.7 nm
Concentration:	6.45e+008 +/- 2.98e+007 particles/ml
	32.8 +/- 1.5 particles/frame
	57.2 +/- 1.6 centres/frame

Zeta Settings and Results

Parabola fit complete

Adjusted r-square:	0.99
Applied Voltage	24.0 V
Dielectric Constant:	80.00
Average Current	1.25 - 1.27 µA

Stats: Mean +/- Standard Error

Mean:	3.5 +/- 0.1 mV
Mode:	4.7 +/- 0.4 mV
SD:	19.2 +/- 2.4 mV
D10:	-18.8 +/- 3.6 mV
D50:	2.9 +/- 0.3 mV
D90:	23.1 +/- 4.2 mV

NANOSIGHT

SC6 2021-05-20 12-03-27

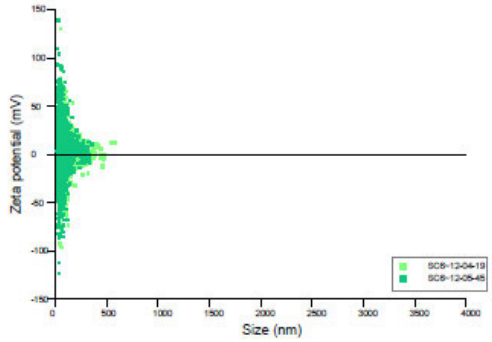

Zeta Potential / Size graph for Experiment:
SC6 2021-05-20 12-03-27

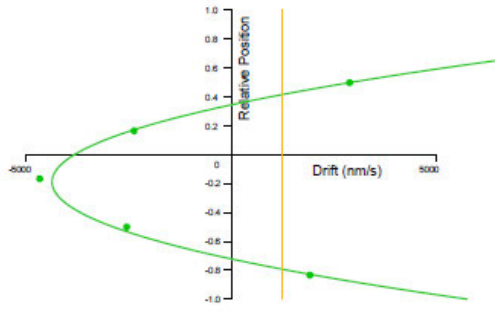

Flow profile for Experiment:
SC6 2021-05-20 12-03-27

NANOSIGHT

SC7 2021-05-21 12-26-27

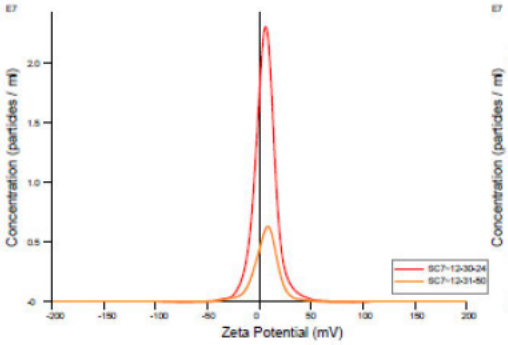

Concentration / Zeta Potential graph for Experiment:
SC7 2021-05-21 12-26-27

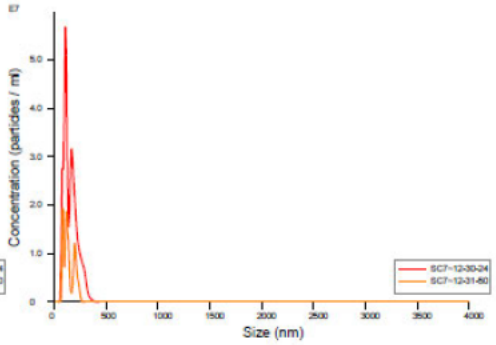

FTLA Concentration / Size graph for Experiment:
SC7 2021-05-21 12-26-27

Included Files

SC7 2021-05-21 12-30-24
SC7 2021-05-21 12-31-50

Details

NTA Version:	NTA 3.2 Dev Build 3.2.16
Script Used:	SC7.txt
Time Captured:	12:26:27 21/05/2021
Operator:	Aliscia
Pre-treatment:	
Sample Name:	SC7
Diluent:	Water
Remarks:	

Capture Settings

Camera Type:	sCMOS
Laser Type:	Blue405
Camera Level:	10
Slider Shutter:	696
Slider Gain:	73
FPS	25.0
Number of Frames:	1498
Temperature:	25.0 ºC
Viscosity:	(Water) 0.9 cP
Dilution factor:	Dilution not recorded

Analysis Settings

Detect Threshold:	7
Blur Size:	Auto
Max Jump Distance:	Auto: 11.9 - 12.6 pix

Results

Stats: Mean +/- Standard Error

Mean:	147.4 +/- 7.4 nm
Mode:	95.4 +/- 12.2 nm
SD:	56.4 +/- 6.3 nm
D10:	73.0 +/- 2.0 nm
D50:	125.4 +/- 9.1 nm
D90:	220.3 +/- 17.4 nm
Concentration:	3.43e+008 +/- 1.80e+008 particles/ml
	17.4 +/- 9.1 particles/frame
	22.4 +/- 12.5 centres/frame

Zeta Settings and Results

Parabola fit complete

Adjusted r-square:	0.98
Applied Voltage	24.0 V
Dielectric Constant:	80.00
Average Current	0.42 - 0.42 µA

Stats: Mean +/- Standard Error

Mean:	5.9 +/- 0.0 mV
Mode:	7.2 +/- 1.1 mV
SD:	13.0 +/- 1.1 mV
D10:	-9.5 +/- 1.1 mV
D50:	5.3 +/- 0.6 mV
D90:	18.5 +/- 0.9 mV

NANOSIGHT

SC7 2021-05-21 12-26-27

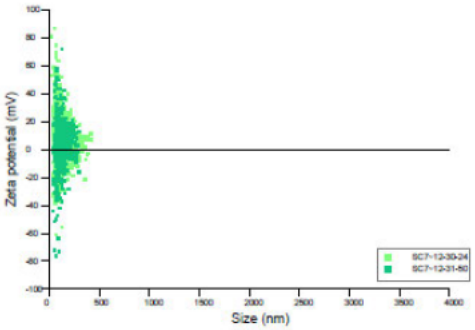

Zeta Potential / Size graph for Experiment:
SC7 2021-05-21 12-26-27

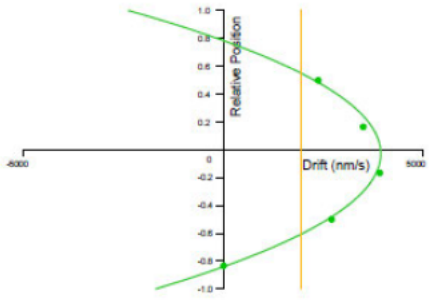

Flow profile for Experiment:
SC7 2021-05-21 12-26-27

APPPENDIX 4A

Laticifers in the leaves of *Tabernaemonatana ventricosa*: Structure, distribution and histophytochemical analysis

C.M. Naidoo, Y. Naidoo
School of Life Sciences, University of KwaZulu-Natal, Westville Campus, Private Bag X54001, Durban 4000, South Africa
E-mail address: naidooclarissa5@gmail.com (C.M. Naidoo)

Tabernaemontana ventricosa (E.A. Omino) is a medicinal plant belonging to the Apocynaceae family which is well known for its milky latex substance. The bark, stems, and leaves of *T. ventricosa* are regularly used in traditional medicine for the treatment of high blood pressure, reduction of fever and restoration of the nervous system. The latex is also used to promote wound healing. Latex occurs within specialized secretory cells that are identified as laticifers. The occurrence of non-articulated laticifers has been noted in the literature for the Apocynaceae family. However, insufficient information is available on the structure and the phytochemical compounds within the leaves of *T. ventricosa*. The aim of this study was to describe the structure and distribution of laticifers, as well as to explore the presence and location of phytochemical compounds within the leaves of *T. ventricosa*. The micromorphology and anatomy of laticifers were determined using light and electron microscopy. Non-articulated, branched and un-branched laticifers displaying intrusive growth were discovered in *T. ventricosa*. Laticiferious cells were found prominently in the midrib region which was closely associated to the vascular system. Preliminary histophytochemistry identified major phytochemical compounds such as; alkaloids, phenolics, and fats and fixed oils. Due to the importance of these compounds further study is essential to establish the potential medicinal properties of this species. In addition, the further classification of laticifers within vegetative and reproductive organs of *T. ventricosa* will assist the field of taxonomy, as many uncertainties exist within the Apocynaceae family regarding prior identification and classification of laticifers present within various species.

doi:10.1016/j.sajb.2018.02.177

plants

MDPI

Article

The Secretory Apparatus of *Tabernaemontana ventricosa* Hochst. ex A.DC. (Apocynaceae): Laticifer Identification, Characterization and Distribution

Clarissa Naidoo [1], Yougasphree Naidoo [1,*] and Yaser Hassan Dewir [2,3]

[1] School of Life Sciences, University of KwaZulu–Natal, Westville Campus, Private Bag X54001, Durban 4000, South Africa; naidooclarissa5@gmail.com

[2] Plant Production Department, P.O. Box 2460, College of Food & Agriculture Sciences, King Saud University, Riyadh 11451, Saudi Arabia; ydewir@ksu.edu.sa

[3] Department of Horticulture, Faculty of Agriculture, Kafrelsheikh University, Kafr El-Sheikh 33516, Egypt

* Correspondence: Naidooy1@ukzn.ac.za; Tel.: +27-(031)-260-7360

Received: 28 April 2020; Accepted: 25 May 2020; Published: 28 May 2020

Abstract: Due to the inconsistencies in the interpretation of laticifers within the Apocynaceae, the current study aimed to distinguish, for the first time, the type and distribution of the laticifers in the embryos, seedlings and adult plants of *Tabernaemontana ventricosa* (Forest Toad tree). The characterization and distribution of laticifers were determined using light and electron microscopy. The findings revealed the presence of articulated anastomosing laticifers. The laticifers were found to have originated from ground meristematic and procambium cells and were randomly distributed in all ground and vascular tissue, displaying complex branching conformations. The presence of chemical constituents within the laticifers and latex determined by histochemical analysis revealed the presence of alkaloids, phenolics, neutral lipids, terpenoids, mucilage, pectin, resin acids, carboxylated polysaccharides, lipophilic, and hydrophilic substances and proteins. These secondary metabolites perform an indispensable role in preventing herbivory, hindering and deterring micro-organisms and may possibly have medicinal importance. The outcomes of the present study outlined the first micromorphology, anatomy, ultrastructural and chemical analysis of the laticifers of *T. ventricosa*. In addition, this investigation similarly established the probable functions of latex and laticifers.

Keywords: laticifers; latex; articulated; anastomosing; alkaloids

1. Introduction

The occurrence of laticifers and latex has been observed in approximately 12,500 plant species representing 22 families [1–3]. Latex is characterized as a sticky suspension of several particles containing a sap of various plant metabolites [3–5]. These naturally occurring secondary metabolites are formed from several constituents which are usually produced via primary and secondary metabolism [6,7]. Plant secondary metabolites can be divided into three chemically distinct groups: Terpenoids, phenolics, and nitrogen/sulfur containing compounds [8–10]. These diverse secondary metabolites are essential for plant growth, development, interactions, and defense systems [6–10].

Natural secondary products such as latex are comprised of a variety of composite chemical constituents which is often species dependent for, e.g., terpenoids (*Hevea brasiliensis*), alkaloids (*Papaver somniferum*), phenolic glucosides (*Cannabis sativa*), proteins (*Ficus callosa*), and tannins (*Musa* sp.) [11]. The occurrence of these chemical constituents could attribute to the appearance of latex as the color varies in plant species and may appear milky white, yellow, orange, red, brown, or

plants

MDPI

Review

Major Bioactive Alkaloids and Biological Activities of *Tabernaemontana* Species (Apocynaceae)

Clarissa Marcelle Naidoo [1], Yougasphree Naidoo [1], Yaser Hassan Dewir [2,3,*], Hosakatte Niranjana Murthy [4], Salah El-Hendawy [2,5] and Nasser Al-Suhaibani [2]

1 School of Life Sciences, Westville Campus, University of KwaZulu-Natal, Private Bag X54001, Durban 4000, South Africa; naidooclarissa5@gmail.com (C.M.N.); naidooy1@ukzn.ac.za (Y.N.)
2 Plant Production Department, College of Food and Agriculture Sciences, King Saud University, P.O. Box 2460, Riyadh 11451, Saudi Arabia; mosalah@ksu.edu.sa (S.E.-H.); nsuhaib@ksu.edu.sa (N.A.-S.)
3 Department of Horticulture, Faculty of Agriculture, Kafrelsheikh University, Kafr El-Sheikh 33516, Egypt
4 Department of Botany, Karnatak University, Dharwad 580003, India; hnmurthy60@gmail.com
5 Department of Agronomy, Faculty of Agriculture, Suez Canal University, Ismailia 41522, Egypt
* Correspondence: ydewir@ksu.edu.sa

Abstract: Several species belonging to the genus *Tabernaemontana* have been well researched and utilized for their wide-ranging biological activities. A few of the most prominent species include *Tabernaemontana divaricata*, *Tabernaemontana catharinensis*, *Tabernaemontana crassa*, and *Tabernaemontana elegans*. These species and many others within the genus often display pharmacological importance, which is habitually related to their chemical constituents. The secondary metabolites within the genus have demonstrated huge medicinal potential for the treatment of infections, pain, injuries, and various diseases. Regardless of the indispensable reports and properties displayed by *Tabernaemontana* spp., there remains a wide variety of plants that are yet to be considered or examined. Thus, an additional inclusive study on species within this genus is essential. The current review aimed to extensively analyze, collate, and describe an updated report of the current literature related to the major alkaloidal components and biological activities of species within the genus *Tabernaemontana*.

Keywords: alkaloids; Apocynaceae; biological activity; pharmacological properties; *Tabernaemontana*

Citation: Naidoo, C.M.; Naidoo, Y.; Dewir, Y.H.; Murthy, H.N.; El-Hendawy, S.; Al-Suhaibani, N. Major Bioactive Alkaloids and Biological Activities of *Tabernaemontana* Species (Apocynaceae). *Plants* 2021, *10*, 313. https://doi.org/10.3390/plants10020313

Academic Editor: Milan Stankovic
Received: 31 December 2020
Accepted: 29 January 2021
Published: 5 February 2021

1. Introduction

The genus *Tabernaemontana* belonging to the family Apocynaceae was named by a German physician and botanist, J. Th. Muller [1]. At present, approximately 100 species belonging to this genus have been distributed in tropical and subtropical regions around the world, including Africa, Asia, Oceania, and the Americas [2]. *Tabernaemontana* species consists of flowering shrubs and small-medium-sized trees, which habitually grow in the savannahs, rocky outcrops, and forest understories [3]. Characteristic features of the genus include tubular white flowers, follicular fruit with seeds embedded within a yellow to reddish aril, and a milky or watery latex exudate, which is often found in wounded species [4]. Due to the latex content, plants within this genus are usually called "milkweed" and are often used for their biological activities [2,5,6]. Plants within the genus *Tabernaemontana* obtain a profusely high alkaloid content, usually displaying pharmacological activity [2]. Furthermore, monoterpene indole and bisindole alkaloids are the major classes of alkaloids within the genus, and other compounds include terpenes, lactones, steroids, phenolics, and flavonoids [1]. Over 67 species have been investigated for indole alkaloids, of which 470 isolations of approximately 240 structurally different bases have been detected [2,3,7].

A few of the most intensively studied *Tabernaemontana* species include *T. divaricata*, also known as "Crape Jasmine", which occurs in the tropical regions of southern China, India, and Thailand [8]. Crape Jasmine is intensively utilized as an aphrodisiac, tonic, and a purgative [8]. According to Van Beek et al. [1], in western India, latex is used for

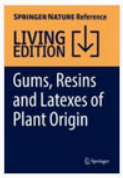

Gums, Resins and Latexes of Plant Origin pp 1-24 | Cite as

Chemistry, Biological Activities, and Uses of Latex from Selected Species of Apocynaceae

Authors | Authors and affiliations

Clarissa Marcelle Naidoo, Ashlin Munsamy, Yougasphree Naidoo, Yaser Hassan Dewir

Living reference work entry
First Online: 02 November 2021

Part of the Reference Series in Phytochemistry book series (RSP)

Abstract

Latex is a complex phytochemical that is mainly involved in the plant defense system. Several species belonging to the Apocynaceae family produce latex that is composed of diverse classes of phytochemicals including proteins, alkaloids, glycolipids, glycosides, acids, sterols, fatty acids, tannins, resins, oils, terpenoids/flavonoids, acetogenins, saponins, and allergens. These phytochemicals contain bioactive compounds with various biological activities such as antibacterial, antifungal, antiviral, antiamebic, anti-inflammatory, anticancer, antioxidant, and antivenom properties. Additionally, species within the Apocynaceae have palliative effects, which frequently promotes the usage of latex-bearing species in traditional and contemporary medical systems. This chapter addresses the chemical composition of latex and provides a summary of its biological activities in selected species of Apocynaceae.

Keywords

Apocynaceae | Alkaloids | Biological activity | Chemistry | Latex